UNIVERSITY OF ANTWERP
UNIVERSITY INSTITUTE AT ANTWERP

Department of Chemistry

# Ab initio study of cluster molecules relevant to materials science and astrophysics



## Development of combined bond-polarization basis sets for the accurate ab initio calculation of dissociation energies



Thesis submitted in partial fulfillment of the requirements for the degree of Doctor of Sciences (Ph.D.) at the University Institute at Antwerp, to be defended in public by

**Jan M. L. MARTIN**
(NFWO Research Assistant, Limburg University Center and UIA)

Thesis Supervisor: Prof. Dr. J.-P. François, Professor at the LUC
Thesis Co-Supervisor: Prof. Dr. R. Gijbels, Full Professor at the UIA



Antwerp, 1991

Nederlandse titel/Dutch title: *Ab initio studie van clustermoleculen van belang in materiaalwetenschappen en astrofysica. Ontwikkeling van gecombineerde bond-polarisatiebasissets voor de nauwkeurige ab initio berekening van dissociatie-energieën.*



## Typographical notes

All fonts used throughout this document are from the Computer Modern (CM) family designed by Donald E. Knuth for use with TEX. The body text was typeset in 12-point CM Roman, with a 6-point leading to enhance readability and reduce super-and subscript clashes. Mathematical formulas are typeset in 12-point CM Math Italic, 8-point type being used for super-and subscripts. Tables were typeset in 11-point CM Roman without leading, with 10-point and 9-point type being used if necessitated by the width of the tabular material. Table captions are in 12-point CM Roman. Footnotes are in 10-point, references in 11-point type. All sectional headings were typeset in CM Bold Extended, 12-point type being used for subsubsection, 14-point for subsection, 17-point for section, and finally 20-point type for chapter headings. All lettering on figures has been done in Helvetica, with mathematical symbols being taken from the Symbol font where necessary.

This work was printed by Omniaprint NV, Hasselt, from camera-ready copy supplied by the author. The final version was entirely typeset using TEXtures 1.3 on an Apple Macintosh SE/30 with 4 MB of RAM and 80 MB of hard disk. The LATEX format was used throughout, with a user-defined style file. Hardcopy was generated on an Apple LaserWriter Plus. Chemical structures were drawn using ChemIntosh 1.41 and imported in TEXtures as `PICT` objects. Graphs were prepared in KaleidaGraph 2.01 and imported as `PICT` files with associated PostScript code. All other artwork was drawn in Aldus Freehand 2.02 and imported as `EPSF` (encapsulated PostScript) files.

# Contents

# Foreword

*The more progress physical sciences make, the more they tend to enter the domain of mathematics, which is a kind of center to which they all converge. We may even judge the degree of perfection to which a science has arrived by the facility with which it may be submitted to calculation.*

A. Quételet, 1796–1874

Being a mathematician himself, Quételet had every reason to arrive at the above conclusion. Yet one cannot deny that there is some truth in this statement. For the areas of physics that are the oldest and most exhaustively researched, like classical mechanics, there exists a closed mathematical formalism. The younger branches of physics, like elementary particle physics, still heavily rely on experiments, though mathematical formalism plays a great role too. Chemistry, that 'junior brother' of physics, is becoming a computational science to an increasing extent. Biologists apply the new insights of nonlinear thermodynamics, and even purely 'empirical' branches like taxonomy rely on numerical techniques (like cluster analysis) today. Economics has an important offspring, econometry, where mathematical models are drafted for systems much more complex than any molecule. And even sociologists rely on computational techniques, not just for statistical data analysis but now also for simulations.

Many scientists still think of chemistry as purely or mainly an empirical branch of science, and this was even more so in the previous century. This opinion is best illustrated by the father of sociology, one of the first science philosophers, and founder of an ill-fated "religion of Humanity":

*Every attempt to employ mathematical methods in the study of chemical questions must be considered profoundly irrational and contrary to the spirit of chemistry. If mathematical analysis should ever hold a prominent place in chemistry — an aberration which is happily almost impossible — it would occasion a rapid and widespread degeneration of that science.*

A. Comte, 1798–1857

One must not forget that Comte — also a mathematician! — made this statement at a time when the second law of thermodynamics was not even known yet, and any progress in the field of chemistry had been made by heroic experiments. Ironically, a contemporary chemist chose to disagree with him:

*We are perhaps not far removed from the time when we shall be able to submit the bulk of chemical phenomena to calculation.*

J. L. Gay-Lussac, 1778–1850

The remainder of the nineteenth century saw first the development of classical ther-

modynamics, which allowed a quantitative description of macroscopic phenomena, such as chemical reactions, from macroscopic experimental data. The tragic genius of Ludwig Boltzmann gave us statistical thermodynamics near the turn of the century, which allowed a quantitative prediction of macroscopic data, such as thermodynamical quantities, from microscopic experimental data such as energy levels. The third stage, the development of quantum machanics, finally served to show, not only how energy levels could be found from spectroscopic constants, but even how these constants themselves can be derived *ab initio* from fundamental quantities — the atomic and electron masses and charges as well as the fundamental physical constants — by solving the wave equation for the system.

Unfortunately there arises the complication that the wave equation for a many-particle system cannot be solved in closed form. The situation in the thirties can be summarized best as follows:

> *The underlying physical laws necessary for the mathematical theory of a large part of physics and the whole of chemistry are thus completely known, and the difficulty is only that the exact application of these laws leads to equations much too complicated to be soluble.*
>
> P. A. M. Dirac, 1902–1984

Numerical solution was the obvious alternative, as the required quantities could then still be obtained anyway. But because all numerical calculations still had to be carried out by hand, there followed a period of slow progress. In a first stage, people developed approximate algorithms which would — hopefully — sacrifice as little accuracy as possible while reducing computational labor as greatly as possible. Much of the foundations of computational chemistry has been laid in that period; practical applications were hindered by the requirement that all calculations still had to be carried out by hand, using mechanical desktop calculators.

The major breakthrough was therefore not one of science but of technology, namely the invention of the digital computer. Now two developments started working in synergy; on one front, theoretical chemists devised increasingly efficient algorithms yielding more accuracy in less floating-point operations; on another, developments in the field of electronics made computers ever faster, smaller, and less expensive. Together they finally created a situation where *ab initio* calculations for small molecules can reach an accuracy comparable to that of good experiments, often at substantially lower cost.

But this is only the beginning. Rare, reactive or short-lived species cannot be studied well by experiment; such problems are totally immaterial for the quantum chemist, who can equally well study the most abundant and stable molecules, such as $H_2O$ and $N_2$, or a transition state for a reaction which has by definition no lifetime at all.

The present state of the art appears to be: chemical accuracy for small molecules, semiquantitative results for medium-sized, and qualitative results for large molecules. As computers grow more and more powerful every day, the medium-sized and finally the large molecules will succumb to the power of 'brute reason'.

> *I would like to emphasize strongly my belief that the era (...) where hundreds if not thousands of chemists will go to the computing machine instead of the laboratory, for increasingly many facets of chemical information, is already at hand.*
>
> R. S. Mulliken, 1896–1986

The present work summarizes the modest contributions of the author to this emerging area of 'computational chemistry'. He hopes the reader enjoys it.

# Reader's guide

Except for some brief introductory and ackowledgment material, this thesis is composed of five main chapters.

In Chapter 1, a discussion of all the computational methods and techniques relevant to this work may be found. The discussion there is aimed at the nonspecialist with some background in general physical chemistry, as well as at quantum chemists who do not have a working experience with electron correlation methods. Monographs could have been written about every single subject touched there; the discussion therefore cannot claim completeness. The principal aim of this Chapter is not to describe the methods in full mathematical or implementational detail, but rather to outline their philosophy, their main advantages and disadvantages, and their mutual relationships.

In Chapter 2, an overview of all the computing equipment and software packages used in this work has been given.

The following three chapters, in which the author's original investigations in the field are reported, constitute the bulk of the present thesis. Chapter 3 deals with the development of a new family of basis sets, with which very accurate determinations of the binding energies of the first-row hydrides could be achieved. Chapter 4 presents various applications of ab initio methods to cluster chemistry. Finally, in Chapter 5 a number of methodological issues are discussed.

The first section of each of these latter chapters consists of a general introduction, the 'hows and whys', and a brief summary of the results presented in the subsequent sections. Each subsequent section is a self-contained unit, that may be read more or less without reference to the other sections of the chapter. With two exceptions (both of them due for publication), each of these sections is an adaptation of an article previously published in an international journal.

Tables and Figures relevant to a Section are presented in the course of the text, rather than grouped at the end of the chapter, in order both to save space and to achieve continuity. Tables and Figures are placed as closely as possible to the first location where they are referenced.

Between two sections in a chapter there may be a fairly large distance in time. This means that different sections may reflect different interpretative insights on the same topic. At the risk of sometimes sounding schizophrenic, the author has deliberately not made attempts to 'bend' the older sections towards the insights in the 'newer' ones.

Bibliographic references are grouped at the end of a chapter. Abbreviations for journal names follow the *Physical Review* recommendations[1]. In-text citations use the American Mathematical Society (AMS) system, with alphanumerical labels enclosed in square

[1] A. Waldron and P. Judd (Eds.), *Physical Review style and notation guide* (American Physical Society, Woodbury, NY, 1983), Appendix A.

brackets. The label consists of the first three letters of the principal author's name, followed by the last two digits of the year of publication and, where necessary to remove ambiguities, a single lowercase letter a–z which is assigned in order of appearance in the reference list. The latter is ordered first by author(s), then by year, then by journal, then by volume, and finally by first page. In the author's opinion, the AMS system represents the best compromise between the numeric system — which is compact but uninformative as well as (without automatic numbering) highly error-prone[2] — and the informative but verbose (Author,Year) system.

Some special cases for label construction are dealt with as follows. If the reference is a collective work published by or for an organization, the organizational acronym is used to create the label. If the material referenced is a personal communication to the present author, the year is replaced by the uppercase letters "PC". If it is a personal communication to some other author quoted in another reference, say [May68], the year of publication of this latter reference is used, and a statement "quoted in [May68]" is added. If the material referenced is a prepublication item that is to be published formally, the year is replaced by the uppercase letters "TBP". If the material referenced is unpublished work without firm plans for formal publication, the year is replaced by the uppercase letters "UP".

The convention for mathematical symbols is as follows.

- Scalar quantities are denoted by uppercase or lowercase letters in math italics, e.g. $A$, $T$, $E$, $D_e$.
- Vectors (or any one-dimensional arrays) are denoted by uppercase or lowercase letters with a vector arrow above, e.g. $\vec{x}$, $\vec{C}$.
- Matrices are indicated by sans serif type, e.g. $\mathsf{F}$, $\mathsf{P}$. Elements of a matrix are however set in math italics (e.g. $F_{pq}$, $P_{rs}$), unless they themselves are matrices.
- Operators are indicated by 'operator hats', e.g. $\hat{H}$, $\hat{T}_n$.

[2]Besides, in the commonly used 'superscript' variant, leading to confusing situations such as "the best result was 9.69 $eV^{17}$" or "this method was applied to $N_2$[18], $CO$[19], and $NO^{+}$[20]".

# Acknowledgments

First and foremost, I should thank Prof. Dr. J. P. François for being the Supervisor of this Thesis and his continued interest in its progress.

Secondly, thanks are due to Prof. Dr. R. Gijbels, who made his considerable skill in managing resources and people available as Assistant Supervisor and suggested the subject for Chapter IV.

The author was supported by the National Fund for Scientific Research (NFWO/FNRS) through a Research Assistant Fellowship. He is therefore perenially indebted to this organization.

This work could never have been completed without the availability of large amounts of computer time on high-performance equipment. The author is therefore indebted to the following organizations or individuals;

- The NFWO and the Services for Science Policy Programming of the Prime Minister's Office (DPWB) for large allotments of computer time on the IBM 3090/400e VF mainframe with vector facilities at the University of Leuven (KUL);
- Prof. Dr. Jean-Marie André of the Facultés Universitaires de Namur (FUN) for generously allowing usage of the IBM/FPS configuration at Namur;
- The DPWB for research grants enabling the purchase of a DEC VAXstation 2000 and its subsequent upgrade to a VAXstation 3100, on which the bulk of the present work has been done;
- The Limburgs Universitair Centrum (LUC) for free access to the campus CDC Cyber 930/11 mainframe, which was used for `BITNET` access, as a front-end to the 3090 and FPS configurations, and for some semiempirical calculations.

The following staff members of the various computer centers should be credited for their kind and helpful technical assistance: Mr. Frans Van De Ven at the KUL; Dr. J. G. Fripiat, Dr. D. Vercauteren, and Mr. Bruno Durasse at the FUN; and finally Mr. Marc Thoelen at the LUC.

During the course of this work, the author has benefited from helpful discussions with a number of people, including but not limited to (in no particular order) Prof. Dr. Chris Van Alsenoy (UIA), Prof. Dr. Paul Geerlings (Brussels Free University), Prof. Dr. Gustavo E. Scuseria (Rice University, Houston, TX), Prof. Dr. Martin Vala (University of Florida, Gainesville, FL), Dr. James R. Heath (University of California, Berkeley, CA), Dr. Zdenek Slanina (Heyrovsky Institute of Physical Chemistry and Electrochemistry, Prague), Prof. Dr. Jan Almlöf (University of Minnesota, Minneapolis, MN), and especially Dr. Peter R. Taylor (NASA Ames Research Center, Moffett Field,

CA), with whom I had the great pleasure and honor of collaborating on a joint project (see Section 4.11).

The following persons should be credited for making available results prior to publication:

- Dr. James R. Heath, whose IR spectroscopic work with Doppler limited resolution on carbon clusters was synergetic with my own ab initio and semiempirical work on these species in characterising $C_7$ and $C_9$;
- Dr. Krishnan Raghavachari, who made available some unpublished UHF/6-31G* infrared intensity data on the clusters $C_6$ to $C_9$;
- Prof. Dr. Martin Vala, who made available a preprint of isotopic substitution work on $C_6$ and (allegedly) $C_8$ long before its appearance in print;
- Prof. Dr. Jan Almlöf, who made available his ab initio work on $C_4$ prior to publication;
- Dr. Peter R. Taylor, who contributed too many prepublication items to mention here;
- Prof. Dr. Gustavo E. Scuseria, who sent me prepublication work on $C_3^+$ and on the CCSD(T) method;
- Dr. V. J. Barclay (University of Ontario, Ottawa, Canada), who sent a copy of his Ph.D. Thesis on bond functions;
- Dr. Ludwik Adamowicz (University of Arizona, Tucson, AZ), Prof. Dr. David W. Ewing (John Carroll University, Cleveland, OH), and many others who sent prepublication material of various kinds.

It goes without saying that I am grateful to my parents, who made it possible for me to study for a University degree, and continued to provide me with miscellaneous logistical support afterwards even though I had decided to live on my own.

And now for the "that's what friends are for" department: I hereby thanks Jos, Roos, Werner (Donné), Werner (Callebaut), Patrick, Dirk, Karin, Jack, Geert-Jan, and all the others (you know who you are) that put up with my company, for moral support and inspiring discussions on all possible kinds of topics outside quantum chemistry. Of these, Jos Gijsenbergs taught me whatever little I know of typography and layout, Patrick Bonckaert converted me from an antiTEXite into a TEX proselite, and Werner Callebaut brought me in contact with the most recent issues in science philosophy.

Thanks are also due to Dr. J.-P. Schneiders (Mathematical Institute, Université de l'Etat à Liège) who provided me with copies of OzTEXand BIBTEX, and to Mrs. M.

Withofs-Ieven, who prepared beautiful Aldus Freehand drawings from my sloppy sketches for the figures in Chapter 1.

And finally, I should of course acknowledge R., who has had to put up with being a 'computer widow' for almost as long as she knows me.

This work is built upon the foundations that many of the finest theoretical physicists and chemists have laid in the past half century, but could never have been completed successfully without someone dreaming up the machine on which to do the actual calculations. I therefore most humbly dedicate it

*to John Von Neumann (1903–1957).*

one of whose many brainchildren is the computer as we know it today.

# Chapter 1

# Theoretical background

*I had not supposed, sons, that we were on such familiar terms with Nature that, in response to a simple and perfunctory salutation, she would condescend to unveil for us her mysteries and bestow on us her blessings...*

*Francis Bacon, 1561–1626*

## 1.1 Hartree-Fock based methods

In this section, we will briefly recapitulate some points about Hartree-Fock theory, as well as discuss some SCF-related topics such as convergence enforcement and acceleration, and stability testing of the wavefunction.

A general introduction to Hartree-Fock theory may be found in the textbooks by Ostlund and Szabo [Sza89, Chapters 2 and 3], and by McWeeny [McW89, especially Chapters 5 and 6] or in the 'review book' by Hehre *et al.* [Heh86a]; the subject is also discussed in the M.Sc. Thesis of the present author [Mar87].

In the latter work, a summary is also given of semiempirical methods, such as: (1) extended Hückel theory [Hof63]; (2) intermediate neglect of differential overlap (INDO) [Pop67] and its reparametrizations MINDO (modified INDO) [Bai69], MINDO/2 [Dew70], and MINDO/3 [Bin75a]; and (3) neglect of diatomic differential overlap (NDDO) [Sus69] and its commonly used variants MNDO (modified neglect of diatomic overlap) [Dew77], AM1 (Austin model 1) [Dew85], and PM3 [Ste89]. A brief summary of these techniques is also given in the introduction to Section 4.7 [Mar90d].

### 1.1.1 Brief recapitulation of Hartree-Fock theory

Under the Hartree-Fock approximation, it is assumed that the many-particle wavefunction contains no explicit coupling terms, i.e.

$$\psi = \hat{A}\phi_1(\vec{r}_1)\phi_2(\vec{r}_2)\ldots\phi_N(\vec{r}_N) \tag{1.1}$$

where the fermion character of the particles is accounted for by the *antisymmetrization operator*

$$\hat{A} = \frac{1}{\sqrt{N!}} \sum_p (-1)^p \hat{P}_p \tag{1.2}$$

and the summation runs over all $N!$ possible permutations of the coordinates [1]. $p$ is the number of pairs that have been permuted. It is easily seen, that $\psi$ may be written in determinant form, and is therefore called a *Slater determinant.*

Each one-particle function is the product of a spatial function and a spin function. The latter can only be one of the functions $\varsigma_\alpha$ or $\varsigma_\beta$ (spin-up and spin-down, respectively); the former can be developed as linear combinations of some appropriate set of quadratically integrable functions called *basis functions*

$$\phi_i = \sum_p c_{ip} \xi_p \tag{1.3}$$

For historical reasons, these basis functions are called the *atomic orbitals* (AOs).[2] We will first consider the general case where all orbitals have different spatial parts, which is called an UHF (*unrestricted Hartree-Fock*) wavefunction. Applying the Rayleigh-Ritz variational principle with the Slater determinant as the trial wave function, we obtain after some straightforward but lengthy variation calculus the *Pople-Nesbet equations* [Pop54]:

$$E = \frac{1}{2} \sum_{pq} [(P^\alpha_{pq} + P^\beta_{pq}) H_{pq} + P^\alpha_{pq} F^\alpha_{pq} + P^\beta_{pq} F^\beta_{pq}] \tag{1.4}$$

$$F^\alpha_{pq} = H_{pq} + \sum_{rs} (P^\alpha_{rs} + P^\beta_{rs}) \langle pr|qs\rangle - \sum_{rs} P^\alpha_{rs} \langle pr|sq\rangle \tag{1.5}$$

$$F^\beta_{pq} = H_{pq} + \sum_{rs} (P^\alpha_{rs} + P^\beta_{rs}) \langle pr|qs\rangle - \sum_{rs} P^\beta_{rs} \langle pr|sq\rangle \tag{1.6}$$

$$\mathsf{F}^\alpha \vec{c}^\alpha_i = \epsilon^\alpha_i \mathsf{S} \vec{c}^\alpha_i \;\forall\, i \tag{1.7}$$

$$\mathsf{F}^\beta \vec{c}^\beta_i = \epsilon^\beta_i \mathsf{S} \vec{c}^\alpha_i \;\forall\, i \tag{1.8}$$

where all summations run over the $n$ basis functions. $E$ denotes the Hartree-Fock energy, $\mathsf{F}^\alpha$ and $\mathsf{F}^\beta$ are called the $\alpha$ and $\beta$ *Fock matrices*, the $\vec{c}^\alpha_i$ and $\vec{c}^\beta_i$ are called the $\alpha$ and $\beta$ *molecular orbitals* (MOs) and the $\epsilon^\alpha_i$ and $\epsilon^\beta_i$ their associated *orbital energies.* The elements of $\mathsf{H}$ are integrals over the *one-electron operator*, which is the sum of the kinetic energy operator $\hat{T}$ and the nuclear attraction operator $\hat{V}$. $\mathsf{S}$ is called the *overlap matrix*; its elements are simply overlap integrals between the basis functions. $\langle pq|rs\rangle$ are the *two-electron integrals*[3]

$$\langle pq|rs\rangle = \int\int \phi_p(\vec{r}_1)\phi_q(\vec{r}_2) r_{12}^{-1} \phi_r(\vec{r}_1)\phi_s(\vec{r}_2) d\tau_1 d\tau_2 \tag{1.9}$$

[1] Or over all possible permutations of the one-particle functions, which is equivalent.

[2] This does by no means imply that they have to be centered on atoms, as is commonly supposed.

[3] This notation, where the bras are on the left and the kets on the right, is called the physicist's notation. The so-called chemical notation would be $[pr|qs]$, where the functions of $\vec{r}_1$ are on the left and those of $\vec{r}_2$ on the right. Except where indicated otherwise, the former notation is used throughout in this work.

Finally, the $\alpha$ and $\beta$ *density matrices* $\mathsf{P}$ are defined through

$$P^{\alpha}_{pq} = \sum_i n^{\alpha}_i c_{ip} c_{iq} \tag{1.10}$$

$$P^{\beta}_{pq} = \sum_i n^{\beta}_i c_{ip} c_{iq} \tag{1.11}$$

where the *occupation numbers* $n^{\alpha}_i$ and $n^{\beta}_i$ are all unity for the UHF wavefunction.

The Pople-Nesbet equations are quite often (e.g. [See76, Pop79]) written in terms of a single set of $2n$ spin-orbitals rather than two disjoint sets of $n$ orbitals for $\alpha$ and $\beta$ spin each. Taking advantage of the fact that $\langle pr|qs\rangle$ vanishes unless $\varsigma_p = \varsigma_q$ and $\varsigma_r = \varsigma_s$, the UHF equations can be written in a particularly compact and elegant form:

$$E = \frac{1}{2}\sum_{pq} P_{pq}(H_{pq} + F_{pq}) \tag{1.12}$$

$$F_{pq} = H_{pq} + \sum_{rs} P_{rs}\langle pr||qs\rangle \tag{1.13}$$

$$\mathsf{P} = \begin{pmatrix} \mathsf{P}^{\alpha} & 0 \\ 0 & \mathsf{P}^{\beta} \end{pmatrix} \tag{1.14}$$

$$\mathsf{F}\vec{c}_i = \epsilon_i \mathsf{S}\vec{c}_i \;\forall\, i \tag{1.15}$$

where $\mathsf{F}$ $\mathsf{S}$, and $\mathsf{P}$ are the Fock, overlap and density matrices in the spin-orbital basis[4] and the indices now run over all the $2n$ spin-orbitals. $\langle pq||rs\rangle$ are the *antisymmetrized two-electron integrals*, expressed in terms of regular two-electron integrals as

$$\langle pq||rs\rangle = \langle pq|rs\rangle - \langle pq|sr\rangle \tag{1.16}$$

The MOs are found by solving the generalized eigenvalue problem (1.15). (In practice, the two coupled problems (1.5) and (1.6) are solved instead.) But as the Fock matrix is itself a function of the MOs through the density matrix, the system has to be solved iteratively:

1. Take some appropriate *initial guess* for the $\alpha$ and $\beta$ MOs (e.g. extended Hückel [Hof63] orbitals or the eigenvectors of the core Hamiltonian matrix $\mathsf{H}$).

2. Construct the density matrix $\mathsf{P}$ from the $\alpha$ and $\beta$ MOs.

3. Construct the Fock matrix $\mathsf{F}$ (i.e. $\mathsf{F}^{\alpha}$ and $\mathsf{F}^{\beta}$).

4. Solve (1.15), i.e. (1.5) and (1.6).

5. Construct a new approximation to $\mathsf{P}$ from the MOs thus obtained.

6. Optionally compute $E$ at this iteration.

[4]The latter symbol is also often used for the *total density matrix* $\mathsf{P} = \mathsf{P}^{\alpha} + \mathsf{P}^{\beta}$, with the related *spin density matrix* being given by $\mathsf{P}^{s} = \mathsf{P}^{\alpha} - \mathsf{P}^{\beta}$.

7. Take the difference between the current and previous P and compute its norm. If it is below some small threshold $\delta$, the iteration has converged; otherwise return to step 3.

The latter criterion may be interpreted as requiring that the orbitals are consistent with the field resulting from themselves; hence the name *self consistent field* (SCF) procedure.

Note that the eigenvalue problem has additional solutions except for the orbitals occurring in the density matrix. These are called the *virtual orbitals*. Throughout the remainder of the work, we will denote the occupied orbitals with indices $ijkl\ldots$ and the virtual orbitals with indices $abcd\ldots$. The indices $pqrs\ldots$ are employed for the basis functions.

In terms of the MOs, the Fock matrix becomes diagonal and the overlap matrix a unit matrix, by definition of the generalized eigenvectors. The energy then becomes

$$E = \frac{1}{2}\sum_{ij}(H_{ii}\delta_{ij} + F_{ii}\delta_{ij} + H_{jj}\delta_{ij} + F_{jj}\delta_{ij}) = \sum_{i}(H_{ii} + F_{ii}) = \sum_{i}(\epsilon_i^0 + \epsilon_i) \quad (1.17)$$

or, alternatively

$$E = \sum_{pq} P_{pq}H_{pq} + \frac{1}{2}\sum_{pqrs} P_{pq}P_{rs}\langle pr||qs\rangle \quad (1.18)$$

$$E = \sum_{i}\epsilon_i^0 + \frac{1}{2}\sum_{ij}\langle ij||ij\rangle = \sum_{i}\epsilon_i^0 + \frac{1}{2}\sum_{ij}(J_{ij} - K_{ij}) \quad (1.19)$$

where we have introduced the *coulomb operator* $\hat{J}$ and the *exchange operator* $\hat{K}$:

$$\hat{J}_i\phi_j = \langle i|r_{12}^{-1}|i\rangle\phi_j \quad (1.20)$$

$$\hat{K}_i\phi_j = \langle i|r_{12}^{-1}|j\rangle\phi_i \quad (1.21)$$

From the definition of $\hat{K}$, it is obvious that $K_{ij}$ vanishes if $\phi_i$ and $\phi_j$ have opposite spins. In the AO basis, we have

$$\hat{J}_i\phi_j = P_{rs}\langle r|r_{12}^{-1}|s\rangle\phi_j \quad (1.22)$$

$$\hat{K}_i\phi_j = P_{rs}\langle r|r_{12}^{-1}|j\rangle\phi_s \quad (1.23)$$

The time-limiting factor in a Hartree-Fock calculation is the computation and processing of the two-electron integrals. In the absence of any molecular symmetry, there are (with $n$ basis functions) $n^4/8$ distinct integrals. The factor $1/8$ comes from the identities:

$$\langle pq|rs\rangle = \langle rq|ps\rangle = \langle ps|rq\rangle = \langle rs|pq\rangle = \langle qp|sr\rangle = \langle sp|qr\rangle = \langle qr|sp\rangle = \langle sr|qp\rangle \quad (1.24)$$

or, in chemical notation:

$$[pr|qs] = [rp|qs] = [pr|sq] = [rp|sq] = [qs|pr] = [sq|pr] = [qs|rp] = [sq|rp] \quad (1.25)$$

In a traditional SCF calculation, these integrals are computed and stored to disk, each together with their four indices. Upon every SCF iteration, the integral file is read sequentially, and the contribution added to the appropriate Fock matrix elements. This integral file is also needed for any subsequent electron correlation treatment (see further sections).

The association with the label indices allows the integrals to be computed and stored in the order most convenient for the integral evaluation program; it also allows the omission of zero or very small integrals from the file. Various fast algorithms [McM78, Pop78, Dup76, Oba86] for the evaluation of these integrals have been developed over the years: a discussion may be found in the M.Sc. thesis of the present author [Mar87], and will not be repeated here.

#### 1.1.1.1 The atomic unit system

Some brief remarks about the units employed should be made.

The atomic unit for energy is the *hartree*, defined as twice the exact nonrelativistic energy of the hydrogen atom in its ground state. Some useful conversion factors:

$$1 \text{ hartree} = 27.21 \text{ eV} = 627.51 \text{ kcal/mol} = 219474.6 \text{ cm}^{-1} \tag{1.26}$$

(The last number is twice the Rydberg constant.)

In the dimensionality of the hartree and electronvolt (eV), a division 'per particle' is actually implicit. The calorie is not the SI unit for energy, but is so commonly used in thermochemical work that the author has adopted its use throughout the present work (with one or two purposely exceptions). Also, whereas the wavenumber ($\text{cm}^{-1}$) definitely does not have the correct dimensionality for an energy, spectroscopists are so accustomed to measuring transition frequencies in it that they actually quote energy differences between states in wavenumbers, and the great majority of quantum chemists has adopted the $\text{cm}^{-1}$ as a second (operational) unit of energy.

The atomic unit of length is the *bohr*, defined as the radius of the $1s$ orbit of the hydrogen atom in the old quantum (Bohr) theory or, alternatively, as the expectation value of the proton-electron distance for the exact nonrelativistic solution of the hydrogen atom in its ground state:

$$1 \text{ bohr} = 5.2917706 \times 10^{-11} \text{ m} = 0.52917706 \text{ Å} \tag{1.27}$$

The atomic unit of mass is *not* the commonly known 'atomic mass unit' (defined as 1/12 of the mass of a single $^{12}$C atom), but the electron mass:

$$1 \text{ a.m.u.} = 1880.860 \text{ electron mass} \tag{1.28}$$

Finally, the atomic unit of charge is simply the elementary charge:

$$1\ e_0 = 1.6021917 \times 10^{-19} \text{ coulomb} \tag{1.29}$$

### 1.1.2 The spin contamination problem

UHF can be applied for any open-shell system, and is a very convenient starting point for open-shell electron correlation methods. Its primary disadvantage is that an UHF determinant is not necessarily an eigenfunction of the squared total spin operator $\hat{S}^2$. Denoting the number of $\alpha$ and $\beta$ spin electrons by $n_\alpha$ and $n_\beta$, respectively, and taking $n_\alpha > n_\beta$ by convention, it can be shown that [5]

$$\langle\psi|\hat{S}^2|\psi\rangle = \frac{n_\alpha + n_\beta}{2} + \frac{(n_\alpha - n_\beta)^2}{4} - \sum_{i,\alpha}\sum_{j,\beta} \vec{c}_i^{\dagger} \mathsf{S} \vec{c}_j \tag{1.30}$$

whereas the value for a pure eigenstate of $\hat{S}^2$ would be

$$\langle\psi|\hat{S}^2|\psi\rangle = [(n_\alpha - n_\beta)/2 + 1][(n_\alpha - n_\beta)/2] \tag{1.31}$$

It is readily seen, that the two expressions can only become identical when the spatial parts are the same for all paired electrons. (This also trivially occurs if there are no paired electrons.) Then the final term of (1.30) reduces to $-n_\beta$, which is of course equivalent to

$$\frac{n_\alpha + n_\beta}{2} - \frac{n_\alpha - n_\beta}{2} \tag{1.32}$$

### 1.1.3 Spin-restricted closed-shell Hartree-Fock (RHF)

The simplest and most common case is the closed-shell Hartree-Fock theory of Roothaan [Roo51]. In the closed-shell case, $n_\alpha = n_\beta$. Let us write the Fock equations in the form

$$\begin{pmatrix} \mathsf{F}_{\alpha\alpha} & \mathsf{F}_{\alpha\beta} \\ \mathsf{F}_{\beta\alpha} & \mathsf{F}_{\beta\beta} \end{pmatrix} \begin{pmatrix} \mathsf{C}_\alpha \\ \mathsf{C}_\beta \end{pmatrix} = \mathsf{S} \begin{pmatrix} \mathsf{C}_\alpha \\ \mathsf{C}_\beta \end{pmatrix} \begin{pmatrix} \mathsf{E}_{\alpha\alpha} & 0 \\ 0 & \mathsf{E}_{\beta\beta} \end{pmatrix} \tag{1.33}$$

$$\mathsf{F}_{\alpha\alpha} = \mathsf{H}_{\alpha\alpha} + \mathsf{J}_{\alpha\alpha} - \mathsf{K}_{\alpha\alpha} \tag{1.34}$$

$$\mathsf{F}_{\beta\beta} = \mathsf{H}_{\beta\beta} + \mathsf{J}_{\beta\beta} - \mathsf{K}_{\beta\beta} \tag{1.35}$$

$$\mathsf{F}_{\alpha\beta} = \mathsf{F}_{\beta\alpha} = \mathsf{J}_{\alpha\beta} \tag{1.36}$$

where $\mathsf{E}_\alpha$ and $\mathsf{E}_\beta$ are of course diagonal for canonical HF orbitals.[6] Now when $\mathsf{C}_\alpha$ is taken identical to $\mathsf{C}_\beta$, it follows that $\mathsf{E}_{\alpha\alpha} = \mathsf{E}_{\beta\beta}$, and we obtain by working out the block products

$$2(\mathsf{F}_{\alpha\alpha} + \mathsf{F}_{\alpha\beta})\mathsf{C}_\alpha = 2\mathsf{S}\mathsf{E}_{\alpha\alpha}\mathsf{C}_\alpha \tag{1.37}$$

or, by expanding the F blocks:

$$\mathsf{FC} = \mathsf{SEC} \tag{1.38}$$

$$\mathsf{F} = \mathsf{H} + 2\mathsf{J} - \mathsf{K} \tag{1.39}$$

[5] As the spin parts of $\alpha$ and $\beta$ orbitals are already orthogonal, the spatial parts of $\alpha$ orbitals do not have to be orthogonal to those of $\beta$ orbitals.

[6] The Hartree-Fock orbitals are not uniquely defined, as there are $n$ orbitals and $n^2$ Lagrange multipliers $\epsilon_{ij}$ in the variation problem. Canonical HF orbitals are defined as those obtained by requiring the off-diagonal Lagrange multipliers to vanish.

which are of course the *Roothaan equations.*[7] The energy expression remains

$$E = \frac{1}{2}\sum_{pq} P_{pq}(H_{pq} + F_{pq}) = \frac{1}{2}\mathrm{Tr}(\mathsf{P}(\mathsf{H}+\mathsf{F})) \tag{1.40}$$

but now with all occupation numbers $n_i = 2$ in the density matrix.

### 1.1.4 Spin-restricted open-shell Hartree-Fock (ROHF)

We will first consider the most common special case, that of a high-spin coupled open-shell state with nondegenerate open-shell orbitals (most nonlinear radicals fall into this category, as do $\Sigma^+$ states of linear molecules).

Let us partition the $\alpha$ space in two parts, namely the closed-shell electrons $\alpha'$ and the open-shell electrons $\alpha''$. This leads to a Fock problem with three partitions in each matrix:

$$\begin{pmatrix} \mathsf{F}_{\alpha'\alpha'} & \mathsf{F}_{\alpha'\alpha''} & \mathsf{F}_{\alpha'\beta} \\ \mathsf{F}_{\alpha''\alpha'} & \mathsf{F}_{\alpha''\alpha''} & \mathsf{F}_{\alpha''\beta} \\ \mathsf{F}_{\beta\alpha'} & \mathsf{F}_{\beta\alpha''} & \mathsf{F}_{\beta\beta} \end{pmatrix} \begin{pmatrix} \mathsf{C}'_\alpha \\ \mathsf{C}''_\alpha \\ \mathsf{C}_\beta \end{pmatrix} = \mathsf{S} \begin{pmatrix} \mathsf{C}'_\alpha \\ \mathsf{C}''_\alpha \\ \mathsf{C}_\beta \end{pmatrix} \begin{pmatrix} \mathsf{E}_{\alpha'\alpha'} & 0 & 0 \\ 0 & \mathsf{E}_{\alpha''\alpha''} & 0 \\ 0 & 0 & \mathsf{E}_{\beta\beta} \end{pmatrix} \tag{1.41}$$

$$\mathsf{F}_{\alpha'\alpha'} = \mathsf{H}_{\alpha'\alpha'} + \mathsf{J}_{\alpha'\alpha'} - \mathsf{K}_{\alpha'\alpha'} \tag{1.42}$$

$$\mathsf{F}_{\alpha'\alpha''} = \mathsf{F}^+_{\alpha''\alpha'} = \mathsf{J}_{\alpha'\alpha''} - \mathsf{K}_{\alpha'\alpha''} \tag{1.43}$$

$$\mathsf{F}_{\beta\beta} = \mathsf{H}_{\beta\beta} + \mathsf{J}_{\beta\beta} - \mathsf{K}_{\beta\beta} \tag{1.44}$$

$$\mathsf{F}_{\alpha'\beta} = \mathsf{F}^+_{\beta\alpha'} = \mathsf{J}_{\alpha'\beta} \tag{1.45}$$

$$\mathsf{F}_{\alpha''\beta} = \mathsf{F}^+_{\beta\alpha''} = \mathsf{J}_{\alpha''\beta} \tag{1.46}$$

Upon working out the block products and substituting the Fock matrices, and considering that

$$\mathsf{J}_{\alpha'\alpha'} = \mathsf{J}_{\alpha'\beta} = \mathsf{J}_{\beta\beta} \equiv \mathsf{J}_{CC} \tag{1.47}$$

$$\mathsf{H}_{\alpha'\alpha''} = \mathsf{H}_{\beta\alpha''} \equiv \mathsf{J}_{CO} \tag{1.48}$$

$$\mathsf{H}_{\alpha''\alpha''} \equiv \mathsf{J}_{OO} \tag{1.49}$$

and similarly for H and K, we obtain the equations

$$[\mathsf{H}_{CC} + 2\mathsf{J}_{CC} - \mathsf{K}_{CC} + \frac{1}{2}(2\mathsf{J}_{CO} - \mathsf{K}_{CO})]\mathsf{C}_C = \mathsf{S}\mathsf{C}_C\epsilon_C \tag{1.50}$$

$$\mathsf{H}_{OO} + \mathsf{J}_{OO} - \mathsf{K}_{OO} + (2\mathsf{J}_{CO} - \mathsf{K}_{CO})\mathsf{C}_O = \mathsf{S}\mathsf{C}_O\epsilon_O \tag{1.51}$$

which were derived by Binkley *et al.* [Bin74]. The energy expression becomes

$$E = \frac{1}{2}\mathrm{Tr}(\mathsf{P}_C(\mathsf{H}+\mathsf{F}_C)) + \frac{1}{2}\mathrm{Tr}(\mathsf{P}_O(\mathsf{H}+\mathsf{F}_O)) \tag{1.52}$$

$$\mathsf{P}_O = \mathsf{P}^\alpha - \mathsf{P}^\beta \tag{1.53}$$

$$\mathsf{P}_C = 2\mathsf{P}^\beta \tag{1.54}$$

[7] Most textbooks present the Roothaan equations first, and then generalise these to the Pople-Nesbet equations. We have deliberately followed the opposite route, treating RHF as a special case of UHF, because it allows for an elegant introduction of ROHF theory.

One additional case of little interest, namely low-spin coupling involving nondegenerate orbitals, can be treated by also partitioning the $\beta$ space in $\beta'$ and $\beta''$ orbitals. More general open-shell cases (involving low-spin coupling in degenerate orbitals) can no longer be treated by applying constraints to the UHF wavefunction, as vanishing of the off-diagonal Lagrange multipliers can no longer be enforced there. Roothaan [Roo60] demonstrates a method of eliminating these. The resulting equations involve an energy expression of the form

$$\begin{aligned} E &= 2\sum_{k} H_k + \sum_{kl} 2J_{kl} - K_{kl} + f[2\sum_{m} H_m + f\sum_{mn}(2aJ_{mn} - bK_{mn}) \\ &\quad + 2\sum_{km}(2J_{km} - K_{km})] \end{aligned} \tag{1.55}$$

where the indices $kl$ run over the closed-shell, and $mn$ over the open-shell orbitals. $f$ is the fractional occupancy of the open shell (e.g. 3/4 for a $\pi^3$ shell), the *coulomb* and *exchange coupling coefficients* $a$ and $b$ depend on the coupling case. This form of ROHF must be resorted to for most spin-restricted open-shell calculations on atoms and linear molecules. Carbo and Riera [Car78] list coupling coefficients for nearly all possible cases; they are also listed in the basis set compilation by Poirier *et al.* [Poi87].

For degenerate cases, such ROHF solutions are no longer single-determinant solutions, strictly speaking, but rather symmetry- and spin-adapted linear combinations of two or more such determinants built from a single set of MOs. Many authors (including the NASA Ames group) use the term *configuration state functions (CSFs)* for these.

As pointed out by Gustavo E. Scuseria to the present author, it is by no means unusual to run ROHF calculations on degenerate point groups in a nondegenerate subgroup, like e.g. running a calculation on a $^3\Pi_u$ state of a symmetric linear molecule (full point group $D_{\infty h}$) in the nondegenerate $D_{2h}$ or even $C_{2v}$ subgroup. In the latter case, the two degenerate components of the partially occupied $\pi_u$ orbital then correspond to an $a_1$ and a $b_1$ or $b_2$ (dependent on the axis frame convention) component, respectively. Because such components cannot have fractional occupations anymore, the two components are no longer degenerate, whereas the total energy is slightly different from that obtained in the full symmetry too. In some situations, notably the evaluation of a bending potential curve, this is desirable, however, as it eliminates the discontinuity in the energy that arises (with a single reference determinant, that is to say) at the point where the symmetry is broken[8].

As RHF/ROHF is rigorously free of spin contamination, it appears to be preferable over UHF for open-shell systems. However, it in general does not exhibit *proper dissociation*: the wavefunction of a molecule with the bonds stretched to infinite distance does not correspond tc that of the separated fragments. For example, the RHF solution for $H_2$ stretched to infinite distance does not correspond to 2 H, but to $H^+ + H^-$, as the former

[8] In multireference techniques, the problem is solved by using both determinants involved as references.

situation can only be reached by changing the occupation number vector. (As no such need arises in the UHF case, an UHF solution dissociates properly and will in general do so.) Similar problems always arise when closed shells dissociate to open shells[9].

### 1.1.5 Internal and external stability of the HF wavefunction

If a Hartree-Fock wavefunction has converged, there is still no guarantee that it corresponds to the lowest state of a given combination of multiplicity and symmetry. For example, a HF calculation with the default INDO-type initial guess [Pop67] of the GAUSSIAN series on the $C_2$ molecule will not converge to the lowest-lying $^3\Pi$ state, but to a $^3\Sigma_u^+$ state.

Furthermore, it is possible that for a particular problem an RHF wavefunction has been obtained, but that a lower energy may be reached by allowing the wave function to become UHF. The physical significance and the desirability of such so-called 'spin-symmetry broken' UHF solutions has been the subject of a lot of discussion: see Bénard and Paldus [Ben80] and Fukutome [Fuk81] for details. Lower energies may sometimes also be reached (such as for the $^1\Delta_g$ state of $O_2$) by allowing the MOs to become complex [Pop71].

A wavefunction that is the lowest solution within the given set of spin, symmetry, RHF-UHF and real-complex constraints, in other terms, that is stable with respect to changes in the occupation numbers, is said to be *internally stable*. A wavefunction whose energy cannot be lowered by relaxing any of the constraints of spin, symmetry, RHF-UHF, and real-complex is said to be *externally stable*. Seeger and Pople [See77] describe a general procedure for determining the stability of an RHF or UHF wavefunction.

The orbitals for the most general form of the Hartree-Fock solution, the GHF (generalized Hartree Fock) determinant, may be written as

$$\chi_i = \sum_p \left( c_{ip}^{\alpha} \phi_p \varsigma_\alpha + c_{ip}^{\beta} \phi_p \varsigma_\beta \right) \tag{1.56}$$

Each of the coefficients may be a complex number. This requires $4N$ real numbers for the specification of each orbital.

The UHF determinant is a special case of the GHF wavefunction, where $\alpha$ and $\beta$ spin are not allowed to become mixed. This leaves only $2N$ real numbers to be determined in the complex UHF case, and only $N$ in the real UHF case.

Any change in any occupation number of the GHF wavefunction corresponds to a single excitation. A number of such changes may occur simultaneously, but independently.

[9] In multireference calculations, correct dissociation may be guaranteed by admitting all configurations to the reference space that can be derived from symmetry-and spin-adapted linear combinations of the fragment states. The CASSCF method (Section 1.4.3) may be seen as an extension of this idea (see below).

If we now introduce a *generator* $\hat{E}_{ia}$ defined by

$$\hat{E}_{ia}\psi_0 = \psi_i^a \tag{1.57}$$

where $\psi_i^a$ denotes the determinant obtained by replacing $\phi_i$ by $\phi_a$ in $\psi_0$, we may introduce (anticipating on Section 1.3) the *excitation operator*

$$\hat{D}_1 = \sum_{ia} D_i^a \hat{E}_{ia} \tag{1.58}$$

$$\hat{D}_1\psi_0 = \sum_{ia} D_i^a \psi_i^a \tag{1.59}$$

Then a wavefunction where individual single replacements may occur simultaneously, but independently, has the mathematical form[10] $\exp(\hat{D}_1)\psi_0$. A variational (expectation value) expression for the energy may be found as[11]

$$E = E_{\mathrm{GHF}} + \frac{\langle \exp(\hat{D}_1)\psi_0 | \hat{H}' | \exp(\hat{D}_1)\psi_0 \rangle}{\langle \exp(\hat{D}_1)\psi_0 | \exp(\hat{D}_1)\psi_0 \rangle} \tag{1.60}$$

where $\hat{H}' \equiv \hat{H} - E_{\mathrm{GHF}}$. The wavefunction is then internally stable if no infinitesimal change in any $D_i^a$ or combination of these will make the second term of (1.60) negative. Expanding its numerator (the denominator is strictly positive anyway), and discarding higher-order terms in $\mathsf{D}_1$ for small displacements, this means that

$$\frac{1}{2}\sum_{st} 2D_s^* D_t \langle s|\hat{H}'|t\rangle + D_s D_t \langle 0|\hat{H}'|st\rangle + D_s^* D_t^* \langle st|\hat{H}'|0\rangle \tag{1.61}$$

must not become negative for any values of $\mathsf{D}$. (The subscripts $s$ and $t$ run over all single excitations.) This may be written in matrix form, by writing (with $D_s \equiv D_i^a$ and $D_t \equiv D_j^b$)

$$A_{st} \equiv \langle s|H'|t\rangle = (\epsilon_a - \epsilon_i)\delta_{st} + \langle ij||ab\rangle \tag{1.62}$$

$$B_{st} \equiv \langle st|H'|0\rangle = \langle ij||ab\rangle \tag{1.63}$$

$$\mathsf{D^*AD + DA^*D^* + DB^*D + D^*BD^* \geq 0} \tag{1.64}$$

Defining the compound arrays $\mathsf{H}$ and $\mathsf{G}$ as

$$\mathsf{H} = \begin{pmatrix} \mathsf{A} & \mathsf{B} \\ \mathsf{B^*} & \mathsf{A^*} \end{pmatrix} \tag{1.65}$$

$$\mathsf{G} = \begin{pmatrix} \mathsf{D} \\ \mathsf{D^*} \end{pmatrix} \tag{1.66}$$

Then the stability condition may be written as

$$\mathsf{G^+HG} \geq 0 \quad \forall\, \delta\mathsf{G} \tag{1.67}$$

[10] In a later Section, this will be recognized to be a coupled cluster wavefunction!

[11] An alternative derivation involving the Hessian of the energy with respect to the MOs has very recently been given by Yamaguchi *et al.* [Yam90].

For condition (1.67) to hold, it is necessary and sufficient that H is positive semidefinite. So it suffices to compute the necessary integrals (for which a partial integral transform is required), to set up H, and to compute its eigenvalues. Zero eigenvalues will occur for any state with a residual electron spin (its direction is indeterminate). Negative eigenvalues indicate an instability; from the eigenvector it can easily be deduced what orbital switchings are involved.

If the original wavefunction is real, both A and B become real and the condition may be factored into a term for real and one for complex displacements as follows:

$$(D + D^*)^+(A + B)(D + D^*) + (D - D^*)^+(A - B)(D - D^*) \geq 0 \tag{1.68}$$

The first term corresponds to the internal stability of a real GHF wavefunction, the second to the external instability with respect to complex GHF. The internal stability condition then becomes that $A + B$, the external one that $A - B$ be positive semidefinite.

For consideration of the stability of a complex UHF wavefunction, the matrix H may be blocked into a spin-conserved part $H'$ and a spin-unconserved part $H''$, these being built up from corresponding $A'$, $A''$, $B'$, and $B''$ arrays. Positive semidefinite character of $H'$ is required for internal complex UHF stability, whereas $H''$ must fulfill the same requirement for external stability with respect to complex GHF.

For the real UHF case, a similar factorization into real and complex displacements as for real GHF may additionally be made. If $A' + B'$ is positive semidefinite, then the real UHF wavefunction is internally stable. (Zero eigenvalues will occur with partially filled degenerate orbitals, such as in $\Pi$ states of linear molecules.) If $A'' + B''$ is positive semidefinite, then the wavefunction is stable with respect to becoming real GHF. Finally, instability of the wavefunction with respect to becoming complex UHF is indicated by negative eigenvalues of $A' - B'$.

Now turning to the complex closed-shell RHF case (we will not treat ROHF cases), we can factor $H'$ into singlet and triplet matrices ${}^1H'$ and ${}^3H'$, with corresponding components ${}^1A'$, ${}^3A'$, ${}^1B'$, ${}^3B'$. Negative eigenvalues of ${}^3H'$ imply external instability with respect to becoming complex UHF, whereas a nonnegative spectrum of ${}^1H'$ indicates that the complex RHF wavefunction is internally stable.

Finally, we arrive at the case of a real RHF wavefunction. There another factorization, this time in ${}^1A' + {}^1B'$ and ${}^1A' - {}^1B'$, applies. The former matrix has nonnegative eigenvalues if the RHF determinant is internally stable, the latter if it is stable against becoming complex RHF. Stability against becoming real UHF may finally be tested from the matrix ${}^3A' + {}^3B'$.

The method is implemented in the GAUSSIAN series. Optionally, a linear search for the lowest energy can be carried out along the eigenvector corresponding to the negative eigenvalue; the resulting MOs can then be used as the 'initial guess' to a new SCF calculation within the same constraints (for internal instability) or with the appropriate

conditions relaxed (for external instability).

Our experience is that this latter procedure often does not work as it should. What generally does work is to save the MOs to disk (which is done through the checkpoint file in the GAUSSIAN series), read in the previous MOs as initial guess to a new SCF calculation, and manually 'switch' the necessary orbitals to obtain the correct symmetry. Sometimes (when the occupation scheme happens to be retained during a classical SCF, or when applying nonstandard SCF procedures that can be relied upon to be 'state-loyal', which means that the final wavefunction will have the same symmetry as the initial guess) it is even sufficient to apply the correct alterations to the initial guess orbitals. All this is made very convenient by the automatic symmetry determination that is done for all MOs in the GAUSSIAN series. In our experience, it is worthwhile, for particularly difficult cases (e.g. $BN_2$ [Mar89c]; see also Section 4.2), to save a copy of the converged MOs in a lower-level calculation and read these in for any subsequent higher-level calculations.

The stability testing procedure is definitely useful, but cannot be regarded as a panacea for finding the ground state. For one thing, the ordering of electronic states is not always predicted correctly at the UHF level. This means that the actual ground state may well be internally unstable at the HF level. Secondly, if low-lying triplet or higher excited states exist, the RHF ground state is usually found to be unstable with respect to becoming UHF. Finally, in cases of UHF bifurcations (encountered in Section 4.10 for $C_3^+$), the stability testing procedure will usually consider the solution with the lowest spin contamination to be unstable, whereas it is precisely that solution that should be preferred for any further ab initio work.

### 1.1.6 Use of symmetry in SCF and related calculations

For molecular systems with some symmetry, judicious use of the latter may greatly reduce computational effort required to obtain the desired result. Two main approaches have been followed in the past.

#### 1.1.6.1 Use of symmetry-adapted basis functions

This procedure is the oldest [Pit73]; it was actually built into the first versions of the pioneering POLYATOM package (see [Mos77] for a description and a modification history).[12] It centers upon the fact, that a two-electron integral $\langle pq|rs\rangle$ can only be nonvanishing if

$$\langle \Gamma_p \otimes \Gamma_q \otimes \Gamma_r \otimes \Gamma_s | \Gamma_1 \rangle \neq 0 \tag{1.69}$$

i.e. when the direct product of the irreducible representations of the four basis functions involved contains the identity. (The $1/r_{12}$ term has spherical symmetry, and thus always

[12] Together with E. Clementi's IBMOL, it was the first ab initio package — however limited — to become accessible to the quantum chemistry community.

transforms as the totally symmetric representation $\Gamma_1$.) For nondegenerate point groups (i.e. $D_{2h}$ and subgroups), this simplifies to

$$\Gamma_p \otimes \Gamma_q \otimes \Gamma_r \otimes \Gamma_s = \Gamma_1 \tag{1.70}$$

as the representations are then simple sets of numbers. In practice, systems with degenerate point groups are treated in the largest nondegenerate subgroup (e.g. $D_{2h}$ for $D_{\infty h}$, or $C_{2v}$ for $D_{3h}$).

All integrals are calculated in the usual way over atomic basis functions. Then symmetry-adapted linear combinations over these are constructed, and the integrals transformed from the regular to the symmetry-adapted basis. Vanishing transformed integrals are simply discarded in the process. (For nondegenerate point groups, the coefficients can only take on the values 0, +1, and -1, so the extra computational effort involved is acceptable.) As a trivial consequence of the 'great orthogonality theorem' of group theory, the Fock matrix is then blocked by symmetry provided that the density matrix has the correct symmetry too. (It is easily seen, that a sufficient condition for this is the initial guess having the correct symmetry.) The blocking greatly reduces the time both to construct the Fock matrix (as the vanishing integrals have previously been discarded), as well as to solve the eigenvalue problem.

In practical calculations the gain in the SCF is often outweighed by the effort required to symmetry-transform the integrals. However, as pointed out by Peter R. Taylor to the present author, it is the method of choice in 'heavier' correlated calculations. There the correlation method dominates the computer time, and the extra effort in the integral package has no appreciable effect on the total CPU time, whereas taking advantage of symmetry in correlated calculations is relatively straightforward in a basis of symmetry-adapted functions. For example, in the integral transformation from $\langle pq|rs\rangle$ to $\langle ij|kl\rangle$, only the cases where

$$\Gamma_i \otimes \Gamma_j \otimes \Gamma_k \otimes \Gamma_l = \Gamma_1 \tag{1.71}$$

have to be considered, since the symmetry-adapted integrals transform as $\Gamma_1$ anyway. In a CI calculation, all matrix elements where the bra and ket are of different irreducible representations can be ignored, leading to a 'blocked' CI matrix. MCSCF and coupled cluster calculations are amenable to similar procedures. For systems with higher symmetries like $D_{2h}$, very substantial reductions in computer time and disk space requirements may thus be obtained.

Pople (e.g. [Heh86a]) always held the opinion that most chemically interesting systems have no symmetry at all anyway (e.g. most organic molecules); therefore the GAUSSIAN series makes comparatively little use of symmetry. No symmetry at all is accounted for in the electron correlation parts of the program, which the present author sees as an important deficiency.

#### 1.1.6.2 Use of a 'petite list'

This procedure is more recent, and allows to eliminate a lot of integral calculation beforehand. It is based on work by Dacre [Dac70] and Elder [Eld73] for nondegenerate point groups, and has found widespread application following the extension by Dupuis and King [Dup77] to any symmetry.

Let G1 denote the set of all basis function shells. When there is molecular symmetry, some of these shells will be equivalent by symmetry. The list of all symmetry-unique shells is called P1, the *petite list* (G1 evidently becomes the *grande list*). With every shell $I$ in P1 a *constituency number* $q(I)$ is associated, given by $g/n(I)$, where $g$ is the order of the point group and $n(I)$ the number of operations that map $I$ onto itself. The direct product of G1 with itself is G2; that of G2 with itself G4, the latter being the set of all possible index combinations for two-electron integrals. There is a corresponding petite list P4; the constituency number of its elements is given by

$$q_4(IJKL) = 8g/n(IJKL) \tag{1.72}$$

The factor eight results from the so-called 'trivial symmetries' involving label permutations.

Let us next define a *skeleton matrix* $\bar{\mathsf{M}}$ by

$$\bar{M}_{ij} = \lambda_{ij} M_{ij} \tag{1.73}$$

where $\lambda_{ij} = q_2(IJ)$ if $IJ \in P2$, and zero otherwise. Now we define a *symmetrization* operation by

$$\mathsf{M}_{\mathrm{sym}} = (2q)^{-1} \sum_{\mathsf{R}\in G} \mathsf{R}^{+}(\mathsf{M} + \mathsf{M}^{+})\mathsf{R} \tag{1.74}$$

where $\mathsf{R}$ runs over the matrix representations of all the symmetry operations in the molecular point group. It can then be proven [Dup77] that $\bar{\mathsf{M}}_{\mathrm{sym}} = \mathsf{M}$. So if the Fock matrix $\mathsf{F}$ is calculated from the grande list by

$$F_{ij} = H_{ij} + \sum_{kl} P_{kl}\langle ik||jl\rangle \tag{1.75}$$

it can be shown [Dup77] that

$$\bar{\mathsf{F}} = \bar{\mathsf{H}} + \sum_{P4} q_4(IJKL)V(IJKL) \tag{1.76}$$

$$V(IJKL) = V_c(IJKL) + V_c(KLIJ) - \frac{1}{2}[V_e(IJKL) + V_e(JIKL) + V_e(IJLK) + V_e(JILK)] \tag{1.77}$$

$$V_c(IJKL) = P_{kl}\langle ij|kl\rangle \tag{1.78}$$

$$V_e(IJKL) = P_{jl}\langle ij|kl\rangle \tag{1.79}$$

So only a subset of the integrals have to be actually computed in this algorithm. The integrals are usually premultiplied by their constituency number before writing them out to disk, so the SCF procedure no longer has to worry about them.

Originally developed for the HONDO 5 [Hon78] program of King and Dupuis, this method is incorporated in the GAUSSIAN series, and reduces both disk space and integral time requirements very substantially for SCF-oriented calculations. The extension of the algorithm to gradients [Dup78] is straightforward, a little less so for frequency calculations [Tak81]. Its extension to correlated methods, however, is far from trivial; some work has been done on the extension to integral transformation [Car84] and coupled cluster calculations [Car87].

Even in its present form, the algorithm has still been very useful in the present work as it allowed SCF frequency calculations for fairly large basis sets to be carried out with the limited disk space available.

### 1.1.7 Enforcement or acceleration of SCF convergence

There is no guarantee that the 'classical SCF' scheme will converge to the right state, or even that it converges at all. In practice, oscillation between nearby states is often observed, and cannot be removed with the 'traditional' bag of tricks (Aitken-type extrapolations and level shifting). Many of the calculations reported in this work, particularly those on the cluster molecules, could not have been completed if it were not for the availability of various SCF enhancers.

#### 1.1.7.1 The DIIS method of Pulay

The *direct inversion of the iterative subspace* is actually one of the most powerful general convergence accelerators available, being applicable to almost any iteration-by-back-substitution scheme for any application. Its prime use, however, is SCF convergence acceleration.

The general idea is the following [Pul80]. Consider any iteration process at the $m+1$-th iteration, with iterates $\vec{p}_i, i = 1, \ldots, m$. The residuum vectors are defined as $\Delta\vec{p}_i = \vec{p}_{i+1} - \vec{p}_i$. Then we define a new update as $\Delta\vec{p} = \sum_i c_i \Delta\vec{p}_i$. (For the conventional iteration, all coefficients are zero except the last, which is unity.) At convergence, the residuum vector should be zero. Of course one could require the residuum vector to approximate the zero vector in the least squares sense, with the constraint that the coefficients all sum up to unity. Applying the method of Lagrange multipliers, we find the linear system

$$\begin{pmatrix} \mathsf{B} & -1 \\ -1 & 0 \end{pmatrix} \begin{pmatrix} \vec{c} \\ \lambda \end{pmatrix} = \begin{pmatrix} \vec{0} \\ -1 \end{pmatrix} \tag{1.80}$$

$$\text{with } B_{ij} = \langle \Delta\vec{p}_i | \Delta\vec{p}_j \rangle \tag{1.81}$$

The Lagrange multiplier $\lambda$ is actually the squared norm of the residuum vector. Note that $\mathsf{B}$ is independent of the definition of $\vec{p}$ or the associated inner product.

In the first application of DIIS to SCF [Pul80], the residuum vector involved the construction of an extra Fock matrix. This is not a problem for semiempirical calculations; it is unacceptable, however, for the ab initio case. A second implementation [Pul82] removes this difficulty.

Let us first partition the orbitals in different *occupation blocks* according to different values for the occupation numbers, and number the blocks in descending order of occupation number. Assume that there are $k$ such blocks (the $k$-th block corresponding to occupation number zero, i.e. the virtual orbitals). Then we can write $\mathsf{P}$ as a linear combination of the different *occupation-block density matrices* $\mathsf{D}_i$:

$$\mathsf{P} = \sum_{i=1}^{k-1} n_i \mathsf{D}_i \tag{1.82}$$

where $n_i$ is the occupation number associated with $\mathsf{D}_i$. A necessary and sufficient condition [Pul82] for SCF convergence is easily seen to be that the Fock matrix in orbital basis is diagonal (for the RHF and UHF cases), or blocked (in degenerate ROHF cases). This is equivalent to the condition that

$$\mathsf{N}_i \mathcal{F} \mathsf{N}_j - \mathsf{N}_j \mathcal{F} \mathsf{N}_i = 0 \tag{1.83}$$

where $\mathcal{F}$ is the Fock matrix in the MO basis and the $\mathsf{N}_i$ are the occupation-block density matrices in the orbital basis (i.e. diagonal matrices built from zeros and ones). The summation indices go over the different groups of orbitals (doubly occupied, singly occupied, and virtual in the simple ROHF case, singly occupied and virtual in the UHF case, doubly occupied and virtual in the RHF case). Back-transforming this to the original AO basis yields the error matrix:

$$\mathsf{e} = \mathsf{f} - \mathsf{f}^{+} \tag{1.84}$$

$$\mathsf{f} = (\mathsf{C}^{-1})^{+} \mathsf{N}_i \mathcal{F} \mathsf{N}_j \mathsf{C}^{-1} \tag{1.85}$$

As $\mathsf{C}^{+}\mathsf{S}\mathsf{C} = 1$, this simplifies to

$$\mathsf{f} = \sum_{i>j} a_{ij} \mathsf{S}\mathsf{D}_i\mathsf{F}\mathsf{D}_j\mathsf{S} \tag{1.86}$$

where the $a_{ij}$ are arbitrary nonzero coefficients and the $\mathsf{D}_i$ represent occupation-block density matrices in the AO basis. Introducing the 'virtual density matrix'

$$\mathsf{D}_k = \mathsf{S}^{-1} - \sum_{i=1}^{k-1} \mathsf{D}_i \tag{1.87}$$

f can be written as

$$\sum_{i>j}^{k-1} (a_{ij} + a_{ki} - a_{kj}) \mathsf{S}\mathsf{D}_i\mathsf{F}\mathsf{D}_j\mathsf{S} + \sum_{j=1}^{k-1} a_{kj} \mathsf{F}\mathsf{D}_\mathsf{j}\mathsf{S} \tag{1.88}$$

If we choose $a_{ij} = a_{kj} - a_{ki}$, the first sum vanishes and $\mathbf{e}$ is given by the simple expression

$$\mathbf{e} = \sum_{j=1}^{k-1} a_j(\mathsf{FD_jS} - \mathsf{SD_jF}) \tag{1.89}$$

The best choice for the $a_j = a_{kj}$ are perhaps the occupation numbers, leading finally to

$$\mathbf{e} = \mathsf{FPS} - \mathsf{SPF} \tag{1.90}$$

Finally, to enhance numerical stability, a more balanced vector can be constructed by transforming $\mathbf{e}$ to an orthonormal basis. This can be readily done by setting

$$\mathbf{e}' = \mathsf{S}^{-1/2}\mathbf{e}\mathsf{S}^{-1/2} \tag{1.91}$$

The scalar product for matrices, necessary for constructing $\mathsf{B}$, is simply $B_{ij} = \mathrm{Tr}(\mathbf{e}_i\mathbf{e}_j)$.

In practice, DIIS is switched on after the first iteration, and a DIIS is subsequently performed at every step. In some cases, some of the previous iterates may be nearly identical, leading to ill-conditioning of the DIIS matrix. This is readily identified by very large DIIS coefficients. In the GAUSSIAN series, the DIIS procedure is simply reset when any coefficient exceeds a given threshold (default value 4.0); i.e., all iterates prior to the current one are ignored in future DIIS extrapolations.

#### 1.1.7.2 Direct minimization SCF methods

Most nonstandard SCF procedures are based upon the fact (a trivial corollary of the variational theorem) that for the converged Hartree-Fock solution, the energy should be a local minimum with respect to changes in the MO coefficients. (Only for the ground state is it a global minimum.) Since the functional dependence of the energy on the MO coefficients is fairly simple (a quartic multivariate polynomial), it becomes appealing to apply the whole familiar machinery for nonlinear multivariate optimizations to the SCF problem.

The Hartree-Fock energy is given by (assuming all real quantities)

$$E = \sum_{pq} H_{pq}P_{pq} + \frac{1}{2}\sum_{pqrs} P_{pq}P_{rs}\langle pr||qs\rangle \tag{1.92}$$

$$P_{pq} = \sum_i n_i c_{ip}c_{iq} \tag{1.93}$$

where the $n_i$ involved in the density matrix $\mathsf{P}$ are the occupation numbers. Taking the first derivative with respect to any MO coefficient yields the expression

$$\begin{aligned}
\frac{\partial E}{\partial c_{it}} &= \sum_{pq} H_{pq}\frac{\partial P_{pq}}{\partial c_{it}} + \sum_{pqrs}\frac{\partial P_{pq}}{\partial c_{it}}P_{rs}\langle pr||qs\rangle \\
&= \sum_{pq} F_{pq}\frac{\partial P_{pq}}{\partial c_{it}} \\
\frac{\partial P_{pq}}{\partial c_{it}} &= n_i(\delta_{qt}c_{ip} + \delta_{pt}c_{iq}) \\
\frac{\partial E}{\partial c_{it}} &= 2n_i\sum_p c_{ip}F_{pt}
\end{aligned} \tag{1.94}$$

While we are at it, we can just as well evaluate the Hessian too:

$$\begin{aligned}\frac{\partial^2 E}{\partial c_{it}\partial c_{ju}} &= \left(\frac{\partial}{\partial c_{it}}\right) 2n_j \sum_p c_{jp} F_{pu} \\ &= 2n_j F_{tu} + 2n_j \sum_p c_{jp} \frac{\partial F_{pu}}{\partial c_{it}} \\ &= 2n_j F_{tu} + 2n_j \sum_p c_{jp} \frac{\partial P_{rs}}{\partial c_{it}} \langle pr||us\rangle \\ &= 2n_j F_{tu} + 4n_i n_j \sum_s c_{is} c_{jp} \langle pt||us\rangle \end{aligned} \tag{1.95}$$

Given the latter, it looks in principle appropriate to use the generalized Newton-Raphson method:

$$\mathsf{C}^{[n+1]} = \mathsf{C}^{[n]} - \mathsf{H}^{-1}\mathsf{g} \tag{1.96}$$

where $\mathsf{C}^{[n]}$ means $\mathsf{C}$ at the $n$-th iteration, $\mathsf{H}$ represents not the Hamiltonian, but the Hessian with elements given by (1.95), and $\mathsf{g}$ the gradient with elements given by (1.94). The main drawback is that, given the large number of unknowns, $\mathsf{H}$ quickly takes on astronomical dimensions; e.g. for a closed-shell RHF calculation with 20 electrons and 120 basis functions we would need no less than $(120 \times 10)^2 = 1.44 \times 10^6$ words of central memory to store it. Furthermore, although Newton-Raphson type methods converge very rapidly in the neighborhood of the solution, they often do not converge at all far from it, i.e. at the beginning of the SCF.

Another possibility is to use only the first derivative, (1.94), and to perform a line search for the minimum along its direction at each iteration, which is of course the steepest-descent method. The application of the steepest-descent method to SCF problems was suggested as early as 1956 by McWeeny [McW56]. Steepest descent has the advantage of unconditional convergence, but converges extremely slowly. It should be noted that the Fock matrix has to be rebuilt for every step in the line search (every *microiteration*), not just for every new line search (every *macroiteration*). Hillier and Saunders [Hil70] achieved considerable acceleration by using energy-weighted 'coordinates'. To ensure orthogonality of the successive line searches, application of the conjugate gradient method [Fle63] has also been considered. As all these techniques are special cases of the variable metric method, which may be proven to be symmetry-conserving [McI71], they are all guaranteed to be 'state-loyal'.

Seeger and Pople [See76] showed that it is more efficient to search along a path that contains the 'classical' iterate at $\lambda = 1$ (where $\lambda$ represents the line seach parameter). To avoid interchange between occupied and virtual orbitals, they keep the mesh size for the search down to 0.4 and select the occupied orbitals by a criterion of maximum overlap with the previous occupieds. The latter procedure guarantees state-loyalty.

Finally, Bacskay [Bac81] implemented a quadratically convergent SCF (QCSCF) method which may be shown to be a Newton-Raphson method where the explicit con-

struction and inversion of the Hessian matrix are avoided by several cunning techniques. It is also state-loyal, but requires some pre-iteration by a steepest-descent method. The latter combination works very well in most cases, and is much faster than the Seeger-Pople method.

In the present author's experience, the following 'sequence of remedies' should be followed when encountering convergence difficulties.

- Look at the initial guess orbitals, especially whether they have the right symmetry. This is normally not a problem with extended Hückel [Hof63] or core Hamiltonian guesses; if the occupation scheme is wrong, the calculation will most likely converge, albeit to the wrong state! With INDO-type [Pop67] initial guesses (the default in the GAUSSIAN series), symmetry breaking may occur, with all the usual consequences.

- Try DIIS. This solves more than 95% of convergence difficulties (even many involving oscillation between states).

- Check if the density matrix update norm does not keep 'hanging' at a small number that is not yet below the threshold. If it is, this suggests an inherent numerical problem in the integral evaluation (often near-linear dependence of the basis set). Try tightening up integral evaluation tolerances, or loosening the SCF criterion, whichever is appropriate for the problem at hand.

- Try QCSCF. This will usually work for the other cases.

- If convergence has been achieved, save the MOs in some way suitable for reading in as the 'initial guess' to further calculations on that system.

- If convergence has not been achieved yet, try enforcing convergence in a minimal or double-zeta basis set first, and read in the converged orbitals as the initial guess.

- Try Seeger-Pople direct minimization SCF.

- Try the same, combined with level shifting.

- If all else fails, report it as an intrinsically divergent case.

Some programs like the GAUSSIAN series do DIIS by default. In that case, convergence problems are very occasionally remedied by turning it off (though the opposite occurs much more often).

### 1.1.8 The direct SCF method

The two most time-consuming parts in an ab initio Hartree-Fock calculation are normally the $O(n^4)$ computation of the integrals (where $n$ represents the number of basis functions), and the repeated $O(n^4)$ construction of the Fock matrix from these. (In semiempirical methods, the integral problem is reduced to a negligible $O(n^2)$ problem; the repeated $O(n^3)$ matrix eigensystem solution then dominates the calculation.) The integral computation involves mainly 'numbercrunching', and is thus *CPU-bound*; the construction of the Fock matrix mainly involves reading an integral file of $O(n^4)$ words, and is thus *I/O bound.*

Over the last two decades, advances in semiconductor technology have had a tremendous impact on the CPU power of commonly available machines; even a humble VAXstation 3100 is rated at 3.5 VAX MIPS (million instructions per second), whereas the theoretical performance of a 'low-end' supercomputer like the Cray X-MP is quoted to be around 400 MFLOPS (million floating point operations per second). Mass storage technology has not kept up with this progress: disk units of today still use essentially the same technology as they did twenty years ago. Some advances have been made, notably in increasing storage capacity; I/O bandwith (the maximum rate at which data can be transferred) has also significantly increased. However, these advances are nowhere near the three or four orders of magnitude booked in CPU technology.

This means that, when the basis set in an SCF calculation exceeds a particular size, the rate-limiting step in the Hartree-Fock calculation is no longer the computation of the integrals, but the construction of the Fock matrix. During the latter, the machine accumulates idle time waiting for the fulfillment of I/O requests, whereas the I/O units themselves are constantly saturated with requests from the SCF program. On an ordinary mainframe, every user will note degraded performance if a couple of SCF jobs are running in the batch queues; on a vector machine, costly CPU time gets lost inevitably unless the CPU can work on a totally CPU-bound job while waiting for the peripheral processor to fetch yet another chunk of integrals. On VMS or UNIX workstations, at the other end of the machine spectrum, CPUs are not so fast, of course, and operate in scalar mode, but I/O devices are often of the same slow breed found in the cheapest personal computers[13].

Additionally, with very large basis sets, the integral file may become much too large to fit in any reasonable amount of scratch disk space. The fact that most large organic molecules, a common application today, have no symmetry to be taken advantage of, only aggravates the problem. For example, lysergic acid ($C_{16}H_{16}N_2O_2$) in a medium-sized basis set like 6-31G* would entail 332 basis functions, or 3,037,332,544 integrals with only trivial symmetries. Taking into account that every integral will require at least

[13]The VAXstations even have an SCSI bus, where the eight bits of a byte even have to be sent in succession! Transfer rates, seek and latency times have better specifications in the Apple Macintosh SE/30 personal computer the author is writing the present work on!

one 32-bit word for the value and another for the label, one has to secure a scratch disk space of 22.6 GB, which is accessible to essentially nobody. (In practice, for a molecule of this size, a substantial portion of these integrals (those between basis functions on atoms that are widely apart) will lead to 'pre-exponential factors' below the evaluation tolerance. Even so, the remaining number of integrals would still be formidable.)

Recent advances in fast and vectorized integral evaluation algorithms have only highlighted the problem, getting to the point where the additional CPU time to re-evaluate the required integrals in situ would be outweighed by the almost complete elimination of idle I/O time. Exactly this is the idea behind the *direct SCF* method devised by Almlöf and coworkers [Alm82].

It is easily seen that the 'loops' involved in the integral evaluation and the SCF calculation are easily combined. Additionally, by constructing a 'skeleton' Fock matrix first and then symmetrizing it, only symmetry-unique integrals (the 'petite list') have to be evaluated.

It has considerable advantages to build the Fock matrix in an incremental fashion:

$$\Delta F_{pq} = \sum_{rs} \Delta P_{rs} \langle pr||qs \rangle \tag{1.97}$$

where $\Delta$P represents the change in the density matrix between two consecutive iterations. Its elements $\Delta P_{rs}$ of course decrease as the SCF calculation progresses, to be (ideally) vanishing at convergence. Now introduce an update threshold $\epsilon$, one may dispense with computing $\langle pr||qs \rangle$ if

$$|\Delta P_{rs} \langle pr||qs \rangle| < \epsilon \tag{1.98}$$

As a result, less and less integrals have to be computed upon every iteration. The value for $\epsilon$ should be made proportional to the SCF convergence criterion $\delta$,

$$\sqrt{\sum_{pq} \Delta P_{pq}^2} < \delta \text{ at convergence} \tag{1.99}$$

Direct SCF has been essential in making very large molecules amenable to ab initio calculations, even though no electron correlation can still be treated. If a direct SCF is possible, geometry optimization with analytical gradients immediately becomes an option since the gradient evaluation becomes negligible compared to the effort in the SCF. Direct frequency calculations become more demanding, as every coupled perturbed Hartree-Fock (CPHF, see Section 1.10) iteration requires the re-evaluation of all the integral derivatives involved.

Some effort has recently been put into the development of direct electron correlation methods, which is not exactly a trivial business because of the additional requirement to avoid the integral transformation entirely. The principles of direct correlated methods were first discussed by Taylor [Tay87]; direct [Sae89, Hea88] and semi-direct [Fri90b] MP2 methods have recently been implemented, as have direct MP2 gradients [Fri90a].

Very recently, prices for central memory have dropped so enormously that even modest workstations are equipped with fairly large amounts of it (32 MB is standard in some product ranges), whereas the users of large mainframes and supercomputers may have even greater core spaces at their disposal (256 MB or more). Such large core spaces are essential for direct correlated methods; in the semi-direct methods, part of the intermediate storage is deferred to disk. For medium-to-large molecules or basis sets, however, they also allow the two-electron integrals to be stored in core, rather than on disk, which combines the CPU savings of conventional SCF with the elimination of I/O overhead in direct SCF. Some versions of GAUSSIAN allow for such 'in-core' SCF. It would perhaps be useful to look at an algorithm with an incremental Fock matrix construction, but where the integrals associated with the largest $\Delta P$ elements would be kept in memory. Then less and less integrals would have to be recomputed as the SCF progresses, until finally all integrals could be fetched from memory.

Such a hybrid algorithm — but based on disk instead of central memory storage — has in fact recently been implemented by Häser and Ahlrichs [Has89]. These authors report time savings on the order of 35–50%.

## 1.2 The electron correlation problem: preliminaries

Part of the material dealt with in the subsequent sections is also discussed in [McW89, Sza89, Heh86a], as well as in a book by Dykstra [Dyk88] that also includes an excellent bibliography on most of the subjects. Wilson [Wil84] discusses most of the material (and some other topics) in a fairly detailed manner. Some of the material is so specialized or new, however, that explicit reference to the primary literature cannot be avoided. As every scientist knows, conciseness and importance of content are more highly valued in the primary literature than clarity and understandability, and rightly so. The author has therefore tried to present the following material in a somewhat personal way in an attempt to satisfy three requirements:

- To avoid verbatim copying of developments, proofs, etc. from other printed texts.
- To make the discussion understandable for a nonspecialist.
- To emphasize the relationship between, and the common logic of, seemingly disparate electron correlation treatments.

### 1.2.1 Form of the $n$-particle solution

It is well known, that the solution for the one-particle problem may be expanded in a countably infinite series of quadratically integrable functions $\Phi_i$

$$\phi(\vec{r}_1) = \sum_i c_i \Phi_i(\vec{r}_1) \tag{1.100}$$

which are then called basis functions.

For a two-particle function, this development may still be made; the coefficients $c_j$ then become functions of the second coordinate $\vec{r}_2$:

$$\Psi(\vec{r}_1, \vec{r}_2) = \sum_j c_j(\vec{r}_2)\Phi_j(\vec{r}_1) \tag{1.101}$$

But nothing stops us from developing the $c_j$ coefficients themselves as a series in the basis functions $\Phi_j$:

$$\Psi(\vec{r}_1, \vec{r}_2) = \sum_{i,j} C_{ij}\Phi_i(\vec{r}_1)\Phi_j(\vec{r}_2) \tag{1.102}$$

where the $C_{ij}$ are now constants. To turn this two-particle function into a valid two-fermion wave function, antisymmetry must be imposed:

$$\Psi(\vec{r}_1, \vec{r}_2) = \sum_{i>j} C_{ij}\hat{A}\Phi_i(\vec{r}_1)\Phi_j(\vec{r}_2) = \sum_{i>j} C_{ij}\psi_{ij} \tag{1.103}$$

where $\psi_{ij}$ represents the Slater determinant generated from one-particle function $\Phi_i$ and $\Phi_j$, and the restriction on the summation avoids unnecessary repetition. (Equal indices lead to vanishing determinants.) This discussion is easily extended to the $n$-particle case, to yield the following result

$$\Psi(\vec{r}_1, \vec{r}_2, \ldots, \vec{r}_n) = \sum_{i>j>k>\ldots} C_{ijk\ldots}\psi_{ijk\ldots} \tag{1.104}$$

In other terms: the $n$-particle solution can always be expanded as an infinite series of all Slater determinants that can be generated from a given infinite one-particle basis set[14]. In practical calculations, a finite subset of the infinite one-particle basis set is chosen. Then the same development can still be made, but the expansion becomes finite.

When this latter expansion is made in a basis of Hartree-Fock orbitals, it is commonly called the full configuration interaction wavefunction (see next section).

### 1.2.2 Definition of the correlation energy

Let $E$ be the exact, nonrelativistic, Born-Oppenheimer energy of the system, and $E_{\mathrm{HF}}$ the exact Hartree-Fock energy under the same constraints. Then the *exact correlation energy* is defined as the difference between the two[15]:

$$\Delta E_{\mathrm{exact}} = E - E_{\mathrm{HF}} \tag{1.105}$$

[14]The argument presented here is originally due to Löwdin [Loe59].

[15]The present definition is usually attributed to Löwdin [Loe59]. The concept *correlation energy* was first introduced by Wigner [Wig33].

This corresponds to an expansion of the form (1.104) for an infinite one-particle basis set. The corresponding energy for a finite one-particle basis set is called the *basis set correlation energy.* It is usually denoted $E_{\mathrm{FCI}}$, where the acronym FCI stands for full configuration interaction.

More generally, the correlation energy at a given level is then defined (using intermediate normalization, $\langle\psi_0|\Psi\rangle = 1$) as

$$\Delta E = \langle\psi_0|\hat{H}'|\Psi\rangle \tag{1.106}$$

where

$$\hat{H}' \equiv \hat{H} - E_{\mathrm{HF}} \tag{1.107}$$

### 1.2.3 The second quantization formalism

Second quantization, or the occupation number representation, is a very powerful formulation of quantum mechanics. The present discussion will be confined to those aspects that are relevant for the remainder of the discussion. A clear and concise introduction has been given by Paldus and Čížek [Pal75]; a monograph by Jørgensen and Simons [Jor81] may also be recommended.

Let us consider a space of one-particle eigenfunctions $\phi_i$ of some one-particle operator. A basis for an $n$-particle fermion system is then spanned by the Slater determinants $\hat{A}\prod_i \phi_i$, where the antisymmetrization operator $\hat{A}$ generates the determinant form from the Hartree product $\prod_i \phi_i$. For completeness, a zero-particle wavefunction is denoted $|\mathrm{vac}\rangle$, the so-called *true vacuum state.* We can then define the so-called *annihilation operators*

$$\hat{a}_i|\phi_i\rangle = |\mathrm{vac}\rangle \tag{1.108}$$

that 'destroy' a particle in the corresponding eigenstate $|\phi_i\rangle$. The Hermitian adjoint of the annihilation operator is the *creation operator*

$$\hat{a}_i^+|\mathrm{vac}\rangle = |\phi_i\rangle \tag{1.109}$$

(This definition of creation and annihilation operators corresponds to the so-called *particle formalism.*) With these operators, any $n$-particle Slater determinant can be represented by a string of $n$ creation operators working on the true vacuum state:

$$|\hat{A}\phi_i\phi_j\phi_k\ldots\phi_n\rangle = \hat{a}_i^+\hat{a}_j^+\hat{a}_k^+\ldots\hat{a}_n^+|\mathrm{vac}\rangle \tag{1.110}$$

Note that, at least for a fermion system, the order in which the operators are written is not immaterial, e.g.:

$$\hat{a}_i^+\hat{a}_j^+|\mathrm{vac}\rangle = |\hat{A}\phi_i\phi_j\rangle \tag{1.111}$$

$$\hat{a}_j^+\hat{a}_i^+|\mathrm{vac}\rangle = |\hat{A}\phi_j\phi_i\rangle = -|\hat{A}\phi_i\phi_j\rangle \tag{1.112}$$

$$\hat{a}_k^+|\hat{A}\phi_j\phi_i\rangle = |\hat{A}\phi_k\phi_j\phi_i\rangle \tag{1.113}$$

As the particles are 'created' in right-to-left order, the determinants are formed by inserting the one-particle functions in the same order between the antisymmetrization operator and any already present Hartree product.

For our present purpose, it is convenient to 'shift origin' from the true vacuum state to a so-called *Fermi vacuum state* $|\psi_0\rangle = |\hat{A}\phi_1\phi_2\ldots\phi_n\rangle$, which is a single $n$-particle Slater determinant. The definitions of creation and annihilation operators then become

$$\hat{a}_a^+|\psi_0\rangle = |\hat{A}\phi_a\phi_1\phi_2\ldots\phi_n\rangle \text{ if } a \text{ virtual} \tag{1.114}$$

$$\hat{a}_i^+|\psi_0\rangle = 0 \text{ if } i \text{ occupied} \tag{1.115}$$

$$\hat{a}_i|\hat{A}\phi_i\phi_1\phi_2\ldots\phi_n\rangle = |\psi_0\rangle \text{ if } i \text{ occupied} \tag{1.116}$$

$$\hat{a}_a|\psi_0\rangle = 0 \text{ if } a \text{ virtual} \tag{1.117}$$

where it is taken into account that a Slater determinant with two identical orbitals vanishes. Henceforth, we will always use the indices $ijkl\ldots$ and $abcd\ldots$ for orbitals that are occupied and virtual, respectively, in the Fermi vacuum.

Defining the *anticommutator* of two operators as $[\hat{A},\hat{B}]_+ \equiv \hat{A}\hat{B} + \hat{B}\hat{A}$, it is easily seen that the creation and annihilation operators obey the following *anticommutation relations*:

$$[\hat{a}_i,\hat{a}_j]_+ = 0 \tag{1.118}$$

$$[\hat{a}_a^+,\hat{a}_b^+]_+ = 0 \tag{1.119}$$

$$[\hat{a}_a^+,\hat{a}_i]_+ = \delta_{ia} \tag{1.120}$$

It is obvious, that the number of particles is only left invariant by a string of creation and annihilation operators if there are precisely as many of the former as there are of the latter.

An alternative definition (leading to the so-called *hole formalism*) of the creator and annihilator is possible, where the annihilator destroys a 'hole' (i.e. creates a particle), and the creator creates one. The anticommutation properties of the operators remain the same.

As demonstrated by Paldus and Čížek [Pal75], it is sometimes advantageous to use a so-called *mixed formalism*, where the annihilators and creators 'change roles' depending upon whether they act on an occupied or virtual orbital. We will denote such 'mixed' hole-particle indices by $xyz\ldots$. They also introduce the *hole* and *particle* functions $h(x)$ and $p(x)$, such that

$$h(x) = 1 \text{ if } x \text{ virtual} \qquad h(x) = 0 \text{ if } x \text{ occupied} \tag{1.121}$$

$$p(x) = 0 \text{ if } x \text{ virtual} \qquad p(x) = 1 \text{ if } x \text{ occupied} \tag{1.122}$$

$$h(x) + p(x) = 1 \qquad \forall x \tag{1.123}$$

Any $n$-particle operator can now be brought in second-quantized form as follows:

$$\hat{O}_n = \frac{1}{n!}\sum_{ijk\ldots xyz\ldots}\langle ijk\ldots|\hat{O}_n|xyz\ldots\rangle\hat{a}_x^+\hat{a}_y^+\hat{a}_z^+\ldots\hat{a}_i\hat{a}_j\hat{a}_k\ldots \tag{1.124}$$

where the division by $n!$ eliminates the need for mutual restrictions on the summation indices. (Terms where indices coincide vanish anyway.) The choice $x = i, y = j, z = k, \ldots$ will leave the wavefunction unaltered; examples are general one-and two-particle potentials:

$$\hat{V} = \sum_i \langle i|\hat{V}|i\rangle \hat{a}_i^+ \hat{a}_i \tag{1.125}$$

$$\hat{W} = \frac{1}{2}\sum_{ij} \langle ij|\hat{W}|ij\rangle \hat{a}_j^+ \hat{a}_i^+ \hat{a}_i \hat{a}_j \tag{1.126}$$

The case where $xyz\ldots$ become hole indices $abc\ldots$ leads to excitation and cluster operators (see below) that figure very prominently in electron correlation theory.

There is obviously a lot more to be said about second quantization. We will terminate the discussion here in order not to digress too far. In order to avoid confusion when reading other texts, it should only be noted that creation-annihilation operators $\hat{a}_y^+ \hat{a}_a^+ \hat{a}_x \hat{a}_i$ are often abbreviated as $\hat{y}^+\hat{a}^+\hat{x}\hat{i}$ or even, when no ambiguity is thus introduced, as $y^+a^+xi$. The latter notation is of course quite convenient for typographical reasons.

### 1.2.4 Integral transformation

Virtually all current electron correlation methods work in a basis of Hartree-Fock orbitals. This means that the two-electron integrals, which are computed in the AO (atomic orbital) basis set for the SCF calculation, must be transformed to the MO (molecular orbital) basis set:

$$\langle ij|kl\rangle = \sum_{pqrs} c_{ip}c_{jq}c_{kr}c_{ls}\langle pq|rs\rangle \tag{1.127}$$

With $n$ AO basis functions, this would imply $O(n^8)$ operations, which is clearly unacceptable. The transformation is therefore split up in four partial transformations [Roo75]:

$$\begin{aligned}
\langle iq|rs\rangle &= \sum_p c_{ip}\langle pq|rs\rangle \\
\langle ij|rs\rangle &= \sum_q c_{jq}\langle iq|rs\rangle \\
\langle ij|ks\rangle &= \sum_r c_{kr}\langle ij|rs\rangle \\
\langle ij|kl\rangle &= \sum_s c_{ls}\langle ij|rs\rangle
\end{aligned} \tag{1.128}$$

In this manner, only $O(4n^5)$ operations are required, as well as $O(n^4)$ external storage for the partially transformed integrals. (Alternatively, the original AO integrals may be deleted after the first step). Usually, the integrals must subsequently be antisymmetrized according to $\langle ij||kl\rangle = \langle ij|kl\rangle - \langle ij|lk\rangle$; as the integrals are already sorted in MO order, with the last index varying most rapidly, this antisymmetrization is quite easy. For most applications, the original $\langle ij|kl\rangle$ integrals may be deleted afterwards. In some integral

transformation algorithms, it is possible to carry out the antisymmetrization already in an inner loop of the transformation.

The integral transformation is one of the time-consuming parts of most electron correlation calculations: for some of the noniterative lower-level treatments, like MP2, it is even the rate-determining step. Hence, much effort has been done for these to avoid a full integral transform (as in the Pople group implementations of Møller-Plesset [Bin75b, Pop76, Kri78, Kri80] and CISD [Pop77] methods), or even to work directly in an AO basis (as in the *self consistent electron pairs* (SCEP) procedure of Meyer [Mey76]).

## 1.3 Configuration interaction (CI)

This is the oldest treatment, being discussed by Slater as early as 1929 [Sla29], and has for considerable time been the most popular. An excellent, though somewhat older, review of configuration interaction methods was made by Shavitt [Sha77] in 1977. Important developments have been made since; some of these are discussed in the book by McWeeny [McW89]. Very recently, the subject has been reviewed [Bau90a]; a discussion of practical computational implementations that discusses the literature *en passant* has been presented by Taylor *et al.* [Tay89].

### 1.3.1 Full configuration interaction

This is nothing but the exact n-particle expansion in a finite basis set of Hartree-Fock orbitals. It corresponds to the eigenvalue problem

$$\hat{H}'\Psi = E_{\mathrm{FCI}}\Psi \tag{1.129}$$

where $\hat{H}' \equiv \hat{H} - E_{\mathrm{HF}}$ and $E_{\mathrm{FCI}}$ is the basis set correlation energy. The matrix elements between the Slater determinants can be conveniently expressed in terms of two-electron integrals (see next subsection). This finally leads to a huge algebraic eigenvalue problem, where the eigenvalues are the energies of ground and excited states, and the elements of the eigenvectors the coefficients of the Slater determinants in the expansion. They satisfy either the *regular normalization condition* $\sum_i C_i^2 = 1$ (i.e. $\langle\Psi|\Psi\rangle = 1$), or the *intermediate normalization condition* $C_0 = 1$ (i.e. $\langle\psi_0|\Psi\rangle = 1$); the latter convention is the more convenient one in discussions of electron correlation techniques.

The Slater determinants involved are commonly called *configurations*, hence the name *configuration superposition* or *configuration interaction* (The term *interaction* refers to the off-diagonal elements of the H matrix).

These configurations consist of the Hartree-Fock ground state or *reference configuration*, and a very large number of Hartree-Fock excited states in which one or more *occupied orbitals* of the ground state are replaced by *virtual orbitals*, i.e. MOs that are unoccupied in the Hartree-Fock ground state. The number of such replacements is called

the *excitation level*; any replacement itself is referred to as an *excitation*. Configurations with excitation levels one, two, three, four, ... are called single, double, triple, quadruple, ... excitations. Such an excited configuration is denoted as $\psi_{ijk\ldots}^{abc\ldots}$, where $ijk\ldots$ represent the indices of the occupied, and $abc\ldots$ those of the virtual, orbitals that are involved in the excitation. The corresponding coefficient is likewise notated $C_{ijk\ldots}^{abc\ldots}$.

Using second quantization notation, the full CI expansion may be written in operator form. Let us define the *excitation operators*

$$\hat{C}_1 = \sum_{i,a} C_i^a \hat{a}_a^+ \hat{a}_i \tag{1.130}$$

$$\hat{C}_2 = \sum_{i>j,a>b} C_{ij}^{ab} \hat{a}_a^+ \hat{a}_b^+ \hat{a}_i \hat{a}_j \tag{1.131}$$

$$\hat{C}_3 = \sum_{i>j>k,a>b>c} C_{ijk}^{abc} \hat{a}_a^+ \hat{a}_b^+ \hat{a}_c^+ \hat{a}_i \hat{a}_j \hat{a}_k \tag{1.132}$$

$$\hat{C}_4 = \sum_{i>j>k>l,a>b>c>d} C_{ijkk}^{abcd} \hat{a}_a^+ \hat{a}_b^+ \hat{a}_c^+ \hat{a}_d^+ \hat{a}_i \hat{a}_j \hat{a}_k \hat{a}_l \tag{1.133}$$

...

which, when applied to the Hartree-Fock determinant $\psi_0$, have the effect

$$\hat{C}_1 \psi_0 = \sum_{i,a} C_i^a \psi_i^a \tag{1.134}$$

$$\hat{C}_2 \psi_0 = \sum_{i>j,a>b} C_{ij}^{ab} \psi_{ij}^{ab} \tag{1.135}$$

$$\hat{C}_3 \psi_0 = \sum_{i>j>k,a>b>c} C_{ijk}^{abc} \psi_{ijk}^{abc} \tag{1.136}$$

$$\hat{C}_4 \psi_0 = \sum_{i>j>k>l,a>b>c>d} C_{ijkl}^{abcd} \psi_{ijkl}^{abcd} \tag{1.137}$$

...

A full CI has the advantage that it represents the exact result within the given basis set. Its principal disadvantage is the explosive growth of the number of configurations with the size of the basis set and the number of electrons. For $m$ orbitals, total spin $S$, and $N$ electrons, and ignoring spatial symmetry, the number of determinants in the full CI expansion is given by the Weyl formula:

$$n(N,S,m) = \frac{2S+1}{m+1} \begin{pmatrix} m+1 \\ N/2-S \end{pmatrix} \begin{pmatrix} m+1 \\ N/2+S+1 \end{pmatrix} \tag{1.138}$$

A rough approximation when $m \gg N \gg S$, i.e. the basis set is sufficiently large and most of the electrons are paired, is given by [Sha77]:

$$n(N,S,m) \approx N^{-2}(2m/N)^N \tag{1.139}$$

Even when CSFs are used instead of determinants to shorten the expansion length, a full CI calculation on e.g. water in a double-zeta basis set [Sax81] still involves 256,473

symmetry- and spin-adapted configurations[16]. It goes without saying that explicit construction of a matrix of 256,473 × 256,473 = 65,778,399,729 elements is simply out of the question. Therefore so-called *direct CI* techniques (see Section 1.3.3), that avoid the explicit construction, are employed.

Some pioneering full CI calculations were made possible through the so-called graphical unitary group approach (GUGA). The theoretical background of the latter — which is beyond the scope of this work — has been reviewed by Paldus [Pal76]; its two practical implementations, the older loop-driven GUGA [Bro79] and the more efficient shape-driven GUGA [Sax82] display excellent performance on scalar computers, but fail to make the most out of vector processing supercomputers as the algorithm is essentially scalar in nature for higher than double excitations [Bau90a]. The determinant-based modification [Kno84] of Siegbahn's factorized direct CI algorithm [Sie84] does not have this disadvantage, and has made it possible, at least with today's fastest supercomputers, to perform full CI calculations in a DZP basis set on small molecules. Their main function is as a 'benchmark' for less expensive and more practical electron correlation methods: Bauschlicher, Taylor and their coworkers at NASA Ames laboratories have published an impressive series of such benchmarks since 1986 (see [Bau90a] for a review).

### 1.3.2 Evaluation of matrix elements

CI matrix elements between Slater determinants are most conveniently written in terms of antisymmetrized two-electron integrals. We will consider a number of different cases:

- Matrix elements between configurations that belong to different irreducible representations of the molecular point group are zero. This is a trivial consequence of the 'great orthogonality theorem' of group theory.

- Matrix elements between configurations of different multiplicity also vanish. This is a consequence of the mutual orthogonality of the $\alpha$ and $\beta$ spin functions.

- The matrix element between $|\psi_0\rangle$ and any singly excited state vanishes for a canonical Hartree-Fock reference, because it corresponds to an off-diagonal element of the Fock operator, which is of course diagonal in the basis of its own eigenfunctions. This is one formulation of the famous Brillouin theorem [Bri34].

- Matrix elements between any two configurations that are more than two excitations apart, i.e. that require more than two creator/annihilator pairs to be mapped onto each other, vanish also. This is a consequence of the fact, that the Hamiltonian contains two-particle interactions at most.

[16] Of course a double-zeta basis set is much too small to produce any chemically useful result at a correlated level.

- The matrix element between two determinants that can be mapped onto each other by the creator/annihilator pairs $\hat{a}_a^+\hat{a}_b^+\hat{a}_i\hat{a}_j$ are given by $\langle ij||ab\rangle$.

- For two CSFs $\psi_K$ and $\psi_L$, the matrix element is given by the more general expression [Roo77]

$$H_{KL} = \sum_{wxyz} B_{wxyz}^{KL}\langle wx|yz\rangle \tag{1.140}$$

in which $wxyz$ run over all MOs and the $B$ denote so-called *(two-electron) coupling coefficients* whose value depends on the occupation and spin of orbitals $wxyz$ in $\psi_K$ and $\psi_L$.

### 1.3.3 Direct CI

The CI problem may be written in a variety of iterative forms, one of which is e.g. (in the CID case)

$$\langle\psi_{ij}^{ab}|H'|(1+\hat{C}_2)\psi_0\rangle = E_{\text{CID}}C_{ij}^{ab} \tag{1.141}$$

$$\langle\psi_0|H'|(1+\hat{C}_2)\psi_0\rangle = E_{\text{CID}} \tag{1.142}$$

On the first iteration, $E_{\text{CID}}$ is set equal to zero in (1.141); this leaves only a homogenous linear system to be solved (which can be handled to much larger sizes than eigenvalue problems). The resulting coefficients are used to compute $E_{\text{CID}}$, which is then substituted back; on the next iteration, an inhomogenous system has to be solved (which is not more difficult than a homogenous). The iterations are repeated until either the energy or the CI amplitudes no longer change appreciably. One disadvantage of this approach is that no energies for the excited states are thus obtained; however these energies would not be very reliable anyway as the CI expansion involved was built on the Hartree-Fock reference for another state.

The other disadvantage is that at least on the first iteration, the CI matrix still must be constructed explicitly. It does have the advantage over the noniterative algorithm that the large eigenvalue problem is reduced to a succession of matrix inversions or linear system solutions (which can be handled to very large dimensions for 'sparse' systems [Ral78]). In matrix form, it corresponds to

$$\Delta E^{[n+1]} = -\vec{B}^+(\mathsf{A}-\Delta E^{[n]}1)^{-1}\vec{B} \tag{1.143}$$

$$B_D = \langle\psi_0|H'|\psi_D\rangle \tag{1.144}$$

$$A_{DD'} = \langle\psi_D|H'|\psi_{D'}\rangle \tag{1.145}$$

where the superscript $[n]$ means 'at the $n$-th iteration'.

The iterative problem can be cast in a more practical form by introducing the *Rayleigh quotient*, defined for general $\vec{x}$ and $\mathsf{A}$ as $\vec{x}^{+}\mathsf{A}\vec{x}/\vec{x}^{+}\vec{x}$. (Of course the expression for the variational principle is readily recognized.)

$$\vec{C}^{[n+1]} = (\Delta E^{[n]})^{-1}\mathsf{H}\vec{C}^{[n]} \tag{1.146}$$

$$\Delta E^{[n+1]} = \frac{\vec{C}^{+[n]}\mathsf{H}\vec{C}^{[n]}}{\vec{C}^{+[n]}\vec{C}^{[n]}} \tag{1.147}$$

We here again set $\vec{C}^{[0]} = 0$; to avoid division by zero, $\Delta E^{[0]} = 1$, after which $\vec{C}^{[n+1]}$ may be normalized.

Actually, this is none other than the familiar *power method* for iterative solution of eigensystems [Ral78]. The method is based upon the fact that, given some vector $\vec{y}$ composed of eigenvectors $\vec{x}$ associated with eigenvalues $\lambda$ of some matrix $\mathsf{A}$, the component corresponding to the largest $\lambda$ (in absolute value) will be enhanced in the product $\mathsf{A}\vec{y}$:

$$\mathsf{A}^n(c_2\vec{x}_2 + c_2\vec{x}_2 + \ldots) = \lambda_1^n c_1\vec{x}_1 + \lambda_2^n c_2\vec{x}_2 + \ldots \tag{1.148}$$

We see that, for sufficiently large $n$, the eigenvector corresponding to the largest $\lambda$ will eventually dominate the result. The error in the eigenvector is given by $O((\frac{\lambda_2}{\lambda_1})^n)$, whereas the eigenvalue computed as a Rayleigh quotient has an error only on the order of $O((\frac{\lambda_2}{\lambda_1})^{2n})$. Convergence acceleration techniques can be applied to the sequence of vectors $\vec{y}^{(n)}$. (It is now readily seen, why low-lying excited states will hamper convergence. Level shifting, which is the addition of a shift parameter $\eta$ to the diagonal elements of $\mathsf{A}$, may alleviate this latter problem.)

The main advantage of this and related techniques (such as the inverse power method [Ral78]) is that it effectively dispenses with the need to construct $\mathsf{H}$ explicitly: it is only necessary to compute and store the vector $\mathsf{H}\vec{C}^{[n]}$, which may be constructed directly from the transformed two-electron integrals on disk.

For more general ROHF cases, including multireference ones, the expressions for $\mathsf{H}\vec{C}$ involve coupling coefficients $A$ that depend on the spin symmetry of the two states involved in the elements of $\mathsf{H}$. These are usually stored on a disk file commonly called a 'formula tape', which is then processed once per iteration. As many of these coefficients are nonzero, the length of the formula tape becomes the limiting factor for large CI calculations.

Siegbahn [Sie84] discovered that by inserting a resolution of the identity, the two-electron coupling coefficients may be factorized as a product of one-electron coupling coefficients:

$$B^{KL}_{wxyz} = \sum_J A^{KJ}_{wx} A^{JL}_{yz} \tag{1.149}$$

This not only considerably shortens the formula tape, but brings the construction of $\mathsf{H}\vec{C}$ into a form that is very well suited for vectorization, and thus achieves maximum

performance on supercomputers. However, for large CI calculations the formula tape still becomes prohibitively large.

Working not in a basis of CSFs but of ordinary determinants generally increases the length of the CI expansion, but eliminates the formula tape as all coupling coefficients become zero or unity, and can be generated on the fly [Kno84]. On a high-end supercomputer like the Cray-2, full CI calculations involving more than 20 million determinants have been performed [Bau86]. Actually, by special techniques [Kno89a] exploiting the sparseness of $\vec{C}$ and $\mathsf{H}\vec{C}$ for very large expansions, pilot calculations including some 400 million determinants have been performed [Kno89b].

Several other updating schemes than the power method have been proposed over the years (see [Roo77] for references). Most of these are based on the observation that the Rayleigh quotient is a stationary point with respect to variation in the coefficients for every eigenvector[17]. An update to the eigenvector is then found as

$$\rho = \frac{\vec{c}^{+}\mathsf{A}\vec{c}}{\vec{c}^{+}\vec{c}} \tag{1.150}$$

$$\delta_i = \frac{\mathsf{A} - \rho\mathsf{1}}{\rho - A_{ii}} \tag{1.151}$$

Among the most popular is the Davidson method [Dav75], which has the advantage that it allows determination of *several* low-lying eigensolutions instead of just the lowest one. It is briefly described below:

- If the $k$-th eigenvalue is desired, take a set of starting vectors $\vec{b}$ of dimension $l \geq k$ that span the dominant components of the corresponding eigenvectors (in our case, e.g. the HF determinants for the desired states). Form all vectors $\mathsf{A}\vec{b}_i$ and store them.
- Build the matrix $\tilde{\mathsf{A}}$ with elements $\tilde{A}_{ij} = \vec{b}_i^{+}\mathsf{A}\vec{b}_j$. Find its eigenvalues $\lambda$ and its eigenvectors $\vec{x}$. Select $\lambda_k$ and $\vec{x}_k$.
- Form $\vec{q}_M = \sum_{i=1}^{M} x_{ki}^{[M]}\mathsf{A}\vec{b}_i - \sum_{i=1}^{M} x_{ki}^{[M]}\lambda_k^{[M]}\vec{b}_i$; $M$ is the dimension of $\tilde{\mathsf{A}}$.
- If $||\vec{q}_k||$ is sufficiently small, then exit.
- Compute $\vec{y}$; $y_i = q_{iM}/(\lambda_k^{[M]} - A_{ii})$.
- Compute $\vec{d}_{M+1} = \prod_{i=1}^{M}(1 - \vec{b}_i\vec{b}_i^{+})\vec{y}_{M+1}$, i.e. orthogonalize it to the previous vectors.
- Normalize it, i.e. $\vec{b}_{M+1} = \vec{d}/||\vec{d}||$.
- Form $\mathsf{A}\vec{b}_{M+1}$ and store it. This is the time-consuming step.
- Return to the second step.

[17] It becomes a minimum for the lowest eigenvector, which is another formulation of the Rayleigh-Ritz variation principle.

(Pulay [Pul80, Pul83] has pointed out the connection between the present method and DIIS.) For very large CI problems, storage for previous iterates becomes exhausted after a number of iterations. The algorithm is then simply 'reset' at the current iteration, and all previous iterates discarded. This may delay convergence by a few cycles, but this may be offset by the elimination of idle I/O time.

### 1.3.4 Limited configuration interaction

This consists of restricting the CI expansion to a subset of the full CI excitation operators. As we have seen under the previous heading that only doubly excited states interact directly with the ground state, restriction to $\hat{C}_2$ is the most obvious choice. This type of limited configuration interaction is called CID (CI with all double excitations).

The single excitations contained in $\hat{C}_1$ actually do interact, indirectly, with the ground state. As their number is small anyway, including them too does not significantly increase the computational cost. A limited CI calculation where only $\hat{C}_1 + \hat{C}_2$ is considered, is called a CISD (configuration interaction with all singles and double excitations) calculation. The latter is by far the most commonly used type of limited configuration interaction.

CISD expansions are much smaller than full CI expansions: given a basis set of size $n$ and $N$ correlated electrons, the total number of distinct $m$-fold excited determinants that can be generated (ignoring spatial and spin symmetry) is

$$\binom{N}{m}\binom{2K-N}{m} \tag{1.152}$$

Typical CISD expansion lengths for a small molecule in a medium-sized basis set are thus on the order of a few thousand configurations. Furthermore, the number of configurations does not increase as explosively with basis set and number of electrons as is the case with a full CI calculation.

CID and CISD calculations can be routinely carried out even for fairly large molecules (especially when GUGA techniques are applied[18]). The energies are variational and are thus upper bounds to the exact energy. Moreover, CISD is exact for a two-electron system.

CID and CISD have one major disadvantage: they are not *size consistent*, i.e. the correlation energy does not scale correctly with molecular size. This is best illustrated by the example of two monomers A and B at infinite distance.

Let the individual CID correlation energies be $E_{\mathrm{CID}}(A)$ and $E_{\mathrm{CID}}(B)$, respectively, corresponding to wavefunctions $(1 + \hat{C}_2(A))\psi_0$ and $(1 + \hat{C}_2^B)\psi_0$. Assume that the effect

[18] A recent new closed-shell CISD implementation even outperforms SDGUGA by a factor of two [Scu88a].

of $\hat{C}_1$ can be neglected[19]. Then the exact energy for the supersystem at infinite distance would be $E_{\text{CID}}(A) + E_{\text{CID}}(B)$, whereas its exact wavefunction would be

$$(1 + \hat{C}_2(A))(1 + \hat{C}_2(B))\psi_0 = (1 + \hat{C}_2(A) + \hat{C}_2(B) + \hat{C}_2(A)\hat{C}_2(B))\psi_0 \tag{1.153}$$

The last term corresponds to so-called *disconnected* quadruple excitations, and cannot possibly be included in a CID calculation because it involves determinants with an excitation level above two. But although these quadruple excitations do not interact directly with the ground state, they interact very appreciably with the doubly excited configurations and thus affect the energy significantly. Their neglect results in the fact that

$$E_{\text{CID}}(AB) > E_{\text{CID}}(A) + E_{\text{CID}}(B) \tag{1.154}$$

The error is far from academic (see e.g. [Ahl74]): for larger molecules, it may well exceed the interaction energy to be evaluated, making CID (and CISD, which exhibits the same problem) useless for the evaluation of any reaction energy.

Actually, the problem is even worse: substitute e.g. two hydrogen molecules for A and B, and one sees that size-consistency errors will be introduced for any system with more than two electrons. Inclusion of the $\hat{C}_4$ operator (i.e., a CIDQ method) would remedy the problem (CISDTQ in the case of the CISD method), but only for the four-electron case; otherwise, the wavefunction for the supersystem will e.g. contain disconnected sextuple excitations, and one is 'back to square one'.

Various approximate correction formulas for the size-consistency error have been developed [Lan74, Pop77, Sie78, Dav77]. A critical analysis [Mar90b] of these is presented in Section 5.3 of this work. All of these formulas, however, have one deficiency or the other; furthermore they cannot be applied to other properties than the energy (like geometrical and electric field derivatives), and give rise to 'noisy' computed potential energy surfaces [Bar79][20].

Very closely related to (and often confused with) size-consistency is the property of *size-extensivity*. For the purpose of the present discussion, a method is size-extensive if the correlation energy contains only terms that scale linearly with the size of the system. (A more rigorous definition will be given in Section 1.5.3.) If the reference wavefunction dissociates correctly, a method that is size-extensive is guaranteed to be size-consistent, but the converse is not true. In this sense, requiring a method to be size-extensive is more severe than imposing size-consistency. (Other fine points between the definitions for size-consistency [Pop76] and size-extensivity [Bar78] are discussed in

[19]This can be done exactly for Brueckner orbitals [Bru54], which are defined by the requirement that the single-excitation contribution to the energy vanishes; for an RHF or ROHF wavefunction and a system that can be adequately described by a single-reference method, this even holds approximately for Hartree-Fock orbitals.

[20]In this paper, a quartic potential energy surface was fitted to computed energies at 36 different geometries for water. The addition of the Davidson correction [Lan74] to the CISD energies leads to a significant increase in the standard deviation of the fit.

[Bar78, Bar81a, Bar81b, Bar89a].) The term 'size-extensive' has the advantage of rigorous mathematical definition, whereas the physical concept of size-consistency is much easier to grasp intuitively. As the difference is fairly academic in most situations, and both terms convey the same concept of 'correct size dependence', many authors speak of 'size-consistency' when they actually are referring to 'size-extensivity' [TayPC].

Higher excitations that cannot be factored into lower excitations like the disconnected ones are called *connected*. The most important ones in practical applications are connected triple excitations: no size consistency correction formula can of course account for these. It should be mentioned here that according to Davidson [Dav74] (quoted in [Car80]), these should become very important for large molecules; he suggested that e.g. for a hydrocarbon chain longer than about 30 atoms, most of the correlation energy should come from higher than quadruple excitations.

## 1.4 Other variational methods

### 1.4.1 Multireference double excitation configuration interaction (MRD-CI)

This method, developed by Buenker and coworkers [Bue74], is not used in the present work. However, its use is fairly widespread, so it is briefly outlined here to be able to assess the quality of literature results obtained through it.

Besides not being size-consistent, single-reference configuration interaction experiences another potential breakdown, which occurs when an excited state of the same symmetry is very close in energy to the Hartree-Fock reference. Then several determinants have large coefficients in the CI expansion, whereas excited states from these determinants would significantly affect the energy if properly included.

There is no a priori objection, however, against using limited CI with more than one reference configuration. This corresponds to a wavefunction

$$\Psi = \sum_R (C_R + \hat{C}_{1(R)} + \hat{C}_{2(R)})\psi_R \tag{1.155}$$

where the index $R$ runs over all the reference configurations. The latter are chosen in such a way that the sum of their squared amplitudes is sufficiently close to unity.

This still gives rise to an expansion too large to be treated (that is to say, at the time when this method was developed). Therefore a further configuration selection was built in: the energy change by inclusion of a certain configuration was estimated by second-order perturbation theory (see Section 1.5.4). If it is greater than a given threshold $T$ (e.g. 10 microhartrees), the configuration was retained, otherwise it is discarded. By running MRD-CIs with varying selection thresholds it is possible to perform an extrapolation to $T = 0$ [Bue75].

Through the choice of the references, the MRD-CI method effectively includes the most important higher excitations. This has two advantages: (a) the size- consistency problem is alleviated, though not remedied; (b) the effect of connected higher excitations is partially accounted for.

One generally successful practical application of MRD-CI is the computation of electronic transition energies (see e.g. [Bue83] for a review). Another is the evaluation of diatomic potential curves: however, MRD-CI curves tend to be 'noisy' and are thus unsuitable for Dunham analyses (Section 1.12.4). For reaction energies, a size consistency correction must still be applied, with the additional complication that such formulas have no firm theoretical ground for multireference calculations, and are more or less empirical [Blo83]. Furthermore, as already said, connected higher excitations are only partially accounted for: these are especially important in multiply-bonded molecules [Heh86a].

### 1.4.2 Multiconfigurational self-consistent field theory (MCSCF) and complete active space SCF (CASSCF)

From a variational point of view, a limited CI expansion is optimal in the configuration amplitudes but not in the orbitals, because these have been optimized for the Hartree-Fock case. One may also consider a wavefunction in which orbitals and configuration amplitudes are optimized simultaneously: this is called an *MCSCF* wavefunction [Wah77]. MCSCF has not been used in the present work, but is again briefly described here in relation to literature values[21].

An MCSCF problem has many, many more unknowns than the corresponding CI problem, and is thus computationally much more demanding. Therefore, only relatively small expansions can be treated, which introduces an annoying empirism in MCSCF results, namely the choice of the configurations.

One possible choice is to include all configurations that are involved in the breaking of a bond one is interested in. For the evaluation of a dissociation energy, this generally involves all possible excited determinants within the valence shell. Such a wavefunction is said to be of the CASSCF (complete active space SCF) type; the expansion is usually denoted by quoting the number of active electrons and orbitals. (The CASSCF method has been developed by Roos and coworkers [Roo80]; an analogous concept called FORS (fully optimized reaction space) was suggested by Ruedenberg [Rue82]. A review of applications may be found in [Roo87]). For example, the $C_2$ molecule has eight valence electrons and eight valence orbitals; when all configurations that can be generated from these are included in the MCSCF expansion, the wavefunction is denoted as an 8/8 CASSCF. Another example: benzene has thirty valence electrons and as much valence orbitals. An MCSCF calculation involving all possible determinants from these (which

[21] Historical note: among the oldest published examples of MCSCF calculations the author could find was the 1939 work of Hartree *et al.* [Har39].

is next to impossible even with the most powerful computers currently available) would be termed a 30/30 CASSCF. If one is only interested in the carbon-carbon bonds, and not in the carbon-hydrogen bonds, one could eliminate the six lowest valence orbitals (corresponding to the carbon-hydrogen $\sigma$ bonds) and the corresponding virtuals, and retain an 18/18 CASSCF. Finally, if only the $\pi$ bonds are of interest, then only the six inner orbitals (three $\pi$ and three $\pi^*$) would form the active space, reducing the problem to a 6/6 CASSCF. While using anything less than the full valence active space may entail serious problems, this serves to illustrate the philosophy behind CASSCF.

Although CASSCF is not size-consistent, strictly speaking, evaluation of dissociation energies is technically possible. The usual procedure is to perform a CASSCF both on the molecule, and on the fragments at large distances.

### 1.4.3 Qualitative partitioning of types of electron correlation

The following terms are often encountered in discussions of electron correlation effects, and are thus briefly explained here.

| | |
|---|---|
| **Fermi correlation** | Repulsion between electrons of like spin; the statistical probability to find them at the same spot should be zero. It is accounted for at the Hartree-Fock level through the exchange integrals. |
| **Near-degeneracy** | Correlation effects caused by the existence of excited states close to the ground state in energy. Also sometimes termed nondynamical correlation. |
| **Dynamical correlation** | Difference between total and near-degeneracy correlation energies. |
| **Internal correlation** | The type of correlation accounted for in a full- valence CASSCF. |
| **External correlation** | The part of the dynamical correlation not directly associated with bond making and breaking. |
| **Core correlation** | Dynamical correlation involving excitations from at least one occupied non-valence orbital. Sometimes partitioned in core-core and core-valence effects: the former involve excitations from core orbitals alone, the latter from both core and valence orbitals. |

Most of these terms were introduced in the pioneering work of Sinanoğlu and coworkers [Sin69].

### 1.4.4 The NASA Ames MRCI procedure

The acronym differs from MRD-CI only by the omission of a single 'D', but the method itself has little more in common with it. The philosophy behind the method, especially the use of CASSCF orbitals for the references, appears to have been put forward first by Taylor [Tay81]. Countless applications have since been made by the NASA Ames group (see [Bau90a] for a recent review).

To generate the reference space, a full CASSCF is first performed. If possible, the CASSCF wavefunction is used as the reference to a CISD calculation in its entirety; such a wavefunction is sometimes called a second order CI (SOCI). Otherwise, all CASSCF configurations whose CAS amplitude exceeds (in absolute value) a given threshold are included in the reference space. No further selection of CI configurations is performed. The level of theory is e.g denoted MRCI(0.05) for a reference selection threshold of 0.05. Usually a succession of thresholds (like MRCI(0.05), MRCI(0.025), and MRCI(0.01)) is performed to assure that the results converge to the SOCI (or MRCI(0.0)) limit. To correct for size-consistency errors, a multireference analog [Blo83] of the Davidson correction is usually applied. With a sufficiently large reference space, this does no longer result in an appreciable error.

Comparisons with full CI calculations have shown that such calculations, with a sufficiently small threshold, approach the full basis set correlation energy. Other advantages are that both internal and external correlation are described well, no empirism is involved in the selection of references, and that the method will happily handle even extreme near-degeneracy effects. Its principal disadvantage is the enormous computational cost involved.

## 1.5 Many-body perturbation theory

The oldest mention of this type of electron correlation treatment is the classic paper by Møller and Plesset [Mol34], who outlined the general theory; practical applications to quantum chemistry were fairly late. A good review of early MBPT work has been given by Kelly [Kel69]. More recent reviews of MBPT application include the combined MBPT/coupled cluster review of Bartlett [Bar81b], and several chapters of the book by the Pople group [Heh86a]. Much of the widespread practical application that MBPT currently gets is due to the work and the authority of these authors, the very cost-effective character, as well as through the easy availability of their GAUSSIAN program series, that include MBPT implementations from GAUSSIAN 80 onwards.

### 1.5.1 General background

It is well known that the Hartree-Fock wavefunction is *not* an eigenfunction of the full Hamiltonian. Now does there exist an approximate Hamiltonian of which it is an eigenfunction? The answer is positive. The one-electron functions $\phi_i$ in the Slater determinant $\psi_0$ are eigenfunctions of the corresponding Fock operator $\hat{F}_i$ with eigenvalue $\epsilon_i$, which is of course the molecular orbital energy. Consequently, $\psi_0$ is an eigenfunction of the sum over all the Fock operators, with the sum of all the orbital energies as an eigenfunction:

$$(\sum_i \hat{F}_i)\psi_0 = (\sum_i \epsilon_i)\psi_0 \tag{1.156}$$

Note that the sum of the orbital energies is not equal to the Hartree-Fock energy, which is $E_{\mathrm{HF}} = \sum_i (\epsilon_i + \epsilon_i^0)$, with $\epsilon_i^0$ representing the eigenvalue of the one-electron operator for $\phi_i$.

We could now consider $\sum_i \hat{F}_i$ as the zero-order Hamiltonian, and $\hat{V} \equiv \hat{H} - \sum_i \hat{F}_i$ as a perturbation, which we treat in the basis of $\psi_0$ and all possible excited determinants therefrom. The zero-order wavefunction is $\psi_0$, the zero-order energy $\sum_i \epsilon_i$. We have thus all the ingredients for Rayleigh-Schrödinger perturbation theory.

The first-order correction to the energy is none other than

$$E_1 = \langle \psi_0 | \hat{V} | \psi_0 \rangle = E_{\mathrm{HF}} - E_0 \tag{1.157}$$

whereas the first-order correction to the wave function is given by

$$\psi_1 = \sum_{i>j,a>b} a_{ijab}^{(1)} = \frac{1}{4} \sum_{ij,ab} a_{ijab}^{(1)} \tag{1.158}$$

$$a_{ijab}^{(1)} = \frac{\langle ij||ab \rangle}{\epsilon_a + \epsilon_b - \epsilon_i - \epsilon_j} \tag{1.159}$$

The denominator of the last expression appears very often in MBPT, and will henceforth be abbreviated by $D_{ijab}$.

So the Hartree-Fock energy is correct to first order in MBPT, but the wavefunction is not. (The Hellmann-Feynman theorem [Hel37] in derivative evaluation is a simple corollary of the latter.) Also, the first-order wavefunction does not contain single excitations, which is a 'nonobvious' MBPT formulation of the Brillouin theorem [Bri34].

The second-order correction to the energy is still found relatively easily by 'sandwiching' $\hat{V}$ between zero- and first-order wavefunctions.

$$E_2 = \langle \psi_0 | \hat{V} | \psi_1 \rangle = \sum_{i>j,a>b} \langle ij||ab \rangle a_{ijab}^{(1)} = \sum_{i>j,a>b} \frac{|\langle ij||ab \rangle|^2}{D_{ijab}} = \frac{1}{4} \sum_{ijab} \frac{|\langle ij||ab \rangle|^2}{D_{ijab}} \tag{1.160}$$

This defines the most cost-effective electron correlation treatment currently around, second-order Møller-Plesset theory (abbreviated MP2 or MBPT(2), depending on the authors). It requires no more than a partial integral transformation and a simple summation over these integrals. The integral transform step is rate-determining, leading to the development of 'in-core' algorithms that avoid the separate transformation.

Given its simplicity, MP2 often recovers a surprisingly high percentage of the basis set correlation energy [Bin75b]; is sometimes even overshoots it! Furthermore, as will be seen below, it is rigorously size-extensive. This encouraged further development of MBPT methods.

The algebra for higher orders of perturbation theory becomes a bit complicated, besides introducing various pitfalls. We shall therefore proceed to introduce a commonly used technique for many-body perturbation theory.

### 1.5.2 Diagrammatic perturbation theory

This technique sprung from the unique mind of Richard P. Feynman, who developed it as a 'shortcut' in the course of his work on quantum electrodynamics [Fey48]. As discussed in his Nobel lecture [Fey66], he had at no point a 'proof' in closed form for the validity of his procedure, let alone a derivation; he only "did know, from fooling around, that everything was in fact equivalent to regular electrodynamics" [Fey66].

For the application of Feynman diagrams to the electron correlation problem, some specialized versions of Feynman's diagrammatic notation have been developed including Hugenholtz diagrams [Hug57], Goldstone diagrams [Gol57], and Brandow or antisymmetrized Goldstone diagrams [Bra67]. The latter are particularly convenient for our purpose, as they translate directly into antisymmetrized two-electron integrals.

The notational convention for Hugenholtz diagrams is the following:

- A perturbation $\hat{V}$ is denoted by a dot. The number of dots in a diagram is therefore equivalent to its order in MBPT.
- The dots are (for convenience and by convention) placed on an imaginary vertical line[22].
- An imaginary horizontal line going through one of the dots is called a vertex.
- A solid line corresponds to a function $\phi_i$.
- Every solid line has an up-going or down-going arrow; an up-going arrow denoted a virtual orbital (the line is then called a 'particle line'), a down-going arrow denotes an occupied orbital (the line is then called a 'hole line').
- A dot with its associated in-and outgoing lines denotes a matrix element of $\hat{V}$ between $\psi_0$ and an excited determinant with occupied orbitals corresponding to the attached hole lines replaced by virtuals corresponding to the attached particle lines.

[22] In the writings of Paldus and coworkers, they are generally placed on a horizontal line. Their variant of the Hugenholtz diagrams is identical to that discussed here, except for a rotation by 90 degrees.

- Every dot has exactly two incoming, and exactly two outgoing lines.
- Every line is connected at both ends.
- An imaginary horizontal line between two vertices must cross at least one hole and one particle line. The excitation level between these two vertices is half the number of lines crossed.
- A line may not start and end at the same point.

The last item is actually a 'nonobvious' consequence of the Brillouin theorem, as such a line would correspond to a matrix element between states that only differ by a single excitation. The prescription for translating Hugenholtz diagrams into algebraic expressions is as follows:

- Label each hole line by unique occupied orbital indices $ijk\ldots$, and each particle line by unique virtual orbital indices $abc\ldots$.
- Set the algebraic expression to an initial value of unity.
- For each dot, multiply the numerator by a factor $\langle \mathrm{in}_1\mathrm{in}_2||\mathrm{out}_1\mathrm{out}_2\rangle$. The labeling 1 and 2 is arbitrary.
- For each adjacent pair of vertices, multiply the denominator by an MBPT denominator constructed as follows:
  - Start it out at zero.
  - For each particle line, add $\epsilon_a$ for the virtual orbital index $a$ that corresponds to it.
  - For each hole line, subtract $\epsilon_i$ for the occupied orbital index $i$ that corresponds to it.
- Sum the expression over all hole and particle indices, without index restrictions, or ignore the next point if they are preferred.
- Divide the expression by $2^k$, where $k$ is the number of equivalent line pairs in the diagram. A pair of lines is equivalent if both lines start and end at the same dots and both go into the same direction.
- Multiply the expression by $(-1)^h$, where $h$ is the number of hole lines (occupied orbital indices).
- Finally, multiply the expression by $(-1)^l$, where $l$ is the number of closed loops in the diagram.

Figure 1.1: Some Hugenholtz diagrams and their algebraic translation.

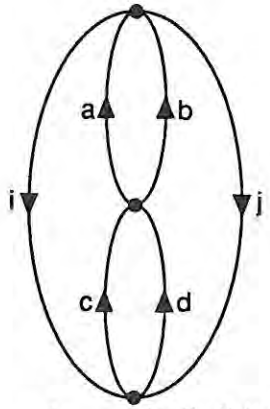


$$= \frac{1}{8} \sum_{ijabcd} \frac{\langle ij||ab\rangle\langle ab||cd\rangle\langle cd||ij\rangle}{D_{ijab}D_{ijcd}}$$

$i \rightarrow a : a \rightarrow c : c \rightarrow i$

$j \rightarrow b : b \rightarrow d : d \rightarrow j$

$k = 3; h = 2; l = 2$

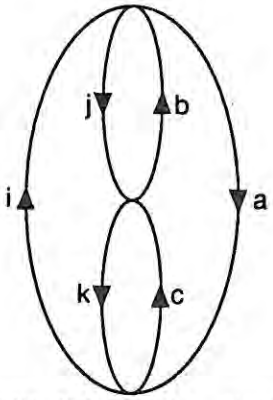


$$= \sum_{ijkabc} \frac{\langle ij||ab\rangle\langle kb||cj\rangle\langle ac||ik\rangle}{D_{ijab}D_{ikac}}$$

$i \rightarrow a : a \rightarrow i$

$j \rightarrow b : b \rightarrow j$

$k \rightarrow c : c \rightarrow k$

$k = 3; h = 2; l = 2$

The number of closed loops is the only thing that cannot be determined by inspection from the diagram. It is a consequence of the fact that the order in which the indices for a given antisymmetrized integral are written is not prescribed. (Yet all possible choices should give algebraically equivalent expressions; the 'closed loop' determination ensures this.) What one does is simply write out the entire numerator, select a particular index, and follow it through the matrix elements $\langle 12||34\rangle$ using the rules $1 \rightarrow 3$ and $2 \rightarrow 4$ until one reaches the same label. The number of times this has to be done before all the labels are exhausted is $l$.

Figure 1.1 shows a few examples of Hugenholtz diagrams and the algebraic expressions corresponding to them. The 'closed loop' procedure is illustrated there too.

The procedure to find the MBPT correction to the energy at any given order is then to set down the right number of dots, generate all possible topologically distinct Hugenholtz diagrams, write down the algebraic expressions, and add them all up. Two diagrams are topologically equivalent if the in-and outgoing lines match for each and every dot, i.e. there is at least one way to distort the lines as to make the diagrams look identical.

The Brandow or antisymmetrized Goldstone diagrams are best looked upon as Hugenholtz diagrams that are 'pulled apart':

- A perturbation $\hat{V}$ is denoted by two dots connected by an interaction line or vertex. The number of vertices is equal to the order of the diagram.

- An interaction line is denoted by a dotted horizontal line.

- Every dot has exactly one incoming, and one outgoing line.
- The remainder of the definition is identical to that for the Hugenholtz diagrams.

The procedure to generate the algebraic expressions is analogous:

- Label each hole line by unique occupied orbital indices $ijk\ldots$, and each particle line by unique virtual orbital indices $abc\ldots$.
- Set the algebraic expression to an initial value of unity.
- For each vertex, multiply the numerator by a factor $\langle \mathrm{in}_{\mathrm{left}}\mathrm{in}_{\mathrm{right}}||\mathrm{out}_{\mathrm{left}}\mathrm{out}_{\mathrm{right}}\rangle$.
- For each adjacent pair of vertices, multiply the denominator by an MBPT denominator constructed as for the Hugenholtz diagrams.
- Sum the expression over all hole and particle indices, without index restrictions, or ignore the next point if they are preferred.
- Divide the expression by $2^k$, where $k$ is the number of equivalent line pairs in the diagram. A pair of line is equivalent if both lines start and end at the same dots and both go into the same direction.
- Multiply the expression by $(-1)^h$, where $h$ is the number of hole lines (occupied orbital indices).
- Finally, multiply the expression by $(-1)^l$, where $l$ is the number of closed loops in the diagram. These are now seen as solid lines forming a closed loop.

The entire algebraic expression can now be derived from the diagram, which is a distinct advantage in complicated diagrammatic MBPT calculations. The procedure to generate all the terms at a given order of MBPT is identical to that for the Hugenholtz diagrams.

Figure 1.2 shows the Brandow diagrams that correspond to the Hugenholtz diagrams of Figure 1.1, to illustrate the relationship between them as well as their evaluation.

Figure 1.2: Antisymmetrized Goldstone diagrams corresponding to the Hugenholtz diagrams in Figure 1.1.

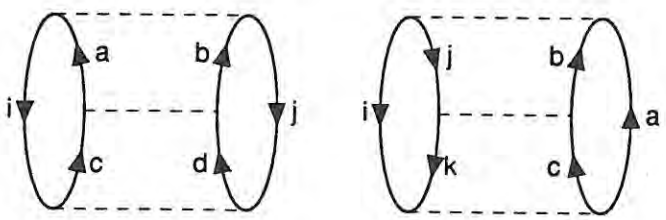

Figure 1.3: Examples of connected, linked disconnected, and unlinked diagrams at fourth order.

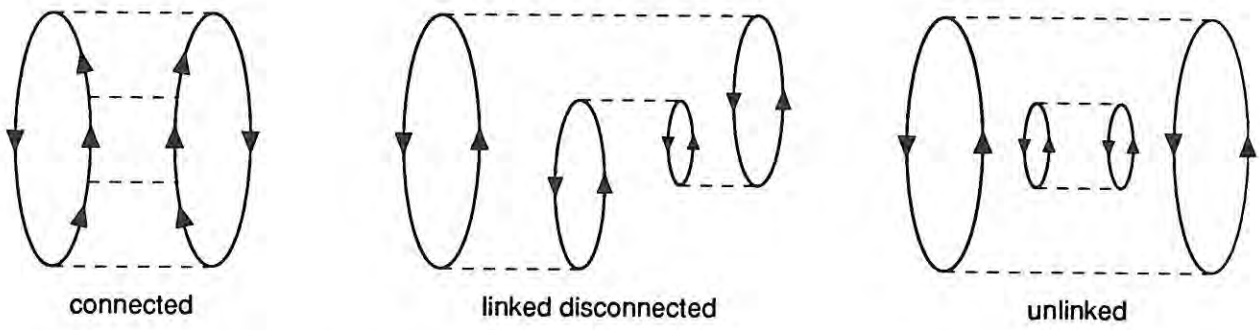


In very complicated calculations, so-called 'unlabeled Hugenholtz' and 'unlabeled Brandow' diagrams are sometimes (e.g. [Kuc86]) introduced. These are simply regular diagrams without arrows; they correspond each to a number of diagrams whose expressions have the same algebraic structure, except for the occupied or virtual nature of the indices. They constitute a very convenient shorthand in diagrammatic calculations involving factorization of diagrams, as only the algebraic structure then matters.

### 1.5.3 Linked and unlinked diagrams: the linked cluster theorem.

A diagram is said to be *linked* if the Hugenholtz diagram is in one piece, i.e. one continuous uninterrupted solid line connects the dots. Diagrams that can be 'taken apart' in two or more disjoint pieces are said to be *unlinked.*

If at any intervertex excitation level the upper or the lower part of the diagram can be taken apart into two or more pieces without breaking any hole, particle, or interaction lines, then the diagram is said to be disconnected; any diagram where this is not possible is said to be connected. An unlinked diagram is of necessity disconnected; a disconnected diagram may be linked, though. To illustrate these concepts, Figure 1.3 depicts a connected, a linked disconnected, and an unlinked diagram, all at fourth order.

Just as in the case of CI, the intermediate normalization introduces a so-called 'renormalization term' into the energy. Siegbahn [Sie78] showed that its exact expression in algebraic MBPT language is given by

$$E_{\mathrm{R}} = \Delta E \langle \psi' | \psi' \rangle \tag{1.161}$$

where $\psi' \equiv \Psi - \psi_0$. ($\Psi$ and $\psi_0$ represent the exact and Hartree-Fock wavefunctions, respectively). Expanding $\psi'$ in an MBPT series

$$\psi' = \psi^{(1)} + \psi^{(2)} + \ldots \tag{1.162}$$

we find that its lowest term is at fourth order [23]. Of course we have seen this term before when we were discussing the size-consistency of CI methods; it was exactly this one that is canceled by the 'unlinked clusters' in coupled cluster theory (Section 1.6).

For finite-order MBPT to be size-extensive, it is required that at any order in MBPT the renormalization term is canceled by unlinked cluster diagrams. One can easily see by trying that it is not possible to construct nonvanishing unlinked diagrams at second and third order for Hartree-Fock references (the only possibility at third order involves a circular line resulting in a factor that cancels because of Brillouin's theorem); size consistency is thus trivial up to and including third order. An explicit demonstration of cancellation at fourth order will be given in the discussion of MP4; it is also not very difficult to do this at fifth order.

It can be shown, through a fairly complicated proof which will not be reproduced here, that the cancellation is valid to all orders. This is one formulation [Rob75] of the famous 'linked cluster' theorem proved by Brueckner [Bru55] for the first few finite orders, and by Goldstone [Gol57] to infinite order. This means that both the renormalization and unlinked terms may be simultaneously ignored; therefore an often heard formulation of the linked cluster theorem is that only linked diagrams are allowed. (This definition is of course only correct if the renormalization term is ignored too.)

Precisely this, namely the exact cancellation of unlinked diagrams with the renormalization term, is the rigorous definition of size-extensivity.

There is an important corollary: not only is MBPT to any order size-extensive, but any method where only certain classes of diagrams are included at any specific order (e.g. where some excitation levels are neglected) is size-extensive too. This is important as it is sometimes very economical to do so at higher orders.

We will now discuss various finite orders of MBPT.

### 1.5.4 Second-order MBPT: MBPT-2 or MP2

There is only one antisymmetrized Goldstone diagram (AGD) possible at second order: it is given in Figure 1.4. The corresponding algebraic expression (now without index restrictions) is:

$$E^{(2)} = \frac{1}{4}\sum_{ijab}\frac{\langle ij||ab\rangle\langle ab||ij\rangle}{D_{ijab}} = \frac{1}{4}\sum_{ijab}\frac{|\langle ij||ab\rangle|^2}{D_{ijab}} \tag{1.163}$$

where $D_{ijab} \equiv \epsilon_a + \epsilon_b - \epsilon_i - \epsilon_j$.

This method has been implemented for RHF and UHF wavefunctions by Binkley and Pople [Bin75b]: as with all other MBPT (and CC, for that matter) methods, the extension to an ROHF wavefunction is by no means trivial. We will evaluate the computational cost for the UHF case.

[23] It is readily seen, that for a set of $L$ noninteracting systems this term will scale as $L^2$ rather than $L$; hence the violation of size extensivity (and consequently of size consistency).

Let $N$ denote the number of electrons, and $n$ the number of basis functions, then (1.163) requires only $O((n-N)^2N^2)$ (leading term $O(n^2)$) operations, and this only once. This is quite different from what we are used to in CI and coupled cluster (Section 1.6) methods, that scale at least as $O(n^6)$ per iteration. The cost of the integral transformation far exceeds that of the actual MP2; a partial index transformation where only the integrals of the $\langle ij||ab\rangle$ type are transformed will scale with leading term $O(Nn^4)$. [24]

If the transformed integrals have not been antisymmetrized yet, this must also be done: it is very convenient to combine antisymmetrization and computation of the MP2 energy in a single set of loops.

When $O(n^3)$ words of main memory are available, it is more efficient to combine the integral transformation and MP2 steps; to minimize I/O, the outer loop should be over occupied orbitals. This in-core MP2 method is implemented in the GAUSSIAN series as subprogram L903; for fast machines with small I/O bandwidths, like our VAXstation 3100, it is far to be preferred over regular MP2. We used this algorithm [Heh86b] repeatedly for various practical applications, and will therefore present it in pseudocode:

```
for all i do
    build ⟨iq|rs⟩ from file in O(n³) array;
    for all j do
        build ⟨ij|rs⟩ from O(n³) in O(n²) array;
        for all k do
            build ⟨ij|ks⟩ from O(n²) in O(n) array a⃗;
            build ⟨ij|sk⟩ from O(n²) in O(n) array b⃗;
            for all l do
                compute ⟨ij|kl⟩ from O(n) array a⃗;
                compute ⟨ij|lk⟩ from O(n) array b⃗;
                form ⟨ij||kl⟩ = ⟨ij|kl⟩ − ⟨ij|lk⟩;
                add contribution to E(2);
            end for;
        end for;
    end for;
end for;
```

This procedure scales as $O(Nn^4)$ in computer time, which is similar to the partial transformation alone. It however only requires $N$ read passes through the entire AO integral file, and no write passes at all. It is furthermore very suitable for vectorization,

[24] Only the first partial transformation goes as $n^4$; in the second one, only $Nn^3$ integrals have to be processed if the first step is done over an occupied orbital. In the third step, only $N^2n^2$ integrals have to be done, and finally only $N^2(N-n)n$ are left for the fourth step.

Figure 1.4: The second-order antisymmetrized Goldstone diagram.

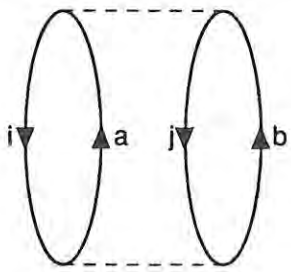


which is relevant to get the most out of a supercomputer version of the program. Replacing the $E^{(2)}$ add-in step by writing out the antisymmetrized integral, the algorithm can also be used for partial or complete integral transformations. For the latter, it will still require $O(n^5)$ operations like the conventional four-step algorithm, but only $O(n^3)$ core storage and no temporary disk storage, whereas the conventional four-step algorithm requires either $O(n^4)$ words of central memory or intermediate disk space. $n$ read passes through the integral file have to be made; the final integrals are written out once.

If $O(n^4)$ words of memory are available (which is no longer very uncommon), then the 'cascade' in the above algorithm may be extended by one outer loop; the original integrals then only have to be read once and for all.

### 1.5.5 Third-order MBPT: MP3 or MBPT(3)

The three AGDs that can be constructed at third order are given in Figure 1.5. They correspond to the following terms:

$$E^{(3)} = \frac{1}{8}\sum_{ij,abcd}\frac{\langle ij||ab\rangle\langle ab||cd\rangle\langle cd||ij\rangle}{D_{ijab}D_{ijcd}} \quad \text{(A)} \tag{1.164}$$

$$+\frac{1}{8}\sum_{ijkl,ab}\frac{\langle ab||ij\rangle\langle ij||kl\rangle\langle kl||ab\rangle}{D_{ijab}D_{klab}} \quad \text{(B)} \tag{1.165}$$

$$+\sum_{ijk,abc}\frac{\langle ij||ab\rangle\langle ic||ak\rangle\langle kj||cb\rangle}{D_{ijab}D_{kjcb}} \quad \text{(C)} \tag{1.166}$$

Some extra transformed integrals are now required, namely those of the $\langle ij||kl\rangle$, $\langle ab||cd\rangle$, and $\langle ia||jb\rangle$ types, which is about the full complement. The three computational steps of the MP3 calculation itself scale as $O(N^2(n-N)^4)$, $O(N^3(n-N)^3)$, and $O(N^4(n-N)^2)$, respectively, which makes a leading term $O(n^4)$, still very cheap compared to the CI/CC situation.

A generally available MP3 implementation was first published by Pople *et al.* [Pop76]. Here they avoid the full integral transformation by rewriting the first diagram (which

Figure 1.5: Third-order antisymmetrized Goldstone diagrams for a Hartree-Fock reference state.

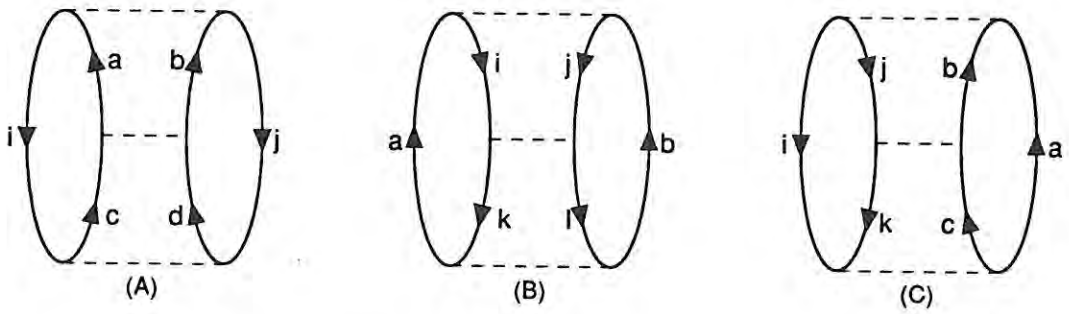


requires the large $\langle ab||cd\rangle$ set) in the following manner:

$$E^{(3)}(A) = \frac{1}{8} \sum_{ij,abcd} a^{(1)}_{ijab} a^{(1)}_{ijcd} \langle ab||cd\rangle \tag{1.167}$$

and then partially back-transforming $a^{(1)}$ to the AO basis

$$\tilde{a}^{(1)}_{ijrs} = \sum_{ab} a^{(1)}_{ijab} c_{ar} c_{bs} \tag{1.168}$$

which allows the first diagram to be written directly in terms of AO integrals as:

$$E^{(3)}(A) = \frac{1}{8} \sum_{ij,pqrs} \tilde{a}^{(1)}_{ijpq} \tilde{a}^{(1)}_{ijrs} \langle pq||rs\rangle \tag{1.169}$$

Then the first diagram requires only $O(n^4N^2)$ operations, whereas only the smaller sets of transformed integrals $\langle ij||kl\rangle$ and $\langle ia||jb\rangle$ must be generated beyond what was already necessary for MP2.

### 1.5.6 Fourth-order MBPT: MP4 or MBPT(4)

This is the first level at which other than double excitations begin to contribute. The only intervertex excitation level that matters is the middle, since the two outer levels are double anyway. The single, double, triple, and quadruple excitation AGDs are shown in Figures 1.6–1.9.

Figure 1.6: Single-excitation diagrams at fourth order for a Hartree-Fock reference state [Bar78, page 565].

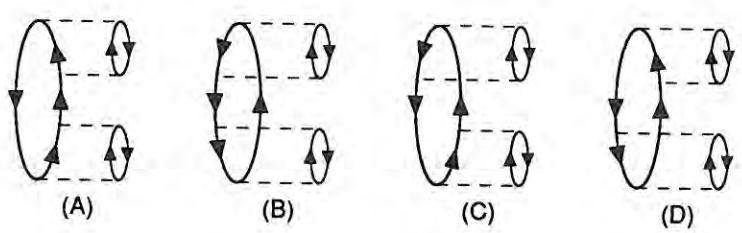

Figure 1.7: Double-excitation diagrams at fourth order for a Hartree-Fock reference state [Bar78, page 566].

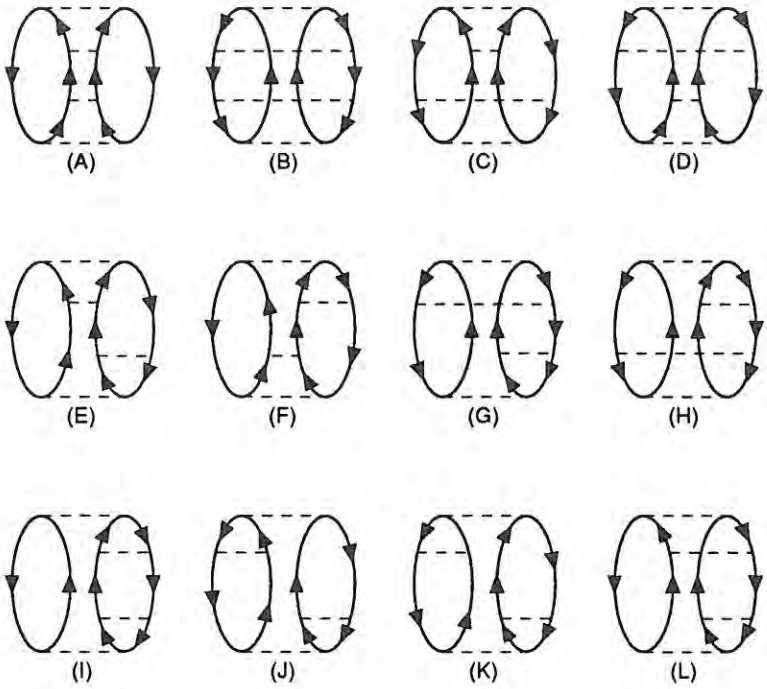


Figure 1.8: Triple-excitation diagrams at fourth order for a Hartree-Fock reference state [Bar78, page 567].

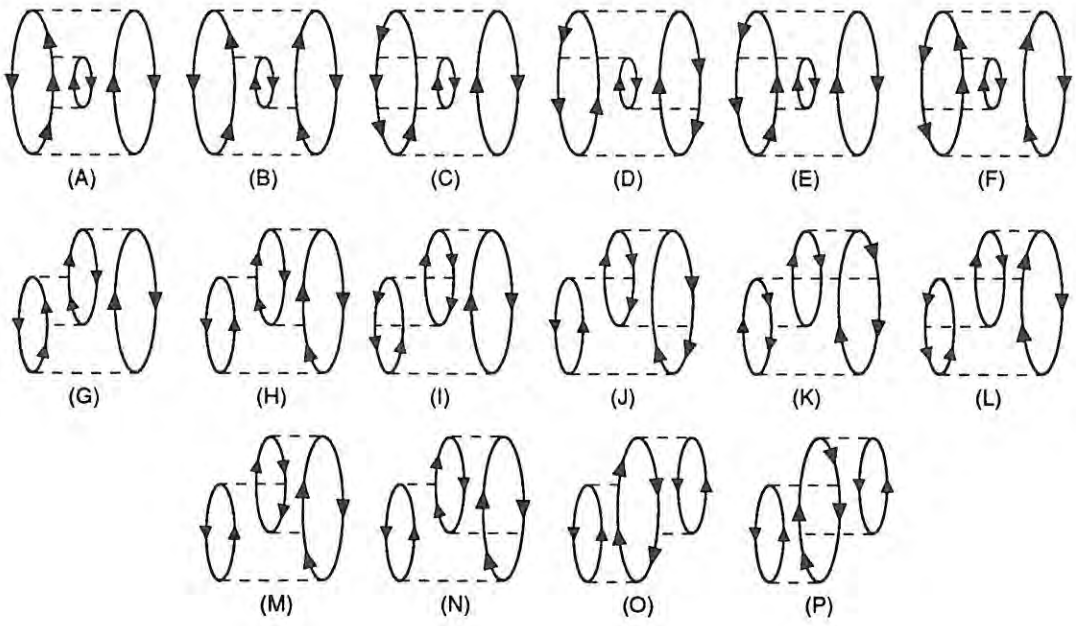

Figure 1.9: Quadruple-excitation diagrams at fourth order for a Hartree-Fock reference state [Bar78, page 568]. All diagrams are disconnected; the last two are unlinked.

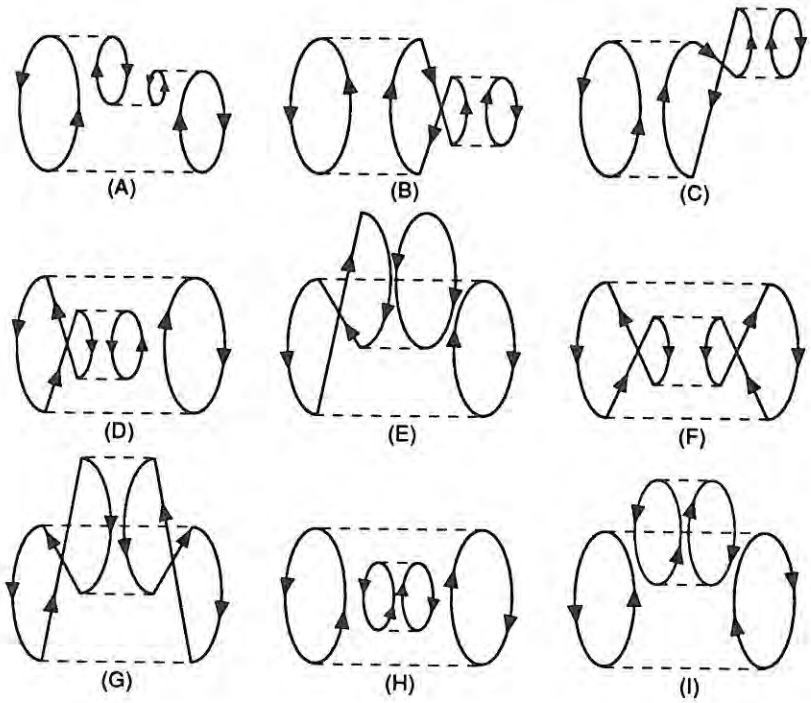


The doubles term is fairly easy to evaluate. An MP4 calculation where only the doubles term is included at fourth order is termed an MP4(D) or D-MBPT(4) calculation. It is identical with L-CCD to fourth order.

The quadruples diagrams in Figure 1.9 are easily seen to be all disconnected. The quadruples term deserves special mention, as it includes two unlinked diagrams (H) and (I). The latter correspond to the expressions:

$$E_{\mathrm{UL}}^{(4)} = \frac{1}{16} \sum_{ijkl,abcd} \frac{|\langle ij||ab\rangle|^2 |\langle kl||cd\rangle|^2}{D_{ijab} D_{ijklabcd} D_{ijab}} + \frac{1}{16} \sum_{ijkl,abcd} \frac{|\langle ij||ab\rangle|^2 |\langle kl||cd\rangle|^2}{D_{ijab} D_{ijklabcd} D_{klcd}} \tag{1.170}$$

Bringing the two sets of terms on common denominators, and realizing that $D_{ijabklcd} = D_{ijab} + D_{klcd}$, it follows that

$$\begin{aligned} E_{\mathrm{UL}}^{(4)} &= \frac{1}{16} \sum_{ijab,klcd} \frac{|\langle ij||ab\rangle|^2 |\langle kl||cd\rangle|^2}{D_{ijab}^2 D_{klcd}} = \frac{1}{16} \sum_{ij,ab} \frac{|\langle ij||ab\rangle|^2}{D_{ijab}} \sum_{abcd} \frac{|\langle kl||cd\rangle|^2}{D_{klcd}} \\ &= \langle \psi^{(1)} | \psi^{(1)} \rangle E^{(2)} \end{aligned} \tag{1.171}$$

But this cancels exactly with the renormalization term at fourth order $-E^{(2)}\langle \psi^{(1)} | \psi^{(1)} \rangle$. Both can thus be dropped from the expansion, leaving only the linked disconnected quadruples diagrams.

(This is perhaps the place to make a little parenthesis on the exclusion-principle violating (EPV) diagrams. These correspond to disconnected diagrams where two particle or hole lines in different 'pieces' of the diagram have a common index. However, it can

Figure 1.10: Example of cancellation of linked and unlinked EPV diagrams at fifth order [Pal75, page 193].

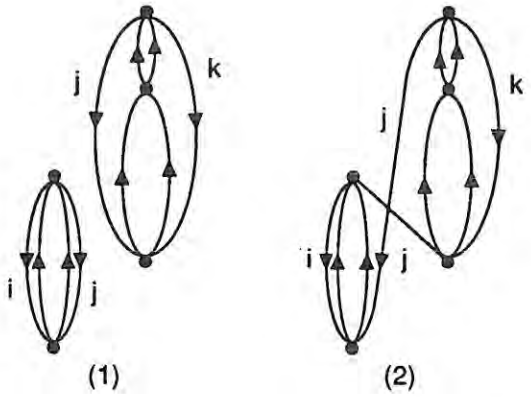


be shown that for any unlinked EPV diagram there exists a corresponding linked EPV diagram that exactly cancels it. To illustrate this, consider the two fifth-order diagrams depicted in Figure 1.10, where an index $j$ occurs twice. The linked diagram can be made from the unlinked one by detaching the two $j$ lines from their endpoints and swapping them. Numerator and denominator for the two are the same, but whereas the unlinked EPV diagram is negative, the linked EPV diagram has one fermion loop less and becomes thus positive. A similar argument may be made at higher orders. In L-CCD, the unlinked EPV diagrams are included, but not the linked ones: hence the fact that L-CCD energies are usually below CCD energies, and often even below full CI. The diagrammatic argument for cancellation was first presented by Paldus and Čížek [Pal75, Appendix F]).

Inclusion of both the doubles and the quadruples terms results in the MP4(DQ) or DQ-MBPT(4) method, which is identical with CCD to fourth order. Implementation is a bit trickier than for the MP4(D) method, but in either case the additional computer time over MP3 is small.

The next step would be to include the single excitations, which require a negligible extra evaluation time. This results in the MP4(SDQ) or SDQ-MBPT(4) method, identical to fourth order with CCSD. The first generally available MP4(SDQ) implementation was by Krishnan and Pople [Kri78] [25].

For molecules without low-lying excited states, MP4(DQ) results are very close to CCD; if no heavy spin contamination is present, MP4(SDQ) results are also close to CCSD. Unfortunately some account of triple excitations is required for molecules with multiple bonds.

[25] Note that R. Krishnan and K. Raghavachari are one and the same person: up to and including 1980, the former form appears on the byline, from 1981 onwards the latter. This bit of trivia just to eliminate some possible confusion.

The problem is, that the most efficient algorithm to evaluate the triples diagrams still scales as $O(n^4N^3)$. It is the dominant step in a full MP4 calculation (also denoted MP4(SDTQ) or SDTQ-MBPT(4)), but practical applications showed that it normally cannot be dispensed with, even for such simple molecules as hydrides. For a molecule like $N_2$, the contribution is of course very important.

The first generally available full MP4 algorithm has been published by Krishnan *et al.* [Kri80].

In well-behaved cases, MP4 recovers a very high percentage of the basis set correlation energy, and is thus the most cost-effective general purpose electron correlation treatment around. In our experience, it takes about one-fifth the time of a QCISD(T) calculation for large cases.

MP4 still has some important deficiencies though, making it useless in some situations:

- The triple excitation contribution is generally overestimated, sometimes grossly.
- The MP series converges very slowly in the presence of low-lying excited states.
- The MP series also converges slowly in cases with spin contamination.

The latter two points have been studied in depth by Handy *et al.* [Han85], who projected out MP energies up to order 48 from a full CI wavefunction[26], and by Gill *et al.* [Gil88] who found that heavy spin contamination in UHF states was precisely caused by the presence of low-lying excited states, and that the two problems are thus one and the same as far as MP is concerned. The problem there is caused by the fact that nearby states will give rise to small MBPT denominators, and thus high MP amplitudes for these states, whose successive contributions will not have 'died out' at fourth order.

The fact that low-lying excited states cause spin contamination is a consequence of the variational and spin-unrestricted nature of the UHF wavefunction: if there is a low-lying excited state of a higher multiplicity, then the total energy may be lowered by allowing the extra determinant (or several of them) to 'mix in'. Especially catastrophic results were found in this work (e.g. for the $^2B_2$ state of $C_3^+$ [Mar90c], Sections 3.9 and 3.10)

[26] This can be done in the following manner [Han85]: Let $\hat{H}_0 \equiv \sum_i \hat{F}_i$ and $E_1 \equiv E_{\mathrm{HF}} - E_0$, then standard Rayleigh-Schrödinger perturbation theory leads to the equation

$$(\hat{H}_0 - E_0)\psi_k + (\hat{W} - E_1)\psi_{k-1} - \sum_{l=2}^{k} E_l \psi_{k-l} = 0$$

If the direct CI update is constructed from the previous MBPT wavefunction, i.e. $\sigma_k = \mathsf{H}\psi_{k-1}$, then $E_k$ and $\psi_k$ may be obtained as

$$\begin{aligned} E_k &= \langle \psi_0 | \sigma_k \rangle \\ \psi_k &= (\mathsf{H}_0 - E_0)^{-1} \left[ \sum_{l=1}^{k} E_k \psi_{k-l} + \mathsf{H}_0 \psi_{k-1} - \sigma_k \right] \end{aligned}$$

when the excited state's HF energy was below that of the ground state (which may well happen because state orderings of nearby states are often incorrect at the Hartree-Fock level). A comparable problem exists when low-lying excited states of a different symmetry exist, and symmetry is not enforced on the HF wavefunction: then the converged SCF orbitals often do not exactly belong to specific irreducible representations of the point group. Occasionally the latter problem can become even more severe, with the total wavefunction no longer having the full symmetry of the molecular point group (so-called symmetry breaking).

## 1.6 Coupled cluster methods

If a single class of emerging electron correlation methods has a chance of becoming the standard electron correlation treatment, it is coupled cluster theory. An excellent review [Bar89a] has been written by Bartlett, currently the leading proponent of CC theory; older reviews include [Ciz80, Bar81a, Bar81b].

### 1.6.1 General background and the CCD and LCCD methods

In the coupled cluster methods, which originated in nuclear physics [Coe58] and were first brought up in a quantum chemical context by Čížek [Ciz66], exact size consistency is guaranteed by the form of the wavefunction. We will illustrate the philosophy involved by the example of $n$ noninteracting monomers.

Let us first look again at the situation with two noninteracting monomers A and B. The CID wavefunctions for the two will be $(1+\hat{C}_2(A))\psi_0$ and $(1+\hat{C}_2(B))\psi_0$, respectively. For the dimer, the equation

$$\hat{C}_2 = \hat{C}_2(A) + \hat{C}_2(B) \tag{1.172}$$

will hold. Now consider the following:

$$\hat{C}_2^2 = \hat{C}_2^2(A) + \hat{C}_2^2(B) + 2\hat{C}_2(A)\hat{C}_2(B) \tag{1.173}$$

The last term is, except for a factor of two, the term that would be needed to restore size-consistency in the CID case. This suggests a wavefunction of the form

$$(1 + \hat{C}_2 + \hat{C}_2^2/2)\psi_0 \tag{1.174}$$

A new, but smaller, error is however introduced because cross-products involving $\hat{C}_2^2(A)$ and/or $\hat{C}_2^2(B)$ are absent, starting at disconnected sextuple excitations. Furthermore, the wavefunction will still break down in the case of three monomers A, B, and C. It is however easily seen that both problems are remedied by extending the wavefunction to

$$(1 + \hat{C}_2 + \hat{C}_2^2/2 + \hat{C}_2^3/6)\psi_0 \tag{1.175}$$

This, however, will again break down for four monomers, and lacks some disconnected octuple excitations. The next term will be $\hat{C}_2^4/24$, then $\hat{C}_2^5/120$, and generally $\hat{C}_2^n/n!$. Extending the summation to infinity, we obtain a wavefunction

$$(\sum_{n=0}^{\infty} \frac{\hat{C}_2^n}{n!})\psi_0 \equiv [\exp(\hat{C}_2)]\psi_0 \tag{1.176}$$

where no cross-terms are left out, and which is exactly size-consistent (actually: size-extensive) for any number of noninteracting monomers. This form of the wavefunction is called the *exponential ansatz*, the argument of the exponential a *cluster operator*. To distinguish them henceforth from the excitation operators $\hat{C}_n$, the cluster operators will be denoted $\hat{T}_n$, which is by the way the standard notation for them. The *cluster amplitudes* in them are denoted by a lowercase letter $t$:

$$\hat{T}_1 = \sum_{i,a} t_i^a \hat{a}_a^+ \hat{a}_i \tag{1.177}$$

$$\hat{T}_2 = \sum_{i>j,a>b} t_{ij}^{ab} \hat{a}_a^+ \hat{a}_b^+ \hat{a}_i \hat{a}_j \tag{1.178}$$

$$\hat{T}_3 = \sum_{i>j>k,a>b>c} t_{ijk}^{abc} \hat{a}_a^+ \hat{a}_b^+ \hat{a}_c^+ \hat{a}_i \hat{a}_j \hat{a}_k \tag{1.179}$$

$$\hat{T}_4 = \sum_{i>j>k>l,a>b>c>d} t_{ijkk}^{abcd} \hat{a}_a^+ \hat{a}_b^+ \hat{a}_c^+ \hat{a}_d^+ \hat{a}_i \hat{a}_j \hat{a}_k \hat{a}_l \tag{1.180}$$

...

Now could we build a computational method on such a wavefunction? Yes we can. Consider the ansatz $\exp(\hat{T}_2)$. This gives rise to the following equations:

$$E_{\mathrm{CCD}} = \langle \psi_0 | H' | (1 + \hat{T}_2 + \ldots)\psi_0 \rangle \tag{1.181}$$

$$E_{\mathrm{CCD}} t_{ij}^{ab} = \langle \psi_{ij}^{ab} | H' | (1 + \hat{T}_2 + \hat{T}_2^2/2 + \ldots)\psi_0 \rangle \tag{1.182}$$

Projecting out the quadruples, sextuples, etc. gives rise to redundant equations for the powers of the $\hat{T}_2$ amplitudes. After elimination of the terms that give rise to vanishing interaction integrals, one obtains the following coupled set of quadratic equations:

$$E_{\mathrm{CCD}} = \langle \psi_0 | H' | (1 + \hat{T}_2)\psi_0 \rangle \tag{1.183}$$

$$E_{\mathrm{CCD}} t_{ij}^{ab} = \langle \psi_{ij}^{ab} | H' | (1 + \hat{T}_2 + \hat{T}_2^2/2)\psi_0 \rangle \tag{1.184}$$

which define the CCD (coupled cluster with all doubles) method. The quadratic equations here are not much more difficult to solve iteratively than the linear equations in the iterative formulation of CID. The computational cost is therefore comparable, except that, in our experience, CCD usually converges more slowly than CID.

Let us now take a closer look at the form of $\hat{T}_2^2/2$, which is not as simple as it looks. The 'catch' is, that more than one product of cluster amplitudes can lead to any given quadruply excited configuration $\psi_{ijkl}^{abcd}$; any permutation of the four 'occupied' indices and any of the four 'virtual' indices is allowed. This leads to 18 different products in all

[Sza89, chapter 5](with an odd number of permutations resulting in a sign change): the sum of all possible permutations is denoted by $t_{ij}^{ab} * t_{kl}^{cd}$

$$\begin{aligned} t_{ij}^{ab} * t_{kl}^{cd} &= t_{ij}^{ab}t_{kl}^{cd} - t_{ik}^{ab}t_{jl}^{cd} + t_{il}^{ab}t_{jk}^{cd} - t_{ij}^{ac}t_{kl}^{bd} + t_{ik}^{ac}t_{jl}^{bd} - t_{il}^{ac}t_{jk}^{bd} \\ &\quad + t_{ij}^{ad}t_{kl}^{bc} - t_{ij}^{ac}t_{kl}^{bd} + t_{ij}^{ad}t_{kl}^{bc} + t_{ij}^{cd}t_{kl}^{ab} - t_{ik}^{cd}t_{jl}^{ab} + t_{il}^{cd}t_{jk}^{ab} \\ &\quad - t_{ij}^{bd}t_{kl}^{ac} + t_{ik}^{bd}t_{jl}^{ac} - t_{il}^{bd}t_{jk}^{ac} + t_{ij}^{bc}t_{kl}^{ad} - t_{ik}^{bc}t_{jl}^{ad} + t_{il}^{bc}t_{jk}^{ad} \\ &\equiv t_{ij}^{ab}t_{kl}^{cd} - \langle t_{ij}^{ab} * t_{kl}^{cd} \rangle \end{aligned} \tag{1.185}$$

What would happen if we were to neglect the permutation terms? This is best seen by writing out the matrix elements involved:

$$\begin{aligned} \sum_{k>l,c>d,m>n,e>f} \langle \psi_{ij}^{ab} | H' | \psi_{klmn}^{cdef} \rangle &= \sum_{k>l,c>d} \langle \psi_{ij}^{ab} | H' | \psi_{klij}^{cdab} \rangle + \sum_{m>n,e>f} \langle \psi_{ij}^{ab} | H' | \psi_{ijmn}^{abef} \rangle \\ &= 2 \sum_{k>l,c>d} \langle \psi_{ij}^{ab} | H' | \psi_{klij}^{cdab} \rangle \\ &= 2 \sum_{k>l,c>d} \langle \psi_0 | H' | \psi_{kl}^{cd} \rangle \end{aligned} \tag{1.186}$$

Substituting this in the amplitude equation (1.184), the factor of two in the numerator cancels with that in the denominator and we obtain

$$\langle \psi_{ij}^{ab} | H' | (1 + \hat{T}_2) \psi_0 \rangle + E_{\mathrm{LCCD}} \langle \psi_{ij}^{ab} | \psi_0 \rangle = E_{\mathrm{LCCD}} t_{ij}^{ab} \tag{1.187}$$

$$\langle \psi_{ij}^{ab} | H' | (1 + \hat{T}_2) \psi_0 \rangle = 0 \tag{1.188}$$

with the energy still given by

$$E_{\mathrm{LCCD}} = \langle \psi_0 | H' | \hat{T}_2 \psi_0 \rangle \tag{1.189}$$

The acronym LCCD stands for *linearized coupled cluster with all doubles.* This method is still size-extensive, but is no longer exact for two electrons. It is also no longer iterative: actually it is equivalent with the first CID iteration in the iterative formulation discussed above. So the iterations apparently make the energy worse rather than better: as the effect of iterating through the energy expression may actually be seen as an intermediate normalization condition, the difference between LCCD and CID is often called the *renormalization term*[27].

[27]The term 'renormalization energy' is perhaps best illustrated by the following. Ahlrichs [Ahl79] showed that the LCCD equations can be found by minimizing the functional

$$F_c = \langle \psi_0 + \psi_{\mathrm{D}} | \hat{H}' | \psi_0 + \psi_{\mathrm{D}} \rangle$$

where $\psi_{\mathrm{D}} \equiv \hat{T}_2 \psi_0$, with respect to the $t_{ij}^{ab}$. This should be compared with the variational expression for the CID energy (intermediate normalization):

$$E_c = \frac{\langle \psi_0 + \psi_{\mathrm{D}} | \hat{H}' | \psi_0 + \psi_{\mathrm{D}} \rangle}{1 + \langle \psi_{\mathrm{D}} | \psi_{\mathrm{D}} \rangle} = F_c(1 - \langle \psi_{\mathrm{D}} | \psi_{\mathrm{D}} \rangle + \ldots)$$

The cluster terms involving the amplitudes $t_{ij}^{ab}t_{kl}^{cd}$ correspond in diagrammatic language to so-called *unlinked cluster diagrams*, which are discussed in the section on MBPT. Their 'neglect' in a CID calculation is actually the cause of the size-inconsistency. The terms involving the permuted products correspond to *linked disconnected diagrams* in MBPT language.

It is perhaps the place here to make a few remarks on the index restrictions in the summation. The first is that the $i < j$ and $k < l$ restrictions are often removed for convenience (e.g. in the writings of Professor Bartlett's group). The case $i = j$ and/or $k = l$ gives rise to vanishing antisymmetrized integrals $\langle ii||kl\rangle$ or $\langle ij||kk\rangle$. The cases $i > j$ and $k > l$ each lead to a duplication of the integrals, and thus each require the introduction of a factor $\frac{1}{2}$. The same applies for the other cluster operators in these papers: the definition of $\hat{T}_n$ there consequently differs from the present definition by a factor $1/2^n$.

Another remark is that in products of the cluster operators, no mutual restrictions are placed between the summation indices of each factor. This gives rise to cluster terms where two or more indices coincide, i.e. where the same particle is created or annihilated twice. Such terms are said to be *exclusion principle violating* (EPV). It should be stressed [Rob75] that these terms are *not* unphysical, and that they should be properly included in any coupled cluster calculation. For the two-electron case, the EPV part of the unlinked disconnected clusters cancels with that of their linked counterparts, which explains why CCD is exact for two electrons whereas L-CCD is not (forgetting about the single excitations for a moment) [Pal82].

Although various types of coupled cluster calculations were performed for very small systems early on (see e.g. [Pal72]), the first practical CCD implementation appears to be that by Taylor *et al.* [Tay76], followed by the work of Bartlett *et al.* [Bar78] and Pople *et al.* [Pop78b].

In common cases, CCD recovers a very high percentage (99% or more) of the basis set correlation energy, even when low-lying excited states are present (as in the case of BH($X^1\Sigma^+$) or Be($^1S$)). LCCD (also sometimes referred to as D-MBPT($\infty$) or CEPA-0) generally overshoots the basis set correlation energy — it should be remembered that coupled cluster methods are not variational — by several procent, sometimes resulting in surprising error compensations with basis set incompleteness.

CCD however does not include single excitations — which may become very important for open-shell UHF calculations [Pop88a] or cases with multireference character [Lee90a, Lee90b], and are indispensable for non-Hartree-Fock reference wavefunctions (with the exception of Brueckner orbitals [Bru54], where they exactly vanish).

### 1.6.2 The CCSD and QCISD methods

A coupled cluster method that includes all single and double substitutions is readily defined by changing the exponential ansatz into $\exp(\hat{T}_1 + \hat{T}_2)$. Now different projection equations are needed for the $\hat{T}_1$ and $\hat{T}_2$ amplitudes; the CCSD [Pur82] (coupled cluster with all singles and doubles) equations then become (with $\langle 0| \equiv \langle \psi_0|$ and $|0\rangle \equiv |\psi_0\rangle$ henceforth, for convenience):

$$E_{\mathrm{CCSD}} = \langle 0|H'(\hat{T}_1 + \hat{T}_2 + \hat{T}_1^2/2)|0\rangle \tag{1.190}$$

$$t_i^a E_{\mathrm{CCSD}} = \langle \psi_i^a|H'(1 + \hat{T}_1 + \hat{T}_2 + T_1^2/2 + \hat{T}_1^3/6 + \hat{T}_1\hat{T}_2)|0\rangle \tag{1.191}$$

$$(t_{ij}^{ab} + (t_i^a t_j^b - t_i^b t_j^a))E_{\mathrm{CCSD}} = \langle \psi_{ij}^{ab}|H'(1 + \hat{T}_1 + \hat{T}_2 + T_1^2/2 + \hat{T}_1^3/6 + \hat{T}_1\hat{T}_2 + \hat{T}_2^2/2 + \hat{T}_1^2\hat{T}_2/2 + \hat{T}_1^4/24)|0\rangle \tag{1.192}$$

The first term in the $E_{\mathrm{CCSD}}$ and $\hat{T}_1$ equations may be omitted for a Hartree-Fock reference state because of Brillouin's theorem.

CCSD is exact for any two-electron system, as is CISD. It again recovers very large percentages of the basis set correlation energy, now also for multireference cases. The breaking of a single bond is described essentially as good as full CI. A traditional test for electron correlation methods is a calculation of a molecule like HF at a highly stretched geometry (like $2r_e$), because a single HF determinant is normally no longer adequate as the reference wavefunction. CCSD handles this essentially as well as full CI, whereas most other single-reference methods fail.

The upshot is CCSD being distinctly more expensive than CISD or even CCD, because a quartic system of coupled equations is involved this time (which generally results in slower convergence). This lead to the development of an approximate method called QCISD (see below) which has only quadratic equations.

However, Scuseria and Schaefer [Scu89] showed recently that the CCSD method can be reformulated in such a way that the equations become quadratic at most. They define (formalism with unrestricted sums) the effective doubles amplitudes $\tau_{ij}^{ab} \equiv \frac{1}{2}t_{ij}^{ab} + t_i^a t_j^b$, which is equivalent to defining the effective doubles cluster operator $\hat{T}_2' \equiv \hat{T}_2 + \hat{T}_1^2/2$. Using this latter notation, the CCSD equations become

$$E_{\mathrm{CCSD}} = \langle 0|H'(\hat{T}_1 + \hat{T}_2')|0\rangle \tag{1.193}$$

$$t_i^a E_{\mathrm{CCSD}} = \langle \psi_i^a|H'(1 + \hat{T}_1 + \hat{T}_2' + \hat{T}_1\hat{T}_2')|0\rangle \tag{1.194}$$

$$(t_{ij}^{ab} + (t_i^a t_j^b - t_i^b t_j^a))E_{\mathrm{CCSD}} = \langle \psi_{ij}^{ab}|H'(1 + \hat{T}_1 + \hat{T}_2' + \hat{T}_1\hat{T}_2' + (\hat{T}_2')^2/2)|0\rangle \tag{1.195}$$

which are not only more readable but also computationally more efficient than the usual formulation of CCSD.

Pople and coworkers developed the *quadratic configuration interaction* (QCI) method [Pop87a] precisely to circumvent the quartic equations. The equations for the singles and

doubles case (QCISD), assuming a HF reference, are given by

$$E_{\mathrm{QCISD}} = \langle 0|H'(\hat{T}_2)|0\rangle \tag{1.196}$$

$$t_i^a E_{\mathrm{QCISD}} = \langle \psi_i^a|H'(1+\hat{T}_1+\hat{T}_2+\hat{T}_1\hat{T}_2)|0\rangle \tag{1.197}$$

$$t_{ij}^{ab} E_{\mathrm{QCISD}} = \langle \psi_{ij}^{ab}|H'(1+\hat{T}_1+\hat{T}_2+T_2^2/2)|0\rangle \tag{1.198}$$

In these equations, all terms that are nonlinear in $\hat{T}_1$ are neglected, as well as the $\hat{T}_1\hat{T}_2$ coupling term in the $\hat{T}_2$ equation. The latter is corrected for in the QCISD(T) method which includes a quasiperturbative treatment for triple excitations. (It should be remarked that the QCISD method was not intended to be used without it.) The higher-order terms in $\hat{T}_1$ are unimportant near equilibrium geometries, at least in the vast majority of cases; for these, QCISD exhibits the same very good performance characteristics as CCSD. For cases with very heavy spin contamination (like $B_3$) or extreme multireference character (like CuH($X^1\Sigma^+$)), however, QCISD yields energies which are several millihartrees too low, whereas CCSD still holds its own. A detailed comparison of the two methods for closed-shell cases has been made by Lee *et al.* [Lee90b].

Quite apart from the good numerical performance, the QCISD method has been the subject of some polemic in the literature between Paldus and coworkers on the one hand [Pal89b] and Pople *et al.* on the other hand [Pop89b]. Much of it centers around the fact that the Pople group chose to present the QCI method as a new class of electron correlation methods, rather than an approximation to CCSD, whereas Paldus *et al.* point out that the extension of the QCISD method to QCISDT (QCI with all singles, doubles, and triples) is not even size-extensive! Furthermore, the latter authors endorse the point of view that the more rigorous method is necessarily the better, whereas the former hold the opinion that only an empirical comparison with full CI (or, with sufficiently large basis sets, experimental dissociation energies) can settle the question as to which method is the better one. More details about this quantum chemical 'tribal quarrel' can be found in [Pal89b] and [Pop89b].

### 1.6.3 Relationship between excitation and cluster operators

It is obvious that the configuration and the cluster expansions must become equivalent for the full CI case, i.e. when all excitation resp. cluster operators are included properly. Setting

$$\hat{C}_1+\hat{C}_2+\hat{C}_3+\hat{C}_4+\ldots = \exp(\hat{T}_1+\hat{T}_2+\hat{T}_3+\hat{T}_4+\ldots) \tag{1.199}$$

this leads to the following useful equalities:

$$\hat{C}_1 = \hat{T}_1 \tag{1.200}$$

$$\hat{C}_2 = \hat{T}_2+\hat{T}_1^2/2 \tag{1.201}$$

$$\hat{C}_3 = \hat{T}_3+\hat{T}_1\hat{T}_2+\hat{T}_1^3/6 \tag{1.202}$$

$$\hat{C}_4 = \hat{T}_4+\hat{T}_1\hat{T}_3+\hat{T}_2^2/2+\hat{T}_1^2\hat{T}_2+\hat{T}_1^4/24 \tag{1.203}$$

The first terms of each excitation operator are the connected, the remaining the disconnected $n$-tuple excitations.

### 1.6.4 An alternative formulation of the coupled cluster equations

For our purposes, it is convienient to cast the coupled cluster equations in a different form (see e.g. [Pal75]). Originally, they were defined through

$$\hat{H}' \exp(\hat{T})|\psi_0\rangle = E \exp(\hat{T})|\psi_0\rangle \tag{1.204}$$

Let us now multiply (1.204) on the left with $\exp(-\hat{T})$, which results in

$$\exp(-\hat{T})\hat{H}' \exp(\hat{T})|\psi_0\rangle = E|\psi_0\rangle \tag{1.205}$$

Note that the operators on the left do not cancel. More specifically, the operator product on the left may, upon expansion of the power series, be written as

$$\begin{aligned} \exp(-\hat{T})\hat{H}' \exp(\hat{T}) &= 1 + [\hat{H}', \hat{T}] + \frac{1}{2}[[\hat{H}', \hat{T}], \hat{T}] + \frac{1}{6}[[[\hat{H}', \hat{T}], \hat{T}], \hat{T}] \\ &\quad + \frac{1}{24}[[[[\hat{H}', \hat{T}], \hat{T}], \hat{T}], \hat{T}] \end{aligned} \tag{1.206}$$

where the square brackets represent the commutator $[\hat{A}, \hat{B}] \equiv \hat{A}\hat{B} - \hat{B}\hat{A}$. Note also that the series truncates after exactly four commutator terms for this case, since the second quantization representation of $\hat{H}$ contains strings of at most four operators.

Through very involved manipulations that require the introduction of various new concepts, it can be shown (see e.g. [Pal75]) that only connected diagrams remain, i.e.

$$\exp(-\hat{T})\hat{H}' \exp(\hat{T}) = [\hat{H}' \exp(\hat{T})]_C \tag{1.207}$$

where the subscript $C$ denotes a restriction to connected terms only. Projecting (1.205) from the left with the ground and excited determinants, we obtain the equations:

$$\langle 0|[\hat{H}' \exp(\hat{T})]_C|0\rangle = \Delta E \tag{1.208}$$

$$\langle \psi_i^a|[\hat{H}' \exp(\hat{T})]_C|0\rangle = 0 \tag{1.209}$$

$$\langle \psi_{ij}^{ab}|[\hat{H}' \exp(\hat{T})]_C|0\rangle = 0 \tag{1.210}$$

$$\langle \psi_{ijk}^{abc}|[\hat{H}' \exp(\hat{T})]_C|0\rangle = 0 \tag{1.211}$$

$$\langle \psi_{ijkl}^{abcd}|[\hat{H}' \exp(\hat{T})]_C|0\rangle = 0 \tag{1.212}$$

$$\ldots$$

Note that there are no more renormalization terms, which is another way of stating that the coupled cluster equations are size-extensive. This is a consequence of the fact that there are no more disconnected terms, of which the unlinked diagrams are a subset.

It is furthermore convenient to partition $\hat{H}'$ into a Fock operator part $\hat{V}$ and a two-electron part $\hat{W}$.

$$\hat{H}' = \hat{F} - E_0 + \hat{W} \equiv \hat{V} + \hat{W} \tag{1.213}$$

Then it can be easily shown (see e.g. [Pal75]) that

$$\begin{aligned}
\langle 0|[\hat{V}\exp(\hat{T})]_C|0\rangle &= 0 && (1.214)\\
\langle \psi_i^a|[\hat{V}\exp(\hat{T})]_C|0\rangle &= -t_i^a D_{ia} && (1.215)\\
\langle \psi_{ij}^{ab}|[\hat{V}\exp(\hat{T})]_C|0\rangle &= -t_{ij}^{ab} D_{ijab} && (1.216)\\
\langle \psi_{ijk}^{abc}|[\hat{V}\exp(\hat{T})]_C|0\rangle &= -t_{ijk}^{abc} D_{ijkabc} && (1.217)\\
\langle \psi_{ijkl}^{abcd}|[\hat{V}\exp(\hat{T})]_C|0\rangle &= -t_{ijkl}^{abcd} D_{ijklabcd} && (1.218)\\
&\ldots
\end{aligned}$$

where the $D_{ijk\ldots abc\ldots}$ are many-body perturbation denominators given by $\epsilon_a + \epsilon_b + \ldots - \epsilon_i - \epsilon_j - \ldots$. Substituting (1.214)–(1.218) in the corresponding relations (1.208)–(1.212) finally leads to the following form of the CC equations:

$$\begin{aligned}
\langle 0|[\hat{W}\exp(\hat{T})]_C|0\rangle &= \Delta E && (1.219)\\
\langle \psi_i^a|[\hat{W}\exp(\hat{T})]_C|0\rangle &= t_i^a D_{ia} && (1.220)\\
\langle \psi_{ij}^{ab}|[\hat{W}\exp(\hat{T})]_C|0\rangle &= t_{ij}^{ab} D_{ijab} && (1.221)\\
\langle \psi_{ijk}^{abc}|[\hat{W}\exp(\hat{T})]_C|0\rangle &= t_{ijk}^{abc} D_{ijkabc} && (1.222)\\
\langle \psi_{ijkl}^{abcd}|[\hat{W}\exp(\hat{T})]_C|0\rangle &= t_{ijkl}^{abcd} D_{ijklabcd} && (1.223)\\
&\ldots
\end{aligned}$$

which is particularly convenient for the remainder of the discussion. The CCSDTQ equations in operator form are then given as

$$\begin{aligned}
\Delta E &= \langle 0|\hat{W}(\hat{T}_2 + \hat{T}_1^2/2)|0\rangle && (1.224)\\
D_1T_1 &= \hat{W}[\hat{T}_1 + \hat{T}_2 + \hat{T}_1^2/2 + \hat{T}_3 + \hat{T}_1\hat{T}_2 + \hat{T}_1^3/6] && (1.225)\\
D_2T_2 &= \hat{W}[1 + \hat{T}_1 + \hat{T}_2 + \hat{T}_1^2/2 + \hat{T}_3 + \hat{T}_1\hat{T}_2 + \hat{T}_1^3/6\\
&\quad + \hat{T}_4 + \hat{T}_1\hat{T}_3 + \hat{T}_2^2/2 + \hat{T}_1^2\hat{T}_2/2 + \hat{T}_1^4/24] && (1.226)\\
D_3T_3 &= \hat{W}[\hat{T}_1 + \hat{T}_2 + \hat{T}_1^2/2 + \hat{T}_3 + \hat{T}_1\hat{T}_2 + \hat{T}_1^3/6\\
&\quad + \hat{T}_4 + \hat{T}_1\hat{T}_3 + \hat{T}_2^2/2 + \hat{T}_1^2\hat{T}_2/2 + \hat{T}_1^4/24\\
&\quad + \hat{T}_1\hat{T}_4 + \hat{T}_2\hat{T}_3 + \hat{T}_1^2\hat{T}_3/2 + \hat{T}_1\hat{T}_2^2/2 + \hat{T}_1^3\hat{T}_2/6 + \hat{T}_1^5/120] && (1.227)\\
D_4T_4 &= \hat{W}[\hat{T}_2 + \hat{T}_1^2/2 + \hat{T}_3 + \hat{T}_1\hat{T}_2 + \hat{T}_1^3/6\\
&\quad + \hat{T}_4 + \hat{T}_1\hat{T}_3 + \hat{T}_2^2/2 + \hat{T}_1^2\hat{T}_2/2 + \hat{T}_1^4/24\\
&\quad + \hat{T}_1\hat{T}_4 + \hat{T}_2\hat{T}_3 + \hat{T}_1^2\hat{T}_3/2 + \hat{T}_1\hat{T}_2^2/2 + \hat{T}_1^3\hat{T}_2/6 + \hat{T}_1^5/120\\
&\quad + \hat{T}_2\hat{T}_4 + \hat{T}_1^2\hat{T}_4/2 + \hat{T}_3^2/2 + \hat{T}_1\hat{T}_2\hat{T}_3 + \hat{T}_1^3\hat{T}_3\\
&\quad + \hat{T}_2^3/6 + \hat{T}_1^4\hat{T}_2/24 + \hat{T}_1^2\hat{T}_2^2/4 + \hat{T}_1^6/720] && (1.228)
\end{aligned}$$

with the restriction to connected terms being understood from now on. $D_1$ is a shorthand notation for $D_{ia}$, $D_2$ for $D_{ijab}$, etc. Part of the terms in these equations are incapable of producing connected contributions, and therefore vanish from the equations: this will become evident below when the equations are translated in diagrammatic languauge. The final equations are [Kuc89, Bar90b]

$$\begin{aligned}
\Delta E &= \langle 0|\hat{W}(\hat{T}_2 + \hat{T}_1^2/2)|0\rangle && (1.229)\\
D_1T_1 &= \hat{W}[\hat{T}_1 + \hat{T}_2 + \hat{T}_1^2/2 + \hat{T}_3 + \hat{T}_1\hat{T}_2 + \hat{T}_1^3/6] && (1.230)\\
D_2T_2 &= \hat{W}[1 + \hat{T}_1 + \hat{T}_2 + \hat{T}_1^2/2 + \hat{T}_3 + \hat{T}_1\hat{T}_2 + \hat{T}_1^3/6 \\
&\quad + \hat{T}_4 + \hat{T}_1\hat{T}_3 + \hat{T}_2^2/2 + \hat{T}_1^2\hat{T}_2/2 + \hat{T}_1^4/24] && (1.231)\\
D_3T_3 &= \hat{W}[\hat{T}_2 + \hat{T}_3 + \hat{T}_1\hat{T}_2 + \hat{T}_4 + \hat{T}_1\hat{T}_3 + \hat{T}_2^2/2 + \hat{T}_1^2\hat{T}_2/2 \\
&\quad + \hat{T}_1\hat{T}_4 + \hat{T}_2\hat{T}_3 + \hat{T}_1^2\hat{T}_3/2 + \hat{T}_1\hat{T}_2^2/2 + \hat{T}_1^3\hat{T}_2/6] && (1.232)\\
D_4T_4 &= \hat{W}[\hat{T}_3 + \hat{T}_4 + \hat{T}_1\hat{T}_3 + \hat{T}_2^2/2 + \hat{T}_1\hat{T}_4 + \hat{T}_2\hat{T}_3 + \hat{T}_1^2\hat{T}_3/2 + \hat{T}_1\hat{T}_2^2/2 \\
&\quad + \hat{T}_2\hat{T}_4 + \hat{T}_1^2\hat{T}_4/2 + \hat{T}_3^2/2 + \hat{T}_1\hat{T}_2\hat{T}_3 + \hat{T}_1^3\hat{T}_3 + \hat{T}_2^3/6 + \hat{T}_1^2\hat{T}_2^2/4] && (1.233)
\end{aligned}$$

The CCSD equations in this formalism are simply (for HF references):

$$\begin{aligned}
\Delta E &= \langle 0|\hat{W}(\hat{T}_2 + \hat{T}_1^2/2)|0\rangle && (1.234)\\
D_1T_1 &= \hat{W}[\hat{T}_1 + \hat{T}_2 + \hat{T}_1^2/2 + \hat{T}_1\hat{T}_2 + \hat{T}_1^3/6] && (1.235)\\
D_2T_2 &= \hat{W}[1 + \hat{T}_1 + \hat{T}_2 + \hat{T}_1^2/2 + \hat{T}_1\hat{T}_2 + \hat{T}_1^3/6 \\
&\quad + \hat{T}_2^2/2 + \hat{T}_1^2\hat{T}_2/2 + \hat{T}_1^4/24] && (1.236)
\end{aligned}$$

whereas the simpler QCISD equations are found as:

$$\begin{aligned}
\Delta E &= \langle 0|\hat{W}\hat{T}_2|0\rangle && (1.237)\\
D_1T_1 &= \hat{W}[\hat{T}_1 + \hat{T}_2 + \hat{T}_1\hat{T}_2] && (1.238)\\
D_2T_2 &= \hat{W}[1 + \hat{T}_1 + \hat{T}_2 + \hat{T}_2^2/2] && (1.239)
\end{aligned}$$

### 1.6.5 Iterative inclusion of connected triple excitations — exact and approximate CCSDT methods

For molecules with multiple bonds, connected triple excitations are since long known to be very important [Kri80]. To reach the full CI limit in these cases, the ansatz should include some account of triple excitations too. The full CCSDT equations are:

$$\Delta E = \langle 0|\hat{W}(\hat{T}_2 + \hat{T}_1^2/2)|0\rangle \quad (1.240)$$

$$D_1T_1 = \hat{W}[\hat{T}_1 + \hat{T}_2 + \hat{T}_1^2/2 + \hat{T}_3 + \hat{T}_1\hat{T}_2 + \hat{T}_1^3/6] \quad (1.241)$$

$$D_2T_2 = \hat{W}[1 + \hat{T}_1 + \hat{T}_2 + \hat{T}_1^2/2 + \hat{T}_3 + \hat{T}_1\hat{T}_2 + \hat{T}_1^3/6 + \hat{T}_1\hat{T}_3 + \hat{T}_2^2/2 + \hat{T}_1^2\hat{T}_2/2 + \hat{T}_1^4/24] \quad (1.242)$$

$$D_3T_3 = \hat{W}[\hat{T}_2 + \hat{T}_3 + \hat{T}_1\hat{T}_2 + \hat{T}_1\hat{T}_3 + \hat{T}_2^2/2 + \hat{T}_1^2\hat{T}_2/2 + \hat{T}_2\hat{T}_3 + \hat{T}_1^2\hat{T}_3/2 + \hat{T}_1\hat{T}_2^2/2 + \hat{T}_1^3\hat{T}_2/6] \quad (1.243)$$

Such a method is not only very difficult to implement, but also very intensive computationally, requiring $O(n^8)$ operations per iteration. Full implementations have been reported by Noga and Bartlett [Nog87] and by Scuseria and Schaefer [Scu88b]. Several approximations that require only $O(n^7)$ operations per iteration have been proposed by Bartlett and coworkers [Lee84, Urb85, Urb87, Nog87]. They are presented below in increasing order of approximation.

In the CCSDT-4 method [Nog87], the nonlinear terms involving $\hat{T}_3$ are dropped from the triples amplitude equations:

$$\Delta E_{\mathrm{CCSDT-4}} = \langle 0|\hat{W}(\hat{T}_2 + \hat{T}_1^2/2)|0\rangle \quad (1.244)$$

$$D_1T_1 = \hat{W}[\hat{T}_1 + \hat{T}_2 + \hat{T}_1^2/2 + \hat{T}_3 + \hat{T}_1\hat{T}_2 + \hat{T}_1^3/6] \quad (1.245)$$

$$D_2T_2 = \hat{W}[1 + \hat{T}_1 + \hat{T}_2 + \hat{T}_1^2/2 + \hat{T}_3 + \hat{T}_1\hat{T}_2 + \hat{T}_1^3/6 + \hat{T}_1\hat{T}_3 + \hat{T}_2^2/2 + \hat{T}_1^2\hat{T}_2/2 + \hat{T}_1^4/24] \quad (1.246)$$

$$D_3T_3 = \hat{W}[\hat{T}_2 + \hat{T}_1\hat{T}_2 + \hat{T}_2^2/2 + \hat{T}_1^2\hat{T}_2/2 + \hat{T}_1\hat{T}_2^2/2 + \hat{T}_1^3\hat{T}_2/6 + \hat{T}_3] \quad (1.247)$$

CCSDT-4 gives results very slightly closer to full CCSDT than the following methods; its computer time requirements still scale as $O(n^8)$ per iteration, however, whereas the others only scale as $O(n^7)$ per iteration.

In the CCSDT-3 method [Urb85, Urb87], all terms involving $\hat{T}_3$ are dropped from the triples amplitude equations. The connected triples can thus no longer affect themselves directly:

$$\Delta E_{\mathrm{CCSDT-3}} = \langle 0|\hat{W}(\hat{T}_2 + \hat{T}_1^2/2)|0\rangle \quad (1.248)$$

$$D_1T_1 = \hat{W}[\hat{T}_1 + \hat{T}_2 + \hat{T}_1^2/2 + \hat{T}_3 + \hat{T}_1\hat{T}_2 + \hat{T}_1^3/6] \quad (1.249)$$

$$D_2T_2 = \hat{W}[1 + \hat{T}_1 + \hat{T}_2 + \hat{T}_1^2/2 + \hat{T}_3 + \hat{T}_1\hat{T}_2 + \hat{T}_1^3/6 + \hat{T}_1\hat{T}_3 + \hat{T}_2^2/2 + \hat{T}_1^2\hat{T}_2/2 + \hat{T}_1^4/24] \quad (1.250)$$

$$D_3T_3 = \hat{W}[\hat{T}_2 + \hat{T}_1\hat{T}_2 + \hat{T}_2^2/2 + \hat{T}_1^2\hat{T}_2/2 + \hat{T}_1\hat{T}_2^2/2 + \hat{T}_1^3\hat{T}_2/6] \quad (1.251)$$

In the CCSDT-2 method [Urb85, Urb87], the terms involving $\hat{T}_1$ are also dropped from the triples equation:

$$\Delta E_{\mathrm{CCSDT-2}} = \langle 0|\hat{W}(\hat{T}_2 + \hat{T}_1^2/2)|0\rangle \quad (1.252)$$

$$D_1 T_1 = \hat{W}[\hat{T}_1 + \hat{T}_2 + \hat{T}_1^2/2 + \hat{T}_3 + \hat{T}_1\hat{T}_2 + \hat{T}_1^3/6] \quad (1.253)$$

$$D_2 T_2 = \hat{W}[1 + \hat{T}_1 + \hat{T}_2 + \hat{T}_1^2/2 + \hat{T}_3 + \hat{T}_1\hat{T}_2 + \hat{T}_1^3/6 + \hat{T}_1\hat{T}_3 + \hat{T}_2^2/2 + \hat{T}_1^2\hat{T}_2/2 + \hat{T}_1^4/24] \quad (1.254)$$

$$D_3 T_3 = \hat{W}[\hat{T}_2 + \hat{T}_2^2/2] \quad (1.255)$$

The CCSDT-1b method [Urb85, Urb87] is still more drastic, as it even eliminates the disconnected quadruples from the triples equation:

$$\Delta E_{\mathrm{CCSDT-1b}} = \langle 0|\hat{W}(\hat{T}_2 + \hat{T}_1^2/2)|0\rangle \quad (1.256)$$

$$D_1 T_1 = \hat{W}[\hat{T}_1 + \hat{T}_2 + \hat{T}_1^2/2 + \hat{T}_3 + \hat{T}_1\hat{T}_2 + \hat{T}_1^3/6] \quad (1.257)$$

$$D_2 T_2 = \hat{W}[1 + \hat{T}_1 + \hat{T}_2 + \hat{T}_1^2/2 + \hat{T}_3 + \hat{T}_1\hat{T}_2 + \hat{T}_1^3/6 + \hat{T}_1\hat{T}_3 + \hat{T}_2^2/2 + \hat{T}_1^2\hat{T}_2/2 + \hat{T}_1^4/24] \quad (1.258)$$

$$D_3 T_3 = \hat{W}[\hat{T}_2] \quad (1.259)$$

Finally, in the CCSDT-1a method (also denoted CCSDT-1) [Lee84, Urb85, Urb87], the term $\hat{T}_1\hat{T}_3$ is furthermore dropped from the $\hat{T}_2$ equation:

$$\Delta E_{\mathrm{CCSDT-1a}} = \langle 0|\hat{W}(\hat{T}_2 + \hat{T}_1^2/2)|0\rangle \quad (1.260)$$

$$D_1 T_1 = \hat{W}[\hat{T}_1 + \hat{T}_2 + \hat{T}_1^2/2 + \hat{T}_3 + \hat{T}_1\hat{T}_2 + \hat{T}_1^3/6] \quad (1.261)$$

$$D_2 T_2 = \hat{W}[1 + \hat{T}_1 + \hat{T}_2 + \hat{T}_1^2/2 + \hat{T}_3 + \hat{T}_1\hat{T}_2 + \hat{T}_1^3/6 + \hat{T}_2^2/2 + \hat{T}_1^2\hat{T}_2/2 + \hat{T}_1^4/24] \quad (1.262)$$

$$D_3 T_3 = \hat{W}[\hat{T}_2] \quad (1.263)$$

A limited numerical comparison can be found in [Urb85] and [Nog87]. All these methods appear to reproduce the energetic effects of triple excitations rather well. Near equilibrium, there appears to be little to choose among them; for water with bonds stretched to $2r_e$, a traditional benchmark for correlation methods that include higher than double excitations, CCSDT-1a and CCSDT-1b fail obviously, whereas CCSDT-2 and CCSDT-3 both produce results close to full CI. The performance of CCSDT-1a and CCSDT-1b is essentially identical, as are those of CCSDT-2 and CCSDT-3. For very heavily spin-contaminated UHF wavefunctions, CCSDT-3 may perform better than CCSDT-2, though, but this has never been explicitly investigated.

Even CCSDT-1a is much too expensive computationally to be used for routine calculations. Alternatives have therefore been sought.

### 1.6.6 Quasiperturbative evaluation of $\hat{T}_3$ effects – the CCD(ST), QCISD(T), and CCSD(T) methods

It is well known in MBPT, that the contribution of connected triples to the molecular energy starts out at fourth order, and that the fourth-order term is given by [Kri80]

$$E_{4\mathrm{T}} = \sum_{s}^{D}\sum_{t}^{T}\sum_{u}^{D} \frac{a_s V_{st} V_{tu} a_u}{D_t} \tag{1.264}$$

where the summation indices $s$ and $u$ extend over all double, and $t$ over all triple excitations, $V_{st}$ represents the matrix element of $\hat{H}'$ between the configurations corresponding to $s$ and $t$; $D_t$ is the appropriate MBPT denominator for $t$. The amplitude of configuration $s$ to first order in MBPT is finally denoted $a_s$. Most important is, that the evaluation of $E_{4\mathrm{T}}$ requires only one step with $O(n^7)$ operations, whereas the CCSDT-n methods require several such steps per iteration.

A first attempt at taking advantage of this expression was the CCSD+T(4) method proposed by Bartlett *et al.* [Bar83]. Here, $E_{4T}$ is simply added to the CCSD energy. However, it is well known (e.g. [Kri80]) that for systems where $\hat{T}_3$ effects are important, $E_{4T}$ significantly overshoots the effect.

Another possibility would be to replace the first-order MBPT wavefunction by converged $\hat{T}_2$ amplitudes from a CCSD calculation, which yields the CCSD+T(CCSD) method of Bartlett and coworkers [Urb85]. (These amplitudes are at least correct to second order, and also include important effects to infinite order. As they are thus certainly correct to first order, the quasiperturbative $\hat{T}_3$ effect from them is at least correct to fourth order; it will however also contain important terms at fifth and higher order.) This method was found to give a good approximation to CCSDT-1 results; however, it broke down completely in a recent study of the harmonic frequencies of ozone [Sta89] (a molecule where $\hat{T}_3$ effects are unusually important), predicting a value $128i$ cm$^{-1}$ for the asymmetric stretch (compared to the experimental value [Bar74a] of 1089 cm$^{-1}$).

Raghavachari [Rag85] also proposed the CCD+ST(CCD) method, which should actually be denoted CCD(ST) by analogy with what follows. Here, the triples are evaluated quasiperturbatively (i.e., as shown above) from converged CCD amplitudes. The single excitations contribution (which requires only minimal computational effort) is evaluated in an analogous manner. (The expression is identical to that for the triples, except that the middle index runs over single instead of triple excitations. It also starts out at fourth order.) The main weak point of this method is exactly this defective account for single excitations, which makes it only useful for well-behaved molecules.

At fifth order in perturbation theory, an additional $\hat{T}_3$ term in the energy arises from the single excitation amplitudes (which start out at second order):

$$E_{5\mathrm{T}} = \sum_{s}^{S}\sum_{t}^{T}\sum_{u}^{D} \frac{a_s V_{st} V_{tu} a_u}{D_t} + \sum_{s}^{D}\sum_{t}^{T}\sum_{u}^{S} \frac{a_s V_{st} V_{tu} a_u}{D_t}$$

$$= 2\sum_{s}^{S}\sum_{t}^{T}\sum_{u}^{D}\frac{a_s V_{st} V_{tu} a_u}{D_t} \tag{1.265}$$

One could now substitute converged $\hat{T}_1$ amplitudes (which are at least correct to second order) instead of their MBPT equivalents. This is done in the QCISD(T) method, together with the $\hat{T}_2$ amplitudes from the same calculation. Both terms can be conveniently collected as

$$\text{QCISD(T)} - \text{QCISD} = (2\sum_{s}^{S} + \sum_{s}^{D})\sum_{t}^{T}\sum_{u}^{D}\frac{a_s V_{st} V_{tu} a_u}{D_t} \tag{1.266}$$

This method also gives a good account of $\hat{T}_3$ effects in practical calculations. Somewhat surprisingly, it gives a quite good representation of the force field of ozone [Rag89b]: the asymmetric stretch is computed at 934 $cm^{-1}$, an error quite typical for the small DZP basis set used. This shows that it actually accounts *better* for the $\hat{T}_3$ effects than T(CCSD). Apparently the fifth-order term neglected in T(CCSD) is too important to be left out at will.

It can easily be accounted for, of course, in a similar manner as in QCISD(T), now by using both $\hat{T}_1$ and $\hat{T}_2$ amplitudes from the converged CCSD calculation. However, the factor of two should now be eliminated to avoid some double-counting: the diagrams that correspond to (1.265) are Hermitian conjugates of diagrams coming from the $\hat{T}_1\hat{T}_2$ cross-term in the CCSD doubles equation. (Exactly this term was the leading difference between the CCSD and QCISD energies.) The CCSD(T) method [Rag89] is thus defined by:

$$\text{CCSD(T)} - \text{CCSD} = (\sum_{s}^{S} + \sum_{s}^{D})\sum_{t}^{T}\sum_{u}^{D}\frac{a_s V_{st} V_{tu} a_u}{D_t} \tag{1.267}$$

This method combines the good performance of QCISD(T) with the rigor of the CCSD vs. the QCISD method. The ozone force field (now a test case for triple excitation inclusion) is handled excellently; using the same DZP basis set as above, the predicted value for the asymmetric stretch is 977 $cm^{-1}$ [Rag89], whereas a very recent large basis set CCSD(T) calculation [Lee90c] yields geometries and anharmonic frequencies with an accuracy comparable to the experiment. Furthermore, multireference character and extreme spin contamination are no longer problems with it, as shown by a recent full CCSDT calculation on the CuH molecule [Scu90]; the CCSD(T) total energy using the same basis set differed from it by only 0.973 millihartree, compared to 10.33 millihartree for the QCISD(T) method.

It is noteworthy here, that CCSDT-1a and CCSDT-1b both predict a much too low value of 680 $cm^{-1}$ for the asymmetric ozone stretch, whereas CCSDT-2 predicts a quite acceptable 1182 $cm^{-1}$ [Mag89]; apparently QCISD(T) and CCSD(T) are better than CCSDT-1, as also suggested in a very recent paper of Raghavachari *et al.* [Rag90], where QCISD(T) gave an energy for water at $2r_e$ virtually identical to the full CCSDT result.

We have seen that the treatment of triples in CCSD(T) and QCISD(T) is identical to fifth order (and probably beyond): this explains the finding of Lee *et al.* [Lee90b] that the difference between QCISD(T) and CCSD(T) is generally much smaller than that between QCISD and CCSD.

Withal, CCSD(T) emerges as the ideal 'black box' high-level electron correlation procedure:

1. It yields correlation energies very close to the basis set limit.
2. No further input on the part of the user is required beyond that already necessary for the previous part of the calculation.
3. Even severely multireference problems may still be treated from a single reference determinant.
4. Computationally, although not exactly cheap, it is still amenable to medium-to-large problems with ordinary high-performance computing facilities.
5. It may usually be relied upon (especially with good convergence accelerators such as the DIIS procedure of Pulay [Pul82]) to converge, and certainly to converge to the correct solution.
6. It is rigorously size-extensive.

Only full CCSDT and perhaps CASSCF/CI will do better on account (1); the former is essentially impossible for medium-to-large scale calculations. This is not as severe a problem with the latter; for large-scale work, computer facilities on the order of a Cray Y-MP are still necessary, though. Both methods thus fail on account (4). Any multireference method except CASSCF and CASSCF/CI will fail on account (2); only CASSCF and CASSCF/CI can do better on account (3). Only single-reference CID and CISD will usually present less convergence problems; MBPT calculations are noniterative and thus ipso facto free from convergence difficulties. These often fail to come sufficiently close to full CI for accurate work, though. Convergence failure, deceptive convergence, and convergence to false variational extrema are relatively common problems with CASSCF calculations. Finally, only MBPT and the other CC methods are rigorously size-extensive; of these, only CCSDT may a priori be relied upon to give better results.

### 1.6.7 Some recent developments

The reference determinant does not necessarily have to be a Hartree-Fock wavefunction. One possibility would be to choose so-called Brueckner orbitals [Bru54], which are defined by the requirement that $\hat{T}_1$ must vanish. Such orbitals could in principle be generated from the Hartree-Fock orbitals; it is however much easier and much more convenient

to introduce them implicitly by requiring the $\hat{T}_1$ amplitudes in a CCSD calculation to vanish. This gives rise to the following equations:

$$E_{\mathrm{BD}} = \langle \Psi_0 | H' \hat{T}_2 | \Psi_0 \rangle \tag{1.268}$$

$$0 = \langle \psi_i^a | H' (1 + \hat{T}_2) | \Psi_0 \rangle \tag{1.269}$$

$$t_{ij}^{ab} E_{\mathrm{BD}} = \langle \psi_{ij}^{ab} | H' (1 + \hat{T}_2 + \hat{T}_2^2/2) | \Psi_0 \rangle \tag{1.270}$$

where the acronym denotes the Brueckner doubles (BD) method [Chi81, Han89]. Note that the orbitals of the Brueckner determinant $\Psi_0$ and those of the Hartree-Fock determinant $\psi_0$ are related by a unitary transformation, the coefficients of which are imposed by condition (1.269). Again, a quasiperturbative correction for triples can be introduced (now the term involving single excitations is superfluous), leading to the BD(T) method [Han89]. Numerical tests [Rag90] indicate that the performance of the BD(T) method is comparable to that of CCSD(T); actually, the method includes some fifth- and higher order terms that are not included in CCSD(T), as does BD compared to CCSD [Rag90].

Connected quadruple excitations $\hat{T}_4$ may potentially be important for multiply-bonded systems, e.g. for polyenes. In MBPT language, $\hat{T}_4$ terms start out at fifth order. A full CCSDTQ method would require $O(n^{10})$ operations per iteration, which is clearly unacceptable. Very recently, Kucharski and Bartlett [Kuc89] proposed the CCSDTQ-1 method, obtained by deleting from the $\hat{T}_4$ equation of full CCSDTQ all cluster operators except $\hat{T}_2$, $\hat{T}_3$ and $\hat{T}_2^2/2$ (which should be the most important terms). Such a method involves $O(n^9)$ operations per iteration. The CCSDT+Q(CCSDT) method, where the $\hat{T}_4$ effects are evaluated quasiperturbatively, was also proposed; this involves only a single $O(n^8)$ step. More recently, Bartlett *et al.* [Bar90b] proposed the CCSD+TQ(CCSD) method, which also has a single $O(n^8)$ term, but is only $O(n^6)$ instead of $O(n^8)$ per iteration (plus a single $O(n^7)$ term).

Raghavachari *et al.* [Rag90] introduced three more methods that include connected quadruples, namely CCSD(TQ) (which differs from CCSD+TQ(CCSD) in the same way as CCSD(T) does from CCSD+T(CCSD)), QCISD(TQ), and BD(TQ). All of these methods scale as $O(n^6)$ per iteration, with one $O(n^7)$ and $O(n^8)$ step. Numerical results for $N_2$, HCN, and the CN radical obtained by these authors with a minimal STO-3G basis set indicate that the $\hat{T}_4$ effect is on the order of 2 millihartrees for these molecules, and that the final QCISD(TQ) and BD(TQ) results are extremely close to full CI. All three methods CCSD(TQ), QCISD(TQ), and BD(TQ) are exactly correct to fifth order in perturbation theory, which CCSD+TQ(CCSD) is not.

Although one of the virtues of coupled cluster methods is precisely that they handle multireference problems well from single-reference wavefunctions, some effort has been put in recent years in the development of multireference coupled cluster methods. The subject has recently been reviewed by Paldus *et al.* [Pal89a] and by Kaldor [Kal89].

Finally, two alternative ansätze for coupled cluster theory, namely *expectation value*

*coupled cluster* (XCC) and *unitary coupled cluster* (UCC) have recently been considered [Bar89b]. XCC is based on an energy expression that is the expectation value for a wavefunction $\exp(\hat{T})\psi_0$

$$\Delta E_{\mathrm{XCC}} = \frac{\langle\psi_0|\exp(\hat{T}^+)\hat{H}'\exp(\hat{T})|\psi_0\rangle}{\langle\psi_0|\exp(\hat{T}^+)\exp(\hat{T})|\psi_0\rangle} \tag{1.271}$$

The XCC($n$) functional is found by making an MBPT expansion of the wavefunction, and discarding all terms in $\Delta E$ that contribute for the first time beyond order $n$. By applying the variation principle to this functional the XCC($n$) equations are then obtained. XCC(2) is equivalent with MP2, XCC(3) with LCCD. XCC(4) corresponds to an approximate CCSDT method, in which all terms that contribute for the first time at fifth or higher order are discarded. XCC(5) is correct to fifth order, although no $\hat{T}_4$ terms appear in the equations. This 'implicit' account for $\hat{T}_4$ is a main asset of XCC(5), as it circumvents the expensive $O(n^9)$ iteration of connected quadruples.

UCC is based on a unitary cluster operator $\hat{\tau} \equiv \hat{T} - \hat{T}^+$. Its energy expression simply becomes

$$\Delta E_{\mathrm{UCC}} = \frac{\langle\psi_0|\exp(\hat{\tau}^+)\hat{H}'\exp(\hat{\tau})|\psi_0\rangle}{\langle\psi_0|\exp(\hat{\tau}^+)\exp(\hat{\tau})|\psi_0\rangle} \tag{1.272}$$

UCC($n$) has the same advantages as XCC($n$), except that it also satisfies the *generalized Hellmann-Feynman* theorem, i.e. the energy is exactly stationary in the cluster amplitudes (like e.g. a CI wavefunction). This means that gradients can be evaluated with comparative ease, as CPHF equations only have to be solved for the orbitals, not for the amplitudes.

More details can be found in a recent review [Bar89b]. As at least the advantage of eliminating the $O(n^9)$ step is also associated with quasiperturbative account of quadruples, and recent advances in response theory [Hel88, Koc90, and references therein] have eliminated much of the problems associated with not satisfying the generalized Hellmann-Feynman theorem, the UCC method appears to have been 'sidetracked'.

## 1.7 Relationship between coupled cluster and MBPT theories

Let us recapitulate the CCSDTQ equations in normal operator form [Kuc89, Bar90b]:

$$\Delta E = \langle 0|\hat{W}(\hat{T}_2 + \hat{T}_1^2/2)|0\rangle \quad (1.273)$$

$$D_1T_1 = \hat{W}[\hat{T}_1 + \hat{T}_2 + \hat{T}_1^2/2 + \hat{T}_3 + \hat{T}_1\hat{T}_2 + \hat{T}_1^3/6] \quad (1.274)$$

$$D_2T_2 = \hat{W}[1 + \hat{T}_1 + \hat{T}_2 + \hat{T}_1^2/2 + \hat{T}_3 + \hat{T}_1\hat{T}_2 + \hat{T}_1^3/6 + \hat{T}_4 + \hat{T}_1\hat{T}_3 + \hat{T}_2^2/2 + \hat{T}_1^2\hat{T}_2/2 + \hat{T}_1^4/24] \quad (1.275)$$

$$D_3T_3 = \hat{W}[\hat{T}_2 + \hat{T}_3 + \hat{T}_1\hat{T}_2 + \hat{T}_4 + \hat{T}_1\hat{T}_3 + \hat{T}_2^2/2 + \hat{T}_1^2\hat{T}_2/2 + \hat{T}_1\hat{T}_4 + \hat{T}_2\hat{T}_3 + \hat{T}_1^2\hat{T}_3/2 + \hat{T}_1\hat{T}_2^2/2 + \hat{T}_1^3\hat{T}_2/6] \quad (1.276)$$

$$D_4T_4 = \hat{W}[\hat{T}_3 + \hat{T}_4 + \hat{T}_1\hat{T}_3 + \hat{T}_2^2/2 + \hat{T}_1\hat{T}_4 + \hat{T}_2\hat{T}_3 + \hat{T}_1^2\hat{T}_3/2 + \hat{T}_1\hat{T}_2^2/2 + \hat{T}_2\hat{T}_4 + \hat{T}_1^2\hat{T}_4/2 + \hat{T}_3^2/2 + \hat{T}_1\hat{T}_2\hat{T}_3 + \hat{T}_1^3\hat{T}_3 + \hat{T}_2^3/6 + \hat{T}_1^2\hat{T}_2^2/4] \quad (1.277)$$

Actually, what these equations allow is to obtain the MBPT wavefunction amplitudes in a convenient iterative manner. Let us introduce for convenience the notation $\hat{T}_n^{(m)}$, denoting the m-th order contribution to $T_n$. Now realize that every multiplication by $\hat{W}$ increases the order by one[28].

At zeroth order, all amplitudes are zero. The only term that contributes anything for a HF reference is the "1" term in the $\hat{T}_2$ equation (1.275). This results in a first-order effect $\hat{T}_2^{(1)}$, which is none other of course than the first-order MBPT amplitude (this can easily be verified by working out the matrix elements).

Now substitute $\hat{T}_2^{(1)}$ in all the other equations. In the $\Delta E$ equation, we obtain a contribution at second order $E^{(2)}$, which is of course identical to the MP2 energy. In the $\hat{T}_1$ equation, a second-order effect $\hat{T}_1^{(2)}$ is produced. (An alternative formulation of Brillouin's theorem is thus that single excitations do not occur in first order in the MBPT wavefunction.) A similar contribution $\hat{T}_3^{(2)}$ is produced in the $\hat{T}_3$ equation. No effect is seen as yet in the $\hat{T}_4$ equation, whereas two terms would contribute to the $\hat{T}_2$ equation, namely $\hat{T}_2$ and $\hat{T}_2^2/2$. The former term produces $\hat{T}_2^{(2)}$; the latter, corresponding to $(\hat{T}_2^{(1)})^2/2$ or $(\hat{T}_2^2)^{(2)}/2$, corresponds to the disconnected quadruple excitations in the second-order wavefunction, but influences the $\hat{T}_2$ amplitudes only in third order.

We have thus obtained the well-known result, that the second-order MBPT wavefunction contains only single, double, triple, and disconnected quadruple excitations.

At the next iteration, we could substitute two terms in $\Delta E$, namely $\hat{T}_2^{(2)}$ and $(\hat{T}_1^{(2)})^2/2$; the latter contributes only at fifth order to the energy, whereas the former is of course $E^{(3)}$. So up to third order, only double excitations contribute to the energy. Three terms affect $\hat{T}_1$, namely $\hat{T}_1^{(2)}$, $\hat{T}_2^{(2)}$, and $\hat{T}_3^{(2)}$; we will denote their contributions $\hat{T}_1^{(3)}(\mathrm{S})$, $\hat{T}_1^{(3)}(\mathrm{D})$, and $\hat{T}_1^{(3)}(T)$, respectively. In the doubles equation, four terms contribute to $\hat{T}_2^{(3)}$, namely $\hat{T}_1^{(2)}$, $\hat{T}_2^{(2)}$, $\hat{T}_3^{(2)}$, and $(\hat{T}_2^{(1)})^2/2$; we will denote their contributions $\hat{T}_2^{(3)}(\mathrm{S})$,

[28]Part of the analysis below has never been published before, to the author's knowledge.

$\hat{T}_2^{(3)}(\mathrm{D})$, $\hat{T}_2^{(3)}(\mathrm{T})$, and $\hat{T}_2^{(3)}(\mathrm{Q_{dd}})$. Three terms affect the triples amplitudes, namely $\hat{T}_2^{(2)}$, $\hat{T}_3^{(2)}$, and $(\hat{T}_2^{(1)})^2/2$; their contributions will be denoted $\hat{T}_3^{(3)}(\mathrm{D})$, $\hat{T}_3^{(3)}(\mathrm{T})$, and $\hat{T}_3^{(3)}(\mathrm{Q_{dd}})$. Finally, connected quadruple excitations make their first entrance through the effect of $\hat{T}_3^{(2)}$ on $\hat{T}_4$. Except for these excitation types, some disconnected terms figure in the third-order wavefunction, namely disconnected triples $\hat{T}_1^{(2)}\hat{T}_2^{(1)}$, disconnected quintuples $\hat{T}_3^{(2)}\hat{T}_2^{(1)}$, and finally disconnected sextuples $(\hat{T}_2^{(2)})^3/6$. (Connected quintuples start only out in the fourth-order, connected sextuples in the fifth-order wavefunction.)

At the fourth iteration, we obtain through $\hat{T}_2^{(3)}$ the four familiar fourth-order energy terms $E^{(4)}(\mathrm{S})$, $E^{(4)}(\mathrm{D})$, $E^{(4)}(\mathrm{T})$, and $E^{(4)}(\mathrm{Q_{dd}})$. To be able to investigate the fifth-order energy term, we will also iterate the $\hat{T}_2$ equation one more time. We now have six terms that should be considered, namely $\hat{T}_1^{(3)}$, $\hat{T}_2^{(3)}$, $\hat{T}_3^{(3)}$, $\hat{T}_2^{(1)}\hat{T}_2^{(2)}$, $\hat{T}_4^{(3)}$, and $\hat{T}_2^{(1)}\hat{T}_1^{(2)}$. All these result in a bunch of $\hat{T}_2^{(4)}$ terms that will be broken down below.

At the fifth iteration, two terms will contribute to $\Delta E$, namely $(\hat{T}_1^{(2)})^2/2$, resulting in an energy term[29] $E^{(5)}(\mathrm{D_{ss}})$, and $\hat{T}_2^{(4)}$, resulting in the set of energy terms $E^{(5)}(\mathrm{SD})$, $E^{(5)}(\mathrm{SS})$, $E^{(5)}(\mathrm{ST})$, $E^{(5)}(\mathrm{DS})$, $E^{(5)}(\mathrm{DD})$, $E^{(5)}(\mathrm{DT})$, $E^{(5)}(\mathrm{DQ_{dd}})$, $E^{(5)}(\mathrm{DQ})$, $E^{(5)}(\mathrm{TS})$, $E^{(5)}(\mathrm{TD})$, $E^{(5)}(\mathrm{TT})$, $E^{(5)}(\mathrm{QT})$, $E^{(5)}(\mathrm{QQ_{dd}})$, and $E^{(5)}(\mathrm{T_{ds}})$. Note that the present notation differs from that used in perturbation theory, corresponding to the hierarchy of terms rather than the intervertex excitation level.

For the remaining terms, we will quote the lowest order in PT at which they affect the energy: for the list ($\hat{T}_1\hat{T}_2$, $\hat{T}_1^2/2$, $\hat{T}_1^3/6$) in the $\hat{T}_1$ equation this is (6,7,9); for the list ($\hat{T}_1T_3$, $\hat{T}_1^2/2$, $\hat{T}_1^2\hat{T}_2/2$, $\hat{T}_1^3/6$, $\hat{T}_1^4/24$) in the $\hat{T}_2$ equation we find (6,6,7,8,10); for the list ($\hat{T}_4$, $\hat{T}_1\hat{T}_2$, $\hat{T}_2T_3$, $\hat{T}_1\hat{T}_3$, $\hat{T}_1\hat{T}_4$, $\hat{T}_2^2\hat{T}_1/2$, $\hat{T}_1^2\hat{T}_2/2$, $\hat{T}_1^2\hat{T}_3/2$, $\hat{T}_1^3\hat{T}_2/6$) in the $\hat{T}_3$ equation we obtain (6,6,6,7,8,7,8,9,10); and finally for the 13 remaining terms in the $\hat{T}_4$ equation ($\hat{T}_4$, $\hat{T}_2^3/6$, $\hat{T}_1^2\hat{T}_4/2$, $\hat{T}_2\hat{T}_3$, $\hat{T}_1\hat{T}_3$, $\hat{T}_2\hat{T}_4$, $\hat{T}_1\hat{T}_2\hat{T}_3$, $\hat{T}_2^2\hat{T}_1/2$, $\hat{T}_3^2/2$, $\hat{T}_2^2\hat{T}_1^2/4$, $\hat{T}_1\hat{T}_4$, $\hat{T}_1^2\hat{T}_3/2$, $\hat{T}_1^3\hat{T}_3/6$) we obtain the lowest energy orders (6,6,10,6,7,7,9,7,7,9,8,9,11).

At what order would connected quintuples and sextuples enter the energy? Well, the lowest terms that can still produce connected quintuples in the $\hat{T}_5$ equation are $\hat{T}_2\hat{T}_3$ and $\hat{T}_4$, all starting at third order. This yields a fourth-order wavefunction contribution affecting $\hat{T}_3$ and $\hat{T}_4$, of which a fifth-order contribution in $\hat{T}_3$ is the lowest order result, which would produce a sixth-order effect on $\hat{T}_2$ and finally only a seventh-order contribution to the energy. The lowest-order connected sextuples can be made by $\hat{T}_5$, $\hat{T}_2\hat{T}_4$, and $\hat{T}_3^2/2$, all starting at fourth order, which yields a fifth-order $\hat{T}_6$ term that affects the $\hat{T}_4$ equation at the lowest. There it produces a sixth-order term in $\hat{T}_4$, which affects the doubles wavefunction at seventh order and finally the energy at eighth order. In other terms, a full CCSDTQ calculation is exact to sixth order in perturbation theory!

[29] $\mathrm{D_{ss}}$ denotes disconnected double excitations from two single excitations. Likewise, $\mathrm{T_{ds}}$ denotes disconnected triple excitations from a double and a single excitation, and so on.

Figure 1.11: Some examples of wavefunction diagrams [Kuc86, page 287].

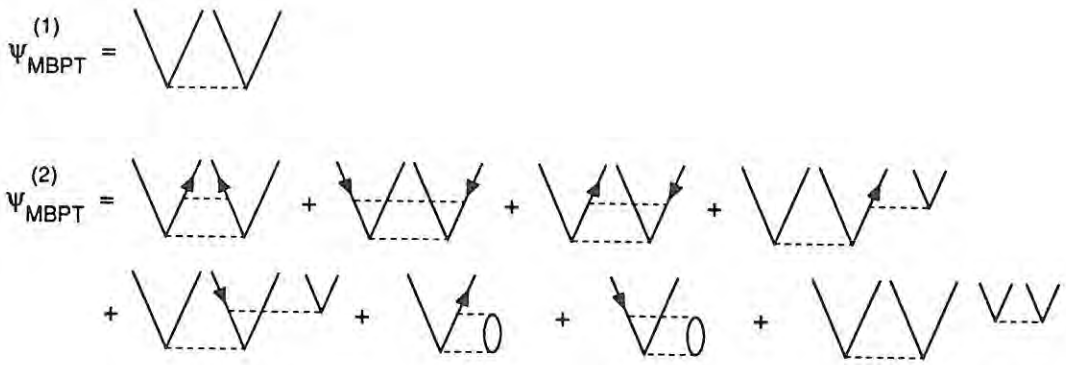


Figure 1.12: Diagrammatic representation of cluster operators $\hat{T}_n$ [Kuc86, top of page 298].

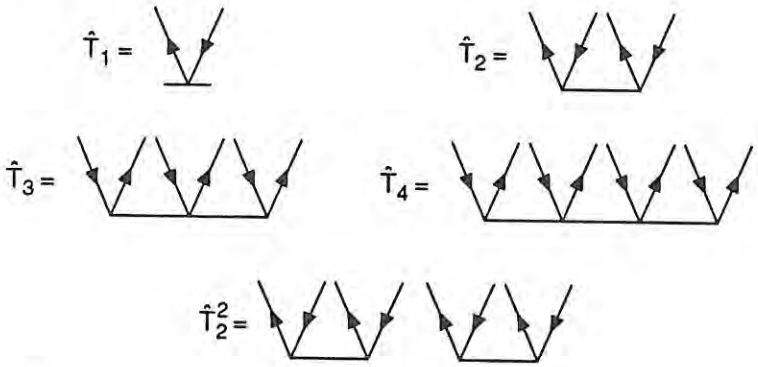


### 1.7.1 Diagrammatic formulation of the coupled cluster equations

MBPT wavefunction terms can just as well be represented by diagrams as MBPT energy terms [Kuc86]. We will use AGDs here.

A wavefunction of finite order corresponds to the lower part of a regular AGD that has been divided horizontally. The number of vertices remaining is the order of the diagram: half the number of 'dangling' ends (i.e. unconnected hole and particle lines) is the excitation level. The diagram is disconnected if it 'falls apart' in two or more pieces, otherwise it is connected. Some examples are given in Figure 1.11.

The cluster terms in the CC equations are represented by similar diagrams, with the bottom vertex replaced by a solid line, which is called an *iteration line.* At any given iteration of the CC equations according to the procedure discussed above, any wavefunction diagram that 'fits' can be inserted into the iteration line. Some examples are presented in Figure 1.12.

Finally, we should have a diagrammatic representation for $\hat{W}$. This is simply a

Figure 1.13: Diagrammatic representation of the normal-form Hamiltonian for a Hartree-Fock reference wavefunction (adapted from [Kuc86, bottom of page 298]).

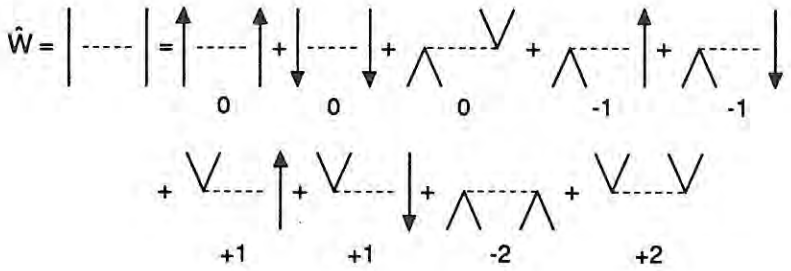


Figure 1.14: Some examples of linked and unlinked cluster terms.

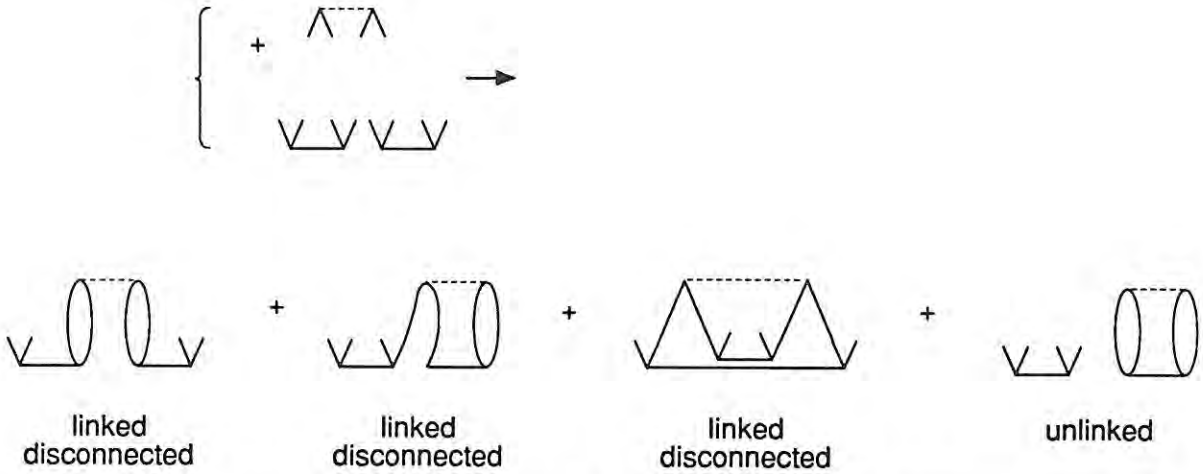


The $\hat{T}_2^2/2$ wavefunction diagram can be connected with the '-2' $\hat{W}$ diagram in four topologically distinct ways shown above. The first three possibilities generate linked diagrams, the fourth leads to an unlinked diagram. Substituting $(\hat{T}_2^{(1)})^2/2$ at the bottom and connecting the '-2' diagram of the $\Delta E$ equation at the top, and considering all distinct relative orderings of the vertices, leads to the nine fourth-order quadruples diagrams shown in Figure 1.9. Diagram (A) there comes from the leftmost possibility; diagrams (B), (C), (D), and (E) from the second one; diagrams (F) and (G) from the third one; and finally the unlinked diagrams (H) and (I) are offspring from the rightmost case.

vertex with two hole and two particle 'dangling ends'. These can be connected in nine topologically distinct ways shown in Figure 1.13. Of these, the first three possibilities leave the excitation level unchanged, the following two reduce the excitation level by one, the next two increase it by one, followed by one which decreases the excitation level by two and finally another which increases it by two.

To find the diagrammatic representation of an $n$-th excitation term in the equation for the $\hat{T}_m$ amplitudes, one should take those $\hat{W}$ diagrams — one at a time — that lower the excitation level from $n$ to $m$ (the term will simply not contribute if there aren't

any), and connect them at the top of the cluster diagrams in all topologically distinct ways. It is then very readily seen whether that particular term in $\hat{T}_m$ is connected, linked disconnected, or unlinked. If the diagram falls apart in two or more pieces, it is disconnected. If any of these pieces is in itself a closed MBPT diagram, the term is unlinked too. Some illustrative examples are given in Figure 1.14.

It is readily seen, that the case +2 for the $\hat{W}$ diagrams always results in disconnected diagrams, except for the "1" term in the $\hat{T}_2$ equation. As a further illustration, let us consider the terms dropping out of the $\hat{T}_3$ equation, which were $\hat{T}_1^n/n!$. The case $n = 1$ can only be made into a triple excitation by applying the +2 term of $\hat{W}$, and will thus fall apart into two disjoint pieces. The case $n = 2$ consists of two disjoint $\hat{T}_1$ diagrams, whose excitation level has to be raised by one to produce a triple excitation. The two +1 diagrams in $\hat{W}$ have only one vacant line end, leaving one of the two pieces 'hanging in the air' and thus resulting in a disconnected diagram. The case $n = 3$ already has the correct excitation level, so the +0 diagrams of $\hat{W}$ have to be applied. All three of these can 'mend' two of the three disjoint pieces together, with one dangling piece remaining: the diagram is disconnected. For the case $n = 4$, the excitation level has to be lowered by one. The two $\hat{W}$ diagrams that can do this can connect up to three diagrams, leaving the fourth disjoint piece hanging loose. And finally, the case $n = 5$ requires the "-2" diagram of $\hat{W}$, which can connect up to four of these pieces, i.e. still one too few.

As an additional illustration, the $\hat{T}_1^2\hat{T}_2/2$ term does not drop out of the $\hat{T}_3$ equation. It falls apart into three pieces, but has an excitation level of four which should be lowered by one. The -1 terms of $\hat{W}$ can connect up to three diagrams, which is enough to fuse it into one piece.

Observing that the "$-k$" terms of $\hat{W}$ have $k+2$ vacant line endings at the bottom and will thus connect $k+2$ diagram pieces at most, we can formulate the following theorem:

> If a cluster diagram of total excitation level $l$ appears in the $\hat{T}_m$ equation, it will not result in any connected contributions if it is composed of more than $m - l + 2$ disjoint pieces.

Figure 1.15 gives the diagrammatic representation of the CCSDT equations. The $\Delta E$ equation is of course obtained by enforcing a final excitation level of zero, which closes the diagram from above.

The iteration procedure of the previous section may now be repeated diagrammatically. Initially, no diagrams can be filled in, leaving the loose +2 diagram in $\hat{W}$ as the only term, this giving the first-order contribution to $\hat{T}_2$. In the next iteration, this diagram is substituted for the $\hat{T}_2$ iteration lines in $\Delta E$, resulting in the familiar second-order energy diagram, as well as in the $\hat{T}_1$ and $\hat{T}_3$ equations, resulting in the corresponding second-order wavefunction diagrams. In the next iteration, the second-order $\hat{T}_2$ diagrams are substituted in the $\Delta E$ equation, giving a third-order skeleton diagram that can be

Figure 1.15: Diagrammatic representation of the CCSDT equations for a Hartree-Fock reference (adapted from [Kuc86, pp. 304–305]).

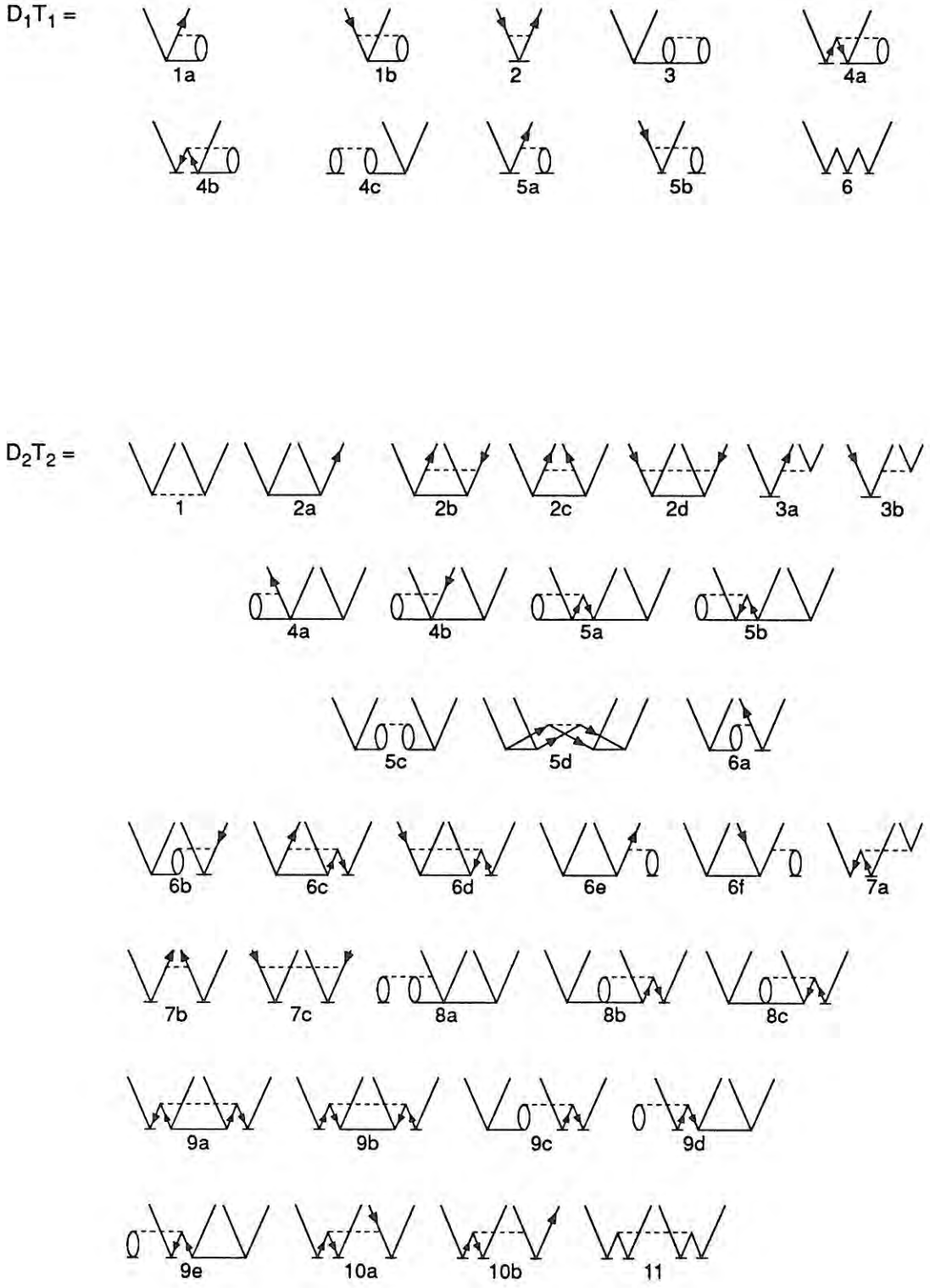

Figure 1.15: (continued)

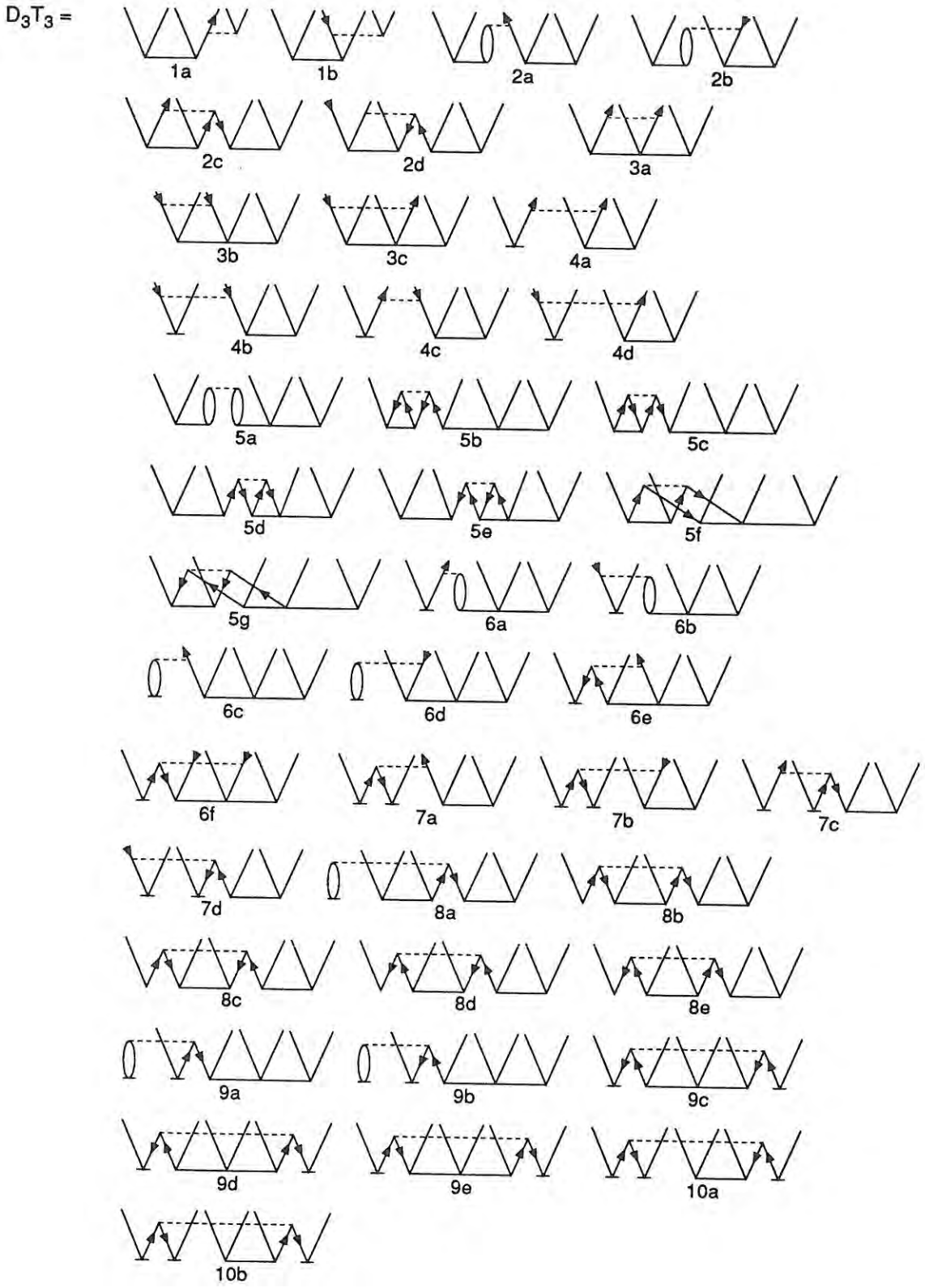

Figure 1.16: Graphical representation of the relationship between cluster terms and MBPT diagrams at fifth order [Kuc86, page 324].

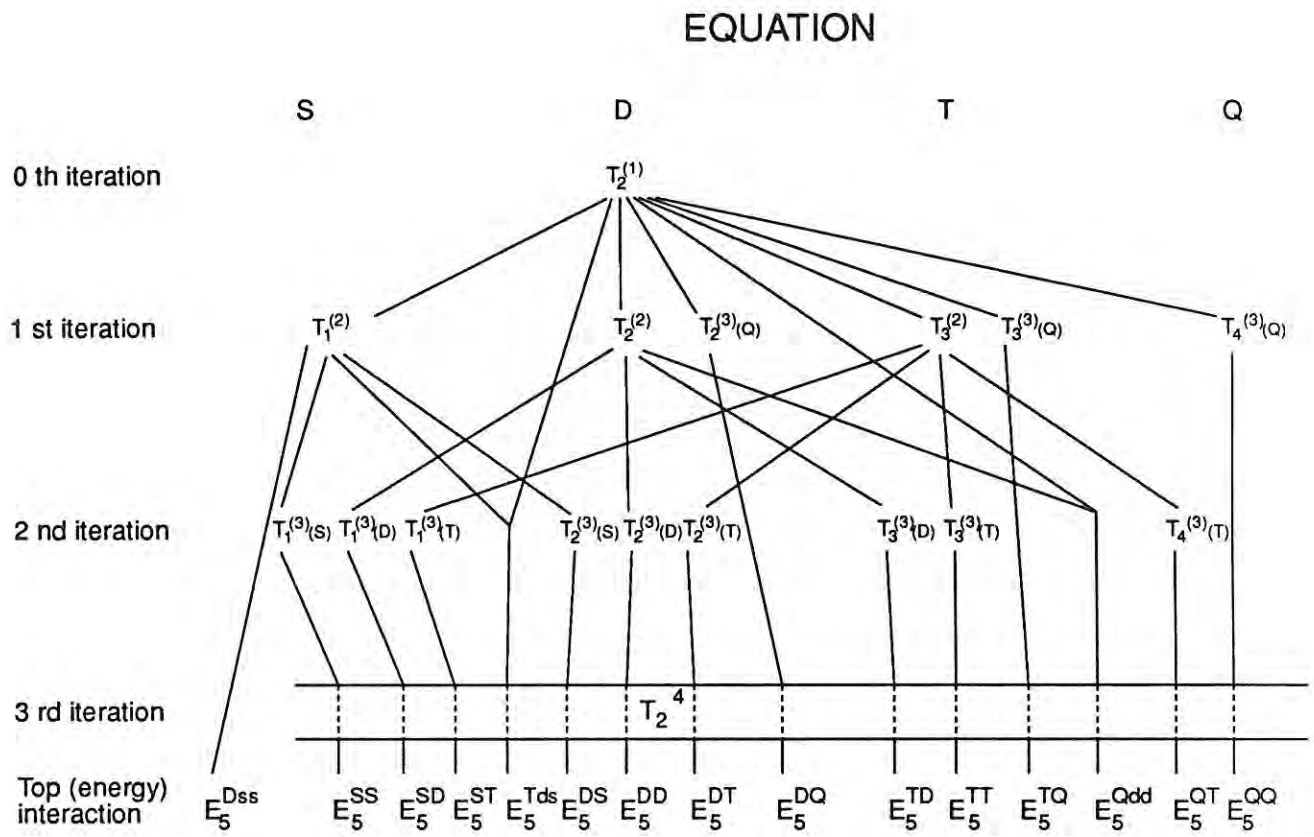


labeled with hole and particle states in three distinct ways, corresponding to the familiar three MP3 diagrams. In the $\hat{T}_2$ equation, it is now time for the $\hat{T}_1$ and $\hat{T}_3$ diagrams to be inserted for the first time, as well as for the second-order $\hat{T}_2$ diagram and for $(\hat{T}_2^{(1)})^2/2$. For this case, as well as for $\hat{T}_3$, there are a number of topologically distinct possibilities, all of which should be included. In the $\hat{T}_2^2/2$ case, only the possibilities that correspond to connected contributions should be retained; here, the only disconnected contribution is unlinked as well, and gives rise, if substituted in the $\Delta E$ equation, to two distinct topological possibilities which are our familiar unlinked fourth-order diagrams (that are here already cancelled against the renormalization energy). This procedure can be continued as long as one likes, and will generate all the same diagrams, order by order, as we have seen in the section on MBPT.

Note that the intervertex excitation levels of the fifth-order diagrams lead to an energy term nomenclature different from that used in the previous section. Figure 1.16 is a graphical representation of the correspondence between terms in various representations. Note that some of the diagrams can actually be found by turning certain others upside down: these diagrams are still topologically different for the purposes of enumerating the

distinct diagrams, but correspond to expressions that are the Hermitian adjoint of each other. In a basis of real orbitals and basis functions, as we are always using, they are numerically equal.

### 1.7.2 Diagrammatic interpretation of quasiperturbative corrections

In Table I, a fifth-order comparison between various approximate coupled cluster methods is found: for each term, it is indicated whether it is accounted for properly at that level of theory.

It is immediately seen that some important terms are missing in QCISD compared to CCSD. We have already stated that this is partially 'fixed up' by the quasiperturbative account of triples in QCISD(T). To illustrate this let us consider the form of the quasiperturbative expression.

First let us address the 'fourth-order like' term, that also appears in CCSD+T(CCSD) and CCD+T(CCD). Actually, it is obtained by taking all diagrams contributing to $E_T^{(4)}$ and replacing the top and bottom vertices with iteration lines. In these, all double-excitation wavefunction diagrams, to infinite order, from a converged CCSD resp. CCD calculation are put in at the bottom, their complex conjugates at the top, and all resulting diagrams are summed over all possibilities and mutual combinations. For the CCSD case, this is easily seen to produce all diagrams, to infinite order, that appear in a CCSDT calculation and that have exactly one intervertex excitation level of three — with two adjacent levels of two — and do not include cross-terms involving $\hat{T}_3$. For the CCD case, the same holds, but now for all the CCDT diagrams that have at most one intervertex excitation level of three and excluding cross-terms in $\hat{T}_3$. Or, in PT language, $E_{4\mathrm{T}}$, $2E_{5\mathrm{DT}}$, $2E_{6\mathrm{TD}x}$, $2E_{6\mathrm{DTD}}$, and similar higher order terms (where $x$ denotes D or $\mathrm{Q_{dd}}$ for CCD(T), and S, D, $\mathrm{T_{ds}}$, or $\mathrm{Q_{dd}}$ for CCSD+T(CCSD)).

The 'fourth-order like' single excitation term in CCD+S(CCD) likewise corresponds to all the single excitation diagrams, with an iteration line substituted at the top and the bottom, and consequently all diagrams from a CCSD calculation that have at most one intervertex excitation level of one and do not involve products of $\hat{T}_1$. Or, in PT language, the terms $E_{4\mathrm{S}}$, $2E_{5\mathrm{SD}}$, $2E_{6\mathrm{SD}x}$, $2E_{6\mathrm{DSD}}$, and similar higher order terms (where $x$ denotes D or $\mathrm{Q_{dd}}$).

Finally, we discuss the 'fifth-order like' term. It consists of the $E_{5\mathrm{ST}}$ and $E_{5\mathrm{TS}}$ diagrams in the MBPT classification — which are of course Hermitian conjugates of each other — with the $\hat{T}_1^{(2)}$ and $\hat{T}_2^{(1)}$ ends replaced by $\hat{T}_1$ and $\hat{T}_2$ iteration lines, respectively. This includes a whole series of diagrams to infinite order, namely all diagrams that involve exactly one instance of $\hat{T}_3$, with one adjacent single and one adjacent double intermediate state. In PT language, this corresponds, besides $2E_{5\mathrm{ST}}$, to $2E_{6x\mathrm{ST}}$, $2E_{6\mathrm{STD}}$, and similar higher-order terms. Half these terms at fifth and higher order are already included in a

Table I: A fifth-order comparison of various electron correlation methods (Adapted from [Kuc86, pp. 322-323]).

| Method | $E_5^{SS}$ | $E_5^{SD}$ | $E_5^{ST}$ | $E_5^{DS}$ | $E_5^{DD}$ | $E_5^{DT}$ | $E_5^{DQ}$ | $E_5^{T_{ds}}$ |
|---|---|---|---|---|---|---|---|---|
| L-CCD | | | | | × | | | |
| CCD | | | | | × | | × | |
| CCD(T) | | | | | × | × | × | |
| CCD(ST) | | × | | × | × | × | × | |
| L-CCSD | × | × | | × | × | | | |
| CCSD | × | × | | × | × | | × | × |
| CCSD+T(CCSD) | × | × | | × | × | × | × | × |
| CCSD(T) | × | × | × | × | × | × | × | × |
| CCSD(TQ) | × | × | × | × | × | × | × | × |
| QCISD | × | × | | × | × | | × | |
| QCISD(T) | × | × | 2× | × | × | × | × | √ |
| QCISD(TQ) | × | × | 2× | × | × | × | × | × |
| BD | × | × | √ | × | × | | × | × |
| BD(T) | × | × | √ | × | × | × | × | × |
| BD(TQ) | × | × | × | × | × | × | × | × |
| CCSDT-1 | × | × | × | × | × | × | × | × |
| CCSDT-2 | × | × | × | × | × | × | × | × |
| CCSDT-3 | × | × | × | × | × | × | × | × |
| CCSDT | × | × | × | × | × | × | × | × |
| CCSDT(Q) | × | × | × | × | × | × | × | × |
| CCSDTQ | × | × | × | × | × | × | × | × |

| Method | $E_5^{TD}$ | $E_5^{TT}$ | $E_5^{TQ}$ | $E_5^{Q_{dd}}$ | $E_5^{QT}$ | $E_5^{QQ}$ | $E_5^{D_{ss}}$ |
|---|---|---|---|---|---|---|---|
| L-CCD | | | | | | | |
| CCD | | | | × | | | |
| CCD(T) | × | | | × | | | |
| CCD(ST) | × | | | × | | | |
| L-CCSD | | | | | | | |
| CCSD | | | | × | | | × |
| CCSD+T(CCSD) | × | | | × | | | × |
| CCSD(T) | × | | | × | | | × |
| CCSD(TQ) | × | × | × | × | × | × | × |
| QCISD | | | | × | | | × |
| QCISD(T) | × | | | × | | | √ |
| QCISD(TQ) | × | × | × | × | × | × | × |
| BD | | | √ | × | | | 2× |
| BD(T) | × | | √ | × | | | 2× |
| BD(TQ) | × | × | × | × | × | × | × |
| CCSDT-1 | × | | | × | | | × |
| CCSDT-2 | × | | × | × | | | × |
| CCSDT-3 | × | | × | × | | | × |
| CCSDT | × | × | × | × | | | × |
| CCSDT(Q) | × | × | × | × | × | × | × |
| CCSDTQ | × | × | × | × | × | × | × |

√ Included through double-counting another term that involves diagrams that are the Hermitian conjugate of those in the present term.

CCSD calculation through the operator $\hat{T}_1\hat{T}_2$ in the doubles equation, and $\hat{T}_1^2/2$ in the triples equation; these terms are lacking in the QCISD equations. So what is done is to include half the 'fifth-order like' correction in the CCSD(T) case, and all of it in the QCISD(T) case, thus taking care that this particular class of terms is included properly in both cases. Of course, the correction is not done in the CCSD+T(CCSD) case, which results in neglecting the $E_{5ST}$ contribution as well as related contributions at higher orders.

The 'fourth-order' and 'fifth-order' like terms together include, of the diagrams that are missing compared to a full CCSDT calculation, all diagrams that involve precisely one connected triple excitation intermediate state, and no further instances of $\hat{T}_3$.

Similarly, a Q(CCSD) or Q(CCSDT) calculation will, except for the fifth-order connected quadruples term, include important higher-order diagrams derived from these.

### 1.7.3 Relationship between limited CI and MBPT

The methodological relationship between limited CI and coupled cluster theory should have been clear from the outset; of course, the relationship between limited CI and MBPT follows by induction. One remark is still due, however.

Let us write the CI matrix in a block-structured fashion, i.e. with all determinants of a given excitation level grouped together. Wilson [Wil84, p.201] then derived the lowest order of MBPT in which any block appears for the first time:

| | $\psi_0$ | $\hat{C}_1$ | $\hat{C}_2$ | $\hat{C}_3$ | $\hat{C}_4$ | $\hat{C}_5$ | $\hat{C}_6$ | $\hat{C}_7$ | ... |
|---|---|---|---|---|---|---|---|---|---|
| $\psi_0$ | 0 | | 2 | | | | | | |
| $\hat{C}_1$ | | 5 | 4 | 5 | | | | | |
| $\hat{C}_2$ | 2 | 4 | 3 | 4 | 4 | | | | |
| $\hat{C}_3$ | | 5 | 4 | 5 | 5 | 6 | | | |
| $\hat{C}_4$ | | | 4 | 5 | 5 | 6 | 6 | | |
| $\hat{C}_5$ | | | | 6 | 6 | 7 | 7 | 8 | |
| $\hat{C}_6$ | | | | | 6 | 7 | 7 | 8 | ... |
| $\hat{C}_7$ | | | | | | 8 | 8 | 9 | ... |
| ... | | | | | | | ... | ... | ... |

(1.278)

where white space denotes vanishing matrix elements. The array can be continued at will in that symmetric pattern to any desired order. Note that the connected or disconnected character of the excitations is not specified, e.g. the $\langle\hat{C}_4|\hat{W}|\hat{C}_2\rangle$ block is actually $\langle\hat{T}_2^2/2|\hat{W}|\hat{T}_2\rangle$ in coupled cluster language. Likewise, the sixth-order terms involving quintuple and hextuple excitations only involve disconnected terms at that order.

## 1.8 Spin projected Hartree-Fock and MBPT

The slow convergence in cases with spin contamination significantly reduces the usefulness of MBPT methods. Extension to ROHF wavefunctions, where the problem is ipso facto

nonexistent, is by no means trivial, contrary to the CI (and, to a lesser extent, CC) cases. Therefore, alternative methods have been sought to allow the application of these very cost-effective methods to spin-contaminated cases.

Equations for a spin-projected UHF method have been known since a long time (see [May80] for a review). Let the Löwdin spin projection operator [Loe55] be defined as

$$\hat{P}_s = \prod_{k \neq s} \frac{\hat{S}^2 - k(k+1)}{s(s+1) - k(k+1)} \tag{1.279}$$

where $s$ is the spin quantum number for the state of interest. The spin-projected UHF energy is then given (in regular normalization) by

$$E_{projUHF} = \frac{\langle \hat{P}_s \psi_0 | \hat{H} | \hat{P}_s \psi_0 \rangle}{\langle \hat{P}_s \psi_0 | \hat{P}_s \psi_0 \rangle} = \frac{\langle \psi_0 | \hat{H} \hat{P}_s | \psi_0 \rangle}{\langle \psi_0 | \hat{P}_s | \psi_0 \rangle} \tag{1.280}$$

Note that the operator $\hat{P}_s$ is idempotent, and commutes with $\hat{H}$. By inserting the closure condition, which states that the identity operator can be written as

$$\hat{I} = |\psi_0\rangle\langle\psi_0| + \sum_j |\psi_j\rangle\langle\psi_j| \tag{1.281}$$

(where $j$ runs over all excited determinants) between $\hat{H}$ and $\hat{P}_s$, we can expand the numerator and obtain

$$E_{\mathrm{projUHF}} = E_{\mathrm{UHF}} + \frac{\sum_i \langle \psi_0 | \hat{H} \hat{P}_s | \psi_i \rangle \langle \psi_i | \hat{P}_s | \psi_0 \rangle}{\langle \psi_0 | \hat{P}_s | \psi_0 \rangle} \tag{1.282}$$

where $i$ only runs over doubly excited states only because of Brillouin's theorem and the fact that $\hat{H}$ contains at most two-electron operators.

In most practical cases, the major part of the spin contamination comes from the next higher spin; e.g. a doublet will have mostly quartet contamination and a triplet mostly quintet contamination. Under such circumstances, the full Löwdin projection operator might be approximated by the $s+1$ factor alone, which is then called a spin annihilator (not to be confused with the annihilation operators in second quantization). The $n$-th spin annihilator is given by

$$\hat{A}_{s+n} = \frac{\hat{S}^2 - (s+n)(s+n+1)}{\langle \psi_0 | \hat{S}^2 | \psi_0 \rangle - (s+n)(s+n+1)} \tag{1.283}$$

where the choice of the denominator ensures that $\hat{A}_{s+n}\psi_0$ is intermediately normalized. (*Important note:* $\hat{A}_{s+n}$ is only idempotent when no other contaminants than the $n$-th are present. The papers by Schlegel on spin-projected methods [Sch86, Sch88] disregard this fact [Mar90a]; see also Section 5.2.)

Selecting $n = 1$, we obtain the following expression for the PUHF energy:

$$E_{\mathrm{PUHF}} = E_{\mathrm{UHF}} + \frac{\sum_i \langle \psi_0 | \hat{H} | \psi_i \rangle \langle \psi_i | \hat{S}^2 | \psi_0 \rangle}{\langle \psi_0 | \hat{S}^2 | \psi_0 \rangle - (s+1)(s+2)} \tag{1.284}$$

$$\hat{A}_{s+1}\psi_0 = \psi_0 + \frac{\sum_j |\psi_j\rangle\langle\psi_j| \hat{S}^2 |\psi_0\rangle}{\langle \psi_0 | \hat{S}^2 | \psi_0 \rangle - (s+1)(s+2)} \equiv \psi_0 + \tilde{\psi}_1 \tag{1.285}$$

where $i$ runs over all double excitations, and $j$ over all single and double excitations (the singles contribute to the wavefunction, but cannot affect the energy).

At the MP2 level, the energy is produced from the first-order wavefunction $\psi_1$, which will contain a $\tilde{\psi}_1$ component too. The correction should then be diminished, as a first approximation, by the magnitude of that component:

$$E_{\mathrm{PMP2}} = E_{\mathrm{UMP2}} + \Delta E_{\mathrm{PUHF}}(1 - \frac{\langle\tilde{\psi}_1|\psi_1\rangle}{\langle\tilde{\psi}_1|\tilde{\psi}_1\rangle}) \tag{1.286}$$

At third order, a similar correction should be made for the second-order wavefunction $\psi_2$, leading to:

$$E_{\mathrm{PMP3}} = E_{\mathrm{UMP3}} + \Delta E_{\mathrm{PUHF}}(1 - \frac{\langle\tilde{\psi}_1|\psi_1 + \psi_2\rangle}{\langle\tilde{\psi}_1|\tilde{\psi}_1\rangle}) \tag{1.287}$$

Then at fourth order, a correction should be introduced for (the doubles in) the third-order wavefunction, but this is normally neglected.

$$E_{\mathrm{PMP4}} = E_{\mathrm{UMP4}} + \Delta E_{\mathrm{PUHF}}(1 - \frac{\langle\tilde{\psi}_1|\psi_1 + \psi_2 + \psi_3\rangle}{\langle\tilde{\psi}_1|\tilde{\psi}_1\rangle}) \tag{1.288}$$

$$\approx E_{\mathrm{UMP4}} + E_{\mathrm{PMP3}} - E_{\mathrm{UMP3}} \tag{1.289}$$

These equations define the PMP$n$ methods. They are programmed in the GAUSSIAN 8X series from GAUSSIAN 86 on.

The main asset of the method is its simplicity and the negligible extra amount of computer time required to apply it. Important disadvantages are the incapability to correct for large single excitation effects, as well as the fact that it is no longer strictly size consistent: the energy of the fragments at very large distances is no longer exactly the sum of the fragment energies (this is caused by the presence of higher contaminants). Also, the method may break down if more than one important contaminant is present.

The latter problem can be overcome by the PMPn(m) methods, where the first $m$ contaminants are annihilated. The equations are very similar, with a product of several spin annihilators now figuring in the PUHF equation, which leads to an expression involving expectation values of powers of $\hat{S}^2$ for the matrix elements over it. The correction for the $\tilde{\psi}_1$ component is done identically.

Incidentally, the multiple projection also remedies the size-consistency problem.

This method is implemented in GAUSSIAN 88. Additional annihilators are added until the energies change by less than 1 microhartree upon doing so. It is perhaps the most cost-effective electron correlation method currently available for very heavily spin-contaminated wavefunctions.

## 1.9 Other nonvariational methods

### 1.9.1 Coupled electron pair approximation (CEPA)

Of the remaining electron correlation methods, the so-called *coupled electron pair approximation* should be briefly discussed. It has not been used in any of the present work, but occasionally comparison is made with CEPA literature values. These can of course not be assessed without some background information on the method. (More detailed information can be found in the reviews by Kutzelnigg [Kut77] and Ahlrichs [Ahl79].)

Let us recapitulate the LCCD equations

$$\langle\psi_{ij}^{ab}|H'|\psi_0\rangle + \frac{1}{2}\sum_{klcd} t_{kl}^{cd}\langle\psi_{ij}^{ab}|H'|\psi_{kl}^{cd}\rangle + \frac{1}{4}\sum_{klcd} t_{ij}^{ab}t_{kl}^{cd}\langle kl||cd\rangle = t_{ij}^{ab}E_{\mathrm{LCCD}} \tag{1.290}$$

that is to say

$$\langle\psi_{ij}^{ab}|H'|\psi_0\rangle + \frac{1}{2}\sum_{klcd} t_{kl}^{cd}\langle\psi_{ij}^{ab}|H'|\psi_{kl}^{cd}\rangle + t_{ij}^{ab}E_{\mathrm{LCCD}} = t_{ij}^{ab}E_{\mathrm{LCCD}} \tag{1.291}$$

where the last term on the left-hand side of course cancels with the right-hand side. But this term includes some EPV contributions (from the cases where two or more of the indices $ijklabcd$ coincide) that should cancel with those from the 'linked' disconnected quadruples that are neglected in LCCD. By correcting for this in a variety of ways, one obtains a new class of approximate methods that are both size-extensive and (more or less) exact for two-electron systems.

We introduce the *pair correlation energies*

$$e_{ij} = \frac{1}{2}\sum_{ab} t_{ij}^{ab}\langle ij||ab\rangle \tag{1.292}$$

that are easily seen to sum up to the total correlation energy:

$$\Delta E = \sum_{ij} e_{ij} \tag{1.293}$$

The last term of (1.290) is then approximated as

$$\frac{1}{4}\sum_{klcd}\langle kl||cd\rangle t_{ij}^{kl}t_{ab}^{cd} \approx t_{ij}^{ab}(\Delta E - A_{ij}) \tag{1.294}$$

where the following methods are defined through the choice of $A_{ij}$:

$$\text{CEPA(0):} \qquad A_{ij} = 0 \tag{1.295}$$

$$\text{CEPA(2):} \qquad A_{ij} = e_{ij} \tag{1.296}$$

$$\text{CEPA(1):} \qquad A_{ij} = \tfrac{1}{2}\textstyle\sum_k (e_{ik} + e_{jk}) \tag{1.297}$$

$$\text{CEPA(3):} \qquad A_{ij} = \tfrac{1}{2}\textstyle\sum_k (e_{ik} + e_{jk}) - e_{ij} \tag{1.298}$$

$$\text{CID:} \qquad A_{ij} = \tfrac{1}{2}\textstyle\sum_{kl} e_{kl} = \Delta E \tag{1.299}$$

CEPA(0) is of course readily seen to be equivalent to LCCD. In CEPA(3), proposed by Kelly [Kel64], all EPV terms are exactly accounted for. In CEPA(2), all terms where $(ij) = (kl)$ are deleted, which is a natural extension of the so-called *independent electron pair approximation* (IEPA) [Kut73], where even the wavefunction is approximated as a pair function:

$$t_{ij}^{ab} = \langle \psi_{ij}^{ab} | H' | \psi_0 + \psi_{ij} \rangle \tag{1.300}$$

$$\psi_{ij} = \frac{1}{2} \sum_{ab} t_{ij}^{ab} \psi_{ij}^{ab} \tag{1.301}$$

Finally, CEPA(1) is just the average between CEPA(3) and CEPA(2). CEPA(1) and CEPA(2) have been proposed by Meyer [Mey73].

IEPA was proposed independently by Sinanoğlu [Sin64] and Nesbet [Nes65]. It is often appropriately called 'pair-at-a-time' CI. It is size-extensive and very cost-effective (being noniterative); important disadvantages are severe overshooting of the correlation energy (120 % of the actual value is not uncommon), as well as noninvariance under transformations between partially occupied degenerate orbitals. [30]

The CEPA methods share the overshooting problem, but exhibit it to a much lesser extent. CEPA(0) $\equiv$ LCCD is invariant under transformations between degenerate orbitals, the other CEPA methods are not, but exhibit the problem to a much lesser extent than IEPA. Up to sixth order in perturbation theory, the following inequalities can be proven:

$$\text{CEPA(0)} < \text{CEPA(2)} < \text{CEPA(1)} < \text{CEPA(3)} < \text{CID} \tag{1.302}$$

Hurley [Hur76] conjectured that these inequalities hold to infinite order. As the difference between CEPA(3) and CCD involves 'repulsive' disconnected quadruple excitation diagrams, the inequalities may probably be extended to

$$\text{CEPA(0)} < \text{CEPA(2)} < \text{CEPA(1)} < \text{CEPA(3)} < \text{CCD} < \text{CID} \tag{1.303}$$

CEPA(n) still involves iterative solution, but this can be formulated in a computationally very efficient way through the *self consistent electron pairs* (SCEP) procedure of Meyer [Mey76]. More specifically, CID and all CEPA variants can be reformulated as minimization of a functional involving pair functions and pair energies[31]. Minimization of that functional involves pair Coulomb and exchange operators, which are essentially no less conveniently constructed in the AO than in the MO basis. This means that the integral transformation can be avoided entirely.

SCEP-CEPA calculations with 150 basis functions and more can routinely be carried out on a high-end scalar computer (see e.g. [Bot89] for an example).

[30] In other words, IEPA produces e.g. different energies for the degenerate $x$ and $y$ components of a $^2\Pi$ state!

[31] Such 'functional' methods are variational or nonvariational, depending on the definition of the functional.

The 'overshooting' makes the CEPA(n) methods less desirable for energy calculation purposes. The CEPA(n) methods have however been applied with great success to the calculation of potential energy surfaces; the work of Botschwina (see [Bot88] for a review) contains many fine examples. In these papers, energies are evaluated for scores or hundreds of displaced geometries, after which a high-order polynomial is fitted to these energies and spectroscopic constants derived from that. Dipole moment functions are constructed by repeating these calculations in positive and negative electric fields and applying a difference formula. The resulting polynomial of the dipole moment in the internal coordinates allows the determination of harmonic and anharmonic infrared intensities.

Mention should be made of the *coupled pair functional* (CPF) method recently developed by Ahlrichs and coworkers [Ahl85], which is closely related to the pair functional formulation of CEPA but has the additional advantage of being invariant under orbital rotations. (Pair function techniques have recently been reviewed by Ahlrichs and Scharf [Ahl87].)

A further modification called the *averaged coupled pair functional* (ACPF) [Gda88] allows the use of multiple reference determinants. The NASA Ames group is currently starting to use MR-ACPF instead of MR-CISD techniques [Bau90a], as the size consistency problem can then rigorously be disposed of. It was used in a collaborative effort between Peter R. Taylor of NASA Ames and the present author on $C_3^+$ (Section 4.11), and is therefore briefly described below.

### 1.9.2 The averaged coupled-pair functional (ACPF) method

Let us assume that $\Psi$ is intermediately normalized. The variational CISD calculation then involves minimising the functional

$$E_c = \frac{\langle \psi_0 + \psi_D | \hat{H}' | \psi_0 + \psi_D \rangle}{1 + \langle \psi_D | \psi_D \rangle} \tag{1.304}$$

Introduction of unlinked clusters 'cancels away' the denominator, and restores size-extensivity. The resulting method, LCCSD, however usually overshoots the correlation energy because no account is made for linked EPV diagrams, that should cancel away their unlinked EPV counterparts. Both CISD and LCCSD are special cases of minimising the functional

$$F_c(\psi_D) = \frac{\langle \psi_0 + \psi_D | \hat{H}' | \psi_0 + \psi_D \rangle}{1 + g_D \langle \psi_D | \psi_D \rangle} \tag{1.305}$$

where the choice $g_D = 1$ leads to the CISD and $g_D = 0$ to the LCCSD equations upon minimization of $F_c$ with respect to $\psi_D$. It becomes tempting to look for an 'intermediate' value of $g_D$ that will restore size-extensivity, but will also take account of unlinked cluster effects as much as possible. It can be shown [Gda88], that for a system of $m$ noninteracting

subsystems with $n$ electrons correlated, $g_D$ should be made proportional to $1/n$ in order to restore size-extensivity. In order to make the method also exact for two-electron systems, the final choice is $g_D = 2/n$.

The extension to a multireference calculation can be made as follows. Let us write $\Psi = \psi_0 + \psi_c$, where $\psi_0$ is the linear combination of the references and $\psi_c$ a linear combination of all single and double excitations out of any of the determinants in $\psi_0$, subject to the constraint that $\langle\psi_0|\psi_c\rangle = 0$. Now let us partition $\psi_c$ into two mutually orthogonal parts $\psi_a + \psi_e$, where $\psi_a$ is the internal or 'active space' portion of $\psi_0$, $\psi_e$ the external part. We then rewrite the functional as

$$F_c(\psi_D) = \frac{\langle\psi_0 + \psi_c|\hat{H}'|\psi_0 + \psi_c\rangle}{1 + g_a\langle\psi_a|\psi_a\rangle + g_e\langle\psi_e|\psi_e\rangle} \tag{1.306}$$

The proper choice for $g_e$ remains $2/n$. For a CAS reference, $g_a = 1$ if proper size extensivity is to be guaranteed. For non-CASSCF references, the choice is less obvious; Gdanitz and Ahlrichs [Gda88] recommend always using $g_e = 1$, which will give an upper bound to the value obtained with the correct $g_e$. If the reference wavefunction is sufficiently close to CASSCF (e.g. in an MRCI(0.01) calculation), the error thus incurred should be negligible.

## 1.10 Analytical derivative evaluation

The energy within the Born-Oppenheimer approximation is an explicit function of the nuclear coordinates. Furthermore, the energy changes upon application of an external electric field. Expanding the energy as a power series in one nuclear coordinate $r$ (for simplicity) and an electric field $x$, we obtain:

$$E = E_0 + \frac{\partial E}{\partial r} + \frac{\partial^2 E}{\partial r^2} + \frac{\partial E}{\partial x} + \frac{\partial^2 E}{\partial x^2} + \frac{\partial^2 E}{\partial r \partial x} + \cdots \tag{1.307}$$

At a stationary point (equilibrium geometry or saddle point), the first derivatives with respect to the geometry should vanish. The second derivatives (the matrix of which is called the Hessian) are related to the harmonic frequencies. The first derivative with respect to the electric field is the energy derivative formulation of the dipole moment, the second is the polarizability. Finally, the cross-derivative is the dipole-moment derivative, related to the (double-harmonic) infrared intensities. (Note: the term double-harmonic refers to the assumption that the potential is harmonic both in the geometric and in the electric field variables.)

The importance of these derivatives is obvious. They can be evaluated by numerical differentiation; however, for higher than first derivatives these procedures are both very time-consuming and numerically unstable. Therefore, considerable attention has gone, especially in the last ten years, to the evaluation of analytical derivatives of the energy according to various ab initio models. The general theory, especially concerning the

most recent developments, is very involved. We will restrict the discussion here to the analytical derivatives used in this work, namely Hartree-Fock first and second derivatives, and MP2 first derivatives. (From the latter, a harmonic force field may be constructed by single numerical differentiation: this process is still sufficiently stable numerically, and is also definitely cheaper than constructing the full Hessian by double numerical differentiation.)

### 1.10.1 General background

Writing the energy as an expectation value $E = \langle\Psi|H|\Psi\rangle$ (regular normalization), the derivative of the energy with respect to a general external perturbation $y$ is given by:

$$\frac{\partial E}{\partial y} = 2\langle\frac{\partial\Psi}{\partial y}|H|\Psi\rangle + \langle\Psi|\frac{\partial H}{\partial y}|\Psi\rangle \tag{1.308}$$

The latter term in the equation is a simple expectation value, often called the Hellmann-Feynman force (see below). The former term involves wavefunction derivatives, the determination of which is a far from trivial task that can be accomplished explicitly by a procedure called *coupled perturbed Hartree-Fock* (CPHF) [Ger69].

The Hellmann-Feynman theorem states, that for an exact wavefunction, the wavefunction force vanishes and the derivative thus only involves the Hellman-Feynman force, the determination of which is normally a trivial task. We will now investigate for what classes of approximate wavefunctions the Hellmann-Feynman theorem is valid and, if not, whether we can find a way around the CPHF procedure.

Let us write the general wavefunction $\Psi$ as a linear combination of Slater determinants $\psi_\alpha$, whose coefficients are some function of an amplitude vector $\vec{C}$. These functions may be linear (as in CI) or nonlinear (as in CC theory). The $\psi_\alpha$ are themselves functions of MO coefficients $\vec{c}_\alpha$ and basis set parameters $\vec{\zeta}$. These latter parameters include exponents, contraction coefficients, and position vectors of the basis functions[32] (this latter fact is not generally appreciated):

$$\Psi = \sum_\alpha f_\alpha(\vec{C})\psi_\alpha(\vec{c}_\alpha, \vec{\zeta}) \tag{1.309}$$

Differentiating $\Psi$ with respect to an external perturbation $y$ and applying the chain rule for partial derivatives, we obtain:

$$\begin{aligned}\frac{\partial\Psi}{\partial y} &= \sum_\alpha \psi_\alpha \sum_\beta \frac{\partial f_\alpha(\vec{C})}{\partial C_\beta}\frac{\partial C_\beta}{\partial y} + \sum_\alpha f_\alpha(\vec{C}) \sum_\beta \frac{\partial\psi_\alpha}{\partial c_{\alpha\beta}}\frac{\partial c_{\alpha\beta}}{\partial y} \\ &\quad + \sum_\alpha f_\alpha(\vec{C}) \sum_\beta \frac{\partial\psi_\alpha}{\partial\zeta_\beta}\frac{\partial\zeta_\beta}{\partial y}\end{aligned} \tag{1.310}$$

[32] These are usually constrained to be those of the nuclei, though there is no reason, strictly speaking, to do so.

The wavefunction derivative will then vanish if the wavefunction is stationary with respect to all the parameters appearing in the previous equation. This is trivially the case for an exact wavefunction, which proves the Hellmann-Feynman theorem. It is also trivially the case for an exact single-determinant (i.e. an infinite-basis set Hartree-Fock) wavefunction. Let us now investigate for what finite-basis cases the theorem holds.

1. Numerical Hartree-Fock. The Hellmann-Feynman theorem holds exactly, as the numerical HF orbitals are the variational optimum with respect to all $c$ and $\zeta$ parameters, whereas there are no $C$ parameters to be determined variationally.

2. Finite basis set HF. The derivative will vanish if all basis set parameters are optimum. One specific example would be a simultaneous optimization of the geometry, the exponents, and the basis function position in a calculation with floating uncontracted Gaussian basis functions: the wavefunction derivative would then vanish exactly at the stationary point. It holds approximately in so-called floating orbital geometry optimizations [Hub80], where positions of nuclei and basis functions are optimized simultaneously, but not the other basis set parameters. For ordinary atom- or bond-centered basis functions, the wavefunction force cannot be neglected: some examples are given in the classic paper of Pulay [Pul69]. Nevertheless, the energy is stationary with respect to the MOs, which means that their explicit derivatives are not required. This is an important result: for Hartree-Fock first derivatives no coupled perturbed Hartree-Fock (CPHF, see Section 1.346) procedure is thus required. Fast algorithms [Sch84] for the computation of the two-electron integral derivatives involved in the remaining terms have reduced the time to evaluate a HF gradient to less than that required for the SCF itself.

3. Finite-basis MCSCF. ( We can safely ignore the special case of optimum basis functions from now on.) Here the energy is stationary with respect to both the configuration amplitudes and the MO coefficients for each configuration. This means that again no CPHF will be required for first derivatives.

4. Finite-basis CI. Here the energy is stationary with respect to the configuration amplitudes[33], but not with respect to the MOs for each configuration. A CPHF will thus have to be performed for the latter.

5. The MBPT and CC cases. These methods are not variational; hence the energy is stationary with respect to neither the amplitudes, nor the MOs for each configuration. In the MBPT case, the amplitudes can generally be written in terms of the MOs, so CPHF is sufficient to solve the problem. The CC case, where the amplitudes are no longer simple functions of the MOs, presents additional complications.

[33] A wavefunction that satisfies this condition is said to obey the *generalized Hellmann-Feynman theorem.*

We will now treat some specific cases in detail.

### 1.10.2 First HF derivatives

For the general UHF case, the energy is given by [Pop79]

$$E = \sum_{pq} P_{pq} H_{pq} + \frac{1}{2} \sum_{pqrs} P_{pq} P_{rs} \langle pr||qs\rangle + V_{nuc} \tag{1.311}$$

with $V_{nuc}$ the nuclear repulsion energy, and the density matrix $P$ being defined by

$$P_{pq} = \sum_{i} \nu_i c_{ip} c_{iq} \tag{1.312}$$

where the occupation numbers $\nu_i$ are always one for occupied, and zero for virtual HF orbitals. (Rational values occur in certain ROHF cases, irrational values in first-order post-SCF density matrices.) Furthermore, the orthonormality condition of the orbitals may be written as

$$\sum_{pq} c_{ip} S_{pq} c_{jq} = \delta_{ij} \tag{1.313}$$

where $\delta_{ij}$ represents the familiar Kronecker delta. Differentiating the energy, we obtain:

$$\begin{aligned} \frac{\partial E}{\partial x} &= \sum_{pq} P_{pq} \frac{\partial H_{pq}}{\partial x} + \frac{1}{2} \sum_{pqrs} P_{pq} P_{rs} \frac{\partial \langle pr||qs\rangle}{\partial x} \\ &\quad + \frac{\partial V_{nuc}}{\partial x} + 2 \sum_{pq} F_{pq} \frac{\partial P_{pq}}{\partial x} \end{aligned} \tag{1.314}$$

But the final term is equivalent to

$$2 \sum_{pq} c_{ip} F_{pq} \frac{\partial c_{iq}}{\partial x} = 2 \sum_{pq} c_{ip} \epsilon_i S_{pq} \frac{\partial c_{iq}}{\partial x} \tag{1.315}$$

Combining this with the derivative of the orthonormality condition (1.313)

$$2 \sum_{pq} c_{ip} s_{pq} \frac{\partial c_{iq}}{\partial x} + \sum_{pq} c_{ip} c_{iq} \frac{\partial S_{pq}}{\partial x} = 0 \tag{1.316}$$

the wavefunction derivatives may be eliminated, leading to

$$\begin{aligned} \frac{\partial E}{\partial x} &= \sum_{pq} P_{pq} \frac{\partial H_{pq}}{\partial x} + \frac{1}{2} \sum_{pqrs} P_{pq} P_{rs} \frac{\partial \langle pr||qs\rangle}{\partial x} \\ &\quad + \frac{\partial V_{nuc}}{\partial x} - \sum_{pq} W_{pq} \frac{\partial S_{pq}}{\partial x} \end{aligned} \tag{1.317}$$

where the energy-weighted density matrix is defined as

$$W_{pq} = \sum_{i} \epsilon_i c_{ip} c_{iq} \tag{1.318}$$

So indeed, as expected, the first HF derivative does not involve a CPHF calculation.

If $x$ is an electric field, neither the overlap nor the two-electron integrals depend, of course, on the perturbation, and the expression reduces to the Hellmann-Feynman force. This is the reason why the dipole moment can be exactly evaluated as an expectation value, rather than an energy derivative, at the Hartree-Fock level.

### 1.10.3 Second HF derivatives

Differentiating the first derivatives with respect to an additional perturbation $y$, we obtain the expression [Pop79]:

$$\begin{aligned}\frac{\partial^2 E}{\partial x \partial y} &= \sum_{pq} P_{pq} \frac{\partial^2 H_{pq}}{\partial x \partial y} + \frac{1}{2} \sum_{pqrs} P_{pq} P_{rs} \frac{\partial^2 \langle pr||qs\rangle}{\partial x \partial y} \\ &+ \frac{\partial^2 V_{nuc}}{\partial x \partial y} - \sum_{pq} W_{pq} \frac{\partial^2 S_{pq}}{\partial x \partial y} + \sum_{pq} \frac{\partial P_{pq}}{\partial y} \frac{\partial H_{pq}}{\partial x} \\ &+ \sum_{pqrs} \frac{\partial P_{pq}}{\partial y} P_{rs} \frac{\partial \langle pr||qs\rangle}{\partial x} - \sum_{pq} \frac{\partial W_{pq}}{\partial y} \frac{\partial S_{pq}}{\partial x} \end{aligned} \tag{1.319}$$

where we can no longer avoid evaluation of the wavefunction derivatives.

If either perturbation $x$ or $y$ is an electric field, then the second derivative expression simplifies again to:

$$\frac{\partial^2 E}{\partial x \partial y} = \sum_{pq} P_{pq} \frac{\partial^2 H_{pq}}{\partial x \partial y} + \frac{\partial^2 V_{nuc}}{\partial x \partial y} + \sum_{pq} \frac{\partial P_{pq}}{\partial y} \frac{\partial H_{pq}}{\partial x} \tag{1.320}$$

because the overlap and two-electron integral derivatives then vanish. The wavefunction derivatives are still necessary, though.

### 1.10.4 Coupled perturbed Hartree-Fock (CPHF)

The Hartree-Fock equations, subject to a perturbation $y$, as written in general matrix form are

$$\mathsf{F}(y)\mathsf{C}(y) = \mathsf{S}(y)\mathsf{C}(y)\mathsf{E}(y) \tag{1.321}$$

$$\mathsf{C}^+(y)\mathsf{S}(y)\mathsf{C}(y) = 1 \tag{1.322}$$

$\mathsf{C}$ must be related to $\mathsf{C}(0)$ by a linear transformation $\mathsf{C}(y) = \mathsf{C}(0)\mathsf{U}(y)$, where $\mathsf{U}$ is called the *first order orbital rotation matrix*. Substituting this transformation in (1.321) and (1.322), and multiplying (1.321) on the left by $\mathsf{C}^+(0)$, we obtain:

$$\mathsf{C}^+(0)\mathsf{F}(y)\mathsf{C}(0)\mathsf{U}(y) = \mathsf{C}^+(0)\mathsf{S}(y)\mathsf{C}(0)\mathsf{U}(y)\mathsf{E}(y) \tag{1.323}$$

$$\mathsf{U}^+(y)\mathsf{C}^+(0)\mathsf{S}(y)\mathsf{C}(0)\mathsf{U}(y) = 1 \tag{1.324}$$

After introducing Fock and overlap matrices transformed by $\mathsf{C}$,

$$\mathcal{F}(y) = \mathsf{C}^+(0)\mathsf{F}(y)\mathsf{C}(0) \tag{1.325}$$

$$\mathcal{S}(y) = \mathsf{C}^+(0)\mathsf{S}(y)\mathsf{C}(0) \tag{1.326}$$

the Fock and overlap equations are reduced to

$$\mathcal{F}(y)\mathsf{U}(y) = \mathcal{S}(y)\mathsf{U}(y)\mathsf{E}(y) \tag{1.327}$$

$$\mathsf{U}^+(y)\mathcal{S}(y)\mathsf{U}(y) = 1 \tag{1.328}$$

Our task is now to solve these equations for small $y$. The discussion is somewhat simplified if we continue in the MO basis. (It is however quite feasible to solve the CPHF equations in the AO basis [Pul83], which is more demanding computationally but minimizes I/O requirements. From GAUSSIAN 86 onwards, the GAUSSIAN series implements both algorithms.) Then $\mathsf{U}(0)$ and $\mathcal{S}(0)$ become unit matrices, and $\mathcal{F}(0) = \mathsf{E}(0)$, which also means it is diagonal.

Expanding the various matrices in power series of $y$, and truncating them (for small $y$) after the linear term:

$$\mathcal{F}(y) = \mathsf{E}(0) + y\mathcal{F}^y + O(y^2) \tag{1.329}$$

$$\mathcal{S}(y) = 1 + y\mathcal{S}^y + O(y^2) \tag{1.330}$$

$$\mathsf{U}(y) = 1 + y\mathsf{U}^y + O(y^2) \tag{1.331}$$

$$\mathsf{E}(y) = \mathsf{E}(0) + y\mathsf{E}^y + O(y^2) \tag{1.332}$$

where the superscript $y$ denotes the first derivative with respect to $y$, (note that $\mathsf{E}^y$ is diagonal since $\mathsf{E}$ is diagonal for all values of $y$) we obtain the equations:

$$\mathcal{F}^y + \mathsf{E}(0)\mathsf{U}^y = \mathcal{S}^y\mathsf{E}(0) + \mathsf{U}^y\mathsf{E}(0) + \mathsf{E}^y \tag{1.333}$$

$$(\mathsf{U}^y)^+ + \mathsf{U}^y + \mathcal{S}^y = 0 \tag{1.334}$$

By reverting to subscript notation and performing some straightforward algebra, the latter two equations can be cast into the form

$$(1 - \mathsf{A})\mathsf{U}^y = \mathsf{B}_0 \tag{1.335}$$

where the elements of the supermatrix $\mathsf{A}$ are given by

$$A_{ijab} = \frac{\langle ij||ab\rangle + \langle ib||aj\rangle}{\epsilon_i - \epsilon_a} \tag{1.336}$$

and those of the matrix $\mathsf{B}_0$ by

$$B_{0(ai)} = \frac{Q^y_{ai}}{\epsilon_i - \epsilon_a} \tag{1.337}$$

$$Q^y_{ai} = H^y_{ai} - S^y_{ai}\epsilon_i - \sum_{kl} S^y_{kl}\langle al||ik\rangle + \sum_{pqrs} c_{ap}c_{iq}P_{rs}\frac{\partial\langle pr||qs\rangle}{\partial y} \tag{1.338}$$

$$H^y_{ij} = \sum_{pq} c_{ip}c_{jq}H^y_{pq} \tag{1.339}$$

$$S^y_{ij} = \sum_{pq} c_{ip}c_{jq}S^y_{pq} \tag{1.340}$$

For M perturbational parameters, there are M such systems to be solved, each of dimension $n^2$ for closed-shell systems, and $4n^2$ for open-shell systems. This is best solved iteratively, by expanding the inverse of $(1 - \mathsf{A})$ in a power series:

$$\mathsf{U}^y = \sum_{n=0}^{\infty} \mathsf{A}^n\mathsf{B}_0 \tag{1.341}$$

This process converges slowly, but can be considerably accelerated by Schmidt orthogonalization of the successive approximations $\mathsf{B}_n$:

$$\mathsf{B}_{n+1} = \mathsf{A}\mathsf{B}_n - \sum_{i=0}^{n} \frac{\langle \mathsf{B}_l | A | \mathsf{B}_n \rangle}{\langle \mathsf{B}_l | \mathsf{B}_l \rangle} \mathsf{B}_l \tag{1.342}$$

and putting

$$\mathsf{U}_n^y = \alpha_0 \mathsf{B}_0 + \alpha_1 \mathsf{B}_1 + \ldots + \alpha_n \mathsf{B}_n \tag{1.343}$$

Then the coefficients $\alpha$ may be obtained from those of the previous iteration, and requiring $\langle (1 - \mathsf{A}) | \mathsf{U}_n^y \rangle - \mathsf{B}_0$ to vanish. (As pointed out by Pulay [Pul83], this process is essentially an application of DIIS [Pul80, Pul82]; see Section 1.1.7.1.) Typically, convergence is reached in six to ten iterations.

### 1.10.5 MP2 first derivatives

These are conveniently expressed as [Pop79]

$$\frac{\partial E_2}{\partial x} = \sum_{ijab} a_{ij}^{ab} X_{ij}^{ab} \tag{1.344}$$

$$\begin{aligned} X_{ij}^{ab} = {} & \frac{1}{2} \sum_{pqrs} c_{ip} c_{jq} c_{ar} c_{bs} \frac{\partial \langle pr || qs \rangle}{\partial x} \\ & + \sum_k \langle ij || ak \rangle U_{kb}^x - \frac{1}{2} a_{kj}^{ab} [F_{ki}^x - \epsilon_i S_{ki}^x] - \frac{1}{2} \langle kj || ab \rangle S_{ik}^x \\ & + \sum_c \langle cj || ab \rangle U_{ci}^x - \frac{1}{2} a_{ij}^{ac} [F_{cb}^x - \epsilon_b S_{cb}^x] - \frac{1}{2} \langle ij || ac \rangle S_{bc}^x \end{aligned} \tag{1.345}$$

Solution in the AO basis is next to impossible. In the MO basis, this approach has the disadvantage that a huge file of integral derivatives has to be stored for the computation. Without symmetry, there are 12 different integral derivatives for each two-electron integral, three of which are redundant because of translational invariance. This implies a `D2E` file of about nine times the size of the `INT` file, which makes large basis set calculations prohibitive. The only alternative would be to recompute the integrals for every CPHF step, which is of course not very desirable.

The only situation where the problem does not arise is in the evaluation of MP2 dipole moments as energy derivatives, since then the two-electron integral derivatives simply vanish.

### 1.10.6 The Z-vector method

Fortunately, Handy and Schaefer [Han84] discovered an important simplification. It is applicable to $n$-th order CPHF problems, but will here be discussed for the case of a first-order CPHF.

Write the CPHF equations (at first order) as

$$\mathsf{G}_0\mathsf{U}^y = \mathsf{B}_0 \tag{1.346}$$

where $\mathsf{G}_0 \equiv 1 - \mathsf{A}$. Now define a vector (actually a supervector, i.e. a matrix) $\mathsf{Z}$ as the solution to

$$\mathsf{G}_0^+\mathsf{Z} = \mathsf{E}_0 \tag{1.347}$$

where $\mathsf{E}_0 \equiv \mathsf{E}(0)$. By multiplying (1.346) on the left with $\mathsf{Z}^+$, we find easily that

$$\mathsf{E}_0^+\mathsf{U}^y = \mathsf{Z}^+\mathsf{B}_0 \tag{1.348}$$

Or, as $\mathsf{E}$ is diagonal,

$$\mathsf{U}^y = \mathsf{E}_0^{-1}\mathsf{Z}^+\mathsf{B}_0 \tag{1.349}$$

This means that, once $\mathsf{Z}$ has been obtained, all sets of CPHF equations are solved at once since $\mathsf{G}_0$ and $\mathsf{E}_0$, and therefore $\mathsf{Z}$, are independent of the perturbation! So for $M$ atoms, the $3M + 3$ (nuclear coordinates + $x$, $y$, and $z$ components of the electric field) CPHF problems are reduced to one: the determination of $\mathsf{Z}$.

Valuable as this result is, the effects are even greater when the MP2 gradient expression is suitably rearranged. More specifically, writing the orbital rotations directly in terms of $Z$, all gradient terms involving the two-electron integral derivatives can be collected. Then the latter have to be processed only once - in the AO basis - for the entire MP2 gradient calculation, and can consequently be computed once, summed into the expression and discarded.

Together, this realizes substantial time savings and effectively does away with the integral derivative file. MP2 gradient calculations can now be performed with fairly large basis sets (100 basis functions or more). Simandiras *et al.* [Sim87] observed that MP2 gradients in this implementation take less than twice the time of the corresponding SCF gradients.

The Z-vector method is implemented in GAUSSIAN 88, but cannot be used if both MP2 first derivatives and HF second derivatives (a sensible option for Newton-Raphson geometry optimizations) are required. Then the integral derivatives are required more than once, making it necessary to store them on disk anyway.

## 1.11 Selection of the finite basis set

The electron correlation method determines the power of an ab initio calculation to reproduce the full CI limit, *within the given finite basis set.* It is the finite basis set itself that determines the ability of the calculation to reproduce the actual properties accurately.

Numerical Hartree-Fock calculations, where the solution spans an infinite basis set by definition, are currently routine for atoms [Fro77], and are starting to become so for diatomics (see e.g.[Mul89]). Very recently, some correlated calculations with numerical orbitals have been done for small diatomics (see e.g. [Ada88]). For polyatomics, finite basis sets are still the only option, whereas they remain the only practical option even for atoms and diatomics.

Basis sets have been extensively reviewed. Older reviews are by Dunning and Hay [Dun77] and by Ahlrichs and Taylor [Ahl81]; basis sets are also discussed in the book by Čársky and Urban [Car80]. More recently, Huzinaga [Huz85] and Davidson and Feller [Dav86] have covered the subject. Poirier *et al.* [Poi87] have published an extensive compilation of Gaussian basis sets; a review in preparation by Almlöf and Taylor will also cover the most recent developments [Alm91]. The situation up to the first quarter of 1987 was reviewed by the present author in his M.Sc. thesis; the present discussion will be more concise and center upon the more recent developments.

The most extensive bibliographies of basis set applications available are to be found in Richards and Walker [Ric81] and Ohno and Morokuma [Ohn82] (the latter with yearly supplements), which include brief summaries of nearly every conceivable practical ab initio calculation (as well as of the most important methodological papers).

### 1.11.1 Types of basis functions

The exact solutions of hydrogen-like atoms are derived in most quantum chemistry textbooks (e.g. [Eyr44]) to be

$$\phi_{nlm}(r,\theta,\phi) = N(Z,n,l,m)Y_{lm}(\theta,\phi)L_{n+l}^{2l+1}(2Zr/n)\exp(-Zr/n) \tag{1.350}$$

where $Y_{lm}$ and $L_{n+l}^{2l+1}$ are a spherical harmonic and an associated Laguerre polynomial, respectively, N is an appropriate normalization constant, $Z$ represents the nuclear charge of the hydrogen-like atom, and $nlm$ are the well-known principal, angular, and magnetic quantum numbers. The set of $2l+1$ basis functions that differ only in the value of $m$ is called a *shell.*

Hydrogen-like orbitals can be written (if $\zeta = Z/n$) as linear combinations of so-called *Slater type orbitals* (STOs) [Sla30]

$$\xi_{nlm}(r,\theta,\phi) = NY_{lm}(\theta,\phi)r^{n-l}\exp(-\zeta r) \tag{1.351}$$

where $\zeta$ is a constant called the *orbital exponent*[34]. However, Slater observed that numerical Hartree-Fock orbitals of many-electron atoms could also be described well by this function, but now with more general values of $n$ and $\zeta$.

[34]Hydrogen-like orbitals and STOs are identical when $l = n-1$ (again for $\zeta = Z/n$); the main distinction when $l < n-1$ lies in the absence of radial nodes in the STO.

Furthermore, a linear combination of STOs can be enforced to satisfy the $r \to 0$ and $r \to \infty$ limits for the exact wavefunction.

Originally Slater proposed to determine the $n$ and $\zeta$ by empirical rules, the well-known *Slater rules* [Sla30]. For the present purpose however, it is much more satisfying to use them as variational parameters, which means minimizing the total energy with respect to them. Clementi and Roetti [Cle74] published an extensive compilation of atomic Hartree-Fock solutions involving Slater orbitals, covering H through Xe. Their expansions involved groups of $K$ STOs for every combination of $n$ and $l$ that was occupied in the atomic state of interest, different exponents being taken for each of the $K$ functions. The case $K = 1$ they termed *single-zeta*, the case $K = 2$ *double-zeta* (DZ), the case $K = 3$ *triple-zeta* (TZ), and so on; these terms are still commonly used today.

In the course of their work they discovered, that at least a double-zeta basis set was necessary to start reproducing the essential quantitative features of the Hartree-Fock solution. Another thing they discovered was that for a given value of $l$, it did not matter much what value of $n$ was taken; a basis where all $n = l$ (i.e. with the $r^{n-l}$ term eliminated) does just as well as any other. This allows for important computational simplifications.

The use of STOs in atomic calculations is fairly straightforward, as simple analytical expression exist for all the necessary integrals, including the $\langle pq|rs\rangle$ that dominate the integral part of the calculation. In the case of diatomics, their evaluation in closed form is still possible through the use of elliptical coordinates. Most of the diatomics calculations done in the IBM laboratory at San Jose by McLean and coworkers since the sixties use STOs; they developed a program suite called ALCHEMY for this purpose.

For polyatomics, some of the two-electron integrals involve three or four centers. The evaluation of three-or four-center integrals over STOs can no longer be carried out in closed form, except for the special case of linear molecules. The only practically useful technique to date is the so-called Shavitt-Karplus transformation [Sha65], where the exponential is written as an integral transform of a Gaussian:

$$\exp(-\alpha r) = \frac{\alpha}{2\sqrt{\pi}} \int_0^\infty s^{-3/2} \exp(-\alpha^2/4s) \exp(-sr^2) ds \tag{1.352}$$

By swapping the order of the spatial integrations and that of the integral transform, and doing the latter by numerical integration, the problem is reduced to evaluating a large number of Gaussian integrals, which are comparatively simple to evaluate. More specifically, e.g. for $s$-type Gaussians [Sha63]

$$\exp(-\alpha_1|\vec{r} - \vec{R}_1|^2) \exp(-\alpha_2|\vec{r} - \vec{R}_2|^2) = K \exp(-(\alpha_1 + \alpha_2)|\vec{r} - \vec{R}_c|^2) \tag{1.353}$$

$$\vec{R}_c = \frac{\alpha_1 \vec{R}_1 + \alpha_2 \vec{R}_2}{\alpha_1 + \alpha_2} \tag{1.354}$$

$$K = \exp\left(-\frac{\alpha_1 \alpha_2}{\alpha_1 + \alpha_2} |\vec{R}_1 - \vec{R}_2|^2\right) \tag{1.355}$$

i.e, the product of two Gaussians on two distinct centers can itself be written as a Gaussian. In this manner, the four-center integral can be reduced to a two-center integral, and (by repeating the process) to a one-center integral. Finally, even $r_{12}^{-1}$ can be brought in Gaussian form by an integral transformation

$$r^{-1} = \int_0^\infty t^{-1/2} \exp(-tr^2) dt \tag{1.356}$$

The final integral involves the incomplete gamma function, which is easily evaluated to any desired accuracy by interpolating a precomputed table.

Similar relations hold for integrals involving functions with higher angular momentum, although the situation is slightly more difficult there.

The reader rightly wonders 'why going through all the trouble of the Shavitt-Karplus transformation when we could have used Gaussian basis functions in the first place?'. The use of Gaussians as basis functions in *ab initio* calculations was first suggested by Boys [Boy50]. Gaussians have the important disadvantage, though, that both their short- and long-range behavior are very different from that of the exact solution. However, it may rightly be argued that a chemist is not principally interested in the behavior of the wavefunction at very small or very large distances, but in the intermediate range. In the intermediate range, the behavior of a single Gaussian does not mimic that of the true solution adequately; a variational calculation on the hydrogen atom gives an error of 100 millihartree (i.e. 20 % !). However, with six simultaneously optimized Gaussians the error is reduced to 54 microhartrees; with ten of them, the error becomes only a single microhartree [Dui71].

A six-to-one ratio in basis set size also means $6^4 = 1296$ times more integrals. Even so, the simplest Gaussian integral package outperforms the Shavitt-Karplus transformation of STOs by a longshot [Oha66].

Originally, the basis functions were simply linear combinations of Gaussians where both the exponents and the expansion coefficients were least-squared fitted to STOs [Oha66]. However, it was quickly realized that a much better Gaussian-to-STO ratio (about 2:1) could be obtained by energy-optimizing all exponents [Huz65]. A single Gaussian is called a *primitive Gaussian type orbital* (GTO). When the $r^{n-l}$ term is dropped, they are called *Cartesian GTOs*; their analytical form is given by

$$\xi_{ijk} = N x^i y^j z^k \exp(-\zeta |\vec{r} - \vec{R}|^2) \tag{1.357}$$

where $N$ is again a normalization constant, and the $ijk$ are positive integers, with $l = i + j + k$. $\vec{R}$ is the position vector of the center, which is usually (but not necessarily) an atomic center.

Pure $d$ functions can be obtained as linear combinations of the second-order cartesian Gaussians (i.e. $l = 2$). Actually, there are six of the latter, namely $xy, xz, yz, x^2, y^2, z^2$, leading to the five pure $d$ functions $xy, xz, yz, x^2-y^2, 3z^2-r^2$ and a redundant $3s$ function

$r^2$. The integrals over pure $d$ functions can be formed by a simple linear transformation of those involving the second-order Gaussians, where the redundant $3s$ function is then discarded. Likewise, the ten third-order Gaussians lead to seven pure $f$ functions and a redundant $4p$ shell.

### 1.11.2 Contracted Gaussian basis sets

An expansion in primitive GTOs (an *uncontracted* GTO basis set) gives rise both to unnecessarily large integral files and ditto eigensystems, let alone the length of any CI or CC expansion! Fortunately linear combinations of these basis functions can be taken with little or no loss in energy. This process is called *contraction*: the resulting basis functions are called *contracted GTOs* (CGTOs).

$$\xi_{ijk} = \sum_{m=1}^{K} C_m N x^i y^j z^k \exp(-\zeta_m(\vec{r} - \vec{R})^2) \tag{1.358}$$

where $K$ is called the *degree of contraction* and the $C_m$ the *contraction coefficients.*

Most integral packages handle all integrals involving the same four CGTO shells at one time; to avoid unnecessary duplication of integral evaluation, different CGTOs of the same symmetry share as few primitives as possible. Any contraction scheme where not all primitives of a given $l$ contribute to all CGTOs of that symmetry is called a *segmented contraction.* Most practical basis sets involve segmented contractions.

In a *general contraction*, all primitives of a given $l$ contribute to all CGTOs of that atomic symmetry. This scheme, devised by Raffenetti [Raf73], allows any amount of contraction, even all the way down to single zeta, without *contraction error* (increase in atomic energy relative to the uncontracted basis set). Raffenetti also devised a special integral evaluation algorithm that eliminates computing duplicate integrals by calculating all integrals $\langle pq|rs\rangle$ of a given combination of angular momenta for $pqrs$ at the same time [Raf73].

It is time to introduce some common notations for uncontracted and contracted basis sets. The uncontracted set is given by listing, between round brackets, all atomic symmetry types in ascending order of $l$ prefixed by the number of primitives for each. For example, a $(9s5p)$ basis set has nine primitive $s$ functions and five primitive $p$ shells ($5 \times 3 = 15$ primitive $p$ functions). When a basis set is defined for elements of different rows in the periodic table, the primitive sets for each row are commonly given in one pair of brackets, with different sets separated by a slash. For example, a $(10s6p/5s)$ primitive set is $(10s6p)$ for Li–Ne, and $(5s)$ for H and He.

The contracted set is denoted in a similar manner, but now between square brackets. For example, a $[4s2p]$ basis set has four contracted $s$ functions and two shells of contracted $p$ functions, whereas a $[5s3p/3s]$ is $[5s3p]$ for Li–Ne and $[3s]$ for H and He. Basis sets are often specified in the literature by writing down the uncontracted and contracted sets in

the manner just stated, like "These calculations were carried out using Dunning's [5*s*3*p*] contraction of Huzinaga's (10*s*6*p*) primitive set."

Another notation for the contracted set, introduced by Huzinaga [Huz85], makes the contraction scheme explicit. It consists of a list of integers which give the degree of contraction for each CGTO, with different angular momenta separated by a slash. (Different rows of the periodic table may be separated by a semicolon.) By convention, the functions are ordered from 'hardest' (highest exponent) to 'softest' (lowest exponent). For example, the [4*s*2*p*] set just mentioned might be (6111/41) in Huzinaga's notation; note that (4311/32) would also be [4*s*2*p*], whereas it would have radically different performance.

The terms single-zeta, double-zeta, and triple-zeta are used here too, where the number of 'zetas' refers to the number of CGTOs this time. For example, a [4*s*2*p*] basis set for carbon is said to be of DZ quality, a [5*s*3*p*] for carbon is said to be of core double zeta and of valence triple zeta quality. Another important term is the *minimal basis set*, defined as a basis that is single-zeta in all core and valence shells. For example, a minimal basis set for Be is of [2*s*1*p*] quality, whereas a single-zeta set would normally only be [2*s*]. But the 2*p* orbitals of Be are occupied in valence-shell excited states, and are involved in molecules as well.

It should be noted that the term 'minimal' does not say anything neither about the quality of the primitive set, nor about the capability to reach the atomic Hartree-Fock limit for the energy. For example, a [2*s*1*p*] general contraction of a very large primitive set, say (30*s*20*p*), may well reach the atomic Hartree-Fock limit. It is however totally useless, both in molecular calculations and in correlated atomic calculations (and a fortiori in correlated molecular calculations), because the orbitals do not have any flexibility left to adapt to a chemical environment or to excited states. A general consensus exists that for any useful result to be obtained in a molecular calculation, the basis set should be of at least double-zeta quality, whereas triple-zeta or better is prerequisite for accurate work.

### 1.11.3 Polarization functions

Let us for example consider the ground state of the carbon atom. At the Hartree-Fock limit, the solution will only contain *s* and *p* components; *d* and higher functions will not result in a further improvement of the energy. *d* and higher orbitals become only occupied in *Rydberg states* (excited states with occupied orbitals outside the valence shell), and will therefore not contribute to the *internal* correlation energy of the atom; a CASSCF calculation on the carbon atom can well be carried out in a basis of only *s* and *p* functions. *d* and higher functions will contribute to the *external* correlation energy, though, and are indispensible for accurate calculations on atoms.

Molecules at the Hartree-Fock level are another matter. When a carbon atom occurs in a molecule, e.g. methane, its environment is no longer isotropic; the electronic charge cloud becomes *polarized* towards the bonding or, in other terms, the center of the charge

cloud for a given orbital no longer coincides with the atomic center. One can either take this into account by allowing the basis functions to shift off the nuclear center, or by admitting $d$ and higher functions to the expansion, which are then called *polarization functions.* The latter approach appears to be first introduced by Nesbet [Nes60]. Its rationale becomes most obvious when a displaced $s$ and a displaced $p$ function are developed in a series of nuclear-centered functions

$$\begin{aligned}\exp[-a(x-r)^2] &= \exp(-ar^2)\exp(-ax^2)[1+2arx+2a^2r^2x^2 \\ &\quad +\frac{4}{3}a^3r^3x^3+\frac{2}{3}a^4r^4x^4+\ldots] \qquad (1.359)\\ (x-r)\exp[-a(x-r)^2] &= \exp(-ar^2)\exp(-ax^2)[-r+\left(1-2ar^2\right)x \\ &\quad +\left(2ar-2a^2r^3\right)x^2+\frac{1}{3}\left(6a^2r^2-4a^3r^4\right)x^3 \\ &\quad +\frac{1}{3}\left(4a^3r^3-2a^4r^5\right)x^4+\ldots] \qquad (1.360)\end{aligned}$$

where the polarization functions are seen to arise in a natural way. [35] The name 'polarization functions' does not cover all of the effects though. $d$, $f$, and higher functions (also $p$ functions in the case of hydrogen) do act as polarization function both at the Hartree-Fock and CASSCF levels; however, both in atoms and in molecules, they also contribute to the external correlation energy and could therefore have been called *correlation functions.* The term 'polarization functions' is preserved for historical reasons, however.

Second-and third order Cartesian Gaussians have six and ten components, respectively, corresponding to the five true $d$ functions plus one redundant $s$ function in the former case and the seven true $f$ functions plus one redundant $p$ shell in the latter case. These redundant functions do lower the total energy, and integrals over them are computed anyway, so one becomes tempted to include them in the basis set. On the other hand, they do lead to an increase in computer time for correlated calculations (because of the extra virtual orbitals). Furthermore, they are often near linear dependence with one of the valence $s$ or $p$ functions, leading sometimes to hampered convergence in the

[35] This fact is sometimes exploited to approximate $p$ and $d$ functions by so-called *lobe functions*, that allow two-electron integrals over these functions with integral packages that cannot handle these functions:

$$\exp[-a(x-r)^2]-\exp[-a(x+r)^2]=\exp(-ar^2)\exp(-ax^2)\left(4arx+\frac{8}{3}a^3r^3x^3+\ldots\right)$$

and, with $r=(2a)^{-1/2}$

$$\begin{aligned}(x-r)\exp[-a(x-r)^2]-(x+r)\exp[-a(x+r)^2] &= \exp(-ar^2)\exp(-ax^2)\left(-\sqrt{\frac{2}{a}}+\sqrt{2a}x^2\right. \\ &\quad \left.+\frac{(2a)^{3/2}}{4}x^4+\ldots\right)\end{aligned}$$

SCF and always to some very large MO coefficients. The latter, in turn, result in a numerically unstable integral transformation, which affects the numerical accuracy of any correlated calculation and in extreme cases leads to nonsensical energies[36]. In the present work the policy of always using 'pure' $d$ and $f$ functions has been adopted, except when necessitated otherwise for comparison with existing results.

### 1.11.4 Basis set superposition error

This is perhaps the correct place to discuss this phenomenon, which we will illustrate by considering the dissociation energy of a diatomic molecule AB. This is simply found as:

$$-D_e = \Delta E = E_{AB} - E_A - E_B \tag{1.361}$$

Now assume that the atomic basis set for A is incomplete, which means that addition of extra basis functions would still lower the atomic energy. If we now place the atom in the molecule, then to a first approximation, all the basis functions of the molecular basis set become available for the atomic energy. Now we have just seen, that the atomic basis functions of B can be developed in a series around the nucleus of A, and then lead to all kinds of *spd*... components centered on A. Hence a lowering of the energy of the atom A in the AB basis set. The same happens, of course, for B. Adding in — again to a first approximation — the true interaction energy at that level, we find that the total energy is artificially lowered and thus the dissociation energy artificially increased. This phenomenon is called *basis set superposition error.* It can be estimated by the Boys-Bernardi formula [Boy70], which readily follows from the above discussion:

$$\text{BSSE} = E_{A(B)} + E_{B(A)} - E_A - E_B \tag{1.362}$$

where $E_{A(B)}$ represents the energy of A in the basis set for AB, and conversely for $E_{B(A)}$. Boys and Bernardi suggested using this as a correction term to the computed interaction energy, and termed this procedure the *counterpoise method* [Boy70]:

$$\Delta E_{\text{CP}} = E_{AB} - E_{A(B)} - E_{B(A)} \tag{1.363}$$

The discussion is readily transferred to dimer interactions between any two monomers.

Of course all this assumes that the BSSE and true interaction energy are additive: it has been shown recently by Mayer and Vibok [May87] that this does not hold exactly.

Other objections against the simple CP correction include supposed violation of the Pauli principle, in the sense that orbitals are made available for charge transfer that are already occupied. Whereas this may be a problem on his part, this argument has never made much sense to the present author. Nevertheless, several approximate schemes have been suggested, in which only the virtual orbitals of the monomers are included [Col86],

[36] By way of diagnostic, GAUSSIAN 88 aborts a correlated calculation if any MO coefficient in the integral transformation exceeds $10^3$.

or even only their polarization functions [Sch85]. Van Duijneveldt and coworkers [Dui87] showed theoretically that this argument is not valid. Anyway, this scheme also assumes additivity of BSSE and interaction energy.

Two related subjects, namely the polarization counterpoise correction [Lou87] and the secondary BSSE [Lat87], should be mentioned here; details can be found in these references.

The present author sees the counterpoise correction mainly as a device to probe basis set incompleteness. Furthermore, as BSSE and basis set incompleteness error usually work in opposite directions, the two often compensate each other to a large extent.

The extension of the counterpoise procedure to many-body interactions is not unique: see the work of Wells and Wilson [Wel83] and Chapter 3.4 of the present work [Mar89g] for details.

### 1.11.5 Bond functions

If one is mainly interested in the 'polarization' effect of polarization functions, one may just as well shortcut the series expansion of displaced atomic functions by displacing them in the first place. A first approach, the *floating orbital geometry optimization* [Hub80], has already been discussed and has the advantage of leading to near-validity of the Hellmann-Feynman theorem. We recall that it basically consists of simultaneously optimizing the nuclear and basis function center coordinates.

Another is to supplement an ordinary atomic basis set by $s$ and $p$ functions that are placed somewhere along the bond axis, which are then called *bond functions* [Rot71, Vla73]. Bond functions usually lead to more compact basis sets than polarization functions, and thus in drastic reductions of computer time. Additionally, integration algorithms for $s$ and $p$ shells like the Pople-Hehre axis transformation [Pop78] are usually much faster than algorithms for $d$ and higher functions (like the Rys polynomial algorithm [Dup76]). For binding energies, several studies have indicated that bond functions are definitely no worse than polarization functions at the Hartree-Fock level [Rot71, Vla73, Nei82].

At correlated levels, the matter is a bit more complicated. At first sight, numerical evidence indicates that bond functions are definitely superior [Mac85]. Some of this improvement may be deceptive, however, in that bond function basis sets lead to excessive basis set superposition error at correlated levels [Bau85]. This is readily explained: an atomic basis set of only $s$ and $p$ functions lacks the $d$ and $f$ functions required for a good account of external correlation, whereas such functions are present — as components in the atomic expansion of the bond functions — in the molecular basis set. Hence an artificial lowering of the atomic energy in the molecule and BSSE. The amounts involved without any polarization functions are so clearly excessive that error compensation with basis set incompleteness can no longer be confidently relied upon.

An obvious remedy would be to add some polarization functions, so that the basis set is no longer overly incomplete; Section 3.3 of the present work [Mar89c] deals with precisely this problem. Suffice to say here that the combination of bond and polarization functions does not lead to any better results than any of the two by themselves at the Hartree-Fock level [Vla73]; at correlated levels, this is definitely no longer true, as witnessed by the fact that unusually accurate dissociation energies can be obtained [Mar89b] using *combined bond-polarization basis sets* developed in Chapter 3 of this work [Mar89g, Mar89c, Mar89c, Mar89a, Mar89f, Mar89b].

### 1.11.6 Diffuse and Rydberg functions

Because of the analytical shape of Gaussian basis functions, they are not capable of describing the tail region of an orbital well. This is not a problem in most cases; however, the highest occupied orbitals of anions usually are very close to the ionization limit and therefore extend rather far in space.

Conventional basis sets are incapable of providing a correct description of the outer regions of such orbitals; therefore performance of ab initio methods for anions used to be disappointing. Schleyer and coworkers discovered [Cha81], that this problem was greatly relieved when so-called *diffuse functions*, i.e. $s$ and $p$ functions with very low exponents, were admitted to the basis set[37]. Subsequent studies by the Pople group [Pop85] revealed that their effect on the dissociation energy should also not be neglected for neutral compounds with lone pairs; their effect on the geometries [Cla83] and harmonic frequencies [DeF86] is also significant for anions.

The use of such functions was already found to be essential [Dun77] for studying $s$ and $p$ Rydberg states, for the simple reason that the orbitals involved are by nature 'softer' than valence orbitals.

The use of diffuse functions is not always without problems. Especially with larger primitive basis sets such as 6-311G and [5s3p], the optimum 'diffuse' functions are often near linear dependence with the outermost functions of the parent basis set, resulting in SCF convergence problems as well as numerically unstable integral transformations. For very accurate work, it appears to be more gratifying to select a parent basis set whose outermost exponents are already 'diffuse' enough, rather than to add additional diffuse functions.

### 1.11.7 Some common basis set families

#### 1.11.7.1 The Huzinaga-Dunning family

Two basis set families are used in the overwhelming majority of practical applications, namely the basis sets introduced by Pople and coworkers and the Huzinaga-Dunning

[37] Actually, this was already suggested by Dunning and Hay [Dun77].

family. The latter, which are the basis sets of choice of many workers despite being second in popularity to those of the Pople group, will be described first.

The uncontracted Huzinaga sets [Huz65] are of $(9s5p/4s)$ and $(10s6p/5s)$ quality. They were developed by optimization of the ROHF energies of the atoms in their respective ground states. For Li and Be, $p$ basis functions cannot be obtained in this manner as these do not contribute to the ground states Li($^2S$) and Be($^1S$).

The Dunning contraction scheme is based on the SCF coefficients from these calculations. We will illustrate it for the $(9s5p)$ primitive set [Dun70].

To obtain a $[2p]$ contraction of the $(5p)$ set, the outermost $p$ function was simply set free and the others renormalized, leading to a (41) contraction pattern. A $[3p]$ contraction is made by setting the outermost of the four contracted functions free and again renormalising the three remaining ones; the contraction pattern then becomes (311). The idea is that the outermost functions are most involved in bonding, and thus should have maximum flexibility. As all the $p$ functions only contribute to one occupied $p$ shell, different contraction patterns of the $p$ shell yield the same HF energy.

This is not true for the $s$ functions, that contribute to two different atomic orbitals. The procedure there is to divide the SCF coefficients for the $1s$ and $2s$ orbitals by that of the 'hardest' primitive, tabulate the orbitals side by side, ordered from the inside out or the outside in (depending on the case), and split the contraction before the first primitive that has a clearly different contribution (e.g. opposite sign) in the two columns. The part that can thus be 'chopped off' is renormalized, and the procedure repeated on the remaining primitives. For $[3s]$, $[4s]$ and $[5s]$ contractions of the $(9s)$ primitive set this leads to contraction patterns (612), (6111), and (42111), respectively. The $s$ and $p$ contractions are subsequently combined to obtain $[3s2p]$, $[4s2p]$, and $[5s3p]$ contracted basis set.

Finally, the hydrogen primitive set is simply uncontracted as (31) to go with the $[3s2p]$ and $[4s2p]$ sets, or (211) to go with the $[5s3p]$ set. The $[4s2p/2s]$ set is used especially often, and is usually abbreviated — rather broadly — as the DZ (double zeta) basis set. It is of double-zeta quality in both the core and valence orbitals.

For most chemically interesting problems (with the study of core ionization potentials as the primary exception), the behavior of the core orbitals is of little interest. Taking this into account, Dunning and Hay recommend a *valence double zeta* (VDZ) quality basis set [Dun77] obtained by doubling up the third outermost primitive and contracting according to a (721) pattern. These basis sets yield atomic energies identical to those of the $[4s2p]$ basis set and are still of double-zeta quality in the valence orbitals, but are only minimal in the core.

For the $(10s6p)$ primitive set, the objective was a basis of triple-zeta quality in the valence shell [Dun71]. This was easily achieved for the $p$ functions by loosening the outermost two functions, leading to a (411) contraction pattern. For the $s$ functions, it

would become necessary to split as (511111) to keep the contraction error down to an acceptable level. By doubling up the sixth $s$ primitive, however, the contraction pattern can be changed into (62111), and a [5$s$3$p$] basis set is obtained. A [5$s$4$p$] set — which is of quadruple zeta quality in the $p$ functions only — has also been recommended. Both sets are commonly denoted TZ (for triple zeta).

Dunning and Hay [Dun77] also suggest polarization functions to go with these basis sets, that are based on optimum values for some molecules at the Hartree-Fock level. These values do not appear to be completely standard, however, and many authors use some more or less reasonable-looking value without further justification. Most authors employ 6$d$ and 10$f$ sets instead of 5$d$ and 7$f$, however questionable the inclusion of the redundant $s$ and $p$ functions is.

### 1.11.7.2 The Pople family

The oldest Pople basis set family is the STO-$n$G one [Heh69], which is mainly of historical interest. These minimal basis sets are obtained by fitting a $n$-term Gaussian expansion to an STO and substituting that for each STO in a minimal STO basis set.

Very heavily used are a number of *split-valence* basis sets developed by Pople and coworkers. The oldest one is the 4-31G basis set [Dit71], which is an (8$s$4$p$) contracted to [3$s$2$p$] according to (431/31). Both exponents and contraction coefficients are obtained by energy optimization at the UHF level, the coefficients subject to the constraint of normalization, the exponent subject to the constraint that the valence $s$ and $p$ exponents be equal. (This equality can easily cut the integral evaluation time in half with the Pople-Hehre axis switching algorithm [Pop78], but does result in some loss of energy. It is enforced in all subsequent Pople group basis sets). The relatively poor representation of the core region is justified by observing that only valence effects are of general chemical interest anyway — at least for first-row atoms!

Finally, the exponents of the valence functions are multiplied by a common *scale factor*: the two scale factors for each atom were optimized in various molecular environments. Except for hydrogen, the optimum values for the scale factors differ on average little from unity[38].

The poor representation of the core proved to be more problematic than previously thought, primarily because of a tendency of the valence functions to 'collapse' into the core during the optimization. For boron, a 4-31G basis set was only obtained with considerable difficulty [Heh72a]; for Li and Be, no 4-31G set could be obtained (the '4-31G' sets available in the GAUSSIAN series for these atoms are actually 5-21G) [Dil75][39].

[38]The procedure of optimizing atomic basis sets in molecular environments is somewhat controversial. On the one hand, it should improve the performance of the basis set in molecular calculations; on the other hand, it will certainly increase BSSE.

[39]It should be remarked that the original basis set, optimized for the $^1S$ ground state of the Be atom, was incapable of predicting binding for tetrahedral $Be_4$; this was corrected in a later publication, where

The problem was solved completely by allowing two more primitives in the core; such optimized basis set is denoted as 6-31G [Heh72b].

Standard polarization exponents have been defined by Hariharan and Pople [Har73], who obtained their recommended values by optimization in molecular environments. (There is no other option at the Hartree-Fock level.) Again the six second order $d$ functions are included instead of the five $l = 2$ spherical harmonics. A 6-31G basis with added $d$ functions is denoted 6-31G* or 6-31G($d$); if $p$ polarization functions are also added to the hydrogen atom the notation 6-31G** or 6-31G($d,p$) is employed. The 6-31G* basis set is usually considered the smallest basis set that is meaningful to use at correlated levels; the polarization functions are also indispensable in describing highly strained compounds even qualitatively correct.

Pulay and coworkers [Pul79] devised a 4-21G basis set for hydrogen and boron to fluorine. The basis set for hydrogen is simply the Huzinaga (21) set, scaled by 1.15. The cores for the other elements were taken from the 4-31G basis set; the valence shells, again with an $s = p$ constraint, were optimized for the closed-shell hydrides at their respective experimental geometries. For geometries and harmonic frequencies, the performance of this basis set is essentially as good as that of the larger 4-31G basis set, whereas it puts much smaller demands on the integral and derivative programs. It is commonly used for geometry and frequency studies on large organic molecules, sometimes supplemented with polarization functions on heteroatoms (see e.g. [Pan82]).

An even smaller (and essentially as good) 3-21G basis set [Bin80] was subsequently developed by the Pople group. It was obtained by taking the core from the 6-31G set, optimizing a (21) valence set to go with it, and then simply replacing the (6$s$) core by a (3$s$) core, which was optimized with the other functions held fixed. The 3-21G basis set is computationally slightly more efficient than the 4-21G basis set, with comparable performance. It lends itself very well for preliminary geometry and frequency calculations, as well as for preparing the 'initial guess' to a larger calculation in cases with convergence difficulties. Timings for geometry and frequency calculations approach those with the inferior STO-3G basis set.

For correlated calculations, such basis sets lead to meaningless results; even 6-31G* is only sufficient for qualitative purposes. With that in mind, the 6-311G** (or 6-311G($d,p$)) basis set has been developed by the Pople group [Kri80b]. The optimizations were carried out at the UMP2 level; polarization exponents were optimized at the MP2 level for the closed-shell hydrides. (These exponents are rather different from those obtained at the SCF level.) The redundant $s$ function in the $d$ shell has been eliminated this time. The use of scale factors has been eliminated, also for hydrogen, where the Huzinaga-Dunning (311) basis set has been used. Performance at correlated levels is satisfactory, but still insufficient for quantitative determination of dissociation energies;

the optimization has been carried out for the $^3P$ excited state [Bin77].

the main weakness is the single set of polarization functions.

Frisch *et al.* [Fri84] investigated the addition of supplementary polarization functions, and arrived at the conclusion that additional $d$ exponents could be derived by the so-called *even scaling rule*: let the exponent for a single $d$ function be $\alpha_d$, then those for two $d$ functions are given by $\alpha_d/2$ and $2\alpha_d$, whereas for three $d$ functions the values $\alpha_d/4$, $\alpha_d$, and $4\alpha_d$ are appropriate. Additionally, $f$ functions were optimized at the MP4 level for the atoms, whereas diffuse functions were obtained at the MP2 level by Clark *et al.* [Cla83]. The notation for these basis sets is e.g. 6-311G$(2df,p)$ for a basis set that is $[4s3p2d1f]$ on the first-row atoms and $[3s1p]$ on hydrogen; the addition of diffuse functions on first-row atoms is denoted by a '+' as in 6-311+G$(2df,p)$. Together with an isogyric correction procedure called *G1 theory* [Pop89a], the 6-311+G$(2df,p)$ basis set allows the prediction of total atomization energies of first-row compounds to an accuracy of $\pm 2$ kcal/mol, provided electron correlation is treated at least at the MP4 level.

Recently it has been suggested [Gre89] that the 6-311G basis is not of valence triple-zeta quality, as the exponents are actually biased towards the core region because of core collapse in the optimization; they suggest that it be replaced by the Huzinaga-Dunning $[5s3p]$ basis set. On the other hand, 6-311G was optimized at a correlated level, whereas the $[5s3p]$ set was only optimized at the Hartree-Fock level.

Nobes *et al.* [Nob82] developed the 6-31G++ basis set, which is simply the 6-31G basis set supplemented with the polarization functions from the 6-311G** basis set. It is slightly more efficient in correlated calculations because of the eliminated redundant $s$ function, and has a performance that is essentially identical to that of the 6-31G** set.

We should also address second-row atoms. The 6-31G** basis set has been extended for these [Fra82] (actually it should be called 66-31G** for these), and should be of valence double-zeta quality; for calculations of triple-zeta quality, the 6-311G** on first-row atoms is combined with the McLean-Chandler $[6s5p]$ contraction of their $(12s9p)$ primitive set [McL80]. The 3-21G basis set has also been extended for second-row atoms [Gor82]; inclusion of a $d$ function on the second-row atoms proved necessary for an adequate description of hypervalent compounds [Pie82]. Diffuse functions have also been published [Spi87]; their effect is much less prominent than for the first-row atoms and can be neglected if the parent basis set is not too small. Additional polarization functions have been published by Wong *et al.* [Won88].

### 1.11.7.3 Some other common basis sets

The following basis sets are not used in the present work, but crop up frequently in other publications.

Van Duijneveldt [Dui71] published a large series of uncontracted SCF-optimized atomic basis sets, that are sometimes encountered in published work. His $(13s8p)$ basis set is sometimes contracted to $[6s5p]$ for very large molecular calculations (see e.g.

[Sim88]).

When the number of primitives becomes very large, optimizations become very difficult since variation of individual exponents becomes associated with very small changes in the energy. The large number of parameters becomes a challenge in itself, whereas many local minima crop up. Ruedenberg decided that individual values of exponents become largely academic when very large basis sets are used, and arrived at the concept of an *even-tempered* basis set [Bar74b][40], where the exponents are constrained to follow a geometric progression, $\alpha_i = \alpha_1 \beta^{i-1}$. Even-tempered basis sets are usually subjected to general contractions, where multiple-zeta basis sets are constructed by doubling up the appropriate number of outer exponents as uncontracted functions.

Optimizations become very simple, involving only two parameters per atomic symmetry type. Schmidt and Ruedenberg even devised a systematic algorithm for reaching the Hartree-Fock limit to any desired degree of accuracy, where additional primitives are added as necessary [Sch79].

Huzinaga and coworkers carried the logic one step further and devised so-called *well-tempered* expansions [Huz83], where all primitive exponents of all symmetry types are derived from a single four-parameter function

$$\zeta_i = \alpha\beta^{i-1}[1 + \gamma(k/K)^\delta], \qquad k = 1, 2, \ldots, K \tag{1.364}$$

where $K$ denotes the contraction degree. A compilation of well-tempered basis sets for lithium through mercury has recently been published [Huz88].

Huzinaga and coworkers also derived a family of basis sets that was optimized for optimum reproduction of shapes and energies of atomic Hartree-Fock orbitals. The minimal variants are denoted MINI-$n$, the split-valence variants MIDI-$n$. A complete compilation and documentation of these basis sets is available in book form [Huz84]; we refer to that work for further details.

Many more types of basis sets exist that cannot be discussed in this short space. The reader is referred to one of the specialized bibliographies for these.

### 1.11.7.4 Atomic natural orbital (ANO) basis sets

These represent perhaps the most important recent development in atom-centered basis sets. In order to discuss them, we should first explain what *natural orbitals* (NOs) are.

The SCF orbitals are easily seen to be eigenvectors of the density matrix with their occupation numbers as eigenvectors:

$$[\mathsf{P}\vec{c}_i]_p = \sum_q P_{pq} c_{iq} = \sum_{jq} n_j c_{jp} c_{jq} c_{iq} = \sum_j n_j c_{jp} \delta_{ij} = n_i c_{ip} \tag{1.365}$$

[40] The term refers to the tuning system commonly used for keyboard instruments since the 18th century (*cf.* J. S. Bach's 'Das wohltemperierte Klavier', BWV 846-893). Even-tempered tuning is defined by dividing the octave — that corresponds to a 2:1 ratio — in twelve equal semitone intervals, each corresponding to a ratio $2^{1/12} = 1.05946\ldots$

Actually, the elements of the density matrix are matrix elements of the Dirac delta-functions $\delta(\vec{r}-\vec{x})$:

$$\langle p|\delta(\vec{r}-\vec{x})|q\rangle = \phi_p(\vec{x})\phi_q(\vec{x}) \tag{1.366}$$

For a correlated wavefunction, a *one-particle density matrix* can still be defined, the elements of which now have the form

$$P_{pq} = \sum_{xy} n_{xy} c_{xp} c_{yx} \tag{1.367}$$

where $xy$ run over both occupied and virtual orbitals. The $n_{xy}$ are functions of the expansion coefficients in the correlated calculation (e.g. the excitation amplitudes in a CI calculation). Expectation values of one-electron operators $\hat{O}$ can be computed completely analogously to the Hartree-Fock case: $\langle O\rangle = \mathrm{Tr}(\mathsf{PO})$.

The Hartree-Fock orbitals are of course no longer eigenfunctions of the correlated density matrix. It is however still possible to seek the eigenvectors of P: these are called the *natural orbitals*, and their associated eigenvalues the *natural occupation numbers*. The beautiful thing about natural orbitals is that a subset of them can be shown to be the optimum approximation to the full basis set, provided those with the largest occupation numbers are chosen [Col63].

This procedure is a bit awkward for reducing the length of CI or CC expansions, as the latter must already be known in their complete form before they can be truncated. Almlöf and Taylor [Alm87] found, however, that it constitutes an ideal device for generating generally contracted basis sets for correlated calculations.

Their *atomic natural orbital* (ANO) basis sets are generated in the following manner:

- Select some sufficiently large uncontracted basis set. One they considered was the Van Duijneveldt $(13s8p)$, supplemented by a $(6d4f2g)$ polarization complement generated from even-tempered sequences with all $\beta = 2.5$. The geometric mean of the exponents from which $\alpha$ is derived, was taken to follow the Ahlrichs-Taylor rule $\zeta_d = 0.02Z^2$, where $Z$ represents the atomic number. The mean $f, g, \ldots$ exponents are always taken to be 1.2 times that of the previous angular momentum.

- Perform a frozen-core CISD calculation on the ground state.

- Compute the one-particle density matrix and obtain the natural orbitals.

- For each desired contraction $[klmn\ldots]$, choose the $k$ $s$ orbitals with the highest occupation numbers, and analogously for the $p, d, f, \ldots$ orbitals.

- The coefficients of the natural orbitals in question form the contraction coefficients.

The basis set for hydrogen cannot be generated according to this recipe, as there is no atomic correlation energy. The expansion coefficients were then derived from the NOs for the $H_2$ molecule. The primitive set was $(8s6p4d)$, with the $(8s)$ taken from Van Duijneveldt [Dui71], and the $p$ and $d$ sets based on mean exponents of 1.00 and geometric ratios of 2.5.

ANO basis sets have the very desirable property that all possible contracted sets are generated at one time, which allows for very systematic extension of the basis set. The huge primitive set just discussed is of course not a prerequisite for the procedure; an example, discussing ANO contractions of the Huzinaga $(9s5p)$ basis set for Ne, is also given. It is found there that only a negligible contraction loss is present in a $[5s4p]$ basis set, and only a fairly small one in a $[4s3p]$ basis set; the common $[4s2p]$ set results in a severe loss of correlation energy.

ANO basis sets have since then mainly been used in the work of the NASA Ames group. The fact that integral packages that can handle general contractions are not widely available places a practical restriction on their general usage, but this should not take too long to be removed.

A noteworthy detail is that ANO basis sets apparently have very low BSSE, which is of course a consequence of the fact that they constitute — for that size of primitive set — the most optimal contraction according to a particular scheme.

Widmark *et al.* [Wid90] very recently published a set of *density matrix averaged ANO* basis sets. The idea was to improve the convergence for spectroscopic and electric properties, which was hampered in the regular ANO basis set by the bias of the NOs towards the ground state of the atoms. Widmark *et al.* therefore averaged the one-particle density matrix over the ground and a number of excited states, as well as calculations involving homogenous electric fields. (Details of the averaging procedure can be found in that reference.) ANOs were then derived from the averaged density matrix. The primitive set was identical to that of Almlöf and Taylor, except that no $g$ functions were included, and that the $(9p)$ functions for Li and Be (which were not determined by Van Duijneveldt as they do not contribute to the ground states of these atoms) were optimized separately at the SCF level for the $^2P$ and $^3P$ states, respectively. These exponents were taken to follow a modified geometric progression $\alpha\beta^k\gamma^{1/k}$. An important detail is that these authors chose to publish a listing of their final basis sets, which was not done by Almlöf and Taylor!

Performance of the new ANO basis sets is only very slightly worse for ground state energies and harmonic frequencies, but very much better for electrical properties, ionization potentials, and electron affinities.

### 1.11.8 Use of isogyric reaction cycles — G1 theory

Even with large basis sets, the direct determination of dissociation energies is still not without problems. Achieving 'chemical accuracy' without some sort of empirical correction is only possible for very small molecules, at least at the current state of the art. The problem is that the convergence behavior of the energy of a two electron-bond with respect to the addition of higher angular momenta to the basis set, after a fairly rapid onset, becomes very slow [Alm91].

For example, Almlöf *et al.* [Alm89] considered the $N_2$ molecule (experimental $D_e$=228.4 kcal/mol [Hub79]) with ANO basis sets including very high angular momenta. With a $[4s3p2d1f]$ ANO basis, they found $D_e$=216.7 kcal/mol at the second order CI level. Increasing the basis to $[5s4p3d2f1g]$ yields a $D_e$ increment of 6.1 kcal/mol; stepping up to $[6s5p4d3f2g1h]$ one of 2.3 kcal/mol; adding a $i$ function still raises the $D_e$ by 0.5 kcal/mol.

It may be argued that $N_2$, with its strong triple bond, is too severe an example; however, Wright and Barclay [Wri87] found similar though somewhat less extreme results for the hydrogen molecule (experimental $D_e$=109.48 kcal/mol [Hub79]). At the CISD level[41], a $(9s)$ basis set[42] contracted to $[4s]$ yields a $D_e$ of 96.84 kcal/mol. Adding a single $p$ function increases this by 9.14 kcal/mol to 105.98 kcal/mol. But then, tripling the $p$ functions adds only 1.84 kcal/mol. Throwing in a $d$ function gives another 0.93 kcal/mol; doubling the $d$ functions a mere 0.28 kcal/mol. Finally, topping it off with an $f$ function brings out a measly 0.14 kcal/mol, leaving the $D_e$ still 0.32 kcal/mol removed from the exact value.

As the remaining errors — particularly in the higher quantum numbers — are fairly small compared to the quantity to be computed, it does not seem unreasonable to expect them to cancel between different bond types. One correction scheme that has met considerable success was introduced by Pople *et al.* [Pop83] in their work on first-row hydrides. Instead of computing the $\Sigma D_e$ directly, i.e. the energy change of the reaction

$$AH_n \rightarrow A + nH \tag{1.368}$$

they computed that of the *isogyric reaction*

$$AH_n + (n-m)H \rightarrow A \tag{1.369}$$

$$m = \frac{1}{2}[n + g(A) - G(AH_n)] \tag{1.370}$$

where $g(A)$ and $g(AH_n)$ represent the spin multiplicities of the species involved. (This choice of $m$ balances the number of unpaired electrons on either side of the equation: hence the term *isogyric*.) Now as the dissociation energy of $H_2$ is very well known

[41] Which is of course equivalent to full CI for this system.

[42] Atomic energy: -0.499998 hartree, compared to the exact value of -0.5 hartree.

experimentally (109.48 kcal/mol, see above), a correction term to the theoretical $\Sigma D_e$ is readily found:

$$\begin{aligned}\Sigma D_e &= [E(\mathrm{AH_n}) - E(\mathrm{A}) - nE(\mathrm{H})] \\ &\quad + m\{109.48 \text{ kcal/mol} - [E(\mathrm{H_2}) - 2E(\mathrm{H})]\}\end{aligned} \tag{1.371}$$

With this scheme applied to MP4/6-311G($2df,p$) calculations, Pople *et al.* [Pop83] achieved accuracies of ± 2 kcal/mol for the total dissociation energies of the first-row hydrides and hydride radicals. Later applications to atomization energies [Pop85], proton affinities and ionization potentials [Pop87b], and electron affinities [Pop88b] of first- and second-row one-heavy-atom hydrides displayed this accuracy throughout [Pop85]. It will be shown in Chapter 3 (*esp.* Section 3.6) of this work, that this accuracy can be improved by an order of magnitude by adding bond functions to the basis set.

The principal disadvantage of this scheme in its present form is its being limited to hydride bonds. However, the difference between computed and experimental energy for $H_2$ could also be seen as a measure for the basis set incompleteness for a more general electron pair. At the QCISD(T)/6-311G** level, the energy for $H_2$ is -1.16832 hartree, compared to the exact value of -1.17446 hartree. This suggests adding -6.14 millihartrees to the total energy (i.e., 3.85 kcal/mol to $\Sigma D_e$) per bound valence electron pair. Likewise, as the energy of the hydrogen atom in the 6-311G** basis is only -0.49981 hartree, we should add -0.19 hartree per unbound valence electron. Together this yields the 'high level correction' formula:

$$\Delta E(\mathrm{HLC}) = -0.19n_\alpha - 5.95n_\beta \text{ millihartree} \tag{1.372}$$

$$\Delta(\Sigma D_e) = 0.12n_\alpha + 3.73n_\beta \text{ kcal/mol} \tag{1.373}$$

Pople and coworkers based a general calculation scheme called *G1 theory* (for: Gaussian-1 theory) on this formula [Pop89a]. It proceeds in the following steps:

- Evaluate HF/6-31G* equilibrium geometries. These are to be used later in the HF/6-31G* frequency calculations.
- Refine these geometries at the MP2/6-31G* level. The final geometry is to be used in the energy calculations.
- Calculate the MP4/6-311G** energy. As is standard practice, all correlated calculations are done with frozen cores[43].
- Calculate the MP4/6-311+G** energy. The difference with the previous energy is taken as a measure of the effect of adding diffuse functions;

$$\Delta E(+) = E(\text{MP4/6-311+G**}) - E(\text{MP4/6-311G**}) \tag{1.374}$$

[43]The effect of neglecting core correlation is extremely small for first-row elements. Its proper inclusion would require splitting the core functions, as well as adding 'hard' (high-exponent) polarization functions.

- Calculate the MP4/6-311G($2df,p$) energy. The difference with the MP4/6-311G** energy is taken as a measure for expanding the polarization space;

$$\Delta E(2df) = E[\text{MP4/6-311G}(2df,p)] - E(\text{MP4/6-311G**}) \tag{1.375}$$

- Calculate the QCISD(T)/6-311G** energy. This level of theory should include higher-order correlation effects well; the basis set extension effects are then accounted for by the additivity approximation

$$E[\text{QCISD(T)/6-311G**}] + \Delta E(2df) + \Delta E(+) \tag{1.376}$$

- Add in the 'high-level correction' (1.372).
- Compute the HF/6-31G* frequencies. Scale them by a factor of 0.8929 (the reciprocal of their average overestimate of the experimental energies [Pop81]) and compute the zero-point energy from these.
- Finally, add everything in to obtain $\Delta D_0$.

According to this recipe, an average error of $\pm$ 2 kcal/mol could still be reached, but now for more general molecules.

For molecules where fourth-order MBPT breaks down (usually because of heavy spin contamination and/or multireference effects), the basis set additivity steps in the unmodified G1 theory are its Achilles' heel[44]. (As diffuse and polarization functions are totally different contributions to the basis set, considering them additive is not in itself the major problem.) In the present work, a slightly modified variant is therefore sometimes applied, in which PMP4($n$), CCD(ST), or QCISD(T) were employed in the additivity calculations, whichever was appropriate or computationally feasible for the problem at hand.

## 1.12 Molecular spectroscopy and statistical thermodynamics

It is all fine and dandy to compute the properties of a single isolated molecule theoretically; in practice a chemist is also (and mainly) interested in the thermodynamic properties of a collection of $N$ identical molecules: an *assembly*. Statistically speaking, a practical assembly is astronomically large; one billionth of a mole still contains six hundred million million ($6 \times 10^{14}$) molecules!

Exactly because of this astronomical assembly size, it is meaningful to describe the thermodynamic properties of an assembly from a statistical distribution of the population

[44] See e.g. [Bau90b] for a clear-cut example.

of its energy levels. This area of science, called *statistical thermodynamics*, forms the bridge between the microscopic properties that the quantum chemist can study and the macroscopic properties that are generally of chemical interest.

There is a class of microscopic properties, though, that are of direct relevance to a chemist: the study of energetic transitions in a molecule that interacts with an external field. The study of the energetic transitions that then occur, as well as their probabilities, is called *molecular spectroscopy*. It is of special interest because a particular type of spectrum is often a 'fingerprint' for a given molecule, and enables its identification.

Molecular spectroscopy and statistical thermodynamics deal with one and the same 'raw matter': the energy levels of the molecule. This is the reason why the two are treated together here.

Lengthy textbooks have been devoted to either subject[45]; there is a lot to be said about them too. In the interest of brevity and readability, the material is presented here in a 'pragmatic' manner, which may differ considerably from how it is treated in more theory-oriented textbooks.

### 1.12.1 Statistical thermodynamics

All expressions below are derived for an ideal gas, i.e. an assembly of noninteracting particles.

We know from quantum mechanics that a molecule may be in a countably infinite number of energetic states: the one corresponding to the lowest energy being called the *ground state*. According to the familiar Boltzmann distribution, the relative probability (with respect to the ground state $\epsilon_0$) that a given energy level $\epsilon_i$ with degeneracy $g_i$ is occupied is given by:

$$w_i = g_i \exp(-\frac{(\epsilon_i - \epsilon_0)}{kT}) \tag{1.377}$$

where $k$, the *Boltzmann constant*, is a fundamental constant whose numerical value can be proven to be $R/N_a$. ($R$ and $N_a$ represent the ideal gas constant and Avogadro's number, respectively.) At thermodynamic equilibrium, the *temperature* $T$ is a parameter of the distribution. (In nonequilibrium situations, the 'statistical' or distribution temperature may not always correspond to other macroscopic 'temperature' concepts.)

To compute the relative probability with respect to the entire assembly that a given level is occupied, one must divide $w_i$ by the sum over all states of $w_i$. This latter function is called the 'state sum' or *partition function*:

$$Q = \sum_i g_i \exp(-\frac{(\epsilon_i - \epsilon_0)}{kT}) \tag{1.378}$$

[45] Valuable reference works on molecular spectroscopy are [Her45, Her50, Her66, Wil55]. Among textbooks on statistical thermodynamics, [Hil60, Fow66, Rus67, May77] are quoted.

The distribution mean and variance are then given by

$$\langle \epsilon \rangle = \sum_i w_i \epsilon_i / Q = kT \sum_i w_i \frac{\epsilon_i}{kT} / Q \tag{1.379}$$

$$\langle \epsilon^2 \rangle - \langle \epsilon \rangle^2 = \sum_i w_i \epsilon_i^2 / Q - (\sum_i w_i \epsilon_i / Q)^2 \tag{1.380}$$

If, following Pitzer and Brewer[Pit61], we now introduce the first and second moments of the partition function:

$$Q' \equiv \sum_i (\frac{\epsilon_i}{kT}) g_i \exp(-\frac{(\epsilon_i - \epsilon_0)}{kT}) \tag{1.381}$$

$$Q'' \equiv \sum_i (\frac{\epsilon_i}{kT})^2 g_i \exp(-\frac{(\epsilon_i - \epsilon_0)}{kT}) \tag{1.382}$$

we obtain the following expressions:

$$\langle \epsilon \rangle = kTQ'/Q \tag{1.383}$$

$$\langle \epsilon^2 \rangle - \langle \epsilon \rangle^2 = k^2 T^2 [Q''/Q - (Q'/Q)^2] \tag{1.384}$$

For one mole, the average energy becomes the sum of all means for the molecules, which is exactly $N_a \langle \epsilon \rangle$. The variance on this quantity is again simply the sum of all the individual variances, being precisely $N_a(\langle \epsilon^2 \rangle - \langle \epsilon \rangle^2)$. Because of the enormous sample size $N_a$, the standard deviation on the energy becomes negligible compared to the quantity itself. For all intents and purposes, the latter is thus a well defined macroscopic thermodynamical property of the assembly called the *internal energy* $E$:

$$E - N_a \epsilon_0 = RT \frac{Q'}{Q} = RT^2 \frac{dQ}{QdT} = RT^2 \frac{d \ln Q}{dT} \tag{1.385}$$

The thermodynamical *heat capacity* or *molar heat* (at constant volume) is defined as the derivative of the internal energy with respect to temperature:

$$C_v = \frac{dE}{dT} = 2RT \frac{d \ln Q}{dT} + RT^2 \frac{d^2 \ln Q}{dT^2} = R[\frac{Q''}{Q} - (\frac{Q'}{Q})^2] \tag{1.386}$$

The heat capacity is thus, except for a factor $kT^2$, the variance on the energy distribution. For one mole of an ideal gas, $pV = RT$ holds, so that $C_p = C_v + R$. This also implies that, for the enthalpy, $H = E + RT$.

Since the $N_a$ molecules in the assembly are indistinguishable, there are always $N_a!$ ways of realizing any population, which means that the partition function and all its moments should be multiplied by a factor $N_a!$. This does not change anything for $E$, $H$, $C_p$, or $C_v$, as the factor will cancel there between numerator and denominator. It does affect the *entropy*, which is found as:

$$\begin{aligned} S &= \int_0^T \frac{C_v}{T} dT \\ &= 2R \ln Q + RT \frac{d \ln Q}{dT} - R \ln Q + 2k \ln N_a! - k \ln N_a! \\ &= R \left( \ln Q + \frac{Q'}{Q} \right) + k \ln N_a! \end{aligned} \tag{1.387}$$

As $N_a$ is astronomically large, Stirlings approximation $\ln N_a! = N_a(\ln N_a - 1)$ may be applied, yielding:

$$S = R\left(\ln Q + \frac{Q'}{Q}\right) + R(\ln N_a - 1) \tag{1.388}$$

For practial computations, two additional functions are usually defined, namely the enthalpy or heat content function

$$\mathrm{hcf}(T) \equiv H(T) - H(T_{\mathrm{ref}}) \tag{1.389}$$

and the free energy or Gibbs energy function

$$\mathrm{gef}(T) \equiv -\frac{G(T) - H(T_{\mathrm{ref}})}{T} \tag{1.390}$$

With the aid of these two functions, the $\Delta H$ and $\Delta G$ of any reaction can be determined from $\Delta H(T_{\mathrm{ref}})$ as

$$\Delta H(T) = \Delta H(T_{\mathrm{ref}}) + \Delta\mathrm{hcf}(T) \tag{1.391}$$

$$\Delta G(T) = \Delta H(T_{\mathrm{ref}}) - T\Delta\mathrm{gef}(T) \tag{1.392}$$

There are two common conventions for the choice of $T_{\mathrm{ref}}$, namely room temperature, 298.15 K, and absolute zero, 0 K. When using or comparing to published functions, one should always check what convention was used. Tabulated functions can be converted from one reference system to another by use of the equations:

$$\mathrm{hcf}_{298}(T) = \mathrm{hcf}_0(T) - \mathrm{hcf}_0(298.15) \tag{1.393}$$

$$\mathrm{hcf}_0(T) = \mathrm{hcf}_{298}(T) - \mathrm{hcf}_{298}(0) \tag{1.394}$$

$$\mathrm{gef}_{298}(T) = \mathrm{gef}_0(T) + \mathrm{hcf}_0(298.15)/T \tag{1.395}$$

$$\mathrm{gef}_0(T) = \mathrm{gef}_{298}(T) + \mathrm{hcf}_{298}(0)/T \tag{1.396}$$

For our purposes, the choice $T_{\mathrm{ref}} = 0$ is the most convenient one, as $H(T_{\mathrm{ref}})$ then reduces to simply $N_a\epsilon_0$, which is the primary output of a quantum mechanical energy calculation (except for the obvious factor $N_a$). We then find the two functions as

$$\mathrm{hcf}(T) = RT\frac{Q'}{Q} \tag{1.397}$$

$$\mathrm{gef}(T) = R\ln Q + R\ln N_a \tag{1.398}$$

This leaves us with the task of determining the molecular energy levels $\epsilon_i$, which are a function of four different sets of state quantum numbers: translational, rotational, vibrational, and electronic. For an ideal gas, the translational energy levels are independent of the other quantum numbers, so the partition function may be factored into a translational and an *internal* part:

$$Q = Q_{\mathrm{trans}}Q_{\mathrm{int}} \quad Q' = Q'_{\mathrm{trans}}Q'_{\mathrm{int}} \quad Q'' = Q''_{\mathrm{trans}}Q''_{\mathrm{int}} \tag{1.399}$$

$$S = S_{\mathrm{trans}} + S_{\mathrm{int}} \quad H = H_{\mathrm{trans}} + H_{\mathrm{int}} \quad \ldots \tag{1.400}$$

The $N_a!$ factor of the partition function is usually gathered with the translational partition function, and similarly for the thermodynamic functions.

The energy levels of translation are these of a particle in a three-dimensional box, substituting $RT/p$ for the volume of the box. Except at very low temperatures (where Boltzmann statistics is also no longer valid), the energy levels may be treated as a continuum — the summation therefore as an integration — and one obtains:

$$S_{\text{trans}} = R(\frac{5}{2}\ln T + \frac{3}{2}\ln M - 1.16487 + \ln p) \tag{1.401}$$

$$\text{gef}_{\text{trans}}(T) = R(\frac{5}{2}(\ln T - 1) + \frac{3}{2}\ln M - 1.16487 + \ln p) \tag{1.402}$$

$$\text{hcf}_{\text{trans}} = \frac{5}{2}RT \tag{1.403}$$

$$C_{p,trans} = \frac{5}{2}R \tag{1.404}$$

where M, the molecular mass, has been expressed in atomic mass units, and the pressure $p$ in atmospheres. Occasionally, tabulations are made for a pressure of 1 bar = $10^5$ Pa; to convert from 1 bar to 1 atmosphere, add $0.013163R$ to $S_{\text{trans}}$ and $\text{gef}_{\text{trans}}(T)$. The expressions have been brought into this form to make them independent of the unit system: output in any desired units is achieved by substituting the correct definition for $R$ in that particular unit system.

Henceforth we will use the convention $Q \equiv Q_{\text{int}}$, and so on. Their new definitions (excluding the indistinguishability term) are:

$$S = R(\ln Q + \frac{Q'}{Q}) \tag{1.405}$$

$$C_p = R[\frac{Q''}{Q} - (\frac{Q'}{Q})^2] \tag{1.406}$$

$$\text{hcf}(T) = RT\frac{Q'}{Q} \tag{1.407}$$

$$\text{gef}(T) = R\ln Q \tag{1.408}$$

As molecular energy levels are usually expressed in $\text{cm}^{-1}$ (though this unit does not have the correct dimensionality), one writes:

$$Q = \sum_{i,n,J} g(i,n,J)\exp(-\frac{c_2\epsilon(i,n,J)}{T}) \tag{1.409}$$

$$Q' = \sum_{i,n,J} g(i,n,J)[\frac{c_2\epsilon(i,n,J)}{T}]\exp(-\frac{c_2\epsilon(i,n,J)}{T}) \tag{1.410}$$

$$Q'' = \sum_{i,n,J} g(i,n,J)[\frac{c_2\epsilon(i,n,J)}{T}]^2\exp(-\frac{c_2\epsilon(i,n,J)}{T}) \tag{1.411}$$

in which the indices $i$, $n$, and $J$ run over electronic, vibrational, and rotational levels, respectively. The *second radiation constant* $c_2 \equiv 100hc/k$ has the numerical value 1.438786 cm K.

## 1.12.2 Essential spectroscopic features of atoms and molecules

The determination of the partition function requires the spectroscopic constants of an atom or molecule. We will therefore briefly discuss essential spectroscopic features of atoms, diatomics, and polyatomics before discussing the actual partition functions.

Although a bit outdated in some respects, especially the quantum mechanical treatment, the monumental reference works of Herzberg still are rightly considered the 'Old Testament' of any spectroscopist. Volume I discusses all spectroscopic features of diatomic molecules in ample detail [Her45]. Volumes II and III deal with the rovibrational and electronic spectra of polyatomic molecules, respectively [Her50, Her66]. Finally, Volume IV (with K. P. Huber) is perhaps the most complete and thorough compilation to date of experimental spectroscopic data on diatomic molecules [Hub79].

### 1.12.2.1 Atoms

The only internal energy levels of an atom are the electronic states. As no closed expressions for the transition energies can be obtained, these have to be obtained individually (from spectroscopic data or ab initio calculations). The partition function is then constructed by direct numerical summation according to (1.409)–(1.411). The degeneracy of the atomic states is $(2L+1)(2S+1)$ without spin-orbit coupling, where $L$ and $S$ are the total angular momentum and total spin quantum numbers, respectively.

For very accurate work, and for calculations on heavy atoms, spin-orbit coupling cannot be neglected. This is a relativistic effect that partially lifts the degeneracy of the atomic states by splitting them up in $2S+1$ component states with spin-orbit quantum numbers $J = L - S_z$, where $S_z$ runs from $-S$ to $+S$. Each component state has a degeneracy $(2J+1)$. For example, the $^3P$ state of carbon ($L = 1$, $S = 1$), with a zero-order degeneracy of nine, splits up in three component states $^3P_0$, $^3P_1$, and $^3P_2$, with degeneracies one, three, and five, respectively. Spin-orbit coupling does not result in a splitting when $L = 0$ ($S$ states) and, trivially, for singlet states ($S = 0$). The spin-orbit coupling is very small for first-row atoms, but increases steeply with $Z$, until its effects become comparable to the electronic transition energies themselves for lanthanides.

The first principles computation of spin-orbit effects in atoms and molecules is technically possible, though by no means trivial. The interested reader should consult the book of Richards, Trivedi, and Cooper [Ric81].

### 1.12.2.2 Diatomic molecules

For the electronic partition function of a diatomic molecule, the same remarks as for atoms hold. The zero-order degeneracy of an electronic state, though, is now $2S+1$ if $L = 0$ ($\Sigma^+$ or $\Sigma^-$ states), and $2(2S+1)$ if $L > 0$ ($\Pi, \Delta, \ldots$ states). Spin-orbit coupling for $L > 0$ will cause an electronic state to split up in $2S+1$ component states $L - S$

to $L + S$, but now each component state has only degeneracy two. For example, the $^2\Pi$ state of NO will split up in two component states $^2\Pi_{-1/2}$ and $^2\Pi_{+1/2}$.

For denoting electronic states, two conventions are employed. The first is the Herzberg-Mulliken convention commonly used by spectroscopists. The ground state is then prefixed by a capital $X$. Any excited states of the same spin multiplicity are labeled $A$, $B$, $C$, ... from the ground state on up, and $a$, $b$, $c$, ... for different multiplicities. For example, the three lowest states of SiC are labeled $X\ ^3\Pi$, $A\ ^3\Sigma^-$, and $a\ ^1\Sigma^+$. The second convention prefixes the state with a digit, which starts at 1 for the lowest state of that symmetry and multiplicity and is incremented for each new state.

The derivation of the symmetry of a Slater determinant from the orbital symmetries deserves mention, as it is seldom discussed in textbooks on group theory. For nondegenerate orbitals, the irreducible representation of the determinant is simply the product of those for the individual orbitals. A direct consequence is that a closed-shell RHF determinant always has the symmetry of the identical representation. The case of degenerate orbitals is complicated by the spin. Let us consider two electrons in two degenerate $\Pi$ orbitals. The product of two $\Pi$ representations can be decomposed in a $\Sigma^+$, a $\Sigma^-$, and a $\Delta$ representation. The first and third cases require the spatial wavefunction to be symmetric, and the spin wavefunction to be antisymmetric; the opposite is true for the second. A symmetric spin wavefunction can only be realized by high-spin coupling of the electrons: as a result, two degenerate $\Pi$ electrons can couple as $^1\Sigma^+$, $^3\Sigma^-$, or $^1\Delta$ states. According to Hund's rules, the ground state will be $^3\Sigma^-$; of the two remaining states, the $^1\Delta$ will normally be the lowest in energy. The case of three electrons in two degenerate orbitals is identical, as far as group theory is concerned, to that of a single Fermi hole in two degenerate orbitals; its treatment is therefore identical to that of a single electron as group theory does not distinguish between Fermi particles and Fermi holes. For example, both a single electron in a $\Pi$ shell and three electrons in a $\Pi$ shell give rise to $^2\Pi$ states. A completely filled degenerate set always transforms as the identity representation, e. g. four electrons in a $\Pi$ shell yield a $^1\Sigma^+$ shell.

Of course, a diatomic molecule also vibrates. The empirical representation of the vibrational levels of a diatomic is as a power series in the vibrational quantum number $n$:

$$G(n) = \omega_e(n + \frac{1}{2}) - \omega_e x_e(n + \frac{1}{2})^2 + \omega_e y_e(n + \frac{1}{2})^3 + \omega_e z_e(n + \frac{1}{2})^4 + \ldots \qquad (1.412)$$

The first term is the vibrational energy for a quantum mechanical harmonic oscillator, with $\omega_e$ representing the *harmonic frequency*. $\omega_e x_e$ is called the (first-order) *anharmonicity constant*; further terms are the higher-order anharmonicity constants: only the first two terms are usually well-determined from the experimental data (the higher-order constants are very small). The vibrational constants are related to the geometrical derivatives of the energy: see Section 1.12.4 on the Dunham analysis for details. The levels are

nondegenerate.

The zero-point energy $G(0)$ is given by

$$G(0) = \frac{1}{2}\omega_e - \frac{1}{4}\omega_e x_e + \frac{1}{8}\omega_e y_e + \frac{1}{16}\omega_e z_e + \ldots \tag{1.413}$$

and the anharmonic first transition by:

$$G(1) - G(0) \equiv \nu = \equiv \Delta G(\frac{1}{2}) = \omega_e - 2\omega_e x_e + \frac{13}{4}\omega_e y_e + 5\omega_e z_e + \ldots \tag{1.414}$$

Every electronic state has a distinct set of vibrational constants.

Finally, a diatomic molecule rotates. An empirical expression for the energy levels is given by:

$$F(n, J) = B_n[J(J+1)] - D_n[J(J+1)]^2 + H_n[J(J+1)^3] + \ldots \tag{1.415}$$

where the subscripts $n$ indicate that the rotational constants are in general dependent on the vibrational state. This dependence is generally expressed as a power series in $(n + 1/2)$:

$$B_n = B_e - \alpha_e(n + \frac{1}{2}) + \gamma_e(n + \frac{1}{2})^2 + \ldots \tag{1.416}$$

$$D_n = D_e - \beta_e(n + \frac{1}{2}) + \ldots \tag{1.417}$$

$\ldots$

The $B_e$ term corresponds to a quantum mechanical rigid rotator: $B_e$ is called the *rotational constant.* It is related to the equilibrium bond distance $r_e$ by the expression

$$B_e = \frac{h}{8\pi^2 c\mu r_e^2} = \frac{16.85763}{\mu r_e^2} \tag{1.418}$$

$$\mu = \frac{m_1 m_2}{m_1 + m_2} \tag{1.419}$$

where $r_e$ and the *reduced mass* $\mu$ are expressed in angstroms and atomic mass units, respectively, and $B_e$ is found in the spectroscopic 'multipurpose unit' $cm^{-1}$.

For general $n$, an averaged $r_n$ can still be defined from

$$B_n = \frac{16.85763}{\mu r_n^2} \tag{1.420}$$

The most commonly encountered value is $r_0$, the zero-point averaged bond distance. It is generally longer than $r_e$ because of the asymmetric shape of a diatomic potential curve, which rises much more steeply towards $r = 0$ than towards $r = \infty$. This is exactly the physical interpretation of the *rotation-vibration coupling constant* $\alpha_e$.

The rotation-vibration coupling is thus an anharmonic effect. The *centrifugal distortion constant* $D_e$ (sometimes also called centrifugal stretching constant) is a harmonic effect though, resulting from the nonrigid character of the rotor. Classically speaking,

the atoms at the ends of the rotor undergo a 'centrifugal force' that will cause a nonrigid bond to 'stretch'.

Usually, experimental data allow the determination of $B_e$, $\alpha_e$, $\omega_e$, and $\omega_e x_e$. $D_e$ can be derived from $\omega_e$ and $B_e$. In less fortunate cases, only $\omega_0$ and $B_0$ can be determined.

All vibrational levels have degeneracy one; the rotational levels have degeneracy $2J+1$. All vibrational levels are always allowed. For heteronuclear diatomics, all rotational levels are allowed too: this is no longer true for homonuclear diatomics. Then, only alternate levels are allowed, namely the odd $J$ values if the nuclear spin function has $\Sigma_u$ symmetry, and the even $J$ values if the nuclear spin function has $\Sigma_g$ symmetry (the nuclear ground state). This latter fact is of little importance spectroscopically (the nuclear levels are very close together), but has consequences for setting up the partition function.

As a final note, for molecules with spin-orbit coupling the two component states have very slightly different rotational constants. This leads to two sets of rotational levels that diverge with rising $J$. This effect is called $\lambda$-doubling: it is not important for the present purpose as it has a negligible effect on the partition function.

### 1.12.2.3 Linear polyatomic molecules

The discussion of electronic states is identical to that for the diatomic.

There are now not one, but several, possible vibrations. The vibrational levels are given by

$$G(\vec{n}) = \sum_i \omega_i (n_i + \frac{g_i}{2}) - \sum_{i,j} X_{ij} (n_i + \frac{g_i}{2})(n_j + \frac{g_j}{2}) + \ldots \tag{1.421}$$

where $n_i$ are the vibrational quantum numbers, $\omega_i$ and $X_{ij}$ represent harmonic frequencies and anharmonicity constants, respectively; the degeneracies $g_i$ equal one for stretching, and two for bending vibrations (as the latter always come in orthogonal but otherwise identical pairs). For a linear polyatomic with $N$ atoms, the degeneracies sum up to $3N-5$. It is easily seen, that there will be $N-1$ nontrivial stretchings and $N-2$ distinct nontrivial bendings.

The theoretical determination of anharmonic force fields for polyatomics is an art in itself; experimental data seldom warrant their full determination. Usually the only quantities that can be determined are the anharmonic frequencies $\nu_i$, given by:

$$\nu_i = \omega_i - 2X_{ii} - \frac{1}{2}\sum_j X_{ij} + \ldots \tag{1.422}$$

The exact zero-point energy is given by

$$G(\vec{0}) = \frac{1}{2}\sum_i \omega_i - \frac{1}{4}\sum_{i,j} X_{ij} + \ldots \tag{1.423}$$

It is readily seen that, given the normal situation of positive anharmonicity constants, the zero-point energy determined as $\sum_i \nu_i/2$ is a lower bound for the correct one.

The harmonic frequencies can be found from the Hessian matrix by solving the generalized eigenvalue problem:

$$\mathsf{F}\vec{x}_i = k_i \mathsf{M}\vec{x} \tag{1.424}$$

or, in matrix form

$$\mathsf{FL} = \mathsf{kML} \tag{1.425}$$

where M is a diagonal matrix of the form $M_{11} = M_{22} = M_{33} = m_1$, $M_{44} = M_{55} = M_{66} = m_2, \ldots$. (Assuming that rows and colums are ordered $x_1$, $y_1$, $z_1$, $x_2$, $y_2$, $z_2$, etc.). This equation is converted into a regular eigenvalue problem by defining the *mass-weighted force constant matrix* $\mathsf{F}' = \mathsf{M}^{-1/2}\mathsf{F}\mathsf{M}^{-1/2}$ and the *mass-weighted normal vibrations* $\vec{x}' = \mathsf{M}^{-1/2}\vec{x}\mathsf{M}^{-1/2}$, which leads to

$$\mathsf{F}'\mathsf{L}' = \mathsf{kL}' \tag{1.426}$$

*Ab initio* calculations yield F in hartree/(electron mass)$\AA^2$. The harmonic frequencies in $\mathrm{cm}^{-1}$ are then obtained as $\omega_i = 5140.5\sqrt{k_i}$.

The bending vibrations will give rise to pairs of degenerate eigenvalues. Five eigenvalues are normally zero (or very small, due to roundoff): these correspond to three translations and two orthogonal rotation planes. These five eigenvectors are often called the 'trivial vibrations'. (The most common cause for nonzero trivial frequencies is an incompletely optimized geometry.) Note that the transformation from Cartesian to normal coordinates is only valid at the equilibrium geometry.

If all the nontrivial eigenvalues are positive, the molecule is a local minimum; a single negative eigenvalue signifies a transition state (with the corresponding eigenvector being the reaction coordinate). A stationary point with $n$ negative eigenvalues is also called an *nth order saddle point.*

We will here also briefly address the infrared intensities. The transition probability $P_{ij}$ for a transition in absorption or emission is given by the matrix element of the dipole moment operator $\hat{\mu}$ between initial and final states $i$ and $j$:

$$P_{ij} = \langle i|\hat{\mu}|j\rangle \tag{1.427}$$

For a diatomic, we could develop $\hat{\mu}$ in a Taylor series about $r_e$, leading to:

$$P_{ij} = \mu_e\langle i|\hat{\mu}|j\rangle + \frac{\partial\mu}{\partial r}\langle i|r|j\rangle + \sum_{n=2}^{\infty}\frac{\partial^n\mu}{\partial r^n}\langle i|r^n|j\rangle/n! \tag{1.428}$$

Assuming electrical harmonicity, the summation drops out; for a harmonic oscillator then, $\langle i|\hat{\mu}|j\rangle = 0$ if $|i-j| \neq 1$. The two together, the so-called *double-harmonic approximation*, lead to the familiar result that no overtones are allowed (when they occur, they are anharmonic effects), and that the transition probability is proportional to the dipole

moment derivative. The integrated intensity is the square of the transition probability; the double-harmonic IR intensities for a polyatomic molecule are then finally given by:

$$I = 42.2547(\mathsf{L}\vec{\nabla}\mu)^2 \text{ km/mol} \tag{1.429}$$

The rotational spectrum of a polyatomic is identical to that of a diatomic, except that there is now more than one rotation-vibration coupling constant:

$$B_n = B_e - \sum_i \alpha_i (n_i + \frac{g_i}{2}) \tag{1.430}$$

$B_e$ is found from the expression

$$B_e = \frac{16.85763}{I_A} \text{ cm}^{-1} \qquad I_A = \sum_i m_i r_i^2 - \frac{1}{M}(\sum_i m_i r_i)^2 \tag{1.431}$$

where $I_A$ denotes the *principal moment of inertia* of the molecule and $M = \sum_i m_i$ is the molecular mass.

Spin-orbit interaction effects again exist for states with both $L$ and $S$ nonzero. Another important effect is that the degeneracy of the bending vibrations will be lifted: this is called the *Renner-Teller effect*. We will illustrate it qualitatively from the example of $N_3$, which has a $X\ ^2\Pi_g$ ground state with one electron in a degenerate $\Pi$ shell. One can now 'bend' the molecule in two orthogonal planes: one parallel, and one orthogonal to the occupied component of the $\Pi$ pair. This will give rise to two different force constants for these two bends, lifting their degeneracy. Renner-Teller effects can be 'weak' (when both force constants are still positive) or 'strong' (when one of the two force constants becomes negative and the molecule will distort to a nonlinear structure).

### 1.12.2.4 Nonlinear polyatomics

The situation for the electronic states is again similar. The degeneracies though are $2S+1$ for a nondegenerate ($A$ or $B$) state, $4S+2$ for a doubly degenerate ($E$) state, and $6S+3$ for a triply degenerate ($T$) one.

The discussion of vibrations is identical to that of the linear molecule, except that there now will be only $3N-6$ nontrivial vibrations (as there are three rotations for a nonlinear molecule), and that the degeneracy of individual vibration types will depend on the molecular point group. Their degeneracies must now sum up to $3N-6$.

The rotational spectrum is different. Let us first consider the rigid case. The equilibrium rotational constants are then found as the eigenvalues of the *inertial tensor*, defined for a rigid rotor as

$$I = \begin{pmatrix} I_{xx} & -I_{xy} & -I_{xz} \\ -I_{xy} & I_{yy} & -I_{yz} \\ -I_{xz} & -I_{yz} & I_{zz} \end{pmatrix} \tag{1.432}$$

$$I_{xx} = \sum_i m_i (y_i^2 + z_i^2) - \frac{1}{M}\left[(\sum_i m_i y_i)^2 - (\sum_i m_i z_i)^2\right] \tag{1.433}$$

$$I_{yz} = \sum_i m_i y_i z_i - \frac{1}{M}\left(\sum_i m_i y_i\right)\left(\sum_i m_i z_i\right) \tag{1.434}$$

where $x_i$, $y_i$, and $z_i$ are the coordinates of the $i$-th atom in an arbitrary coordinate system. (The expressions for $I_{yy}$ and $I_{zz}$ on the one hand, and $I_{xy}$ and $I_{xz}$ on the other hand, are found as cyclic permutations of those for $I_{xx}$ and $I_{yz}$, respectively.) The eigenvectors correspond to the principal axes of inertia; the corresponding moments yield three rotational constants $A, B, C$. Depending on the molecular point group, these are classified as:

**spherical tops** where $A = B = C$. This occurs for tetrahedral, octahedral, and higher polyhedral point groups, which all have at least triply degenerate irreducible representations. Only spherical tops can have triply degenerate electronic states.

**symmetric tops** where $A = B \neq C$. This occurs for all other point groups that have a higher than twofold symmetry axis. Distinction is usually made between *prolate* symmetric tops (where $A = B < C$), and *oblate* symmetric tops (where $A = B > C$). These point groups have twofold, but no threefold, degenerate representations, and can have doubly degenerate electronic states.

**asymmetric tops** where $A \neq B \neq C$. This occurs for all remaining point groups, which only have nondegenerate irreducible representations and can thus only have nondegenerate electronic states.

The energy levels of a symmetric top are given by

$$F(J,K) = BJ(J+1) + (C-B)K^2 \qquad K = -J, \ldots, J \tag{1.435}$$

where each $(J, K)$ level will have degeneracy $2J + 1$. The levels for a spherical top are readily found by substituting $C = B$, which yields levels $BJ(J+1)$ with degeneracy $(2J+1)^2$. For the levels of an asymmetric top, finally, there is no expression in closed form.

Centrifugal and rotation-vibration effects also exist here: their treatment is by no means trivial, however, and they can seldom be determined accurately from the experimental data.

Again, spin-orbit effects exist for states with both $L$ and $S$ nonzero, the treatment of which involves relativistic corrections. Furthermore, however, such states give rise to a well-known degeneracy-lifting distortion called the *Jahn-Teller effect.* Discussions can even be found in freshman general and inorganic chemistry courses (primarily because of its common occurence in transition metal complexes with octahedral or tetrahedral

symmetry). Important for the present discussion is that the Born-Oppenheimer approximation breaks down, and that a single determinant is no longer appropriate to describe the wavefunction even qualitatively; a single-determinant wavefunction will break symmetry.

The potential energy surface of an order $n$ Jahn-Teller molecule has $n+1$ equivalent minima on its potential energy surface, all corresponding to geometrically equivalent distortions of the parent symmetry. However, the barrier towards the parent structure may sometimes be so low that the effective structure becomes symmetric at practical temperatures [Ham71].

Another noteworthy term here is the pseudo-Jahn-Teller effect. This occurs when the reference determinant is nondegenerate, but there is considerable interaction with a degenerate state that would undergo Jahn-Teller distortion.

## 1.12.3 Construction of partition functions

### 1.12.3.1 Rotational partition functions

One can of course always construct the partition function by direct numerical summation. This 'brute-force' approach has the advantage that it is exact, but can become very time-consuming if a very large number of nonfactorizable electronic states is involved, and especially for polyatomic molecules.

For a diatomic molecule, and neglecting the higher-order stretching terms, the partition function would become (with $y \equiv c_2 B/T$ and $\delta \equiv D/B$)

$$Q_{\text{rot}} = \sum_{J=0}^{\infty} (2J+1) \exp[-yJ(J+1)] \exp[\delta y J^2 (J+1)^2] \tag{1.436}$$

For $\delta = 0$, an asymptotic series for $Q_{\text{rot}}$ can be obtained through the Euler-MacLaurin summation formula [Kas33]

$$Q_{\text{rot}} = \frac{1}{\sigma y}\left(1 + \frac{y}{3} + \frac{y^2}{15} + \frac{4y^3}{315} + \frac{y^4}{315} + \frac{4y^5}{3465} + \ldots\right) \tag{1.437}$$

where the *symmetry number* $\sigma$ equals one for heteronuclear, and two for homonuclear molecules (see above). This series usually reaches its asymptotic value after only a few terms, except for the case of $H_2$ at low temperatures, which is best handled by direct numerical summation. The approximation to handle the 'alternate levels' rule by simply halving the partition function also holds very well at practical temperatures.

A correction for centrifugal distortion can be made by expanding the second exponential in $Q_{\text{rot}}$ as a MacLaurin series, swapping the order of summation, and summing over $J$ term by term. As that contribution is only important for large $T$ (and so for very small $y$), the summations may be approximated by integrals and one obtains:

$$\Delta Q_\delta = \sum_{m=0}^{\infty} \frac{\delta^m (2m)!}{y^m m!} \tag{1.438}$$

This series will rapidly reach its asymptotic value if $\delta/y$ is not too large; otherwise it will blow up, and direct numerical summation must be performed.

Terms involving higher stretching constants will only enter the summation at very high temperatures (4000 K or more). These very small effects can very well be approximated from their first-order terms:

$$\begin{aligned} \Delta Q_\eta &\approx \frac{6\eta}{y^2} \\ &\ldots \end{aligned} \tag{1.439}$$

where $\eta \equiv H/B$.

The rotational partition function for the linear polyatomic can be treated identically. That for a semirigid (i.e. not centrifugally distorting) symmetric top can again be evaluated through the Euler-MacLaurin summation, although the algebra is rather unwieldy. Introducing $y \equiv c_2 B/T$, $x \equiv c_2 C/T$, and $z \equiv (1 - B/C)y$, the result can be expressed as [Kas33]:

$$Q_{\text{rot}} = \exp(y/4)\sqrt{\frac{\pi}{xy^2}}\left(1 + \frac{z}{12} + \frac{7z^2}{480} + \frac{31z^3}{8064} + \frac{127z^4}{92160} + \frac{511z^5}{811008} + \ldots\right) \tag{1.440}$$

This expansion usually converges much faster, since the rotational constants involved are much smaller for polyatomics than for diatomics. The expression for the spherical top follows very simply by setting $z = 0$ and $x = y$.

The partition functions for linear molecules [McD88], spherical tops [McD87], and symmetric tops [McD90] have recently been reconsidered by McDowell. He showed that a much more rapidly converging expansion for rigid rotators could be obtained by premultiplying the series by $\exp(y/3)$. For a linear molecule this leads to

$$Q_{\text{rot}}(y) = \frac{e^{y/3}}{y}\left(1 + \frac{y^2}{90} + \frac{8y^3}{2835} + \frac{5y^4}{4536} + \frac{148y^5}{280665} + \ldots\right) \tag{1.441}$$

and for a symmetric top, with $y$ and $z$ being defined as in (1.440), to

$$Q_{\text{rot}}(y) = \frac{e^{y/3}}{y}\sqrt{\frac{\pi}{xy^2}}\left(1 + \frac{z^2}{90} + \frac{8z^3}{2835} + \frac{5z^4}{4536} + \frac{148z^5}{280665} + \ldots\right) \tag{1.442}$$

He then proceeded to show that the effect of centrifugal stretching terms for linear molecules could be accounted for by multiplying the partition function with a correction factor

$$f_c = 1 + 2d\frac{3-y}{3y} + 6\frac{2d^2 - h}{y^2} + 24\frac{5d^3 - 5dh - l}{y^3} \tag{1.443}$$

where $d \equiv D/B$, $h \equiv H/B$, and $l \equiv L/B$, for an energy level expression of the form

$$F(J) = BJ(J+1) - DJ^2(J+1)^2 + HJ^3(J+1)^3 + LJ^4(J+1)^4 + \ldots \tag{1.444}$$

This differs only by a small quantum correction from the previous expression (1.438).

The corresponding expressions [McD90] for the symmetric top are complex and not very relevant to the present discussion.

The case of an asymmetric top (including centrifugal stretching effects) can only be treated exactly by direct numerical summation. However, it has been found empirically [Gor34] that the expression for the symmetric top, with $B$ substituted by $\sqrt{AB}$, results in errors of less than 0.1% even in highly unfavorable cases. Very recently, Watson [Wat88] derived the partition function for a semirigid asymmetric top with rotational constants $A$, $B$, and $C$. By two different methods, he obtained the expression

$$Q' = \sqrt{\frac{\pi}{abc}} \exp(f_1)(1 + f_2' + f_3' + \ldots) \tag{1.445}$$

$$f_1 = \frac{1}{12}\left[2\sum a - \sum \frac{ab}{c}\right] \tag{1.446}$$

$$f_2' = \frac{1}{90}\sum \frac{ab(c-a)(c-b)}{c^2} \tag{1.447}$$

$$f_3' = \frac{1}{2835}\sum \frac{(c-a)(c-b)}{c^3}[(a-b)^2c^2 + 4(a+b)abc - 8a^2b^2] \tag{1.448}$$

(1.449)

where $a \equiv c_2A/T$, $b \equiv c_2B/T$, $c \equiv c_2C/T$, and each sum runs over the three cyclic permutations $(abc), (bca), (cab)$. Two important limiting cases are readily verified: by substituting $a = c$, the expressions simplify to McDowell's form [McD90] for the partition function of a semirigid symmetric top, while substituting $a = b = c$ leads to the expression for the spherical top.

At practical temperatures, all three cases reach the classical equipartition limit, where

$$Q_{\text{rot}} = \frac{1}{\sigma}\sqrt{\frac{\pi T^3}{c_2^3 ABC}} \tag{1.450}$$

The symmetry number, by which the abovementioned expressions should also be divided, enters the expression for similar reasons as in the diatomic cases. It corresponds to one plus the number of distinct rotations that map the molecule onto itself, and is given below for all common point groups:

- 1 for the point groups $C_1$, $C_s$, $C_i$, and $C_{\infty v}$;
- 2 for $D_{\infty h}$;
- $n$ for $C_n$, $C_{nv}$, and $C_{nh}$;
- $2n$ for $D_n$, $D_{nh}$, and $D_{nd}$;
- 12 for $T$ and $T_d$;
- 24 for $O$ and $O_h$.

### 1.12.3.2 Vibrational partition functions

For a diatomic molecule, this can easily be constructed by direct numerical summation. The rovibrational partition function is then found as (with $x(n) \equiv c_2[\epsilon_{\rm vib}(n) - \epsilon_{\rm vib}(0)]$):

$$Q_{\rm rv} = \sum_{n=0}^{\infty} Q_{\rm rot}(n) \exp[-x(n)] \tag{1.451}$$

$$Q'_{\rm rv} = \sum_{n=0}^{\infty} [Q_{\rm rot}(n)x(n) + Q'_{\rm rot}(n)] \exp[-x(n)] \tag{1.452}$$

$$Q''_{\rm rv} = \sum_{n=0}^{\infty} [Q_{\rm rot}(n)x(n)^2 + 2Q'_{\rm rot}(n)x(n) + Q''_{\rm rot}(n)] \exp[-x(n)] \tag{1.453}$$

Partition functions for two coupled phenomena are always constructed in this manner.

For a rigid rotor and a harmonic oscillator, the two partition functions are factorizable. The vibrational partition function is then found as:

$$Q_{\rm vib} = \sum_{n=0}^{\infty} \exp(-nc_2\omega_e/T) = \frac{1}{1 - \exp(-nc_2\omega_e/T)} \tag{1.454}$$

For a polyatomic molecule, we obtain the familiar result:

$$\ln Q_{\rm vib} = \sum_i -g_i \ln[1 - exp(-c2\omega_i/T)] \tag{1.455}$$

### 1.12.3.3 Electronic partition function

This can only be constructed by direct numerical summation. In general, the electronic states have different rotational and vibrational constants, and the internal partition function is constructed from:

$$Q_{\rm int} = \sum_i Q_{rv,i} \exp(-x_i) \tag{1.456}$$

$$Q'_{\rm int} = \sum_i [Q_{rv,i}x_i + Q'_{rv,i}] \exp(-x_i) \tag{1.457}$$

$$Q''_{\rm int} = \sum_i [Q_{rv,i}x_i^2 + 2Q'_{rv,i}x_i + Q''_{rv,i}] \exp(-x_i) \tag{1.458}$$

where $x_i \equiv c_2(\epsilon_i - \epsilon_0)/T$. In some situations though (e.g., for very high-lying states or for component states of a spin-orbit coupled level), some levels can safely be factored out.

The relative abundances of the various electronic states/isomers can be conveniently calculated as:

$$a_i = \exp(-x_i)Q_{rv,i}/Q_{\rm int} \tag{1.459}$$

## 1.12.4 Dunham analysis

We have not yet discussed the relationship between the potential curve of a diatomic molecule and the spectroscopic constants. It is convenient to transform it to the dimensionless variable $\xi = (r - r_e)/r_e$. Then the potential around $r_e$ is given by:

$$E(\xi) = a_0\xi^2(1 + a_1\xi + a_2\xi^2 + a_3\xi^3 + \ldots) \tag{1.460}$$

where it is easily found that $\omega_e = \sqrt{4B_e a_0}$. The effective Schrödinger equation for the rotating vibrator then becomes

$$\frac{d^2\psi}{d\xi^2} + \frac{2\mu}{\hbar^2}[E - V - \frac{B_e J(J+1)}{(1+\xi)^2}]\psi = 0 \tag{1.461}$$

where we used the identity $r = r_e(1+\xi)$. The rotational term can then also be expanded in a power series, becoming:

$$B_e J(J+1)(1 - 2\xi + 3\xi^2 - 4\xi^3 + \ldots) \tag{1.462}$$

Using the Wentzel-Brillouin-Kramers method, the evaluation of the energy level expression becomes a straightforward but tedious task. After many manipulations it is found [Dun32] that:

$$E(n,J) = \sum_{i=0,j=0}^{\infty} Y_{ij}(n+\frac{1}{2})^i[J(J+1)]^j \tag{1.463}$$

The $Y_{ij}$ are called the *Dunham coefficients*. Comparison with the empirical energy level expressions yields the equivalences:

$$\begin{aligned}
Y_{10} &= \omega_e \quad Y_{20} = -\omega_e x_e \quad Y_{30} = \omega_e y_e \quad \ldots \\
Y_{01} &= B_e \quad Y_{02} = -D_e \quad Y_{03} = H_e \quad \ldots \\
Y_{11} &= -\alpha_e \quad Y_{12} = -\beta_e \quad Y_{21} = \gamma_e \quad \ldots \\
&\ldots
\end{aligned} \tag{1.464}$$

The first fifteen Dunham coefficients are given by:

$$Y_{00} = \frac{B_e}{8}\left(3a_2 - \frac{7a_1^2}{4}\right) \tag{1.465}$$

$$Y_{10} = \omega_e + \frac{B_e^2}{4}\left(25a_4 - 95a_1a_3 - \frac{67a_2^2}{4} + \frac{459a_1^2a_2}{8} - \frac{1155a_1^4}{64}\right) \tag{1.466}$$

$$\begin{aligned}
Y_{20} = {} & \frac{B_e}{2}\left(3a_2 - \frac{15a_1^2}{4}\right) + \frac{B_e^3}{4\omega_e^2}\left(245a_6 - \frac{1365a_1a_5}{2} - \frac{885a_2a_4}{2} - \frac{1085a_3^2}{4}\right. \\
& + \frac{8535a_1^2a_4}{8} + \frac{1707a_2^3}{8} + \frac{7335a_1a_2a_3}{4} - \frac{23865a_1^3a_3}{16} - \frac{62013a_1^2a_2^2}{32} \\
& \left. + \frac{239985a_1^4a_2}{128} - \frac{209055a_1^6}{512}\right)
\end{aligned} \tag{1.467}$$

$$Y_{30} = \frac{B_e^2}{2\omega_e}\left(10a_4 - 35a_1a_3 - \frac{17a_2^2}{2} + \frac{225a_1^2a_2}{4} - \frac{705a_1^4}{32}\right) \tag{1.468}$$

$$\begin{aligned}
Y_{40} = {} & \frac{5B_e^3}{\omega_e^2}\left(\frac{7a_6}{2} - \frac{63a_1a_5}{4} - \frac{33a_2a_4}{4} - \frac{63a_3^2}{8} + \frac{543a_1^2a_4}{16} + \frac{75a_2^3}{16}\right. \\
& \left. + \frac{483a_1a_2a_3}{8} - \frac{1953a_1^2a_3}{32} - \frac{4989a_1^2a_2^2}{64} + \frac{23265a_1^4a_2}{256} - \frac{23151a_1^6}{1024}\right)
\end{aligned} \tag{1.469}$$

$$Y_{01} = B_e + \frac{B_e^3}{2\omega_e^2}\left(15 + 14a_1 - 9a_2 + 15a_3 - 23a_1a_2 + \frac{21(a_1^2 + a_1^3)}{2}\right) \tag{1.470}$$

$$Y_{11} = \frac{6B_e^2}{\omega_e}(1+a_1) + \frac{B_e^2}{\omega_e^2}\left(175 + 285a_1 - \frac{332a_2}{2} + 190a_3 - \frac{225a_4}{2} + 175a_5 + \frac{2295a_1^2}{8} - 459a_1a_2 + \frac{1425a_1a_3}{4} - \frac{795a_1a_4}{2} + \frac{1005a_2^2}{8} - \frac{715a_2a_3}{2} + \frac{1155a_1^3}{4} - \frac{9639a_1^2a_2}{16} + \frac{5145a_1^2a_3}{8} + \frac{4677a_1a_2^2}{8} - \frac{14259a_1^3a_2}{16} + \frac{31185(a_1^4+a_1^5)}{128}\right) \quad (1.471)$$

$$Y_{21} = \frac{6B_e^3}{\omega_e^2}\left(5 + 10a_1 - 3a_2 + 5a_3 - 13a_1a_2 + \frac{15(a_1^2+a_1^3)}{2}\right) \quad (1.472)$$

$$Y_{31} = \frac{20B_e^4}{\omega_e^3}\left(7 + 21a_1 - \frac{17a_2}{2} + 14a_3 - \frac{9a_4}{2} + 7a_5 + \frac{225a_1^2}{8} - 45a_1a_2 + \frac{105a_1a_3}{4} - \frac{51a_1a_4}{2} + \frac{51a_2^2}{8} - \frac{45a_2a_3}{2} + \frac{141a_1^3}{4} - \frac{945a_1^2a_2}{16} + \frac{435a_1^2a_3}{8} + \frac{411a_1a_2^2}{8} - \frac{1509a_1^3a_2}{16} + \frac{3807(a_1^4+a_1^5)}{128}\right) \quad (1.473)$$

$$Y_{02} = -\frac{4B_e^3}{\omega_e^2} - \frac{2B_e^5}{\omega_e^4}\left(163 + 199a_1 - 119a_2 + 90a_3 - 45a_4 + \frac{205a_1a_3}{2} - 207a_1a_2 - \frac{333a_1^2a_2}{2} + \frac{693a_1^2}{4} + 46a_2^2 + 126a_1^3 + \frac{63a_1^4}{2}\right) \quad (1.474)$$

$$Y_{12} = -\frac{12B_e^4}{\omega_e^3}\left(\frac{19}{2} + 9a_1 + \frac{9a_1^2}{2} - 4a_2\right) \quad (1.475)$$

$$Y_{22} = -\frac{24B_e^5}{\omega_e^4}\left(65 + 125a_1 - 61a_2 + 30a_3 - 15a_4 + \frac{495a_1^2}{4} - 117a_1a_2 + 26a_2^2 + \frac{95a_1a_3}{2} - \frac{207a_1^2a_2}{2} + 90a_1^3 + 45a_1^4\right) \quad (1.476)$$

$$Y_{03} = \frac{16B_e^5}{\omega_e^4}(3+a_1) \quad (1.477)$$

$$Y_{13} = \frac{12B_e^6}{\omega_e^5}\left(233 + 279a_1 + 189a_1^2 + 63a_1^3 - 88a_1a_2 - 120a_2 + \frac{80a_3}{3}\right) \quad (1.478)$$

$$Y_{04} = -\frac{64B_e^7}{\omega_e^6}\left(13 + 9a_1 - a_2 + \frac{9a_1^2}{4}\right) \quad (1.479)$$

A number of things in this impressive array of equations are noteworthy:

- There is a zero-point rotational term $Y_{00}$ that should be added to the zero-point energy.

- Apparently, the 'mechanical' $B_e$ and $\omega_e$ are not exactly equal to the 'empirical' $B_e$ and $\omega_e$. The difference terms are unimportant for most practical purposes, but nevertheless detectable in careful experimental work. Most experimental publications (like the Huber-Herzberg compilation) adhere to the 'empirical' rather than the 'mechanical' definition.

- The terms involving $(B_e^2/\omega_e^2)$ in the equations for $Y_{10}$, $Y_{20}$, $Y_{01}$, $Y_{11}$, and $Y_{02}$ are generally omitted, resulting in errors on the order of 1 part in $10^4$. Within this approximation, all spectroscopically important terms may be derived from a quartic potential; it is equivalent to equating the 'empirical' and 'mechanical' spectroscopic constants.

- A term on the order of $B_e^3/\omega_e^2$ has been omitted from the $Y_{00}$ expression. It is totally unimportant in practice.

This procedure was originally intended to allow the extraction of potential curves from spectroscopical data. For this, it has the disadvantage of being numerically highly unstable. It is however perfectly suited for the reverse process: the derivation of spectroscopic constants from an existing potential curve.

The Dunham potential can be evaluated *ab initio* by computing the energy for various bond distances, fitting a polynomial of some suitable degree, locating its minimum, and transforming the polynomial to the dimensionless variable $\xi$. The zero-order coefficient is the energy at $r_e$; the first-order coefficient should vanish; the second-order coefficient $a_0$ allows the extraction of the mechanical $\omega_e$ (the mechanical $B_e$ is of course easily found from $r_e$). The higher-order coefficients should simply be divided by $a_0$ to obtain $a_1$, $a_2$, .... Obtaining the various spectroscopic constants then becomes a trivial procedure.

The Dunham potential has some important disadvantages, though. It diverges when $r > 2r_e$, whereas the usual range of convergence is often much less. Furthermore, it does not have the correct limiting behavior at $r = 0$ (where it should reach $\infty$) or $r = \infty$ (where it should reach the dissociation limit). Also, the coefficients $a_n$ grow very rapidly with increasing $n$. In ab initio calculations with very sharp convergence thresholds, where the energies can usually be relied upon to be correct to eight or nine decimal places, this poses little problems when only $a_1$ and $a_2$ are required, because only a very small range of $r$ is then required. Even so, the stepsize and number of points should be chosen carefully and adapted to the 'steepness' of the potential. For MRD-CI type calculations, where energies are only reliable to five decimal places or worse, large ranges are necessary where the Dunham potential will always diverge. (In such calculations, an often used procedure is to fit a Morse or generalized Morse potential to the curve and compute any spectroscopic constants from that [Bar90a].)

Simons, Parr, and Finlan [Sim73] (SPF) suggested an alternative form for the potential, namely a power series expansion in $\rho = (r - r_e)/r$:

$$E(\rho) = b_0\rho^2(1 + b_1\rho + b_2\rho^2 + b_3\rho^3 + \ldots) \tag{1.480}$$

This expansion may be shown to have a perturbation theoretical basis. Also, it is easily seen that

$$\rho = \xi/(1+\xi) = \xi - \xi^2 + \xi^3 - \xi^4 + \ldots \tag{1.481}$$

which means that higher order terms are implicitly introduced into the expansion. Also, the Simons-Parr-Finlan expansion has the right behavior in the $r = 0$ and $r \to \infty$ limits, and has no upper limit on $r$ for convergence.

An infinite Dunham and an infinite SPF expansion should be equal in their convergence regions, which means that their derivatives with respect to $r$ should be identical at $r_e$. This leads to the following relationship between the Dunham and SPF coefficients:

$$a_n = b_n + \sum_{i=1}^{n-1} (-1)^i b_{n-i} \begin{pmatrix} n+1 \\ i \end{pmatrix} + (-1)^n (n+1) \tag{1.482}$$

So one can fit an SPF expansion, obtain the Dunham coefficients from that, and extract the spectroscopic constants from these. The $b_n$ coefficients are usually smaller than unity and even tend to decay with increasing $n$.

Over small ranges, the SPF expansion has no obvious advantages over the Dunham expansion. Over large ranges however (with less accurate energies or when a high-order expansion is required), an SPF function will usually result in a much better fit and thus more reliable spectroscopic constants.

When enough experimental energy levels are available, a numerical potential curve may be derived using the Rydberg-Klein-Rees (RKR) method [Ree47, Hur76]. Comparison of Dunham and SPF expansions has shown that SPF expansions reproduce the RKR potential curves accurately over a much larger range than the regular Dunham expansion.

The radius of convergence for the Dunham potential is $0 < r < 2r_e$, that of the SPF expansion $r_e/2 < r < \infty$. Yet another expansion, with convergence radius $0 < r < \infty$, has been suggested by Tipping and Ogilvie (quoted in [Bec76]) and uses the parameter

$$z = \frac{r - r_e}{r + r_e} \tag{1.483}$$

Its expansion coefficients are related to the Dunham coefficients by

$$a_0 = \frac{1}{4} C_0 \tag{1.484}$$

$$a_n = \frac{1}{2^n} \left( C_n + \sum_{i=1}^{n-1} (-1)^i C_{n-i} \begin{pmatrix} n+1 \\ i \end{pmatrix} + (-1)^n (n+1) \right) \tag{1.485}$$

A comparative investigation of the Dunham, SPF and Ogilvie-Tipping expansions has been made by Wilson [Wil78]. This latter author also discusses the fitting of the SCF and the correlation energy to separate polynomials; SCF energies are quite anharmonic and generally known to higher precision than the correlation energy, which suggests using a high-order polynomial for the SCF and a low-order one for the correlation energy. The subject is also briefly touched in Section 4.5.

# References


[Ada88] L. Adamowicz and R. J. Bartlett, *Phys. Rev. A* **37**, 1 (1988) and references therein.

[Ahl74] R. Ahlrichs, *Theor. Chim. Acta* **35**, 59 (1974).

[Ahl79] R. Ahlrichs, *Comp. Phys. Commun.* **17**, 31 (1979).

[Ahl81] R. Ahlrichs and P. R. Taylor, *J. Chim. Phys.* **78**, 315 (1981).

[Ahl85] R. Ahlrichs, P. Scharf, and C. Ehrhardt, *J. Chem. Phys.* **82**, 890 (1985).

[Ahl87] R. Ahlrichs and P. Scharf, *Adv. Chem. Phys.* **67**, 501 (1987).

[Alm82] J. Almlöf, K. Faegri Jr., and K. Korsell, *J. Comp. Chem.* **3**, 385 (1982).

[Alm87] J. Almlöf and P. R. Taylor, *J. Chem. Phys.* **86**, 4070 (1987); *J. Chem. Phys.* **92**, 551 (1990).

[Alm89] J. Almlöf, B. J. DeLeeuw, P. R. Taylor, C. W. Bauschlicher Jr., and P. E. M. Siegbahn, *Int. J. Quantum Chem. Symp.* **23**, 345 (1989).

[Alm91] J. Almlöf and P. R. Taylor, *Adv. Quantum Chem.*, to appear.

[Bac81] G. B. Bacskay, *Chem. Phys.* **61**, 385 (1981).

[Bai69] N. C. Baird and M. J. S. Dewar, *J. Chem. Phys.* **50**, 1262 (1969).

[Bar74a] A. Barbe, C. Secroun, and P. Jouve, *J. Mol. Spectr.* **49**, 171 (1974).

[Bar74b] R. D. Bardo and K. Ruedenberg, *J. Chem. Phys.* **60**, 918 (1974).

[Bar78] R. J. Bartlett and G. D. Purvis, *Int. J. Quantum Chem.* **14**, 561 (1978).

[Bar79] R. J. Bartlett, I. Shavitt, and G. D. Purvis III, *J. Chem. Phys.* **71**, 281 (1979).

[Bar81a] R. J. Bartlett and G. D. Purvis III, *Phys. Scr.* **21**, 255 (1981).

[Bar81b] R. J. Bartlett, *Ann. Rev. Phys. Chem.* **32**, 359 (1981).

[Bar83] R. J. Bartlett, H. Sekino, and G. D. Purvis III, *Chem. Phys. Lett.* **98**, 66 (1983).

[Bar89a] R. J. Bartlett, *J. Phys. Chem.* **93**, 1697 (1989).

[Bar89b] R. J. Bartlett, S. A. Kucharski, J. Noga, J. D. Watts, and G. W. Trucks, in *Many-body methods in quantum chemistry* (ed. U. Kaldor), Lecture Notes in Chemistry **52**, Springer Verlag, Berlin, Heidelberg, New York, 1989, p.125.

[Bar90a] V. J. Barclay, Ph. D. thesis, University of Ontario, Ottawa, Canada, 1990.

[Bar90b] R. J. Bartlett, J. D. Watts, S. A. Kucharski, and J. Noga, *Chem. Phys. Lett.* **165**, 513 (1990).

[Bau85] C. W. Bauschlicher Jr., *Chem. Phys. Lett.* **122**, 572 (1985) and references therein.

[Bau86] C. W. Bauschlicher Jr. and P. R. Taylor, *J. Chem. Phys.* **85**, 2779 (1986).

[Bau90a] C. W. Bauschlicher, Jr., S. R. Langhoff, and P. R. Taylor, *Adv. Chem. Phys.* **77**, 103 (1990).

[Bau90b] C. W. Bauschlicher, Jr., S. R. Langhoff, and P. R. Taylor, *Chem. Phys. Lett.* **171**, 42 (1990).

[Bec76] C. L. Beckel, *J. Chem. Phys.* **65**, 4319 (1976).

[Ben80] M. Bénard and J. Paldus, *J. Chem. Phys.* **72**, 6546 (1980).

[Bin74] J. S. Binkley, J. A. Pople, and P. A. Dobosh, *Mol. Phys.* **28**, 1423 (1974).

[Bin75a] R. C. Bingham, M. J. S. Dewar, and D. H. Lo, *J. Am. Chem. Soc.* **97**, 1285 (1975).

[Bin75b] J. S. Binkley and J. A. Pople, *Int. J. Quantum Chem.* **9**, 229 (1975).

[Bin77] J. S. Binkley and J. A. Pople, *J. Chem. Phys.* **66**, 879 (1977).

[Bin80] J. S. Binkley, J. A. Pople, and W. J. Hehre, *J. Am. Chem. Soc.* **102**, 939 (1980).

[Blo83] M. R. A. Blomberg and P. E. M. Siegbahn, *J. Chem. Phys.* **78**, 5682 (1983).

[Bot88] P. Botschwina, *J. Chem. Soc. Faraday II* **84**, 1263 (1988).

[Bot89] P. Botschwina and P. Sebald, *Chem. Phys. Lett.* **160**, 485 (1989).

[Boy50] S. F. Boys, *Proc. Royal Soc.* **A 200**, 542 (1950).

[Boy70] S. F. Boys and F. Bernardi, *Mol. Phys.* **19**, 553 (1970).

[Bra67] B. H. Brandow, *Rev. Mod. Phys.* **39**, 771 (1967).

[Bri34] L. Brillouin, *Actual. Sci. Ind.* p.71(1933); p.159(1934).

[Bro79] B. R. Brooks and H. F. Schaefer III, *J. Chem. Phys.* **70**, 5092 (1979).

[Bru54] K. A. Brueckner, *Phys. Rev.* **96**, 508 (1954); *Phys. Rev.* **97**, 1353 (1955).

[Bru55] K. A. Brueckner, *Phys. Rev.* **100**, 36 (1955).

[Bue74] R. J. Buenker, S. D. Peyerimhoff, and W. Butscher, *Mol. Phys.* **35**, 771 (1978); R. J. Buenker and S. D. Peyerimhoff, *Theor. Chim. Acta* **35**, 33 (1974); R. J. Buenker and R. A. Phillips, *J. Mol. Struct. (THEOCHEM)* **123**, 291 (1985).

[Bue75] R. J. Buenker and S. D. Peyerimhoff, *Theor. Chim. Acta* **39**, 217 (1975).

[Bue83] R. J. Buenker and S. D. Peyerimhoff, in *New horizons of quantum chemistry* (eds. P.O.Löwdin and B. Pullman), D. Reidel, Dordrecht, Boston, 1983.

[Car78] R. Carbo and J. M. Riera, *A general SCF theory*, Lecture Notes in Chemistry vol. 8 (Springer Verlag, Berlin, 1978).

[Car80] P. Čársky and M. Urban, *Ab initio calculations: methods and applications in chemistry*, Lecture Notes in Chemistry vol. 16 (Springer Verlag, Berlin, 1980).

[Car84] P. Čársky, B. A. Hess Jr., and L. J. Schaad, *J. Comp. Chem.* **5**, 280 (1984).

[Car87] P. Čársky, L. J. Schaad, B. A. Hess Jr., M. Urban, and J. Noga, *J. Chem. Phys.* **87**, 411 (1987).

[Cha81] J. Chandrasekar, J. G. Andrade, and P. von Ragué Schleyer, *J. Am. Chem. Soc.* **103**, 5609 (1981).

[Chi81] R. A. Chiles and C. E. Dykstra, *J. Chem. Phys.* **74**, 4544 (1981).

[Ciz66] J. Čížek, *J. Chem. Phys.* **45**, 4256 (1966).

[Ciz80] J. Čížek and J. Paldus, *Phys. Scr.* **21**, 251 (1980).

[Cla83] T. Clark, J. Chandrasekar, G. W. Spitznagel, and P. Von Ragué Schleyer, *J. Comp. Chem.* **4**, 294 (1983).

[Cle74] E. Clementi and C. Roetti, *Atom. Data Nucl. Data Tables* **14**, 177 (1974) and references therein.

[Coe58] F. Coester, *Nucl. Phys.* **1**, 421 (1958); F. Coester and H. Kümmel, *Nucl. Phys.* **17**, 477 (1960).

[Col63] A. J. Coleman, *Rev. Mod. Phys.* **35**, 668 (1963).

[Col86] J. R. Collins and G. A. Gallup, *Chem. Phys. Lett.* **123**, 56 (1986).

[Dac70] P. D. Dacre, *Chem. Phys. Lett.* **7**, 47 (1970).

[Dav74] E. R. Davidson, in: The world of quantum chemistry (Ed. R. Daudel and B. Pullman), D. Reidel, Dordrecht, 1974, p. 17.

[Dav75] E. R. Davidson, *J. Comp. Phys.* **17**, 87 (1975).

[Dav77] E. R. Davidson and D. W. Silver, *Chem. Phys. Lett.* **52**, 403 (1977).

[Dav86] E. R. Davidson and D. Feller, *Chem. Rev.* **86**, 681 (1986).

[DeF86] D. J. DeFrees and A. D. McLean, *J. Comp. Chem.* **7**, 321 (1986).

[Dew70] M. J. S. Dewar and E. Haselbach, *J. Am. Chem. Soc.* **92**, 590 (1970).

[Dew77] M. J. S. Dewar and W. Thiel, *J. Am. Chem. Soc.* **99**, 4899 (1977).

[Dew85] M. J. S. Dewar, E. G. Zoebisch, E. F. Healy, and J. J. P. Stewart, *J. Am. Chem. Soc.* **107**, 3902 (1985).

[Dil75] J. D. Dill and J. A. Pople, *J. Chem. Phys.* **62**, 2921 (1975).

[Dit71] R. Ditchfield, W. J. Hehre, and J. A. Pople, *J. Chem. Phys.* **54**, 724 (1971).

[Dui71] F. B. Van Duijneveldt, *IBM Technical Research Report* RJ945 (1971).

[Dui87] J. H. Van Lenthe, J. C. G. M. van Duijneveldt-van de Rijdt, and F. B. van Duijneveldt, *Adv. Chem. Phys.* **69**, 521 (1987) and references therein.

[Dun32] J. L. Dunham, *Phys. Rev.* **41**, 721 (1932).

[Dun70] T. H. Dunning Jr., *J. Chem. Phys.* **53**, 2823 (1970).

[Dun71] T. H. Dunning Jr., *J. Chem. Phys.* **55**, 716 (1971).

[Dun77] T. Dunning and P. Hay, in *Modern theoretical chemistry* (ed. H. F. Schaefer III), Plenum press, New York, London, 1977, p.1.

[Dup76] M. Dupuis, J. Rys, and H. F. King, *J. Chem. Phys.* **65**, 111 (1976); H. F. King and M. Dupuis, *J. Comp. Phys.* **21**, 144 (1976); J. Rys, M. Dupuis, and H. F. King, *J. Comp. Chem.* **4**, 154 (1983).

[Dup77] M. Dupuis and H. F. King, *Int. J. Quantum Chem.* **11**, 613 (1977).

[Dup78] M. Dupuis and H. F. King, *J. Chem. Phys.* **68**, 3998 (1978).

[Dyk88] C. E. Dykstra, *Ab initio calculation of the structures and properties of molecules* (Elsevier, Amsterdam, 1988).

[Eld73] M. Elder, *Int. J. Quantum Chem.* **7**, 75 (1973).

[Eyr44] H. Eyring, J. Walter, and G. E. Kimball, *Quantum Chemistry* (J. Wiley, New York, 1944).

[Fey48] R. P. Feynman, *Rev. Mod. Phys.* **20**, 367 (1948).

[Fey66] R. P. Feynman, *Science* **153**, 699 (1966).

[Fle63] R. Fletcher and M. J. D. Powell, *Comput. J.* **6**, 163 (1963).

[Fow66] R. H. Fowler, *Statistical Mechanics* (Cambridge University Press, Cambridge, 1966); R. H. Fowler and E. A. Guggenheim, *Statistical thermodynamics* (Cambridge University Press, Cambridge, 1965).

[Fra82] M. M. Francl, W. J. Pietro, W. J. Hehre, J. S. Binkley, M. S. Gordon, D. J. DeFrees, and J. A. Pople, *J. Chem. Phys.* **77**, 3654 (1982).

[Fri84] M. J. Frisch, J. A. Pople, and J. S. Binkley, *J. Chem. Phys.* **80**, 3265 (1984).

[Fri90a] M. J. Frisch, M. Head-Gordon, and J. A. Pople, *Chem. Phys. Lett.* **166**, 275 (1990).

[Fri90b] M. J. Frisch, M. Head-Gordon, and J. A. Pople, *Chem. Phys. Lett.* **166**, 281 (1990).

[Fro77] C. Froese Fischer, *Atomic Hartree-Fock calculations*, (Wiley, New York, 1977).

[Fuk81] H. Fukutome, *Int. J. Quantum Chem.* **20**, 955 (1981).

[Gda88] R. J. Gdanitz and R. Ahlrichs, *Chem. Phys. Lett.* **143**, 413 (1988).

[Ger69] J. Gerratt and I. M. Mills, *J. Chem. Phys.* **49**, 1719 (1968); *J. Chem. Phys.* **49**, 1730 (1968).

[Gil88] P. M. W. Gill, J. A. Pople, L. Radom, and R. H. Nobes, *J. Chem. Phys.* **89**, 7307 (1988).

[Gol57] J. Goldstone, *Proc. Royal Soc. (London)* **A 239**, 267 (1957).

[Gor34] A. R. Gordon, *J. Chem. Phys.* **2**, 65 (1934).

[Gor82] M. S. Gordon, J. S. Binkley, J. A. Pople, W. Pietro, and W. J. Hehre, *J. Am. Chem. Soc.* **104**, 2797 (1982).

[Gre89] R. S. Grev and H. F. Schaefer III, *J. Chem. Phys.* **91**, 7305 (1989).

[Ham71] Frank S. Ham, *Int. J. Quantum Chem.* Symp. **5**, 191 (1971).

[Han84] N. C. Handy and H. F. Schaefer III, *J. Chem. Phys.* **81**, 5031 (1984).

[Han85] N. C. Handy, P. J. Knowles, and K. Somasundram, *Theor. Chim. Acta* **68**, 87 (1985);P. J. Knowles, K. Somasundram, N. C. Handy, and K. Hirao, *Chem. Phys. Lett.* **113**, 8 (1985).

[Han89] N. C. Handy, J. A. Pople, M. Head-Gordon, K. Raghavachari, and G. W. Trucks, *Chem. Phys. Lett.* **164**, 185 (1989).

[Har39] D. R. Hartree, W. Hartree, and B. Swirles, *Phil. Trans. Royal Soc. (London)* **A238**, 229 (1939).

[Har73] P. C. Hariharan and J. A. Pople, *Chem. Phys. Lett.* **16**, 217 (1972); *Theor. Chim. Acta* **28**, 213 (1973).

[Has89] M. Häser and R. Ahlrichs, *J. Comp. Chem.* **10**, 104 (1989).

[Hea88] M. Head-Gordon, J. A. Pople, and M. J. Frisch, *Chem. Phys. Lett.* **153**, 503 (1988).

[Heh69] W. J. Hehre, R. F. Stewart, and J. A. Pople, *J. Chem. Phys.* **51**, 2657 (1969).

[Heh72a] W. J. Hehre and J. A. Pople, *J. Chem. Phys.* **56**, 4233 (1972).

[Heh72b] W. J. Hehre, R. Ditchfield, and J. A. Pople, *J. Chem. Phys.* **56**, 2257 (1972).

[Heh86a] W. J. Hehre, L. Radom, P. von Ragué Schleyer, and J. A. Pople, *Ab initio molecular orbital theory*, Wiley, New York, 1985.

[Heh86b] W. J. Hehre *et al.*, *op. cit.* (pp. 56–58).

[Hel37] H. Hellmann, *Einführung in die Quantumchemie* (Franz Deuticke & Co., Leipzig, 1937.); R. P. Feynman, *Phys. Rev.* **56**, 440 (1939).

[Hel88] T. Helgaker and P. Jørgensen, *Adv. Quantum Chem.* **19**, 183 (1988).

[Her45] G. Herzberg, *Infrared and Raman spectra* (Van Nostrand Reinhold, New York, 1945).

[Her50] G. Herzberg, *Spectra of diatomic molecules* (Van Nostrand Reinhold, New York, 1950).

[Her66] G. Herzberg, *Electronic spectra of polyatomic molecules* (Van Nostrand Reinhold, New York, 1966).

[Hil60] T. L. Hill, *Introduction to statistical thermodynamics* (Addison-Wesley, Reading, MA, 1960).

[Hil70] I. H. Hillier and V. R. Saunders, *Int. J. Quantum Chem.* **4**, 503 (1970); *Proc. Royal Soc. (London)* **A320**, 161 (1970).

[Hof63] R. Hoffmann, *J. Chem. Phys.* **39**, 1397 (1963).

[Hon78] M. Dupuis, J. Rys, and H. F. King, HONDO 5, QCPE 401 (CDC version) and QCPE 403 (IBM version), Quantum Chemistry Program Exchange, Bloomington, IN.

[Hub79] K. P. Huber and G. Herzberg, *Constants of diatomic molecules* (Van Nostrand Reinhold, New York, 1979).

[Hub80] H. P. Huber, *Chem. Phys. Lett.* **62**, 95 (1979); *Chem. Phys. Lett.* **70**, 353 (1980); H. P. Huber, *Theor. Chim. Acta* **55**, 117 (1980).

[Hug57] N. H. Hugenholtz, *Physica* **23**, 481 (1957).

[Hur76] A. C. Hurley, *Electron correlation in small molecules* (Academic Press, London, 1976).

[Huz65] S. Huzinaga, *J. Chem. Phys.* **42**, 1293 (1965).

[Huz83] S. Huzinaga, M. Klobukowski, H. Tatewaki, *Can. J. Chem.* **63**, 1812 (1985).

[Huz84] S. Huzinaga, J. Andzelm, M. Klobukowski, and E. Radzio-Andzelm, *Gaussian basis sets for molecular calculations* (Elsevier, Amsterdam, 1984).

[Huz85] S. Huzinaga, *Computer Physics Reports* **2**, 279 (1985).

[Huz88] S. Huzinaga and M. Klobukowski, *J. Mol. Struct. (THEOCHEM)* **167**, 1 (1988).

[Jor81] P. Jørgensen and J. Simons, *Second quantization methods in chemistry*, Academic Press, New York, 1981.

[Kal89] U. Kaldor, in *Many-body methods in quantum chemistry* (ed. U. Kaldor), Lecture Notes in Chemistry **52**, Springer Verlag, Berlin, Heidelberg, New York, 1989, p.199.

[Kas33] L. S. Kassel, *J. Chem. Phys.* **1**, 576 (1933).

[Kel64] H. P. Kelly and A. M. Sessler, *Phys. Rev.* **132**, 2091 (1963); H. P. Kelly, *Phys. Rev. A* **134**, 1450 (1964).

[Kel69] H. P. Kelly, *Adv. Chem. Phys.* **14**, 129 (1969).

[Kno84] P. J. Knowles and N. C. Handy, *Chem. Phys. Lett.* **111**, 315 (1984).

[Kno89a] P. J. Knowles, *Chem. Phys. Lett.* **155**, 513 (1989).

[Kno89b] P. J. Knowles and N. C. Handy, *J. Chem. Phys.* **91**, 2396 (1989).

[Koc90] H. Koch, H. J. A. Jensen, P. Jørgensen, T. Helgaker, G. E. Scuseria, and H. F. Schaefer III, *J. Chem. Phys.* **92**, 4924 (1990).

[Kri78] R. Krishnan and J. A. Pople, *Int. J. Quantum Chem.* **14**, 91 (1978).

[Kri80] R. Krishnan, J. S. Binkley, R. Seeger, and J. A. Pople, *J. Chem. Phys.* **72**, 650 (1980).

[Kri80b] R. Krishnan, M. J. Frisch, and J. A. Pople, *J. Chem. Phys.* **72**, 4244 (1980).

[Kuc86] S. A. Kucharski and R. J. Bartlett, *Adv. Quantum Chem.* **18**, 281 (1986).

[Kuc89] S. A. Kucharski and R. J. Bartlett, *Chem. Phys. Lett.* **158**, 550 (1989).

[Kut73] W. Kutzelnigg, *Top. Current Chem.* **41**, 31 (1977).

[Kut77] W. Kutzelnigg, in *Modern Theoretical Chemistry Vol. 3* (ed. H. F. Schaefer III), Plenum Press, New York, London, 1977, p.129.

[Lan74] S. R. Langhoff and E. R. Davidson, *Int. J. Quantum Chem.* **8**, 61 (1974).

[Lat87] Z. Latajka and S. Scheiner, *J. Chem. Phys.* **87**, 1194 (1987).

[Lee84] Y. S. Lee, S. A. Kucharski, and R. J. Bartlett, *J. Chem. Phys.* **81**, 5906 (1984).

[Lee90a] T. J. Lee and P. R. Taylor, *Int. J. Quantum Chem. Symp.* **23**, 199 (1990).

[Lee90b] T. J. Lee, A. P. Rendell, and P. R. Taylor, *J. Phys. Chem.* **94**, 5463 (1990).

[Lee90c] T. J. Lee and G. E. Scuseria, *J. Chem. Phys.* **93**, 489 (1990).

[Loe55] P. O. Löwdin, *Phys. Rev.* **97**, 1509 (1955).

[Loe59] P. O. Löwdin, *Adv. Chem. Phys.* **2**, 207 (1959).

[Lou87] S. K. Loushin and C. E. Dykstra, *J. Comp. Chem.* **8**, 81 (1987); S. K. Loushin, S. Liu, and C. E. Dykstra, *J. Chem. Phys.* **84**, 2720 (1986).

[Mac85] P. Mach and O. Kysel, *J. Comp. Chem.* **6**, 312 (1985).

[Mag89] D. H. Magers, W. N. Lipscomb, R. J. Bartlett, and J. F Stanton, *J. Chem. Phys.* **91**, 1945 (1989).

[Mar87] J. M. L. Martin, M. Sc. Thesis (University of Antwerp, Wilrijk, 1987).

[Mar89a] J. M. L. Martin, J. P. François, and R. Gijbels, *Chem. Phys. Lett.* **157**, 217 (1989); *erratum* **159**, 122 (1989).

[Mar89b] J. M. L. Martin, J. P. François, and R. Gijbels, *Chem. Phys. Lett.* **163**, 387 (1989).

[Mar89c] J. M. L. Martin, J. P. François, and R. Gijbels, *J. Chem. Phys.* **90**, 6469 (1989); *Colloque de Physique* **50 C 5**, 873 (1989).

[Mar89c] J. M. L. Martin, J. P. François, and R. Gijbels, *J. Comp. Chem.* **10**, 875 (1989).

[Mar89c] J. M. L. Martin, J. P. François, and R. Gijbels, *J. Comp. Chem.* **10**, 152 (1989).

[Mar89f] J. M. L. Martin, J. P. François, and R. Gijbels, *J. Chem. Phys.* **91**, 4425 (1989).

[Mar89g] J. M. L. Martin, J. P. François, and R. Gijbels, *Theor. Chim. Acta* **76**, 195 (1989).

[Mar90a] J. M. L. Martin, J. P. François, and R. Gijbels, *Chem. Phys. Lett.* **166**, 295 (1990).

[Mar90b] J. M. L. Martin, J. P. François, and R. Gijbels, *Chem. Phys. Lett.* **172**, 346 (1990).

[Mar90c] J. M. L. Martin, J. P. François, and R. Gijbels, *J. Chem. Phys.* **93**, 5037 (1990).

[Mar90d] J. M. L. Martin, J. P. François, and R. Gijbels, *J. Comp. Chem.* **11**, xxx (1990).

[May77] J. E. Mayer and M. G. Mayer, *Statistical mechanics* (Wiley Interscience, New York, 1977).

[May80] I. Mayer, *Adv. Quantum Chem.* **12**, 189 (1980).

[May87] I. Mayer and A. Vibok, *Chem. Phys. Lett.* **140**, 558 (1987); see also I. Mayer, *Theor. Chim. Acta* **72**, 207 (1987).

[McD87] R. S. McDowell, *J. Quant. Spectr. Radiat. Transfer* **38**, 337 (1987).

[McD88] R. S. McDowell, *J. Chem. Phys.* **88**, 356 (1988).

[McD90] R. S. McDowell, *J. Chem. Phys.* **93**, 2801 (1990).

[McI71] J. W. McIver Jr. and A. Komornicki, *Chem. Phys. Lett.* **10**, 303 (1971).

[McL80] A. D. McLean and G. S. Chandler, *J. Chem. Phys.* **72**, 5639 (1980).

[McM78] L. E. McMurchie and E. R. Davidson, *J. Comp. Phys.* **26**, 218 (1978).

[McW56] R. McWeeny, *Proc. Royal Soc. (London)* **A235**, 496 (1956).

[McW89] R. McWeeny, *Methods of molecular quantum mechanics*, Second Edition (Academic Press, London, 1989).

[Mey73] W. Meyer, *Int. J. Quantum Chem.* **5**, 341 (1971); *J. Chem. Phys.* **58**, 1017 (1973).

[Mey76] W. Meyer, *J. Chem. Phys.* **64**, 2901 (1976); C. E. Dykstra, H. F. Schaefer III, and W. Meyer, *J. Chem. Phys.* **65**, 2740 (1976); *J. Chem. Phys.* **65**, 5141 (1976).

[Mol34] C. Møller and M. S. Plesset, *Phys. Rev.* **46**, 618 (1934).

[Mos77] J. Moskowitz and L. C. Snyder, in *Modern Theoretical Chemistry* (ed. H. F. Schaefer III), Plenum Press, New York, London, 1977, p.387.

[Mul89] F. Müller-Plathe and L. Laaksonen, *Chem. Phys. Lett.* **160**, 175 (1989).

[Nei82] D. Neisius and G. Verhaegen, *Chem. Phys. Lett.* **89**, 228 (1982); *Chem. Phys.* **78**, 147 (1981); *Chem. Phys. Lett.* **66**, 358 (1979).

[Nes60] R. K. Nesbet, *Rev. Mod. Phys.* **32**, 272 (1960).

[Nes65] R. K. Nesbet, *Adv. Chem. Phys.* **9**, 321 (1965).

[Nob82] R. H. Nobes, W. R. Rodwell, and L. Radom, *J. Comp. Chem.* **3**, 561 (1982).

[Nog87] J. Noga and R. J. Bartlett, *J. Chem. Phys.* **86**, 7041 (1987); *erratum***89**, 3401 (1988).

[Oba86] S. Obara and A. Saika, *J. Chem. Phys.* **84**, 3963 (1986); M. Head-Gordon and J. A. Pople, *J. Chem. Phys* **89**, 5777 (1988); P. M. W. Gill, M. Head-Gordon, and J. A. Pople, *J. Phys. Chem.* **94**, 5564 (1990).

[Oha66] K. O-Ohata, H. Taketa, and S. Huzinaga, *J. Phys. Soc. of Japan* **21**, 2306 (1966); H. Taketa, S. Huzinaga, and K. O-Ohata, *ibid.* **21**, 2313 (1966).

[Ohn82] K. Ohno and K. Morokuma (eds.), *Quantum chemistry literature data base – Bibliography of ab initio calculations for 1978-1980*, (Elsevier, Amsterdam, 1982); Supplement for 1981, *J. Mol. Struct. (THEOCHEM)* **91**, 1 (1982); Supplement for 1982, *ibid.* **106**, 1 (1983); Supplement for 1983, *ibid.* **119**, 1 (1984); Supplement for 1984, *ibid.* **134**, 1 (1985); Supplement for 1985, *ibid.* **148**, 1 (1986); Supplement for 1986, *ibid.* **154**, 1 (1987); Supplement for 1987, *ibid.* **182**, 1 (1988); Supplement for 1988, *ibid.* **203**, 1 (1989); Supplement for 1989, *ibid.* **211**, 1 (1990).

[Pal72] J. Paldus, J. Čížek, and I. Shavitt, *Phys. Rev. A* **5**, 50 (1972).

[Pal75] J. Paldus and J. Čížek, *Adv. Quantum Chem.* **9**, 105 (1975).

[Pal76] J. Paldus, in *Theoretical chemistry, advances and perspectives* (eds. H. Eyring and D. Henderson), Academic Press, New York, London, 1976, p.132.

[Pal82] J. Paldus, P. E. S. Wormer, F. Visser, and A. van der Avoird, *J. Chem. Phys.* **76**, 2458 (1982).

[Pal89a] J. Paldus, L. Pylypow, and B. Jeziorski, in *Many-body methods in quantum chemistry* (ed. U. Kaldor), Lecture Notes in Chemistry **52**, Springer Verlag, Berlin, Heidelberg, New York, 1989, p.151.

[Pal89b] J. Paldus, J. Čížek, and B. Jeziorski, *J. Chem. Phys.* **90**, 4356 (1989); *J. Chem. Phys.* **93**, 1485 (1990).

[Pan82] F. Pang, P. Pulay, and J. E. Boggs, *J. Mol. Struct. (THEOCHEM)* **88**, 79 (1982).

[Pie82] W. J. Pietro, M. M. Francl, W. J. Hehre, D. J. DeFrees, J. A. Pople, and J. S. Binkley, *J. Am. Chem. Soc.* **104**, 5039 (1982).

[Pit61] K. S. Pitzer and L. Brewer, *Thermodynamics* (McGraw-Hill, New York, 1961), ch. 27.

[Pit73] N. W. Winter, W. C. Ermler, and R. M. Pitzer, *Chem. Phys. Lett.* **19**, 179 (1973); R. M. Pitzer, *J. Chem. Phys.* **58**, 3111 (1973).

[Poi87] R. A. Poirier, R. Kari, and I. G. Czismadia, *Handbook of Gaussian basis sets* (Elsevier, Amsterdam, 1985).

[Pop54] J. A. Pople and R. K. Nesbet, *J. Chem. Phys.* **22**, 571 (1954).

[Pop67] J. A. Pople, D. L. Beveridge, and P. A. Dobosh, *J. Chem. Phys.* **47**, 2027 (1967).

[Pop71] J. A. Pople, *Int. J. Quantum Chem.* Symp. **5**, 175 (1971).

[Pop76] J. A. Pople, J. S. Binkley, and R. Seeger, *Int. J. Quantum Chem. Symp.* **10**, 1 (1976).

[Pop77] J. A. Pople, R. Seeger, and R. Krishnan, *Int. J. Quantum Chem. Symp.* **11**, 149 (1977).

[Pop78] J. A. Pople and W. J. Hehre, *J. Comp. Phys.* **27**, 161 (1978).

[Pop78b] J. A. Pople, R. Krishnan, H. B. Schlegel, and J. S. Binkley, *Int. J. Quantum Chem.* **14**, 545 (1978).

[Pop79] J. A. Pople, R. Krishnan, H. B. Schlegel, and J. S. Binkley, *Int. J. Quantum Chem. Symp.* **13**, 225 (1979).

[Pop81] J. A. Pople, H. B. Schlegel, R. Krishnan, D. J. DeFrees, J. S. Binkley, M. J. Frisch, R. A. Whiteside, R. F. Hout, and W. J. Hehre, *Int. J. Quantum Chem. Symp.* **15**, 269 (1981).

[Pop83] J. A. Pople, M. J. Frisch, B. T. Luke, and J. S. Binkley, *Int. J. Quantum Chem. Symp.* **17**, 307 (1983).

[Pop85] J. A. Pople, B. T. Luke, M. J. Frisch, and J. S. Binkley, *J. Phys. Chem.* **89**, 2198 (1985).

[Pop87a] J. A. Pople, M. Head-Gordon, and K. Raghavachari, *J. Chem. Phys.* **87**, 5968 (1987); K. Raghavachari, J. A. Pople, and M. Head-Gordon, in *Many-body methods in quantum chemistry* (ed. U. Kaldor), Lecture Notes in Chemistry 52, Springer Verlag, Berlin, Heidelberg, New York, 1989, p.215.

[Pop87b] J. A. Pople and L. A. Curtiss, *J. Phys. Chem.* **91**, 155 (1987); **91**, 3637 (1987); L. A. Curtiss and J. A. Pople, *J. Phys. Chem.* **92**, 894 (1988).

[Pop88a] J. A. Pople, M. Head-Gordon, and K. Raghavachari, *Int. J. Quantum Chem. Symp.* **22**, 377 (1988).

[Pop88b] J. A. Pople, P. Von Ragué Schleyer, J. Kaneti, and G. W. Spitznagel, *Chem. Phys. Lett.* **145**, 359 (1988).

[Pop89a] J. A. Pople, M. Head-Gordon, D. J. Fox, K. Raghavachari, and L. A. Curtiss, *J. Chem. Phys.* **90**, 5622 (1989); L. A. Curtiss, C. Jones, G. W. Trucks, K. Raghavachari, and J. A. Pople, *J. Chem. Phys.* **93**, 2537 (1990).

[Pop89b] J. A. Pople, M. Head-Gordon, and K. Raghavachari, *J. Chem. Phys.* **90**, 4635 (1989); *J. Chem. Phys.* **93**, 1486 (1990).

[Pul69] P. Pulay, *Mol. Phys.* **17**, 197 (1969).

[Pul79] P. Pulay, G. Fogarasi, F. Pang, and J. E. Boggs, *J. Am. Chem. Soc.* **101**, 2550 (1979).

[Pul80] P. Pulay, *Chem. Phys. Lett.* **73**, 393 (1980).

[Pul82] P. Pulay, *J. Comp. Chem.* **3**, 556 (1982).

[Pul83] P. Pulay, *J. Chem. Phys.* **78**, 5043 (1983).

[Pur82] G. D. Purvis III and R. J. Bartlett, *J. Chem. Phys.* **76**, 1910 (1982).

[Raf73] R. C. Raffenetti, *J. Chem. Phys.* **58**, 4452 (1973).

[Rag85] K. Raghavachari, *J. Chem. Phys.* **82**, 4607 (1985).

[Rag89] K. Raghavachari, G. W. Trucks, J. A. Pople, and M. Head-Gordon, *Chem. Phys. Lett.* **157**, 479 (1989).

[Rag89b] K. Raghavachari, G. W. Trucks, J. A. Pople, and E. Replogle, *Chem. Phys. Lett.* **158**, 207 (1989).

[Rag90] K. Raghavachari, J. A. Pople, E. S. Replogle, and M. Head-Gordon, *J. Phys. Chem.* **94**, 5579 (1990).

[Ral78] A. Ralston and P. Rabinowitz, *A first course in numerical analysis* (McGraw-Hill, New York, 1978).

[Ree47] A. L. G. Rees, *Proc. Phys. Soc.* **59**, 998 (1947); O. Klein, *Z. Physik* **76**, 226 (1931); R. Rydberg, *Z. Physik* **73**, 376 (1931); **80**, 514 (1933).

[Ric81] W. G. Richards, H. P. Trivedi, and D. L. Cooper, *Spin-orbit couping in molecules* (Clarendon Press, Oxford, 1981).

[Rob75] M. A. Robb, in *Computational Methods in Quantum Chemistry and Molecular Physics* (eds. G. H. F. Diercksen, B. T. Sutcliffe, and A. Veillard), D. Reidel, Dordrecht, Boston, 1975, p.435.

[Roo51] C. C. J. Roothaan, *Rev. Mod. Phys.* **23**, 69 (1951).

[Roo60] C. C. J. Roothaan, *Rev. Mod. Phys.* **32**, 179 (1960).

[Roo75] B. Roos, in *Computational Methods in Quantum Chemistry and Molecular Physics* (eds. G. H. F. Diercksen, B. T. Sutcliffe, and A. Veillard), D. Reidel, Dordrecht, Boston, 1975, p.251.

[Roo77] B. Roos and P. Siegbahn, in *Modern Theoretical Chemistry* (ed. H. F. Schaefer III), Plenum Press, New York, London, 1977, p.277.

[Roo80] B. O. Roos, P. R. Taylor, and P. E. M. Siegbahn, *Chem. Phys.* **48**, 157 (1980).

[Roo87] B. O. Roos, *Adv. Chem. Phys.* **69**, 399 (1987).

[Rot71] S. Rothenberg and H. F. Schaefer III, *J. Chem. Phys.* **54**, 2764 (1971).

[Rue82] K. Ruedenberg, M. W. Schmidt, M. M. Gilbert, and S. T. Elbert, *Chem. Phys.* **71**, 41 (1982) and references therein.

[Rus67] G. S. Rushbrooke, *Introduction to statistical mechanics* (Clarendon Press, Oxford, 1967).

[Sae89] S. Saebø and J. Almlöf, *Chem. Phys. Lett.* **154**, 83 (1989).

[Sax81] P. Saxe, H. F. Schaefer III, and N. C. Handy, *Chem. Phys. Lett.* **79**, 202 (1981).

[Sax82] P. Saxe, D. J. Fox, H. F. Schaefer III, and N. C. Handy, *J. Chem. Phys.* **77**, 5584 (1982).

[Sch79] M. W. Schmidt and K. Ruedenberg, *J. Chem. Phys.* **71**, 3951 (1979).

[Sch84] H. B. Schlegel, J. S. Binkley, and J. A. Pople, *J. Chem. Phys.* **80**, 1976 (1984).

[Sch85] D. W. Schwenke and D. G. Truhlar, *J. Chem. Phys.* **82**, 2418 (1985).

[Sch86] H. B. Schlegel, *J. Chem. Phys.* **84**, 4530 (1986); C. Sosa and H. B. Schlegel, *Int. J. Quantum Chem.* **29**, 1001 (1986); C. Sosa and H. B. Schlegel, *J. Am. Chem. Soc.* **109**, 4193 (1987).

[Sch88] H. B. Schlegel, *J. Phys. Chem.* **92**, 3075 (1988).

[Scu88a] G. E. Scuseria, C. L. Janssen, and H. F. Schaefer III, *J. Chem. Phys.* **89**, 7382 (1988).

[Scu88b] G. E. Scuseria and H. F. Schaefer III, *Chem. Phys. Lett.* **152**, 382 (1988).

[Scu89] G. E. Scuseria and H. F. Schaefer III, *J. Chem. Phys.* **90**, 3700 (1989).

[Scu90] G. E. Scuseria and T. J. Lee, *J. Chem. Phys.* **93**, 5851 (1990).

[See76] R. Seeger and J. A. Pople, *J. Chem. Phys.* **65**, 265 (1976).

[See77] R. Seeger and J. A. Pople, *J. Chem. Phys.* **66**, 3045 (1977).

[Sha63] I. Shavitt, in *Methods of Computational Physics vol.2* (eds. B. Alder, S. Fernbach, and M. Rotenberg), Academic Press, New York, 1963, p.1.

[Sha65] I. Shavitt and M. Karplus, *J. Chem. Phys.* **36**, 550 (1965).

[Sha77] I. Shavitt, in *Modern Theoretical Chemistry* (ed. H. F. Schaefer III), Plenum Press, New York, London, 1977, p.189.

[Sie78] P. E. M. Siegbahn, *Chem. Phys. Lett.* **55**, 386 (1978).

[Sie84] P. E. M. Siegbahn, *Chem. Phys. Lett.* **109**, 417 (1984).

[Sim73] G. Simons, R. G. Parr, and J. M. Finlan, *J. Chem. Phys.* **59**, 3229 (1973).

[Sim87] E. D. Simandiras, R. D. Amos, and N. C. Handy, *Chem. Phys.* **114**, 9 (1987) and references therein.

[Sim88] E. D. Simandiras, J. E. Rice, T. J. Lee, R. D. Amos, and N. C. Handy, *J. Chem. Phys.* **88**, 3187 (1988).

[Sin64] O. Sinanoğlu, *Adv. Chem. Phys.* **6**, 315 (1964).

[Sin69] I. Oksüz and O. Sinanoğlu, *Phys. Rev.* **181**, 42 (1969) and references therein.

[Sla29] J. C. Slater, *Phys. Rev.* **34**, 1293 (1929); quoted by E. R. Davidson, in *The world of quantum chemistry* (eds. R. Daudel, B. Pullman), D. Reidel, Dordrecht, Boston, 1974, p. 17.

[Sla30] J. C. Slater, *Phys. Rev.* **36**, 57 (1930).

[Spi87] G. W. Spitznagel, T. Clark, and P. Von Ragué Schleyer, *J. Comp. Chem.* **8**, 1109 (1987).

[Sta89] J. F. Stanton, W. N. Lipscomb, D. H. Magers, and R. J. Bartlett, *J. Chem. Phys.* **90**, 1077 (1989).

[Ste89] J. J. P. Stewart, *J. Comp. Chem.* **10**, 209 (1989); *ibid.* **10**, 221 (1989).

[Sus69] R. Sustmann, J. E. Williams, M. J. S. Dewar, L. C. Allen, and P. von Ragué Schleyer, *J. Am. Chem. Soc.* **91**, 5350 (1969).

[Sza89] A. Szabo and N. S. Ostlund, *Modern quantum chemistry* (revised first edition), McGraw-Hill, New York, 1989.

[Tak81] T. Takada, M. Dupuis, and H. F. King, *J. Chem. Phys.* **76**, 332 (1981).

[Tay76] P. R. Taylor, G. B. Backskay, N. S. Hush, and A. C. Hurley, *Chem. Phys. Lett.* **41**, 444 (1976).

[Tay81] P. R. Taylor, *J. Chem. Phys.* **74**, 1256 (1981).

[Tay87] P. R. Taylor, *Int. J. Quantum Chem.* **31**, 521 (1987).

[Tay89] P. R. Taylor, C. W. Bauschlicher Jr., and D. W. Schwenke, in *Methods in computational chemistry vol. 3* (Ed. S. Wilson), Plenum Publishing Corporation, New York, 1989.

[TayPC] P. R. Taylor, personal communication.

[Urb85] M. Urban, J. Noga, S. J. Cole, and R. J. Bartlett, *J. Chem. Phys.* **83**, 4041 (1985).

[Urb87] J. Noga, R. J. Bartlett, and M. Urban, *Chem. Phys. Lett.* **134**, 126 (1987).

[Vla73] T. Vladimiroff, *J. Phys. Chem.* **77**, 1983 (1973).

[Wah77] A. Wahl and G. Das, in *Modern Theoretical Chemistry* (ed. H. F. Schaefer III), Plenum Press, New York, London, 1977, p.51.

[Wat88] J. K. G. Watson, *Mol. Phys.* **65**, 1377 (1988).

[Wel83] B. H. Wells and S. Wilson, *Chem. Phys. Lett.* **101**, 429 (1983).

[Wid90] P. O. Widmark, P. A. Malmqvist, and B. O. Roos, *Theor. Chim. Acta* **77**, 291 (1990).

[Wig33] E. P. Wigner, *Phys. Rev.* **46**, 1002 (1934); E. P. Wigner and F. Seitz, *Phys. Rev.* **43**, 824 (1933).

[Wil55] E. B. Wilson Jr., J. C. Decius, and P. C. Cross, *Molecular vibrations* (McGraw-Hill, New York, 1955).

[Wil78] S. Wilson, *Mol. Phys.* **35**, 1 (1978).

[Wil84] S. Wilson, *Electron correlation in molecules* (Clarendon Press, Oxford, 1984).

[Won88] M. W. Wong, P. W. M. Gill, R. H. Nobes, and L. Radom, *J. Phys. Chem.* **92**, 4875 (1988).

[Wri87] J. S. Wright and V. J. Barclay, *J. Chem. Phys.* **86**, 3054 (1987).

[Yam90] Y. Yamaguchi, I. L. Alberts, J. D. Goddard, and H. F. Schaefer III, *Chem. Phys.* **147**, 309 (1990).

# Chapter 2

# Hardware and software

*Nullius in verba (Words alone are nothing).*

*Motto of the Royal Society*

## 2.1 Ab initio molecular orbital packages

These have been restricted to the GAUSSIAN series, developed by the group of Professor Pople at Carnegie-Mellon University. This seminal series started out with the GAUSSIAN 70 package [Gau70], which was limited to single-point RHF and UHF calculations in an (*sp*) basis set. Its main assets at the time were its easy availability and the highly efficient Pople-Hehre axis-switching algorithm for two-electron integrals [Pop78]. The next version, GAUSSIAN 76 [Gau76], was extended to *d* orbitals using the Rys polynomial algorithm [Dup76], but was still limited to single-point calculations. A significant step-up was marked by GAUSSIAN 80 [Gau80], which included geometry optimization with analytical gradients, CID, CISD, MP2, and MP3 single-point calculations, and integrals over up to *f* orbitals. This was the last program to be available through the Quantum Chemistry Program Exchange, a non-profit organization that centralises the distribution of quantum chemical and related computer codes[1]. The subsequent versions, GAUSSIAN 82 [Gau82] and GAUSSIAN 86 [Gau86], were to be obtained directly from the Carnegie-Mellon Quantum Chemistry Publishing Unit, that charged a nominal amount ($250 resp. $300 for academic groups, $500 resp. $1,000 for corporate clients) for handling and distribution costs. From there on, increasing development and follow-up requirements suggested establishing a semi-commercial company, Gaussian, Inc., with a number of full-time employees. Hence, public versions of GAUSSIAN 88 [Gau88] and the newly released GAUSSIAN 90 [Gau90] go for $2,000 for academic, and $10,000 for corporate clients. Gaussian, Inc. also markets an auxillary program called BROWSE, developed

[1] Quantum Chemistry Program Exchange, c/o Mr. Richard W. Counts, Indiana University, Bloomington, IN 47401. E-mail: `COUNTSR@IUBACS.BITNET`

for the management of archived results and various postprocessing, at costs of $1,000 (academic) and $5,000 (corporate), respectively.

Payment of these license fees entitles the client to unlimited use on one particular computer at a site of their choice, provided the use of the program is acknowledged in any published work. It may be used by third parties on that particular computer under the same condition. It may not be used on a second computer (with the possible exception of nodes in a VAXcluster) without paying the fee for additional licences, which is $600 (academic) and $3,000 (corporate) for GAUSSIAN 88 and GAUSSIAN 90. Copies may not be given to third parties, except when these obtain a license too. The program may be converted to other platforms, but such conversions may not be passed on to third parties, even if they are registered GAUSSIAN users.

All of these packages were originally developed on VAX computers. Due to their size and complexity (at least from GAUSSIAN 82 on), as well as the highly machine-dependent nature of several parts of the code, porting them to another platform is far from trivial. Gaussian, Inc. releases some conversions itself, namely those that it has certified itself.

Virtually all the *ab initio* calculations reported in this work were performed using GAUSSIAN 82, GAUSSIAN 86, and GAUSSIAN 88. Below follows a brief survey of their capabilities.

### 2.1.1 GAUSSIAN 82

This large package (130,000 lines of Fortran code, and some 15,000 lines of assembly language and operating system interface) has the following features:

- RHF and UHF single point, gradient, and analytical force constant matrix calculations in an (*spdf*) basis set;
- single-point ROHF calculations. Their utility is rather limited, as the post-SCF and gradient codes do not support ROHF wavefunctions;
- analytical MP2 and closed-shell CID and CISD gradients;
- single-point CID and CISD calculations (both from RHF and UHF references);
- Single-point MP2, MP3, partial and full MP4 energies;
- Single-point CCD calculations;
- Internal and external instability testing of the Hartree-Fock wavefunction [See77];
- SCF by direct minimization of the energy [See76] (for handling difficult convergence);

- Automatic generation of an archive entry containing the most relevant computational data. This is intended for addition to a central database, which can be manipulated using the BROWSE program or, in our case, by some user-written software.

A version was also available at the Facultés Universitaires de Namur, where it ran on the IBM 4381. The code was modified to take advantage of two attached FPS array processors for two-electron integrals and derivatives; for correlated calculations, it is extremely slow. The results in Section 3.2 of the present work have been obtained with it, if only failing anything better.

### 2.1.2 GAUSSIAN 86

This version has been extended to about 170,000 lines of Fortran code (and another 15,000 lines of assembly language and operating system interface). It has the following additional capabilities over GAUSSIAN 82:

- Single-point CCD(ST) calculations;
- Single point spin-projected UHF, MP2, and MP3 calculatiosn;
- Electric field, dipole and polarizability derivatives. Determination of infrared intensities and Raman activities in analytical force constant calculations, and of infrared intensities alone in numerical force constant calculations (provided an analytical gradient is available);
- Acceleration of SCF convergence through Pulay's DIIS procedure [Pul82];
- Generalized valence bond (GVB) calculations [Bob77];
- The semiempirical MOPAC 3 package has been integrated in the system;
- Substantial speedups and partial vectorization of existing routines.

The lion's share of the present work was executed with GAUSSIAN 86 on the VAXstation 2000. Furthermore, a version was available on the IBM 3090/400e VF at the University of Leuven, as well as on the IBM/FPS configuration at the Facultés Universitaires de Namur. This latter version ran entirely within the FPS units, with the IBM only being used as a front-end system.

### 2.1.3 GAUSSIAN 88

By now, the program has crossed the psychological barrier of 200,000 lines of Fortran code (and some 25,000 lines of assembler and operating system interface). Its main additional capabilities over GAUSSIAN 86 are:

- Single-point QCISD(T) calculations;
- Single point multiply spin-projected UHF, MP2, and MP3 calculations;
- Quadratically convergent SCF [Bac81] (QCSCF) for handling cases with difficult convergence;
- Implementation of the Handy-Schaefer Z-vector method [Han84] for MP2 and CI derivatives. This results in a drastic reduction of computer time and especially disk space requirements for these types of calculations;
- Direct SCF, including direct gradients and direct QCSCF;
- The semiempirical section was upgraded to MOPAC 4 level;
- Further substantial speedups and partial vectorization of existing sections of the program.

This program was only available at a later stage of the present work, but quickly proved indispensable because of the QCISD and PMP4($n$) sections, as well as the Z-vector based frequencies. Versions were used on the VAXstation 2000 (later replaced by the VAXstation 3100) as well as on the IBM 3090/400e VF at the University of Leuven.

## 2.2 Semiempirical molecular orbital packages

All semiempirical calculations reported in this work have been performed with a CDC conversion [Ste90] by the present author of the semiempirical MO package MOPAC 5.0 by J. J. P. Stewart [Ste89b]. This program comprises about 23,000 lines of source code, and can do calculations with the MINDO/3 [Bin75], MNDO [Dew77], AM1 [Dew85], and PM3 [Ste89a] semiempirical Hamiltonians, both with standard and user-defined parameters. Single-point calculations, geometry optimizations with analytical gradients, and numerical frequency calculations (including an undocumented infrared intensity evaluation) can all be performed with RHF, UHF, and ROHF wavefunctions, as can transition state searches, numerical polarizability calculations, and various other types of runs.

## 2.3 User-written software

Not each and every task could be performed with the available quantum chemical packages. Below follows an inventory of some software items developed by the present author for the purpose of 'getting the job done'. Some of these programs deal with molecular statistical thermodynamics, others with spectroscopy, still others are utilities for a specific purpose.

DUNHAM A Fortran program (about 1,000 lines) that accepts a series of energies and bond distances for a diatomic molecule, fits them to a regular Dunham or a Simons-Parr-Finlan expansion of ascending degrees, and determines the significance level of the addition of each next term. Based on these, the operator selects an expansion order, after which the program locates the stationary point, re-expands the polynomial, and performs a Dunham analysis. Standard deviations for the various spectroscopic constants are obtained through propagation of the standard deviations in the fit. Dunham's formulas up to eighth order (i.e. up to $\omega_e z_e$) are implemented.

DIATHERM A Pascal program (about 700 lines) to set up the partition function of a diatomic molecule by modified direct numerical summation. For each electronic state, the input consists of the multiplicity, the electronic transition energy, and a set of spectroscopic constants, including anharmonic, rotation-vibration coupling, and centrifugal stretching constants. The summation over electronic and vibrational states is carried out directly; the effective rotational and centrifugal stretching constants for each vibronic level are then computed. Asymptotic series for rotation and centrifugal distortion are summed to convergence; if any of these diverges (usually the second), the rotational sublevels are summed directly. Effects of higher-order centrifugal stretching terms are truncated at first order (as these are very very small anyway). If so desired, direct summation over all rovibronic levels can be enforced too, but this usually does not affect results perceptibly and often increases computer time by one or two orders of magnitude.

ISOSTAR A Fortran program to evaluate vibrational isotopic substitution spectra for polyatomic molecules. Given a GAUSSIAN 8X archive entry, it will extract the required force constant matrix and atom numbers, search a database for isotope masses, and loop over all possible combinations, transforming the force field to mass-weighted coordinates and computing the harmonic frequencies. The output is given as a table ready for pasting into a TEX input file.

THERMOS A related program; given a GAUSSIAN 8X archive entry and the cartesian coordinates of the corresponding geometry, it will compute the required frequencies and rotational constants, and will set up the partition functions within the rigid rotor-harmonic oscillator (RRHO) approximation. Isotope effects are included by looping over all possible isotope combinations and weighing the computed partition functions based on the product of the natural abundances for the given isotopomer. Thermodynamic functions are computed and output in a format suitable for pasting into a TEX document.

RRHO A more general RRHO program, allowing the treatment of multiple electronic states and/or isomers with and without different rotation and vibration constants. Outputs a table of the thermodynamic functions, as well as of the relative abundances of the isomers and/or electronic states.

PAROPT A companion utility to MOPAC 5.0 to allow for parameter optimizations. Employs a derivative-free nonlinear least-squares procedure. CDC version only.

WORDTEX Not a theoretical chemistry program, but a utility (about 1,000 lines Pascal code) that converts Microsoft Word documents into LaTeX input files while preserving most formatting attributes and even mathematical formulas. It is included here as it was written specifically for the purpose of the present work, for which it was necessary to convert several hundred pages worth of Microsoft Word documents preferably without user intervention.

Furthermore, a couple of dozen utilities were written on the VAX, Cyber and MacIntosh computers to enhance productivity and to tailor the working environment to our group's specific needs.

## 2.4 Overview of the hardware used in the present work

### 2.4.1 Workstations and mainframes

The bulk of the present work has been done on a succession of two VAXstations, namely a VAXstation 2000 and a VAXstation 3100. These machines, manufactured and marketed by Digital Equipment Corporation, Inc, were originally developed with the CAD/CAM market in mind, but are excellent value for money in numbercrunching applications. They run under Digital's proprietary VMS (Virtual Memory System) operating system, one of the first commercial operating systems to support virtual memory. Versions running under Ultrix (the DEC implementation of Unix) are also available under the name DECstation.

The VAX CPU is a scalar CISC (complex instruction set computer[2]). The instruction set is very large even by CISC standards; there is even a machine code instruction for polynomial evaluation according to the Horner scheme, as well as a complete set of character string manipulation instructions. The CPU of the VAXstation supports the entire VAX instruction set, with the string instructions being emulated in software.

Our VAXstation 2000 consisted of a CPU running at 0.9 VAX MIPS (million instructions per second) — compared to a 1.1 MIPS rating for the VAX 11/750 mainframe —

[2]As opposed to a RISC (Reduced Instruction Set Computer).

a single SCSI hard disk of 159 MB, a TK50 tape streamer with a capacity of 95 MB per cartridge, and a 15" black-and-white console. An RS-232 port in the back allowed attachment of one extra terminal; at most two users could work on it interactively at the same time. This port was attached to the TDI (Terminal Device Interface) of the CDC, allowing passthrough access via CDCNET from any terminal attached to it. It was generally accessed (for interactive login and text-only file transfer) from an Apple Macintosh computer running VersaTerm 2.2 (a terminal emulation program with VT100 emulation capabilities). Installed system software included MicroVMS 4.7 (a subset of full VMS, lacking certain utilities) and VAX Fortran 4.8; the VAX Macro Assembler is a standard VMS component.

At a later stage, this was replaced by a VAXstation 3100 model 38, with a CPU rated at 3.5 VAX MIPS and two SCSI hard disks of 104 MB. (The remainder of the configuration was identical). Installed system software included full VMS 5.3 and VAX Fortran 4.8, as well as the DECwindows console front-end (Digital's equivalent of the X-Windows graphical user interface developed at MIT for the UNIX operating system).

Semiempirical calculations were performed on the campus CDC Cyber 930-11, which is rated at 1.8 VAX MIPS (double precision) and has a disk capacity of 4 × 414 MB. This machine, which has a BITNET connection, was also used for storage and manipulation of the output files from the external computers, as well as for E-mail access.

The configuration at Namur consists of an IBM 4381 mainframe with two attached FPS-M64 array processors. The IBM itself is so slow and so heavily loaded that running ab initio calculations on it is only meaningful if nothing else is available. The FPS units are rated at about 10 VAX MIPS, although, from our experience, this number appears to be on the high side for GAUSSIAN 8X. The IBM runs under the VM/SP operating system; the FPS units run under the proprietary FPS Manager 1.0. The latter has no virtual memory facilities, and only very limited multi-user capability. The GAUSSIAN 86 version running on it left a lot to be desired; several bugs had to be fixed by the combined efforts of Drs. J.G. Fripiat and D. Vercauteren, as well as the system engineer, Bruno Durasse. The first FPS had a central memory of 8 MB and a disk space of 4 × 135 MB; the second of 28 MB and 3 × 625 MB, respectively.

Finally, the very largest calculations have been performed on the IBM 3090/400e VF at the University of Leuven. The IBM machine is actually a high-end scalar mainframe with vector processing facilities (four vector processors). The machine runs both under VM/XA and the more evolved MVS/XA operating system, the latter of which does support virtual address spaces. Its theoretical performance per vector processor is rated at 116 MFLOPS (million floating point operations per second) for a fully vectorized program. As a maximum of three vector units can be used by a single program under MVS, this leads to a theoretical peak performance of 348 MFLOPS. In our experience, a more realistic figure for the GAUSSIAN 8X series is about 60–70 VAX MIPS. Very large

amounts of scratch disk space can be secured without too many problems; as no volume spillover is possible for GAUSSIAN 8X, a practical upper bound of 1.6 GB (the size of a single disk unit) is placed on the size of each scratch file.

### 2.4.2 Personal computing equipment

The task of writing up the present manuscript, preparing the tables, and performing various intermediate manipulations on the raw data was done entirely with the Apple Macintosh SE personal computers that constitute the campus AppleTalk network, and an Apple Macintosh SE/30 at home. The former have a 16-bit Motorola 68000 CPU clocked at 8 MHz, 1 MB RAM, and two 800 KB floppy disk drives, as well as an AppleTalk outlet connecting them to a 580 MB CDC Wren disk drive, partitioned into several public and private server volumes, and various hardcopy units including a PostScript-driven [Ado86] 300 dpi (dots per inch) Apple LaserWriter Plus. The SE/30 has a 32-bit Motorola 68030 clocked at 16 MHz, a Motorola 68882 floating point accelerator, 4 MB of 120ns dynamic RAM, one dual-format 800 KB and 1.44 MB floppy disk drive, and a 40 MB internal hard disk drive. The Macintosh Finder graphical user interface is not just proverbially user-friendly, but also extremely responsive, and allows an experienced user to work much more rapidly than on any other personal computer. It also allows seamless and virtually transparent communication of data between (sometimes radically) different programs, eliminating the need for manual retyping or cumbersome conversion procedures.

The software packages (commercial, shareware, and public domain) used on this machine are plainly too many to be listed here. Among the most heavily used were the WYSIWIG (What You See Is What You Get) word processors Microsoft Word (versions 3.02 and 4.0) and Nisus 3.04 (Paragon Concepts), the spreadsheet Microsoft Excel (various versions), the power text editors QUED-M 2.01 and 2.09 (Paragon Concepts), McSink 7.0 (Signature Software), and Vantage 1.5.1 (Preferred Publishers), the programming environments MacFortran (Absoft Language Systems) and Think Pascal 2.0 (Symantec), the bibliographic database EndNote (Niles Associates), the scientific graphics programs Cricket Graph 1.3 and KaleidaGraph 2.1 (Abelbeck Software, distributed by Synergy Software), and, last but certainly not least, two implementations of Donald E. Knuth's extremely powerful computer typography system TEX [Knu84], namely OzTEX 1.2 (public domain software by Andy Trevorrow of Aston University) and TEXtures 1.3 (Blue Sky Research). The latter has the advantage that import of various graphics formats is possible. With both TEX versions, Leslie E. Lamport's macro package LATEX [Lam86] has been used throughout.

For checking of certain algebraic derivations, occasional use was made of the computer algebra system MATHEMATICA (Wolfram Research Inc.) [Wol88] running on the MacIntosh SE/30.

# References


[Ado86] Adobe Systems Inc., *PostScript language reference manual*, Addison-Wesley, Reading, MA, 1986.

[Bac81] G. B. Backskay, *Chem. Phys.* **61**, 385 (1981).

[Bin75] R. C. Bingham, M. J. S. Dewar, and D. H. Lo, *J. Am. Chem. Soc.* **97**, 1285 (1975).

[Bob77] F. Bobrowicz and W. A. Goddard III, in *Modern Theoretical Chemistry Vol.3* (ed. H. F. Schaefer III), Plenum Press, New York, London, 1977, p.79.

[Dew77] M. J. S. Dewar and W. Thiel, *J. Am. Chem. Soc.* **99**, 4899 (1977).

[Dew85] M. J. S. Dewar, E. G. Zoebisch, E. F. Healy, and J. J. P. Stewart, *J. Am. Chem. Soc.* **107**, 3902 (1985).

[Dup76] M. Dupuis, J. Rys, and H. F. King, *J. Chem. Phys.* **65**, 111 (1976); H. F. King and M. Dupuis, *J. Comp. Phys.* **21**, 144 (1976); J. Rys, M. Dupuis, and H. F. King, *J. Comp. Chem.* **4**, 154 (1983).

[Gau70] W. J. Hehre, W. A. Lathan, R. Ditchfield, M. D. Newton, and J. A. Pople, GAUSSIAN 70, Quantum Chemistry Program Exchange, Program No. 236 (IBM), 237 (VAX).

[Gau76] J. S. Binkley, R. A. Whiteside, P. C. Hariharan, R. Seeger, J. A. Pople, W. J. Hehre, and M. D. Newton, GAUSSIAN 76, Carnegie- Mellon University, Pittsburgh, PA 15213 (VAX) and Quantum Chemistry Program Exchange, Program No. 368 (CDC), 391 (IBM).

[Gau80] J. S. Binkley, R. A. Whiteside, R. Krishnan, R. Seeger, D. J. DeFrees, H. B. Schlegel, S. Topiol, L. R. Kahn, and J. A. Pople, GAUSSIAN 80, Carnegie-Mellon Quantum Chemistry Publishing Unit, Pittsburgh, PA 15213.

[Gau82] J. S. Binkley, M. J. Frisch, D. J. DeFrees, R. Krishnan, R. A. Whiteside, E. M. Fluder, and J. A. Pople, GAUSSIAN 82, Carnegie-Mellon Quantum Chemistry Publishing Unit, Pittsburgh, PA 15213.

[Gau86] M. J. Frisch, J. S. Binkley, H. B. Schlegel, K. Raghavachari, C. F. Melius, R. L. Martin, J. J. P. Stewart, F. W. Bobrowicz, C. M. Rohlfing, L. R. Kahn, D. J. DeFrees, R. Seeger, R. A. Whiteside, D. J. Fox, E. M. Fluder, and J. A. Pople, GAUSSIAN 86, Carnegie-Mellon Quantum Chemistry Publishing Unit, Pittsburgh, PA 15213.

[Gau88] M. J. Frisch, M. Head-Gordon, H. B. Schlegel, K. Raghavachari, J. S. Binkley, C. Gonzalez, D. J. DeFrees, D. J. Fox, R. A. Whiteside, R. Seeger, C. F. Melius, J. Baker, R. L. Martin, L. R. Kahn, J. J. P. Stewart, E. M. Fluder, S. Topiol, and J. A. Pople, GAUSSIAN 88, gaussian, Inc., Pittsburgh, PA, 1989.

[Gau90] M. J. Frisch, M. Head-Gordon, G. W. Trucks, J. B. Foresman, H. B. Schlegel, K. Raghavachari, M. A. Robb, J. S. Binkley, C. Gonzalez, D. J. DeFrees, D. J. Fox, R. A. Whiteside, R. Seeger, C. F. Melius, J. Baker, R. L. Martin, L. R. Kahn, J. J. P. Stewart, S. Topiol, and J. A. Pople, GAUSSIAN 90, Gaussian, Inc., 6823 North Lakewood, Chicago, IL 60626.

[Han84] N. C. Handy and H. F. Schaefer III, *J. Chem. Phys.* **81**, 5031 (1984).

[Knu84] D. E. Knuth, *The TEXbook*, Addison-Wesley, Reading, MA, 1984.

[Lam86] L. E. Lamport, LaTeX *user's guide and reference manual*, Addison-Wesley, Reading, MA, 1986.

[Pop78] J. A. Pople and W. J. Hehre, *J. Comp. Phys.* **27**, 161 (1978).

[Pul82] P. Pulay, *J. Comp. Chem.* **3**, 556 (1982).

[See76] R. Seeger and J. A. Pople, *J. Chem. Phys.* **65**, 265 (1976).

[See77] R. Seeger and J. A. Pople, *J. Chem. Phys.* **66**, 3045 (1977).

[Ste89a] J. J. P. Stewart, *J. Comp. Chem.* **10**, 209 (1989).

[Ste89b] J. J. P. Stewart, MOPAC *5.0, a general purpose molecular orbital package*, QCPE 455/VAXM.

[Ste90] J. J. P. Stewart, J. M. L. Martin and J. P. François, MOPAC 5.0 (CDC version), QCPE 455/CDCM; see also *QCPE bulletin* **10**, 9 (1990).

[Wol88] S. Wolfram, MATHEMATICA, *a system for doing mathematics by computer*, Addison-Wesley, Reading, MA, 1988.

# Chapter 3

# Combined bond-polarization basis sets

*New ideas are always suspected, and usually opposed, without any other reason than that they are not already common.*

*John Locke, 1632–1704*

## 3.1 Summary and general introduction

If electron correlation is treated well (and this is technically possible with present-day methods) the accuracy-determining factor for an ab initio calculation becomes the choice of the finite basis set. This is especially true for the most common type of calculation, namely that of the total dissociation energy of the molecule.

We have seen in Chapter 1 that, even at the Hartree-Fock level, an isotropic basis set (i.e. one containing only the symmetry types of the occupied atomic orbitals) is no longer sufficient, and that either bond or polarization functions must be added. Accounting for external correlation, on the other hand, always requires polarization functions.

Bond and polarization functions both have their advantages and disadvantages, which will be discussed in detail in the next sections. Those for bond functions can be briefly summarized as follows:

- Pros:
  - bond functions lead to more compact basis sets, and thus to much less expensive calculations;
  - the $s$ and $p$ functions involved allow the use of fast integral algorithms;
  - they generally recover a larger percentage of the experimental dissociation energy, at least when electron correlation is included.

- Cons:
  - excessive basis set superposition effects;
  - no account for lone pair-lone pair and bond-lone pair interactions;
  - implicit assumption of directional bonding;
  - basis sets are less general and less straightforward to generate.

The pros and cons of polarization functions are of course the 'mirror image' of these:

- Pros:
  - less excessive basis set superposition effects;
  - lone pair-lone pair and bond-lone pair interactions can be handled as well as regular bonding;
  - no implicit assumption of directional bonding;
  - basis sets are general and straightforward to generate.
- Cons:
  - larger basis sets, and thus more expensive calculations;
  - high angular momentum functions result in complicated integrals;
  - computed dissociation energy converges slowly with expansion of polarization complement.

As either type has its obvious advantages and disadvantages, the idea suggests itself to apply them 'with joined forces' in what might be called a combined bond-polarisation basis set. A few preliminary calculations yielded very encouraging results, so this trail was pursued further in the present work.

In a first investigation, reported in Section 3.2[a], a more or less standard basis set of double zeta plus diffuse plus polarization quality, namely 6-31+G($d,p$), was supplemented with a single *sp* shell along the bond axis, the exponent of which was optimized at the CISD level for the closed-shell hydrides of Li to F. This basis set was then applied to the first-row hydrides and hydride radicals, a set of compounds that has been studied in great detail over the years. Electron correlation was incorporated at the MP4 level. It was shown that results are competitive even with basis sets as large as 6-311++G($3df,3pd$), while computation times are reduced by a factor of 4 to 20. Computed total atomization energies are on the average less than 2 kcal/mol removed from the experimental values if an isogyric correction is applied. Even without an isogyric correction, the computed

[a]This section has been adapted from J. M. L. Martin, J. P. François, and R. Gijbels, *J. Comp. Chem.* 10, 152 (1989).

values are fairly close to the experimental ones. Basis set superposition errors were considered for the diatomic species, and found to be as large as 7 kcal/mol for HF. Correcting for BSSE, however, completely destroys the good agreement with the experimental atomization energies. We therefore advocated neglecting BSSE altogether on empirical grounds.

This decision is of course not entirely satisfactory, as it introduces an error compensation that cannot necessarily be relied upon. What basically causes the BSSE problem with bond functions, however, is an imbalance in the treatment of intra-atomic external correlation between atomic and molecular calculations. External correlation in the atoms requires $d$, $f$, and higher angular momentum functions. Only one $d$ function is present in the 6-31+G($d,p$)B basis set, which is more than in a bare 'DZ+bond function' basis set but still far from enough. In the molecular calculation, on the other hand, the bond functions expand as additional $d, f, \ldots$ functions about the atoms, as do the basis functions on the other atoms. Hence intra-atomic external correlation is better accounted for in the molecular than in the atomic calculation, which results in the large BSSE just noted.

An obvious solution would be to add additional polarization functions to the atoms, which would saturate the basis with respect to atomic external correlation and thus restore the balance. However, this would make the basis set just as or perhaps more expensive than a regular polarization-only basis set, so this is only justifiable if the performance of the new basis set is definitely superior to the latter.

Additionally, the 6-31+G($d,p$)B basis set still exhibits some BSSE even at the Hartree-Fock level. This may well be caused by the valence shell not being near the Hartree-Fock limit, and can conceivably be remedied by expanding the valence shell, perhaps to 6-311+G($d,p$)B.

The answer to all these issues is given in Section 3.3[b], where the BSSE and the performance for the total dissociation energies of the first-row hydrides are investigated as a function of the parent basis set. It is found that expansion of the valence part from 6-31 to 6-311 very effectively reduces the Hartree-Fock BSSE, as well as slightly improves general performance, at a moderate additional cost. Doubling up the $d$ functions helps little, whereas addition of an $f$ function dramatically reduces the BSSE. The resulting basis set, 6-311+G($2df,p$)B, has a computational cost only slightly larger than that of the parent polarization-only 6-311+G($2df,p$) basis set, but has distinctly superior performance.

A more detailed investigation of the BSSE issue was apparently still called for, though. Hitherto, only diatomic BSSEs were considered, as the extension of the counterpoise method to polyatomic BSSEs is not unique. In Section 3.4[c], three possible many-body

[b] Adapted from J. M. L. Martin, J. P. François, and R. Gijbels, *J. Comp. Chem.* **10**, 875 (1989).
[c] Adapted from J. M. L. Martin, J. P. François, and R. Gijbels, *Theor. Chim. Acta* **76**, 195 (1989).

extensions of the counterpoise method, two from the literature [Wel83] and a new one, were compared for the first-row polyatomic hydrides and hydride radicals. It is found that the BSSEs without bond functions are about half those with bond functions, and still quite sizeable in their own right. Some systematic trends are seen, notably the increase of BSSE from left to right in the periodic table. As the number of electrons, and thus the basis set incompleteness error, also increases from left to right in the periodic table, the part of the BSSE that is additive with the interaction energy (the presence of a nonadditive component, which invalidates much of the reasoning behind counterpoise-like methods, was recently demonstrated by Mayer [May87a, May87b]) will conceivably cancel out the error in the interaction energy to a large extent, leading to the good agreement with experiment for the uncorrected values observed here. Both with and without bond functions, attempting BSSE corrections leads to severe errors in the computed dissociation energies.

Some overshooting in the hydrides of the heavier elements is still present. Is this a BSSE effect, or an artifact of the electron correlation procedure resulting from the MP series not being converged yet? This is investigated in Section 3.5[d], where the calculations reported in Section 3.3 are repeated at the CCD(ST) level [Rag85a]. Also investigated in this section is the reliability of Pople's geometric extrapolation formula for the MP series. The latter is shown to be reliable as long as triple excitations were not too important. A modification is proposed which is slightly less sensitive to the latter problem. At the CCD(ST) level, most of the previously observed overshooting tendency in the computed dissociation energies is removed. The new computed dissociation energies are extremely close to the experimental values, the mean absolute error at the CCD(ST)/6-311+G(2*df*,*p*)B level being 0.46 kcal/mol, compared to 1.99 kcal/mol for the CCD(ST)/6-311+G(2*df*,*p*) level (i.e., no bond functions). The accuracy with the small 6-311+G(*d*,*p*)B basis set is still respectable, the mean absolute error being 0.69 kcal/mol.

In Section 3.6[e] however, the reference geometries, previously determined at the UHF/6-31G* level, were taken at the CID/6-31G* level in an attempt to 'squeeze the last bit of performance' out of the results. Except for $H_2$, the absolute values of the dissociation energies are not much affected; however, the modified value of $H_2$ leads to effects on the isogyrically corrected values in excess of 0.5 kcal/mol. The final values have a mean absolute error of 0.12 kcal/mol per bond, an accuracy which is unprecedented in the theoretical literature. Some predicted values for experimentally poorly known $\Sigma D_0$ values ($\Delta H_f^0$ at 0 K) are (in kcal/mol): BeH 45.6 ±0.12 (82.5 ±1.3); $BeH_2$ 139.1 ±0.24 (40.6 ±1.4); BH 82.4 ±0.12 (105.1±3); $BH_2$ 159.4 ±0.24 (76.5±3.2); $BH_3$ 265.3 ±0.36 (22.3±3.3); NH 77.8 ±0.12 (86.3±0.22); $NH_2$ 170.3 ±0.24(45.5±0.35) kcal/mol. The

[d] Adapted from J. M. L. Martin, J. P. François, and R. Gijbels, *Chem. Phys. Lett.* **157**, 217 (1989).
[e] Adapted from J. M. L. Martin, J. P. François, and R. Gijbels, *Chem. Phys. Lett.* **163**, 387 (1989).

limiting factor in their accuracy is the heat of formation of the central atoms.

An example application to the BH molecule is reported in Section 3.7[f]. It is shown there with absolute certainty that the previously proposed experimental $D_e$ of 78.9 kcal/mol is in error, and that the actual value is quite close to the predissociation limit of 82.6±0.4 kcal/mol. This conclusion, previously conjectured by Curtiss and Pople [Cur89], has in the meantime been confirmed by the NASA Ames group [Bau90] using a huge [5*s*4*p*3*d*2*f*1*g*] atomic natural orbital basis set and MRCI techniques.

Summing up, combined bond-polarization basis sets developed in this study, are shown to be a powerful tool in the ab initio prediction of dissociation energies, allowing an accuracy competitive with the best experimental techniques at moderate computational cost.

[f] Adapted from J. M. L. Martin, J. P. François, and R. Gijbels, *J. Chem. Phys.* **91**, 4425 (1989).

## 3.2 Initial investigation: basis sets of DZP + bond function quality

### 3.2.1 Introduction

*Ab initio* molecular orbital (MO) methods have achieved the status of being accepted as reliable tools for the prediction of molecular properties. Two examples in which theory is actually preceding experiment are the properties of methylene (as documented in [Sch86a]), and the prediction of proton affinities ([Dew86] includes a comprehensive bibliography; see also [Mar89f]).

A primary objective is the prediction of thermochemical data, most of which involve in some way the molecular binding energy. Exactly this problem has always remained a big challenge in quantum chemistry, as it involves calculating the very small difference between very large electronic energies. To make things worse, little or no similarities exists between reactants and products of a dissociation reaction in most cases, so error compensation of some kind cannot be relied on. To use the very eloquent expression by Coulson [Cou64]: one is "weighing the captain of a ship by weighing the ship with and without the captain on board, then taking the difference".

One solution is to apply some kind of empirical adjustment: the bond and atom equivalent schemes by Wiberg [Wib84] and Ibrahim and Schleyer [Ibr85] are one example, semiempirical MO theory in all its varieties [Pop70, Bin75a, Dew77, Thi81, Dew85] is another. The parametrization in these methods is mostly obtained by least-squares fitting to empirical data, to the point where they start resembling numerical fitting procedures. If this criticism appears a little harsh, it is still true that such methods always depend to some extent upon the similarity between the reference compounds and the ones being investigated.

The other solution then, is to apply *ab initio* theory to whatever level is necessary to produce the required accuracy. It is now well established, that a good description of electron correlation is essential: unless the molecule is very small, the only methods that are feasible in terms of both quality and cost appear to be: CISD with some kind of size consistency correction (such as those by Langhoff and Davidson [Lan74] or Pople *et al.* [Pop77]), coupled cluster theory [Bar81, Bar89], and particularly finite-order many-body perturbation theory [Mol34, Bin75b, Pop76, Kri80b]. Another substantial factor however is the choice of the basis set (see Huzinaga [Huz85] and Davidson and Feller [Dav86] for excellent reviews). This not only because of a good description of the molecule at the Hartree-Fock level, but also because correlation theories strongly rely upon the quality of the virtual orbital description.

It was already pointed out by Nesbet [Nes60] that a so-called isotropic basis set (i.e. only containing the basis function types necessary to reach the atomic Hartree-Fock

Table I: Recommended exponents for the 6-31G$(d,p)$B and 6-31+G$(d,p)$B basis sets.

| Atom | Polarization exponent | Diffuse exponent | Bond-ftn. exponent |
|---|---|---|---|
| H | | | |
| in $H_2$ | 0.70 | N/A | 0.32 |
| in LiH | 0.36 | N/A | N/A |
| otherwise | 0.75 | N/A | N/A |
| Li | 0.067966 | 0.0135 | 0.28 |
| Be | 0.25 | 0.02932 | 0.21 |
| B | 0.44 | 0.03544 | 0.47 |
| C | 0.72 | 0.04454 | 0.95 |
| N | 0.95 | 0.08782 | 1.1737 |
| O | 1.27 | 0.08607 | 1.45 |
| F | 1.65 | 0.1032 | 1.53 |

limit) could not possibly account for the polarization in molecular binding. Since then, basically two different roads towards reaching this goal have been pursued. The first (and by far the most popular) is the one already indicated by Nesbet [Nes60] himself. It consists of adding one or more shells of functions with higher angular momentum ($d$ and $f$ functions on first-and second row elements, $p$ and $d$ functions on hydrogen) on every atom. Standardized basis sets with polarization functions as generated by Pople and coworkers [Har72, Har73, Kri80a, Fra82] have now become quite popular in molecular calculations. On the other hand, even at high levels of electron correlation theory, these basis sets are still not sufficient for accurate predictions of dissociation energies, as witnessed among others by the work of Pople *et al.* [Pop78]. Very recently, a promising new approach based on atomic natural orbitals (ANOs) has been introduced by Almlöf and Taylor [Alm87]. These ANOs provide an excellent basis for molecular electronic structure calculations, and large primitive sets can be contracted to a relatively limited number of functions without significant loss in either SCF or correlation energy. The method has been applied [Alm87] with encouraging results to the dissociation energy of the $N_2$,$H_2O$, and SO molecules.

Another possibility consists of adding $s$- and $p$-type functions at some point on the bond axis between bonded atoms. Such so-called bond functions are in no way inferior to polarization-type basis sets (see e.g. Neisius and Verhaegen [Nei79, Nei81] or the papers by Vladimiroff [Vla73, Vla74], in which early references on the subject can be found) for most compounds at the Hartree-Fock level; at correlated levels, they are even markedly superior to them [Mac85]. Also, they are generally more compact than their polarized counterparts, resulting in much less expensive calculations. They are not of much use, however, when multicenter bonds or Vanderwaals-type interactions are involved. Also, they are less suited to describe dense electronic populations; for example, they completely fail to describe the bond angles around heteroatoms properly [MarUP]. A minor disadvantage is also, that different exponents and relative placements

are necessary for different bonds, not just for different atoms.

Here, a third alternative imposes itself: to combine both approaches into a hybrid bond/polarized basis set. A similar approach has already been followed in a MRD-CI study on the dissociation of the $N_2$ molecule by Butscher *et al.* [But77] and in a CEPA study of diazine by Burton [Bur77]. Also, Schwenke and Truhlar [Sch85a] considered some bond-function augmented polarization basis sets among the many examined in their extensive SCF study of the dimerization energy of hydrogen fluoride. Given the rather encouraging results obtained in these treatments, it is surprising that hardly any systematic investigations of that type of basis set have been undertaken: one rare example is a series of papers by Wright and coworkers [Wri83b, Wri83a, Wri84]. At the SCF level, Vladimiroff [Vla73] even arrived at the conclusion that "The use of a mixed basis of $3d$ functions and bond functions does not seem to be a very good idea". It is however in correlated calculations (such as in [But77, Bur77]) that the forte of bond functions seems to be. So this study was undertaken, in order to assess the performance of a combined bond-polarization basis set with full fourth-order Møller-Plesset theory on a moderately-sized class of molecules. Eventually, the first-row open and closed shell hydride species were selected, because for this particular case, high-quality calculations by Pople *et al.* [Pop83] using multiple polarization functions, full fourth-order Møller-Plesset theory and various assumptions, were available for direct comparison, as well as experimental data.

### 3.2.2 Methods, results and discussion

As a nucleus, the standard 6-31G basis [Heh72] was used. It is known to be the smallest basis set appropriate for post-Hartree-Fock calculations (e.g. DeFrees *et al.* [DeF79]). Subsequent optimizations were carried out for the first row hydrides $H_2$, LiH, BeH, $BH_2$, $CH_4$, $NH_3$, $H_2O$, and HF, all of them selected because of their well-defined experimental geometries. The optimizations were performed at the CISD level, using the direct CI algorithm of Roos and Siegbahn [Roo77] as implemented in the MONSTER-GAUSS 81 program [Pet81] by Peterson and Poirier. Since minimizations towards an energy are to be performed in the optimization procedure, a variational CI procedure seemed more appropriate than a perturbation technique here.

The calculations were performed on the Control Data Cyber 930 computer at the Limburgs Universitair Centrum. Optimizations were carried out by first bracketing the minimum by varying the parameter to be optimized in increments of about 1 unit on the second significant digit, and then passing a cubic polynomial through four points around the minimum. The minimum of the polynomial was then found analytically. Because of the relatively flat energy surfaces, not using a more sophisticated method seemed to be warranted. Any effort towards simultaneous optimization of several variables, for example using a variable metric method, was totally out of the question with the available computing resources. For the open shell species, restricted open-shell Hartree-Fock theory

Table II: Total energies (hartree) for first-row atoms and hydride species using the 6-31G$(d,p)$B and 6-31+G$(d,p)$B basis sets*.

| Species | SCF | MP2 | MP3 | MP4(SDQ) | MP4 | MPextrp. |
|---|---|---|---|---|---|---|
| | | | 6-31G$(d,p)$B | | | |
| H | 0.49823 | 0.49823 | 0.49823 | 0.49823 | 0.49823 | 0.49823 |
| $H_2$ | 1.13135 | 1.15983 | 1.16607 | 1.16762 | 1.16762 | 1.16806 |
| Li | 7.43124 | 7.43124 | 7.43124 | 7.43124 | 7.43124 | 7.43124 |
| LiH | 7.98396 | 8.00844 | 8.01512 | 8.01707 | 8.01707 | 8.01781 |
| Be | 14.56676 | 14.59342 | 14.60399 | 14.60881 | 14.60881 | 14.61222 |
| BeH | 15.14896 | 15.17809 | 15.18557 | 15.18763 | 15.18780 | 15.18860 |
| $BeH_2$ | 15.76861 | 15.82289 | 15.83552 | 15.83856 | 15.83885 | 15.83989 |
| B | 24.52267 | 24.56014 | 24.57349 | 24.57852 | 24.57886 | 24.58198 |
| BH | 25.12008 | 25.18577 | 25.20348 | 25.20905 | 25.20974 | 25.21227 |
| $BH_2$ | 25.75242 | 25.82582 | 25.84111 | 25.84426 | 25.84510 | 25.84621 |
| $BH_3$ | 26.39299 | 26.49561 | 26.51488 | 26.51839 | 26.51974 | 26.52094 |
| C | 37.68077 | 37.73246 | 37.74645 | 37.75027 | 37.75071 | 37.75235 |
| CH ($^2\Pi$) | 38.26730 | 38.35262 | 38.37080 | 38.37510 | 38.37617 | 38.37775 |
| CH ($^4\Sigma^-$) | 38.27843 | 38.34309 | 38.35491 | 38.35697 | 38.35770 | 38.35835 |
| $CH_2$ ($^1A_1$) | 38.87712 | 38.99844 | 39.01899 | 39.02292 | 39.02489 | 39.02624 |
| $CH_2$ ($^3B_1$) | 38.92550 | 39.02729 | 39.04348 | 39.04591 | 39.04736 | 39.04816 |
| $CH_3$ | 39.56427 | 39.70496 | 39.72396 | 39.72647 | 39.72898 | 39.72987 |
| $CH_4$ | 40.20121 | 40.38290 | 40.40274 | 40.40522 | 40.40940 | 40.41041 |
| N | 54.38501 | 54.45555 | 54.46855 | 54.47044 | 54.47090 | 54.47143 |
| NH | 54.96234 | 55.07334 | 55.08934 | 55.09157 | 55.09287 | 55.09351 |
| $NH_2$ | 55.56515 | 55.72293 | 55.73910 | 55.74108 | 55.74384 | 55.74449 |
| $NH_3$ | 56.19653 | 56.40338 | 56.41673 | 56.41871 | 56.42344 | 56.42412 |
| O | 74.78307 | 74.88488 | 74.89789 | 74.89942 | 74.90008 | 74.90041 |
| OH | 75.38825 | 75.54531 | 75.55776 | 75.55931 | 75.56118 | 75.56153 |
| $H_2O$ | 76.02491 | 76.24272 | 76.24965 | 76.25183 | 76.25584 | 76.25623 |
| F | 99.36364 | 99.50463 | 99.51431 | 99.51535 | 99.51615 | 99.51630 |
| HF | 100.01193 | 100.22248 | 100.22572 | 100.22784 | 100.23034 | 100.23052 |
| | | | 6-31+G$(d,p)$B | | | |
| H | 0.49823 | 0.49823 | 0.49823 | 0.49823 | 0.49823 | 0.49823 |
| $H_2$ | 1.13135 | 1.15983 | 1.16607 | 1.16762 | 1.16762 | 1.16806 |
| Li | 7.43124 | 7.43124 | 7.43124 | 7.43124 | 7.43124 | 7.43124 |
| LiH | 7.98404 | 8.00854 | 8.01522 | 8.01716 | 8.01716 | 8.01791 |
| Be | 14.57003 | 14.59614 | 14.60622 | 14.61080 | 14.61080 | 14.61391 |
| BeH | 15.15008 | 15.17930 | 15.18678 | 15.18884 | 15.18901 | 15.18982 |
| $BeH_2$ | 15.76902 | 15.82338 | 15.83602 | 15.83905 | 15.83935 | 15.84039 |
| B | 24.52690 | 24.56459 | 24.57785 | 24.58277 | 24.58313 | 24.58616 |
| BH | 25.12480 | 25.19040 | 25.20780 | 25.21314 | 25.21388 | 25.21627 |
| $BH_2$ | 25.75420 | 25.82796 | 25.84327 | 25.84640 | 25.84728 | 25.84839 |
| $BH_3$ | 26.39358 | 26.49641 | 26.51566 | 26.51915 | 26.52054 | 26.52174 |
| C | 37.68378 | 37.73614 | 37.75022 | 37.75405 | 37.75455 | 37.75621 |
| CH ($^2\Pi$) | 38.27148 | 38.35794 | 38.37612 | 38.38035 | 38.38152 | 38.38310 |
| CH ($^4\Sigma^-$) | 38.28077 | 38.34636 | 38.35828 | 38.36036 | 38.36116 | 38.36184 |
| $CH_2$ ($^1A_1$) | 38.88162 | 39.00416 | 39.02451 | 39.02830 | 39.03044 | 39.03177 |
| $CH_2$ ($^3B_1$) | 38.92798 | 39.03097 | 39.04718 | 39.04961 | 39.05118 | 39.05200 |
| $CH_3$ | 39.56662 | 39.70873 | 39.72763 | 39.73010 | 39.73279 | 39.73369 |
| $CH_4$ | 40.20166 | 40.38424 | 40.40398 | 40.40644 | 40.41078 | 40.41181 |
| N | 54.38608 | 54.45754 | 54.47064 | 54.47261 | 54.47317 | 54.47374 |
| NH | 54.96499 | 55.07787 | 55.09392 | 55.09627 | 55.09781 | 55.09852 |
| $NH_2$ | 55.56877 | 55.72925 | 55.74517 | 55.74730 | 55.75047 | 55.75119 |
| $NH_3$ | 56.20173 | 56.41257 | 56.42500 | 56.42721 | 56.43262 | 56.43338 |
| O | 74.78610 | 74.88975 | 74.90282 | 74.90460 | 74.90549 | 74.90590 |
| OH | 75.39390 | 75.55483 | 75.56671 | 75.56872 | 75.57118 | 75.57165 |
| $H_2O$ | 76.03321 | 76.25698 | 76.26369 | 76.26511 | 76.27016 | 76.27056 |
| F | 99.37036 | 99.51524 | 99.52443 | 99.52608 | 99.52742 | 99.52767 |
| HF | 100.02553 | 100.24401 | 100.24461 | 100.24831 | 100.25216 | 100.25245 |

* The minus sign was omitted everywhere.

Table III: Dissociation energies (kcal/mol) for the first-row hydride species obtained with the 6-31G$(d,p)$B and 6-31+G$(d,p)$B basis sets.

| Species | SCF | MP2 | MP3 | MP4(SDQ) | MP4 | Extrp. |
|---|---|---|---|---|---|---|
| | | | 6-31G$(d,p)$B | | | |
| $H_2$ | 84.64 | 102.51 | 106.43 | 107.40 | 107.40 | 107.68 |
| LiH | 34.19 | 49.55 | 53.75 | 54.97 | 54.97 | 55.44 |
| BeH | 52.69 | 54.24 | 52.30 | 50.57 | 50.67 | 49.04 |
| $BeH_2$ | 128.88 | 146.21 | 147.51 | 146.38 | 146.56 | 145.08 |
| BH | 62.24 | 79.95 | 82.68 | 83.02 | 83.24 | 82.87 |
| $BH_2$ | 146.39 | 168.94 | 170.15 | 168.97 | 169.29 | 168.03 |
| $BH_3$ | 235.71 | 276.59 | 280.30 | 279.35 | 279.99 | 278.78 |
| CH ($^2\Pi$) | 55.41 | 76.51 | 79.14 | 79.44 | 79.83 | 79.80 |
| CH ($^4\Sigma^-$) | 62.39 | 70.53 | 69.17 | 68.06 | 68.24 | 67.63 |
| $CH_2$ ($^1A_1$) | 125.43 | 169.12 | 173.24 | 173.31 | 174.27 | 174.09 |
| $CH_2$ ($^3B_1$) | 155.79 | 187.23 | 188.60 | 187.73 | 188.37 | 187.84 |
| $CH_3$ | 243.98 | 299.83 | 302.97 | 302.14 | 303.45 | 302.98 |
| $CH_4$ | 331.02 | 412.60 | 416.26 | 415.42 | 417.77 | 417.88 |
| NH | 49.64 | 75.03 | 76.91 | 77.12 | 77.65 | 77.72 |
| $NH_2$ | 115.26 | 170.00 | 171.99 | 172.04 | 173.49 | 173.57 |
| $NH_3$ | 198.81 | 284.35 | 284.57 | 284.62 | 287.30 | 287.39 |
| OH | 67.11 | 101.78 | 101.43 | 101.45 | 102.20 | 102.21 |
| $H_2O$ | 153.98 | 226.77 | 222.95 | 223.36 | 225.46 | 225.50 |
| HF | 94.16 | 137.81 | 133.77 | 134.44 | 135.52 | 135.53 |
| | | | 6-31+G$(d,p)$B | | | |
| $H_2$ | 84.64 | 102.51 | 106.43 | 107.40 | 107.40 | 107.68 |
| LiH | 34.24 | 49.62 | 53.81 | 55.03 | 55.03 | 55.50 |
| BeH | 51.34 | 53.29 | 51.66 | 50.08 | 50.19 | 48.74 |
| $BeH_2$ | 127.08 | 144.81 | 146.42 | 145.45 | 145.63 | 144.33 |
| BH | 62.54 | 80.06 | 82.66 | 82.92 | 83.15 | 82.76 |
| $BH_2$ | 144.85 | 167.49 | 168.77 | 167.65 | 167.97 | 166.77 |
| $BH_3$ | 233.42 | 274.30 | 278.06 | 277.16 | 277.80 | 276.66 |
| CH ($^2\Pi$) | 56.14 | 77.54 | 80.11 | 80.36 | 80.79 | 80.73 |
| CH ($^4\Sigma^-$) | 61.97 | 70.28 | 68.92 | 67.82 | 68.01 | 67.39 |
| $CH_2$ ($^1A_1$) | 126.36 | 170.40 | 174.34 | 174.31 | 175.34 | 175.13 |
| $CH_2$ ($^3B_1$) | 155.45 | 187.22 | 188.56 | 187.68 | 188.36 | 187.83 |
| $CH_3$ | 243.57 | 299.88 | 302.90 | 302.05 | 303.42 | 302.95 |
| $CH_4$ | 329.42 | 411.12 | 414.67 | 413.82 | 416.23 | 415.83 |
| NH | 50.63 | 76.61 | 78.47 | 78.70 | 79.32 | 79.41 |
| $NH_2$ | 116.86 | 172.72 | 174.48 | 174.59 | 176.23 | 176.32 |
| $NH_3$ | 201.40 | 288.86 | 288.44 | 288.59 | 291.64 | 291.75 |
| OH | 68.75 | 104.70 | 103.95 | 104.10 | 105.08 | 105.12 |
| $H_2O$ | 157.28 | 232.66 | 228.67 | 228.44 | 231.06 | 231.04 |
| HF | 98.48 | 144.66 | 139.27 | 140.56 | 142.14 | 142.16 |

Table IV: Dissociation energies (kcal/mol) for the first-row hydride species as calculated from the total energies given by Pople *et al.* [Pop83].

| Species | 6-311G** MP4 | 6-311G** extrp. | Diff.*sp* extrp. | Double *d* extrp. | Single *f* extrp. | Combined extrp. |
|---|---|---|---|---|---|---|
| $H_2$ | 105.43 | 105.79 | 105.79 | 105.79 | 105.79 | 105.79 |
| LiH | 52.51 | 53.02 | 53.08 | 53.46 | 54.15 | 54.64 |
| BeH | 47.96 | 45.84 | 45.86 | 46.45 | 46.85 | 47.48 |
| $BeH_2$ | 141.76 | 139.80 | 139.82 | 140.74 | 141.48 | 142.44 |
| BH | 79.73 | 79.42 | 79.62 | 80.14 | 80.74 | 81.65 |
| $BH_2$ | 162.68 | 161.55 | 161.51 | 162.54 | 163.87 | 164.83 |
| $BH_3$ | 270.24 | 269.13 | 268.99 | 270.56 | 272.23 | 273.52 |
| CH ($^2\Pi$) | 76.41 | 76.39 | 76.90 | 77.23 | 78.57 | 79.93 |
| CH ($^4\Sigma^-$) | 64.36 | 63.76 | 63.75 | 63.33 | 64.95 | 64.51 |
| $CH_2$ ($^1A_1$) | 167.61 | 166.87 | 167.58 | 168.64 | 170.59 | 173.08 |
| $CH_2$ ($^3B_1$) | 181.34 | 180.83 | 180.98 | 181.24 | 183.87 | 184.44 |
| $CH_3$ | 292.97 | 292.51 | 292.75 | 293.71 | 297.11 | 298.55 |
| $CH_4$ | 402.40 | 402.01 | 401.64 | 403.92 | 407.32 | 408.85 |
| NH | 73.32 | 73.42 | 74.54 | 74.12 | 76.10 | 77.91 |
| $NH_2$ | 164.48 | 164.60 | 166.67 | 165.98 | 169.34 | 172.80 |
| $NH_3$ | 274.36 | 274.49 | 277.48 | 275.88 | 280.81 | 285.18 |
| OH | 97.31 | 97.37 | 99.34 | 97.91 | 99.35 | 101.86 |
| $H_2O$ | 215.20 | 215.28 | 219.58 | 215.80 | 218.70 | 223.52 |
| HF | 131.19 | 131.19 | 135.04 | 131.81 | 132.51 | 136.97 |

(ROHF) according to Binkley *et al.* [Bin74] was used.

First, a set of 5 pure *d* functions was added to the central atom, along with a set of *p*-functions on the hydrogen atoms. For the hydrogen molecule itself, the *p*-exponents were optimized: in the remaining molecules, the standard value of 0.75, well accepted in molecular calculations [Pop76, Kri80a], was used to reduce the optimization overhead. Since the potential surface for these is known to be very flat, this does not represent a serious restriction. Optimum values (at the CISD level) for the *d* exponents are presented in Table I. These seem to be in good accordance with those for the 6-311G** basis set [Kri80a]. The basis set obtained is subsequently denoted as 6-31G$(d,p)$.

Subsequently, a single *sp*-shell was added halfway every bond. The additional *s* function is included in the integral evaluation anyway, so it seemed reasonable to include it in the basis set for what it was worth. Such displaced *s*-functions expand as *p*-functions with contaminations from higher angular momenta, so the absence of a third valence shell is perhaps partially compensated for. Ideally, the fractional distance should have been optimized too, but such a problem would be intractable with the present computer facilities. Optimum values (at the CISD level) for the exponents are presented in Table I. The resulting basis set is denoted 6-31G$(d,p)$B,for convenience.

The optimization was also repeated with the polarization functions removed. Oddly, quite different values for the optimum exponents were obtained.

Since their contribution is known to be considerable for molecules with free electrons or ditto pairs, diffuse *sp*-shells on the nonhydrogen atoms were also optimized as additions upon the 6-31G$(d,p)$ basis. For $CH_4$ and LiH, the optimization failed (as was expected). Here, it was repeated with the $CH_3$ radical and the $Li^-$ singlet anion, respectively. Optimum values (at the CISD level) are again presented in Table I. They seem to be in qualitative agreement with those obtained by Clark *et al.* [Cla83] at a much lower level, for anions. These exponents were then transferred without reoptimization to the 6-31G$(d,p)$B basis set, yielding 6-31+G$(d,p)$B.

Using 6-31G$(d,p)$B and 6-31+G$(d,p)$B, energy calculations for all the species listed in Table II were performed at the MP4 level [Mol34, Kri80b] using the GAUSSIAN 82 [Gau82] package running on the IBM 4381 at the Facultés Universitaires de Namur. Geometries at the HF/6-31G* level were taken from the work of DeFrees *et al.* [DeF79], just as in the paper by Pople *et al.* [Pop83], to enable direct comparison between both. SCF, MP2 [Bin75b], MP3 [Pop76], MP4(SDQ) [Kri78], and full MP4 energies are given in Table II, along with those extrapolated to infinite order using the geometric-progression formula suggested by Pople *et al.* [Pop83]. From the dissociation equation, the dissociation energies can be obtained directly. They are presented in Table III; MP-extrapolated dissociation energies for all the different basis sets used by Pople *et al.* [Pop83] are given in Table IV for comparison. Experimental data can be found in the last column of Table V.

It is quickly seen, that the basis sets presented here generally recover a much larger percentage of the binding energy than the polarization-only basis sets. Only the case of LiH is a bit problematic: given the weak, long and very polar nature of the bond, it doesn't come as a surprise. The result is much improved when an optimized value is used for the hydrogen *p* exponent: given the nature of the $H^-$ ion, this is also readily understood. The improvements are most spectacular for the ten-electron hydrides. Incidentally, convergence of the Møller-Plesset series should also be fastest for these closed-shell singlets [Han85].

Also very important is the fact that these calculations are consistently three to five times cheaper than the corresponding ones with the classical basis sets. This is explained in Table VI, where the relative magnitudes of $N^4$ and $N^5$ are listed for several different basis sets ($N$ is the dimension of the basis set). It is noted here, that in all known geometry optimization, integral + Hartree-Fock, and Møller-Plesset applications, steps increasing as $N^4$ consume most or almost all of the time. In most CI programs, an integral transformation step, increasing as $N^5$, consumes a sizeable fraction of the time. In large calculations, the choice between e.g. 4 and 20 hours of computer time should be obvious.

However, Pople *et al.* [Pop83] could achieve much better agreement with experiment

Table V: Comparison of theoretical results (this work and Pople *et al.* [Pop83]) for the dissociation energy with experiment [a].

| | Theory | | Experiment | |
|---|---|---|---|---|
| Species | Pople *et al.* [Pop83] | This work * | ZPE[b] | TAE[b] |
| LiH | 58.3 | 57.29 | 1.99 | 58.0[c] |
| BeH | 47.5 | 48.74 | 2.92 | 55.8±7[d],49.8[c] |
| $BeH_2$ | 146.1 | 146.13 | | |
| BH | 85.3 | 84.55 | 3.35 | 81.6±2[e],82.2[c] |
| $BH_2$ | 168.5 | 168.57 | 9.30[f] | 196.2±15[f] |
| $BH_3$ | 280.9 | 280.25 | 17.97[g] | 278.1±10[g] |
| CH ($^2\Pi$) | 83.6 | 82.53 | 4.04 | 84.4±.1[h],83.9[c] |
| CH ($^4\Sigma^-$) | 64.5 | 67.39 | 4.44[i] | 67.2[i] |
| $CH_2$ ($^3B_1$) | 188.1 | 189.63 | 10.20[j] | 189.8±.6[j] |
| $CH_2$ ($^1A_1$) | 180.4 | 178.73 | 10.76[k] | 182.3±.5[k] |
| $CH_3$ | 305.9 | 306.54 | 18.27[l] | 307.2±.2[l] |
| $CH_4$ | 419.9 | 421.22 | 27.3[m] | 419.8±.1[m] |
| NH | 81.6 | 81.20 | 4.64 | 78.8±4[n],≤84.7[c] |
| $NH_2$ | 180.2 | 179.91 | 11.28[o] | 180.9±1.5[o] |
| $NH_3$ | 296.2 | 297.14 | 20.60[p] | 297.3±.1[p] |
| OH | 105.5 | 106.91 | 5.28 | 106.6±.3[q],106.6[c] |
| $H_2O$ | 230.9 | 234.63 | 12.88[r] | 232.2[r] |
| HF | 140.6 | 143.96 | 5.85 | 141.2[c] |
| $H_2$ | 105.4 | 107.68 | | 109.48[a] |

* MPextrp./6-31+G(*d*,*p*)B

(a) All energies in kcal/mol. 1 kcal/mol = $1.59348 \times 10^{-3}$ hartree = .0433611eV =349.73 $cm^{-1}$ ; from [Coh76]. $D_e(H_2) = D_0(H_2) + \omega_e/2 - \omega_e x_e/4$= 38289 $cm^{-1}$ = 109.48 kcal/mol = 0.17446 hartree; all data taken from [Hub79].

(b) The zero-point vibrational energy (ZPE) for each molecule was calculated as follows. For diatomic molecules, ZPE = $\omega_e/2 - \omega_e x_e/4$, with the spectroscopic constants taken from [Hub79]. For polyatomic molecules, ZPE = $\sum_i \nu_i/2$, with the source of the $\nu_i$ listed below. The total atomization energy (TAE) is calculated using either experimental dissociation energies ($D_0$) or heats of formation ($\Delta H_f^0$), corrected for the ZPE of the $AH_n$ molecule.

(c) Determined from $D_e = D_0$ + ZPE. $D_0$ is from [Hub79].

(d) $\Delta H_f^0$(Be) and $\Delta H_f^0$(BeH) from [Jan71], $\Delta H_f^0$(H) from [Cha82].

(e) $\Delta H_f^0$(B) and $\Delta H_f^0$(BH) from [Jan71], $\Delta H_f^0$(H) from [Cha82].

(f) $\Delta H_f^0$(B) and $\Delta H_f^0$($BH_2$) from [Jan71],$\Delta H_f^0$(H) from [Cha82];$\nu_i$ are from the MC-CI calculation of [Per81].

(g) $\Delta H_f^0$(B) and $\Delta H_f^0$($BH_3$) from [Jan71],$\Delta H_f^0$(H) from [Cha82];$\nu_i$ (calculated and observed) from [Kal71].

(h) $\Delta H_f^0$(C) and $\Delta H_f^0$(H) from [Cha82], $\Delta H_f^0$(CH) from [Jan71].

(i) Calculated from $D_e$ of $^2\Pi$ state and $T_e(^4\Sigma^- - ^2\Pi)$=5844 $cm^{-1}$, taken from [Hub79]. $\omega_e$ and $\omega_e x_e$ are from the CI calculation of [Lie73].

(j) $\Delta H_f^0$(C) and $\Delta H_f^0$(H) are from [Cha82], $\Delta H_f^0(CH_2)$=93.6±.6 taken from [Len78]; $\nu_i$ are from [Jen82].

(k) calculated by assuming a $^1A_1$-$^3B_1$ separation of 8.1±.8 kcal/mol [Len78]. $\nu_1$ and $\nu_3$ are assumed to be the same as in the $^3B_1$ state (see footnote j), while the bending frequency ($\nu_2$) is from [Her66].

(l) $\Delta H_f^0$(C) and $\Delta H_f^0$(H) from [Cha82], $\Delta H_f^0(CH_3)$ from [Jan71]; $\nu_i$ (calculated and observed) from [Sne70].

(m) $\Delta H_f^0$(C) and $\Delta H_f^0$(H) from [Cha82], $\Delta H_f^0(CH_4)$ from [Jan71]; $\nu_i$ from [Her63].

(n) $\Delta H_f^0$ data from [Cha82].

(o) $\Delta H_f^0$ data from [Cha82];$\nu_i$ (calculated and observed) are from [Mil65].

(p) $\Delta H_f^0$ data from [Cha82];$\nu_i$ from [Ben60].

(q) $\Delta H_f^0$ data from [Cha82].

(r) $\Delta H_f^0$(O) and $\Delta H_f^0$(H) are from [Cha82], $\Delta H_f^0(H_2O)$ from [Jan71]; $\nu_i$ from [Hoy72].

Table VI: Relative magnitudes of $N^4$ and $N^5$ as a function of the basis set, where $N$ represents the basis set dimension.

| Basis set | Species | $N$ | $(N/N_0)^4$ | $(N/N_0)^5$ |
|---|---|---|---|---|
| 6-311G($2df, 2p$) | HF | 39 | 8.27 | 14.02 |
| | $H_2O$ | 48 | 5.06 | 7.59 |
| | $NH_3$ | 57 | 3.74 | 5.19 |
| | $CH_4$ | 66 | 3.04 | 4.01 |
| 6-311G($2df, 2pd$) | HF | 44 | 13.39 | 25.62 |
| | $H_2O$ | 58 | 10.79 | 19.56 |
| | $NH_3$ | 72 | 9.51 | 16.70 |
| | $CH_4$ | 86 | 8.75 | 15.05 |
| 6-31G($d, p$)B | HF | 23 | 1.00 | 1.00 |
| | $H_2O$ | 32 | 1.00 | 1.00 |
| | $NH_3$ | 41 | 1.00 | 1.00 |
| | $CH_4$ | 50 | 1.00 | 1.00 |
| 6-31G($d, p$)2B | HF | 27 | 1.90 | 2.23 |
| | $H_2O$ | 40 | 2.44 | 3.05 |
| | $NH_3$ | 53 | 2.79 | 3.61 |
| | $CH_4$ | 66 | 3.04 | 4.01 |

$N_0$ represents the smallest value of $N$ for the molecule concerned.

using isogyric reactions involving molecular hydrogen. Consider for example:

$$N(^4S) + 3H(^2S) \rightarrow NH_3(^1A_1) \tag{3.1}$$

Then the reaction

$$N(^4S) + 3H_2(^1\Sigma_g^+) \rightarrow NH_3(^1A_1) + 3H(^2S) \tag{3.2}$$

has the same number of unpaired spins on each side, and should present less problems. Now using the binding energy of $H_2$ according to highly accurate experimental data [Hub79], or the very accurate calculations of Kolos and Wolniewicz [Kol68], the energy of (3.1) can be obtained using a very simple reaction cycle. Energies obtained using this method are given in Table VII, with those from Pople *et al.* [Pop83] given for comparison in Table VIII. A synthetic comparison between the two theoretical models and experimental data can be found in Table V, with references for the experimental data given as footnotes. For the sake of completeness, the Wright and Williams [Wri83a] values at the MRD-CI level are given: $H_2$ 109.54, BH 84.6, CH($^2\Pi$) 81.9, NH 79.1, OH 105.6, and finally HF 142.3 kcal/mol.

Generally, the results obtained using the 6-31+G($d, p$)B basis set seem to be at least as good as those with the much larger 6-311+G($2df, p$) basis. Also, the energies quoted by Pople *et al.* [Pop83] come from an additivity approximation, which overestimates energy differences by 1.5, 0.9, and 0.3 kcal/mol for $NH_3$, $H_2O$ and HF respectively. Taking this into account, the picture shifts slightly in favour of the basis set presented here.

Table VII: Dissociation energies (kcal/mol) for the first-row hydride species obtained with the 6-31G$(d,p)$B and 6-31+G$(d,p)$B basis sets, through an isogyric reaction cycle.

| Species | SCF | MP2 | MP3 | MP4(SDQ) | MP4 | Extrp. |
|---|---|---|---|---|---|---|
| | | | 6-31G$(d,p)$B | | | |
| LiH | 59.03 | 56.51 | 56.79 | 57.04 | 57.04 | 57.23 |
| BeH | 52.69 | 54.24 | 52.30 | 50.57 | 50.67 | 49.04 |
| $BeH_2$ | 153.71 | 153.17 | 150.56 | 148.46 | 148.64 | 146.88 |
| BH | 87.07 | 86.91 | 85.72 | 85.10 | 85.32 | 84.66 |
| $BH_2$ | 171.23 | 175.90 | 173.19 | 171.05 | 171.37 | 169.82 |
| $BH_3$ | 285.38 | 290.52 | 286.39 | 283.50 | 284.14 | 282.37 |
| CH ($^2\Pi$) | 80.24 | 83.48 | 82.19 | 81.52 | 81.91 | 81.59 |
| CH ($^4\Sigma^-$) | 62.39 | 70.53 | 69.17 | 68.06 | 68.24 | 67.63 |
| $CH_2$ ($^1A_1$) | 175.10 | 183.05 | 179.33 | 177.46 | 178.42 | 177.68 |
| $CH_2$ ($^3B_1$) | 180.63 | 194.19 | 191.65 | 189.81 | 190.45 | 189.64 |
| $CH_3$ | 293.65 | 313.75 | 309.06 | 306.30 | 307.60 | 306.57 |
| $CH_4$ | 405.52 | 433.48 | 425.40 | 421.65 | 424.60 | 422.76 |
| NH | 74.47 | 81.99 | 79.95 | 79.19 | 79.72 | 79.51 |
| $NH_2$ | 164.93 | 183.93 | 178.09 | 176.20 | 177.65 | 177.16 |
| $NH_3$ | 273.31 | 305.24 | 293.71 | 290.85 | 293.53 | 292.78 |
| OH | 91.95 | 108.74 | 104.48 | 103.52 | 104.28 | 104.01 |
| $H_2O$ | 203.65 | 240.69 | 229.04 | 227.51 | 229.62 | 229.09 |
| HF | 118.99 | 144.77 | 136.82 | 136.52 | 137.59 | 137.33 |
| | | | 6-31+G$(d,p)$B | | | |
| LiH | 59.08 | 56.58 | 56.86 | 57.11 | 57.11 | 57.29 |
| BeH | 51.34 | 53.29 | 51.66 | 50.08 | 50.19 | 48.74 |
| $BeH_2$ | 151.92 | 151.77 | 149.47 | 147.53 | 147.71 | 146.13 |
| BH | 87.37 | 87.02 | 85.70 | 84.99 | 85.23 | 84.55 |
| $BH_2$ | 169.68 | 174.45 | 171.82 | 169.73 | 170.05 | 168.57 |
| $BH_3$ | 283.09 | 288.22 | 284.15 | 281.31 | 281.96 | 280.25 |
| CH ($^2\Pi$) | 80.98 | 84.50 | 83.16 | 82.44 | 82.86 | 82.53 |
| CH ($^4\Sigma^-$) | 61.97 | 70.28 | 68.92 | 67.82 | 68.01 | 67.39 |
| $CH_2$ ($^1A_1$) | 176.03 | 184.33 | 180.43 | 178.46 | 179.49 | 178.73 |
| $CH_2$ ($^3B_1$) | 180.29 | 194.19 | 191.61 | 189.76 | 190.44 | 189.63 |
| $CH_3$ | 293.24 | 313.80 | 309.00 | 306.20 | 307.58 | 306.54 |
| $CH_4$ | 403.92 | 432.01 | 423.81 | 420.05 | 422.46 | 421.22 |
| NH | 75.46 | 83.58 | 81.51 | 80.78 | 81.40 | 81.20 |
| $NH_2$ | 166.53 | 186.64 | 180.58 | 178.74 | 180.38 | 179.91 |
| $NH_3$ | 275.91 | 309.75 | 297.58 | 294.82 | 297.87 | 297.14 |
| OH | 93.59 | 111.66 | 107.00 | 106.17 | 107.16 | 106.91 |
| $H_2O$ | 206.95 | 246.58 | 234.76 | 232.60 | 235.21 | 234.63 |
| HF | 123.32 | 151.62 | 142.32 | 142.64 | 144.21 | 143.96 |

Table VIII: Dissociation energies (kcal/mol) of the first-row hydride species calculated from the total energies given by Pople *et al.* [Pop83], using isogyric reactions.

| Species | 6-311G** MP4 | 6-311G** extrp. | Diff.*sp* extrp. | Double *d* extrp. | Single *f* extrp. | Combined extrp. |
|---|---|---|---|---|---|---|
| LiH | 56.55 | 56.71 | 56.76 | 57.14 | 57.83 | 58.32 |
| BeH | 47.96 | 45.84 | 45.86 | 46.45 | 46.85 | 47.48 |
| $BeH_2$ | 145.80 | 143.48 | 143.50 | 144.42 | 145.17 | 146.13 |
| BH | 83.77 | 83.11 | 83.30 | 83.82 | 84.43 | 85.34 |
| $BH_2$ | 166.72 | 165.23 | 165.20 | 166.22 | 167.56 | 168.52 |
| $BH_3$ | 278.32 | 276.50 | 276.36 | 277.93 | 279.60 | 280.89 |
| CH ($^2\Pi$) | 80.45 | 80.07 | 80.58 | 80.92 | 82.25 | 83.61 |
| CH ($^4\Sigma^-$) | 64.36 | 63.76 | 63.75 | 63.33 | 64.95 | 64.51 |
| $CH_2$ ($^1A_1$) | 175.69 | 174.23 | 174.95 | 176.01 | 177.96 | 180.45 |
| $CH_2$ ($^3B_1$) | 185.39 | 184.51 | 184.66 | 184.93 | 187.56 | 188.12 |
| $CH_3$ | 301.05 | 299.87 | 300.11 | 301.08 | 304.47 | 305.92 |
| $CH_4$ | 414.53 | 413.06 | 412.69 | 414.97 | 418.37 | 419.90 |
| NH | 77.37 | 77.11 | 78.23 | 77.80 | 79.79 | 81.60 |
| $NH_2$ | 172.56 | 171.96 | 174.04 | 173.35 | 176.71 | 180.17 |
| $NH_3$ | 286.48 | 285.54 | 288.53 | 286.93 | 291.86 | 296.23 |
| OH | 101.36 | 101.05 | 103.02 | 101.59 | 103.04 | 105.55 |
| $H_2O$ | 223.29 | 222.65 | 226.95 | 223.17 | 226.07 | 230.89 |
| HF | 135.23 | 134.88 | 138.72 | 135.49 | 136.19 | 140.66 |

To obtain some more definitive data, energies from DeFrees and McLean [DeF86] and Frisch *et al.* [Fri86] for models up to MP4SDTQ/6-311++G($3df, 3pd$) at a CID/6-31G** geometry are supplemented with calculations for C,N,and F, to obtain the best available binding energies for the ten-electron series. Results are presented in Tables IX, X, and XI: it is obvious, that even here 6-31+G($d,p$)B holds its own, even when costing *very* much less (about 18 times for water and ammonia).

The overshooting in some of the binding energies is almost certainly due to basis set superposition error (BSSE). In Table XII, counterpoise corrections according to the Boys and Bernardi method [Boy70] are presented for the first-row diatomic hydrides, using the 6-31+G($d,p$), 6-31+G($d,p$)B and 6-311+G($2df,p$) basis sets. The calculations necessary for obtaining these corrections were performed with the GAUSSIAN 86 [Gau86] package running on a MicroVAX 2000 workstation, under the VMS 4.7 operating system. The BSSEs on OH and HF with the 6-31+G($d,p$)B basis set seem somewhat frightening: comparing the 6-31+G($d,p$) and 6-31+G($d,p$)B BSSEs, 4 kcal/mol may result from the bond functions alone! Significant BSSE corrections when using bond functions are also found by Bauschlicher [Bau80]. However, the counterpoise method is known to overestimate BSSEs [Joh73], and it has been shown repeatedly, that at best a crude estimate may be obtained [Sch85a, Fri86]. Also, in view of the unmistakable agreement between the uncorrected 6-31+G($d,p$)B binding energies and the experimental data, it is suggested not to make any counterpoise correction at all. (A similar argument was made

Table IX: Total electronic energies (hartree) of the hydrogen molecule and of the ten-electron series, as well as the corresponding atoms, using the 6-311++G($3df, 3pd$) basis set.

| Species | SCF | MP2 | MP3 | MP4 | MPextrp. |
|---|---|---|---|---|---|
| H (a) | -0.499818 | -0.499818 | -0.499818 | -0.499818 | -0.499818 |
| $H_2$ (a) | -1.133034 | -1.164926 | -1.170450 | -1.171924 | -1.172263 |
| C (c) | -37.690253 | -37.756851 | -37.771674 | -37.776423 | -37.777925 |
| $CH_4$ (b) | -40.212404 | -40.411905 | -40.429799 | -40.437712 | -40.438778 |
| N (c) | -54.398893 | -54.494367 | -54.508465 | -54.511727 | -54.512341 |
| $NH_3$ (b) | -56.218411 | -56.456757 | -56.467088 | -56.477050 | -56.477935 |
| O (b) | -74.809340 | -74.952421 | -74.966984 | -74.970935 | -74.971461 |
| $H_2O$ (b) | -76.057999 | -76.324196 | -76.326757 | -76.338641 | -76.339316 |
| F (c) | -99.401809 | -99.602117 | -99.612300 | -99.617310 | -99.617700 |
| HF (b) | -100.056754 | -100.332600 | -100.331435 | -100.342866 | -100.343310 |

(a) Frisch *et al.* [Fri84]
(b) DeFrees and McLean [DeF86]
(c) This work

Table X: Dissociation energies of $H_2$ and the ten-electron series using the 6-311++G($3df, 3pd$) basis set, calculated from the energies given in Table IX.

| Species | SCF | MP2 | MP3 | MP4 | Extrp. |
|---|---|---|---|---|---|
| $H_2$ | 83.71 | 103.72 | 107.19 | 108.11 | 108.33 |
| $CH_4$ | 328.11 | 411.51 | 413.44 | 415.42 | 415.15 |
| $NH_3$ | 200.84 | 290.50 | 288.13 | 292.34 | 292.51 |
| $H_2O$ | 156.26 | 233.52 | 225.99 | 230.97 | 231.06 |
| HF | 97.34 | 144.74 | 137.62 | 141.65 | 141.69 |

Table XI: Dissociation energies of the ten-electron series using the 6-311++G($3df, 3pd$) basis set, calculated from total energies in Table IX and an isogyric reaction cycle.

| Species | SCF | MP2 | MP3 | MP4 | Extrp. |
|---|---|---|---|---|---|
| $CH_4$ | 405.41 | 428.77 | 420.30 | 419.51 | 418.60 |
| $NH_3$ | 278.14 | 307.76 | 295.00 | 296.43 | 295.96 |
| $H_2O$ | 207.80 | 245.03 | 230.57 | 233.69 | 233.36 |
| HF | 123.11 | 150.50 | 139.91 | 143.02 | 142.84 |

Table XII: Basis Set Superposition Errors estimated by the counterpoise method for the 6-31+G($d,p$)B, 6-311+G($2df,p$) and 6-31+G($d,p$) basis sets.

| | 6-31+G($d,p$)B | | 6-311+G($2df,p$) | | 6-31+G($d,p$) | |
|---|---|---|---|---|---|---|
| Species | SCF | MP4 | SCF | MP4 | SCF | MP4 |
| $H_2$ | 0.36 | 0.36 | 0.00 | 0.00 | 0.17 | 0.17 |
| LiH | 0.74 | 0.74 | 0.01 | 0.01 | 0.38 | 0.38 |
| BeH | 1.06 | 1.41 | 0.01 | 0.05 | 0.44 | 0.46 |
| BH | 1.39 | 3.09 | 0.01 | 0.02 | 0.83 | 1.31 |
| CH($^2\Pi$) | 0.89 | 2.43 | 0.08 | 0.28 | 0.74 | 1.16 |
| CH($^4\Sigma^-$) | 0.90 | 2.52 | 0.08 | 0.30 | 0.76 | 1.20 |
| NH | 0.46 | 4.35 | 0.07 | 0.44 | 0.29 | 1.77 |
| OH | 0.76 | 5.71 | 0.20 | 0.67 | 0.59 | 2.28 |
| HF | 1.27 | 7.11 | 0.45 | 1.07 | 0.78 | 2.64 |

in [Wri83a, Wri84].) Furthermore, applying it to dissociation energies of polyatomic molecules is in itself by no means a trivial matter [Wel83]. At this point, the justification for neglecting the BSSE must be regarded as purely empirical.

The estimated corrections were not reduced appreciably as the *sp*-part of the atomic basis set was expanded from 6-31G to 6-311G; neither did the computed $D_e$ values change much.

Other sources of error will include the geometry and the relative positioning of the bond functions. Correcting for both, as well as for the basis set incompleteness, will increase binding energy, whereas correcting for the BSSE should decrease binding energy. It can then be imagined, that the errors cancel to some extent, resulting in the good agreement found here.

### 3.2.3 Conclusions

A new family of basis sets, hybrid bond/polarization basis sets, is defined, and the 6-31G($d,p$)B and 6-31+G($d,p$)B basis sets are presented for the first-row hydrides. For the dissociation energies, the 6-31+G($d,p$)B basis set proves to be competitive with polarization-only basis sets as large as 6-311++G($3df,3pd$), while being much more cost-effective than any of these. On empirical grounds, the basis set superposition error should be neglected entirely. Overall, hybrid basis sets seem to be a promising road for high-quality *ab initio* calculations.

## 3.3 Effect of improving the parent polarization complement

### 3.3.1 Introduction

One of the determining factors for the quality of an *ab initio* calculation is the choice of the molecular basis set. A number of excellent review articles exist on this subject: the reader is especially referred to Huzinaga [Huz85] and Davidson and Feller [Dav86].

For overcoming the so-called 'molecular polarization problem', two widely different approaches exist. One of them, originally introduced by Nesbet [Nes60], consists of introducing functions of higher angular momentum on the atoms, so-called 'polarization functions' [Har72, Har73, Fra82]. Because of its wide and straightforward applicability, this approach has by far become the most popular one now. Another one, suggested by Rothenberg and Schaefer [Rot71] and investigated by Vladimiroff [Vla73, Vla74] and Neisius and Verhaegen [Nei79, Nei81, Nei82] among others, consists of adding $s$ and $p$ functions at some point along the bond axis. Such 'bond functions', when it comes to reproducing bond dissociation energies, are in no way inferior to polarization-type functions [Nei79, Nei81, Nei82]; at correlated levels, they are even markedly superior to them [Mac85]. In other areas they are inferior: for example, they completely fail to describe the bond angle around heteroatoms correctly [MarUP]. They are also less straightforward in their application: as pointed out by Hehre *et al.* [Heh86]:

> ...Also, while the positions of non-nuclear-centered basis functions are easily and uniquely specified in molecules characterized by 2-center, 2-electron bonds, their placement is not obvious in molecules involving multi-center bonding. (...) The only apparent recourse in such situations is to allow for bond functions between all pairs of atoms, a solution which results in an enormous increase in computational expense with increasing molecular size. Even then, the exact placement of the functions along the bonds would need to be specified in detail for each and every case. This is clearly undesirable.

The latter objections, however, are only relevant for some less frequent types of problems: weakly bonding interactions like in the hydrogen fluoride dimer and $\pi$-complexes like ferrocene are among them. However, they do not apply to normal more or less covalently-bonded molecules, as most compounds ever investigated by means of *ab initio* methods.

Because of the obvious advantages of either method, one may ask: "why not combine the two types of basis set?". Such an approach was considered a few times in literature for specific cases:among others, Refs. [But77, Bur77, Sch85a] are quoted. Wright and coworkers [Wri83b, Wri83a, Wri84] investigated the performance of a DZP (Double-Zeta

plus Polarization) basis set, supplemented by a single set of bond functions, on the dissociation energy and spectroscopic constants of the diatomic hydrides BH, CH, NH, OH, and HF at the MRD-CI [Bue74] (Multi-Reference Double-excitation Configuration Interaction) level, and obtained excellent agreement with experiment. Bauschlicher however discovered [Bau80], that a lot of the 'improved' dissociation energy could be ascribed to basis set superposition error (BSSE). However, in view of the unmistakable agreement between theoretical and experimental properties for their limited set of molecules, Wright and coworkers suggested balancing the BSSE against the remaining basis set incompleteness error in an empirical manner [Wri83a, Wri84]. The validity of the counterpoise (CP) method [Boy70] as a measure of BSSE is still a matter of controversy. Several authors [Sch85a, Fri86] stated on empirical grounds that it provides only a crude estimate of the BSSE, while some recent publications [Hob88, Sza88, Van87], which are also valuable as reviews on the subject, clearly demonstrate its usefulness. In a very recent paper, however, Mayer and Vibok [May87b] computed SCF interaction energies using a 'chemical Hamiltonian' formalism [May83] which is rigorously free of BSSE, and arrived at the conclusion that

> "the non-additivity [May87a] ... (of BSSE and interaction energy) ... makes meaningless the polemy about whether or not the Boys-Bernardi scheme overestimates BSSE: in fact, it can overestimate or underestimate the value of BSSE (see also ref. [Lou86]) or even give a wrong sign. This rules out all the conventional schemes used for correcting BSSE"

To sum things up, no definitive conclusion as to the ultimate accuracy of the counterpoise procedure appears to be reached at this stage.

Martin *et al.* [Mar89e] made a systematic investigation of the dissociation energies of the closed- and open-shell diatomic and polyatomic first-row hydrides. They added to a standard 6-31G basis [Heh72] polarization functions optimized at the CISD (Section 1.3) level, as well as a set of diffuse functions [Cla83] optimized at the same level, and then supplemented it with a single *sp*-shell halfway along each bond, whose exponents were optimized at the CISD level for the closed-shell species. This basis set was subsequently used in determining dissociation energies at the MP4(SDTQ) [Bin75b, Pop76, Kri78, Kri80b] level (Section 1.5). It proved competitive with results obtained with basis sets as large as 6-311+G(3*df*, 3*pd*) [Fri84], while being much less costly. In this study, the basis set superposition error was also estimated by the counterpoise method for the diatomic species: BSSEs were found to increase from left to right in the periodic table, and to be as large as 7 kcal/mol for HF! In view of the excellent agreement between theoretical and experimental dissociation energies, one can still justify neglect of BSSE on empirical grounds. However, it would be interesting to see if and how the BSSE can be reduced.

One logical way of reducing BSSE, would be to improve the atomic orbital (AO) basis set itself. At the self-consistent field (SCF) level, this would simply mean expanding the valence part towards the isotropic limit, and not to contract it too much in order to still attain enough flexibility in the molecule. At the correlated level, however, the isotropic limit is certainly not equivalent to the basis set limit, and lots of BSSE will come from insufficiently saturated first and maybe second polarization spaces in the atom. This explains why BSSE will in general be larger at correlated than at SCF levels. Since the expansion of bond functions in an AO basis would involve $d$ and $f$ functions, as well as components from higher angular momenta, a logical explanation for the large BSSE caused by bond functions is readily found. Now if one would increase the polarization space in the AO basis set, the BSSE would certainly decrease. The three questions the present work tries to answer are:

1. Will BSSE decrease by a significant amount?
2. If so, is the required expansion of the polarization space manageable?
3. Do the bond functions still improve the dissociation energy in this expanded basis set by a significant amount?

### 3.3.2 Computational methods

All calculations were carried out using the GAUSSIAN 86 program system [Gau86] running on a DEC VAXStation 2000 under the VMS 4.7 operating system. Optimizations of basis set parameters were carried out by plotting the energy against the basis set parameter over a sufficiently wide range with a point spacing of 0.1 for the larger, and 0.05 for the smaller exponents. The global minima were then determined from a cubic spline interpolation on the graph. Because multiple minima occurred in a number of cases, we had to resort to this rather brute-force method. All Møller-Plesset calculations were done using frozen cores. For UHF (Unrestricted Hartree-Fock) wavefunctions, the PUMP [Sch86b] (Projected Unrestricted Møller-Plesset, *cfr.* Section 1.9) energies produced by annihilation of the principal spin contaminant are also determined.

In this case, optimum exponents were always obtained from the diatomic hydrides in their respective ground states. In general, the energy surfaces were found to be rather flat. Optimum exponents differed somewhat from MP2 to MP3 to MP4 levels, but only about 0.1 at most. Because of the apparent insensitivity of the optimum bond function exponent towards the order of many-body perturbation theory, the decision to abandon the CI level optimizations (CID and MP3 are equal to third order [Pop77]) in favor of the less expensive MP optimizations seems to be warranted. The energy changes involved amounted to less than 100 $\mu$Hartree, so only the MP4 optimal exponents are quoted. (In the subsequent discussion and tables, the abbreviation "MP4" always refers to full

Table XIII: Molecular energies (hartree; minus sign omitted) of the first-row hydride species and atoms using the 6-311+G($d,p$)B basis set.

| Species | UHF | UMP2 | UMP3 | UMP4 | PUHF | PUMP2 | PUMP3 |
|---|---|---|---|---|---|---|---|
| HF | 100.05530 | 100.28860 | 100.28688 | 100.29632 | 100.05530 | 100.28860 | 100.28688 |
| (a) | 100.05501 | 100.28775 | 100.28633 | 100.29565 | 100.05501 | 100.28775 | 100.28633 |
| F | 99.39990 | 99.55959 | 99.56749 | 99.57112 | 99.40225 | 99.56081 | 99.56820 |
| $H_2O$ | 76.05443 | 76.28922 | 76.29299 | 76.30258 | 76.05443 | 76.28922 | 76.29299 |
| OH | 75.41518 | 75.58689 | 75.59778 | 75.60310 | 75.41789 | 75.58852 | 75.59877 |
| O | 74.80740 | 74.92178 | 74.93443 | 74.93724 | 74.80995 | 74.92336 | 74.93544 |
| $NH_3$ | 56.21572 | 56.43341 | 56.44518 | 56.45351 | 56.21572 | 56.43341 | 56.44518 |
| $NH_2$ | 55.58263 | 55.74930 | 55.76470 | 55.77053 | 55.58564 | 55.75115 | 55.76579 |
| $NH(^3\Sigma^-)$ | 54.97854 | 55.09764 | 55.11343 | 55.11759 | 54.98210 | 55.09993 | 55.11480 |
| N | 54.39889 | 54.47657 | 54.48998 | 54.49251 | 54.40009 | 54.47738 | 54.49048 |
| $CH_4$ | 40.20987 | 40.39766 | 40.41705 | 40.42435 | 40.20987 | 40.39766 | 40.41705 |
| $CH_3$ | 39.57469 | 39.72245 | 39.74110 | 39.74668 | 39.57767 | 39.72434 | 39.74219 |
| $CH_2(^3B_1)$ | 38.93538 | 39.04320 | 39.05938 | 39.06364 | 38.93806 | 39.04498 | 39.06046 |
| $CH_2(^1A_1)$ | 38.88944 | 39.01586 | 39.03603 | 39.04219 | 38.88944 | 39.01586 | 39.03603 |
| $CH(^2\Pi)$ | 38.27860 | 38.36901 | 38.38733 | 38.39291 | 38.28108 | 38.37042 | 38.38805 |
| $CH(^4\Sigma^-)$ | 38.28737 | 38.35683 | 38.36896 | 38.37199 | 38.28802 | 38.35726 | 38.36923 |
| C | 37.68957 | 37.74587 | 37.76072 | 37.76520 | 37.69157 | 37.74703 | 37.76132 |
| $BH_3$ | 26.39791 | 26.50500 | 26.52370 | 26.52854 | 26.39791 | 26.50500 | 26.52370 |
| $BH_2$ | 25.75809 | 25.83527 | 25.85026 | 25.85425 | 25.75892 | 25.83573 | 25.85050 |
| $BH(^1\Sigma^+)$ | 25.12836 | 25.19611 | 25.21325 | 25.21931 | 25.12836 | 25.19611 | 25.21325 |
| B | 24.53035 | 24.56973 | 24.58321 | 24.58852 | 24.53244 | 24.57084 | 24.58372 |
| $BeH_2$ | 15.77109 | 15.82764 | 15.83983 | 15.84303 | 15.77109 | 15.82764 | 15.83983 |
| BeH | 15.15185 | 15.18237 | 15.18952 | 15.19165 | 15.15215 | 15.18258 | 15.18964 |
| Be | 14.57194 | 14.59864 | 14.60859 | 14.61308 | 14.57194 | 14.59864 | 14.60859 |
| LiH | 7.98591 | 8.01089 | 8.01715 | 8.01898 | 7.98591 | 8.01089 | 8.01715 |
| Li | 7.43203 | 7.43203 | 7.43203 | 7.43203 | 7.43203 | 7.43203 | 7.43203 |
| $H_2$ | 1.13259 | 1.16141 | 1.16765 | 1.16920 | 1.13259 | 1.16141 | 1.16765 |
| H | 0.49981 | 0.49981 | 0.49981 | 0.49981 | 0.49981 | 0.49981 | 0.49981 |

(a) with counterpoise-optimized bond function exponent (see text)

fourth-order Møller-Plesset theory, i.e. MP4(SDTQ).) For radical systems, the values obtained from PUMP2, PUMP3, and PUMP4 energies are almost identical with those from their unprojected counterparts.

With the basis sets retained for further study, MP4 calculations of the dissociation energy of all open- and closed-shell first-row hydrides were performed. Computed total energies for all species involved are given in Tables XIII, XIV, and XV. To remain consistent with Section 3.2 [Mar89e], HF/6-31G* geometries [DeF79] were used throughout the present study. PUMP2 to PUMP4 energies were also computed. Spin contamination was small for all species: the single spin annihilation method of Schlegel [Sch88] removed it entirely in all cases. Since the method involves virtually no additional computation time, is available by default in the GAUSSIAN 86 package, and has small, but non-negligible (up to 1 kcal/mol) effects on computed dissociation energies, we advise that it be applied to all such cases in the future. The method has also proven invaluable [Mar89c] in an extensive study of the relative stabilities of the isomers and states of $B_3$, $B_2N$, $BN_2$, and

Table XIV: Molecular energies (hartree;minus sign omitted) of the first-row hydride species and atoms using the 6-311+G($2d,p$)B basis set.

| Species | UHF | UMP2 | UMP3 | UMP4 | PUHF | PUMP2 | PUMP3 |
|---|---|---|---|---|---|---|---|
| HF | 100.05586 | 100.30906 | 100.30736 | 100.31745 | 100.05586 | 100.30906 | 100.30736 |
| (a) | 100.05551 | 100.30835 | 100.30697 | 100.31682 | 100.05551 | 100.30835 | 100.30697 |
| F | 99.40054 | 99.57860 | 99.58721 | 99.59155 | 99.40328 | 99.58001 | 99.58797 |
| $H_2O$ | 76.05616 | 76.30472 | 76.30810 | 76.31831 | 76.05616 | 76.30472 | 76.30810 |
| OH | 75.41676 | 75.60192 | 75.61313 | 75.61906 | 75.41978 | 75.60370 | 75.61906 |
| O | 74.80806 | 74.93517 | 74.94879 | 74.95231 | 74.81089 | 74.93690 | 74.94985 |
| $NH_3$ | 56.21743 | 56.44419 | 56.45544 | 56.46444 | 56.21743 | 56.44419 | 56.45544 |
| $NH_2$ | 55.58481 | 55.76017 | 55.77550 | 55.78187 | 55.58796 | 55.76211 | 55.77661 |
| $NH(^3\Sigma^-)$ | 54.97987 | 55.10721 | 55.12347 | 55.12820 | 54.98355 | 55.10958 | 55.12486 |
| N | 54.39889 | 54.48485 | 54.49922 | 54.50238 | 54.40009 | 54.48566 | 54.49971 |
| $CH_4$ | 40.21132 | 40.40387 | 40.42295 | 40.43076 | 40.21132 | 40.40387 | 40.42295 |
| $CH_3$ | 39.57578 | 39.72857 | 39.74714 | 39.75314 | 39.57882 | 39.73049 | 39.74824 |
| $CH_2(^3B_1)$ | 38.93607 | 39.04864 | 39.06498 | 39.06962 | 38.93878 | 39.05043 | 39.06606 |
| $CH_2(^1A_1)$ | 38.89113 | 39.02310 | 39.04335 | 39.04985 | 38.89113 | 39.02310 | 39.04335 |
| $CH(^2\Pi)$ | 38.28003 | 38.37505 | 38.39369 | 38.39964 | 38.28280 | 38.37667 | 38.39453 |
| $CH(^4\Sigma^-)$ | 38.28764 | 38.36128 | 38.37379 | 38.37715 | 38.28829 | 38.36171 | 38.37406 |
| C | 37.69019 | 37.75083 | 37.76627 | 37.77119 | 37.69243 | 37.75216 | 37.76698 |
| $BH_3$ | 26.39888 | 26.50765 | 26.52647 | 26.53152 | 26.39888 | 26.50765 | 26.52647 |
| $BH_2$ | 25.75904 | 25.83774 | 25.85290 | 25.85709 | 25.75992 | 25.83824 | 25.85317 |
| $BH(^1\Sigma^+)$ | 25.12907 | 25.19906 | 25.21631 | 25.22246 | 25.12907 | 25.19906 | 25.21631 |
| B | 24.53102 | 24.57199 | 24.58556 | 24.59106 | 24.53347 | 24.57343 | 24.58629 |
| $BeH_2$ | 15.77129 | 15.82806 | 15.84056 | 15.84390 | 15.77129 | 15.82806 | 15.84056 |
| BeH | 15.15201 | 15.18285 | 15.19024 | 15.19247 | 15.15232 | 15.18306 | 15.19036 |
| Be | 14.57194 | 14.59887 | 14.60860 | 14.61303 | 14.57194 | 14.59887 | 14.60860 |
| LiH | 7.98599 | 8.01126 | 8.01744 | 8.01924 | 7.98599 | 8.01126 | 8.01744 |
| Li | 7.43203 | 7.43203 | 7.43203 | 7.43203 | 7.43203 | 7.43203 | 7.43203 |
| $H_2$ | 1.13259 | 1.16141 | 1.16765 | 1.16920 | 1.13259 | 1.16141 | 1.16765 |
| H | 0.49981 | 0.49981 | 0.49981 | 0.49981 | 0.49981 | 0.49981 | 0.49981 |

(a) with counterpoise-optimized bond function exponent (see text)

$N_3$ (Section 4.2). In order to estimate higher-order effects, the extrapolation formula suggested in [Pop83] was used for the unprojected as well as the projected energies.

Pulay's DIIS (Direct Inversion of the Iterative Subspace) procedure [Pul82] (Section 1.1.7.1) was used throughout to accelerate SCF convergence. This did not present any problems, except in the case of BH with the 6-311+G($2df,p$) basis set, where it converged to an excited state. This phenomenon is known to occur occasionally with DIIS [Sch87].

## 3.3.3 Results and discussion

### 3.3.3.1 The 6-311+G($d,p$)B basis set

A first extension that was considered, is the expansion of the *sp*-part in the AO space from 6-31G to 6-311G. Addition of a set of bond functions to the 6-311+G** basis set [Kri80a, Cla83] is denoted here as 6-311+G($d,p$)B. Optimum values at the MP4 level for the bond function exponents are presented in Table XVI. Double minima (one local

Table XV: Molecular energies (hartree;minus sign omitted) of the first-row hydride species and atoms using the 6-311+G($2df,p$)B basis set.

| Molecule | UHF | UMP2 | UMP3 | UMP4 | PUHF | PUMP2 | PUMP3 |
|---|---|---|---|---|---|---|---|
| HF | 100.05602 | 100.32750 | 100.32711 | 100.33723 | 100.05602 | 100.32750 | 100.32711 |
| (a) | 100.05559 | 100.32614 | 100.32604 | 100.33593 | 100.05559 | 100.32614 | 100.32604 |
| F | 99.40169 | 99.59856 | 99.60892 | 99.61344 | 99.40474 | 99.60010 | 99.60972 |
| $H_2O$ | 76.05629 | 76.31715 | 76.32116 | 76.33146 | 76.05629 | 76.31715 | 76.32116 |
| OH | 75.41755 | 75.61592 | 75.62810 | 75.63414 | 75.42079 | 75.61781 | 75.62917 |
| O | 74.80921 | 74.95004 | 74.96471 | 74.96843 | 74.81223 | 74.95186 | 74.96579 |
| $NH_3$ | 56.21748 | 56.45201 | 56.46347 | 56.47260 | 56.21748 | 56.45201 | 56.46347 |
| $NH_2$ | 55.58502 | 55.76866 | 55.78435 | 55.79084 | 55.58830 | 55.77066 | 55.78549 |
| $NH(^3\Sigma^-)$ | 54.97996 | 55.11557 | 55.13212 | 55.13697 | 54.98367 | 55.11795 | 55.13351 |
| N | 54.39889 | 54.49299 | 54.50721 | 54.51042 | 54.40009 | 54.49380 | 54.50769 |
| $CH_4$ | 40.21126 | 40.40822 | 40.42714 | 40.43510 | 40.21126 | 40.40822 | 40.42714 |
| $CH_3$ | 39.57582 | 39.73292 | 39.75143 | 39.75754 | 39.57892 | 39.73487 | 39.75254 |
| $CH_2(^3B_1)$ | 38.93607 | 39.05296 | 39.06928 | 39.07403 | 38.93880 | 39.05476 | 39.07035 |
| $CH_2(^1A_1)$ | 38.89119 | 39.02868 | 39.04883 | 39.05538 | 38.89119 | 39.02868 | 39.04883 |
| $CH(^2\Pi)$ | 38.28020 | 38.38053 | 38.39897 | 38.40487 | 38.28305 | 38.38219 | 38.39981 |
| $CH(^4\Sigma^-)$ | 38.28764 | 38.36507 | 38.37758 | 38.38106 | 38.28829 | 38.36550 | 38.37785 |
| C | 37.69020 | 37.75604 | 37.77094 | 37.77569 | 37.69244 | 37.75737 | 37.77164 |
| $BH_3$ | 26.39891 | 26.51014 | 26.52882 | 26.53391 | 26.39891 | 26.51014 | 26.52882 |
| $BH_2$ | 25.75911 | 25.84010 | 25.85512 | 25.85933 | 25.76002 | 25.84062 | 25.85540 |
| $BH(^1\Sigma^+)$ | 25.12909 | 25.20174 | 25.21840 | 25.22438 | 25.12909 | 25.20174 | 25.21840 |
| B | 24.53103 | 24.57468 | 24.58756 | 24.59279 | 24.53349 | 24.57613 | 24.58828 |
| $BeH_2$ | 15.77109 | 15.82764 | 15.83983 | 15.84303 | 15.77109 | 15.82764 | 15.83983 |
| BeH | 15.15185 | 15.18237 | 15.18952 | 15.19165 | 15.15215 | 15.18258 | 15.18964 |
| Be | 14.57194 | 14.59974 | 14.60880 | 14.61306 | 14.57194 | 14.59974 | 14.60880 |
| LiH | 7.98600 | 8.01178 | 8.01794 | 8.01975 | 7.98600 | 8.01178 | 8.01794 |
| Li | 7.43203 | 7.43203 | 7.43203 | 7.43203 | 7.43203 | 7.43203 | 7.43203 |
| $H_2$ | 1.13259 | 1.16141 | 1.16765 | 1.16920 | 1.13259 | 1.16141 | 1.16765 |
| H | 0.49981 | 0.49981 | 0.49981 | 0.49981 | 0.49981 | 0.49981 | 0.49981 |

(a) with counterpoise-optimized bond function exponent (see text)

and one global) occurred for HF (shallow local minimum), OH, and BeH. Dissociation energies with and without bond functions for the first-row diatomic hydrides are given in Table XVII, whereas Table XVIII lists the same obtained through an isogyric reaction cycle involving molecular hydrogen discussed in detail in [Pop83]. Table XIX contains the basis set superposition errors in the diatomic hydrides for the 6-31+G($d,p$), 6-31+G($d,p$)B, 6-311+G($d,p$), and 6-311+G($d,p$)B basis sets at the UHF and MP4 levels. Table XX presents the dissociation energies for the first-row open- and closed shell hydrides computed directly from the MP4 energies, while Table XXI lists those obtained via the isogyric reaction cycle [Pop83]. The various molecular energies are given in Table XIII.

It is seen, that BSSE consistently decreases somewhat in absolute value. In relative terms, the improvements for $H_2$, LiH, and BeH are most spectacular: a significant improvement is also still seen for BH. It is noted here, that H has no correlation energy, and Li has none in the frozen-core approximation. Be($^1S$) has only $s$ functions in the

Table XVI: Optimized values (MP4) for bond function exponents in the 6-311+G($d,p$)B, 6-311+G($2d,p$)B, 6-311+G($2df,p$)B, and 6-311+G($3df,p$)B basis sets.

| Bond | 6-311+G($d,p$)B | 6-311+G($2d,p$)B | 6-311+G($2df,p$)B | 6-311+G($3df,p$)B |
|---|---|---|---|---|
| H–F | 1.14 | 1.13 | 1.08 | 1.23 |
| (a) | 1.46 | 2.08 | 2.03 | N/A |
| O–H | 1.70 | 1.78 | 1.71 | 0.93 |
| N–H | 1.32 | 1.52 | 1.41 | 1.24 |
| C–H | 1.03 | 1.19 | 1.13 | 1.19 |
| B–H | 0.91 | 0.84 | 0.86 | 1.06 |
| Be–H | 0.63 | 0.46 | 0.62 | 0.73 |
| Li–H | 0.19 | 0.24 | 0.25 | 0.20 |
| H–H | 0.237 | 0.237 | 0.237 | 0.237 |

(a) counterpoised optimization (see text)

Table XVII: PUMP4 dissociation energies (kcal/mol) with and without bond functions of the first-row diatomic hydrides.

| Molec. | 6-311+G ($d,p$) | 6-311+G ($d,p$)B | 6-311+G ($2d,p$) | 6-311+G ($2d,p$)B | 6-311+G ($2df,p$) | 6-311+G ($2df,p$)B | 6-311+G ($3df,p$) | 6-311+G ($3df,p$)B |
|---|---|---|---|---|---|---|---|---|
| HF | 134.57 | 140.99 | 134.95 | 141.40 | 136.21 | 140.05 | 137.36 | 141.41 |
| (a) | 134.57 | 140.57 | 134.95 | 141.01 | 136.21 | 139.24 | N/A | N/A |
| OH | 99.24 | 104.18 | 99.63 | 107.81 | 101.42 | 104.10 | 102.61 | 105.38 |
| NH | 74.97 | 79.16 | 75.62 | 79.63 | 77.83 | 80.10 | 78.77 | 80.63 |
| CH | 76.99 | 80.33 | 77.77 | 80.79 | 79.52 | 81.27 | 80.06 | 81.53 |
| BH | 79.61 | 81.87 | 80.09 | 82.12 | 81.08 | 82.24 | 81.12 | 82.25 |
| BeH | 48.08 | 49.50 | 48.70 | 50.05 | 49.65 | 49.51 | 49.74 | 50.59 |
| LiH | 52.56 | 54.68 | 52.99 | 54.85 | 54.19 | 55.16 | 54.17 | 55.13 |
| $H_2$ | 105.43 | 106.42 | 105.43 | 106.42 | 105.43 | 106.42 | 105.43 | 106.42 |

(a) with counterpoise-corrected exponent (see text)

Hartree-Fock limit, so the $p$ functions of the 6-311+G basis can be regarded as first polarization space here. B($^2P$) has only one electron in a $p$ orbital. Also noteworthy is the improvement of the dissociation energy in LiH as compared to the 6-31+G($d,p$)B result. The dissociation energy for $H_2$ gets worse; however, the very good value at the 6-31+G($d,p$)B level was an accidental hit caused by error compensation, the energy of the H atom at the 6-31G level being not quite close to the exact value of .5 hartree.

The trend of increasing BSSE with increasing atomic number of the central atom is reproduced for all other basis sets, as evident from Tables XIX and XXII. It is remarked here, that all basis sets considered have equal numbers of primitive functions for all first-row atoms: it is readily imagined, that an atom with seven correlating electrons will need a larger basis set to reach the correlated limit than one with three correlating electrons.

Summing up, it can be stated that the expansion from 6-31G to 6-311G will have a significant effect, which will especially be evident for the lighter atoms.

Table XVIII: PUMP4 dissociation energies (kcal/mol) with and without bond functions of the first-row diatomic hydrides using isogyric reactions.

| Molec. | 6-311+G $(d,p)$ | 6-311+G $(d,p)$B | 6-311+G $(2d,p)$ | 6-311+G $(2d,p)$B | 6-311+G $(2df,p)$ | 6-311+G $(2df,p)$B | 6-311+G $(3df,p)$ | 6-311+G $(3df,p)$B |
|---|---|---|---|---|---|---|---|---|
| HF | 138.61 | 144.05 | 139.00 | 144.47 | 140.26 | 143.11 | 141.41 | 144.48 |
| (a) | 138.61 | 143.63 | 139.00 | 144.07 | 140.26 | 142.30 | N/A | N/A |
| OH | 103.29 | 107.25 | 103.68 | 110.88 | 105.47 | 107.17 | 106.66 | 108.45 |
| NH | 79.01 | 82.22 | 79.66 | 82.70 | 81.88 | 83.16 | 82.82 | 83.69 |
| CH | 81.04 | 83.39 | 81.82 | 83.86 | 83.57 | 84.34 | 84.11 | 84.59 |
| BH | 83.65 | 84.94 | 84.14 | 85.19 | 85.12 | 85.30 | 85.17 | 85.31 |
| BeH | 48.08 | 49.50 | 48.70 | 50.05 | 49.65 | 49.51 | 49.74 | 50.59 |
| LiH | 56.61 | 57.75 | 57.04 | 57.91 | 58.24 | 58.23 | 58.22 | 58.19 |

(a) with counterpoise-corrected exponent (see text)

Table XIX: Basis Set Superposition Errors (kcal/mol) for the first-row diatomic hydrides using the 6-31+G$(d,p)$ and 6-31+G$(d,p)$B basis sets [Mar89e], as well as the 6-311+G$(d,p)$, 6-311+G$(d,p)$B, 6-311+G$(2d,p)$, and 6- 311+G$(2d,p)$B basis sets.

| Molecule | 6-31+G$(d,p)$ | | 6-31+G$(d,p)$B | | 6-311+G$(d,p)$ | | 6-311+G$(d,p)$B | | 6-311+G$(2d,p)$ | | 6-311+G$(2d,p)$B | |
|---|---|---|---|---|---|---|---|---|---|---|---|---|
| | UHF | MP4 | UHF | MP4 | UHF | MP4 | UHF | MP4 | UHF | MP4 | UHF | MP4 |
| HF | 0.78 | 2.64 | 1.27 | 7.11 | 0.76 | 2.93 | 1.11 | 6.64 | 0.60 | 1.47 | 1.18 | 5.90 |
| (a) | – | – | – | – | 0.76 | 2.93 | 1.02 | 6.12 | 0.60 | 1.47 | 0.90 | 4.64 |
| OH | 0.59 | 2.28 | 0.76 | 5.71 | 0.28 | 2.12 | 0.35 | 4.71 | 0.27 | 1.12 | 0.33 | 3.39 |
| NH | 0.29 | 1.77 | 0.46 | 4.35 | 0.06 | 1.46 | 0.08 | 3.29 | 0.06 | 0.80 | 0.09 | 2.31 |
| CH | 0.76 | 1.20 | 0.90 | 2.52 | 0.30 | 0.70 | 0.34 | 1.47 | 0.07 | 0.41 | 0.09 | 1.10 |
| BH | 0.83 | 1.31 | 1.39 | 3.09 | 0.11 | 0.32 | 0.13 | 0.66 | 0.04 | 0.20 | 0.05 | 0.62 |
| BeH | 0.44 | 0.46 | 1.06 | 1.41 | 0.01 | 0.03 | 0.02 | 0.17 | 0.01 | 0.03 | 0.02 | 0.22 |
| LiH | 0.38 | 0.38 | 0.74 | 0.74 | 0.01 | 0.01 | 0.04 | 0.04 | 0.01 | 0.01 | 0.04 | 0.04 |
| $H_2$ | 0.17 | 0.17 | 0.36 | 0.36 | 0.00 | 0.00 | 0.00 | 0.00 | 0.00 | 0.00 | 0.00 | 0.00 |

(a) with counterpoise-corrected exponent (see text)

### 3.3.3.2 The 6-311+G$(2d,p)$B basis set

As a second extension, the doubling of the $d$ polarization functions was considered. Addition of a set of bond functions to the 6-311+G$(2d,p)$ basis set [Fri84] yields the basis set denoted here as 6-311+G$(2d,p)$B. Optimum values for the bond function exponents are again presented in Table XVI. Here, only HF exhibits a (less shallow) second minimum, while BeH forms a little ripple on one side of the energy valley. Dissociation energies with and without bond functions for the first-row diatomic hydrides are once more given in Tables XVII and XVIII. Table XIX contains the basis set superposition errors in the diatomic hydrides. Table XX presents the dissociation energies computed directly from the MP4 energies, while Table XXI lists those obtained via the isogyric reaction cycle involving molecular hydrogen. The energies of all the species involved in the latter two tables are given in Table XIV.

It is seen, that the effect is rather small: the decrease in BSSE seems to come mainly from the parent basis set itself. This taken into account, the loss in BSSE really is not

Table XX: Experimental (from [Pop83]) and theoretical dissociation energies (kcal/mol) of the first-row hydrides computed with a number of bond-polarization function basis sets.

| Molecule | 6-311+G($d,p$)P | | 6-311+G(2$d,p$)B | | 6-311+G(2$df,p$)B | | Experimental |
|---|---|---|---|---|---|---|---|
| | MPxtrp. | PMPxtrp. | MPxtrp. | PMPxtrp. | MPxtrp. | PMPxtrp. | (ref.18,27) |
| HF | 141.47 | 141.03 | 141.89 | 141.43 | 140.57 | 140.07 | 141.2 |
| (a) | 141.06 | 140.62 | 141.50 | 141.03 | 139.75 | 139.26 | 141.2 |
| $H_2O$ | 229.60 | 228.98 | 229.96 | 229.31 | 228.10 | 227.43 | 232.2 |
| OH | 104.28 | 104.26 | 104.80 | 107.96 | 104.15 | 104.15 | 106.6,106.6±.3 |
| $NH_3$ | 289.81 | 289.50 | 290.41 | 290.10 | 290.52 | 290.22 | 297.3±.1 |
| $NH_2$ | 174.84 | 175.21 | 175.71 | 176.09 | 176.33 | 176.73 | 180.9±1.5 |
| NH ($^3\Sigma^-$) | 78.73 | 79.27 | 79.16 | 79.71 | 79.64 | 80.20 | 78.8±4,≤84.7 |
| $CH_4$ | 413.73 | 413.36 | 413.95 | 413.52 | 414.01 | 413.59 | 419.8±.1 |
| $CH_3$ | 302.04 | 302.34 | 302.28 | 302.52 | 302.38 | 302.64 | 307.2±.2 |
| $CH_2(^3B_1)$ | 186.99 | 187.29 | 186.94 | 187.17 | 187.05 | 187.29 | 189.8±.6 |
| $CH_2(^1A_1)$ | 173.85 | 173.48 | 174.84 | 174.41 | 175.63 | 175.20 | 182.3±.5 |
| CH($^2\Pi$) | 80.19 | 80.26 | 80.62 | 80.69 | 81.18 | 81.26 | 84.4±.1,83.9 |
| CH($^4\Sigma^-$) | 66.51 | 66.31 | 65.96 | 65.69 | 65.76 | 65.50 | 67.2 |
| $BH_3$ | 275.34 | 275.02 | 275.63 | 275.19 | 276.34 | 275.91 | 278.1±10 |
| $BH_2$ | 165.80 | 165.63 | 166.01 | 165.73 | 166.61 | 166.35 | 196.2±15 |
| BH($^1\Sigma^+$) | 81.79 | 81.47 | 82.14 | 81.70 | 82.42 | 81.99 | 81.6±2,82.2 |
| $BeH_2$ | 143.28 | 143.28 | 143.99 | 143.99 | 143.62 | 143.62 | |
| BeH | 48.03 | 48.11 | 48.69 | 48.77 | 48.36 | 48.44 | 49.8,55.8±7 |
| LiH | 55.09 | 55.09 | 55.23 | 55.23 | 55.54 | 55.54 | 58.0 |
| $H_2$ | 106.69 | 106.69 | 106.69 | 106.69 | 106.69 | 106.69 | 109.48 |

(a) with counterpoise-corrected exponent (see text)

Table XXI: Dissociation energies (kcal/mol) of the first-row hydrides computed with a number of bond-polarization function basis sets, using an isogyric reaction cycle.

| Molecule | 6-311+G($d,p$)B | | 6-311+G(2$d,p$)B | | 6-311+G(2$df,p$)B | | Experimental |
|---|---|---|---|---|---|---|---|
| | MPxtrp. | PMPxtrp. | MPxtrp. | PMPxtrp. | MPxtrp. | PMPxtrp. | (ref.18,27) |
| HF | 144.25 | 143.81 | 144.68 | 144.21 | 143.35 | 142.86 | 141.2 |
| (a) | 143.84 | 143.40 | 144.28 | 143.81 | 142.53 | 142.04 | 141.2 |
| $H_2O$ | 235.17 | 234.54 | 235.53 | 234.87 | 233.66 | 233.00 | 232.2 |
| OH | 107.06 | 107.04 | 107.59 | 110.74 | 106.94 | 106.93 | 106.6,106.6±.3 |
| $NH_3$ | 298.15 | 297.85 | 298.75 | 298.45 | 298.87 | 298.57 | 297.3±.1 |
| $NH_2$ | 180.41 | 180.77 | 181.27 | 181.65 | 181.89 | 182.29 | 180.9±1.5 |
| NH($^3\Sigma^-$) | 81.51 | 82.05 | 81.94 | 82.49 | 82.42 | 82.98 | 78.8±4,≤84.7 |
| $CH_4$ | 422.07 | 421.70 | 422.29 | 421.86 | 422.36 | 421.94 | 419.8±.1 |
| $CH_3$ | 307.60 | 307.90 | 307.85 | 308.09 | 307.95 | 308.20 | 307.2±.2 |
| $CH_2(^3B_1)$ | 189.78 | 190.07 | 189.72 | 189.96 | 189.83 | 190.07 | 189.8±.6 |
| $CH_2(^1A_1)$ | 179.42 | 179.05 | 180.41 | 179.98 | 181.19 | 180.77 | 182.3±.5 |
| CH($^2\Pi$) | 82.98 | 83.04 | 83.40 | 83.47 | 83.96 | 84.04 | 84.4±.1,83.9 |
| CH($^4\Sigma^-$) | 66.51 | 66.31 | 65.96 | 65.69 | 65.76 | 65.50 | 67.2 |
| $BH_3$ | 280.90 | 280.59 | 281.19 | 280.75 | 281.90 | 281.47 | 278.1±10 |
| $BH_2$ | 168.58 | 168.42 | 168.79 | 168.52 | 169.39 | 169.13 | 196.2±15 |
| BH($^1\Sigma^+$) | 84.57 | 84.25 | 84.92 | 84.48 | 85.20 | 84.77 | 81.6±2,82.2 |
| $BeH_2$ | 146.07 | 146.07 | 146.77 | 146.77 | 146.40 | 146.40 | |
| BeH | 48.03 | 48 11 | 48.69 | 48.77 | 48.36 | 48.44 | 49.8,55.8±7 |
| LiH | 57.87 | 57.87 | 58.01 | 58.01 | 58.32 | 58.32 | 58.0 |

(a) with counterpoise-corrected exponent (see text)

Table XXII: Basis Set Superposition Errors (kcal/mol) for the first-row diatomic hydrides using the 6-311+G($2df,p$), 6-311+G($2df,p$)B, 6-311+G($3df,p$), and 6-311+G($3df,p$)B basis sets.

| Molecule | 6-311+G($2df,p$) | | 6-311+G($2df,p$)B | | 6-311+G($3df,p$) | | 6-311+G($3df,p$)B | |
|---|---|---|---|---|---|---|---|---|
| | UHF | MP4 | UHF | MP4 | UHF | MP4 | UHF | MP4 |
| HF | 0.45 | 1.07 | 0.72 | 3.74 | 0.40 | 0.87 | 0.51 | 3.36 |
| (a) | 0.45 | 1.07 | 0.47 | 2.34 | – | – | – | – |
| OH | 0.20 | 0.67 | 0.22 | 1.76 | 0.17 | 0.54 | 0.26 | 2.47 |
| NH | 0.07 | 0.44 | 0.09 | 1.28 | 0.07 | 0.39 | 0.11 | 1.27 |
| CH | 0.08 | 0.28 | 0.09 | 0.78 | 0.05 | 0.29 | 0.07 | 0.76 |
| BH | 0.01 | 0.02 | 0.05 | 0.46 | 0.04 | 0.21 | 0.05 | 0.43 |
| BeH | 0.01 | 0.05 | 0.02 | 0.18 | 0.02 | 0.05 | 0.02 | 0.17 |
| LiH | 0.01 | 0.01 | 0.04 | 0.04 | 0.01 | 0.01 | 0.04 | 0.04 |
| $H_2$ | 0.00 | 0.00 | 0.00 | 0.00 | 0.00 | 0.00 | 0.00 | 0.00 |

(a) with counterpoise-corrected exponent (see text)

worth the additional computational effort.

#### 3.3.3.3 The 6-311+G($2df,p$)B basis set

Thirdly, the 6-311+G($2df,p$)B basis set was generated by addition of a set of bond functions to 6-311+G($2df,p$) [Fri84]. Optimum values for the bond function exponents are once more presented in Table XVI. Here, only HF exhibits a somewhat wavy character (Figure 3.1), while the ripple for BeH is still present. Dissociation energies with and without bond functions for the first-row diatomic hydrides are again given in Tables XVII and XVIII. Table XXII contains the associated basis set superposition errors. Table XX presents the dissociation energies computed directly from the MP4 energies, while Table XXI lists those obtained via the isogyric reaction cycle involving molecular hydrogen. The total energies involved in these last two tables are given in Table XV.

This addition proves to be rather beneficial. The additional BSSE caused by the bond functions falls below 1 kcal/mol, except for HF (vide infra). Calculated bond dissociation energies are still significantly improved relative to the 6-311+G($2df,p$) basis set, although the improvement is not as spectacular as in the case of the 6-31+G($d,p$) basis set. The 6-311+G($2df,p$)B direct dissociation reaction energies are even in about the same range as those obtained indirectly with the 6-311+G($2df,p$) basis set through the isogyric reaction cycle. Consideration of the spin-projected dissociation energies for the radical species brings the values even closer to the experimental result.

It is thus seen, that by simply including the appropriate expansions of the AO basis set, the BSSE for bond functions as estimated by the counterpoise method can be reduced by a factor of 3 to 5.

An interesting feature at this point is the remarkably good linear correlation between the optimum exponents and the number of valence electrons (viz. the 'effective core

Figure 3.1: MP4 energy, BSSE, and counterpoise corrected MP4 energy versus the bond function exponent of HF in the 6-311+G($2df,p$) basis set.

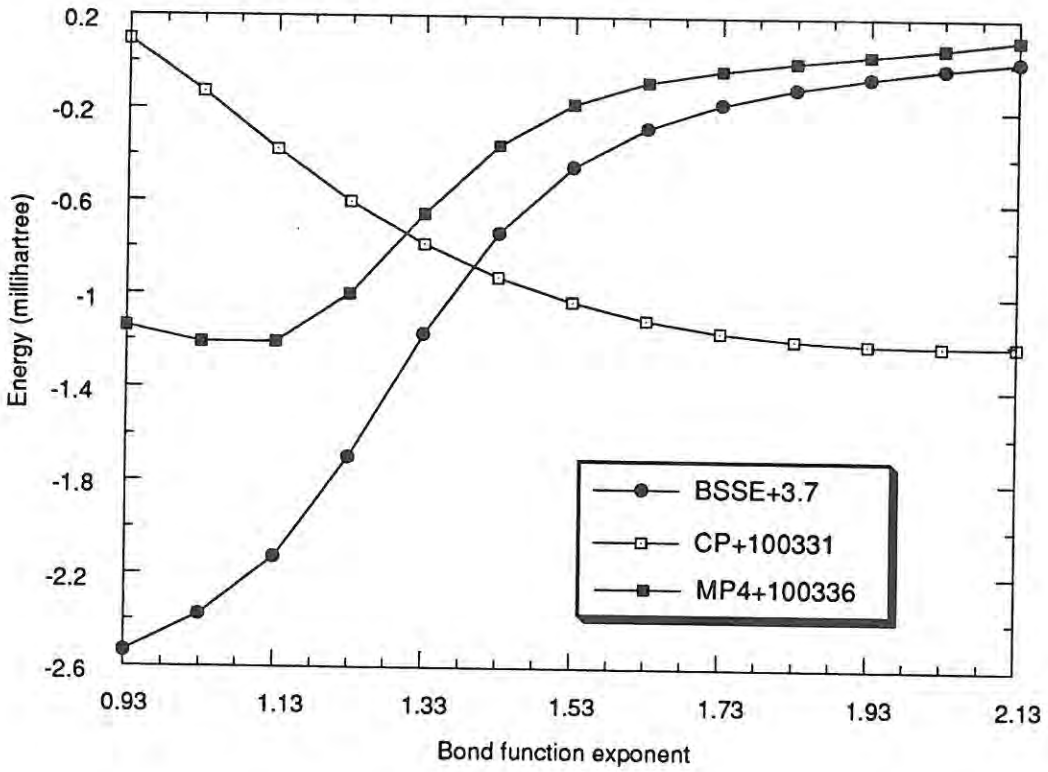


charge'). (In this context, an older paper by Metzgar and Vladimiroff [Met77] discussing the good linear relationship between bond function optimum position and the electronegativity scales of Pauling [Pau32] and Allred and Rochow [All58] is worth mentioning.) For the 6-311+G($d,p$)B, 6-311+G($2d,p$)B, and 6-311+G($2df,p$)B basis sets, linear regression parameters are y=0.1508+0.2053x (R=0.819), y=0.1121+0.2243x (R=0.875), and y=0.1812+0.2017x (R=0.868), respectively. HF is clearly an outlier: if it is eliminated, the relationships become y=-0.0228+0.2809x (R=0.991), y=-0.1018+0.3138x (R=0.998), and y=-0.0178+0.2884x (R=0.999), or essentially perfect fits in the latter two cases. Now the BSSEs in the case of HF are anomalously high too, so it doesn't seem unlikely that the optimal exponents presented here are false minima caused by basis set superposition error. In order to check this, the basis set superposition error was measured in this range, too. Figure 3.1 shows the behavior of uncorrected MP4 energy, BSSE (as estimated by the counterpoise method), and corrected MP4 energy as a function of the exponent in the 6-311+G($2df,p$)B case. It is quickly seen, that a counterpoise corrected minimum is found at almost exactly the location predicted from the linear regression model. BSSE in this case is reduced by no less than 1.4 kcal/mol, while the computed dissociation energy is lowered by only 0.8 kcal/mol. Although the procedure of optimizing exponents with respect to the counterpoise corrected energy is somewhat amenable to discussion,

it is recommended that the exponents obtained in this manner (given as the second entries for HF in Table XVI) be used for the H-F bond. They are in good agreement with the values predicted from the linear regression models (2.12 and 2.00, respectively) for the 6-311+G($2d,p$)B and 6-311+G($2df,p$)B basis sets; this is not the case for the 6-311+G($d,p$)B basis set (predicted value 1.94). As to the other bond types, effects of counterpoised optimization on optimum values as well as on dissociation energies and basis set superposition errors are insignificant.

The 6-311+G($2df,p$)B basis set will be more costly than its counterpart without polarization functions. The increase in cost will not be very large, on the other hand, while the dissociation energies are definitely very much improved. If compared to the use of very much larger polarization-only basis sets, like 6-311++G($3df,3pd$), it will still be significantly cheaper, while it is equal or better on the point of reproducing experimental dissociation energies.

Note that the value predicted for the singlet-triplet splitting of methylene, 9.30 kcal/mol using isogyric reactions, is in perfect agreement with a recent experimental result [McK83] of 9.05 ± 0.06 kcal/mol ($T_0$, between zero-point levels), or 9.08 ± 0.18 kcal/mol ($T_e$, in the hypothetical motionless state) [Sha85]. The computational method by which it was achieved is nevertheless perhaps two orders of magnitude less expensive than the full CI, MRD-CI, and very large basis sets used in some recent studies [Bau87]. The splitting is lowered by about 1 kcal/mol when spin contamination is neglected, which exhibits again the great value of the Schlegel method.

#### 3.3.3.4 The 6-311+G($df,p$)B basis set

Since the effect of doubling the $d$ functions was seen to be minimal, and that of adding $f$ functions rather significant, the 6-311+G($df,p$)B basis set was considered too. However, the optimizations were so problematic, both with and without counterpoise correction during the optimization, that this particular basis set was abandoned. Because of the well-known non-additivity between the 2d and $f$ effects (see e.g. [Fri84]), it would probably have run into other trouble.

#### 3.3.3.5 The 6-311+G($3df,p$) basis set

Finally, tripling the $d$ functions was considered. Table XVI presents the optimum exponents: here only OH exhibits a ripple, while all other exponents present a distinct single minimum. Tables XVII, XVIII, and XXII present the dissociation energies and basis set superposition error, respectively. Here, both the OH and HF bond function exponents are shifted because of BSSE: however, even after performing counterpoise-corrected optimizations BSSEs were not appreciably smaller than those with the ($2df,p$)B basis set. Henceforth, this basis set was left alone, also because it started to put too high a

computational demand on the MicroVAX system.

#### 3.3.3.6 Concluding remarks

It would be interesting to include $g$ and $h$ functions in the comparison. However, no program capable of handling functions of that type is available to us presently. As a means of reaching the molecular correlated basis set limit, however, the use of bond functions, where applicable, seems a more logical and efficient way to proceed than the use of progressively higher angular momenta, resulting in integrals which are progressively more difficult to evaluate, and basis set dimensions which become progressively more prohibitive. For example, Almlöf and Taylor [Alm87] quote a CISD dissociation energy ($D_e$) for $H_2O$ of 216.1 kcal/mol with a [5s4p3d/4s3p] Atomic Natural Orbital (ANO) contraction of a (13s8p6d/8s6p) basis set, while our simple 6-31+G($d,p$)B basis set [Mar89e] yields 223.45 kcal/mol at the HF/6-31G* geometry. They also present a dissociation energy for $H_2$ with the same basis set of 108.2 kcal/mol (our basis: 108.0 kcal/mol at HF/6-31G* geometry), yielding a $D_e$ via isogyric reaction of 218.7 kcal/mol, while 6-31+G($d,p$)B yields 227.78 kcal/mol, or 230.79 kcal/mol after performing the Pople size-consistency correction [Pop77]. It should be noted that the former and the latter basis sets have 58 and 36 contracted functions, 55 and 24 primitive shells, and 119 and 53 primitive functions, respectively. For the $N^4$ parts of SCF and post-Hartree-Fock procedures, this leads to a computer time ratio of 6.74 (for a $4N^5$ integral transformation, the ratio would be 10.85); the same ratio applies to the size of the integral files. For the integral evaluation, the ratio based on the number of shells is 27.6, and that on the number of primitives is 25.4. The present method has the additional advantage, that it is practical to perform using standard *ab initio* packages like GAUSSIAN 82 and GAUSSIAN 86, which run on a variety of simple scalar machines and are widely available.

### 3.3.4 Conclusions

Three new basis sets have been defined, denoted 6-311+G($d,p$)B, 6-311+G($2d,p$)B, and 6-311+G($2df,p$)B. BSSE for the first-row hydrides seems to have a uniform behavior of increase with increasing atomic number of the central atom. Expansion of the valence part of the basis set from 6-31G to 6-311G has a significant effect on the BSSE. This is especially the case for the hydrides of H, Li, Be and B; the computed dissociation energy of LiH, which was pathological for 6-31+G($d,p$)B, is very much improved.

The use of Schlegel's spin-projection method, although negligible in extra cost, does indeed have small but significant effects on reaction energies, even when spin contamination is not strictly a problem.

Doubling the $d$ functions does not seem to have a large effect on the BSSE: the opposite is true for the addition of $f$ functions. Except for the case of HF, additional BSSEs

incurred by bond functions are less than or equal to 1 kcal/mol for the 6-311+G($2df,p$)B basis set. For the first-row hydride species, dissociation energies of chemical accuracy can be obtained even without resorting to isogyric reaction cycles. For high-quality calculations, adding bond functions seems to have definite advantages over expanding the polarization space beyond the [$2d1f$] level.

## 3.4 Basis set superposition error in polyatomic systems

### 3.4.1 Introduction

For overcoming the so-called 'molecular polarization problem' in the choice of basis sets for *ab initio* calculations, a promising approach, the so-called combined bond-polarization basis sets, was introduced recently [Wri83b, Wri83a, Wri84, Mar89e, Mar89c, Mar89g] (In the subsequent discussion, papers [Mar89e], [Mar89c], and [Mar89g] will be referred to as Sections 3.2, 3.3, and 3.5, respectively). The literature and theoretical discussion of the subject can be found in these papers (especially Section 3.3), and will not be repeated here.

The main objection against bond functions in correlated *ab initio* calculations, the exaggerated basis set superposition error (BSSE) [Bau80, Bau85], was shown to be greatly remedied by sufficiently saturating the polarization complement with respect to the atomic correlation energy (Section 3.3). However, this was only shown for the diatomic first-row hydrides. On the basis of these results, basis set superposition error was neglected entirely for both diatomic and polyatomic hydrides, resulting in excellent agreement with experiment (2 kcal/mol or better). The evaluation of polyatomic BSSEs is no trivial matter; in this paper, a tentative effort to investigate these separately is made.

### 3.4.2 Theoretical aspects

The familiar counterpoise method of Boys and Bernardi [Boy70] can be formulated as follows. Suppose it is required to calculate the interaction energy between the systems (atoms, molecules) A and B, usually called monomers, with energies $E(A)$ and $E(B)$. The interaction energy $\Delta E$ of the supersystem $AB$ at some nuclear geometry is given by

$$\Delta E = E(AB) - E(A) - E(B) \tag{3.3}$$

In this equation, however, the effect of basis set superposition is not taken into account. Following Boys and Bernardi's idea, that "the full set of expansion functions used

in the dimer calculation must also be used in the monomer calculations", the interaction energy $\Delta E$ should be written as

$$\Delta E' = E(AB) - E(AG_B) - E(BG_A) \tag{3.4}$$

where $E(AG_B)$ represents the energy of monomer A with the basis functions for B added to the basis set (so-called 'ghost orbitals'), and analogeously for $E(BG_A)$. The BSSE is then defined as follows:

$$\text{BSSE} = \Delta E - \Delta E' = E(AG_B) - E(A) + E(G_AB) - E(B) \tag{3.5}$$

The Boys and Bernardi method has received firm theoretical support over the years [Van87, Hob88, and references therein], in contrast to the results of empirical studies [Sch85a, Fri86], which have indicated that it is not quantitative and suggest that it can only be used as a crude indicator for basis set saturation.

In a recent paper, however, Mayer and Vibok [May87b] computed SCF interaction energies using a 'chemical Hamiltonian' formalism [May83] which is rigorously free of BSSE, and concluded that the interaction energy and its BSSE correction are not additive; to quote these authors,

> "the non-additivity of the BSSE" (and the interaction energy, author's note) "makes meaningless the polemy about whether or not the Boys-Bernardi scheme overestimates BSSE: in fact, it can overestimate or underestimate the value of BSSE (see also ref. [Lou86]) or even give a wrong sign. This rules out all the conventional schemes used for correcting BSSE".

Mayer also gave a theoretical proof [May87a] for the nonadditivity of BSSE and interaction energy in the simplest possible case.

Summing things up, no definitive conclusion as to the validity of the counterpoise procedure appears to be reached at this stage.

The generalization to polyatomic systems (or many-body molecular interactions) is not unique. Wells and Wilson [Wel83] present two possible approaches. In the *pairwise additive function counterpoise* (PAFC) approach, the basis set superposition error is approximated as a sum of Boys-Bernardi BSSEs on pair interactions:

$$\text{PAFC} = \sum_{i \neq j} (E(A_iG_j) - E(A_i)) \tag{3.6}$$

where the summation indices i and j run over all the monomers in the system. In the *site-site function counterpoise* (SSFC) approach, however, it is assumed that all orbitals in the many-body system are available to any of the monomers, and thus the total basis set superposition error may be written as:

$$\text{SSFC} = \sum_{i} (E(A_iG_{jkl\ldots}) - E(A_i)) \tag{3.7}$$

where i again runs over all the monomers, and $G_{jkl...}$ represents the ghost orbitals on all the other monomers. The SSFC expression has the advantage that a meaningful decomposition of the total interaction energy is still possible. Its main disadvantage is the necessity to evaluate the quadratically increasing number of different terms in (3.7), so the PAFC (3.6) is certainly more economical. Wells and Wilson concluded from SCF calculations on helium dimers and trimers that the PAFC tends to overestimate the BSSE (with respect to the SSFC approach), and that the difference between either approach was to some extent a function of the geometric arrangement of the monomers in the adduct. A recent example of an application of SSFC may be found in [Wai89]

However, to our knowledge no systematic comparisons of both approaches at SCF or correlated levels have as yet been undertaken. The present work attempts to provide such a comparison for a moderately-sized class of molecules, the open-and closed-shell first-row hydride species in their respective ground states, for six different basis sets. Three of these are standard [Fri84, and references therein] (6-311+G($d,p$), 6-311+G($2d,p$), and 6-311+G($2df,p$)), the remaining three basis sets contain a single *sp*-shell halfway each bond [Part 2] (6-311+G($d,p$)B, 6-311+G($2d,p$)B and 6-311+G($2df,p$)B). Electron correlation is included using full fourth-order Møller-Plesset theory (MP4(SDTQ), frozen core) [Kri80b, and references therein].

All these basis sets have the common property, that the basis set for hydrogen is nearly saturated: in two-atom counterpoise calculations, its energy was lowered by 10 microhartree or less by the basis functions of the heavy atom, whereas the BSSE in $H_2$ is even much smaller. Henceforth, to a very good approximation, the terms in eqs. (3.6) and (3.7) containing only hydrogen atoms may be neglected. This leads for $AH_n$ to the following simplified expressions:

$$\text{PAFC} = n\,(E(AG_H) - E(A) + E(HG_A) - E(H)) \tag{3.8}$$

$$\text{SSFC} = E(AG_{H_n}) - E(A) + n\,(E(HG_A) - E(H)) \tag{3.9}$$

In other terms, the PAFC of $AH_n$ is exactly $n$ times the counterpoise-BSSE for AH, whereas the SSFC is not. Therefore, one is here comparing plain additivity with nonadditivity.

If the basis set for hydrogen were completely saturated, (3.8) and (3.9) could be further simplified as:

$$\text{PAFC} = n\,(E(AG_{\text{H}}) - E(A)) \tag{3.10}$$

$$\text{SSFC} = E(AG_{\text{H}_n}) - E(A) \tag{3.11}$$

A third alternative imposes itself, besides the PAFC and SSFC approaches: the stepwise formation of the polyatomic molecule. In that case, the total formation reaction can be written as a sequence of binary formation reactions, and the BSSE for each of them can be computed using the normal counterpoise procedure; this eliminates all worries about

nonadditivity. For general cases, this approach has the disadvantage that its application is not unique; for $AH_n$ molecules however, there is an obvious way to proceed. We will illustrate it by considering water. The first step in the formation of water from its atoms will be

$$O(^3P) + H(^2S) \rightarrow OH(^2\Sigma^+) \tag{3.12}$$

The counterpoise energy for this step is of course easily written as

$$\mathrm{BSSE} = E(OG_H) - E(O) + E(HG_O) - E(H) \tag{3.13}$$

Next comes the second association

$$OH + H \rightarrow H_2O \tag{3.14}$$

for which the counterpoise energy can be written as

$$\mathrm{BSSE} = E(OHG_H) - E(OH) + E(HG_{OH}) - E(H) \tag{3.15}$$

The total BSSE then becomes

$$\begin{aligned} \mathrm{BSSE} \;=\; & (E(OHG_H) - E(OH)) + (E(HG_{OH}) - E(H)) \\ & + (E(OG_H) - E(O)) + (E(HG_O) - E(H)) \end{aligned} \tag{3.16}$$

Of course, this definition is not unique. One might just as well consider the following scheme:

$$H + H \rightarrow H_2 \tag{3.17}$$

$$H_2 + O \rightarrow H_2O \tag{3.18}$$

which leads to the following counterpoise expression

$$\mathrm{BSSE} = (E(OG_{H_2}) - E(O)) + (E(H_2G_O) - E(H_2)) + (E(HG_H) - E(H)) \tag{3.19}$$

However, if we consider the H basis set saturated, the second and third terms of (3.19) vanish, and (3.11) for the SSFC method under the same assumption is recovered. Henceforth, we will be using (3.16) as a basis set superposition error estimate, which we will term *successive reaction counterpoise* method (SRCP).

For more than triatomic systems, geometry changes can present additional problems. For example in the $CH_3 + H \rightarrow CH_4$ reaction, $CH_3$ has point group $D_{3h}$, whereas $CH_4$ has point group $T_d$. We may split the reaction in two imaginary steps:

1. the geometry change $CH_3(D_{3h}) \rightarrow CH_3(C_{3v})$, for which no BSSE applies;
2. the reaction $CH_3(C_{3v}) + H \rightarrow CH_4(T_d)$, for which the counterpoise amounts to

$$\begin{aligned} \mathrm{BSSE} \;=\; & (E(CH_3(C_{3v})G_H) - E(CH_3(C_{3v}))) \\ & + \left(E(HG_{CH_3(C_{3v})}) - E(CH_3(C_{3v}))\right) \end{aligned} \tag{3.20}$$

Table XXIII: Basis Set Superposition Error increments (kcal/mol) as estimated by the Site-Site Function Counterpoise Method (SSFC).

| | 6-311+G($d,p$)B | | | | 6-311+G($2d,p$)B | | | | 6-311+G($2df,p$)B | | | |
|---|---|---|---|---|---|---|---|---|---|---|---|---|
| Species | UHF | MP2 | MP3 | MP4 | UHF | MP2 | MP3 | MP4 | UHF | MP2 | MP3 | MP4 |
| HF | 1.02 | 5.61 | 5.88 | 6.12 | 0.90 | 4.28 | 4.49 | 4.64 | 0.47 | 2.32 | 2.24 | 2.34 |
| OH | 0.35 | 4.27 | 4.53 | 4.71 | 0.33 | 3.26 | 3.30 | 3.39 | 0.22 | 1.83 | 1.72 | 1.76 |
| $OH_2$ | 0.81 | 6.70 | 7.16 | 7.29 | 0.57 | 5.11 | 5.37 | 5.44 | 0.25 | 2.87 | 2.81 | 2.84 |
| NH | 0.08 | 3.13 | 3.18 | 3.29 | 0.09 | 2.44 | 2.29 | 2.31 | 0.09 | 1.44 | 1.27 | 1.28 |
| $NH_2$ | 0.09 | 2.87 | 2.89 | 2.98 | 0.09 | 2.19 | 2.04 | 2.05 | 0.10 | 1.28 | 1.13 | 1.13 |
| $NH_3$ | 0.10 | 2.45 | 2.42 | 2.49 | 0.10 | 1.94 | 1.80 | 1.80 | 0.10 | 1.20 | 1.05 | 1.05 |
| CH | 0.34 | 1.68 | 1.46 | 1.47 | 0.09 | 1.36 | 1.12 | 1.10 | 0.09 | 0.97 | 0.79 | 0.78 |
| $CH_2$ | -0.16 | 2.65 | 2.62 | 2.62 | 0.07 | 2.29 | 2.11 | 2.04 | 0.08 | 1.33 | 1.16 | 1.12 |
| $CH_3$ | 0.21 | 1.95 | 1.85 | 1.86 | 0.09 | 1.52 | 1.35 | 1.31 | 0.09 | 0.91 | 0.78 | 0.76 |
| $CH_4$ | 0.20 | 0.81 | 0.60 | 0.60 | 0.07 | 0.60 | 0.41 | 0.40 | 0.07 | 0.46 | 0.30 | 0.30 |
| BH | 0.13 | 0.96 | 0.71 | 0.66 | 0.05 | 0.91 | 0.67 | 0.62 | 0.05 | 0.66 | 0.48 | 0.46 |
| $BH_2$ | 0.21 | 1.93 | 1.71 | 1.64 | 0.07 | 1.49 | 1.22 | 1.10 | 0.07 | 0.89 | 0.69 | 0.63 |
| $BH_3$ | 0.10 | 0.56 | 0.36 | 0.35 | 0.03 | 0.41 | 0.22 | 0.21 | 0.03 | 0.27 | 0.15 | 0.14 |
| BeH | 0.02 | 0.45 | 0.21 | 0.17 | 0.02 | 0.52 | 0.27 | 0.22 | 0.02 | 0.39 | 0.21 | 0.20 |
| $BeH_2$ | 0.01 | 0.28 | 0.09 | 0.07 | 0.02 | 0.28 | 0.12 | 0.09 | 0.02 | 0.20 | 0.09 | 0.09 |
| LiH | 0.04 | 0.04 | 0.04 | 0.04 | 0.04 | 0.04 | 0.04 | 0.04 | 0.04 | 0.04 | 0.04 | 0.04 |
| $H_2$ | 0.00 | 0.00 | 0.00 | 0.00 | 0.00 | 0.00 | 0.00 | 0.00 | 0.00 | 0.00 | 0.00 | 0.00 |
| | 6-311+G($d,p$) | | | | 6-311+G($2d,p$) | | | | 6-311+G($2df,p$) | | | |
| Species | UHF | MP2 | MP3 | MP4 | UHF | MP2 | MP3 | MP4 | UHF | MP2 | MP3 | MP4 |
| HF | 0.76 | 2.55 | 2.76 | 2.93 | 0.60 | 1.34 | 1.39 | 1.47 | 0.45 | 0.99 | 1.00 | 1.07 |
| OH | 0.28 | 1.77 | 1.97 | 2.12 | 0.27 | 1.04 | 1.07 | 1.12 | 0.20 | 0.66 | 0.64 | 0.67 |
| $OH_2$ | 0.32 | 2.75 | 2.99 | 3.14 | 0.16 | 1.51 | 1.58 | 1.66 | 0.20 | 1.05 | 1.02 | 1.07 |
| NH | 0.06 | 1.24 | 1.36 | 1.46 | 0.06 | 0.83 | 0.78 | 0.80 | 0.07 | 0.50 | 0.44 | 0.44 |
| $NH_2$ | 0.06 | 1.23 | 1.33 | 1.42 | 0.07 | 0.81 | 0.76 | 0.77 | 0.08 | 0.50 | 0.44 | 0.45 |
| $NH_3$ | 0.07 | 1.16 | 1.23 | 1.30 | 0.08 | 0.80 | 0.74 | 0.76 | 0.08 | 0.51 | 0.45 | 0.46 |
| CH | 0.30 | 0.73 | 0.68 | 0.70 | 0.07 | 0.49 | 0.42 | 0.41 | 0.08 | 0.34 | 0.28 | 0.28 |
| $CH_2$ | -0.15 | 1.25 | 1.34 | 1.38 | 0.05 | 1.03 | 0.95 | 0.92 | 0.06 | 0.62 | 0.54 | 0.52 |
| $CH_3$ | 0.19 | 1.01 | 1.03 | 1.07 | 0.09 | 0.72 | 0.65 | 0.64 | 0.09 | 0.51 | 0.45 | 0.44 |
| $CH_4$ | 0.17 | 0.38 | 0.31 | 0.31 | 0.07 | 0.42 | 0.34 | 0.33 | 0.07 | 0.24 | 0.19 | 0.19 |
| BH | 0.11 | 0.41 | 0.33 | 0.32 | 0.04 | 0.31 | 0.22 | 0.20 | 0.01 | 0.03 | 0.02 | 0.02 |
| $BH_2$ | 0.21 | 1.08 | 1.02 | 1.03 | 0.05 | 0.77 | 0.63 | 0.57 | 0.07 | 0.65 | 0.50 | 0.46 |
| $BH_3$ | 0.07 | 0.25 | 0.18 | 0.17 | 0.03 | 0.20 | 0.12 | 0.11 | 0.03 | 0.17 | 0.11 | 0.11 |
| BeH | 0.01 | 0.16 | 0.05 | 0.03 | 0.01 | 0.15 | 0.05 | 0.03 | 0.01 | 0.12 | 0.05 | 0.05 |
| $BeH_2$ | 0.01 | 0.15 | 0.06 | 0.05 | 0.01 | 0.16 | 0.07 | 0.06 | 0.01 | 0.09 | 0.04 | 0.04 |
| LiH | 0.01 | 0.01 | 0.01 | 0.01 | 0.01 | 0.01 | 0.01 | 0.01 | 0.01 | 0.01 | 0.01 | 0.01 |
| $H_2$ | 0.00 | 0.00 | 0.00 | 0.00 | 0.00 | 0.00 | 0.00 | 0.00 | 0.00 | 0.00 | 0.00 | 0.00 |

Also, if more than three atoms are involved, a number of supplementary reaction schemes can be constructed. We will avoid these here, since only the scheme adopted in (3.16) corresponds to the sequential association we are interested in.

SRCP will be by far the most expensive method considered here, and requires an operational definition based on the reaction scheme. On the other hand, it is entirely defined in terms of two-body BSSEs, and will thus not suffer from many-body nonadditivity effects.

### 3.4.3 Computational methods

All calculations were carried out using the GAUSSIAN 86 program system [Gau86] running on a MicroVAX 2000 workstation under the VMS 4.7 operating system. To remain consistent with Parts 1, 2 and 4, HF/6-31G* geometries [DeF79] were used throughout the present study.

For the systems $CHG_H$ and $OHG_H$, the SCF criterion had to be loosened from the standard value of 1.0D-9 (Euclidean norm of difference between consecutive density matrices) to 1.0D-5 and 1.0D-6, respectively, in order to obtain convergence. Both with and without DIIS [Pul82], as well as when doing steepest-descent direct minimization SCF [See76], the iteration started cycling indefinitely when better convergence was requested. This effect did not occur in any of the other systems.

### 3.4.4 Results, discussion, and conclusions

Total energies for the atomic systems may be found in Section 3.3, and are not repeated here. The BSSE increments per bond according to the SSFC expression (3.9) are given in the upper part of Table XXIII for the 6-311+G$(d,p)$B, 6-311+G$(2d,p)$B, and 6-311+G$(2df,p)$B basis sets, and in the lower part for the corresponding polarization-only basis sets, i.e. 6-311+G$(d,p)$, 6-311+G$(2d,p)$, and 6-311+G$(2df,p)$. The BSSE increments per bond for the PAFC method defined in (3.8) are of course all identical to the BSSE for the first step. Table XXIV presents the same analysis as Table XXIII, but now for the SRCP method and omitting the 6-311+G$(2d,p)$ and 6-311+G$(2d,p)$B basis sets. Finally, in Table XXV binding energies (without BSSE correction) at the corresponding levels of theory have been given, as well as experimental values corrected for zero-point energy. The numerical values in Table XXV for the 6-311+G$(2d,p)$ and 6-311+G$(2df,p)$ basis sets differ from those given in [Pop83], in that they were computed directly, whereas an additivity approximation was used in [Pop83]. Noticeable nonadditivity errors occur only for the 6-311+G$(2df,p)$ basis set; they are largest in ammonia (1.5 kcal/mol), methane (1.2 kcal/mol), methyl radical (0.9 kcal/mol), and water (0.8 kcal/mol). All other nonadditivity errors are less than or equal to 0.5 kcal/mol.

First and foremost, it is obvious that the basis set superposition error globally increases with increasing atom number of the central atom, both with and without bond functions: this was also seen in Section 3.3. The largest BSSEs in this study are seen for the water molecule, becoming an alarming 12.00 kcal/mol with the 6-311+G$(d,p)$B basis set.

The BSSEs also greatly increase upon inclusion of electron correlation, except of course for $H_2$ and LiH, where the separated atoms have no correlation energy in the frozen-core approximation adopted here. The BSSEs also exhibit a marked decrease from MP2 to MP3, much less from MP3 to MP4, for the lighter hydrides; for the heaviest hydrides there is a slight increase. This decrease is more marked for the larger than for the smaller basis sets: the difference between BSSEs with and without bond func-

Table XXIV: Basis Set Superposition Error increments (kcal/mol) as estimated by the Successive Reaction Counterpoise Method (SRCP).

| | 6-311+G($d,p$)B | | | | 6-311+G(2$df,p$)B | | | |
|---|---|---|---|---|---|---|---|---|
| Species | UHF | MP2 | MP3 | MP4 | UHF | MP2 | MP3 | MP4 |
| HF | 1.02 | 5.61 | 5.88 | 6.12 | 0.47 | 2.32 | 2.24 | 2.34 |
| OH | 0.35 | 4.27 | 4.53 | 4.71 | 0.22 | 1.83 | 1.72 | 1.76 |
| $OH_2$ | 0.58 | 5.41 | 5.68 | 5.86 | 0.27 | 2.17 | 2.05 | 2.15 |
| NH | 0.08 | 3.13 | 3.18 | 3.29 | 0.09 | 1.44 | 1.27 | 1.28 |
| $NH_2$ | 0.19 | 3.29 | 3.37 | 3.50 | 0.13 | 1.43 | 1.29 | 1.33 |
| $NH_3$ | 0.52 | 4.05 | 4.12 | 4.24 | 0.22 | 1.71 | 1.56 | 1.63 |
| CH | 0.34 | 1.68 | 1.46 | 1.47 | 0.09 | 0.97 | 0.79 | 0.78 |
| $CH_2$ | 0.26 | 2.73 | 2.67 | 2.69 | 0.12 | 1.32 | 1.15 | 1.14 |
| $CH_3$ | 0.12 | 1.60 | 1.61 | 1.70 | 0.12 | 0.80 | 0.73 | 0.76 |
| $CH_4$ | 0.18 | 1.83 | 1.82 | 1.90 | 0.12 | 1.01 | 0.91 | 0.95 |
| BH | 0.13 | 0.96 | 0.71 | 0.66 | 0.05 | 0.66 | 0.48 | 0.46 |
| $BH_2$ | 0.08 | 1.36 | 1.09 | 1.03 | 0.05 | 0.68 | 0.48 | 0.46 |
| $BH_3$ | 0.03 | 0.72 | 0.64 | 0.62 | 0.03 | 0.35 | 0.25 | 0.24 |
| BeH | 0.02 | 0.45 | 0.21 | 0.17 | 0.02 | 0.39 | 0.21 | 0.20 |
| $BeH_2$ | 0.10 | 0.27 | 0.29 | 0.29 | 0.04 | 0.18 | 0.18 | 0.18 |
| LiH | 0.04 | 0.04 | 0.04 | 0.04 | 0.04 | 0.04 | 0.04 | 0.04 |
| $H_2$ | 0.00 | 0.00 | 0.00 | 0.00 | 0.00 | 0.00 | 0.00 | 0.00 |
| | 6-311+G($d,p$) | | | | 6-311+G(2$df,p$) | | | |
| Species | UHF | MP2 | MP3 | MP4 | UHF | MP2 | MP3 | MP4 |
| HF | 0.76 | 2.55 | 2.76 | 2.93 | 0.45 | 0.99 | 1.00 | 1.07 |
| OH | 0.28 | 1.77 | 1.97 | 2.12 | 0.20 | 0.66 | 0.64 | 0.67 |
| $OH_2$ | 0.41 | 2.51 | 2.71 | 2.87 | 0.23 | 0.89 | 0.87 | 0.94 |
| NH | 0.06 | 1.24 | 1.36 | 1.46 | 0.07 | 0.50 | 0.44 | 0.44 |
| $NH_2$ | 0.19 | 1.51 | 1.64 | 1.76 | 0.10 | 0.59 | 0.54 | 0.57 |
| $NH_3$ | 0.47 | 2.12 | 2.24 | 2.35 | 0.17 | 0.82 | 0.77 | 0.82 |
| CH | 0.30 | 0.73 | 0.68 | 0.70 | 0.08 | 0.34 | 0.28 | 0.28 |
| $CH_2$ | 0.23 | 1.49 | 1.56 | 1.61 | 0.09 | 0.64 | 0.57 | 0.57 |
| $CH_3$ | 0.09 | 0.80 | 0.86 | 0.92 | 0.09 | 0.43 | 0.41 | 0.43 |
| $CH_4$ | 0.16 | 0.92 | 0.98 | 1.04 | 0.09 | 0.48 | 0.45 | 0.49 |
| BH | 0.11 | 0.41 | 0.33 | 0.32 | 0.01 | 0.03 | 0.02 | 0.02 |
| $BH_2$ | 0.03 | 0.72 | 0.64 | 0.62 | 0.03 | 0.35 | 0.25 | 0.24 |
| $BH_3$ | 0.17 | 0.59 | 0.60 | 0.63 | 0.07 | 0.31 | 0.28 | 0.29 |
| BeH | 0.01 | 0.16 | 0.05 | 0.03 | 0.01 | 0.12 | 0.05 | 0.05 |
| $BeH_2$ | 0.09 | 0.22 | 0.23 | 0.24 | 0.03 | 0.13 | 0.14 | 0.14 |
| LiH | 0.01 | 0.01 | 0.01 | 0.01 | 0.01 | 0.01 | 0.01 | 0.01 |
| $H_2$ | 0.00 | 0.00 | 0.00 | 0.00 | 0.00 | 0.00 | 0.00 | 0.00 |

tions is also affected, and decreases for all cases with the greatest basis set employed. It was generally observed, that BSSEs decrease upon proceeding from MP3 to MP4(DQ), whereas they again increase upon proceeding from MP4(DQ) to MP4(SDTQ). Extrapolating for higher-order effects according to the formula suggested in Part 4 resulted in BSSE changes of only about 0.01 kcal/mol, which enables us to say that, at least for this type of molecules, BSSE is adequately described at the MP4 level.

BSSEs are more than doubled when bond functions are added: this increase is somewhat less spectacular than expected from the work of Bauschlicher. It is remarked here, that the MP4/6-311+G($d,p$) BSSE still amounts to 5.26 kcal/mol for $H_2O$, which although less than half the 12.00 kcal/mol when bond functions are included, is still anything but desirable. The largest MP4/6-311+G($2df,p$) BSSE is 1.74 kcal/mol for $H_2O$, where only 2.86 kcal/mol is added on top by using the bond functions; the difference in binding energy amounts to 10.0 kcal/mol for the smaller, and 5.4 kcal/mol for the larger basis set. For $NH_3$, the picture is more clear-cut: 4.58 kcal/mol extra BSSE results from addition of bond functions to the smaller, 2.11 to the larger basis set, compared to the large differences in binding energy of 12.3 and 6.7 kcal/mol, respectively. For $CH_4$, the extra BSSE is 1.53 kcal/mol with the largest, and 3.09 with the smallest basis sets; this should be compared to extra binding energies of 6.5 and 12.1 kcal/mol, respectively.

If the BSSE differences caused by the bond functions are studied, it becomes clear that they are not markedly affected by the addition of a second set of $d$ functions; they are, on the other hand, decreased by a factor of two or more when a set of $f$ functions is added, from the boron hydrides on. For $H_2$, LiH and the beryllium hydrides, the $d$ functions are already second polarization space for the separated atoms, so $f$ functions (which are then third polarization space) do not contribute appreciably.

For the BSSE without bond functions however, doubling the $d$ functions decreases the BSSE more significantly than the subsequent addition of a set of $f$ functions.

The total BSSEs when using bond functions are decreased by a factor of about three when extra $d$ and $f$ functions are added at the same time. The final values are a bit large in some instances, but still acceptable when compared to the other errors inherent in the calculations.

Considering now the difference between the three methods, Wells and Wilson expect the PAFC to be larger than the SSFC, and thus overestimate the basis set superposition error. From Tables XXIII and XXIV, it is quickly seen that PAFC may both over-and underestimate the SSFC BSSE. Additivity holds better for the UHF than for the correlated levels. The additivity also improves with the basis set: at the UHF/6-311+G($2df,p$) and ($2df,p$)B levels, additivity holds best; incidentally, the BSSE is also smallest here. The SRCP, on the average, tends to yield the highest BSSEs of all three methods, except for the case of $H_2O$, where it is in between the SSFC and PAFC results. Generally, the agreement between SSFC and SRCP appears to be better than either that between SSFC and PAFC, or SRCP and PAFC.

Wells and Wilson also observed, that additivity is strongly influenced by the symmetry of the system. This is particularly noticeable for $CH_3$ and $CH_4$; however, a tendency towards lowered BSSEs due to nonadditivity is seen in all cases where the point group of the adduct is of a more symmetric type than that of its lower hydride monomer (e.g. $CH_3$, $BH_3$: $C_{2v} \rightarrow D_{3h}$, $CH_4$ : $D_{3h} \rightarrow T_d$, but not $NH_3$ : $C_{2v} \rightarrow C_{3v}$). (Also, the wavefunction

for $CG_{H_4}$ (i.e., carbon atom in the basis set for methane) has only $C_{3v}$ symmetry; if it were constrained to $T_d$ symmetry (which is unfortunately impossible with GAUSSIAN 86), the BSSE would even be slightly lower in the $CH_4$ case.) The same argument applies for $BeH_2$ ($C_{\infty v} \rightarrow D_{\infty h}$); the effect is only seen here when bond functions are included. The SRCP method, on the other hand, does not exhibit this phenomenon (except for $BH_3$ and $CH_3$); apparently some BSSE might be involved in the geometrical rearrangement.

The bond function contributions are also strongly nonadditive, reaching 1.56 kcal/mol for $H_2O$ in the 6-311+G$(d,p)$B basis set. Here, an overestimate is generally observed, except for $H_2O$, where PAFC underestimates the SSFC result.

It was found in Sections 3.2 and 3.3, that computed dissociation energies using the 6-31+G$(d,p)$B and 6-311+G$(d,p)$B basis sets and an isogyric reaction cycle involving molecular hydrogen [Pop83] were too large by amounts up to 2 kcal/mol at the MP4 level, when using bond functions; the overshoot was somewhat smaller with the 6-311+G$(2df,p)$B basis set. It would be natural to ascribe this effect to the basis set superposition error (which is of course reduced in the 6-311+G$(2df,p)$B basis set). However, in Section 3.5 it was found that a fair part of the overestimate was not due to BSSE, but to truncation of the Møller-Plesset series: when an augmented coupled cluster method was used instead, mean absolute errors were reduced to 0.42 kcal/mol for the 6-311+G$(2df,p)$B basis set, and 0.68 kcal/mol for 6-311+G$(d,p)$B. The tendency towards overestimation remained, while it should also be noted that the use of optimum geometries at the levels involved would further increase the computed dissociation energy by at most 0.3 kcal/mol [Pop83]. This produces a net overestimation of 1 kcal/mol or less, which is definitely small if compared to the sometimes overly large BSSE values found by all three methods here. This is hard to explain from the viewpoint that the counterpoise method produces an accurate description of basis set superposition error.

The only possible explanation would be, that BSSE and basis set incompleteness error follow the same trend, and thus compensate each other. Since both the basis set incompleteness error and the BSSE increase from left to right in the periodic table, this seems plausible, at least for the case of diatomic molecules; in the case of polyatomic molecules however, this argument becomes more difficult to sustain.

In the light of Mayer's conclusion however, that BSSE and interaction energy are generally nonadditive, our findings are readily understood. As far as the additive part of the BSSE is concerned, the above argument may still apply; the nonadditive part, of course, is also found in the true interaction energy. Since it is hardly desirable to compensate for the latter, and the former error will cancel to a great extent with the basis set incompleteness error, it may be best not to compensate at all for BSSE in dissociation energy calculations using bond functions, until perhaps a correlated extension of Mayer's BSSE-free method becomes generally available. The most powerful argument supporting this conclusion is and remains the excellent agreement between calculated

Table XXV: Theoretical and experimental dissociation energies (kcal/mol; no BSSE correction).

| Species | 6-311+G($d,p$)B | | | | 6-311+G($d,p$) | | | | Experimental |
|---|---|---|---|---|---|---|---|---|---|
| | UHF | MP2 | MP3 | MP4 | UHF | MP2 | MP3 | MP4 | [Pop83, Mar89e] |
| HF | 97.5 | 143.3 | 137.4 | 141.0 | 96.2 | 137.7 | 131.5 | 135.0 | 141.2 |
| $H_2O$ | 155.3 | 230.8 | 225.2 | 229.5 | 154.5 | 221.5 | 215.3 | 219.5 | 232.2 |
| OH | 67.8 | 103.7 | 102.6 | 104.2 | 67.4 | 99.2 | 97.7 | 99.3 | 106.6,106.6±.3 |
| $NH_3$ | 199.2 | 287.0 | 286.0 | 289.6 | 198.5 | 275.5 | 273.9 | 277.3 | 297.3±.1 |
| $NH_2$ | 115.5 | 171.4 | 172.6 | 174.7 | 115.1 | 163.8 | 164.6 | 166.5 | 180.9±1.5 |
| NH | 50.1 | 76.1 | 77.6 | 78.6 | 49.8 | 72.2 | 73.5 | 74.4 | 78.8±4,≤84.7 |
| $CH_4$ | 327.0 | 409.5 | 412.3 | 414.1 | 326.5 | 398.0 | 400.7 | 402.0 | 419.8±.1 |
| $CH_3$ | 242.0 | 299.4 | 301.8 | 302.5 | 241.4 | 290.6 | 292.7 | 293.2 | 307.2±.2 |
| $CH_2$ | 154.5 | 186.8 | 187.7 | 187.5 | 154.0 | 181.1 | 181.7 | 181.5 | 189.8±.6 |
| CH | 56.0 | 77.4 | 79.6 | 80.3 | 55.8 | 74.2 | 76.3 | 76.9 | 84.4±.1,83.9 |
| $BH_3$ | 231.0 | 273.5 | 276.8 | 276.5 | 230.5 | 267.1 | 270.4 | 270.1 | 278.1±10 |
| $BH_2$ | 143.1 | 166.9 | 167.8 | 167.0 | 142.8 | 162.5 | 163.5 | 162.6 | 196.2±15 |
| BH | 61.6 | 79.4 | 81.7 | 82.2 | 61.5 | 77.1 | 79.4 | 79.9 | 81.6±2,82.2 |
| $BeH_2$ | 125.2 | 143.9 | 145.3 | 144.5 | 124.9 | 141.1 | 142.6 | 141.8 | |
| BeH | 50.3 | 52.7 | 50.9 | 49.4 | 50.1 | 51.2 | 49.5 | 48.0 | 49.8,55.8±7 |
| LiH | 33.9 | 49.6 | 53.5 | 54.7 | 33.8 | 48.1 | 51.5 | 52.6 | 58.0 |
| $H_2$ | 83.4 | 101.5 | 105.4 | 106.4 | 83.4 | 100.8 | 104.5 | 105.4 | 109.5 |
| Species | 6-311+G(2$d,p$)B | | | | 6-311+G(2$d,p$) | | | | Experimental |
| | UHF | MP2 | MP3 | MP4 | UHF | MP2 | MP3 | MP4 | [Pop83, Mar89e] |
| HF | 97.4 | 144.3 | 138.0 | 141.5 | 96.3 | 138.6 | 132.0 | 135.4 | 141.2 |
| $H_2O$ | 155.9 | 232.1 | 225.7 | 229.9 | 154.7 | 222.5 | 215.6 | 219.7 | 232.2 |
| OH | 68.3 | 104.8 | 103.2 | 104.8 | 67.7 | 100.0 | 98.2 | 99.6 | 106.6,106.6±.3 |
| $NH_3$ | 200.2 | 288.6 | 286.6 | 290.3 | 199.2 | 277.6 | 275.2 | 278.6 | 297.3±.1 |
| $NH_2$ | 116.9 | 173.0 | 173.6 | 175.6 | 116.3 | 165.6 | 165.9 | 167.8 | 180.9±1.5 |
| NH | 50.9 | 76.9 | 78.1 | 79.1 | 50.6 | 73.1 | 74.1 | 75.1 | 78.8±4,≤84.7 |
| $CH_4$ | 327.5 | 410.3 | 412.6 | 414.4 | 326.9 | 400.4 | 402.5 | 404.1 | 419.8±.1 |
| $CH_3$ | 242.3 | 300.1 | 302.1 | 302.8 | 241.8 | 292.2 | 294.0 | 294.5 | 307.2±.2 |
| $CH_2$ | 154.5 | 187.1 | 187.7 | 187.5 | 154.2 | 181.8 | 182.2 | 181.9 | 189.8±.6 |
| CH | 56.5 | 78.1 | 80.1 | 80.7 | 56.4 | 75.1 | 77.1 | 77.7 | 84.4±.1,83.9 |
| $BH_3$ | 231.2 | 273.7 | 277.0 | 276.8 | 231.1 | 268.5 | 271.8 | 271.5 | 278.1±10 |
| $BH_2$ | 143.3 | 167.0 | 168.0 | 167.2 | 143.2 | 163.5 | 164.4 | 163.6 | 196.2±15 |
| BH | 61.7 | 79.9 | 82.2 | 82.6 | 61.6 | 77.8 | 80.1 | 80.5 | 81.6±2,82.2 |
| $BeH_2$ | 125.3 | 144.1 | 145.8 | 145.1 | 125.3 | 142.0 | 143.5 | 142.8 | |
| BeH | 50.4 | 52.8 | 51.3 | 50.0 | 50.3 | 51.6 | 50.0 | 48.6 | 49.8,55.8±7 |
| LiH | 34.0 | 49.8 | 53.7 | 54.8 | 33.9 | 48.5 | 52.0 | 53.0 | 58.0 |
| $H_2$ | 83.4 | 101.5 | 105.4 | 106.4 | 83.4 | 100.8 | 104.5 | 105.4 | 109.5 |
| Species | 6-311+G(2$df,p$)B | | | | 6-311+G(2$df,p$) | | | | Experimental |
| | UHF | MP2 | MP3 | MP4 | UHF | MP2 | MP3 | MP4 | [Pop83, Mar89e] |
| HF | 96.7 | 142.9 | 136.4 | 139.7 | 96.2 | 140.0 | 133.4 | 136.7 | 141.2 |
| $H_2O$ | 155.3 | 230.6 | 223.9 | 228.0 | 154.6 | 225.3 | 218.6 | 222.6 | 232.2 |
| OH | 68.1 | 104.2 | 102.6 | 104.1 | 67.8 | 101.6 | 100.0 | 101.4 | 106.6,106.6±.3 |
| $NH_3$ | 200.3 | 288.4 | 286.7 | 290.4 | 199.5 | 281.8 | 280.1 | 283.7 | 297.3±.1 |
| $NH_2$ | 117.0 | 173.2 | 174.2 | 176.2 | 116.6 | 168.8 | 169.7 | 171.7 | 180.9±1.5 |
| NH | 51.0 | 77.0 | 78.5 | 79.5 | 50.8 | 74.8 | 76.3 | 77.3 | 78.8±4,≤84.7 |
| $CH_4$ | 327.5 | 409.7 | 412.2 | 414.3 | 327.0 | 403.3 | 406.0 | 407.8 | 419.8±.1 |
| $CH_3$ | 242.3 | 299.6 | 301.9 | 302.7 | 242.0 | 294.9 | 297.2 | 298.0 | 307.2±.2 |
| $CH_2$ | 154.5 | 186.6 | 187.5 | 187.4 | 154.3 | 183.4 | 184.4 | 184.3 | 189.8±.6 |
| CH | 56.6 | 78.2 | 80.5 | 81.2 | 56.5 | 76.4 | 78.7 | 79.4 | 84.4±.1,83.9 |
| $BH_3$ | 231.2 | 273.6 | 277.3 | 277.2 | 231.1 | 270.3 | 274.1 | 274.0 | 278.1±10 |
| $BH_2$ | 143.4 | 166.8 | 168.1 | 167.5 | 143.3 | 164.6 | 166.0 | 165.4 | 196.2±15 |
| BH | 61.7 | 79.8 | 82.2 | 82.7 | 61.6 | 78.5 | 81.0 | 81.5 | 81.6±2,82.2 |
| $BeH_2$ | 125.2 | 143.2 | 145.2 | 144.5 | 125.3 | 142.8 | 145.0 | 144.5 | |
| BeH | 50.3 | 52.0 | 50.8 | 49.4 | 50.3 | 51.9 | 50.8 | 49.6 | 49.8,55.8±7 |
| LiH | 34.0 | 50.2 | 54.0 | 55.2 | 33.9 | 49.3 | 53.1 | 54.2 | 58.0 |
| $H_2$ | 83.4 | 101.5 | 105.4 | 106.4 | 83.4 | 100.8 | 104.5 | 105.4 | 109.5 |

and experimental values using this approximation: in the end, that is what quantum chemistry is all about. Also, it is by no means general practice to include BSSEs in dissociation energy calculations without bond functions. As is seen above, BSSEs according to all three generalizations of the counterpoise method are also anything but small in that case: so there hardly is any good reason either for dismissing bond function basis sets as BSSE-prone, or for advocating that BSSE corrections are more appropriate for calculations with bond functions than for calculations without them. Ultimately, in our opinion, the chief usefulness of counterpoise-related methods in dissociation energy calculations is as a qualitative indicator for basis set incompleteness.

Finally, however, we wish to stress that these conclusions do not necessarily apply for the case of weak molecular interactions, where bond functions, with their inherent reliance on a more or less directional covalent-type bonding, would be of limited use anyway.

## 3.5 Effect of improving electron correlation

### 3.5.1 Introduction

For evaluating the so-called 'basis set correlation energy', i.e. the difference between the full CI and Hartree-Fock energies within a given basis set, a number of approaches have been developed over the years, including limited configuration interaction (CI) [Sha77a], full CI within small basis set using unitary group techniques [Sha77b], the coupled pair functional (CPF) [Ahl85], Møller-Plesset (MP) many-body perturbation (MBP) theory [Mol34], and coupled cluster (CC) techniques [Bar81, Pur82, Urb85, Lee84]. Of these methods, MP theory is computationally by far the most efficient.

The first-order MP energy is already incorporated in the Hartree-Fock energy. Second-order [Bin75b], third-order [Pop76], and fourth-order [Kri78, Kri80b] energies can be routinely evaluated. The formulae for higher than fourth-order energies are prohibitively complex, so their efficient implementation may never see the light of day[1]

Consequently, the MP series is generally truncated at fourth order for the computation of dissociation energies, an idea which is shown to be less than satisfactory in many cases [Han85, Kno85]. Bartlett and Shavitt [Bar77] put forward a series of extrapolation methods based on Padé approximants. Pople and coworkers [Pop83] introduced a simple formula based on the assumption, that the MP2, MP3, and MP4 corrections follow a geometric series:

$$E_{\text{corr}} \approx \frac{E_2 + E_3}{1 - E_4/E_2} \tag{3.21}$$

[1] An MP5 implementation has been published [Kuc89] after going to press of this Section [Mar89g]. Its dominant step, the calculation of $E_{5TT}$, scales as $O(n^8)$, i.e. with the eighth power of basis set size. The $E_{5QQ}$ step, which scales at first sight as $O(n^{10})$, was rewritten as a sequence of $O(n^6)$ steps.

In a recent book on *ab initio* MO theory, co-authored by Pople [Heh86], it was stated that "This assumption is as yet untested; at the present time, it is put forward as a more reasonable procedure than total neglect of higher-order contributions.". In their own work [Pop83] they found it to bring the computed dissociation energies into closer agreement with experiment; the landmark paper of Handy *et al.* [Han85] on the convergence of the MP series was also favorable to it in cases where the MP series converged rapidly. However, to our knowledge no systematic comparison with more accurate post-Hartree-Fock theories has been attempted.

Recently, a number of new combined bond-polarization basis sets were developed in our laboratory [Mar89e, Mar89g], which yield especially good results for computed dissociation energies of first-row hydrides. The most important objection against bond functions, the overly large basis set superposition error, was shown to be removed for the greatest part when the polarization complement was expanded to the $(2df)$ level [Mar89g]. In that study, energies were evaluated using fourth-order MP theory as well as Pople's extrapolation formula, both with and without spin projection [Sch86b]. Computed dissociation energies using an isogyric reaction cycle were systematically slightly too high; application of the extrapolation brought the values into the right direction. The remaining overestimation of 2 kcal/mol or less was then ascribed to basis set superposition error. These effects are investigated in a separate study [Mar89h]. However, there also exists the possibility that the extrapolations were not adequate.

Therefore, in the present study, more accurate correlation energies have been evaluated using the CCD+ST(CCD) method [Rag85a]. In this augmented coupled-cluster with all double substitutions (CCD) method, the single and triple substitution contributions were evaluated using the same formula as for the corresponding MP4 contribution, except that the first-order wavefunction in these expressions has been replaced by the converged CCD wavefunction. The resulting method is identical with MP4 to fourth order; however, the terms arising from $\hat{T}_2^n$ and $(\hat{T}_1 + \hat{T}_3)\hat{T}_2^{n+1}$ are included to all orders, whereas $(\hat{T}_1 + \hat{T}_3)\hat{T}_2$ is correct to fifth order. This method bears a close relationship to the CCSD+T(CCSD) method [Urb85]; this latter method is itself a noniterative and reportedly excellent approximation to the CCSDT-1 [Lee84] method, which itself is known (for molecules involving no multiple bonds) to be quite comparable to full CI near equilibrium geometries [Bar83, Bar87]. It is also much less sensitive towards spin contamination than the MP4 method; actually, the CCSD energy [Pur82] was shown to be invariant towards single spin annihilation [Sch88].

### 3.5.2 Computational methods

All calculations were carried out using the GAUSSIAN 86 program system [Gau86] running on a VAXstation 2000 under the VMS 4.7 operating system. To remain consistent with the previous work [Mar89e, Mar89g], HF/6-31G* geometries [DeF79] were used

throughout the present study.

### 3.5.3 Results and discussion

Total energies at the MP2, MP3, and MP4 levels, as well as the corresponding projected levels, may be found in [Mar89g], and will not be repeated here. CCD, CCD+ST(CCD) energies, and MP4(DQ) total energies (vide infra), as well as the energies obtained from several extrapolations, are presented in Table XXVI for the 6-311+G($d,p$)B and 6-311+G($2df,p$)B basis sets. Table XXVII presents computed dissociation energies for the first-row hydrides using an isogyric reaction cycle discussed in detail in reference [Pop83], as well as the experimental values. The direct dissociation energies, without recourse to a reaction cycle, can be easily computed from the data given in Table XXVII.

It is quickly seen by comparing the CCD+ST(CCD) and PMPx dissociation energies in Table XXVII, that Pople's higher-order correction results in errors of about 1 kcal/mol, which, oddly enough, are larger for the larger basis set. It is remarked here, that MP2 and MP3 contain only double excitation terms, whereas MP4 contains, apart from double and simultaneous double substitutions, single and triple substitutions. Henceforth, an extrapolation formula based upon MP2, MP3, and MP4(DQ) appears more logical; such a formula would extrapolate the double and simultaneous double substitution terms to infinite order, i.e. to the CCD energy. (It has also been suggested, that the fourth-order triples contribution is often an overestimate [Bar83, Rag85a, Rag85b].) These energies are denoted CCx in Tables XXVI and XXVII; it it immediately seen, that this approximation holds to a surprising degree of accuracy (about 10 $\mu$hartrees) in a number of closed-shell cases, and that, except for CH($^2\Pi$), $CH_2$($^1A_1$), BH($^1\Sigma^+$), and Be($^1$S), the error is at most on the order of 400 $\mu$hartree, or 0.25 kcal/mol. In the latter four systems, the error amounts to one millihartree or more. Incidentally, all these systems have low-lying excited states, while the others have not. It is quite well known [Bar78], that CC methods behave well in cases of quasidegeneracy, whereas finite order MBPT and limited CI methods do not, unless a multireference wavefunction is employed. Within the CCD framework, the presence of some dominant excited configurations means that some of the amplitudes in $\hat{T}_2$ will be quite large: hence, these amplitudes will produce a large contribution from $\hat{T}_2^2/2$, which appears for the first time, but is far from complete, in fourth order. Also, Knowles *et al.* [Kno85] found for $CH_2$($^1A_1$), BH($^1\Sigma^+$), and Be($^1S$) that the fifth to seventh order terms of the perturbation series have rather large contributions, summing up to about 4 mhartrees. Taking the singles and triples contribution from the MP4 energy, we suggest the following alternative to Pople's higher-order correction (with $E_4 = E_{4DQ} + E_{4ST}$):

$$E_{\text{corr}} \approx \frac{E_2 + E_3}{1 - E_{4\text{DQ}}/E_2} + E_{4\text{ST}} \tag{3.22}$$

This formula requires no additional computational effort: it may however be expected to be more accurate than Pople's formula, whereas it may even be regarded as a cheap

Table XXVI: Coupled cluster and extrapolated energies (hartree, minus sign omitted) for the first-row hydrides in the 6-311+G$(d,p)$B and 6-311+G$(2df,p)$B basis sets.

| | | | 6-311+G$(d,p)$B | | | | |
|---|---|---|---|---|---|---|---|
| Species | MP4(DQ) | CCx[a] | CCD | CCD+ST | CCx+ST4[b] | MPx[c] | PMPx[d] |
| HF | 100.28841 | 100.28842 | 100.28842 | 100.29464 | 100.29566 | 100.29598 | 100.29598 |
| F | 99.56824 | 99.56828 | 99.56861 | 99.57158 | 99.57116 | 99.57139 | 99.57209 |
| $H_2O$ | 76.29471 | 76.29475 | 76.29483 | 76.30197 | 76.30262 | 76.30315 | 76.30315 |
| OH | 75.59876 | 75.59883 | 75.59926 | 75.60383 | 75.60316 | 75.60361 | 75.60458 |
| O | 74.93562 | 74.93576 | 74.93600 | 74.93806 | 74.93738 | 74.93763 | 74.93863 |
| $NH_3$ | 56.44627 | 56.44634 | 56.44647 | 56.45359 | 56.45357 | 56.45431 | 56.45431 |
| $NH_2$ | 55.76595 | 55.76608 | 55.76642 | 55.77158 | 55.77065 | 55.77130 | 55.77236 |
| NH | 55.11509 | 55.11534 | 55.11551 | 55.11880 | 55.11784 | 55.11832 | 55.11966 |
| N | 54.49175 | 54.49210 | 54.49192 | 54.49310 | 54.49286 | 54.49304 | 54.49353 |
| $CH_4$ | 40.41857 | 40.41875 | 40.41879 | 40.42510 | 40.42452 | 40.42543 | 40.42543 |
| $CH_3$ | 39.74288 | 39.74313 | 39.74327 | 39.74787 | 39.74693 | 39.74763 | 39.75031 |
| $CH_2(^3B_1)$ | 39.06126 | 39.06159 | 39.06163 | 39.06486 | 39.06396 | 39.06448 | 39.06554 |
| $CH_2(^1A_1)$ | 39.03923 | 39.03984 | 39.04134 | 39.04594 | 39.04280 | 39.04355 | 39.04355 |
| $CH(^2\Pi)$ | 38.39111 | 38.39207 | 38.39297 | 38.39613 | 38.39387 | 38.39448 | 38.39518 |
| $CH(^4\Sigma^-)$ | 38.37065 | 38.37099 | 38.37092 | 38.37300 | 38.37233 | 38.37268 | 38.37294 |
| C | 37.76449 | 37.76583 | 37.76599 | 37.76753 | 37.76654 | 37.76687 | 37.76746 |
| $BH_3$ | 26.52661 | 26.52721 | 26.52707 | 26.52971 | 26.52914 | 26.52966 | 26.52966 |
| $BH_2$ | 25.85296 | 25.85360 | 25.85356 | 25.85559 | 25.85489 | 25.85529 | 25.85552 |
| BH | 25.21818 | 25.21992 | 25.22134 | 25.22371 | 25.22105 | 25.22159 | 25.22159 |
| B | 24.58795 | 24.59044 | 24.59063 | 24.59208 | 24.59101 | 24.59145 | 24.59195 |
| $BeH_2$ | 15.84259 | 15.84335 | 15.84335 | 15.84408 | 15.84379 | 15.84395 | 15.84395 |
| BeH | 15.19134 | 15.19191 | 15.19212 | 15.19281 | 15.19222 | 15.19234 | 15.19246 |
| Be | 14.61295 | 14.61574 | 14.61676 | 14.61714 | 14.61587 | 14.61599 | 14.61599 |
| LiH | 8.01890 | 8.01950 | 8.01955 | 8.01970 | 8.01958 | 8.01962 | 8.01962 |
| Li | 7.43203 | 7.43203 | 7.43203 | 7.43203 | 7.43203 | 7.43203 | 7.43203 |
| $H_2$ | 1.16915 | 1.16957 | 1.16967 | 1.16976 | 1.16963 | 1.16965 | 1.16965 |
| H | 0.49981 | 0.49981 | 0.49981 | 0.49981 | 0.49981 | 0.49981 | 0.49981 |
| | | | 6-311+G$(2df,p)$B | | | | |
| Species | MP4(DQ) | CCx | CCD | CCD+ST | CCx+ST4 | MPx | PMPx |
| HF | 1100.32713 | 100.32714 | 100.32709 | 100.33474 | 100.33589 | 100.33630 | 100.33630 |
| F | 99.60917 | 99.60919 | 99.60941 | 99.61386 | 99.61368 | 99.61379 | 99.61457 |
| $H_2O$ | 76.32200 | 76.32202 | 76.32204 | 76.33060 | 76.33150 | 76.33205 | 76.33205 |
| OH | 75.62845 | 75.62847 | 75.62878 | 75.63476 | 75.63448 | 75.63472 | 75.63577 |
| O | 74.96559 | 74.96569 | 74.96583 | 74.96932 | 74.96866 | 74.96892 | 74.96999 |
| $NH_3$ | 56.46384 | 56.46386 | 56.46395 | 56.47244 | 56.47271 | 56.47344 | 56.47344 |
| $NH_2$ | 55.78502 | 55.78508 | 55.78531 | 55.79174 | 55.79113 | 55.79165 | 55.79276 |
| NH | 55.13338 | 55.13355 | 55.13365 | 55.13821 | 55.13724 | 55.13776 | 55.13912 |
| N | 54.50867 | 54.50891 | 54.50877 | 54.51126 | 54.51052 | 54.51103 | 54.51151 |
| $CH_4$ | 40.42823 | 40.42834 | 40.42835 | 40.43570 | 40.43522 | 40.43623 | 40.43623 |
| $CH_3$ | 39.75284 | 39.75302 | 39.75308 | 39.75863 | 39.75778 | 39.75853 | 39.75961 |
| $CH_2(^3B_1)$ | 39.07088 | 39.07113 | 39.07113 | 39.07526 | 39.07427 | 39.07492 | 39.07597 |
| $CH_2(^1A_1)$ | 39.05163 | 39.05210 | 39.05358 | 39.05907 | 39.05734 | 39.05672 | 39.05672 |
| $CH(^2\Pi)$ | 38.40242 | 38.40319 | 38.40416 | 38.40818 | 38.40661 | 38.40639 | 38.40721 |
| $CH(^4\Sigma^-)$ | 38.37910 | 38.37939 | 38.37928 | 38.38218 | 38.38124 | 38.38182 | 38.38208 |
| C | 37.77439 | 37.77540 | 37.77584 | 37.77828 | 37.77714 | 37.77722 | 37.77789 |
| $BH_3$ | 26.53168 | 26.53225 | 26.53215 | 26.53514 | 26.53438 | 26.53505 | 26.53505 |
| $BH_2$ | 25.85775 | 25.85835 | 25.85834 | 25.86075 | 25.85992 | 25.86038 | 25.86065 |
| BH | 25.22304 | 25.22449 | 25.22621 | 25.22880 | 25.22755 | 25.22640 | 25.22640 |
| B | 24.59196 | 24.59389 | 24.59469 | 24.59656 | 24.59552 | 24.59525 | 24.59594 |
| $BeH_2$ | 15.84485 | 15.84563 | 15.84570 | 15.84645 | 15.84387 | 15.84395 | 15.84395 |
| BeH | 15.19283 | 15.19340 | 15.19363 | 15.19435 | 15.19244 | 15.19234 | 15.19246 |
| Be | 14.61294 | 14.61524 | 14.61686 | 14.61723 | 14.61698 | 14.61547 | 14.61547 |
| LiH | 8.01967 | 8.02024 | 8.02035 | 8.02049 | 8.02043 | 8.02035 | 8.02035 |
| Li | 7.43203 | 7.43203 | 7.43203 | 7.43203 | 7.43203 | 7.43203 | 7.43203 |
| $H_2$ | 1.16915 | 1.16957 | 1.16967 | 1.16976 | 1.16973 | 1.16965 | 1.16965 |
| H | 0.49981 | 0.49981 | 0.49981 | 0.49981 | 0.49981 | 0.49981 | 0.49981 |

(a) from (3.22) without the $E_{4ST}$ term
(b) from (3.22)
(c) from (3.21)
(d) from (3.21), using PMP energies.

Table XXVII: Dissociation energies (kcal/mol) for the first-row hydrides with different theoretical models, using isogyric reaction cycles.

| | 6-311+G($d,p$)B | | | | | | |
|---|---|---|---|---|---|---|---|
| Species | CCx | CCD | CCD+ST | CCx+ST4 | MPx | PMPx | Experiment[Mar89e, Pop83] |
| HF | 141.09 | 140.82 | 142.80 | 143.79 | 143.84 | 143.40 | 141.2 |
| $H_2O$ | 231.17 | 230.94 | 234.01 | 235.01 | 235.17 | 234.54 | 232.2 |
| OH | 105.27 | 105.33 | 106.85 | 106.94 | 107.06 | 107.04 | 106.6±.3, 106.6 |
| $NH_3$ | 293.88 | 293.90 | 297.45 | 297.84 | 298.15 | 297.85 | 297.3±.1 |
| $NH_2$ | 177.82 | 178.03 | 180.41 | 180.14 | 180.41 | 180.77 | 180.9±1.5 |
| NH | 80.28 | 80.44 | 81.71 | 81.34 | 81.51 | 82.05 | 78.8±4, ≤84.7 |
| $CH_4$ | 418.68 | 418.42 | 421.23 | 421.75 | 422.07 | 421.70 | 419.8±.1 |
| $CH_3$ | 305.53 | 305.39 | 307.19 | 307.40 | 307.60 | 308.92 | 307.2±.2 |
| $CH_2(^1A_1)$ | 188.66 | 188.52 | 189.52 | 189.67 | 189.78 | 190.07 | 189.8±.6 |
| $CH_2(^3B_1)$ | 177.84 | 178.56 | 180.36 | 179.19 | 179.42 | 179.05 | 182.3±.5 |
| $CH(^2\Pi)$ | 82.17 | 82.57 | 83.52 | 82.82 | 82.98 | 83.04 | 84.4±.1, 83.9 |
| $CH(^4\Sigma^-)$ | 66.11 | 65.96 | 66.30 | 66.51 | 66.51 | 66.31 | 67.2 |
| $BH_3$ | 280.10 | 279.77 | 280.40 | 280.88 | 280.90 | 280.59 | 278.1±10 |
| $BH_2$ | 168.21 | 168.00 | 168.30 | 168.62 | 168.58 | 168.42 | 196.2±15 |
| BH | 84.20 | 84.91 | 85.43 | 84.51 | 84.57 | 84.25 | 81.6±2, 82.2 |
| $BeH_2$ | 145.90 | 145.20 | 145.36 | 146.06 | 146.07 | 146.07 | |
| BeH | 47.92 | 47.41 | 47.60 | 48.03 | 48.03 | 48.11 | 55.8±7, 49.8 |
| LiH | 57.84 | 57.81 | 57.85 | 57.86 | 57.87 | 57.87 | 58.0 |
| $H_2$ (a) | 106.65 | 106.71 | 106.77 | 106.68 | 106.69 | 106.69 | 109.48 |

| | 6-311+G(2$df,p$)B | | | | | | 6-311+G(2$df,p$) | | | |
|---|---|---|---|---|---|---|---|---|---|---|
| Species | CCx | CCD | CCD ST | CCx +ST4 | MPx | PMPx | CCx | CCD | CCD +ST | Experiment [Mar89e, Pop83] |
| HF | 139.71 | 139.48 | 141.44 | 142.52 | 142.53 | 142.04 | 137.80 | 137.57 | 139.42 | 141.2 |
| $H_2O$ | 229.50 | 229.30 | 232.37 | 233.58 | 233.66 | 233.00 | 226.34 | 226.14 | 228.96 | 232.2 |
| OH | 105.09 | 105.14 | 106.64 | 106.85 | 106.94 | 106.93 | 103.51 | 103.56 | 104.96 | 106.6±.3, 106.6 |
| $NH_3$ | 294.33 | 294.29 | 297.88 | 298.62 | 298.87 | 298.57 | 290.99 | 290.93 | 294.17 | 297.3±.1 |
| $NH_2$ | 179.19 | 179.31 | 181.66 | 181.67 | 181.89 | 182.29 | 176.93 | 177.04 | 179.18 | 180.9±1.5 |
| NH | 81.16 | 81.25 | 82.49 | 82.28 | 82.42 | 82.98 | 79.99 | 80.08 | 81.23 | 78.8±4, ≤84.7 |
| $CH_4$ | 418.69 | 418.24 | 421.14 | 422.08 | 422.36 | 421.94 | 415.68 | 415.20 | 417.72 | 419.8±.1 |
| $CH_3$ | 305.72 | 305.37 | 307.20 | 307.78 | 307.95 | 308.20 | 303.25 | 302.87 | 304.45 | 307.2±.2 |
| $CH_2(^1A_1)$ | 188.64 | 188.30 | 189.31 | 189.76 | 189.83 | 190.07 | 186.67 | 186.32 | 187.17 | 189.8±.6 |
| $CH_2(^3B_1)$ | 179.53 | 180.06 | 181.85 | 181.00 | 181.19 | 180.77 | 178.37 | 178.89 | 180.50 | 182.3±.5 |
| $CH(^2\Pi)$ | 83.14 | 83.41 | 84.34 | 83.83 | 83.96 | 84.04 | 84.17 | 82.75 | 83.60 | 84.4±.1, 83.9 |
| $CH(^4\Sigma^-)$ | 65.37 | 65.03 | 65.32 | 65.78 | 65.76 | 65.50 | 63.96 | 63.62 | 63.85 | 67.2 |
| $BH_3$ | 281.09 | 280.40 | 280.99 | 281.90 | 281.90 | 281.47 | 280.18 | 279.44 | 279.85 | 278.1±10 |
| $BH_2$ | 169.02 | 168.45 | 168.73 | 169.45 | 169.39 | 169.13 | 168.06 | 167.46 | 167.62 | 196.2±15 |
| BH | 84.90 | 85.42 | 85.81 | 85.18 | 85.20 | 84.77 | 84.87 | 85.33 | 85.65 | 81.6±2, 82.2 |
| $BeH_2$ | 147.64 | 146.61 | 146.79 | 146.38 | 146.40 | 146.40 | 147.23 | 146.14 | 146.26 | |
| BeH | 49.16 | 48.29 | 48.52 | 48.34 | 48.36 | 48.44 | 48.40 | 47.51 | 47.71 | 55.8±7, 49.8 |
| LiH | 58.30 | 58.31 | 58.34 | 58.32 | 58.32 | 58.32 | 58.35 | 58.34 | 58.36 | 58.0 |
| $H_2$ (a) | 106.65 | 106.71 | 106.77 | 106.68 | 106.69 | 106.69 | 105.63 | 105.69 | 105.78 | 109.48 |

(a) direct dissociation energy

alternative for CCD (excluding $E_{4ST}$), CCD+ST(MP4) or CCD+ST(CCD) calculations, especially for 'well-behaved' closed-shell systems (MP4(DQ) calculations take only a small extra time over MP3 calculations [Kri78]). The full expression is best seen as a computationally efficient approximation to CCD+ST(MP4).

From Table XXVI, it is seen that the two extrapolation formulas produce quite comparable results for the lighter molecules (where little or no triples contribution is present), but that the energies from (3.22) are consistently higher by several hundred $\mu$hartree (and

Table XXVIII: MP4(DQ), coupled cluster, and extrapolated energies (hartree, minus sign omitted) for the first-row hydrides in the 6-311+G($2df,p$) basis set.

| Species | MP4(DQ) | CCx | CCD | CCD+ST |
|---|---|---|---|---|
| HF | 100.32246 | 100.32246 | 100.32242 | 100.32995 |
| H2O | 76.31373 | 76.31375 | 76.31378 | 76.32202 |
| OH | 75.62429 | 75.62432 | 75.62464 | 75.63050 |
| $NH_3$ | 56.45363 | 56.45367 | 56.45375 | 56.46179 |
| $NH_2$ | 55.77814 | 55.77822 | 55.77846 | 55.78463 |
| NH | 55.12988 | 55.13006 | 55.13016 | 55.13462 |
| $CH_4$ | 40.41852 | 40.41868 | 40.41866 | 40.42551 |
| $CH_3$ | 39.74561 | 39.74582 | 39.74588 | 39.75109 |
| $CH_2(^3B_1)$ | 39.06609 | 39.06637 | 39.06636 | 39.07027 |
| $CH_2(^1A_1)$ | 39.04648 | 39.04701 | 39.04849 | 39.05376 |
| $CH(^2\Pi)$ | 38.40175 | 38.40321 | 38.40149 | 38.40542 |
| $CH(^4\Sigma^-)$ | 38.37684 | 38.37714 | 38.37703 | 38.37984 |
| $BH_3$ | 26.52689 | 26.52755 | 26.52738 | 26.53017 |
| $BH_2$ | 25.85453 | 25.85520 | 25.85515 | 25.85740 |
| BH | 25.22125 | 25.22281 | 25.22445 | 25.22697 |
| $BeH_2$ | 15.84247 | 15.84335 | 15.84334 | 15.84403 |
| BeH | 15.19155 | 15.19219 | 15.19237 | 15.19307 |
| LiH | 8.01812 | 8.01869 | 8.01879 | 8.01894 |
| $H_2$ | 1.16756 | 1.16795 | 1.16805 | 1.16818 |

closer to the CCD+ST(CCD) result) than those from (3.21) for the heavier molecules with significant triples terms. This is to be expected from the difference between (3.21) and (3.22), which has leading terms

$$\frac{E_{4\mathrm{ST}}}{E_2}\left[E_3+(E_{4\mathrm{ST}}+2E_{4\mathrm{DQ}})\left(1+\frac{E_3}{E_2}\right)\right]+\ldots \tag{3.23}$$

This means that when a large triples contribution is present (especially in multiply-bonded molecules), (3.22) will certainly be preferable over (3.21). However, the main source of error as compared to the CCD+ST(CCD) results is clearly $E_{4ST}$ itself. For accurate determination of dissociation energies when $E_{4ST}$ is large, CCD+ST(CCD), which in our experience takes only about twice the time of MP4(SDTQ), should certainly be considered. If only MP4 is feasible, (3.21) will be numerically more stable than (3.21), but overestimation of the triples contribution will still occur. When $E_{4ST}$ is small, on the other hand, there is little to choose between both formulae.

The same trends are seen for the molecular dissociation energies as for the total energies, although less pronounced. Clearly, some error cancellation exists between the central atom and the molecule.

From Table XXVII, CCD+ST(CCD) dissociation energies using the 6-311+G($2df,p$)B basis set are seen to be in extremely good agreement (deviations of only a few tenths of a kcal/mol) with the well established experimental values for HF, OH, $H_2O$, and $NH_3$; perhaps, the computed dissociation energies for the less well-known species are the most

accurate ones available at this point. Especially regarding the beryllium and boron hydrides, where the experimental values are associated with large uncertainties, they might be of considerable value. This again exhibits the great potential inherent in combined bond-polarization basis sets. The larger systems ($NH_3$, $CH_4$) reveal a slight tendency to overestimate the dissociation energy. This may or may not be caused by basis set superposition error.

In order to obtain a definitive assessment of the effect of adding bond functions, CCD+ST(CCD) calculations were also performed using the 6-311+G(2*df*,*p*) basis set, i.e.without bond functions. It is quickly seen from Tables XXVII and XXVIII, that these results are definitely inferior to those obtained with the 6-311+G(2*df*,*p*)B, and even the much cheaper 6-311+G(*d*,*p*)B basis sets. Based on the isogyric reaction results, the mean absolute error (10 data points) for the 6-311+G(2*df*,*p*) basis set is 1.99 kcal/mol, compared to 0.68 kcal/mol for 6-311+G(*d*,*p*)B and 0.42 kcal/mol for 6-311+G(2*df*,*p*)B. When the open-shell species are excluded, these values become 2.12, 1.03, and 0.53 kcal/mol, respectively.

Comparable results with very large 'classical' polarization-only basis sets (eg. using atomic natural orbitals [Alm87]) would require up to several hours per molecule on a Cray; the results presented in this Section are obtained within the same time span on a humble VaxStation 2000. If supercomputers are accessible, the dissociation energies of small-to-medium sized polyatomic molecules might be obtained with high accuracy using the relatively inexpensive CCD+ST(CCD)/6-311+G(2*df*,*p*)B level. For well-behaved closed-shell species, a further reduction by about a factor of two in computer time may be obtained by using the MP4 method within the same basis set, together with (3.22).

## 3.6 Accurate ab initio predictions of the dissociation energy and heat of formation of first-row hydride species

### 3.6.1 Introduction

It is unnecessary to stress the great importance of dissociation energies $D_0$ in thermochemistry. Such values refer to 0 K, and thus include zero-point energy; for the hypothetical motionless state the notation $D_e$ is utilized. Their experimental determination is, however, not always straightforward, especially with short-lived species or reaction intermediates. For these cases, *ab initio* calculations, which are effectively independent of such considerations as lifetime and abundance for their accuracy, have recently acquired the status of a valuable alternative.

The quality of such theoretical determinations is strongly dependent on the basis set employed and the inclusion of electron correlation. Recently, a new family of so-

called 'combined bond-polarization' basis sets has been developed in our laboratory [Mar89e, Mar89g, Mar89a, Mar89h]. We showed that for the first-row hydrides with well-established dissociation energies, the 6-311+G(2*df*,*p*)B basis set [Mar89g] combined with the CCD+ST(CCD) treatment [Rag85a] (which may also be denoted as QCID(ST) [Pop88]) of electron correlation could reach a mean absolute error of 0.46 kcal/mol, with a tendency for positive errors. These calculations were carried out using HF/6-31G* geometries [DeF79]: it will be shown below that an even better accuracy can be achieved using correlated geometries.

An accuracy of ±1 kcal/mol is considered to be "of chemical accuracy", whereas precise determinations can claim accuracies of perhaps ±0.1 kcal/mol. Although the first goal now appears within the reach of theoretical chemistry, the second one has hitherto remained elusive, except for some very small systems. Pople *et al.* [Pop83] obtained an accuracy of ±2 kcal/mol for the first-row hydride species; Martin *et al.* [Mar89a] tightened this to ±0.46 kcal/mol. Bringing this down to perhaps ±0.1 kcal/mol sounds like every theoretical chemist's dream; we will demonstrate here that we are very close to achieving this aim.

In Ref. [Pop83] as well as Ref. [Mar89h], HF/6-31G* geometries were used throughout. Electron correlation tends to have a significant effect on equilibrium geometries, and the change in the latter could possibly affect the dissociation energies too. This effect can be quite pronounced for molecules involving multiple bonds; not only are these bonds quite strong (i.e., have large force constants), their length is also particularly sensitive to the theoretical level at which they are determined. One does not expect this type of behavior with A-H bonds, so it was taken for granted in [Mar89h] and [Pop83] that correlated geometries would not change the computed dissociation energies very much. However, some of the bonds are indeed quite strong, especially the H-H bond (which has the largest known harmonic frequency). The correlation effect on some of the associated bond lengths is quite significant, albeit still small. Now since an isogyric reaction cycle involving molecular hydrogen [Pop83] was used in both Refs. [Mar89h] and [Pop83], any error in the theoretical dissociation energy of $H_2$ is multiplied several times for some of the polyatomic species, so an insignificant error of, say, 0.15 kcal/mol for $H_2$ may become something on the order of 0.5 kcal/mol for the actual molecule. This is perhaps unimportant if one is only concerned with 'chemical accuracy'; for the kind of accuracy that we are dealing with here, it is however quite important!

For most first-row hydride species, the $D_e$ or $\Sigma D_e$ is well established: this is however not the case for the beryllium and boron hydrides, or for imidogen (NH). Their experimental values are associated with uncertainties of 5 to 15 kcal/mol; for $BeH_2$, no experimental data at all are even available. One purpose of the present paper is to present perhaps the best theoretical values currently achievable for these species.

### 3.6.2 Computational methods

All calculations were carried out using the GAUSSIAN 86 program package [Gau86] running on a VAXStation 2000 under the VMS 4.7 operating system. Both the 6-311+G$(d,p)$B and 6-311+G$(2df,p)$B basis sets were used. As opposed to our earlier papers, all calculations were carried out using CID/6-31G* geometries [DeF79, second entry]. For $BeH_2$, $BH_3$, $CH_2(^1A_1)$ and $CH(^4\Sigma^-)$, these were calculated; all others were taken from [DeF79]. Dissociation energies were calculated using the isogyric reaction cycle discussed in detail in [Pop83]. For the sake of clarity, we here present the general expression. Let the direct dissociation reaction be

$$AH_n \rightarrow A + nH \tag{3.24}$$

which has $g(A) + n - 1$ unpaired electrons on the right hand side, and $g(AH_n) - 1$ on the left hand; g(A) and g($AH_n$) here represent the multiplicity of atom and hydride, respectively. Combining (3.24) with the dissociation reaction for molecular hydrogen, we obtain

$$AH_n + mH \rightarrow A + (n-m)H + mH_2 \tag{3.25}$$

$$m = [g(A) - g(AH_n) + n]/2 \tag{3.26}$$

having the same number of unpaired electrons on each side. Combining with the very accurately known experimental dissociation energy [Hub79] for $H_2$, one obtains (with $m$ defined as in (3.26)):

$$-\Sigma D_e = [E(AH_n) - E(A) - nE(H)] + m\{-D_e(H_2) - [E(H_2) - 2E(H)]\} \tag{3.27}$$

The 6-311+G$(2df,p)$B basis set [Mar89g] consists of the standard 6-311+G$(2df,p)$ basis set [Fri84] augmented by a single $sp$ shell midway between each bond, with exponents optimized at the MP4(SDTQ) level [Kri80b] for the first row diatomic hydrides.

### 3.6.3 Results and discussion

All total energies ($E$) and $\Sigma D_e$, as well as the available experimental data corrected for zero-point energy (ZPE) [Mar89f, Pop83] are given in Table XXIX. The effects on the direct $\Sigma D_e$ are quite small, except for the hydrogen molecule, which increases about 0.12 kcal/mol in $D_e$. As outlined above, if taken into account in the isogyric reaction cycle, this results in $\Sigma D_e$ decreases of 0.1 to 0.4 kcal/mol. Since the errors on the $\Sigma D_e$ tended to be positive at the HF geometries, the theoretical $\Sigma D_e$'s now approach the experimental values even closer. For the well-established binding energies of HF and $H_2O$, coincidence has in fact been achieved. The mean absolute error per bond, computed from the more accurate experimental values, is now 0.12 kcal/mol, an agreement never achieved, to our knowledge, by any theoretical model. The largest deviation is seen for methane, of about

Table XXIX: total energies (hartree), zero-point energies (kcal/mol) and $\Sigma D_e$ values (kcal/mol) at the CCD+ST(CCD) level using CID/6-31G* geometries.

| | 6-311+G(*d*,*p*)B | | 6-311+G(2*df*,*p*)B | | Experiment [Pop83, Mar89e] | |
|---|---|---|---|---|---|---|
| | -E | $\Sigma D_e$ | -E | $\Sigma D_e$ | ZPE | $\Sigma D_e$ |
| HF | 100.29452 | 142.62 | 100.33453 | 141.19 | 5.85 | 141.2 |
| F | 99.57158 | – | 99.61386 | – | – | – |
| $H_2O$ | 76.30186 | 233.72 | 76.33066 | 232.17 | 12.88 | 232.2 |
| OH | 75.60374 | 106.68 | 75.63477 | 106.53 | 5.28 | 106.6±.3, 106.6 |
| O | 74.93806 | – | 74.96932 | – | – | – |
| $NH_3$ | 56.45380 | 297.24 | 56.47272 | 297.72 | 20.60 | 297.3±.1 |
| $NH_2$ | 55.77179 | 180.32 | 55.79194 | 181.56 | 11.28 | 180.9±1.5 |
| NH | 55.11887 | 81.64 | 55.13829 | 82.43 | 4.64 | 78.8±4, ≤84.7 |
| N | 54.49310 | – | 54.51126 | – | – | – |
| $CH_4$ | 40.42523 | 420.97 | 40.43581 | 420.87 | 27.30 | 419.8±.1 |
| $CH_3$ | 39.74797 | 307.03 | 39.75872 | 307.03 | 18.27 | 307.2±.2 |
| $CH_2(^3B_1)$ | 39.06501 | 189.51 | 39.07544 | 189.30 | 10.20 | 189.8±.6 |
| $CH_2(^1A_1)$ | 39.04623 | 180.32 | 39.05927 | 181.75 | 10.76 | 181.3±.8[a] |
| $CH(^2\Pi)$ | 38.39622 | 83.47 | 38.40824 | 84.26 | 4.04 | 84.4±.1, 83.9 |
| $CH(^4\Sigma^-)$ | 38.37317 | 66.40 | 38.38237 | 65.44 | 4.44 | 67.2 |
| C | 37.76753 | – | 37.77828 | – | – | – |
| $BH_3$ | 26.52971 | 280.17 | 26.53515 | 280.77 | 17.97 | 278.1±10 |
| $BH_2$ | 25.85565 | 168.23 | 25.86084 | 168.67 | 9.30 | 196.2±15 |
| BH | 25.22372 | 85.32 | 25.22881 | 85.70 | 3.35 | 81.6±2, 82.2 |
| B | 24.59208 | – | 24.59656 | – | – | – |
| $BeH_2$ | 15.84407 | 145.23 | 15.84644 | 146.67 | | |
| BeH | 15.19278 | 47.59 | 15.19434 | 48.51 | 2.92 | 55.8±7, 49.8 |
| Be | 14.61714 | – | 14.61723 | – | – | – |
| LiH | 8.01961 | 57.67 | 8.02038 | 58.16 | 1.99 | 58.0 |
| Li | 7.43203 | – | 7.43203 | – | – | – |
| $H_2$ | 1.16994 | – | 1.16994 | – | 6.21 | 109.48 |
| H | 0.49981 | – | 0.49981 | – | – | – |

(a) From the $T_0$ value of 9.024±0.014 kcal/mol given in [Bun86].

0.25 kcal/mol per bond. Taking everything into account, we estimate the errors in the computed theoretical energies for the other species to be on the order of 0.12 kcal/mol per bond, which is far better than any available experimental result.

For the diatomic species, anharmonicity was corrected for exactly in the zero-point energies. For the polyatomic species however, the 'harmonic' zero-point energy formula was taken, but using the experimental and experimentally derived frequencies. Although this practice, failing anything better, is quite common in thermochemical tables (e.g. JANAF [Jan85]), it would be much more desirable to calculate zero-point energies using perturbational or variational methods from the anharmonic force field. Unfortunately, more or less complete experimental anharmonic force fields are only available for a few polyatomic molecules. To compute them theoretically, e.g. from correlated harmonic

force fields with very large basis sets [Sim88] and anharmonic SCF force fields [Cla88, Amo88, and references therein], could be a possible alternative; a systematic evaluation of such quantities is planned in the near future.

Turning our attention to the less well-known species, we predict $D_e$ and $D_0$ of BeH to be 48.5 and 45.6 kcal/mol, respectively. Combined with the CODATA enthalpies of formation [Cod78] for Be(g) and H(g), this leads to a theoretical $\Delta H_f^0$ of 82.5±1.3 kcal/mol. (All heats of formation in the present paper refer to 0 K.) For $BeH_2$, $\Sigma D_e$ is predicted as 146.7 kcal/mol. Unfortunately, no experimental frequencies are available: using HF/6-31G* frequencies scaled by 0.89 [Pop85] yields a $D_0$ of 139.1 kcal/mol, or a $\Delta H_f^0$ of 40.6±1.4 kcal/mol. For BH, we find $D_e$ and $D_0$ values of 85.7 and 82.35 kcal/mol, respectively, leading to a $\Delta H_f^0$ of 105.1±3 kcal/mol. It has already been shown previously [Cur89, Mar89d] that the observed 'predissociation limit' [Joh67], which is very close to our predicted $D_0$, should actually be quite close to the real $D_0$. For $BH_2$, the $\Sigma D_e$ and $\Sigma D_0$ values are 168.7 and 159.4 kcal/mol, leading to a $\Delta H_f^0$ of 76.5±3.2 kcal/mol. For $BH_3$, 280.8±0.36 kcal/mol is predicted as $\Sigma D_e$. Experimental frequencies are available; however, theoretical calculations have shown repeatedly that the degenerate bend is in error [Hou82]. We prefer the scaled HF/6-31G* ZPE [Pop85] of 15.5 kcal/mol,which leads to 265.3 kcal/mol for $\Sigma D_0$ and a $\Delta H_f^0$ of 22.3 ±3.3 kcal/mol. The limiting factor to the accuracy of these predictions is the experimental uncertainty of the $\Delta H_f^0$ of boron gas, which itself is caused by the difficulty of preparing boron in high purity. If heats of formation for any boron hydride could be determined experimentally to high accuracy, a much improved value for the $\Delta H_f^0$ of gaseous boron could be obtained in combination with our theoretical data. The same remarks apply, if less markedly, for BeH and $BeH_2$. For NH, we predict $D_e$ and $D_0$ values of 82.4 and 77.8 kcal/mol, respectively, leading to a $\Delta H_f^0$ of 86.3±0.22 kcal/mol, which is in between the two available experimental values. For the amino radical $NH_2$, finally, a $\Sigma D_e$ of 181.56±0.24 and a $\Sigma D_0$ of 170.3 kcal/mol are predicted, along with a theoretical $\Delta H_f^0$ of 45.5±0.35 kcal/mol, in excellent agreement with experiment.

As a final note, we would like to stress again that all of the calculations reported here can be carried out in a matter of several hours CPU time on a simple VAXstation 2000. Anyone trying to obtain the kind of agreement with experiment reported here using 'classical' (polarization-only) basis sets (e.g. atomic natural orbitals [Alm87]) should be prepared for a computational investment larger by at least one order of magnitude, whereas the demands on disk space and memory would certainly preclude any but a very large computer.

# 3.7 Comment on "A theoretical study of the dissociation energy of BH using quadratic configuration interaction"

## 3.7.1 Introduction

The dissociation energy of boron hydride has been the subject of some discussion recently. Huber and Herzberg [Hub79] (HH) list a ground state $D_0$ of 78.9 kcal/mol. This value was based on the assumption, that the experimental predissociation limit [Joh67] of 82.6±0.4 kcal/mol was the energy required to attain an outer repulsive maximum in the $^1\Pi$ potential curve, the height of which was estimated by Hurley [Hur61] as 0.16 eV. Several *ab initio* calculations [Sch85b, Car88] appeared to corroborate the HH value: however, in both cases rather small basis sets were used.

Curtiss and Pople [Cur88b] (CP) found a much larger value $D_e$=82.8, $D_0$=86.0 kcal/mol using their G1 theory [Cur88a, Pop89], which is based on both basis set additivity and isogyric comparisons. As the general accuracy of this model is about 2 kcal/mol, this discrepancy is somewhat unexpected. In [Cur89], on which the present work is a comment, they used their new quadratic configuration interaction (QCISD(T)) [Pop87] method, together with a large 6-311++G(3*df*, 3*pd*) basis set [Fri84] and an isogyric comparison [Pop83, Pop85], to obtain a $D_0$ value of 84.9 kcal/mol, which they expected to be accurate to ± 1 kcal/mol. Combined with a precise calculation of the zero-point energy by Botschwina [Bot86] of 3.36 kcal/mol, this amounts to a $D_0$ value of 81.5 kcal/mol, which certainly is not consistent with the value proposed by HH. As the value is quite close to the predissociation limit in [Joh67], they suggested that the predissociation limit itself is perhaps quite close to the actual dissociation energy.

Recently, a new family of combined bond-polarization function basis sets has been developed in our laboratory [Mar89e, Mar89g], specially aimed at the cost-effective and accurate calculation of dissociation energies. Combined with an augmented coupled cluster method CCD+ST(CCD) [Rag85a], which actually is quite comparable to the QCISD(T) method used by CP, mean absolute errors for the well-determined first-row hydride dissociation energies of 0.68 and 0.42 kcal/mol were achieved [Mar89a] for the 6-311+G(*d*, *p*)B and 6-311+G(2*df*, *p*)B basis sets [Mar89g], respectively. The corresponding value for the regular 6-311+G(2*df*, *p*) basis set is 1.99 kcal/mol [Mar89h]. Since the largest absolute errors were found in the polyatomic hydrides, expected errors for the diatomic hydrides are even less, perhaps on the order of 0.2 kcal/mol at most. So the determination of the dissociation energy using this theoretical model should be of some value regarding the present issue.

Table XXX: CCD+ST(CCD)/6-311+G(2*df*,*p*)B energies (hartree).

| R(Å) | Energy | R(Å) | Energy |
|---|---|---|---|
| | H | | B |
| | -0.499810 | | -24.596562 |
| | $H_2$ | | BH |
| 0.730 | -1.169763 | 1.214 | -25.228681 |
| 0.735 | -1.169857 | 1.224 | -25.228791 |
| 0.740 | -1.169917 | 1.234 | -25.228826 |
| 0.745 | -1.169942 | 1.244 | -25.228792 |
| 0.750 | -1.169935 | – | – |

## 3.7.2 Results and discussion

Using the CCD+ST(CCD)/6-311+G(2*df*,*p*)B basis set, which for BH and $H_2$ consists of the regular 6-311+G(2*df*,*p*) basis set with a single *sp* shell (exponents 0.86 and 0.237, respectively) halfway each bond, we found a direct dissociation energy of 83.1 kcal/mol at the HF/6-31G* geometry $R_e$=1.225 Å. According to the isogyric reaction

$$B(^2P) + H_2(^1\Sigma_g^+) \rightarrow BH(^1\Sigma_g^+) + H(^2S) \tag{3.28}$$

which is also employed by CP, this leads to a $D_e$ value of 85.8 kcal mol$^{-1}$, which corresponds to a $D_0$ of 82.5 kcal/mol, in perfect agreement with the predissociation limit. The same basis set without bond functions leads to values of 85.7 kcal/mol $D_e$, and 82.3 kcal/mol $D_0$, again in good agreement with the predissociation limit. Finally, the 6-311+G(*d*,*p*)B basis set comes up with values of 85.4 and 82.1 kcal/mol for $D_e$ and $D_0$, respectively. This latter value, which again points to the predissociation limit, might be underestimated, as the same basis set exhibits this behavior for the relatively well-established dissociation energies of both LiH and CH. For OH and HF, overshooting is caused by elevated basis set superposition error for these species [Mar89h].

In order to assess the effect of the geometry on this result, we have adopted the same cubic interpolation procedure, using the same reference geometries, as CP. The results are presented in Table XXX. For the BH molecule, cubic interpolation leads to an optimum bond distance of 1.234 Å, and a total energy of -25.2288263 hartree. For the hydrogen molecule, involved in the isogyric comparison, the corresponding values are 0.746 Åand -1.1699432 hartree, respectively. The net result on the direct dissociation energy (83.1 kcal/mol) is negligible; however, in the isogyric comparison a $D_e$ lowering of about 0.1 kcal/mol is observed, leading to 106.9 kcal/mol for $H_2$ and a $D_e$ value for BH of 85.7 kcal/mol. Since the small errors observed for the diatomic hydrides with this theoretical model from the UHF/6-31G* geometry were always positive rather than negative, this value should be even more accurate than the previous one. All taken into account, we here propose a theoretical dissociation energy for BH of 82.4 ± 0.2 kcal/mol, which is in perfect agreement with the observed predissociation limit. This result confirms the

conclusion of CP that the 'outer repulsive hump' of the predissociation state should be investigated more fully, and that the observed predissociation limit is quite close to the actual dissociation energy.

At the time of writing this comment, no program capable of quadratic configuration interaction was available to us. We feel however quite confident that the use of QCI would lead to essentially the same results, and have therefore included in the text all data necessary to rerun our calculations using this theoretical model.

The study in [Mar89h] has recently been repeated using CID/6-31G* instead of HF/6-31G* geometries (Section 3.6). It was found that at the CCD+ST(CCD)/6-311+G(2*df*,*p*)B level, a mean absolute error of 0.12 kcal/mol per bond could be achieved [Mar89b]. The dissociation energy of BH using these geometries is identical to two decimal places with the result in this paper. This supports our claims concerning the accuracy of the calculation.

### 3.7.3 Aftermath

After publication of the paper on which this Section is based, the NASA Ames group published their own investigation [Bau90], where huge [5*s*4*p*3*d*2*f*1*g*] basis sets have been used. These authors arrived at a best estimate of 81.4 ± 0.5 kcal/mol; Peter R. Taylor kindly suggested that the discrepancy with our present result could have been caused by an imbalance in the polarization complements, as we had used a 2*df* polarization set for B and only a single *p* function on H. The author then optimized bond functions for the B–H and H–H bonds to go with a 6-311+G(2*df*,2*pd*) basis set. Repeating the previous analysis leads to a final value of 81.8 kcal/mol, in very good agreement with the result in [Bau90].

# References


[Ahl85] R. Ahlrichs, P. Scharf, and C. Ehrhardt, *J. Chem. Phys.* **82**, 890 (1985).

[All58] A. L. Allred and E. G. Rochow, *J. Inorg. Nucl. Chem.* **5**, 264 (1958).

[Alm87] J. Almlöf and P. R. Taylor, *J. Chem. Phys.* **86**, 4070 (1987).

[Amo88] R. D. Amos, J. F. Gaw, N. C. Handy, and S. Carter, *J. Chem. Soc. Faraday II* **84**, 1247 (1988) and references therein.

[Bar77] R. J. Bartlett and I. Shavitt, *Chem. Phys. Lett.* **50**, 190 (1977).

[Bar78] R. J. Bartlett and G. D. Purvis III, *Int. J. Quantum Chem.* 14 (1978) 561; K. Jankowski and J. Paldus, *Int. J. Quantum Chem.* **18**, 1243 (1980).

[Bar81] R. J. Bartlett, *Ann. Rev. Phys. Chem.* **32**, 359 (1981).

[Bar83] R. J. Bartlett, H. Sekino, and G. D. Purvis III, *Chem. Phys. Lett.* **98**, 66 (1983).

[Bar87] S. J. Cole and R. J. Bartlett, *J. Chem. Phys.* **86**, 873 (1987). R. J. Bartlett, S. J. Cole, G. D. Purvis, W. C. Ermler, H. C. Hsieh, and I. Shavitt, *J. Chem. Phys.* **87**, 6579 (1987).

[Bar89] R. J. Bartlett, *J. Phys. Chem.* **93**, 1697 (1989).

[Bau80] C.W.Bauschlicher Jr., *CI superposition error caused by bond functions*, ICASE report 80-9, NASA Langley Research Center, Hampton, VA, 1980; reference quoted in [Dav86].

[Bau85] C. W. Bauschlicher Jr., *Chem. Phys. Lett.* **122**, 572 (1985) and references therein.

[Bau87] see e.g. C. W. Bauschlicher Jr. and P. R. Taylor, *Theor. Chim. Acta* **71**, 263 (1987). For reviews of this challenging problem, see among others Refs. [Sha85, Sch86a], as well as: P. R. Bunker, in *Comparison of ab initio quantum chemistry with experiment for small molecules* (ed. R. J. Bartlett), D. Reidel, Dordrecht, Boston, 1985, p.141.

[Bau90] C. W. Bauschlicher Jr., S. R. Langhoff, and P. R. Taylor, *J. Chem. Phys.* **93**, 502 (1990).

[Ben60] W. S. Benedict and E. K. Plyler, *Can. J. Phys.* **35**, 1235 (1957); W. S. Benedict, E. K. Plyler, and E. D. Tidwell, *J. Chem. Phys.* **32**, 32 (1960).

[Bin74] J. S. Binkley, J. A. Pople, and P. A. Dobosh, *Mol. Phys.* **28**, 1423 (1974).

[Bin75a] R. C. Bingham, M. J. S. Dewar, and D. H. Lo, *J. Am. Chem. Soc.* **97**, 1285 (1975).

[Bin75b] J. S. Binkley and J. A. Pople, *Int. J. Quantum Chem.* **9**, 229 (1975).

[Bot86] P. Botschwina, *J. Mol. Spectr.* **118**, 76 (1986).

[Boy70] S. F. Boys and F. Bernardi, *Mol. Phys.* **19**, 553 (1970).

[Bue74] R. J. Buenker, S. D. Peyerimhoff, and W. Butscher, *Mol. Phys.* **35**, 771 (1978); R. J. Buenker and S. D. Peyerimhoff, *Theor. Chim. Acta* **35**, 33 (1974); R. J. Buenker and R. A. Phillips, *J. Mol. Struct. (THEOCHEM)* **123**, 291 (1985).

[Bun86] P. R. Bunker, P. Jensen, W. P. Kraemer, and R. Beardsworth, *J. Chem. Phys.* **85**, 3724 (1986).

[Bur77] P. G. Burton, *Mol. Phys.* **34**, 51 (1977).

[But77] W. Butscher, S. K. Shih, R. J. Buenker, and S. D. Peyerimhoff, *Chem. Phys. Lett.* **52**, 457 (1977).

[Car88] E. A. Carter and W. A. Goddard III, *J. Chem. Phys.* **88**, 3132 (1988).

[Cha82] M. W. Chase Jr., J. L. Curnutt, J. R. Downey Jr., R. A. McDonald, A. N. Syverud, E. A. Valenzuela, *J. Phys. Chem. Ref. Data* **11**, 695 (1982).

[Cla83] T. Clark, J. Chandrasekar, G. W. Spitznagel, and P. Von Ragué Schleyer, *J. Comp. Chem.* **4**, 294 (1983).

[Cla88] D. A. Clabo Jr., W. D. Allen, R. B. Remington, Y. Yamaguchi, and H. F. Schaefer III, *Chem. Phys.* **123**, 187 (1988).

[Cod78] CODATA Task Group, *J. Chem. Thermodyn.* **10**, 903 (1978).

[Coh76] E. R. Cohen, *At.Data Nucl. Data Tables* **18**, 587 (1976).

[Cou64] C. A. Coulson, *Valence* (Clarendon Press, Oxford, 1964).

[Cur88a] L. A. Curtiss and J. A. Pople, J. Chem. Phys. **88**, 7405 (1988).

[Cur88b] L. A. Curtiss and J. A. Pople, J. Chem. Phys. **89**, 614 (1988).

[Cur89] L. A. Curtiss and J. A. Pople, *J. Chem. Phys.* **90**, 2522 (1989).

[Dav86] E. R. Davidson and D. Feller, *Chem. Rev.* **86**, 681 (1986).

[DeF79] D. J. DeFrees, B. A. Levi, S. K. Pollack, W. J. Hehre, J. S. Binkley, and J. A. Pople, *J. Am. Chem. Soc.* **101**, 4086 (1979); *erratum* **102**, 2513(1980); D. J. DeFrees, K. Raghavachari, H. B. Schlegel, and J. A. Pople, *J. Am. Chem. Soc.* **104**, 5576 (1982).

[DeF86] D. J. DeFrees and A. D. McLean, *J. Comp. Chem.* **7**, 321 (1986).

[Dew77] M. J. S. Dewar and W. Thiel, *J. Am. Chem. Soc.* **99**, 4899 (1977); *Theor. Chim. Acta* **46**, 89 (1977).

[Dew85] M. J. S. Dewar, E. G. Zoebisch, E. F. Healy, and J. J. P. Stewart, *J. Am. Chem. Soc.* **107**, 3902 (1985).

[Dew86] M. J. S. Dewar and K. M. Dieter, *J. Am. Chem. Soc.* **108**, 8075 (1986).

[Fra82] M. M. Francl, W. J. Pietro, W. J. Hehre, J. S. Binkley, M. S. Gordon, D. J. DeFrees, and J. A. Pople, *J. Chem. Phys.* **77**, 3654 (1982).

[Fri84] M. J. Frisch, J. A. Pople, and J. S. Binkley, *J. Chem. Phys.* **80**, 3265 (1984).

[Fri86] M. J. Frisch, J. E. Del Bene, J. S. Binkley, and H. F. Schaefer III, *J. Chem. Phys.* **84**, 2279 (1986).

[Gau82] J. S. Binkley, M. J. Frisch, D. J. DeFrees, R. Krishnan, R. A. Whiteside, R. Seeger, H. B. Schlegel, J. A. Pople, GAUSSIAN 82, Carnegie-Mellon University, Pittsburgh, PA,1982.

[Gau86] J. S. Binkley, M. J. Frisch, K. Raghavachari, D. J. DeFrees, H. B. Schlegel, R. A. Whiteside, E. M. Fluder, R. Seeger, D. J. Fox, M. Head-Gordon, S. Topiol, and J. A. Pople, GAUSSIAN 86 Release C, Carnegie-Mellon University, Pittsburgh, PA, 1987.

[Han85] N. C. Handy, P. J. Knowles, and K. Somasundram, *Theor. Chim. Acta* **68**, 87 (1985).

[Har72] P. C. Hariharan and J. A. Pople, *Chem. Phys. Lett.* **16**, 217 (1972).

[Har73] P. C. Hariharan and J. A. Pople, *Theor. Chim. Acta* **28**, 213 (1973).

[Heh72] W. J. Hehre, R. Ditchfield, and J. A. Pople, *J. Chem. Phys.* **56**, 2257 (1972).

[Heh86] W. J. Hehre, L. Radom, P. von Ragué Schleyer, and J. A. Pople, *Ab initio molecular orbital theory* (J.Wiley & sons, New York, 1986), pp. 80-81.

[Her63] J. Herranz and B. P. Stoicheff, *J. Mol. Spectry.* **10**, 448 (1963); J. Herranz, J. Morcillo, and A. Gomez, *J. Mol. Spectry.* **19**, 266 (1966).

[Her66] G. Herzberg and J. W. C. Johns, *Proc. Royal Soc. (London)* **A 295**, 107 (1966); D. Feldman, K. Meier, H. Zacharias, and K. H. Welge, *Chem. Phys. Letts.* **59**, 171 (1978).

[Hob88] P. Hobza and R. Zahradník, *Chem. Rev.* **88**, 871 (1988).

[Hou82] R. F. Hout, B. A. Levi, and W. J. Hehre, *J. Comp. Chem.* **3**, 234 (1982); J. F. Stanton, R. J. Bartlett, and W. N. Lipscomb, *Chem. Phys. Lett.* **138**, 525 (1987).

[Hoy72] A. R. Hoy, I. M. Mills, and G. Strey, Mol. Phys. **24**,1265 (1972).

[Hub79] K. P. Huber and G. Herzberg, *Constants of diatomic molecules* (Van Nostrand Reinhold, New York, 1979).

[Hur61] A. C. Hurley, *Proc. Royal Soc.(London)* **A 261**, 237 (1961).

[Huz85] S. Huzinaga, *Computer Physics Reports* **2**, 279 (1985).

[Ibr85] M. R. Ibrahim and P. von Ragué Schleyer, *J. Comp. Chem.* **6**, 157 (1985).

[Jan71] D.R.Stull and H.R.Prophet (eds.), *JANAF Theormochemical Tables, 2nd Edition*, NSRDS-NBS 37, US Government Printing Office, Washington, DC, 1971.

[Jan85] M. W. Chase Jr., C. A. Davies, J. R. Downey Jr., D. J. Frurip, R. A. McDonald, and A. N. Syverud, *JANAF thermochemical tables, third edition* (Published by the American Chemical Society and the American Institute of Physics for the National Bureau of Standards, New York, 1985).

[Jen82] P. Jensen, P. R. Bunker, and A. R. Hoy, *J. Chem. Phys.* **77**, 5370 (1982).

[Joh67] J. W. C. Johns, F. A. Grimm, and R. F. Porter, *J. Mol. Spectrosc.* **22**, 435 (1967).

[Joh73] A. Johansson, P. Kollman, and S. Rothenberg, *Theor. Chim. Acta* **29**, 167 (1973); K. Morokuma and K. Kitaura, in *Chemical applications of atomic and molecular electrostatic potentials* (Ed. P. Politzer), Plenum Press, New York, 1981.

[Kal71] A. Kaldor and R. F. Porter, *J. Am. Chem. Soc.* **93**, 2140 (1971).

[Kno85] P. J. Knowles, K. Somasundram, N. C. Handy, and K. Hirao, *Chem. Phys. Lett.* **113**, 8 (1985).

[Kol68] W. Kolos and L. Wolniewicz, J. Chem. Phys. 49,404(1968).

[Kri78] R. Krishnan and J. A. Pople, *Int. J. Quantum Chem.* **14**, 91 (1978).

[Kri80a] R. Krishnan, J. S. Binkley, R. Seeger, and J. A. Pople, *J. Chem. Phys.* **72**, 650 (1980).

[Kri80b] R. Krishnan, M. J. Frisch, and J. A. Pople, *J. Chem. Phys.* **72**, 4244 (1980).

[Kuc89] S. A. Kucharski, J. Noga, and R. J. Bartlett, *J. Chem. Phys.* **90**, 7287 (1989).

[Lan74] S. R. Langhoff and E. R. Davidson, *Int. J. Quantum Chem.* **8**, 61 (1974).

[Lee84] Y. S. Lee and R. J. Bartlett, *J. Chem. Phys.* **80**, 4371 (1984); Y. S. Lee, S. A. Kucharski, and R. J. Bartlett, *J. Chem. Phys.* **81**, 5906 (1984).

[Len78] R. K. Lengel and R. N. Zare, *J. Am. Chem. Soc.* **100**, 7695 (1978).

[Lie73] G. C. Lie, J. Hinze, and B. Liu, *J. Chem. Phys.* **59**,1872,1877 (1973).

[Lou86] S. K. Loushin, S. Liu, and C. E. Dykstra, *J. Chem. Phys.* **84**, 2720 (1986); S. K. Loushin and C. E. Dykstra, *J. Comp. Chem.* **8**, 81 (1987). The closely related subject of "secondary basis set superposition error" is discussed in: G. Karlstrøm and A. J. Sadlej, *Theor. Chim. Acta* **61**, 1 (1982); Z. Latajka and S. Scheiner, *J. Chem. Phys.* **87**,1194 (1987).

[Mac85] P. Mach and O. Kysel, *J. Comp. Chem.* **6**, 312 (1985).

[Mar89a] J. M. L. Martin, J. P. François, and R. Gijbels, *Chem. Phys. Lett.* **157**, 217 (1989).

[Mar89b] J. M. L. Martin, J. P. François, and R. Gijbels, *Chem. Phys. Lett.* **163**, 387 (1989).

[Mar89c] J. M. L. Martin, J. P. François, and R. Gijbels, *J. Chem. Phys.* **90**, 6469 (1989).

[Mar89d] J. M. L. Martin, J. P. François, and R. Gijbels, *J. Chem. Phys.* **91**, 4425 (1989).

[Mar89e] J. M. L. Martin, J. P. François, and R. Gijbels, *J. Comp. Chem.* **10**, 152 (1989).

[Mar89f] J. M. L. Martin, J. P. François, and R. Gijbels, *J. Comp. Chem.* **10**, 346 (1989).

[Mar89g] J. M. L. Martin, J. P. François, and R. Gijbels, *J. Comp. Chem.* **10**, 875 (1989).

[Mar89h] J. M. L. Martin, J. P. François, and R. Gijbels, *Theor. Chim. Acta* **76**, 195 (1989).

[MarUP] J. M. L. Martin, unpublished calculations.

[May83] I. Mayer, *Int. J. Quantum Chem.* **23**, 341 (1983); I. Mayer and A. Vibok, *Chem. Phys.Lett.* **136**,115 (1987).

[May87a] I. Mayer, *Theor. Chim. Acta* **72**, 207 (1987).

[May87b] I. Mayer and A. Vibok, *Chem. Phys. Lett.* **140**, 558 (1987).

[McK83] A. R. W. McKellar, P. R. Bunker, T. J. Sears, K. M. Evenson, R. J. Saykally, and S. R. Langhoff, *J. Chem. Phys.* **79**, 5251 (1983).

[Met77] T. D. Metzgar and T. Vladimiroff, *Theor. Chim. Acta* **45**, 235 (1977).

[Mil65] D. E. Milligan and M. E. Jacox, *J. Chem. Phys.* **43**, 4487 (1965); M. Kroll, *J. Chem. Phys.* **63**, 319 (1975); F. W. Briss, *J. Mol. Spectry.* **85**, 493 (1981).

[Mol34] C. Møller and M. S. Plesset, *Phys. Rev.* **46**, 618 (1934).

[Nei79] D. Neisius and G. Verhaegen, *Chem. Phys. Lett.* **66**, 358 (1979).

[Nei81] D. Neisius and G. Verhaegen, *Chem. Phys.* **78**, 147 (1981).

[Nei82] D. Neisius and G. Verhaegen, *Chem. Phys. Lett.* **89**, 228 (1982).

[Nes60] R. K. Nesbet, *Rev. Mod. Phys.* **32**, 272 (1960).

[Pau32] L. Pauling, *J. Am. Chem. Soc.* **54**, 3570 (1932); see also F. A. Cotton and G. Wilkinson, *Advanced Inorganic Chemistry, 3rd Edition* (Wiley Interscience Publishers, New York, 1972), p.115.

[Per81] M. Perič, S. D. Peyerimhoff, and R. J. Buenker, *Can. J. Chem.* **59**,1318 (1981).

[Pet81] M. R. Peterson and R. A. Poirier,MONSTER-GAUSS 81, University of Toronto, 1981.

[Pop70] J. A. Pople and D. L. Beveridge, *Approximate MO theory* (McGraw-Hill, New York, 1970).

[Pop76] J. A. Pople, J. S. Binkley, and R. Seeger, *Int. J. Quantum Chem. Symp.* **10**, 1 (1976).

[Pop77] J. A. Pople, R. Seeger, and R. Krishnan, *Int. J. Quantum Chem. Symp.* **11**, 149 (1977).

[Pop78] J. A. Pople, R. Krishnan, H. B. Schlegel, and J. S. Binkley, *Int. J. Quantum Chem.* **14**, 545 (1978).

[Pop83] J. A. Pople, M. J. Frisch, B. T. Luke, and J. S. Binkley, *Int. J. Quantum Chem. Symp.* **17**, 307 (1983).

[Pop85] J. A. Pople, B. T. Luke, M. J. Frisch, and J. S. Binkley, *J. Phys. Chem.* **89**, 2198 (1985); J. A. Pople and L. A. Curtiss, *J. Phys. Chem.* **91**, 155 (1987); *ibid.* **91**, 3637 (1987); L. A. Curtiss and J. A. Pople, *J. Phys. Chem.* **92**, 894 (1988).

[Pop87] J. A. Pople, M. Head-Gordon, and K. Raghavachari, *J. Chem. Phys.* **87**, 5968 (1987).

[Pop88] J. A. Pople, M. Head-Gordon, and K. Raghavachari, *Int. J. Quantum Chem. Symp.* **22**, 377 (1988).

[Pop89] J. A. Pople, M. Head-Gordon, D. J. Fox, K. Raghavachari, and L. A. Curtiss, *J. Chem. Phys.* **90**, 5622 (1989).

[Pul82] P. Pulay, *J. Comp. Chem.* **3**, 556 (1982).

[Pur82] G. D. Purvis III and R. J. Bartlett, *J. Chem. Phys.* **76**, 1910 (1982).

[Rag85a] K. Raghavachari, *J. Chem. Phys.* **82**, 4607 (1985).

[Rag85b] K. Raghavachari, *J. Chem. Phys.* **82**, 4142 (1985).

[Roo77] B. Roos and P. E. M. Siegbahn, in *Modern Theoretical Chemistry* (ed. H. F. Schaefer III), Plenum Press, New York, London, 1977, p.277.

[Rot71] S. Rothenberg and H. F. Schaefer III, *J. Chem. Phys.* **54**, 2764 (1971).

[Sch85a] D. W. Schwenke and D. G. Truhlar, *J. Chem. Phys.* **82**, 2418 (1985); *erratum* **84**, 4113 (1986).

[Sch85b] M. W. Schmidt, M. B. T. Lam, S. T. Elbert, and K. Ruedenberg, *Theor. Chim. Acta* **68**, 69 (1985).

[Sch86a] H. F. Schaefer III, *Science* **231**, 1100 (1986).

[Sch86b] H. B. Schlegel, *J. Chem. Phys.* **84**, 4530 (1986).

[Sch87] M. W. Schmidt and S. T. Elbert, *GAMESS program documentation*, North Dakota State University, Fargo, ND, 1987.

[Sch88] H. B. Schlegel, *J. Phys. Chem.* **92**, 3075 (1988).

[See76] R. Seeger and J. A. Pople, *J. Chem. Phys.* **65**, 265 (1976).

[Sha77a] I. Shavitt, in *Modern Theoretical Chemistry* (ed. H. F. Schaefer III), Plenum Press, New York, London, 1977, p.189.

[Sha77b] I. Shavitt, *Int.J.Quantum Chem.Symp.* **11**, 131 (1977); **12**, 5 (1978); B. R. Brooks and H.F.Schaefer III, *J. Chem. Phys.* **70**, 5092 (1979); P. Saxe, D. J. Fox, H. F. Schaefer III, and N. C. Handy, *J. Chem. Phys.* **77**, 5584 (1982); H. Lischka, R. Shepard, F. B. Brown, and I.Shavitt, *Int. J. Quantum Chem. Symp.* **15**, 91 (1985).

[Sha85] see discussion in: I. Shavitt, *Tetrahedron* **41**,1531 (1985).

[Sim88] E. D. Simandiras, J. E. Rice, T. J. Lee, R. D. Amos, and N. C. Handy, *J. Chem. Phys.* **88**, 3187 (1988); E. D. Simandiras, N. C. Handy, and R. D. Amos, *Chem. Phys. Lett.* **133**, 324 (1987).

[Sne70] A. Snelson, *J. Phys. Chem.* **74**, 537 (1970).

[Sza88] K. Szalewicz, S. J. Cole, W. Kolos, and R. J. Bartlett, *J. Chem. Phys.* **89**, 3662 (1988).

[Thi81] W. Thiel, *J. Am. Chem. Soc.* **103**, 1413 (1981).

[Urb85] M. Urban, J. Noga, S. J. Cole, and R. J. Bartlett, *J. Chem. Phys.* **83**, 4041 (1985); J. Noga, R. J. Bartlett, and M. Urban, *Chem. Phys. Lett.* **134**, 126 (1987).

[Van87] J. H. Van Lenthe, J. C. G. M. van Duijneveldt-van de Rijdt, and F. B. van Duijneveldt, *Adv. Chem. Phys.* **69**, 521 (1987).

[Vla73] T. Vladimiroff, *J. Phys. Chem.* **77**, 1983 (1973).

[Vla74] T. Vladimiroff, *Chem. Phys. Lett.* **24**, 340 (1974).

[Wai89] J. Waite and M. G. Papadopoulos, *Theor. Chim. Acta* **75**, 53 (1989).

[Wel83] B. H. Wells and S. Wilson, *Chem. Phys. Lett.* **101**, 429 (1983).

[Wib84] K. B. Wiberg, *J. Comp. Chem.* **5**, 197 (1984).

[Wri83a] J. S. Wright and R. J. Williams, *J. Chem. Phys.* **78**, 5264 (1983).

[Wri83b] J. S. Wright and R. J. Williams, *J. Chem. Phys.* **79**, 2893 (1983); J. S. Wright, D. J. Donaldson, and R. J. Williams, *J. Chem. Phys.* **81**, 397 (1984).

[Wri84] J. S. Wright and R. J. Buenker, *Chem. Phys. Lett.* **106**, 570 (1984).

# Chapter 4

# Theoretical study of cluster molecules

*The hardest bones, containing the richest marrow, can be conquered only by a united crunching of the teeth of all dogs.*

*Franz Kafka, 1883–1924*

## 4.1 Summary and general introduction

In recent years, an enormous and still increasing amount of effort is spent on the theoretical and experimental study of cluster molecules [a]. An introductory review on metallic, ionic, and Van Der Waals clusters is given by Sattler [Sat85]; the focus here is on covalent clusters, i.e. reactive, generally open-shell, compounds that are fairly tightly bound.

The importance of this latter class of molecules extends in many areas of science, including but not limited to the following.

First of all there is the fairly 'applied' topic of materials science. In chemical vapor deposition and related techniques for surface coating, the aim is to improve the physical (hardness, durability) and chemical (e.g. resistance against corrosion) properties of a substrate by deposition of a thin solid film of a very hard and corrosion-resistent material like diamond, carborundum, $\beta$-boron nitride, .... Most techniques for doing this are based on deposition from a 'cold' plasma. The 'natural bridge' between the plasma with its individual atoms and ions and the solid state is cluster growth. There is one major complication: virtually all compounds of interest have several crystalline phases (besides the amorphous material), of which only one has the desired physical and/or chemical properties. Additionally, the latter is often thermodynamically a metastable modification. In order to be able to steer the surface coating process in the right direction, it has proven necessary to obtain a quantitative insight into the cluster growth process, which implies the availability of thermodynamical data for the cluster molecules and ions

[a] Not to be confused with the 'cluster compounds' of transition elements.

involved. Because of the high reactivity of these compounds, experimental studies are often exceedingly difficult and the results associated with large uncertainties.

The study of elementary reactions in atmospheric and combustion processes is a second and related topic, although somewhat more fundamental. The required data are similar, except that interaction with radiation may also be involved (especially in atmospheric processes).

The 'basic' science of astrophysics is a third area where covalent cluster molecules are of high importance. Radio and infrared astronomers detect many different bands in interstellar spectra. In certain cases, the observed features are readily identified as some rotational or vibrational band of some well-known molecule; more often than not, however, such an identification is not possible and an assignment can only be conjectured. Most of these latter cases involve cluster molecules [Tur87]. Again, their reactivity often precludes isolation and hence accurate experimental study.

Other areas which are named in passing are analytical chemistry (especially mass spectrometrical and plasma spectroscopical techniques), general inorganic chemistry (insight in chemical bonding), photography (silver clusters), semiconductor technology (silicon clusters) and homo-and heterogenous catalysis.

None of the problems connected with experimental work on these species is relevant for *ab initio* or semiempirical calculations. The former, if judiciously applied, can presently provide an accuracy competitive with or even exceeding that of the best experimental techniques for the smaller clusters. Adequate, if not as accurate, data can be obtained with the latter for even very large systems. As will be shown below, a combination of the two may even remove the accuracy problem for large systems.

The first few applications in this chapter concern clusters primarily of interest in materials science.

In Section 4.2[b], the boron-nitrogen clusters $B_3$, $B_2N$, $BN_2$, and $N_3$ are investigated. For the first three molecules, the papers from which this section is adapted present the first data available in the open literature; for $B_2N$ and $BN_2$ even the first data at all[c]. For a number of different structures and states of these clusters, optimum geometries and harmonic spectra were obtained at the HF/6-31G* level. The relative stability of the isomers was determined using full fourth-order Møller-Plesset theory, both with and without spin projection, as well as coupled cluster methods. Estimates for dissociation energies are based on scaled CCD+ST(CCD) binding energies. Koopmans' vertical ionization potentials and Mulliken charge distributions, both at the UHF/6-31G* level, are quoted for the most stable isomers. $B_3$ is found to be an equilateral triangle in its $^2A_1'$

[b]Adapted from J. M. L. Martin, J. P. François, and R. Gijbels, *J. Chem. Phys.* **90**, 6469 (1989) and J. M. L. Martin, J. P. François, and R. Gijbels, *Colloque de Physique* **50 C 5**, 873 (1989).

[c]The $B_3$ molecule has previously been considered, if somewhat elliptically, in a Ph.D. Thesis [Whi81]. The present author was not aware of this work until after publication of the papers mentioned in the previous footnote.

ground state. $B_2N$ has a symmetric linear arrangement in its $^2\Sigma_u^+$ ground state with an extremely low bending frequency (73 $cm^{-1}$), and an unusually low vertical ionization potential (6.75 eV). Its asymmetric stretching (2021 $cm^{-1}$) is found to be extremely intense (8782 km/mol). $BN_2$ has four rather closely spaced states, of which an isosceles triangle is the absolute minimum ($^2A_1$ state). However, at high temperatures, an asymmetric linear arrangement ($^2\Pi$ state) is found to have equal importance, whereas a $^4\Sigma^-$ state plays a role there too. The same theoretical methods correctly predict for $N_3$ a symmetric linear arrangement in the $^2\Pi_g$ ground state; the spectroscopic constants are found to be in reasonable agreement with experiment. Estimated dissociation energies (expected accuracy $\pm$ 4 kcal/mol) are: $B_3$ 197.9, $B_2N$ 265.0, $BN_2$ 224.9, $N_3$ 210.1 kcal/mol. From a statistical thermodynamical analysis, $B_3$ is stable against dissociation to $B_2$ and B up to very high temperatures, $B_2N$ is extraordinarily stable, whereas $BN_2$ and $N_3$ dissociate spontaneously to B+$N_2$ and N+$N_2$ at all temperatures. From these results, the presence of $B_2N^+$ and $B_3^+$, the high abundance of $B_2N^+$, as well as the absence of $BN_2^+$ and $N_3^+$ in laser mass spectra of boron nitride is explained.

For $N_3$, some data outside our own, both theoretical and experimental, were available, but for the dissociation energy these all disagreed with each other. It therefore seemed desirable to treat this problem at a very high level of theory that would settle the differences for once and for all. In Section 4.3[d], the dissociation energy of $N_3$ has been computed ab initio using coupled cluster techniques and large basis sets. Our best theoretical estimates (accuracy $\pm$ 2 kcal/mol) are $\Sigma D_e = 234.0$, $\Sigma D_0 = 228.4$, $\Delta H^0_{f,0} = 109.3$, and $\Delta H^0_{f,298} = 108.4$ kcal/mol. These values are in excellent agreement with an ICR determination of $\Delta H^0_f = 112 \pm 5$ kcal/mol. Very large basis set effects are observed.

While presenting the work discussed in Section 4.2 at the Seventh European Conference on Chemical Vapor Deposition (EURO-CVD 7), the Chairman of that conference, Prof. G. Ducarroir, drew our attention to the SiC molecule, which is very important for chemical vapor deposition of carborundum but also has considerable astrophysical importance. Despite it being only a diatomic, no sufficiently accurate data were available and particularly the ground state had not been characterized unambiguously. Given the small size of the molecule, it seemed desirable to treat it at the highest level of accuracy we could technically reach. In Section 4.4[e], the spectroscopic properties of the three lowest-lying states $X\ ^3\Pi$, $A\ ^3\Sigma^-$, and $a\ ^1\Sigma^+$ of SiC have been computed accurately using augmented coupled cluster methods and different basis sets. Partition functions have been set up, accounting for anharmonicity, rotation-vibration coupling, and isotope effects. Thermodynamic properties are tabulated in JANAF style from 100 to 6000 K. A critical analysis of the effects of the various contributions is made.

---

[d] Adapted from J. M. L. Martin, J. P. François, and R. Gijbels, *J. Chem. Phys.* **93**, 4485 (1990).
[e] Adapted from J. M. L. Martin, J. P. François, and R. Gijbels, *J. Chem. Phys.* **92**, 6655 (1990).

In Section 4.5[f], the lowest $^1\Sigma^+$ and $^3\Pi$ states of the BN molecule have been studied using the quadratic configuration interaction method and (*spdf*) basis sets. The lowest $^1\Sigma^+$ and $^3\Pi$ states lie extremely closely ($T_e \approx 100$ cm$^{-1}$) together; it is not clear which is the ground state. The very small separation should form a useful benchmark for basis sets and electron correlation methods. The dissociation energy $D_0$ is computed to be 103.9±2 kcal/mol. A self-consistent set of spectroscopic constants is derived from a combination of ab initio and experimental data. JANAF-style thermodynamic functions in the range 100-6000 K, including anharmonic, rovibrational coupling, centrifugal stretching, and spin-orbit coupling effects are computed using direct numerical summation over the 25 lowest electronic states.

Perhaps the single most intensively studied family of clusters are the neutral $C_n$ species [Wel89], which generate high interest from many areas, most recently mainly in astrophysics. It is therefore surprising that a definitive spectroscopical characterization beyond $C_3$ had not yet been achieved. Thompson *et al.* (TDW) [Tho71] had trapped carbon vapor in an argon matrix, recorded infrared spectra (including isotopic substitution and thermal annealing experiments), and conjectured an assignment of the various detected IR bands to various species. Despite some major drawbacks (like the assumption that all clusters were linear chains), this assignment was considered a paradigm for many years.

The first indication that something was not correct came in 1987 and 1988, when Michalska *et al.* [Mic87] and Bernholdt *et al.* [Ber88b] made theoretical studies of the linear and cyclic structures of $C_4$ (which are very close in energy) and discovered that no IR-active band came even close to the 2164 cm$^{-1}$ band assigmed to $C_4$ by TDW, but that the linear form had a strong band that could correspond to the 1544 cm$^{-1}$ assigned to $C_5$ by TDW. Swapping the assignment seemed logical; a theoretical study of the vibrational frequencies of $C_5$ could settle the issue.

Such a study is reported in Section 4.6[g], where the geometry and infrared spectrum of $C_5$ have been computed ab initio using the MP2/6-31G* theoretical model. The inner and outer bond lengths are 1.291 and 1.300 Å, respectively. A very intense (1243 km/mol) $\Sigma_u$ band is predicted at 2193 cm$^{-1}$, while another $\Sigma_u$ mode at 1368 cm$^{-1}$ is found to be much less intense (64 km/mol). The results confirm the assignment of the experimental IR frequencies of $C_4$ and $C_5$ suggested by Bernholdt *et al.* [Ber88b].

As a direct consequence of this work, and an isotopic substitution experiment by Vala *et al.* [Val89], an experimental characterization was made simultaneously and independently by Bernath *et al.* [Ber89] (University of Arizona and Kitt Peak National Observatory), who succeeded in demonstrating $C_5$ in the atmosphere of the carbon star IRC+10216, and Heath *et al.* [Hea89] (Berkeley) who recorded the rotational fine struc-

[f] Adapted from J. M. L. Martin, J. P. François, and R. Gijbels, *Chem. Phys.*, submitted.
[g] Adapted from J. M. L. Martin, J. P. François, and R. Gijbels, *J. Chem. Phys.* **90**, 3403 (1989).

ture of the $C_5$ vibration with Doppler-limited resolution. Furthermore, Shen and Graham [She89] performed isotopic substitution experiments that rather unambiguously assign the 1544 $cm^{-1}$ band to linear $C_4$.

Applying ab initio theory to the larger clusters did not seem technically possible at this stage. We therefore tried to investigate what could be done at semiempirical levels of theory, which was done in Section 4.7[h]. Dissociation energies and potential energy surface features for the carbon clusters $C_2$ to $C_{10}$ are compared with ab initio or experimental results for the semiempirical methods MINDO/3, MNDO, AM1, and PM3. Quite surprisingly, MINDO/3 gives a rather good account of the various structures and electronic states, unlike the other three methods. MINDO/3 tends towards systematic overestimates of binding energies, the other methods to systematic gross underestimates. Reparametrization of the diatomic parameters $\alpha$, $\beta_s$, and $\beta_p$ for exact reproduction of the experimental data for $C_3$ results in much improved values for binding energies, but fails to correct the state splittings. Also reparametrizing $U_{ss}$, $U_{pp}$, $\zeta_s$, and $\zeta_p$ to reproduce the ab initio linear-rhombic energy difference in $C_4$ results in a much improved description of the other states. For the linear structures, computed harmonic frequencies with the latter parameters are in surprisingly good agreement with experimental or correlated ab initio data, where available; experimental values are consistently overestimated by about 40 $cm^{-1}$. Other results are comparable in quality to good ab initio treatments. The experimental IR bands at 2128 and 1892 $cm^{-1}$, formerly assigned to $C_9$, should be reassigned to linear $C_7$. The intense 1997 $cm^{-1}$ feature almost certainly belongs to $C_9$; bands at 1952 and 1197 $cm^{-1}$ both belong to linear $C_6$. Tentative assignments of bands in the 1600–1850 $cm^{-1}$ region to various cyclic structures of $C_6$, $C_8$, and $C_{10}$ have been made. As such, this suggests a new and promising procedure for the theoretical study of large molecules in general, and of large clusters in particular.

It seemed desirable to corroborate the assignment for linear $C_6$ to $C_9$, which implied a complete revision of the original TDW assignment, by ab initio calculations. In Section 4.8[i], such an independent verification is presented. The harmonic frequencies, infrared intensities, and isotopic substitution bands of $C_6$ have been evaluated at the MP2/6-31G* level. They confirm previous assignments of the 1952 and 1197 $cm^{-1}$ matrix IR bands to $C_6$. Isotopic substitution spectra at the MP2/6-31G* and HF/4-21G level, as well as those with the newly developed *ad hoc* MNDO method are shown to be in good agreement with experiment for $C_4$, $C_5$, and $C_6$. On the basis of RHF/4-21G, RHF/6-31G*, MP2/4-21G, MP2/6-31G*, and *ad hoc* MNDO data, including theoretical frequencies, IR intensities, and isotopic substitution spectra, it is shown with virtual certainty that the 2128 and 1893 $cm^{-1}$ matrix IR bands belong to $C_7$. A recent assignment of the very intense 1997 $cm^{-1}$ matrix IR feature to $C_8$ is contradicted on the same grounds, and an alternative

[h] Adapted from J. M. L. Martin, J. P. François, and R. Gijbels, *J. Comp. Chem.* **11**, xxxx (1990).
[i] Adapted from J. M. L. Martin, J. P. François, and R. Gijbels, *J. Chem. Phys.* **93**, 8850 (1990).

assignment to $C_9$ put forward with virtual certainty. In other terms: the *ad hoc* MNDO assignment is completely confirmed.

During the final stage of this work, contact was made with the experimentalists at Berkeley. Using the present, at that stage still unpublished, assignments as guidelines, they succeeded in unambiguous confirmation of the $C_7$ [Hea90a, Hea91b, HeaTBP] and $C_9$ [Hea90b] assignments as well as the first experimental characterization of these molecules. Further experimental work on the other species is still under way.

One issue which has been puzzling both theorists and experimentalists for more than a decade is the ground state of $C_4$. It was first shown in an *ab initio* study in 1981 [Whi81b] that a linear and a rhombic structure are very close in energy; a semiempirical study had previously come to the same conclusion [Sla77]. Subsequent theoretical studies disagreed on whether the linear or the cyclic form was the ground state; the computed energy difference appeared to be very sensitive to the theoretical procedure employed. Experimental evidence was contradictory; while IR spectroscopy finds only absolute evidence for the linear form [She89], Coulomb explosion experiments [Alg89] indicate that a large proportion of the detected molecules has a rhombic structure. One aspect which had not gotten sufficient attention in previous studies was the choice of the basis set; in Section 4.9[(j)], the lowest-lying $^1A_g$ and $^3\Sigma_g^-$ states of $C_4$ have been studied using basis sets including $f$ functions, quadratic configuration interaction, and full fourth-order Møller-Plesset perturbation theory with multiple spin projection. Basis set effects on the linear-cyclic separation have been found to be fairly significant. Use of the 6-311G* and [5$s$3$p$1$d$] basis sets leads to qualitatively different conclusions; this problem is remedied by expansion of the polarization space. At the highest level of theory considered, the cyclic structure lies about 1 kcal/mol below the linear structure. A G1-type estimate of its heat of formation at 0 K of 249.6 kcal/mol is proposed. This value is in disagreement with the generally quoted experimental values, but in good agreement with third-law values by Drowart *et al.* corrected for improved partition functions. Geometries and harmonic frequencies are reported. It is tentatively suggested that a matrix IR band at 1284 $cm^{-1}$ may belong to cyclic $C_4$; to aid experimentalists in confirming or rejecting this assignment, theoretical isotope shifts are reported.

The 'building block' for the larger clusters appears to be $C_3$ [Bro87]; for the cationic clusters, this becomes the $C_3^+$ cation. The available Coulomb explosion data [Fai87] indicate a cyclic structure, but can also be rationalized in terms of a linear molecule with a very low bending frequency (analogous to $C_3$) [Vag89b]. Theoretical studies could settle the issue; such a study is reported in Section 4.10[(k)], where the potential energy surface of the $C_3^+$ cation has been investigated using coupled cluster techniques and large basis sets. The results are particularly sensitive towards the level of electron correlation. Spin

[(j)] Adapted from J. M. L. Martin, J. P. François, and R. Gijbels, *J. Chem. Phys.* **94**, xxxx (1991).
[(k)] Adapted from J. M. L. Martin, J. P. François, and R. Gijbels, *J. Chem. Phys.* **93**, 5037 (1990).

contamination even produces a 'false stationary point' at the UHF/6-31G* level. $C_3^+$ has a cyclic $^2B_2$ ground state with predicted geometry $r = 1.3242\AA, \theta = 73.06°$ (MP2/6-311G*, empirically corrected bond distance). At the highest level of theory considered, the linear structure ($^2\Sigma_u^+$ state) lies about 2 kcal/mol above the ground state: this might imply quasilinearity. There is also a low barrier towards degenerate isomerization: at high temperatures, $C_3^+$ will be extremely floppy. Harmonic frequencies (UHF/6-31G*) as well as double-harmonic IR and Raman intensities are given for various structures of $C_3^+$. Interesting analogies of $C_3^+$ with $B_3$ and $B_2N$ are pointed out. The heat of formation at 298.15 K, vertical and adiabatic ionization potentials of $C_3$ are predicted as 194.9 $\pm$ 2 kcal/mol, 11.92 $\pm$ 0.1 eV, and 11.84 $\pm$ 0.1 eV, respectively.

Simultaneously and independently, two other theoretical studies of this ion were performed, namely by Grev *et al.* [Gre90] and by Raghavachari [Rag90]. Both also arrived at the conclusion that the ion is cyclic with a barrier of a few kcal/mol towards the linear structure, but there was a substantial difference between the fairly high number predicted in [Gre90] and the fairly low values found by Raghavachari [Rag90] and ourselves. Much of this discrepancy was removed, when Grev *et al.* discovered an input error in their calculations and published substantially revised data as an erratum. Nevertheless, it was thought desirable to perform a more detailed study on this molecule, as the computed energy difference proved to be extremely sensitive to the nature of the electron correlation method employed.

At this point, Peter R. Taylor of NASA Ames offered to pool his own massive expertise in multireference calculations with my own modest knowledge of quantum chemistry in a joint effort, the results of which are reported in Section 4.11[(l)] In this work, the energy difference between the $^2\Sigma_u^+$ and $^2B_2$ structures of $C_3^+$ has been investigated using large [5*s*3*p*2*d*1*f*] basis sets and multireference electron correlation treatments, including complete active space SCF (CASSCF), multireference CI (MRCI), and averaged coupled pair functional (ACPF) methods, as well as the single-reference quadratic configuration interaction (QCISD(T)) method. Our best estimate for the energy separation, including a correction for further basis set incompleteness, is 5.5$\pm$1.3 kcal/mol. An attempt to explain discrepancies with previous (single-reference) ab initio studies has been made. The $^2\Sigma_u^+$ state is probably not a transition state, but a local minimum. It is shown that $C_3^+$ is extremely demanding of the electron correlation treatment used: of all the single-reference methods previously considered, CCSD(T) and QCISD(T) perform best. The MRCI+Q(0.01)/[4*s*2*p*1*d*] energy separation of 1.68 kcal/mol should provide a benchmark for other electron correlation methods applied to this system.

---

[(l)]Adapted from P. R. Taylor, J. M. L. Martin, J. P. François, and R. Gijbels, *J. Chem. Phys.*, submitted.

## 4.2 Ab initio study of boron, nitrogen, and boron-nitrogen clusters. Isomers and thermochemistry of $B_3$, $B_2N$, $BN_2$, and $N_3$

### 4.2.1 Introduction

Boron nitride (BN) is a chemically inert refractory material. Many applications have been found: for a review, see [Gme88]. Boron nitride forms several phases, analogous to those of carbon: hexagonal $\alpha$-BN resembling graphite, the sphalerite type $\beta$-BN, and the wurtzite type $\gamma$-BN, resembling cubic and hexagonal diamond, respectively. Like their carbon counterparts, the latter two phases are metastable under normal temperature and pressure conditions. They can only be formed from $\alpha$-BN under very high temperature and pressure.

BN can be obtained from several reactions, including diborane-ammonia, boron trifluoride-ammonia, and borane triethylamine-ammonia. Thin solid BN films can be obtained among others by the following methods [Gme88]: r.f. sputtering, 'chemical vapor deposition' (CVD), 'laser pulse vapor deposition' (LPVD), 'ionized cluster beam deposition' (ICB) [Tak86]. It has proven extremely difficult to obtain $\beta$ or $\gamma$ BN as a thin solid film. BN films, prepared by r.f. sputtering from an $\alpha$ BN target under $N_2$ or $N_2$–Ar atmosphere, were shown to be $\alpha$ BN by IR and TEM investigations [Rot85, Wig84]. BN films containing the $\beta$ and $\gamma$ phases, along with $\alpha$ BN, were obtained by plasma deposition [Sok79], [Szm83] and by deposition from boron vapor irradiated with a $N_2^+$ ion beam [Sat83].

$\gamma$-BN depositions on a substrate were obtained by LPVD with a $\gamma$-BN target under nitrogen atmosphere [Kes87]. Experimental research is now conducted [Zfi87] as to the relationship between the target state, the plasma composition, and the composition and phase distribution of the deposited product. Important components of the plasma are $B_n$, $N_n$, and $B_mN_n$ clusters, as well as their positive and negative ions. It is seen, that the cluster composition of the plasma is of essential importance for the properties of the deposited BN material. The clusters form a 'natural bridge', as it were, between individual BN molecules and the solid state. For that reason, the abundance distributions of the clusters are used for plasma diagnostics; additionally, the cluster properties are of importance for understanding the mechanism of formation and the evolution of the deposited product.

However, scarcely any experimental data are available as to the properties of these clusters, except for $N_2$, where a vast amount of theoretical [Ric71, Ohn82] as well as experimental [Hub79] data can be found in literature. Ab initio molecular orbital calculations seem a helpful alternative at this stage: because of this, such a study was undertaken in our laboratory, starting with the neutral $B_mN_{3-m}$ (m=0–3) clusters dis-

cussed in this Section.

Besides the practical importance of these results, the properties of such clusters are also of theoretical interest. Carbon clusters have been well studied now [Rag87]. Boron and nitrogen clusters are 'neighbors' in the periodic table, while the mixed clusters and their ions are sometimes isoelectronic with the carbon species (but with lower symmetry). From a purely theoretical viewpoint, it would be interesting to compare the chemical bonding in these clusters with each other, especially with regards to the nature of the various stationary points.

For $B_2$, reliable experimental [Hub79] and theoretical [Dup78, Rag85] data also exist. For BN, the experimental data [Hub79] are already incomplete; MRD-CI calculations have been performed by Karna and Grein [Kar85]. A survey of the theoretical and experimental data regarding the higher clusters would be very brief: the only more or less systematic investigation was conducted by Novaro *et al.* [Mur82] for the $N_3$ surface, here considered in comparison with the $P_3$ surface. Their investigation was conducted using a simple split-valence basis set and Hartree-Fock theory, so it seems somewhat outdated. On the other hand, there have been numerous calculations (e.g. [Bak86]) on the electron affinity of the azide ion, in which the $N_3$ species also appears. However, no potential surface study was conducted in these studies. For $N_3$, good experimental (spectroscopical) data have been given recently [Tia88]. No theoretical or experimental data at all are available for $B_3$, $B_2N$, or $BN_2$. The only exception is a very recent study of boron-nitrogen clusters by Seifert *et al.* [Sei88], using a simplified LCAO-LDA (Local Density Approximation) method [Bie85] which is questionable for obtaining quantitative and even qualitative results. It should also be remarked, that no geometry optimization was carried out by these authors: they assumed linear geometries with fixed bond distances for the three-membered clusters. No distinction was made between electronic states. Results for $N_2$ and $B_2$ are so blatantly imprecise (errors of about 100 % on the binding energy) that any conclusions presented in that paper should be taken with some caution.

### 4.2.2 Computational methods

All computations were carried out using the GAUSSIAN 86 [Gau86] program package, running on a MicroVAX 2000 workstation under VMS 4.7. Unrestricted Hartree-Fock theory [Pop54] has been used throughout.

Firstly, a small topological study was made with the help of some MNDO [Dew77a, Dew77b] calculations, for identifying some probable structures. Although very helpful in obtaining reasonable starting geometries, the results per se are often deceptive: for example, a false Jahn-Teller distortion was found for the cyclic $B_3$ doublet structure, in complete contradiction with the results at the ab initio level shown below.

Table I: Molecular energies (hartree) of the different boron, nitrogen, and boron-nitrogen species.

| | 3-21G | | | 6-31G* | | |
|---|---|---|---|---|---|---|
| Species | UHF | UHF | UMP2 | UMP3 | UMP4 | $UMP_{xtrp}$ |
| $B(^2P)$ | -24.38976 | -24.52204 | -24.55872 | -24.57097 | -24.57594 | -24.57865 |
| $N(^4S)$ | -54.10539 | -54.38544 | -54.45701 | -54.47065 | -54.47326 | -54.47387 |
| $B_2(^3\Sigma_g^-)$ | N/A | -49.07534 | -49.21704 | -49.23907 | -49.25697 | -49.26274 |
| $B_2(^5\Sigma_u^-)$ | N/A | -49.15784 | -49.23514 | -49.24967 | -49.25484 | -49.25625 |
| $BN(^3\Pi)$ | N/A | -78.99016 | -79.16792 | -79.18092 | -79.19225 | -79.19391 |
| $BN(^1\Sigma^+)$ | N/A | -78.88262 | -79.16898 | -79.13851 | -79.20672 | -79.21852 |
| $N_2$ | N/A | -108.94395 | -109.24819 | -109.24534 | -109.26649 | -109.26785 |
| B003 | -73.32724 | -73.73515 | -73.90462 | -73.92623 | -73.94296 | -73.94715 |
| B004 | -73.34438 | -73.74998 | -73.92346 | -73.94392 | -73.96100 | -73.96510 |
| B004′ | N/A | -73.76153 | -73.90452 | -73.92933 | -73.94286 | -73.94687 |
| B005 | -73.33762 | -73.77207 | -73.96619 | -73.98639 | -74.01157 | -74.01833 |
| B006 | -73.33525 | -73.76226 | -73.92471 | -73.94846 | -73.96392 | -73.96804 |
| B008 | -73.33826 | -73.76446 | -73.92987 | -73.95343 | -73.96933 | -73.97353 |
| B010 | -73.32756 | -73.75490 | -73.91762 | -73.94158 | -73.95773 | -73.96215 |
| BN007 | -103.08248 | -103.64980 | -103.85619 | -103.88224 | -103.89800 | -103.90145 |
| BN007′ | N/A | -103.60368 | -103.78796 | -103.81589 | -103.82494 | -103.82685 |
| BN008 | -103.04528 | -103.61869 | -103.82797 | -103.85245 | -103.86678 | -103.86964 |
| BN009 | -103.10589 | -103.67388 | -103.97065 | -103.97768 | -104.00814 | -104.01243 |
| BN010 | -103.10491 | -103.67471 | -103.90626 | -103.91639 | -103.93212 | -103.93400 |
| BN012 | -103.05041 | -103.65425 | -103.91438 | -103.92107 | -103.93971 | -103.94166 |
| BN003 | -132.69312 | -133.44899 | -133.79635 | -133.81133 | -133.83753 | -133.84089 |
| BN003′ | N/A | -133.45591 | -133.78817 | -133.80164 | -133.82704 | -133.83026 |
| BN004 | -132.73161 | -133.48455 | -133.79289 | -133.80709 | -133.82789 | -133.83043 |
| BN005 | N/A | -133.37573 | -133.76866 | -133.76340 | -133.82600 | -133.83686 |
| BN005′ | N/A | -133.39343 | -133.73017 | -133.74515 | -133.77866 | -133.78402 |
| BN006 | -132.73387 | -133.46989 | -133.74337 | -133.77332 | -133.78914 | -133.79195 |
| BN011 | N/A | -133.45913 | -133.81891 | -133.82492 | -133.84748 | -133.84939 |
| BN013 | -132.64732 | -133.43089 | -133.79429 | -133.80409 | -133.83094 | -133.83386 |
| BN014 | -132.62432 | -133.40403 | -133.74791 | -133.75392 | -133.77820 | -133.78051 |
| N003 | -162.20604 | -163.18059 | -163.60228 | -163.61593 | -163.64560 | -163.64887 |
| N004 | -162.03997 | -162.95953 | -163.43001 | -163.42500 | -163.46721 | -163.47088 |
| N005 | -162.21359 | -163.19668 | -163.62366 | -163.63613 | -163.66618 | -163.66940 |
| N006 | -162.14525 | -163.09895 | -163.51309 | -163.52420 | -163.55241 | -163.55528 |
| N007 | N/A | -163.19193 | -163.64279 | -163.64836 | -163.67636 | -163.67859 |
| N008 | -162.16989 | -163.09846 | -163.50167 | -163.51580 | -163.54353 | -163.54662 |
| N009 | -162.28927 | -163.24580 | -163.68687 | -163.68989 | -163.72416 | -163.72731 |
| N010 | -162.24286 | -163.15734 | -163.52146 | -163.54505 | -163.57055 | -163.57424 |
| N010′ | N/A | -163.24428 | -163.59920 | -163.62479 | -163.64833 | -163.65182 |

Table I: (continued)

| | | 6-31G* | | | |
|---|---|---|---|---|---|
| Species | PUHF | PMP2 | PMP3 | PMP4 | $PMP_{xtrp}$ |
| $B(^2P)$ | -24.52372 | -24.55947 | -24.57125 | -24.57623 | -24.57894 |
| $N(^4S)$ | -54.38651 | -54.45765 | -54.47099 | -54.47360 | -54.47420 |
| | | | | | |
| $B_2(^3\Sigma_g^-)$ | -49.07687 | -49.21801 | -49.23963 | -49.25752 | -49.26326 |
| $B_2(^5\Sigma_u^-)$ | -49.15793 | -49.23519 | -49.24970 | -49.25486 | -49.25627 |
| $BN(^3\Pi)$ | -78.99281 | -79.17019 | -79.18264 | -79.19397 | -79.19559 |
| $BN(^1\Sigma^+)$ | -78.88262 | -79.16898 | -79.13851 | -79.20672 | -79.21852 |
| $N_2$ | -108.94395 | -109.24819 | -109.24534 | -109.26649 | -109.26785 |
| | | | | | |
| B003 | -73.73314 | -73.90258 | -73.92417 | -73.94089 | -73.94509 |
| B004 | -73.75116 | -73.92420 | -73.94437 | -73.96146 | -73.96554 |
| B004′ | -73.76269 | -73.90569 | -73.93044 | -73.94397 | -73.94797 |
| B005 | -73.79933 | -73.99218 | -74.00929 | -74.03447 | -74.04082 |
| B006 | -73.76759 | -73.92981 | -73.95294 | -73.96840 | -73.97246 |
| B008 | -73.76907 | -73.93426 | -73.95719 | -73.97309 | -73.97722 |
| B010 | -73.76108 | -73.92352 | -73.94673 | -73.96287 | -73.96722 |
| | | | | | |
| BN007 | -103.68916 | -103.89504 | -103.92003 | -103.93578 | -103.93916 |
| BN007′ | -103.60546 | -103.78904 | -103.81648 | -103.82553 | -103.82742 |
| BN008 | -103.62563 | -103.83447 | -103.85795 | -103.87228 | -103.87507 |
| BN009 | -103.67810 | -103.97331 | -103.97911 | -104.00957 | -104.01375 |
| BN010 | -103.68335 | -103.91348 | -103.92165 | -103.93737 | -103.93913 |
| BN012 | -103.65726 | -103.91666 | -103.92262 | -103.94125 | -103.94316 |
| | | | | | |
| BN003 | -133.45706 | -133.80292 | -133.81586 | -133.84206 | -133.84527 |
| BN003′ | -133.47420 | -133.80581 | -133.81811 | -133.84351 | -133.84663 |
| BN004 | -133.50067 | -133.80618 | -133.81654 | -133.83734 | -133.83962 |
| BN005 | -133.39274 | -133.78238 | -133.77171 | -133.83431 | -133.84425 |
| BN005′ | -133.43191 | -133.76591 | -133.77557 | -133.80909 | -133.81390 |
| BN006 | -133.48379 | -133.75511 | -133.78205 | -133.79787 | -133.80052 |
| BN011 | -133.46043 | -133.81986 | -133.82562 | -133.84817 | -133.85007 |
| BN013 | -133.43475 | -133.79658 | -133.80524 | -133.83209 | -133.83493 |
| BN014 | -133.41077 | -133.75286 | -133.75694 | -133.78122 | -133.78339 |
| | | | | | |
| N003 | -163.20537 | -163.62430 | -163.63275 | -163.66242 | -163.66532 |
| N004 | -162.96666 | -163.43421 | -163.42674 | -163.46894 | -163.47239 |
| N005 | -163.21930 | -163.64332 | -163.65041 | -163.68046 | -163.68330 |
| N006 | -163.10703 | -163.51805 | -163.52671 | -163.55491 | -163.55763 |
| N007 | -163.19651 | -163.64615 | -163.65053 | -163.67854 | -163.68069 |
| N008 | -163.10643 | -163.50680 | -163.51867 | -163.54640 | -163.54934 |
| N009 | -163.26293 | -163.70052 | -163.69845 | -163.73272 | -163.73546 |
| N010 | -163.17491 | -163.53644 | -163.55619 | -163.58169 | -163.58512 |
| N010′ | -163.26324 | -163.61546 | -163.63707 | -163.66061 | -163.66384 |

Table II: Molecular binding energies (kcal/mol) of the boron, nitrogen, and boron-nitrogen species.

| | 3-21G | 6-31G* | | | | |
|---|---|---|---|---|---|---|
| Species | UHF | UHF | UMP2 | UMP3 | UMP4 | $UMP_{xtrp}$ |
| | | | B-clusters | | | |
| $B_2(^3\Sigma_g^-)$ | N/A | 19.62 | 62.50 | 60.96 | 65.94 | 66.16 |
| $B_2(^5\Sigma_u^-)$ | N/A | 71.39 | 73.86 | 67.61 | 64.60 | 62.09 |
| B003 | 99.12 | 106.08 | 143.37 | 133.87 | 134.99 | 132.53 |
| B004 | 109.88 | 115.38 | 155.18 | 144.97 | 146.31 | 143.80 |
| B004′ | N/A | 122.63 | 143.30 | 135.82 | 134.93 | 132.35 |
| B005 | 105.64 | 129.24 | 182.00 | 171.62 | 178.05 | 177.20 |
| B006 | 104.15 | 123.08 | 155.97 | 147.82 | 148.15 | 145.64 |
| B008 | 106.04 | 124.47 | 159.21 | 150.94 | 151.54 | 149.08 |
| B010 | 99.32 | 118.47 | 151.52 | 143.50 | 144.26 | 141.94 |
| | | | BN-clusters | | | |
| $BN(^3\Pi)$ | N/A | 51.88 | 95.50 | 87.42 | 89.77 | 88.72 |
| $BN(^1\Sigma^+)$ | N/A | -15.60 | 96.17 | 60.80 | 98.84 | 104.16 |
| BN007 | 123.98 | 138.23 | 176.80 | 169.21 | 171.22 | 169.60 |
| BN007′ | N/A | 109.29 | 133.98 | 127.57 | 125.37 | 122.79 |
| BN008 | 100.63 | 118.71 | 159.09 | 150.52 | 151.63 | 149.64 |
| BN009 | 138.66 | 153.34 | 248.62 | 229.10 | 240.34 | 239.25 |
| BN010 | 138.05 | 153.86 | 208.22 | 190.64 | 192.63 | 190.03 |
| BN012 | 103.85 | 141.02 | 213.31 | 193.58 | 197.39 | 194.84 |
| BN003 | 58.10 | 97.94 | 203.07 | 187.66 | 197.71 | 197.35 |
| BN003′ | N/A | 102.28 | 197.94 | 181.59 | 191.13 | 190.68 |
| BN004 | 82.24 | 120.25 | 200.90 | 185.00 | 191.66 | 190.79 |
| BN005 | N/A | 51.97 | 185.70 | 157.59 | 190.47 | 194.82 |
| BN005′ | N/A | 63.07 | 161.55 | 146.13 | 160.77 | 161.66 |
| BN006 | 83.66 | 111.05 | 169.82 | 163.81 | 167.35 | 166.64 |
| BN011 | N/A | 104.30 | 217.23 | 196.19 | 203.95 | 202.68 |
| BN013 | 29.36 | 86.58 | 201.78 | 183.12 | 193.58 | 192.94 |
| BN014 | 14.92 | 69.72 | 172.67 | 151.64 | 160.48 | 159.46 |
| | | | N-clusters | | | |
| $N_2$ | N/A | 108.60 | 209.70 | 190.78 | 200.79 | 200.87 |
| N003 | -69.11 | 15.22 | 145.11 | 128.00 | 141.71 | 142.61 |
| N004 | -173.3 | -123.5 | 37.01 | 8.19 | 29.77 | 30.92 |
| N005 | -64.37 | 25.32 | 158.53 | 140.67 | 154.63 | 155.49 |
| N006 | -107.3 | -36.00 | 89.15 | 70.44 | 83.23 | 83.88 |
| N007 | N/A | 22.34 | 170.53 | 148.35 | 161.01 | 161.25 |
| N008 | -91.79 | -36.31 | 81.98 | 65.16 | 77.66 | 78.44 |
| N009 | -16.88 | 56.14 | 198.20 | 174.41 | 191.01 | 191.83 |
| N010 | -46.00 | 0.64 | 94.40 | 83.52 | 94.61 | 95.78 |
| N010′ | N/A | 55.191 | 143.18 | 133.56 | 143.43 | 144.46 |

Table II: (continued)

| | 6-31G* | | | | |
|---|---|---|---|---|---|
| Species | PUHF | PMP2 | PMP3 | PMP4 | $PMP_{xtrp}$ |
| | | B-clusters | | | |
| $B_2(^3\Sigma_g^-)$ | 18.47 | 62.17 | 60.95 | 65.93 | 66.13 |
| $B_2(^5\Sigma_u^-)$ | 69.34 | 72.95 | 67.27 | 64.26 | 61.75 |
| B003 | 101.65 | 140.67 | 132.05 | 133.17 | 130.69 |
| B004 | 112.96 | 154.24 | 144.72 | 146.07 | 143.53 |
| B004′ | 120.19 | 142.62 | 135.98 | 135.10 | 132.50 |
| B005 | 143.18 | 196.90 | 185.46 | 191.89 | 190.77 |
| B006 | 123.26 | 157.76 | 150.10 | 150.43 | 147.87 |
| B008 | 124.19 | 160.55 | 152.76 | 153.37 | 150.86 |
| B010 | 119.18 | 153.81 | 146.20 | 146.96 | 144.58 |
| | | BN-clusters | | | |
| $BN(^3\Pi)$ | 51.82 | 96.06 | 88.10 | 90.45 | 89.39 |
| $BN(^1\Sigma^+)$ | -17.33 | 95.29 | 60.41 | 98.45 | 103.77 |
| BN007 | 160.15 | 199.84 | 192.36 | 194.36 | 192.70 |
| BN007′ | 107.63 | 133.32 | 127.38 | 125.17 | 122.58 |
| BN008 | 120.28 | 161.83 | 153.40 | 154.51 | 152.48 |
| BN009 | 153.21 | 248.95 | 229.43 | 240.67 | 239.50 |
| BN010 | 156.50 | 211.41 | 193.37 | 195.36 | 192.68 |
| BN012 | 140.13 | 213.40 | 193.98 | 197.79 | 195.21 |
| BN003 | 100.60 | 205.92 | 189.90 | 199.95 | 199.50 |
| BN003′ | 111.36 | 207.73 | 191.31 | 200.86 | 200.36 |
| BN004 | 127.97 | 207.96 | 190.33 | 196.99 | 195.96 |
| BN005 | 60.24 | 193.03 | 162.20 | 195.09 | 198.86 |
| BN005′ | 84.82 | 182.70 | 164.62 | 179.26 | 179.82 |
| BN006 | 117.37 | 175.92 | 168.69 | 172.22 | 171.42 |
| BN011 | 102.72 | 216.55 | 196.03 | 203.78 | 202.51 |
| BN013 | 86.60 | 201.94 | 183.24 | 193.69 | 193.01 |
| BN014 | 71.56 | 174.51 | 152.93 | 161.77 | 160.67 |
| | | N-clusters | | | |
| $N_2$ | 107.26 | 208.89 | 190.36 | 200.36 | 200.46 |
| N003 | 28.76 | 157.73 | 137.91 | 151.62 | 152.30 |
| N004 | -121.0 | 38.44 | 8.63 | 30.21 | 31.24 |
| N005 | 37.51 | 169.66 | 148.99 | 162.95 | 163.58 |
| N006 | -32.95 | 91.06 | 71.37 | 84.16 | 84.73 |
| N007 | 23.21 | 171.44 | 149.07 | 161.74 | 161.95 |
| N008 | -33.32 | 84.00 | 66.32 | 78.82 | 79.53 |
| N009 | 64.88 | 205.56 | 179.13 | 195.74 | 196.32 |
| N010 | 9.65 | 102.60 | 89.87 | 100.96 | 101.98 |
| N010′ | 65.08 | 152.19 | 140.62 | 150.49 | 151.38 |

From these results, geometry optimizations were carried out at the UHF/3-21G [Bin80] level, using the built-in BERNY optimization method by Schlegel [Sch82]. Since the initial estimate [Sch84] for the Hessian is inappropriate for cyclic and 'outlandish' structures, the second derivative matrix has been calculated analytically on the first step. Problems were less prone than at the MNDO level; however, compared with the 6-31G* final results, the 3-21G equilibrium geometries were far more problematic than their 6-31G* counterparts. On the $N_3$ surface, some of the 6-31G* stationary points even failed to converge at the 3-21G level.

From the 3-21G equilibrium geometry, an optimization using the standard 6-31G* basis [Heh72] was carried out. The updated force constant matrix from the 3-21G calculation was used to start the optimization: the final wave function of the latter was projected to obtain a reliable initial guess. The convergence criteria were tightened, to reduce translational and rotational contamination in the subsequent force constant matrix calculation.

Subsequently, a harmonic frequency calculation was carried out using analytic second derivatives [Pop79]. The most abundant isotopes, i.e. $^{11}B$ and $^{14}N$, are used throughout. The results, along with the symmetry assignment of the normal vibrations, are shown in Table IV. The computed zero point energy is given in the last column of that table: for transition states, the imaginary frequency was disregarded. At very little extra expense, the IR and Raman intensities of the vibrations were obtained too. For the more stable species, they are reported in Table VI. Although quantitative agreement with experiment is somewhat illusory at this level of theory, the qualitative features are known to be reproduced quite well [Hes86].

For determining the relative stabilities of the several isomers, full fourth-order Møller-Plesset theory [Mol34, Bin75b, Pop76, Kri78, Kri80b] was applied to these structures using the 6-31G* basis set. In order to reduce the effects of spin contamination, the projected unrestricted Møller-Plesset method (PMP) of Schlegel [Sch86] was applied, by which only the next higher spin state is annihilated (i.e. single annihilation). For the PMP4 result, the extrapolation formula suggested by Schlegel [Sch86] was used:

$$E_{\mathrm{PMP4}} \approx E_{\mathrm{UMP4}} + E_{\mathrm{PMP3}} - E_{\mathrm{UMP3}} \tag{4.1}$$

In order to obtain an idea of the effect of higher-order terms, the Aitken-type extrapolation of Pople *et al.* [Pop83] was used too:

$$E_{\mathrm{xtrp}} \approx \frac{E_2 + E_3}{1 - E_4/E_2} \tag{4.2}$$

The total energies at the various levels are reported in Table I, the dissociation energies for the hypothetical motionless state are found in Table II.

The Hartree-Fock wave function was always tested for internal instability [See77]. If any such instability was found, a search along the direction of instability was carried out

and the wave function reoptimized using a steepest-descent direct minimization method [See76]. In a number of cases, this resulted in wavefunctions not belonging to any irreducible representation of the molecular point group. If such an event occurred, the wave function was constrained to the proper point group symmetry anyway. This decision was justified on empirical grounds by Farnell *et al.* [Far83]; in the same paper, it was also shown that the problem was strongly related to basis set incompleteness. Where investigated, the asymmetric wave function always yielded markedly higher post-Hartree-Fock energies than the symmetric one: this conclusion is in complete agreement with Farnell *et al.*

The spin-projection proved invaluable in this study. Nevertheless, it breaks down in some cases, or does not annihilate the contamination satisfactorily. Since the convergence of the Møller-Plesset series is very sensitive towards spin contamination [Han85], coupled-cluster calculations with all powers of double excitations (CCD) were augmented with the singles and triples contribution to fourth-order for the most stable isomers of each species, in the CCD+ST(CCD) fashion of Raghavachari [Rag85]. This method was applied in order to obtain a more reliable picture of the mutual separations, since the coupled cluster method is nowhere near as sensitive towards spin contamination as many-body perturbation theory. Actually, the CCSD energy can be proven to be invariant towards projection of any single spin contaminant [Sch88]. The results are presented in Table V.

### 4.2.3 Results and discussion

An overview of the stationary points for the $B_3$, $B_2N$, $BN_2$, and $N_3$ clusters at the UHF/6-31G* level can be found in Figures 4.1, 4.2, 4.3, and 4.4, respectively. The relevant geometrical parameters are also indicated in these figures. The molecular energies, binding energies, and electronic configurations of the clusters under study are given in Tables I, II, and III, respectively. (In the subsequent discussion, the term 'binding energy' will always refer to the molecule in a hypothetical motionless state (i.e., no zero-point vibration), contrary to the 'dissociation energy', where the zero-point vibration is included.) The point groups, electronic states, and expectation values for $\hat{S}^2$ are presented in the latter table. The UHF/6-31G* harmonic frequencies and the zero-point energies are collected in Table IV. The Mulliken charge distributions [Mul55] at the UHF/6-31G* level for the most important clusters are presented in Figure 4.5. For the most stable species, the first vertical ionization potentials obtained by applying Koopmans' theorem [Koo34] to the UHF/6-31G* wave function are presented in the relevant portions of the text. Such ionization potentials are known to be generally in satisfactory agreement with experiment [Sch77] when a basis set of at least double-zeta quality is used.

Figure 4.1: Stationary points (UHF/6-31G*) for $B_3$. Bond distances in Ångstrom units.

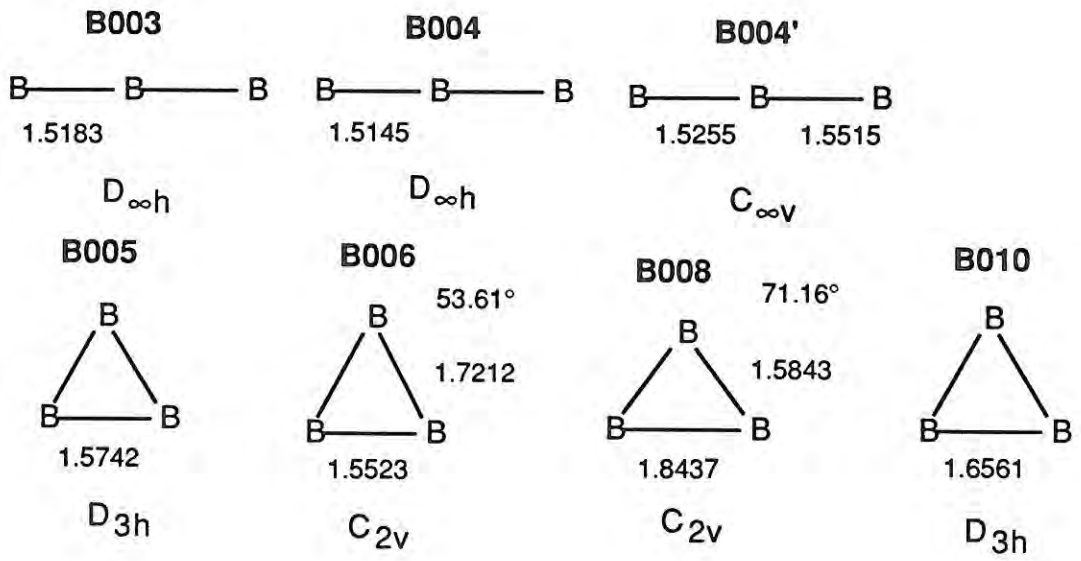


Figure 4.2: Stationary points (UHF/6-31G*) for $B_2N$. Bond distances in Ångstrom units.

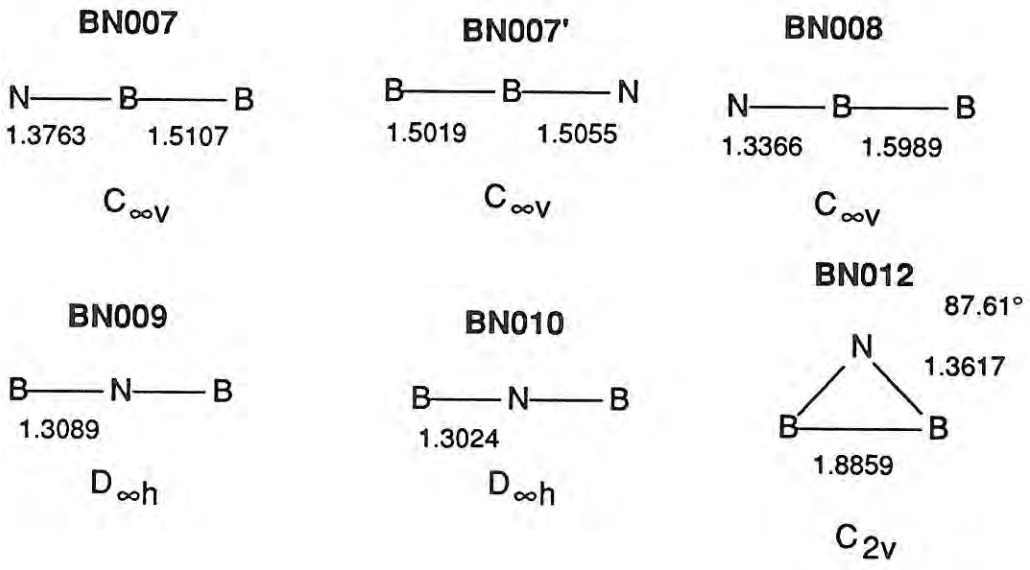

Figure 4.3: Stationary points (UHF/6-31G*) for $BN_2$. Bond distances in Ångstrom units.

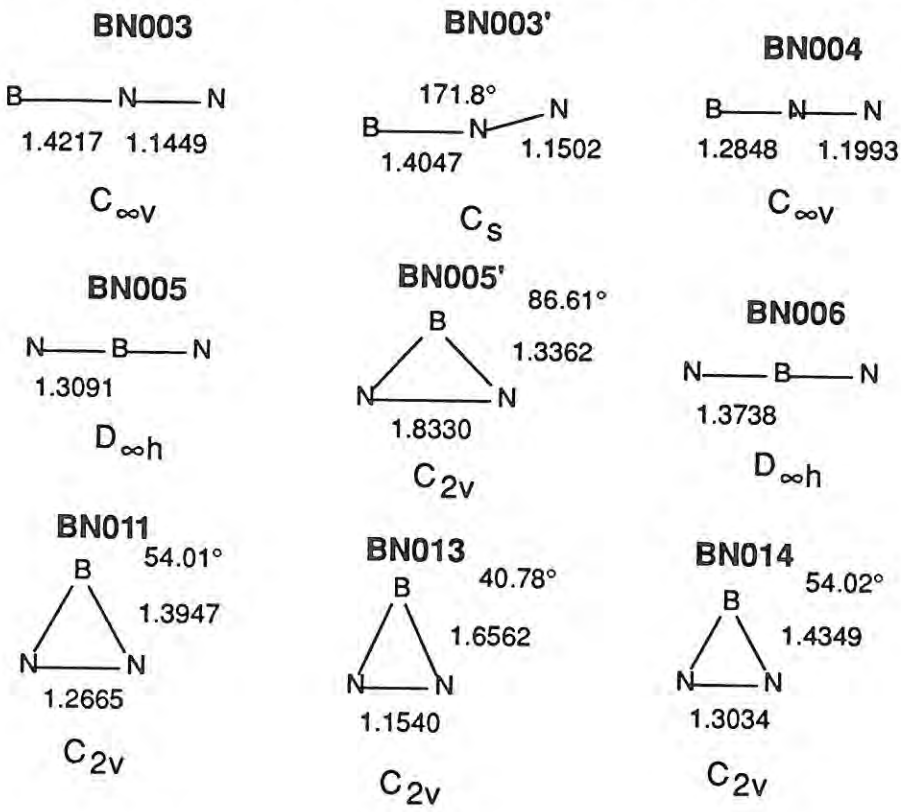


#### 4.2.3.1 Diatomic clusters $B_2$, BN, and $N_2$

These clusters are discussed here for two reasons: (i) to assess the quality of our theoretical model for these species; (ii) to obtain the data necessary in the thermochemical analysis for the larger clusters.

It is quickly seen, that only at the MP4 level of MBPT, the correct ground state for $B_2$ is predicted; a similar observation was made by Raghavachari [Rag85] with the much larger 6-311+G(3*df*) basis set [Fri84]. At the MP4 and PMP4 levels, $^3\Sigma_g^- - {}^5\Sigma_u^-$ splittings of only 1.34 and 1.67 kcal/mol, respectively, are found. When extrapolation for higher order effects is performed, this rises to 4.07 and 4.38 kcal/mol for the unprojected and projected methods, respectively. CCD calculations yielded the wrong ground state (again in agreement with Raghavachari), whereas CCD+ST(CCD) yields 2.09 kcal/mol for the splitting. The best theoretical value for the splitting, using a very large STO basis set and MCSCF/MRCI methods, is 3.6 kcal/mol [Dup78]. whereas Raghavachari [Rag85] found 3.3 kcal/mol at the CCD+ST(CCD)/6-311+G(3*df*) level.

For the low-lying $^1\Sigma^+$ excited state of BN, the MP series exhibits oscillation; so does the predicted ground state. Henceforth, only the coupled cluster values are in any way reliable. CCD predicts the correct ground state ($^3\Pi$), but gives an exaggerated value for the $^1\Sigma^+$ - $^3\Pi$ splitting: CCD+ST(CCD) yields 4.25 kcal/mol, in qualitative agreement

Table III: Electronic configurations and expectation values for $\hat{S}^2$.

| Species | Point group | Term | $\langle\hat{S}^2\rangle$ (1) | $\langle\hat{S}_1^2\rangle$ (2) | $\langle\hat{S}^2\rangle$ (3) | Electronic configuration |
|---|---|---|---|---|---|---|
| $B_2$ | $D_{\infty h}$ | $^3\Sigma_g^-$ | 2.011 | 2.003 | 2.000 | $(\sigma_g)^2(\sigma_u)^2(\sigma_g)^2(\sigma_u)^2(\pi_u)^2$ |
| $B_2$ | $D_{\infty h}$ | $^5\Sigma_u^-$ | 6.001 | 6.000 | 6.000 | $(\sigma_g)^2(\sigma_u)^2(\sigma_g)^2(\sigma_u)(\sigma_g)(\pi_u)^2$ |
| BN | $C_{\infty v}$ | $^3\Pi$ | 2.043 | 2.031 | 2.000 | $(\sigma)^2(\sigma)^2(\sigma)^2(\sigma)^2(\pi)^3(\sigma)$ |
| BN | $C_{\infty v}$ | $^1\Sigma^+$ | 0.000 | 0.000 | 0.000 | $(\sigma)^2(\sigma)^2(\sigma)^2(\sigma)^2(\pi)^4$ |
| $N_2$ | $D_{\infty h}$ | $^1\Sigma_g^+$ | 0.000 | 0.000 | 0.000 | $(\sigma_g)^2(\sigma_u)^2(\sigma_g)^2(\sigma_u)^2(\sigma_g)^2(\pi_u)^4$ |
| | | | | | | $B_3$ |
| B003 | $D_{\infty h}$ | $^2\Pi_g$ | 1.775 | 1.801 | 0.834 | $(\sigma_g)^2(\sigma_u)^2(\sigma_g)^2(\sigma_g)^2(\sigma_u)^2(\sigma_g)(\sigma_u)(\pi_u)^3$ |
| B004 | $D_{\infty h}$ | $^4\Pi_g$ | 3.759 | 3.752 | 3.750 | $(\sigma_g)^2(\sigma_u)^2(\sigma_g)^2(\sigma_g)^2(\sigma_u)^2(\sigma_g)(\sigma_u)(\pi_u)^3$ |
| B004′ | $C_{\infty v}$ | $^4\Pi$ | 4.392 | 4.395 | 3.759 | $(\sigma)^2(\sigma)^2(\sigma)^2(\sigma)^2(\sigma)^2(\sigma)(\sigma)(\pi)^3$ |
| B005 | $D_{3h}$ | $^2A_1$′ | 1.542 | 1.441 | 1.193 | $(a_1')^2(e')^4(a_1')^2(e')^4(a_1')(a_2')^2$ |
| B006 | $C_{2v}$ | $^4B_1$ | 4.115 | 4.084 | 3.754 | $(a_1)^2(a_1)^2(b_2)^2(a_1)^2(a_1)^2(b_2)^2(a_1)(b_1)(a_1)$ |
| B008 | $C_{2v}$ | $^4A_2$ | 4.050 | 4.022 | 3.755 | $(a_1)^2(b_2)^2(a_1)^2(a_1)^2(b_2)^2(a_1)^2(a_1)(b_1)(b_2)$ |
| B010 | $D_{3h}$ | $^4$fuzzy | 4.139 | 4.103 | 3.762 | fuzzy symmetry |
| | | | | | | $B_2N$ |
| BN007 | $C_{\infty v}$ | $^2\Sigma^+$ | 2.315 | 2.231 | 2.621 | $(\sigma)^2(\sigma)^2(\sigma)^2(\sigma)^2(\sigma)^2(\sigma)^2(\sigma)(\pi)^4$ |
| BN007′ | $C_{\infty v}$ | $^6\Sigma^+$ | 8.763 | 8.753 | 8.750 | $(\sigma)^2(\sigma)^2(\sigma)^2(\sigma)^2(\sigma)^2(\sigma)^2(\pi)^2(\sigma)(\pi)^2$ |
| BN008 | $C_{\infty v}$ | $^4\Sigma^+,\Delta$ | 4.046 | 4.008 | 3.753 | $(\sigma)^2(\sigma)^2(\sigma)^2(\sigma)^2(\sigma)^2(\sigma)^2(\pi)^3(\sigma)(\pi)$ |
| BN009 | $D_{\infty h}$ | $^2\Sigma_u^+$ | 0.776 | 0.757 | 0.750 | $(\sigma_g)^2(\sigma_u)^2(\sigma_g)^2(\sigma_g)^2(\sigma_u)^2(\pi_u)^4(\sigma_g)^2(\sigma_u)$ |
| BN010 | $D_{\infty h}$ | $^4\Pi_u$ | 3.924 | 3.866 | 3.754 | $(\sigma_g)^2(\sigma_u)^2(\sigma_g)^2(\sigma_g)^2(\sigma_u)^2(\sigma_g)^2(\pi_u)^4(\sigma_u)(\pi_g)$ |
| BN012 | $C_{2v}$ | $^4B_2$ | 3.787 | 3.769 | 3.750 | $(a_1)^2(a_1)^2(b_2)^2(a_1)^2(a_1)^2(b_2)^2(a_1)(b_1)^2(b_2)(a_1)$ |
| | | | | | | $BN_2$ |
| BN003 | $C_{\infty v}$ | $^2\Pi$ | 0.818 | 0.792 | 0.753 | $(\sigma)^2(\sigma)^2(\sigma)^2(\sigma)^2(\sigma)^2(\sigma)^2(\pi)^4(\sigma)^2(\pi)$ |
| BN003′ | $C_s$ | $^2A$" | 1.345 | 1.296 | 0.899 | $(a')^2(a')^2(a')^2(a')^2(a')^2(a')^2(a')^2(a")^2(a')^2(a')^2(a")$ |
| BN004 | $C_{\infty v}$ | $^4\Sigma^-$ | 3.991 | 3.901 | 3.769 | $(\sigma)^2(\sigma)^2(\sigma)^2(\sigma)^2(\sigma)^2(\sigma)^2(\pi)^4(\sigma)(\pi)^2$ |
| BN005 | $D_{\infty h}$ | $^2\Pi_g$ | 0.909 | 0.846 | 0.755 | $(\sigma_g)^2(\sigma_u)^2(\sigma_g)^2(\sigma_g)^2(\sigma_u)^2(\sigma_g)^2(\pi_u)^4(\sigma_u)^2(\pi_g)$ |
| BN005′ | $C_{2v}$ | $^2A_2$ | 1.416 | 1.293 | 1.085 | $(a_1)^2(b_2)^2(a_1)^2(a_1)^2(b_2)^2(a_1)^2(b_1)^2(b_2)^2(a_1)^2(a_2)$ |
| BN006 | $D_{\infty h}$ | $^4\Pi_u$ | 4.005 | 3.925 | 3.755 | $(\sigma_u)^2(\sigma_g)^2(\sigma_g)^2(\sigma_g)^2(\sigma_u)^2(\sigma_g)^2(\pi_u)^3(\sigma_u)^2(\pi_g)^2$ |
| BN011 | $C_{2v}$ | $^2A_1$ | 0.760 | 0.754 | 0.750 | $(a_1)^2(b_2)^2(a_1)^2(a_1)^2(b_2)^2(a_1)^2(a_1)^2(b_1)^2(b_2)^2(a_1)$ |
| BN013 | $C_{2v}$ | $^2B_2$ | 0.763 | 0.752 | 0.750 | $(a_1)^2(b_2)^2(a_1)^2(a_1)^2(b_2)^2(a_1)^2(a_1)^2(b_1)^2(b_2)(a_1)^2$ |
| BN014 | $C_{2v}$ | $^4B_1$ | 3.811 | 3.778 | 3.751 | $(a_1)^2(b_2)^2(a_1)^2(a_1)^2(b_2)^2(a_1)^2(b_1)^2(a_1)^2(a_1)(b_2)(a_2)$ |
| | | | | | | $N_3$ |
| N003 | $D_{3h}$ | $^2$fuzzy | 1.078 | 1.003 | 0.766 | fuzzy symmetry |
| N004 | $D_{3h}$ | $^4A_1$′ | 3.788 | 3.756 | 3.751 | $(e')^4(a1')^2(a1')^2(e')^4(e')^4(a1')(e")^2$ |
| N005 | $C_{2v}$ | $^2A_2$ | 1.009 | 0.940 | 0.759 | $(a_1)^2(a_1)^2(b_2)^2(a_1)^2(b_2)^2(a_1)^2(b_1)^2(a_1)^2(b_2)^2(a_1)^2(a_2)$ |
| N006 | $C_{2v}$ | $^4B_2$ | 3.794 | 3.760 | 3.751 | $(a_1)^2(b_2)^2(a_1)^2(a_1)^2(b_2)^2(a_1)^2(b_1)^2(a_1)^2(b_2)^2(a_1)(a_2)(b_1)$ |
| N007 | $C_{2v}$ | $^2B_1$ | 0.772 | 0.760 | 0.750 | $(a_1)^2(b_2)^2(a_1)^2(a_1)^2(a_1)^2(b_2)^2(b_1)^2(a_1)^2(a_1)^2(b_2)^2(b_1)$ |
| N008 | $C_{2v}$ | $^4A_1$ | 3.798 | 3.763 | 3.751 | $(a_1)^2(a_1)^2(b_2)^2(a_1)^2(a_1)^2(b_2)^2(b_1)^2(a_1)^2(a_1)^2(b_2)(b_1)(a_2)$ |
| N009 | $D_{\infty h}$ | $^2\Pi_g$ | 0.881 | 0.827 | 0.754 | $(\sigma_g)^2(\sigma_u)^2(\sigma_g)^2(\sigma_g)^2(\sigma_u)^2(\sigma_g)^2(\pi_u)^4(\sigma_u)^2(\pi_g)^3$ |
| N010 | $D_{\infty h}$ | $^4\Pi_g$ | 4.047 | 3.957 | 3.760 | $(\sigma_u)^2(\sigma_g)^2(\sigma_g)^2(\sigma_g)^2(\sigma_u)^2(\sigma_g)^2(\pi_u)^4(\sigma_u)^2(\pi_g)^2(\pi_g)$ |
| N010′ | $C_{2v}$ | $^4B_1$ | 4.061 | 3.970 | 3.761 | $(a_1)^2(a_1)^2(b_2)^2(a_1)^2(b_2)^2(a_1)^2(b_1)^2(b_2)^2(a_1)^2(b_2)(a_2)(a_1)$ |

(1) for UHF wave function
(2) for first-order MBPT wave function
(3) for spin-projected UHF wave function

Figure 4.4: Stationary points (UHF/6-31G*) for $N_3$. Bond distances in Ångstrom units.

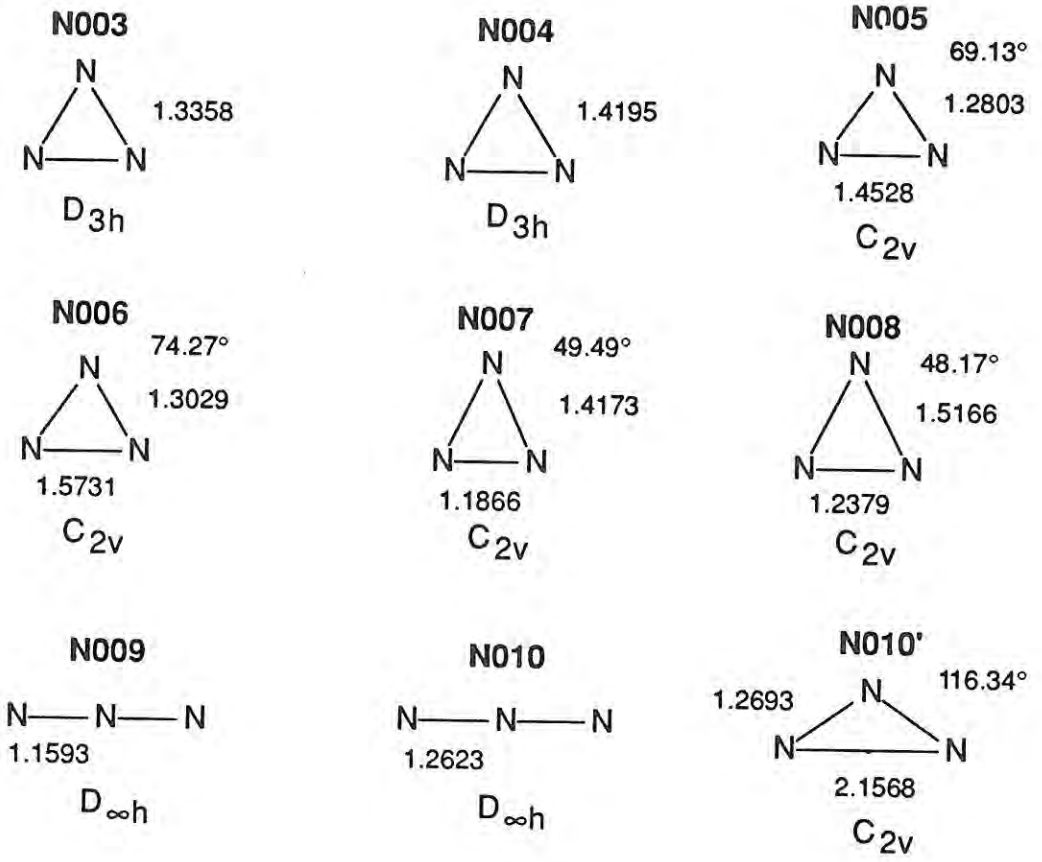


with the Karna and Grein MRD-CI/DZP result of 0.1 eV.

If one looks at the binding energies of $B_2$ and $N_2$ (for BN no experimental data are available), it can be seen that they are all underestimated. Experimental data (Huber and Herzberg, corrected for zero-point energy) are 3.08 eV (± about 0.1 eV) for $B_2$, and 9.90 eV for $N_2$ (from a very accurate dissociation energy). CCD+ST(CCD) yields 2.74 and 8.62 eV, whereas PMP extrapolated for higher order effects yields 2.87 and 8.69 eV, respectively. In other words, CCD+ST(CCD)/6-31G* recovers 89.5 and 87 %, respectively, of the binding energies. A similar observation was made by Raghavachari and Binkley [Rag87], who found that the same theoretical model recovered ca. 90% of the binding energies for $C_2$ and $C_3$, and suggested that the calculated binding energies be scaled by 1.1, yielding excellent agreement with the available experimental data for $C_2$ to $C_7$. A similar argument was presented in a study of silicon clusters [Rag86a]. Following the same lines, we suggest that our calculated CCD+ST(CCD)/6-31G* binding energies be scaled by 1.15, yielding the values 3.15 and 9.91 eV for $B_2$ and $N_2$, respectively, in excellent agreement with experiment. For the molecules under study here, we estimate (by analogy with the carbon and silicon cluster results) that binding energies estimated

Figure 4.5: Mulliken charge distributions (UHF/6-31G*) for the most important clusters.

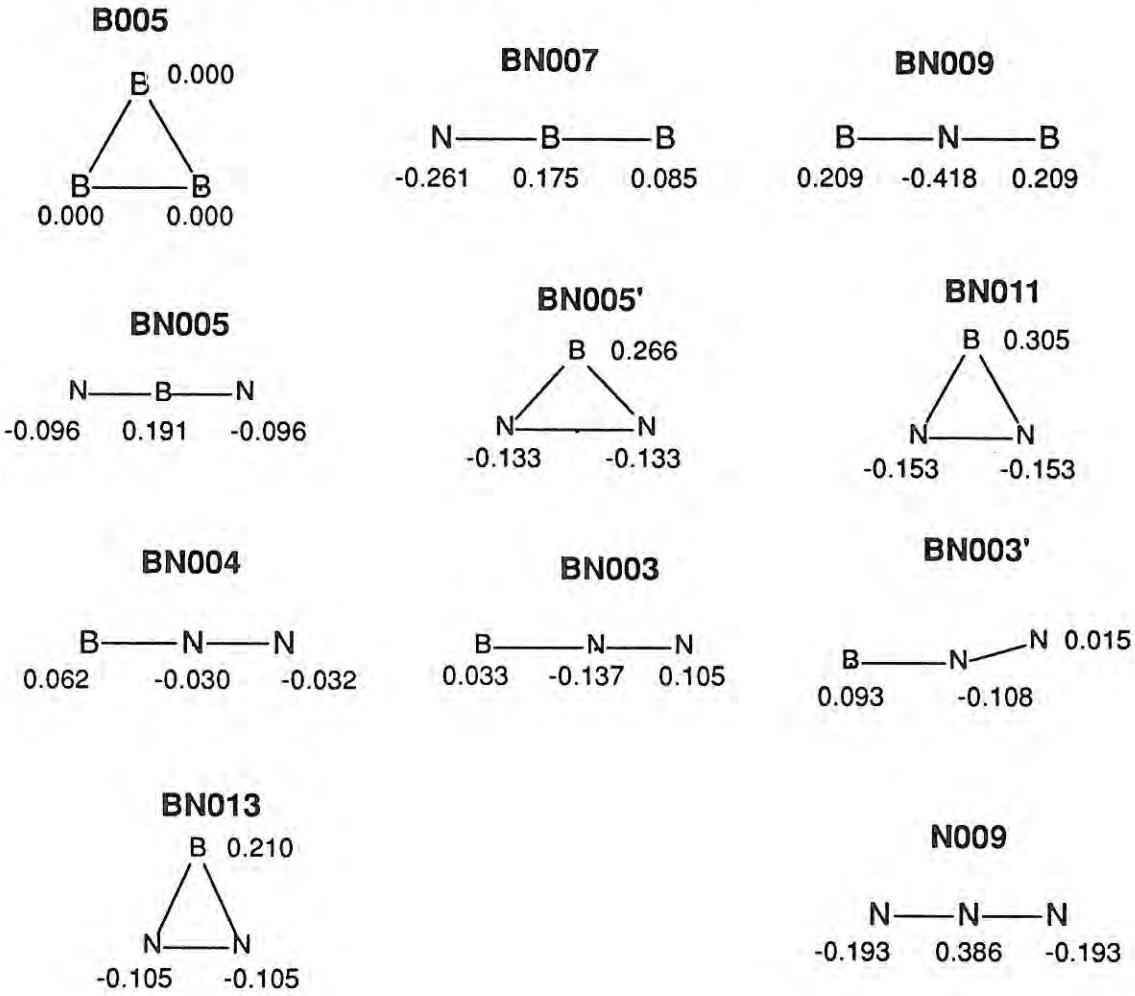


in this way will be off by at most 0.2 eV (actual errors for the three-membered clusters will rather be on the order of 0.1 eV, or about 2 kcal/mol). At 4000 K, an error of 0.2 eV signifies an error on $\log K$ of 0.25 only, so binding energies estimated in this way should be of some value.

From scaling by 1.15, we can then predict here a binding energy of 101.9 kcal/mol for BN, or a dissociation energy of 99.6 kcal/mol. This is in agreement with an extrapolation from the spectroscopic data by Gaydon [Gay53] of 4.0±0.5 eV, or 92 ± 12 kcal/mol. Other values of 5.7 and 6.2 eV [Jan71], as well as estimates of 5.4, 5.6, 6.0, and 6.4 eV [Jan71] based on parent molecules seem to be in error.

#### 4.2.3.2 $B_3$

At the 3-21G level, the linear quartet B004 would be lowest in energy (see Table I), while it is actually a transition state towards deformation to the $C_{\infty v}$ structure. On the contrary, at the 6-31G* level, the equilateral triangle B005 sinks below B004 by no less

Table IV: Point group,term,normal modes, and zero point energy.

| Species | Formula | Point group | Term | Frequencies ($cm^{-1}$) | $E_{zp}$ (kcal/mol) |
|---|---|---|---|---|---|
| | | | Diatomic species | | |
| $B_2$ | $B_2$ | $D_{\infty h}$ | $^3\Sigma_g^-$ | $1086(\Sigma_g)$ | 1.55 |
| $B_2$ | $B_2$ | $D_{\infty h}$ | $^5\Sigma_u^-$ | $1395(\Sigma_g)$ | 1.99 |
| BN | BN | $C_{\infty v}$ | $^1\Sigma^+$ | $1890(\Sigma)$ | 2.70 |
| BN | BN | $C_{\infty v}$ | $^3\Pi$ | $1767(\Sigma)$ | 2.53 |
| $N_2$ | $N_2$ | $D_{\infty h}$ | $^1\Sigma_g^+$ | $2758(\Sigma)$ | 3.94 |
| | | | $B_3$ isomers | | |
| B003 | $B_3$ | $D_{\infty h}$ | $^2\Pi_g$ | $89.1(\Pi_u)$, $139(\Pi_u)$, $965(\Sigma_g)$, $1574(\Sigma_u)$ | 3.96 |
| B004 | $B_3$ | $D_{\infty h}$ | $^4\Pi_g$ | $541i(\Sigma_u)$, $131(\Pi_u)$, $193(\Pi_u)$, $958(\Sigma_g)$ | 1.83 |
| B004′ | $B_3$ | $C_{\infty v}$ | $^4\Pi$ | $241(\Pi)$, $369(\Pi)$, $878(\Sigma)$, $1266(\Sigma)$ | 3.94 |
| B005 | $B_3$ | $D_{3h}$ | $^2A_1$' | 972(E'), 972(E'), $1217(A_1')$ | 4.52 |
| B006 | $B_3$ | $C_{2v}$ | $^4B_1$ | $518i(B_2)$, $888(A_1)$, $1230(A_1)$ | 3.03 |
| B008 | $B_3$ | $C_{2v}$ | $^4A_2$ | $523(A_1)$, $756(B_2)$, $1113(A_1)$ | 3.42 |
| B010 | $B_3$ | $D_{3h}$ | $^4$fuzzy | $1532i$(??), 776(??), 1112(??) | 2.70 |
| | | | $B_2N$ and $BN_2$ isomers | | |
| BN007 | $B_2N$ | $C_{\infty v}$ | $^2\Sigma^+$ | $302(\Pi)$, $302(\Pi)$, $927(\Sigma)$, $1616(\Sigma)$ | 4.50 |
| BN007′ | $B_2N$ | $C_{\infty v}$ | $^6\Sigma^+$ | $370(\Pi)$, $370(\Pi)$, $857(\Sigma)$, $1541(\Sigma)$ | 4.49 |
| BN008 | $B_2N$ | $C_{\infty v}$ | $^4\Sigma^+, \Delta$ | $270(\Pi)$, $394(\Pi)$, $879(\Sigma)$, $1257(\Sigma)$ | 4.00 |
| BN009 | $B_2N$ | $D_{\infty h}$ | $^2\Sigma_u^+$ | $82(\Pi_u)$, $82(\Pi_u)$, $1245(\Sigma_g)$, $2271(\Sigma_u)$ | 5.26 |
| BN010 | $B_2N$ | $D_{\infty h}$ | $^4\Pi_u$ | $273(\Pi_u)$, $451(\Pi_u)$, $1293(\Sigma_g)$, $1504(\Sigma_u)$ | 5.03 |
| BN012 | $B_2N$ | $C_{2v}$ | $^4B_2$ | $786(A_1)$, $1203(B_2)$, $1525(A_1)$ | 5.02 |
| BN003 | $BN_2$ | $C_{\infty v}$ | $^2\Pi$ | $114i(\Pi)$, $287(\Pi)$, $1016(\Sigma)$, $2003(\Sigma)$ | 4.72 |
| BN003′ | $BN_2$ | $C_s$ | $^2A$" | 305(A"), 1051(A'), 1822(A') | 4.54 |
| BN004 | $BN_2$ | $C_{\infty v}$ | $^4\Sigma^-$ | $461(\Pi)$, $461(\Pi)$, $1304(\Sigma)$, $1619(\Sigma)$ | 5.50 |
| BN005 | $BN_2$ | $D_{\infty h}$ | $^2\Pi_g$ | $945i(\Pi_u)$, $211(\Pi_u)$, $1127(\Sigma_g)$, $1905(\Sigma_u)$ | 4.64 |
| BN005′ | $BN_2$ | $C_{2v}$ | $^2A_2$ | $1163i(B_2)$, 399 $(A_1)$, $1376(A_1)$ | 2.54 |
| BN006 | $BN_2$ | $D_{\infty h}$ | $^4\Pi_u$ | $269(\Pi_u)$, $390(\Pi_u)$, $946(\Sigma_g)$, $1215(\Sigma_u)$ | 4.03 |
| BN011 | $BN_2$ | $C_{2v}$ | $^2A_1$ | $1221(B_2)$, $1290(A_1)$, $1760(A_1)$ | 6.10 |
| BN013 | $BN_2$ | $C_{2v}$ | $^2B_2$ | $251i(B_2)$, $732(A_1)$, $2156(A_1)$ | 4.13 |
| BN014 | $BN_2$ | $C_{2v}$ | $^4B_1$ | $193i(B_2)$, $1217(A_1)$, $1538(A_1)$ | 3.94 |
| | | | $N_3$ isomers | | |
| N003 | $N_3$ | $D_{3h}$ | $^2$fuzzy | $173i$(??), 1121(??), 1606(??) | 3.90 |
| N004 | $N_3$ | $D_{3h}$ | $^4A_1$' | 818 (E'), 818(E'), $1358(A_1')$ | 4.28 |
| N005 | $N_3$ | $C_{2v}$ | $^2A_2$ | 566 $(B_2)$, $1024(A_1)$, $1658(A_1)$ | 4.64 |
| N006 | $N_3$ | $C_{2v}$ | $^4B_2$ | $276i$ $(B_2)$, $696(A_1)$, $1563(A_1)$ | 3.23 |
| N007 | $N_3$ | $C_{2v}$ | $^2B_1$ | 985 $(A_1)$, $2040(A_1)$, $2788(B_2)$ | 8.31 |
| N008 | $N_3$ | $C_{2v}$ | $^4A_1$ | $302i$ $(B_2)$, $543(A_1)$, $1796(A_1)$ | 3.34 |
| N009 | $N_3$ | $D_{\infty h}$ | $^2\Pi_g$ | 530 $(\Pi_u)$, 679 $(\Pi_u)$, $1504(\Sigma_g)$, $1703(\Sigma_u)$ | 6.31 |
| N010 | $N_3$ | $D_{\infty h}$ | $^4\Pi_g$ | $1019i$ $(\Pi_u)$, $257(\Pi_u)$, $1110(\Sigma_g)$, $1341(\Sigma_u)$ | 3.87 |
| N010′ | $N_3$ | $C_{2v}$ | $^4B_1$ | 676 $(A_1)$, 967, $(B_2)$, $1299(A_1)$ | 4.21 |

than 14 kcal/mol. The other cyclic structures are also lowered quite a lot in energy. This observation is in agreement with the known fact [Har72], that polarization functions are required for an adequate description of strained rings. At the UHF/6-31G* level, B005 is only slightly below the quartet structure B008. At the Møller-Plesset level, on the other hand, the separation is much enlarged. The same happens when spin projection is performed. Finally, at the highest level of theory indicated in this table, the equilateral triangle B005 markedly comes out as the most stable structure. The separation with its 'lowest neighbor' amounts to 39.9 kcal/mol, which still gives rise to an isomerization equilibrium constant of about 150 even at 4000 K. The differences in partition functions are not capable of changing this conclusion significantly. Henceforth, the equilibrium structure of $B_3$ can be taken as B005 for all intents and purposes. It is stabilized by resonance:

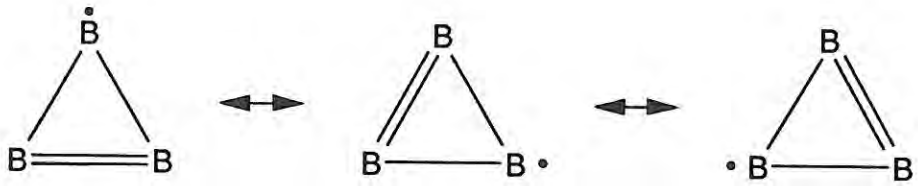


A further glance at the potential surface of the doublet state yields the linear structure B003 as the other minimum, situated 60.1 kcal/mol above the ground state (B005). B003 has an extremely low bending frequency (101.5 $cm^{-1}$ after scaling by 0.89, as suggested by Pople *et al.* [Pop81]), in which it parallels the theoretical [Lis72] and experimental [Gau63, Gau65] behavior of $C_3$. Because of this, it may be expected not to have an appreciable lifetime, if ever formed. An isosceles triangle with an apex angle greater dan 60 degrees may be expected as the transition state between B003 and B005.

The situation is a little different for the quartet state. The isosceles triangle B010 is a Jahn-Teller crossing, deforming towards the isosceles triangle B008 having an apex angle of 71.16 degrees. The structure B006, with apical angle 53.61 degrees, corresponds to three equivalent transition states connecting three equivalent local minima with structure B008 on the Jahn-Teller surface via $C_s$ intermediate structures. B004 is a transition state towards deformation to an asymmetric ($C_{\infty v}$) linear structure B004'. At all correlated levels, however, this structure is distinctly higher in energy than B004, so the deformation must be regarded as an artifact of the optimization level.

Summing up, the equilibrium structure of $B_3$ may unambiguously be predicted as an equilateral triangle with term symbol $^2A_1'$ and spectroscopic parameters predicted at this level as: bond distance of 1.574 Å, harmonic frequencies 1083 $cm^{-1}$ ($A_1$', medium/strong Raman) and 865 $cm^{-1}$ (E', medium/strong IR). From the scaled CC procedure (vide supra), the binding energy is predicted to be 202.0 kcal/mol; together with the zero-point energy, this yields a dissociation energy of 197.9 kcal/mol. The vertical ionization potential according to Koopmans' theorem (at the UHF/6-31G* level) is 9.52 eV ($a_2'$

Table V: Molecular energies (hartree) and binding energies (kcal/mol) of the clusters at the CCD/6-31G* and CCD+ST(CCD)/6-31G* levels, as well as scaled CCD+ST(CCD)/6-31G* binding energies.

| | Molecular energy | | | Binding energy | | | |
|---|---|---|---|---|---|---|---|
| Species | UHF | CCD | CCD+ST | UHF | CCD | +ST | scaled[a] |
| $B(^2P)$ | -24.52204 | -24.57835 | -24.57962 | | | | |
| $N(^4S)$ | -54.38544 | -54.47291 | -54.47375 | | | | |
| $B_2(^3\Sigma_g^-)$ | -49.07687 | -49.24063 | -49.26003 | 20.58 | 52.67 | 63.25 | 72.74 |
| $B_2(^5\Sigma_u^-)$ | -49.15784 | -49.25181 | -49.25670 | 71.39 | 59.68 | 61.16 | 70.33 |
| $BN(^3\Pi)$ | -78.99016 | -79.18314 | -79.19453 | 51.88 | 82.76 | 88.58 | 101.87 |
| $BN(^1\Sigma_u^+)$ | -78.88262 | -79.15290 | -79.18776 | -15.60 | 63.78 | 84.33 | 96.98 |
| $N_2$ | -108.94395 | -109.24925 | -109.26412 | 108.60 | 190.40 | 198.68 | 228.48 |
| B005 | -73.77207 | -73.99026 | -74.01873 | 129.24 | 160.15 | 175.62 | 201.96 |
| BN007 | -103.64980 | -103.88566 | -103.90322 | 138.23 | 160.67 | 169.57 | 195.01 |
| BN009 | -103.6739 | -103.97974 | -104.00672 | 153.34 | 219.71 | 234.52 | 269.70 |
| BN003 | -133.44899 | -133.81823 | -133.83930 | 97.93 | 184.53 | 195.90 | 225.29 |
| BN003′ | -133.45591 | -133.80730 | -133.82980 | 102.28 | 177.67 | 189.93 | 218.42 |
| BN004 | -133.48455 | -133.80964 | -133.82930 | 120.25 | 179.14 | 189.62 | 218.06 |
| BN005 | -133.37573 | -133.76507 | -133.81001 | 51.96 | 151.17 | 177.52 | 204.15 |
| BN005′ | -133.39343 | -133.74782 | -133.77873 | 63.07 | 140.35 | 157.89 | 181.57 |
| BN011 | -133.45913 | -133.82664 | -133.84636 | 104.30 | 189.81 | 200.33 | 230.38 |
| BN013 | -133.43089 | -133.81037 | -133.83139 | 86.58 | 179.60 | 190.94 | 219.58 |
| N009 | -163.24578 | -163.69141 | -163.72017 | 56.14 | 171.11 | 187.58 | 215.72 |

(a) CCD+ST(CCD)/6-31G* binding energies scaled by 1.15 (see text)

orbital, leading to a $^3A_2'$ state for the ion).

#### 4.2.3.3 $B_2N$

At the 3-21G level, the two symmetric linear structures BN009 and BN010 are the most stable ones, with a difference of only 0.5 kcal/mol. The asymmetric linear doublet BN007 follows 14.5 kcal/mol higher. At the 6-31G* level, on the other hand, the bent quartet BN012 is found most stable, in agreement with the earlier remarks about the effect of polarization functions. A bent doublet structure was not found as a stationary point.

Spin projection results in a marked stabilization of BN007. Inspection of $\langle \hat{S}^2 \rangle$ reveals an excessive amount of spin contamination: annihilation of the first contaminant actually increases, rather than decreases, spin contamination. This suggests that strong contamination by states with even higher multiplicity (sextuplets, octuplets) is present. Because of the B-B-N structure, and given the fact that $B_2$ is known to have a very

Table VI: Harmonic frequencies (scaled by 0.89) and corresponding zero-point energies (kcal/mol), IR intensities (km/mol) and Raman activities (Å$^4$/a.m.u.) of the most important clusters.

| Structure | Point group | Term | Frequency (symmetry, IR, Raman) ($cm^{-1}$) | $E_{zp}$ |
|---|---|---|---|---|
| $B_2$ | $D_{\infty h}$ | $^3\Sigma_g^-$ | 967($\Sigma_g$, 0, 99) | 1.38 |
| $B_2$ | $D_{\infty h}$ | $^5\Sigma_u^-$ | 1242($\Sigma_g$, 0, 180) | 1.78 |
| BN | $C_{\infty v}$ | $^3\Pi$ | 1572($\Sigma$, 27, 80) | 2.25 |
| BN | $C_{\infty v}$ | $^1\Sigma^+$ | 1682($\Sigma$, 75, inf) | 2.40 |
| $N_2$ | $D_{\infty h}$ | $1\Sigma_g^+$ | 2455($\Sigma_g$, 0, 18) | 3.51 |
| B005 | $D_{3h}$ | $^2A_1'$ | 865 (E', 32, 0.4), 865 (E', 32, 0.4), 1084($A_1$', 0, 43) | 4.02 |
| BN007 | $C_{\infty v}$ | $^2\Sigma^+$ | 269($\Pi$, 9, 22), 269($\Pi$, 9, 22), 825($\Sigma$, 4, 36), 1438($\Sigma$, 160, 536) | 4.01 |
| BN009 | $D_{\infty h}$ | $^2\Sigma_u^+$ | 73($\Pi_u$, 5, 0), 73($\Pi_u$, 5, 0), 1108($\Sigma_g$, 0, 24), 2021($\Sigma_u$, 8782, 0) | 4.68 |
| BN003 | $C_{\infty v}$ | $^2\Pi$ | 101$i$($\Pi$, 13, 141), 255($\Pi$, 21, 7), 904($\Sigma$, 147, 134), 1783($\Sigma$, 3, 250) | 4.20 |
| BN003' | $C_s$ | $^2A$" | 271(A", 20, 533), 935(A', 51, 78), 1622(A', 68, 45) | 4.04 |
| BN004 | $C_{\infty v}$ | $^4\Sigma^-$ | 410($\Pi$, 0.4, 4), 410($\Pi$, 0.4, 4), 1160($\Sigma$, 16, 19), 1441($\Sigma$, 196, 136) | 4.89 |
| BN005 | $D_{\infty h}$ | $^2\Pi_g$ | 841$i$ ($\Pi_u$, 128, 0), 188($\Pi_u$, 19, 0), 1003 ($\Sigma_g$, 0, inf), 1696($\Sigma_u$, 1225, 16) | 4.13 |
| BN005' | $C_{2v}$ | $^2A_2$ | 1035$i$($B_2$, 1695, 49471), 355($A_1$, 31, inf), 1224($A_1$, 58, 41938) | 2.26 |
| BN011 | $C_{2v}$ | $^2A_1$ | 1087($B_2$, 1, 4), 1148($A_1$, 27, 14), 1566($A_1$, 26, 28) | 5.43 |
| BN013 | $C_{2v}$ | $^2B_2$ | 223$i$, ($B_2$, 11, 0.3), 652($A_1$, 186, 109), 1919($A_1$, 34, 104) | 3.68 |
| N009 | $D_{\infty h}$ | $^2\Pi_g$ | 472($\Pi_u$, 18, 0), 605($\Pi_u$, 15, 0), 1238($\Sigma_g$, 0, 186), 1516($\Sigma_u$, 654, 0) | 5.62 |

`inf` signifies numerical overflow (100000 or more)

low-lying $^5\Sigma_u^-$ state besides the ground $^3\Sigma_g^-$ state, this observation is explainable from a diatomics-in-molecules viewpoint: the sextuplets follow naturally from connecting the $^5\Sigma_u^-$ $B_2$ to the $^4S$ nitrogen atom. Indeed, a $^6\Sigma^+$ state BN007′ was found to lie only 28.9 kcal/mol above the doublet state at the Hartree-Fock level: given the high value of $\langle\hat{S}^2\rangle$ for a sextuplet (8.75 exact, 8.763 for BN007′), the above explanation seems plausible.

When electron correlation is taken into account, BN009 markedly sinks below the other states, because of the stronger dynamical correlation effects in a doublet as opposed to the corresponding quartet. (The Fermi correlation between electrons of like spin is already accounted for by the Hartree-Fock model [Roo77]). For the sextuplets contaminating BN007, the dynamical correlation would be even smaller. Indeed, BN007′ lies 45.8 kcal/mol above BN007 at the UMP4 level, and 69.2 kcal/mol at the PMP4 level. The lowest-lying excited structure would be the bent BN012, 44.3 kcal/mol higher in energy. BN007 and BN010 are about equal in energy at the PMP4 level, both about 47 kcal/mol above the ground state. Any improved treatment is unlikely to bridge this gap for BN007.

At this level of theory, $B_2N$ is predicted to have a symmetric linear ($D_{\infty h}$) structure with a $^2\Sigma_u^+$ ground state, with the following spectroscopical parameters: bond distance 1.309 Å, harmonic frequencies 2021 $cm^{-1}$ ($\Sigma_u$), 1108 $cm^{-1}$ ($\Sigma_g$), and 73 $cm^{-1}$ ($\Pi_u$).

The $\Sigma_u$ mode is predicted to be extremely intense (Table VI). It has a surprisingly low Koopmans vertical ionization potential of only 6.75 eV ($\sigma_g^+$, leading to a $^3\Sigma_u^+$ state): BN007 is more reluctant at 9.95 eV ($\pi$, leading to a $^1\Pi$ state). As can be seen from the Mulliken charge distributions in Figure 4.5, BN009 has a very polar character, with a high negative charge on the central nitrogen atom. Concerning the extremely low bending frequency, the analogy with the behavior of $C_3$ should be noted: $B_2N$ is isoelectronic with $C_3$ except for one electron. BN009 is stabilized by resonance:

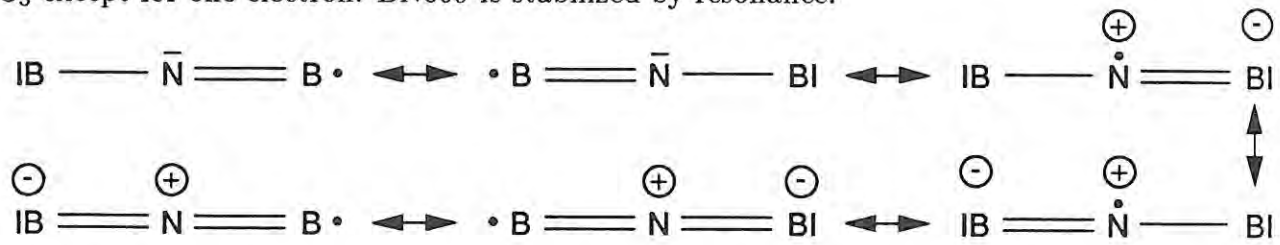

For the quartet state, the $C_{2v}$ structure BN012 will be most stable. It is isoelectronic with $B_3$ except for two unpaired electrons, but appears to have a quite different electronic structure, as judged from the large B-B distance. Its resonance structures are

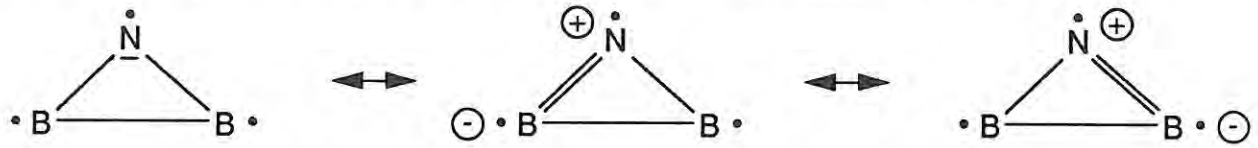

A certain analogy with the triplet state of $C_3$ can again be seen, in that the cyclic structure lies lower than the linear one ($B_2N^-$ is isoelectronic with $C_3$). In $C_3$, the $^3A_2'$ state lies 24.4 kcal/mol above the $^1\Sigma_g^+$ ground state at the UMP4/6-31G* level [Whi81a], whereas the $^3\Pi_u$ state lies 47.0 kcal/mol above the ground state in a MRD-CI/DZ(+bond functions) treatment [Per77], and 48.4 kcal/mol experimentally [Wel64, Wel66].

Finally, from the scaled CC procedure, a binding energy of 269.7 kcal/mol is predicted; this correspond to a dissociation energy of 265.0 kcal/mol.

#### 4.2.3.4 $BN_2$

The situation here is rather complex. At the 3-21G level, convergence failure was even observed for structure BN005. Here, the linear quartet structures BN006 (symmetric) followed by BN004 (asymmetric) are predicted to be most stable. At the DZP level (6-31G*) on the other hand, the order of BN006 and BN004 is reversed and the bent doublet structure BN013 is stabilized. Inclusion of electron correlation lets BN004 and BN013 approach each other in energy. When spin projection is included, the symmetric linear doublet structure BN005 approaches BN004 (again because of larger correlation energy). An asymmetric linear doublet BN003 was only found after considerable numerical difficulty. Even then, a state with a lower Hartree-Fock energy persisted, having a nonzero gradient component on the bond angle. Reoptimization without the linearity

constraint led to divergence of the geometry optimization, because of apparent crossing of several states. At the correlated level, BN003 appears to be the most stable structure at this point. With inclusion of spin projection, BN005 is only very little above.

Both BN003 and BN005 are cases of 'strong' Renner-Teller effect, in that one of both zero-order Renner-Teller frequencies is imaginary. This corresponds to case (c) in the paper by Lee *et al.* [Lee84a]. Perturbation of the linear geometry leads in the case of BN003 to a slightly bent structure BN003′, which was only reached after considerable numerical effort due to oscillation between several states. There is, however, a distinct possibility that the bent structure is an artifact of the theoretical model: a very strong spin contamination should be noted. It should also be remarked that if a lower energy wavefunction exists at the Hartree-Fock level, the HF frequency calculation may give imaginary frequencies for some modes; this may be the problem with BN003 too. At the MP2 to MP4 levels, the bent structure is less stable than the linear one. At the PMP2 to PMP4 levels, on the other hand, the Hartree-Fock result is confirmed, but the separation is less than 1 kcal/mol at the PMP4 level. At both the CCD and CCD+ST(CCD) levels, the linear structure becomes distinctly more stable, by 6.9 and 6.0 kcal/mol respectively. Clearly, recalculation of the force constant matrix at a correlated level with a greater basis set would only lead to 'weak' Renner-Teller effects. It is noted, that a false angular distortion of linear $C_3$ was found at the CI level with a $(9s5p2d)/[4s2p1d]$ basis set by Liskow *et al.* [Lis72]. Perturbation of the bond angle in BN005 leads to a $^2A_2$ state BN005′ first, but at a bond angle around 60 degrees crossing with an $^2A_1$ state BN011 is observed, which seems to represent the global minimum. BN005′ lies significantly higher than BN005 at any correlated level, so the 'strong' Renner-Teller effect might be an artifact of the UHF/6-31G* force constant matrix. Again, a potential surface study at some correlated level would be very helpful. BN011 is separated only 3.01 kcal/mol from BN003, and 3.86 kcal/mol from BN005 at the extrapolated PMP level. At the CCD and CCD+ST(CCD) levels, however, the separation from BN005 becomes quite marked (22.8 kcal/mol); with respect to BN003 the separation remains modest at 4.4 kcal/mol. At elevated temperatures, this separation does not mean too much: it corresponds to an isomerization constant of merely 1.7 at 4000 K. BN011 is also only 10.71 kcal/mol removed from the quartet state BN004, which may thus become more important at higher temperatures because of the additional degeneracy entropy. BN005 will be less important. Therefore, at this stage, the structure of $BN_2$ in a cluster plasma is best thought of as a mixture of BN011 and BN003 in about equal amounts, with also significant contributions from BN004. This makes three different states in all to be considered for $BN_2$. A detailed analysis follows in Section 4.2.4.

On pure energy grounds, BN011 represents the ground state. Based on the Mulliken population analysis and the calculated bond distances, the Lewis structure of BN011 is best thought of as

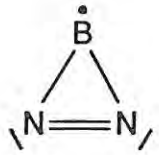

The corresponding Lewis structures for BN003 and BN004 are resonance hybrids

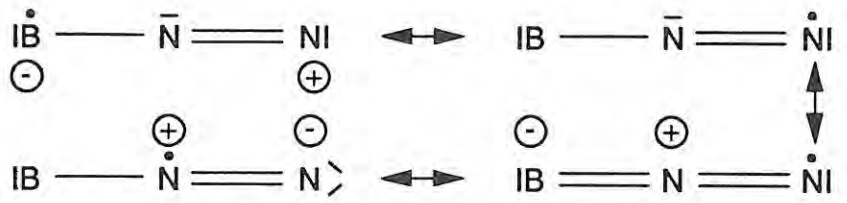

and

respectively. Judged from these resonance structures, BN003 and BN011 are best thought of as a $N_2$ molecule with a B atom attached to it, BN003 representing the axial, and BN011 the lateral adduct. This is not the case for BN004, where the calculated B-N and N-N bond distances differ much less, and the N-N distance is markedly higher than that of the $N_2$ molecule. Note also that BN011 has a rather high degree of charge polarization in the Mulliken population analysis, while this is much less the case for BN003. BN004 has essentially almost equal charges on all atoms, which is readily seen to be in agreement with the resonance hybrids.

BN013 lies relatively low: however, it is found to be a transition state at the UHF/6-31G* level. However, evaluation of the force constant matrix at some correlated level and/or with a larger basis set may characterize it as a local minimum. It also does not benefit from the additional degeneracy entropy of BN004, so it will be even less important, even at higher temperatures.

For the four lowest-lying states and their UHF/6-31G* Renner-Teller distortions (for the linear cases), harmonic frequencies, IR and Raman intensities are given in Table VI. BN003 has two ionization potentials that are about equal: 9.95 eV ($\pi$, leading to a $^1\Sigma^+$ state), and 9.96 eV ($\sigma$, leading to a $^3\Pi$ state). BN003′ has its VIP1 at 9.80 eV ($a$", leading to a $^1A$" state). BN005 has a VIP1 of 11.83 eV ($\pi_u$, leading to a $^3\Delta_u$ state). BN011 has its VIP1 at 11.13 eV ($b_2$, leading to a $^3B_2$ state), while the VIP1 of BN004 lies at 10.11 eV ($\pi$, leading to a $^3\Pi$ state). Finally, the scaled CC binding energies (dissociation energies between parentheses) are given: BN003 225.3 (221.1) kcal/mol, BN004 218.1 (213.2) kcal/mol, BN005 204.1 (200.0) kcal/mol, BN011 230.4 (224.9) kcal/mol, and BN013 219.6 (215.9) kcal/mol.

#### 4.2.3.5 $N_3$

With the 3-21 G basis, most species appear to be unbound (Table II), even the linear doublet N009 corresponding to the experimental ground state. On progressing to the 6-31G* basis set, this problem is partially relieved. The increases in dissociation energy are nevertheless spectacular: on the order of 80 kcal/mol for the cyclic structures! This agrees with the statement about polarization functions and ring strain: however, the effect is on a much larger scale here. The phenomenon also appears with the two linear structures, be it to a lesser extent. It is however known, that calculations on $N_2$ are very sensitive towards expansion of the polarization basis [Bin83]. When electron correlation is taken into account, the picture changes considerably. The tendance for oscillation of the Møller-Plesset series observed [Fri84] for $N_2$ is not seen here.

Spin projection has a non-negligible effect on the dissociation energy at the MP2 level, a little less at the MP4 level.

At the highest level of theory considered here, the linear $^2\Pi_g$ state found experimentally is most stable, followed ca. 33 kcal/mol higher by the $C_{2v}$ structure N005 with an apical angle of 69.13 degrees. The N007 structure with apex angle 49.49 degrees is also a local minimum, now at ca. 35 kcal/mol above the ground state. Both structures are connected by the Jahn-Teller crossing N003, which should be regarded as the crossing between a $^2A_2$ state (N005) and a $^2B_1$ state (N007).

N010 exhibits 'strong' Renner-Teller effect: it deforms to the structure N010′, which lies 50 kcal/mol or more below N010 at all levels.

All other structures lie much higher. N006 and N008, both $C_{2v}$, are found as transition states along their $B_2$ mode: considering the low imaginary frequencies, and the already very high location of both states, the possible $C_s$ local minimum is left out of consideration here. A $D_{3h}$ structure with term $^4A_1'$ is found as a local minimum: it is however so high-lying, that it may safely be neglected.

The structures N005 and N007 might eventually play minor roles at very high temperatures (4000 K or more). The lifetime of these species under such conditions is still open to debate.

N005 was not found in the study by Novaro *et al.* : these authors used the simple split-valence 4-31G basis set, however, and no electron correlation at all. So, any results can only be deceptive for the kind of problem under study, in regard of the high sensitivity to the polarization space. In the present study, plainly absurd geometries were often found at the 3-21G level. In the case of N006, divergence was even observed. None of these problems appeared at the 6-31G* level.

At this level, the spectroscopic parameters for $N_3$ are predicted as: $^2\Pi_g$, bond length 1.1593 Å, frequencies 1516 $cm^{-1}$ ($\Sigma_u$, 654 km/mol), 1238 $cm^{-1}$ ($\Sigma_g$, IR inactive) and 538 $cm^{-1}$ ($\Pi_u$, 18 km/mol). The latter value is simply the average of the two zero-

order Renner-Teller frequencies. All predictions are in reasonable agreement with the experimental result (in a noble gas matrix) of 1.1815 Å, and IR peaks at 1657 $cm^{-1}$ (strong, $\Sigma_u$), 2945 $cm^{-1}$ (weak, combination mode $\Sigma_g$ and $\Sigma_u$), and 473 $cm^{-1}$ (weak, $\Pi_u$). Analogous results were found by the experimentalists with a 6-311G* basis set. A very recent Fourier transform IR study [Bra88] predicts a value of 1.18115 Å in the gas phase, and 1644.6784 $cm^{-1}$ for the $\Sigma_u$ mode. Adamowicz [Ada88] finds 1.186 Å at the MP4 level, and 1.181 Å at the CCSD level, in either case with a 6-311G* basis set. We further predict a vertical ionization ionization potential of 10.77 eV ($\pi_g$, leading to a $^3\Sigma_g^-$ state), which is in fair agreement with the experimental value [Dyk82] of 11.06 eV, as well as with the observed [Dou65] triplet ground state and $D_{\infty h}$ point group for $N_3^+$.

Note that all canonical structures for N009

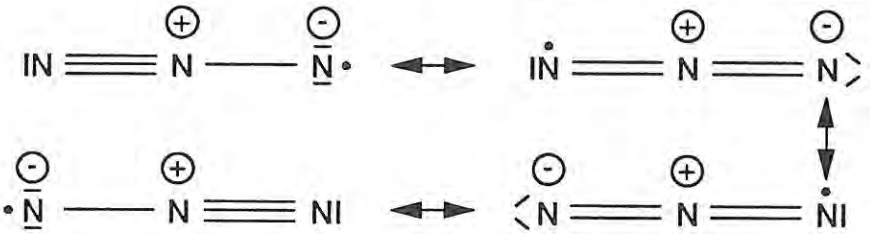

have a positive formal charge on the central nitrogen atom: this explains the very high degree of charge polarization found in the Mulliken population analysis (Figure 4.5).

Finally, the scaled CC method predicts a binding energy of 215.7 kcal/mol, or a dissociation energy of 210.1 kcal/mol. Experimentally, the heat of formation at absolute zero of $N_3$ is given [Pel81] as 468±21 kJ/mol or 111.9±5.0 kcal/mol. Combined with the heat of formation at absolute zero of the N atom [Crc84] (112.534 kcal/mol), this yields a dissociation energy of 225.7 ± 5 kcal/mol. Older references [Cha75] give a value of 99.7±5 kcal/mol for the heat of formation, resulting in a dissociation energy of 237.9±5 kcal/mol. The discrepancy between theoretical and experimental values is somewhat overly large: errors in the experimental values cannot be ruled out. This problem is addressed in more detail in Section 4.3.

### 4.2.4 Some thermochemical considerations

Seifert *et al.* [Sei88] made some thermochemical considerations about the possible fragmentation schemes for the boron-nitrogen clusters. They, however, did not investigate the temperature dependance of the equilibria. For $B_2N$, basically three different fragmentation schemes are possble (they only considered linear structures):

1. BBN → $B_2$ + N
2. BBN → B + BN
3. BNB → BN + B

Table VII: Reaction energies (eV) at the UMP4, PMP4, CCD, and CCD+ST(CCD) levels (this work), and with the local density approximation [Sei88].

| Reaction | MP4 | PMP4 | $MP_x$ | $PMP_x$ | CCD | CCD+ST | scaled[a] | LDA[b] |
|---|---|---|---|---|---|---|---|---|
| $B_3 \rightarrow B_2+B$ | 4.86 | 5.46 | 4.815 | 5.41 | 2.51 | 4.87 | 5.60 | – |
| $N_3 \rightarrow N_2 + N$ | -0.42 | -0.20 | -0.39 | -0.18 | -2.27 | -0.48 | -0.55 | – |
| $B_2N \rightarrow BN + B$ | 6.53 | 6.513 | 6.53 | 6.51 | 4.40 | 6.33 | 7.28 | 9.3 |
| $B_2N \rightarrow B_2 + N$ | 7.56 | 7.577 | 7.51 | 7.52 | 3.55 | 7.43 | 8.54 | 17.7 |
| $BN_2 \rightarrow BN + N$ | 4.95 | 4.914 | 4.94 | 4.91 | 2.27 | 4.85 | 5.58 | 10.9 |
| $BN_2 \rightarrow N_2 + B$ | 0.14 | 0.15 | 0.08 | 0.09 | -0.19 | 0.07 | 0.08 | 1.5 |

(a) from CCD+ST(CCD) binding energies scaled by 1.15 (see text)
(b) [Sei88]

Figure 4.6: Relative abundances of the $^3\Sigma_g^-$ and $^5\Sigma_u^-$ states of $B_2$ as a function of temperature.

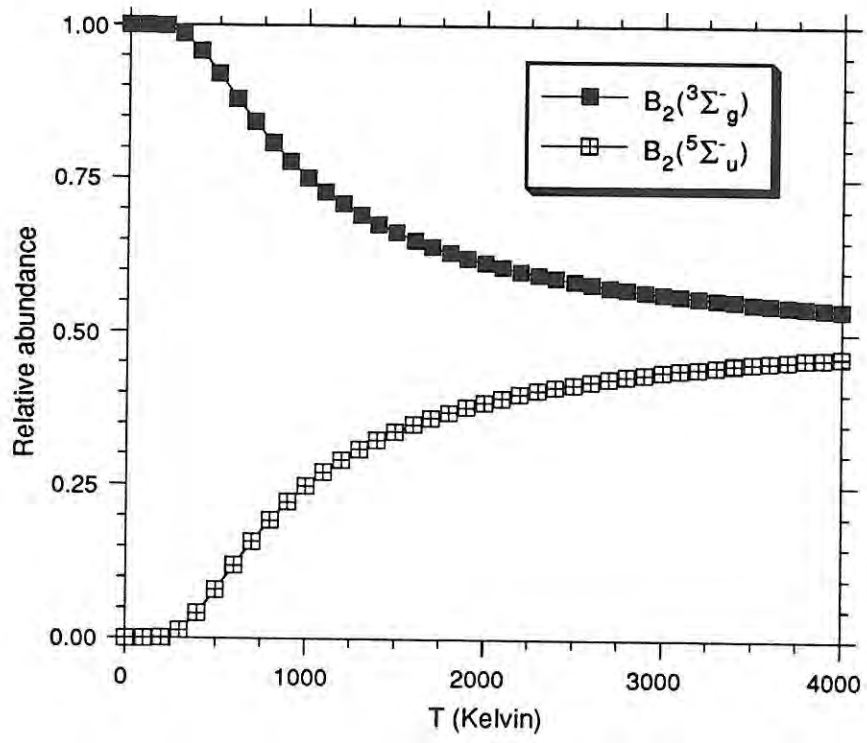

Figure 4.7: Relative abundances of the $^3\Pi$ and $^1\Sigma^+$ states of BN as a function of temperature.

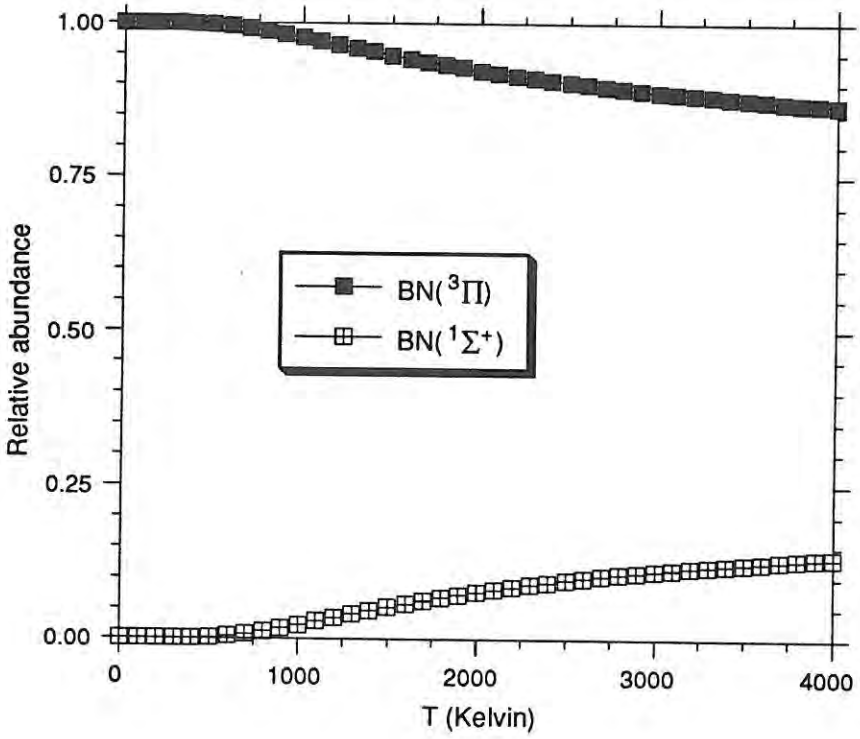


Figure 4.8: Relative abundances of the $^2A_1$ (BN011), $^2\Pi$ (BN003), and $^4\Sigma^-$ (BN004) states of $BN_2$ as a function of temperature.

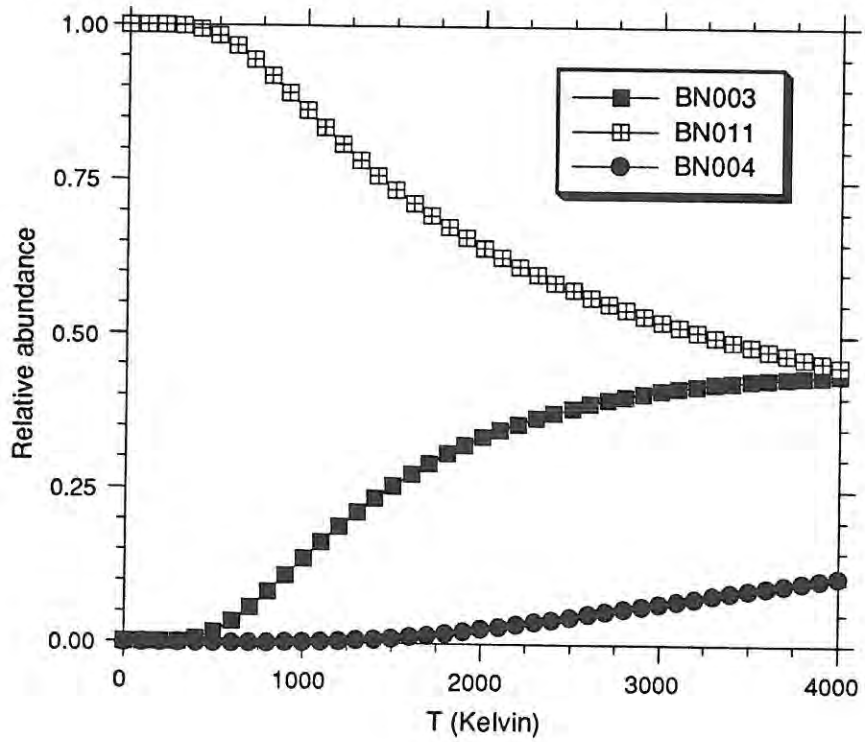

For $BN_2$, the following three fragmentation reactions were considered:

1. $BNN \rightarrow B + N_2$
2. $BNN \rightarrow BN + N$
3. $NBN \rightarrow BN + N$

They concluded from their calculations that BNN will be more stable than NBN, and that BNN readily decays to $N_2$ and B. On the other hand, BNB will be more stable than NBB, and does not decay spontaneously. This is in agreement with the fact, that $B_2N$ is observed in mass spectra, while $BN_2$ is not.

Table VII lists the reaction energies obtained at the MP4/6-31G*, PMP4/6-31G*, CCD/6-31G*, and CCD+ST(CCD)/6-31G* levels, along with the LCAO-LDA values from Seifert *et al.* [Sei88]. It is immediately seen, that although the different ab initio theories all give values within the same range, the LCAO-LDA reaction energies are greatly exaggerated. It is also evident from these results that the triples contribution is very important.

Comparing the qualitative conclusions of Seifert *et al.* with ours, it is confirmed that BNB (our structure BN009) is more stable than BBN (our structure BN007), and that BNB will not dissociate spontaneously in either BN+B or $B_2$+N. We also find confirmation for their conclusion that BNN is more stable than NBN, but find a cylic structure (not considered by them) to be the global minimum.

To investigate the effect of temperature on the equilibrium constants of the various reactions involved, partition functions were set up using moments of inertia from the UHF/6-31G* structures, and harmonic frequencies scaled by 0.89. The formulae concerned are discussed in every textbook on statistical thermodynamics [Hil60]; convenient numerical expressions may also be found in Herzberg [Her45], although the most recent values for the fundamental constants [Pac79] were used in the present work. The individual contributions of the isomers and/or states were then weighed [Sla75] to obtain the global thermodynamic quantities.

Several possible errors may arise in these calculations. The first one is the error in the computed binding energies. Since we are primarily interested in the high temperature behavior, the expected magnitude of errors will not change any conclusions significantly.

The second one is the error in the computed frequencies. Here, the use of a common scaling factor based on a very large sample of IR frequencies will generally result in error cancellation (note the excellent agreement between calculated and experimental zero-point energies for $N_3$), whereas the small magnitude of the zero-point corrections will make any remaining errors completely negligible.

The third one is the use of HF/6-31G* geometries and frequencies for the calculation of reaction entropies. As pointed out in a study by Hout *et al.* [Hou82], computed

Table VIII: Calculated thermodynamic properties at some selected temperatures.

| T (K) | $B_2$ | BN | $N_2$ | $B_3$ | $B_2N$ | $BN_2$ | $N_3$ |
|---|---|---|---|---|---|---|---|
| | | | Association enthalpy (kcal/mol) | | | | |
| 0 | -71.36 | -99.62 | -224.98 | -197.94 | -265.02 | -224.94 | -210.09 |
| 300 | -72.19 | -100.51 | -225.87 | -199.93 | -266.39 | -226.99 | -211.02 |
| 1000 | -72.78 | -101.96 | -227.75 | -202.07 | -268.06 | -229.12 | -210.23 |
| 2000 | -73.60 | -103.06 | -229.49 | -203.50 | -268.81 | -229.56 | -206.98 |
| 3000 | -74.53 | -104.02 | -230.79 | -204.64 | -269.10 | -229.76 | -203.26 |
| 4000 | -75.50 | -104.97 | -231.95 | -205.71 | -269.25 | -229.96 | -199.42 |
| | | | Association entropy (e.u.) | | | | |
| 0 | -0.57 | -1.95 | -5.51 | -2.76 | -4.13 | -5.51 | -6.89 |
| 300 | -29.84 | -31.02 | -36.82 | -60.60 | -60.52 | -65.00 | -71.24 |
| 1000 | -30.99 | -33.72 | -40.14 | -64.72 | -63.68 | -69.34 | -75.16 |
| 2000 | -31.55 | -34.49 | -41.37 | -65.74 | -64.24 | -69.67 | -75.69 |
| 3000 | -31.93 | -34.88 | -41.91 | -66.20 | -64.36 | -69.75 | -75.80 |
| 4000 | -32.21 | -35.16 | -42.24 | -66.51 | -64.40 | -69.81 | -75.84 |
| | | | Free energy of association (kcal/mol) | | | | |
| 0 | -71.36 | -71.36 | -224.98 | -197.94 | -265.02 | -224.94 | -210.09 |
| 300 | -63.24 | -91.20 | -214.83 | -181.75 | -248.23 | -207.49 | -190.84 |
| 1000 | -41.79 | -68.24 | -187.61 | -137.35 | -204.37 | -159.78 | -139.05 |
| 2000 | -10.50 | -34.07 | -146.74 | -72.03 | -140.33 | -90.22 | -63.54 |
| 3000 | 21.26 | 0.63 | -105.08 | -6.04 | -76.01 | -20.50 | 12.21 |
| 4000 | 53.33 | 35.65 | -62.99 | 60.32 | -11.63 | 49.28 | 88.03 |
| | | | Absolute entropy (e.u.) | | | | |
| 0 | 2.18 | 2.18 | 0.00 | 1.38 | 1.38 | 1.38 | 1.38 |
| 300 | 48.52 | 49.43 | 45.73 | 56.94 | 59.11 | 56.73 | 52.58 |
| 1000 | 59.33 | 58.70 | 54.37 | 70.76 | 73.89 | 70.33 | 66.61 |
| 2000 | 65.66 | 64.81 | 60.02 | 80.08 | 83.66 | 80.33 | 76.40 |
| 3000 | 69.31 | 68.45 | 63.52 | 85.65 | 89.59 | 86.29 | 82.34 |
| 4000 | 71.89 | 71.03 | 66.04 | 89.63 | 93.83 | 90.52 | 86.59 |

HF/6-31G* absolute and reaction entropies are in good agreement with experiment at room temperature. The discrepancies might become larger at higher temperatures, but will then be linked to the fourth possible source of error: the RRHO (Rigid Rotator - Harmonic Oscillator) approximation [Zah74]. For a variety of reactions and molecules, it was shown not to present any problem [Zah74] up to even 2000 K. For the species with low bending vibrations however, such as $B_2N$, the same problems will occur for the entropy as for $C_3$, where anharmonicity and vibration-rotation coupling had to be taken into account to obtain satisfactory agreement between the experimental second- and third-law entropies [Str67]. The difference, on the order of 4 e. u. for $C_3$, might have significant consequences for the equilibrium constants at high temperatures. The solution is not trivial. To predict harmonic bending frequencies for multiple bonded molecules accurately, MP2 force constants with a basis set of at least TZ(2*df*) quality seem prerequisite [Sim88]. For the anharmonic corrections, cubic and quartic HF/DZP force constants can be used together with formulae derived from perturbation theory

Figure 4.9: Plot of log $K$ vs $4000/T$ for the reactions $2B \rightarrow B_2$, $3B \rightarrow B_3$, and $B_2 + B \rightarrow B_3$.

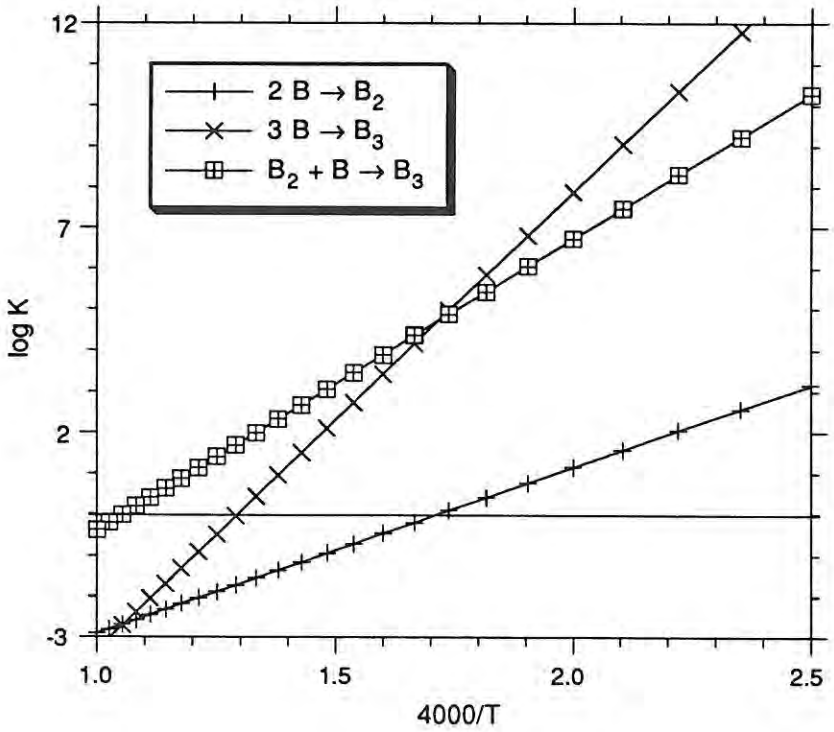


[Cla88]. Since correlated frequencties would also remedy the qualitative misbehavior in the UHF/6-31G* force fields in some instances, we plan to perform such an analysis in the near future.

The fifth potential error source has to do with the relative energies of the different states. Judged from the CCD+ST(CCD) results for $B_2$ and BN, the sequence of states is probably reliable, but improved values for the state splittings might also affect the partition functions. To this end, calculations with greater basis sets also seem appropriate. This might also achieve a lesser dependency on scaling procedures for the binding energies: combined bond-polarization function basis sets [Mar89d] are possible candidates. For the isomeric composition at higher temperatures, however, the problem is also strongly related to the previous one.

Finally, the proper isotopic composition of B has not been accounted for. The most abundant isotope used thoughout in this work, $^{11}$B, has an abundance of 80.22 %; the other naturally occurring isotope $^{10}$B makes up 19.78 % of the total. For species composed entirely of the lighter isotope, vibrational frequencies would be higher by a factor $\sqrt{11/10}$, or 1.05. Translational entropies would be lowered somewhat for these species. For the global entropy, the errors incurred will however be negligible against the other errors inherent in this treatment. The error in the case of nitrogen, with a $^{14}N$ abundance of 99.63 %, is of course negligible whatsoever.

Figure 4.10: Plot of log $K$ vs $4000/T$ for the reactions $2B \rightarrow B_2$, $B + N \rightarrow BN$, $2B + N \rightarrow B_2N$, $B_2 + N \rightarrow B_2N$, and $BN + B \rightarrow B_2N$.

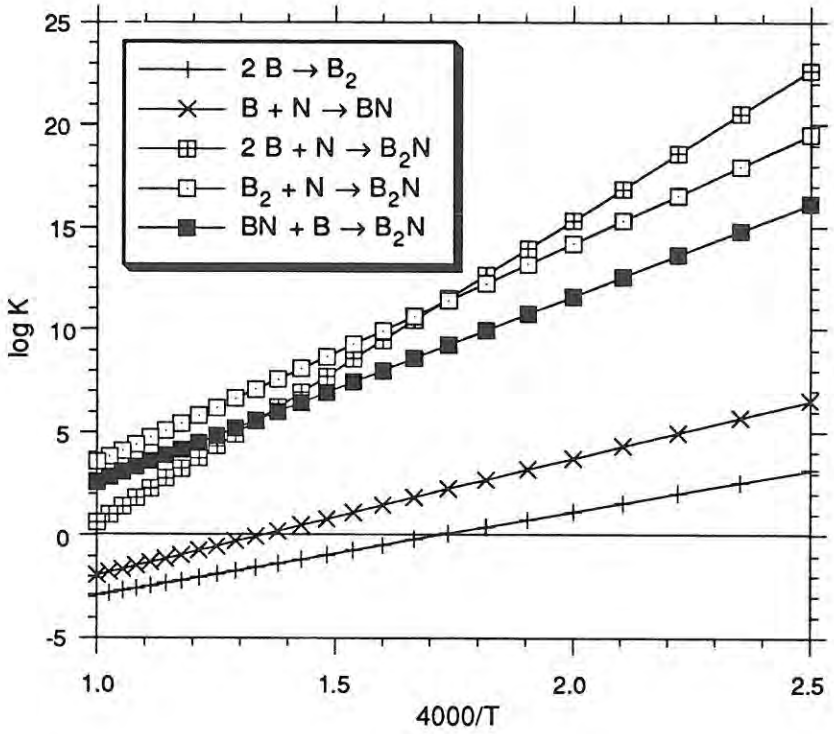


Figure 4.11: Plot of log $K$ vs $4000/T$ for the reactions $B + N \rightarrow BN$, $2N \rightarrow N_2$, $B + 2N \rightarrow BN_2$, $BN + N \rightarrow B_2N$, and $N_2 + B \rightarrow BN_2$.

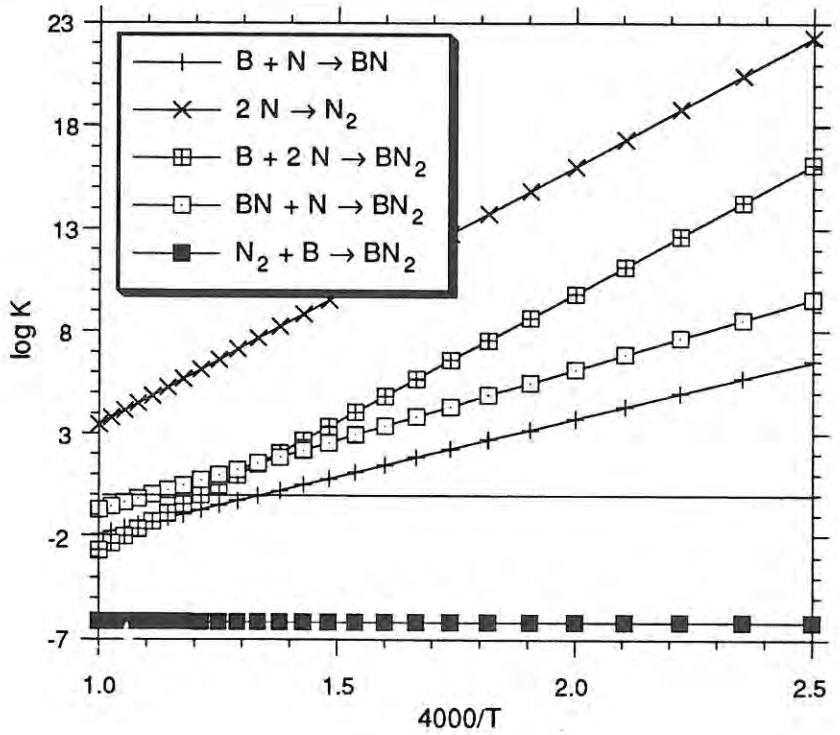

Figure 4.12: Plot of log $K$ vs $4000/T$ for the reactions $2N \rightarrow N_2$, $3N \rightarrow N_3$, and $N_2 + N \rightarrow N_3$.

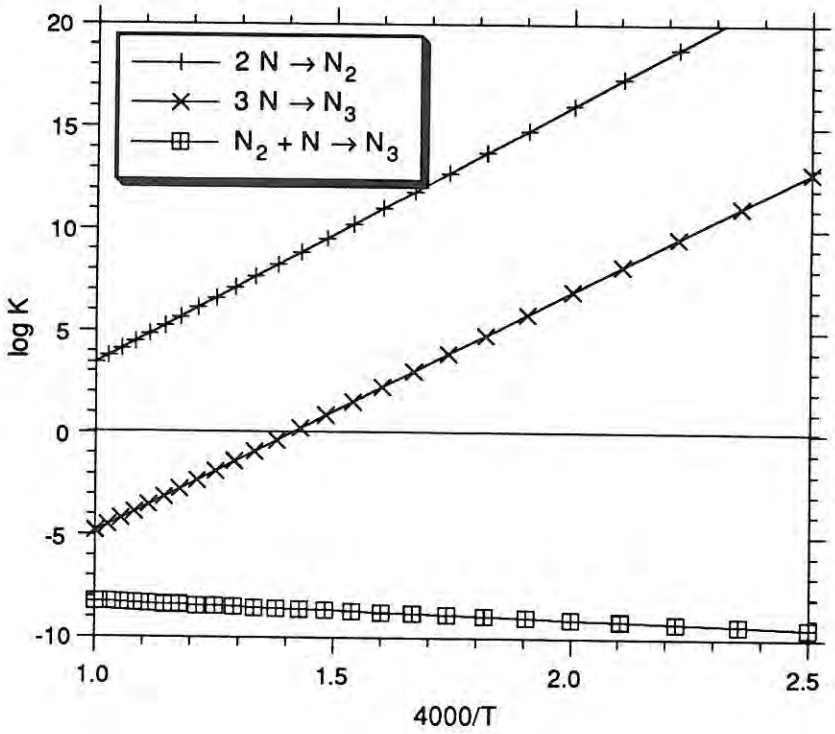


Figure 4.6 presents the relative abundances of the ${}^3\Sigma_g^-$ and ${}^5\Sigma_u^-$ states of $B_2$ as a function of temperature. It is clearly seen, how unimportant the small excitation energy becomes at elevated temperatures. Figure 4.7 presents the same for the ${}^1\Sigma^+$ and ${}^3\Pi$ states of BN. Here, the triplet state benefits from its additional degeneracy entropy, and still makes up 85 % of the total even at 4000 K. Figure 4.8 then, presents the relative abundances of structures BN003, BN004, and BN011 in $BN_2$. (The false Renner-Teller distortion in BN003 presented a problem here; therefore, it was decided to use the BN003 binding energy, but to set up the partition functions using data from BN003′. ) Here, BN011 outweighs the others at lower temperatures, but might become slightly surpassed by BN003 at higher temperatures, where BN004 can play a role too because of its additional degeneracy entropy. The relative behavior of BN003 and BN011 might however be shifted in favor of the latter when the anharmonic behavior of the low bending frequencies of BN003 (replaced here by the low bending frequency of BN003′) were properly accounted for in the entropy.

Table VIII presents values for the dissociation enthalpy, entropy, and free energy from the partition functions, as well as values for the absolute entropy. Figures 4.9 to 4.12 present plots of log K against reciprocal temperature for all dissociation reactions of the $B_3$, $B_2N$, $BN_2$, and $N_3$ systems respectively. Note the high degree of linearity in all curves.

$B_3$ is clearly stable against decay to $B_2$ and B at all temperatures except the very highest, and against atomization up to about 3100 K. So it may be expected to be present at lower plasma temperatures. It is found [Bec86] in double-focussed mass spectra from a laser plasma [Die85].

$B_2N$ will only atomize above 4000 K. It is distincly stable against decay to BN and B, as well as to $B_2$ and N. It is indeed found in laser mass spectra of solid boron nitride, and in high abundance [Bec86].

$BN_2$ is stable against atomization up to about 3300 K, but the dissociation to B and $N_2$ proceeds completely at all temperatures. This explains the absence of $BN_2$ in the mass spectra mentioned above. It is however stable towards dissociation to BN and N up to about 3600 K.

$N_3$ is stable against atomization up to about 2850 K: if our calculated dissociation energy is indeed an underestimate, this temperature will shift even higher. However, due to the extraordinary stability of the $N_2$ molecule, the dissociation in $N_2$ and N proceeds completely at all temperatures concerned. This explains, why $N_3$ is not found in the mass spectra either.

### 4.2.5 Conclusions

The potential surfaces of $B_3$, $B_2N$, $BN_2$, and $N_3$ have been studied using the 6-31G* basis sets and UHF, MP4, PMP4, CCD, and CCD+ST(CCD) methods. Spin contamination is shown to present severe problems with the MP4 procedure, which are for the most part remedied by the PMP4 procedure. Vibrational frequencies and intensities for all the different stationary points found have been given. The description of the potential surface is shown to be not entirely adequate at the UHF level, even not qualitatively.

$B_3$ is unambiguously predicted to be an equilateral triangle in its $^2A_1'$ ground state. $B_2N$ is found to have a symmetric linear structure and a $^2\Sigma_u^+$ ground state, with the asymmetric linear structure possibly being present in small amounts at higher temperatures. The $\Sigma_u$ mode of the ground state is predicted to be extremely intense. The ground state of $BN_2$ is found to be an isosceles triangle in a $^2A_1$ ground state, but $^2\Pi$ and $^4\Sigma^-$ asymmetric linear structures are close contenders, in that order. The predicted spectroscopic parameters for $N_3$ agree well with experiment.

For the lowest-lying states, dissociation energies (with an uncertainty on the order of 4 kcal/mol) are estimated using scaled CCD+ST(CCD)/6-31G* binding energies. Their predicted values are: BN 99.6, $B_3$ 197.9, $B_2N$ 265.0, $BN_2$ 224.9, and $N_3$ 210.1 kcal/mol. For $N_3$, a discrepancy exists with the approximate experimental data in literature; it cannot be ruled out that these are in error.

Using these estimated dissociation energies, the UHF/6-31G* structural parameters, and the harmonic frequencies, partition functions have been set up within the RRHO approximation. Plots of log K versus temperature for the dissociation and fragmentation

reactions of the clusters are given over the 1600-4000 K range. Absolute and reaction entropies, as well as reaction enthalpies and free energies are given at selected temperatures.

The absence of $N_3$ and $BN_2$, as well as the presence of $B_2N$ and $B_3$, in the mass spectra, are explained from a fragmentation analysis. The abundance of $B_2N^+$ can be explained from the surprisingly low VIP1 of $B_2N$, as well as its stability.

## 4.3 The dissociation energy of $N_3$

### 4.3.1 Introduction

Unlike the substantial amount of information available on the azide anion $N_3^-$ [Pol87], studies on the $N_3$ radical are relatively limited. Recently, a Fourier transform IR study [Bra88] yielded a very precise $r_0$ = 1.18115 Å for the $X\ ^2\Pi_g$ ground state, as well as a $\sigma_u$ fundamental of 1644.6784 $cm^{-1}$. Unpublished *ab initio* calculations by Adamowicz [Ada88] yielded $r_e$=1.181 Å at the CCSD/6-311G* level, and 1.186 Å at the MP4/6-311G* level. Matrix IR spectra were published by Tian *et al.* [Tia88], who found the $\sigma_u$ fundamental at 1657.5 $cm^{-1}$, a $\sigma_u - \sigma_g$ combination mode at 2944.9 $cm^{-1}$, and a zero-order Renner-Teller average for the bending frequency of 472.7 $cm^{-1}$. The spin-orbit coupling constant is 71.3 $cm^{-1}$ [Dou65], whereas the $A\ ^2\Sigma_u^+$ state has a $T_e$ of 36811 $cm^{-1}$ [Dou65].

The dissociation energy is not very accurately known. The most recent value was obtained by Pellerite *et al.* [Pel81] using ion cyclotron resonance, which yielded $\Delta H_f^0(N_3(g))$ = 112 ± 5 kcal/mol, which corresponds to $\Sigma D_0$ = 225.6 ± 5 kcal/mol (from $\Delta H_f^0(N(g))$ = 112.529 kcal/mol [Jan85]). Older work yielded $\Delta H_f^0(N_3(g))$ = 99.7 ± 5 kcal/mol [Cha75, Cla70], or $\Sigma D_0$ = 237.9 ± 5 kcal/mol. In our own work on boron-nitrogen clusters [Mar89c], we obtained $\Sigma D_0$ = 210.9 kcal/mol from CCD(ST)/6-31G* [Rag85] energies and a scaling procedure as proposed by Raghavachari [Rag86a, Rag87], which is expected to be accurate to 0.2 eV. The only other theoretical determination was a paper by Petrongolo [Pet88], who computed $D_e$ = 2.25 eV for the lowest dissociation products [$N_2$ and $N(^2D)$] using a [5*s*3*p*2*d*] basis set augmented by (*spd*) bond functions and the MRD-CI procedure [Bue74] with 9 reference configurations and energy extrapolation. Combining this with the $D_e(N_2)$ = 9.90 eV [Hub79], $T_e(^2D - ^4S)$ = 19224.464 $cm^{-1}$ [Jan85], and a zero-point energy (ZPE) from the experimental frequencies of 5.6 kcal/mol, a $\Sigma D_0$ of 219.6 kcal/mol is obtained, in marginal agreement with the newer experimental result. However, an accurate ab initio determination is apparently desirable to settle the issue.

Table IX: Total energies (hartree;minus sign omitted) of 3N and $N_3$ and total atomization energy (TAE, kcal/mol) of $N_3$.

| Method | 6-31G* | TAE | 6-311G* | TAE | 6-311+G* | TAE | 6-311G(2*df*) | TAE | (a) |
|---|---|---|---|---|---|---|---|---|---|
| | | | | | 3 N | | | | |
| UHF | 163.156327 | | 163.193941 | | 163.196678 | | 163.193941 | | |
| MP4(SDQ) | 163.418412 | | 163.470988 | | 163.475595 | | 163.522031 | | |
| MP4 | 163.419769 | | 163.472685 | | 163.477524 | | 163.526664 | | |
| QCISD | 163.419420 | | 163.471785 | | 163.476796 | | 163.522715 | | |
| QCISD(T) | 163.421441 | | 163.474285 | | 163.479607 | | 163.529098 | | |
| | | | | | $N_3$ | | | | |
| UHF | 163.245792 | 56.14 | 163.280996 | 54.63 | 163.284143 | 54.89 | 163.296994 | 64.67 | 64.92 |
| MP4(SDQ) | 163.701424 | 177.59 | 163.761530 | 182.32 | 163.766954 | 182.83 | 163.842787 | 201.28 | 201.79 |
| MP4 | 163.724165 | 191.01 | 163.789834 | 199.01 | 163.795913 | 199.79 | 163.874534 | 218.29 | 219.07 |
| QCISD | 163.707520 | 180.79 | 163.768221 | 186.02 | 163.773728 | 186.33 | 163.848940 | 204.71 | 205.02 |
| QCISD(T) | 163.726744 | 191.58 | 163.791603 | 199.12 | 163.797606 | 199.55 | 163.878199 | 219.06 | 219.49 |

(a) using additivity approximation (see text)

### 4.3.2 Computational methods

All calculations were carried out at the experimental $r_0$ [Bra88], using the GAUSSIAN 88 package [Gau88] running on the IBM 3090/400e VF at the University of Leuven, under the MVS/XA operating system.

Standard 6-311G* [Kri80a], 6-311+G* [Cla83], and 6-311G(2*df*) [Fri84] basis sets were used. Electron correlation was included using the QCISD(T) model [Pop87], which was very recently shown [Lee90] to be a very good approximation to CCSD(T) [Rag89]. Singly [Sch86] and multiply [Sch88] projected MP2 and MP3 energies, as well as the unprojected MP4(SDQ) energy, are obtained *en passant* in the calculations. Full MP4 [Kri80] energies were obtained in separate runs for all three basis sets.

Atomization energies were then obtained using both standard G1 theory [Pop89], and a variation in which all MP4 energy differences are replaced by their more accurate QCISD(T) counterparts. This was done because a recent study of the NASA Ames group [TayPC] on the C–H dissociation energy of acetylene has indicated that the regular G1 recipe is perhaps not appropriate for highly spin-contaminated species. It was already shown some time ago [Sch88, Mar90a] on theoretical grounds that the CCSD energy (and, by extrapolation, its QCISD approximation) is not affected by a single spin contaminant.

### 4.3.3 Results and discussion

Because of high spin contamination ($\langle \hat{S}^2 \rangle \geq 0.90$), single excitations will be very important. We therefore evaluated the binding energies of $N_2$ and $N_3$ using the QCISD(T)/6-31G* model from UHF/6-31G* geometries [Mar89c], which yielded 198.5 and 191.6 kcal/mol, respectively. Scaling the binding energy with 1.15 yields a very good value of 228.3 kcal/mol for the $D_e$ of $N_2$, and a $D_e$ of 220.4 kcal/mol ($D_0$ = 214.7 kcal/mol).

Thus, the quasiperturbative treatment of single excitations in CCD(ST) explains part, but not all, of the disagreement between our previously computed value and experiment. (It is perhaps also worth mentioning that the MP4(DQ) and CCD binding energies differ only slightly, and that the MP2 and MP3 values converge smoothly to that value: this indicates that no convergence problem exists as far as the $\hat{T}_2$ effects are concerned.)

Table IX presents total and dissociation energies obtained using the three basis sets listed above, as well as from assuming additivity of the effects of diffuse functions and expansion of the polarization space. As these two effects are very different, this assumption should hold quite well.

It is immediately seen, that the QCISD total energy for $N_3$ is underestimated by 6 to 7 millihartrees at the MP4(SDQ) level, as well as that the triple excitation effect is significantly overestimated at the MP4 level. Oddly, the two effects compensate each other, leading to a relatively small difference between the full MP4 and the QCISD(T) binding energies (there also exists some cancellation between the separated atoms and the molecule). Furthermore, the differences work in opposite directions for the various basis sets, underestimating the binding energy by 0.11 and 0.77 kcal/mol for the 6-311G* and 6-311G(2*df*) basis sets respectively, and overestimating it by about 0.24 kcal/mol for the 6-311+G* basis set. For the combined binding energy, this finally results in a net underestimate of 0.42 kcal/mol. The G1 correction amounts to 14.46 kcal/mol; the corrected QCISD(T)/6-311+G(2*df*) binding energy within the basis set additivity approximation, is then 233.95 kcal/mol, compared to 233.64 kcal/mol using the conventional G1 recipe. Apparently the G1 value benefits from the fortuitous cancellation, which might not have been observed if oscillation of the MP series were also present.

Basis set effects are strikingly large, including an increase in binding energy by some 7 kcal/mol upon going from 6-31G* to 6-311G*, and an increase by some 20 kcal/mol upon expansion of the polarization space. Because of this extreme sensitivity to the basis set, it is not very surprising that Raghavachari's scaling procedure fails here. It remains to be seen how well it performs for the other species considered in Section 4.2 [Mar89c]: possibly, a bond equivalent scheme may have to be developed. This and other issues will be addressed in full in the near future.

The ZPE as obtained from the UHF/6-31G* harmonic frequencies [Mar89c] scaled by a recommended factor of 0.89 [Pop81] is 5.62 kcal/mol, compared to the 5.56 kcal/mol obtained from the experimental bands. Assuming positive anharmonicity constants (which is the normal situation), the latter value will be a lower bound to the true ZPE. We will therefore use the 5.62 kcal/mol value (in keeping with the G1 model) as a 'second best' alternative to the ZPE obtained from a full anharmonic force field. We then finally obtain a $\Sigma D_0$ of 228.35 kcal/mol and a heat of formation at 0 K of 109.25 kcal/mol, in excellent agreement with the result of Pellerite *et al.* [Pel81].

In order to obtain the heat of formation at 298.15 K, we have set up the partition

functions using the available experimental data and a RRHO approximation. Except perhaps for the bending frequency, the relatively high frequencies and the fact that the experimental data correspond to the first vibrational transitions (which will dominate the partition function), the use of this model is certainly warranted. One other term which should be included is the spin-orbit coupling, for which we assumed that the computed ground state splits up in two levels $\pm 71.3/2$ cm$^{-1}$. At very high temperatures, the levels will have comparable populations and may be treated as degenerate: at room temperature however, we find an atomization enthalpy increase of 0.119 kcal/mol. The degenerate bending vibration contributes -0.308 kcal/mol, the two others together only -0.009 kcal/mol. The rotational enthalpy using the first four terms of the well-known asymptotic series [Kas36] is indistinguishable from the classical result (-0.592 kcal/mol). Finally, the translation enthalpy difference adds up to -2.962 kcal/mol. Together, the thermal atomization enthalpy is 2.173 kcal/mol. Combining this with $\Delta H^0_{f,298}(N(g)) =$ 112.973 kcal/mol, we finally find $\Delta H^0_{f,298}(N_3(g)) = 108.4 \pm 2$ kcal/mol.

## 4.4 Accurate ab initio spectroscopic and thermodynamic properties for the SiC molecule

### 4.4.1 Introduction

Silicon carbide (one of whose crystalline phases is also known under the name 'carborundum') is of great industrial importance, among others as an abrasive [Kir78], for applications in high-temperature ceramics [San84], and with potential as a semiconductor [Par85].

The SiC molecule has aroused much interest among astrophysicists. It is believed to be an abundant component in carbon stars [Roh86], stellar atmospheres [Tsu65], and dense interstellar clouds [Suz79]. Only very recently some spectroscopic data on some of its excited states have become available [Ber88a]. Its ground and first excited states have been predicted unambigously to be $X\ ^3\Pi$ and $A\ ^3\Sigma^-$, respectively, in several ab initio studies [Roh86, Lut74, Bru80, Bau87]. However, neither of them has been well characterized experimentally.

Recently, the study of small molecules appearing in the vapor of neoceramic materials has attracted much attention from researchers in the area of 'chemical vapor deposition', as the possible key to an understanding of mechanism and optimal conditions for CVD [Mar89c]. For work with SiC, the availability of adequate thermochemical data for the SiC molecule would be helpful [DucPC]. However, present-day theoretical methods are quite capable of producing the kind of accuracy required, if judiciously applied.

The purpose of the present paper is threefold:

1. to calculate accurate spectroscopic constants of the three lowest-lying states of SiC;

2. to present thermodynamic functions of chemical accuracy over a wide temperature range;

3. to critically investigate the anharmonic and rotation-vibration effects on the thermodynamic functions. As the RRHO (rigid rotor-harmonic oscillator) approximation is generally applied in thermodynamic studies of polyatomic clusters, such an analysis may indicate whether or not moving beyond this approximation is desirable.

### 4.4.2 Theoretical methods

We first give an overview of the recent theoretical studies on SiC. Bruna *et al.* [Bru80] calculated potential energy curves of a number of electronic states using the MRD-CI method of Buenker and Peyerimhoff [Bue74] and a DZP basis augmented with bond functions. No dissociation energies nor anharmonic constants were computed in this study: the main emphasis appeared to be on the electronic transition energies between the ground and the lower excited states. Two subsequent papers [Bru81] and [Ang83] discuss the ionization potential and electron affinity, respectively. Cooper [Coo83] investigated the spin-orbit coupling in the $X\ ^3\Pi$ state at the SCF level using a double zeta STO basis set. Rohlfing and Martin (RM) [Roh86] studied just the ground state with MP4 and CASSCF/CCI (contracted configuration interaction) methods. They present both dissociation energies and anharmonicity constants, but these are scattered over a wide range among the methods employed. Bauschlicher and Langhoff (BL) [Bau87] studied the $X\ ^3\Pi$ and $A\ ^3\Sigma^-$ states using a large atomic natural orbital (ANO) [Alm87] basis set and several sophisticated CI methods. Based on comparisons with $C_2$ and $Si_2$, they proposed a 'best estimate' of 4.4 eV for the dissociation energy, compared to an experimental upper bound listed in Huber and Herzberg [Hub79] as 4.66 eV. They also noted that the IR intensity would be very weak, and that an accurate rotational constant would be more useful. To this end, they produced a best estimate of 1.719 Å for the bond length. In Bernath *et al.* (BROBM) [Ber88a], single- or two-reference CISD calculations with large (*spdf*) STO basis sets were made to predict the bond distance differences between the various states. Combined with their experimental results for the excited $b\ ^1\Pi$ state, these authors predict $r_e$ and $r_0$ values, respectively, of 1.719 and 1.723 Å for the ground state, both of which are expected to be accurate to $\pm 0.001$ Å. Finally, Müller-Plathe and Laaksonen [Mue89] present numerical Hartree-Fock properties in a recent paper.

Given the apparent necessity for a multi-reference expansion in the CI treatments, as well as the high degree of spin contamination in the UHF wavefunction, it is surprising that no coupled cluster calculations have been attempted. It is well known that coupled cluster theory handles quasidegeneracy quite well even with a single reference determinant [Jan80], as well as that the CCSD energy is not affected by the presence of only a single

spin contaminant [21,23]. Since it was found in [Roh86] that a single spin annihilation reduced the value of $\langle S^2 \rangle$ from 2.50 to 2.02 (compared to 2.0 for a pure triplet state), the decision for a coupled cluster treatment is obvious. From references [Roh86] and [Bau87], it is also apparent that whereas triple excitations are not as important as in $C_2$, they should certainly not be neglected. In a multireference-CISD treatment, the most important triple excitations will be included anyway, as excitations to some of the reference configurations. However, in a single-reference coupled cluster treatment some attempt should be made as to including the $\hat{T}_3$ operator.

For heavily spin-contaminated wavefunctions, it has recently been noted [Pop88], that single excitations have a large effect on the dissociation energy, which is underestimated by 50 % or more when the $\hat{T}_1$ operator is only evaluated perturbatively. Martin *et al.* [Mar90a] (Section 5.2) have also shown, that single excitations have a rather large effect on bond distances and harmonic frequencies under the same circumstances. An ideal treatment would then be CCSD+T(CCSD) [Lee84] or QCISD(T) [Pop87], the latter of which is now available to us. QCISD is actually an approximation to CCSD; however, its perturbative triples correction QCISD(T) has the advantage over that in CCSD+T(CCSD), that it is correct to fifth order [Rag89]. In Section 5.4 we will show [Mar90b] that effects of single excitations in heavily contaminated systems can be surprisingly well accounted for using a combination of CID and CISD, using the Davidson-Silver formula [Dav77] to correct for size inconsistency.

Comparable methods have recently been applied with great success to the $N_3$ molecule [Ada88, Mar90d] using DZP and TZP basis sets, which is in many respects similar to the present one (triplet ground state, spin contamination, large triplet contribution). Regarding the basis set, we had to settle for a compromise between quality and computation time, so we decided on the 6-311G* [Kri80a] basis for carbon, and the McLean-Chandler [6*s*5*p*1*d*] basis set [McL80] for silicon, with polarization exponents modified for correlation calculations as suggested by Wong *et al.* [Won88]. This basis set is denoted below as MC-311G(1*d*). Several basis set extensions were considered to assess their effect on the computed properties. Diffuse functions on C and Si were taken from references [Cla83] and [Spi87], respectively. Standard values [Fri84] were used for the additional C polarization exponents; for Si, the *d* functions were taken as $\alpha/2$ and 2 $\alpha$ ($\alpha$ being the single *d* function exponent), whereas the *f* function exponent was taken as the standard value [Won88]. To further correct for basis set incompleteness, the G1 theory of Pople and coworkers was then applied [Pop89].

Part of the calculations were performed using the GAUSSIAN 86 program system [Gau86], part with the GAUSSIAN 88 package [Gau88], running on a VaxStation 2000 under VMS 4.7.

Potential curves for the $X\ ^3\Pi$, $A\ ^3\Sigma^-$, and $a\ ^1\Sigma^+$ states were evaluated in a range of +0.06 and -0.06 Å around the predicted bond distances in [Ber88a], with a step

size of 0.02 Å. $r_e$ was determined by least-squares fitting of a fourth-degree polynomial through the energies and finding its minimum. The quartic polynomial in $r$ was then transformed to the dimensionless variable $(r - r_e)/r_e$; from the resulting coefficients, the spectroscopic constants of the most abundant isotopomer $^{12}C^{28}Si$ were obtained using expressions derived by Dunham [Dun32] (Section 1.12.4).

The partition functions were evaluated using the direct summation technique (Section 1.12). From the partition function Q as well as its associated moment sums $Q'$ and $Q"$, the thermodynamic functions can then easily be constructed [Pit61]. The summation was carried out over all electronic, vibrational and rotational levels, including anharmonicity, rotation-vibration coupling and centrifugal distortion. No approximate factorization of the three partition functions was carried out. Only the translational contribution was evaluated separately. The threshold for summation was set for any temperature at the energy where a given nondegenerate vibronic level would only contribute 1 part in $10^8$ to the total partition function.

Isotope effects on the spectroscopic constants were incorporated using the approximate formula suggested by Dunham [Dun32]:

$$Y_{ij}(\text{iso})/Y_{ij} \approx (m/m_{\text{iso}})^{(i+2j)/2} \tag{4.3}$$

in which $Y_{10} = \omega_e$, $Y_{20} = -\omega_e x_e$, $Y_{01} = B_e$, $Y_{02} = D_e$, $Y_{11} = -\alpha_e$, etc., except for some very small correction terms. The partition functions are then constructed for each isotopomer separately and finally averaged using the products of the natural isotope abundances as weight factors. This latter approximation, which holds very well except perhaps for the $H_2/D_2$ system, was made in the JANAF tables [Jan85]. It is equivalent to assuming the equilibrium constants for isotopic exchange reactions among the different isotopic species to be all unity.

At higher temperatures, excited states above the three lowest should also be accounted for. Since these contributions will be small, we have adopted here the approximation of setting up the partition functions for these using ab initio and experimental data for three more excited states $b\ ^1\Pi$, $c\ ^1\Delta$, and $d\ ^1\Sigma^+$ given in BROBM [Ber88a] and Bruna *et al.* [Bru80], and deriving the missing constants using some well-known approximate relationships between spectroscopic constants (vide infra) [Her50].

Finally, spin-orbit coupling should be accounted for. Herzberg [Her50] gives a first-order expression for the splitting between components of a molecular term as

$$E = E_0 + A\Lambda\Sigma \tag{4.4}$$

in which A is the spin-orbit coupling constant, and $\Lambda$ and $\Sigma$ represent the components of the electronic angular momentum and of $\hat{S}$ along the nuclear axis, respectively. ($\Lambda$ is 0 for a $\Sigma^+$ or $\Sigma^-$ state, 1 for a $\Pi$ state, 2 for a $\Delta$ state, etc.). $E_0$ denotes the energy in the absence of spin-orbit coupling. The A value for the ground state is computed as -37.3

Table X: Computed spectroscopic constants for the $X\ ^3\Pi$ state (MC-311G($d$)).

| Method | $D_e$ (eV) | $D_0$ (eV) | $r_e$ (Å) | $r_0$ (Å) | $B_e$ ($cm^{-1}$) | $\omega_e$ ($cm^{-1}$) | $\omega_e x_e$ ($cm^{-1}$) | $10^3\alpha_e$ ($cm^{-1}$) |
|---|---|---|---|---|---|---|---|---|
| UHF | 2.55 | 2.49 | 1.765 | 1.769 | 0.64466 | 826.5 | 2.72 | 5.85 |
| MP2 | 3.49 | 3.43 | 1.706 | 1.711 | 0.69005 | 892.3 | 6.76 | 8.53 |
| MP3 | 3.37 | 3.32 | 1.709 | 1.714 | 0.68750 | 886.4 | 6.62 | 8.53 |
| MP4DQ | 3.27 | 3.22 | 1.712 | 1.717 | 0.68508 | 884.2 | 6.46 | 8.40 |
| MP4SDQ | 3.37 | 3.31 | 1.711 | 1.716 | 0.68604 | 905.0 | 7.39 | 8.43 |
| MPx[a] | 3.22 | 3.17 | 1.713 | 1.718 | 0.68424 | 882.6 | 6.37 | 8.36 |
| CCD | 3.24 | 3.18 | 1.713 | 1.718 | 0.68385 | 885.2 | 6.27 | 8.19 |
| CCD(T) | 3.36 | 3.31 | 1.710 | 1.715 | 0.68647 | 894.3 | 6.83 | 8.36 |
| CCD(ST) | 3.50 | 3.44 | 1.711 | 1.716 | 0.68547 | 924.0 | 7.54 | 7.98 |
| PUHF | 2.74 | 2.69 | 1.763 | 1.767 | 0.64579 | 879.7 | 5.53 | 6.07 |
| PMP2 | 3.71 | 3.65 | 1.712 | 1.717 | 0.68451 | 936.5 | 7.00 | 7.62 |
| PMP3 | 3.59 | 3.53 | 1.718 | 1.723 | 0.68012 | 918.9 | 6.35 | 7.42 |
| PMP4 | 3.49 | 3.43 | 1.721 | 1.725 | 0.67800 | 917.5 | 6.35 | 7.35 |
| PMPx[a] | 3.44 | 3.38 | 1.722 | 1.726 | 0.67722 | 915.9 | 6.30 | 7.31 |
| CID | 3.02 | 2.96 | 1.718 | 1.723 | 0.68008 | 874.3 | 5.66 | 7.99 |
| CID+PC | 3.24 | 3.19 | 1.713 | 1.718 | 0.68412 | 883.8 | 6.39 | 8.33 |
| CID+DC | 3.21 | 3.16 | 1.712 | 1.718 | 0.68459 | 884.7 | 6.45 | 8.35 |
| CID+RDC | 3.24 | 3.18 | 1.712 | 1.717 | 0.68515 | 886.2 | 6.57 | 8.41 |
| CID+DSC | 3.27 | 3.22 | 1.711 | 1.716 | 0.68586 | 888.1 | 6.72 | 8.47 |
| CISD | 3.22 | 3.17 | 1.720 | 1.725 | 0.67858 | 924.6 | 7.08 | 7.32 |
| CISD+PC | 3.68 | 3.62 | 1.720 | 1.724 | 0.67824 | 988.9 | 11.05 | 6.10 |
| CISD+DC | 3.63 | 3.57 | 1.719 | 1.723 | 0.67899 | 983.3 | 10.47 | 6.28 |
| CISD+RDC | 3.71 | 3.65 | 1.720 | 1.724 | 0.67848 | 999.5 | 11.54 | 5.96 |
| CISD+DSC | 3.83 | 3.76 | 1.721 | 1.725 | 0.67760 | 1024.4 | 13.26 | 5.50 |
| CCD(T)+S(DSC) | 3.92 | 3.85 | 1.721 | 1.724 | 0.67810 | 1029.6 | 13.22 | 5.43 |
| QCISD | 3.72 | 3.66 | 1.727 | 1.731 | 0.67281 | 970.4 | 8.27 | 6.04 |
| QCISD(T) | 3.93 | 3.87 | 1.732 | 1.735 | 0.66936 | 976.4 | 8.88 | 5.69 |

(a) Corrected using Pople's infinite-order extrapolation formula [Pop83]

$cm^{-1}$by Cooper [Coo83], who expects his empirically corrected SCF value to be correct to a few $cm^{-1}$; the other five states included in this calculation do not exhibit first-order term splitting. We here make the assumption that the partition functions of the three component states of $X\ ^3\Pi$ are very much similar, so the spin-orbit coupling term can be factored out.

## 4.4.3 Results and discussion

### 4.4.3.1 Spectroscopic Constants

Computed spectroscopic constants for the $X\ ^3\Pi$ state using the MC-311G(1$d$) basis set and a variety of theoretical models, including normal and projected UHF, MP2, MP3, and MP4(DQ), Pople's infinite-order extrapolation formula, CID and CISD with four different size-consistency corrections, CCD and CCD+ST(CCD) theory, and finally QCISD and

QCISD(T), are listed in Table X. The size-consistency corrections considered were the Davidson (DC) [Lan74], Pople (PC) [Pop77], renormalized Davidson (RDC) [Sie78], and Davidson-SIlver [Dav77] formulas. It is easily seen, that all spectroscopic constants are quite sensitive to the electron correlation method employed. This is an exception to the general rule, that anharmonic force constants are quite well described at the Hartree-Fock level [Gaw86]. However, in that study, only closed-shell molecules were considered, whereas we are dealing with a heavily spin-contaminated UHF wavefunction here. When the anharmonic constants at other levels are considered relative to the PUHF constants, a much smaller variation is observed.

It would be interesting to see, how much of the remaining difference is due to geometry change effects. Since the coefficients of the Dunham polynomial are not explicitly dependent on bond length, one could make the assumption that the Dunham coefficients $a_0$, $a_1$ and $a_2$ are approximately constant across the different methods. It is then easily shown, that

$$\omega_e x_e(r_1)/\omega_e x_e(r_2) = (r_2/r_1)^2 \tag{4.5}$$

$$\alpha_e(r_1)/\alpha_e(r_2) = (r_2/r_1)^3(4) \tag{4.6}$$

Upon changing from the PUHF to the PMP2 geometry, this would result in 10 % and 6 % increase in $\alpha_e$ and $\omega_e x_e$, respectively. Oddly enough, this approximation holds better with increasing order of perturbation theory, but fails when single or triple excitations are introduced for the first time. Apparently, both of them have some influence, not only on the equilibrium bond length and the harmonic force constant, but even on the anharmonicity. This itself is again a consequence of the spin-contaminated radical character of the wavefunction.

Projection and annihilation of higher contaminants than quintuplet shows almost no change in energy or $\langle \hat{S}^2 \rangle$: the spin contamination is adequately removed by a single projector. As neither the CCSD nor the CISD or QCISD energies are affected by a single spin contaminant [21,23], these methods should be no less reliable than usual.

The Davidson-corrected CISD potential curves all exhibit excessive anharmonicity, which is not seen in the uncorrected curves, nor in the corrected CID curves. Incidentally, the size consistency corrections are all very large, $(1\text{-}c_0)^2$ being about 0.12 and varying quite substantially even over the small distance sampled. All coefficients are quite sensitive to the degree of the fit or interpolation, which is not the case with any of the other methods.

The QCISD and QCISD(T) frequencies are in excellent agreement with the 'best theoretical estimate' of 975±10 $cm^{-1}$ by RM, which was produced using an empirical error correction. Very good agreement is also observed for both methods with the best estimate of 962 $cm^{-1}$ by BL. It should be noted that the basis set employed here is only of TZP quality, whereas the RM basis set was of TZ(2*d*) quality and BL used a TZ(2*df*)

Table XI: Computed spectroscopic constants for the $A\ ^3\Sigma^-$ state (MC-311G($d$)).

| Method | $D_e$ (eV) | $D_0$ (eV) | $r_e$ (Å) | $r_0$ (Å) | $B_e$ ($cm^{-1}$) | $\omega_e$ ($cm^{-1}$) | $\omega_e x_e$ ($cm^{-1}$) | $10^3\alpha_e$ ($cm^{-1}$) |
|---|---|---|---|---|---|---|---|---|
| UHF | 1.86 | 1.80 | 1.765 | 1.768 | 0.64401 | 1002.6 | 4.61 | 4.14 |
| MP2 | 3.40 | 3.35 | 1.810 | 1.814 | 0.61275 | 865.1 | 5.67 | 5.46 |
| MP3 | 3.34 | 3.28 | 1.808 | 1.811 | 0.61421 | 881.2 | 4.81 | 5.01 |
| MP4(DQ) | 3.22 | 3.16 | 1.804 | 1.808 | 0.61663 | 894.7 | 4.54 | 4.79 |
| MP4(SDQ) | 3.26 | 3.21 | 1.809 | 1.812 | 0.61356 | 879.9 | 4.81 | 4.46 |
| CCD | 3.16 | 3.11 | 1.803 | 1.806 | 0.61762 | 898.0 | 4.47 | 4.78 |
| CCD+T(CCD) | 3.33 | 3.27 | 1.813 | 1.817 | 0.61063 | 868.7 | 4.50 | 5.03 |
| CCD+ST(CCD) | 3.37 | 3.32 | 1.818 | 1.822 | 0.60759 | 855.2 | 4.48 | 5.17 |
| PUHF | 1.81 | 1.75 | 1.765 | 1.768 | 0.64427 | 1003.9 | 4.60 | 4.13 |
| PMP2 | 3.38 | 3.33 | 1.810 | 1.814 | 0.61298 | 866.1 | 5.67 | 5.46 |
| PMP3 | 3.33 | 3.28 | 1.808 | 1.811 | 0.61434 | 881.6 | 4.84 | 5.01 |
| PMP4 | 3.21 | 3.16 | 1.804 | 1.808 | 0.61675 | 895.1 | 4.31 | 4.77 |
| CISD | 2.91 | 2.85 | 1.799 | 1.803 | 0.62001 | 907.7 | 4.40 | 4.71 |
| CISD+PC | 3.25 | 3.19 | 1.814 | 1.817 | 0.61036 | 869.4 | 3.30 | 4.62 |
| QCISD | 3.22 | 3.17 | 1.808 | 1.812 | 0.61384 | 881.4 | 4.83 | 4.45 |
| QCISD(T) | 3.39 | 3.34 | 1.819 | 1.823 | 0.60656 | 851.2 | 4.89 | 4.53 |

ANO contraction of a very large primitive set. Apparently, the QCISD and QCISD(T) electron correlation methods are complete enough to obtain good accuracy even with smaller basis sets. The extrapolated value of 1.719±0.001 Å for the bond distance by BROBM is quite well reproduced by the projected MP methods, as well as by the size-consistency corrected CISD methods. Oddly enough, the QCISD and QCISD(T) methods produce longer bond lengths, which might be a basis set effect; computed MP2-4 bond lengths are consistently longer (by 0.008, 0.007, and 0.006 Å, respectively) than with the RM basis.

Concerning the dissociation energies, the most remarkable feature is the large effect of single excitations. Taken as the difference between CCD and QCISD values, it is no less than 0.48 eV! The triple excitation contribution, with 0.21 eV, is comparable to the 0.18 eV difference between MP4(SDQ) and MP4(SDTQ) in the RM study. This value is itself intermediate between the large 0.41 eV contribution in the $a^3\Pi$ state of $C_2$, and the small 0.13 eV contribution in the $X^3\Sigma^-$ state of $Si_2$. The difference with the RM basis set is quite small (0.01 eV at the MP4(DQ) level), whereas the difference between the RM and the BL basis sets was 0.20 eV at the Davidson-corrected MRD-CI level. This indicates that the effect of $f$ functions on the dissociation energy should not be neglected.

As expected, the situation for the $A\ ^3\Sigma^-$ state is quite different. Table XI lists the computed spectroscopic constants with several methods. Projected and unprojected MP results are virtually identical to each other, because no appreciable spin contamination is present. Correspondingly, single excitations have no anomalous effects on the dissociation energy and the CCD+ST(CCD) spectroscopic parameters given should be very close to

Table XII: Computed spectroscopic constants for the $a\ ^1\Sigma^+$ state (MC-311G($d$)).

| Method | $D_e$ (eV) | $D_0$ (eV) | $r_e$ (Å) | $r_0$ (Å) | $B_e$ ($cm^{-1}$) | $\omega_e$ ($cm^{-1}$) | $\omega_e x_e$ ($cm^{-1}$) | $10^3\alpha_e$ ($cm^{-1}$) |
|---|---|---|---|---|---|---|---|---|
| HF | -0.45 | -0.52 | 1.626 | 1.629 | 0.75953 | 1148.2 | 6.51 | 5.28 |
| MP2 | 3.06 | 3.00 | 1.684 | 1.687 | 0.70819 | 989.1 | 6.70 | 6.23 |
| MP3 | 2.38 | 2.31 | 1.652 | 1.655 | 0.73523 | 1088.0 | 6.61 | 5.52 |
| MP4DQ | 2.35 | 2.29 | 1.661 | 1.664 | 0.72746 | 1058.7 | 6.44 | 5.67 |
| MP4SDQ | 2.69 | 2.63 | 1.669 | 1.672 | 0.72091 | 1035.2 | 6.65 | 5.95 |
| MPx | 2.29 | 2.22 | 1.661 | 1.664 | 0.72769 | 1060.6 | 6.38 | 5.64 |
| CCD | 2.36 | 2.30 | 1.663 | 1.667 | 0.72557 | 1052.8 | 6.71 | 5.78 |
| CCD+T(CCD) | 2.83 | 2.77 | 1.678 | 1.682 | 0.71266 | 1004.6 | 6.94 | 6.24 |
| CCD+ST(CCD) | 3.07 | 3.01 | 1.682 | 1.686 | 0.70977 | 992.8 | 7.10 | 6.43 |
| QCISD | 2.96 | 2.89 | 1.657 | 1.660 | 0.73154 | 1080.8 | 7.04 | 5.75 |
| QCISD(T) | 3.39 | 3.33 | 1.666 | 1.670 | 0.72299 | 1053.1 | 7.36 | 6.02 |

Table XIII: Computed spectroscopic constants for the $X\ ^3\Pi$ state (MC-311G($2d$)).

| Method | $D_e$ (eV) | $D_0$ (eV) | $r_e$ (Å) | $r_0$ (Å) | $B_e$ ($cm^{-1}$) | $\omega_e$ ($cm^{-1}$) | $\omega_e x_e$ ($cm^{-1}$) | $10^3\alpha_e$ ($cm^{-1}$) |
|---|---|---|---|---|---|---|---|---|
| UHF | 2.59 | 2.54 | 1.759 | 1.763 | 0.64880 | 825.1 | 2.41 | 5.89 |
| MP2 | 3.51 | 3.46 | 1.699 | 1.704 | 0.69560 | 888.3 | 7.20 | 9.26 |
| MP3 | 3.35 | 3.29 | 1.703 | 1.709 | 0.69189 | 876.4 | 6.92 | 9.30 |
| MP4DQ | 3.18 | 3.13 | 1.707 | 1.713 | 0.68873 | 871.4 | 6.53 | 9.10 |
| MP4SDQ | 3.32 | 3.26 | 1.707 | 1.712 | 0.68907 | 892.2 | 7.44 | 9.00 |
| PUHF | 2.78 | 2.72 | 1.759 | 1.764 | 0.64854 | 878.2 | 5.89 | 6.17 |
| PMP2 | 3.72 | 3.67 | 1.708 | 1.713 | 0.68807 | 929.2 | 7.10 | 8.05 |
| PMP3 | 3.56 | 3.50 | 1.715 | 1.720 | 0.68263 | 905.0 | 6.25 | 7.89 |
| QCISD | 3.65 | 3.59 | 1.725 | 1.729 | 0.67439 | 952.7 | 6.89 | 6.32 |
| QCISD(T) | 3.88 | 3.82 | 1.730 | 1.734 | 0.67057 | 959.3 | 6.49 | 5.84 |

the full CI limit within this basis set. Indeed, the QCISD(T) results are hardly different from those at the CCD+ST(CCD) level. From the QCISD(T) $D_e$'s for each state, a rather high $T_e$ value of 4356 $cm^{-1}$ is found. Neglect of triple excitations reduces this value to 4037 $cm^{-1}$, compared to the large basis set MR-SOCI result of 3619 $cm^{-1}$ by BROBM. BL suggest a value of "about 4000 $cm^{-1}$ " based on their high-level calculations. It should be remarked that neither treatment includes triple excitations properly, which might be responsible for part of the disagreement.

As can be seen from Table XII, the computational behavior of the $a\ ^1\Sigma^+$ state could hardly be more different from that of the $X\ ^3\Pi$ state. With the exception of MP2, the anharmonic constants at the other levels can be approximated quite well using the displaced-curve approximation outlined in eqs. (3) and (4). The state is unbound at

the HF level, but has a markedly high correlation energy. Oscillation of the MP series occurs. As a consequence of this, the MP2 spectroscopic constants benefit from a fortunate error compensation to yield values in excellent agreement with those at the CCD+ST(CCD)level, which one should expect to be quite close to the full CI limit for this closed-shell species. Note the small, but nonnegligible effect of single excitations on $r_e$, as well as the quite significant triple excitation effect. The harmonic frequency was computed as 955 $cm^{-1}$ by BROBM, using a very large QZ($3d2f$) STO basis set and Davidson-corrected multi-reference second-order CI. A prediction of 927 $cm^{-1}$ was made using the same method (and an ROHF wavefunction) for the $X\ ^3\Pi$ state, so, based on the deviation of this value from the 'best theoretical estimates', the CCD(ST) value should be quite close to the actual one. Similar considerations apply for the bond length. Oddly enough, when the calculations were repeated at the QCISD and QCISD(T) levels, all spectroscopic constants were affected significantly. Apparently the problems associated with not including the $\exp(\hat{T}_1 + \hat{T}_2)$ ansatz to infinite order are not necessarily restricted to UHF species with heavy spin contamination. Also, the account for triple excitations is much more complete in the present method than in CCD+ST(CCD), which explains the difference in triple excitation contribution. At this level, the $a\ ^1\Sigma^+$ state lies much closer ($T_e$=4355 $cm^{-1}$) to the ground state than was previously believed (*cf.* the $T_e$ values of 6856 $cm^{-1}$ by Bruna *et al.* [Bru81], and of 6628 $cm^{-1}$ by Lutz and Ryan [Lut74]); in this sense, it compares well to the MR-SOCI result of 5079 $cm^{-1}$ obtained by BROBM.

Because the size-consistency corrected CI methods apparently fail to produce a good rendition of the potential curve for the ground state, these methods were abandoned in the study of basis set effects.

Adding a second set of $d$ functions to each atom results in the spectroscopic parameters for the $X\ ^3\Pi$ state given in Table XIII. Principal features are: (a) a systematic shortening of the bond distance, which decreases as the electron correlation method is improved; (b) an almost negligible effect on the dissociation energy; (c) a consistent lowering of the harmonic frequency by about 15 $cm^{-1}$. The QCISD(T) value of 959 $cm^{-1}$ is in excellent agreement with the empirically corrected value of 962 $\pm$ 10 $cm^{-1}$ by RM. Although the MC-311G($2d$) basis set is quite comparable to the one used by RM, slightly lower (about 0.05 eV) $D_e$ values are consistently obtained. The main difference between both basis sets appears to lie in the values for the polarization exponents. Our computed harmonic frequencies and anharmonicity constants are also consistently lower.

One might argue, that since Si has a greater tendency than C to form compounds with significant $d$-character, the Si atom should be given more polarization functions than the C atom, as Larsson [Lar86] did in his study. We investigated the effect of this by using the 6-311G($d$) basis on C and its MC-311G($2d$) partner on Si. Our findings, summarized in Table XIV, are that the $D_e$ is hardly affected; however, a much smaller decrease of about 4 $cm^{-1}$ (compared to the singly polarized basis set) is found for the

Table XIV: Computed spectroscopic constants for the $X\ ^3\Pi$ state (MC-311G(2$d$ on Si, 1$d$ on C)).

| Method | $D_e$ (eV) | $D_0$ (eV) | $r_e$ (Å) | $r_0$ (Å) | $B_e$ ($cm^{-1}$) | $\omega_e$ ($cm^{-1}$) | $\omega_e x_e$ ($cm^{-1}$) | $10^3\alpha_e$ ($cm^{-1}$) |
|---|---|---|---|---|---|---|---|---|
| UHF | 2.59 | 2.54 | 1.757 | 1.761 | 0.65003 | 830.8 | 2.47 | 5.83 |
| MP2 | 3.49 | 3.44 | 1.697 | 1.703 | 0.69667 | 903.0 | 6.98 | 8.83 |
| MP3 | 3.34 | 3.29 | 1.701 | 1.706 | 0.69378 | 895.7 | 6.78 | 8.81 |
| MP4DQ | 3.19 | 3.14 | 1.704 | 1.710 | 0.69095 | 891.8 | 6.49 | 8.64 |
| MP4SDQ | 3.32 | 3.27 | 1.704 | 1.710 | 0.69112 | 910.3 | 7.29 | 8.57 |
| PUHF | 2.79 | 2.74 | 1.758 | 1.762 | 0.64979 | 883.8 | 5.81 | 6.07 |
| PMP2 | 3.71 | 3.65 | 1.706 | 1.711 | 0.68942 | 943.8 | 6.97 | 7.72 |
| PMP3 | 3.56 | 3.50 | 1.712 | 1.717 | 0.68485 | 924.5 | 6.25 | 7.53 |
| QCISD | 3.66 | 3.60 | 1.722 | 1.726 | 0.67661 | 966.3 | 6.51 | 6.14 |
| QCISD(T) | 3.88 | 3.82 | 1.727 | 1.731 | 0.67309 | 972.6 | 6.00 | 5.68 |

harmonic frequency, whereas the bond distance is significantly shorter (and thus closer to the 'experimental' value) than with the full (2$d$) basis set. However, some sensitivity to the values for the exponents cannot be ruled out; this effect should decrease with increasing basis set.

Adding a set of $f$ functions changes the picture dramatically, as witnessed in Table XV. The dissociation energy is increased by no less than 0.25 eV at the QCISD(T) level, whereas the bond distance is shortened by 0.006 Å. The QCISD value for $r_e$ is in exact agreement with the 'experimental' value of 1.719 Å by BROBM. However, the triples contribution again lengthens the bond by 0.005 Å. The $D_e$ results are readily understood in terms of Dunnings finding [Dun89] (which is supported by our studies on combined bond-polarization basis sets [Mar89e]), that [1$d$] and [2$d$1$f$] polarization complements are well balanced, whereas [2$d$] is not. It is possible that further expansion of the polarization complement would result in a shorter bond length; however, the CISD+(DC)/[3$d$2$f$] $r_e$ of BROBM is 0.004 Å longer than our CISD+DC/[1$d$] result, which is a counterindication. In the Dunning sense, the next well-balanced basis set would have a [3$d$2$f$1$g$] polarization complement; however, the hardware and software available to us preclude such a large basis set. Another factor involved might be core-valence correlation. Its proper inclusion would require a basis set of at least double zeta quality in the cores, as well as (most desirably) inner-shell polarization functions. The same remarks apply here. Comparison with BL's [2$d$1$f$] ANO set shows that our computed $r_e$ is much closer to the 'experimental' value. As the triple excitations significantly improve the quality of the computed $D_e$, their neglect does not seem warranted. Finally, the 'experimental' estimate [Ber88a] assumes that their computed CISD+DC values [Ber88a] for the $b\ ^1\Pi$ and $X\ ^3\Pi$ states are in error by almost equal amounts, which implies that triple excitations and higher-order effects are similar for both states. It is easily verified from our results, that this assumption does

Table XV: Computed spectroscopic constants for the $X\ ^3\Pi$ state (MC-311G(2*df*)).

| Method | $D_e$ (eV) | $D_0$ (eV) | $r_e$ (Å) | $r_0$ (Å) | $B_e$ ($cm^{-1}$) | $\omega_e$ ($cm^{-1}$) | $\omega_e x_e$ ($cm^{-1}$) | $10^3\alpha_e$ ($cm^{-1}$) |
|---|---|---|---|---|---|---|---|---|
| UHF | 2.66 | 2.61 | 1.757 | 1.761 | 0.64993 | 826.0 | 2.90 | 5.94 |
| MP2 | 3.72 | 3.66 | 1.690 | 1.695 | 0.70301 | 909.0 | 8.51 | 9.28 |
| MP3 | 3.58 | 3.53 | 1.694 | 1.700 | 0.69957 | 899.1 | 8.22 | 9.26 |
| MP4DQ | 3.38 | 3.32 | 1.698 | 1.704 | 0.69606 | 893.1 | 7.74 | 9.05 |
| MP4SDQ | 3.56 | 3.51 | 1.698 | 1.704 | 0.69591 | 915.6 | 8.49 | 8.92 |
| PUHF | 2.86 | 2.80 | 1.758 | 1.763 | 0.64915 | 879.0 | 5.88 | 6.14 |
| PMP2 | 3.93 | 3.87 | 1.701 | 1.706 | 0.69415 | 946.9 | 7.96 | 8.11 |
| PMP3 | 3.80 | 3.74 | 1.707 | 1.712 | 0.68903 | 923.8 | 7.12 | 7.91 |
| QCISD | 3.89 | 3.83 | 1.719 | 1.723 | 0.67951 | 971.6 | 6.94 | 6.18 |
| QCISD(T) | 4.13 | 4.07 | 1.724 | 1.728 | 0.67502 | 978.7 | 6.24 | 5.63 |

not hold for the three states considered in the present work; upon proceeding from CCD to CCD+T(CCD) (the basis set always being MC-311G(*d*)), the $A\ ^3\Sigma^-$ state lengthens by 0.010 Å, whereas the $a\ ^1\Sigma^+$ state lengthens by no less than 0.015 Å and the $X\ ^3\Pi$ state even shortens by 0.003 Å. Considering the argument that the QCISD - QCISD(T) difference would be more appropriate for the latter state, we find lengthenings of 0.005, 0.011, and 0.009 Å for the $X\ ^3\Pi$, $A\ ^3\Sigma^-$, and $a\ ^1\Sigma^+$ states, respectively. It is not very likely that these differences would suddenly cease to exist upon proceeding to a larger basis set.

As we did compute spectroscopic parameters using the large basis set for the $A\ ^3\Sigma^-$ state (which are listed in Table XVI), we could compare the computational behavior with that of the $X\ ^3\Pi$ state. And indeed, the effect of triple excitations is quite different in both states. Although the effect on the dissociation energy is smaller for the upper than for the lower state, the bond is lengthened by no less than 0.013 Å, compared to the 0.005 Å of the lower state. If a difference of 0.008 Å is introduced by the neglect of triple excitations, even with this rather large basis set and sophisticated electron correlation model, it is not very unlikely that the relative bond lengths determined by BROBM with a somewhat larger basis set using size-consistency corrected CI are in error by a similar amount.

We attempted calculations on the $^1\Pi$ state using the MC-311G(*d*) basis set. However, this open-shell singlet resulted in a heavily contaminated wave function ($\langle\hat{S}^2\rangle \approx 1.0$), for which SCF convergence could only be obtained by using the QCSCF (Quadratically Convergent SCF [Bac81]) option in the program. For the spin-projected UHF and MP energies, the Dunham analysis was even divergent. The QCISD calculations result in an unrealistically small (about 1800 $cm^{-1}$) value for $T_e$ (BROBM found 7259 $cm^{-1}$). Apparently, this is due to the neglect of some 'repulsive' cluster terms involving $\hat{T}_1$ in a QCISD calculation (Bartlett already pointed out in his review article [Bar89] that

Table XVI: Computed spectroscopic constants for the $A\ ^3\Sigma^-$ state (MC-311G(2*df*)).

| Method | $D_e$ (eV) | $D_0$ (eV) | $r_e$ (Å) | $r_0$ (Å) | $B_e$ ($cm^{-1}$) | $\omega_e$ ($cm^{-1}$) | $\omega_e x_e$ ($cm^{-1}$) | $10^3\alpha_e$ ($cm^{-1}$) |
|---|---|---|---|---|---|---|---|---|
| UHF | 2.05 | 1.99 | 1.763 | 1.766 | 0.64575 | 1005.8 | 4.47 | 4.04 |
| MP2 | 3.70 | 3.64 | 1.805 | 1.809 | 0.61600 | 871.2 | 5.52 | 5.33 |
| MP3 | 3.61 | 3.56 | 1.804 | 1.807 | 0.61699 | 883.4 | 4.77 | 4.95 |
| MP4DQ | 3.39 | 3.34 | 1.799 | 1.802 | 0.62026 | 900.2 | 4.45 | 4.70 |
| MP4SDQ | 3.52 | 3.46 | 1.803 | 1.807 | 0.61745 | 886.9 | 4.64 | 4.87 |
| PUHF | 1.99 | 1.93 | 1.763 | 1.765 | 0.64604 | 1007.0 | 4.47 | 4.03 |
| PMP2 | 3.66 | 3.61 | 1.805 | 1.809 | 0.61622 | 872.1 | 5.51 | 5.32 |
| PMP3 | 3.60 | 3.55 | 1.804 | 1.807 | 0.61712 | 883.9 | 4.77 | 4.95 |
| QCISD | 3.47 | 3.42 | 1.802 | 1.806 | 0.61789 | 888.6 | 4.70 | 4.87 |
| QCISD(T) | 3.66 | 3.61 | 1.815 | 1.818 | 0.60968 | 854.6 | 4.75 | 5.17 |

these terms could be important for a pathological reference wavefunction which results in very high $\hat{T}_1$ amplitudes; such a case is definitely at hand here). For what it is worth, the bond length increases by 0.009 Å upon incorporating triple excitations; at the same level of theory, the effect on the $X\ ^3\Pi$ state is only 0.005 Å. This picture might well change completely when a restricted open-shell wavefunction could be used, but it does indicate again that the assumption of BROBM about constant bond length errors in their calculations is not valid.

At this point, we prefer to think of the 1.719 Å 'best estimate' as a lower bound, with our own value of 1.725 Å as an upper bound for $r_e$ ($X\ ^3\Pi$). So until the X-A transition has been resolved experimentally, we propose preliminary $r_e$ and $r_0$ values of 1.722±0.003 and 1.726±0.003 Å, respectively.

Finally, the addition of diffuse functions results in a small increase (about 0.02 eV) in binding energy, but has a negligible effect on the other spectroscopic constants. It is therefore not considered further.

Assuming additivity of corrections between the diffuse functions and the additional polarization functions, this results in a direct $D_e$ of 4.15 eV. Applying the G1 theory [Pop89] would then result in a basis set incompleteness correction of 0.16 eV. As the G1 theory has a general level of accuracy of ±0.1 eV, this results in a 'best estimate' of 4.31±0.10 eV for the dissociation energy $D_e$ of SiC. This is about 0.1 eV lower than the best previous determination by BL, who suggested 4.4 eV based on an empirical correction for the errors in $C_2$ and $Si_2$. It is remarked here that the G1 theory does not correct for inner-shell effects, being developed for first-row compounds. However, the effect of this on the dissociation energy of a mixed first-second row molecule should be negligible. Further improvement of the basis set (particularly the addition of *g* functions) could also slightly increase the computed $D_e$, but for the philosophy behind G1 theory to remain valid, this should also imply improvements in the basis set used to calculate

Table XVII: Spectroscopic constants used in thermochemistry for SiC.

| State | $g_i$ | $T_e$ ($cm^{-1}$) | $\omega_e$ ($cm^{-1}$) | $\omega_e x_e$ ($cm^{-1}$) | $B_e$ ($cm^{-1}$) | $10^3\alpha_e$ ($cm^{-1}$) |
|---|---|---|---|---|---|---|
| $X\ ^3\Pi_2$ | 2 | -37.3[j] | 979[a] | 6.24[a] | 0.67502[a] | 5.63[a] |
| $X\ ^3\Pi_1$ | 2 | 0 | 979[a] | 6.24[a] | 0.67502[a] | 5.63[a] |
| $X\ ^3\Pi_0$ | 2 | 37.3[j] | 979[a] | 6.24[a] | 0.67502[a] | 5.63[a] |
| $A\ ^3\Sigma^-$ | 3 | 3831[a] | 855[a] | 4.75[a] | 0.60968[a] | 5.17[a] |
| $a\ ^1\Sigma^+$ | 1 | 4355[b] | 1053[b] | 7.36[b] | 0.72299[b] | 6.02[b] |
| $b\ ^1\Pi$ | 2 | 7259[c] | 963[c] | 8.31[i] | 0.67466[d] | 9.32[c] |
| $c\ ^1\Delta$ | 2 | 9306[g] | 855[f] | 7.07[i] | 0.60535[c] | 10.57[c] |
| $d\ ^1\Sigma^+$ | 1 | 11614[h] | 980[e] | 10.19[i] | 0.62083[d] | 2.76[c] |

$D_e(X\ ^3\Pi) = 4.36 \pm 0.05$ eV $= 35167 \pm 400$ $cm^{-1}$

(a) This work, QCISD(T)/MC-311G(2*df*)
(b) This work, QCISD(T)/MC-311G(*d*)
(c) BROBM [Ber88a], ab initio
(d) Calculated using experimental $B_0$ and ab initio $\alpha_e$ from BROBM [Ber88a]
(e) Estimated from experimental $D_0$ and $B_0$ values and computed $\alpha_e$, all from BROBM [Ber88a]
(f) MRD-CI value from Bruna *et al.* [Bru80]
(g) $c\ ^1\Delta - A\ ^3\Sigma^-$ separation from BROBM [Ber88a] (ab initio); $X\ ^3\Pi - A\ ^3\Sigma^-$ separation from this work
(h) $d\ ^1\Sigma^+$ - $a\ ^1\Sigma^+$ separation from BROBM [Ber88a] (observed); $X\ ^3\Pi - a\ ^1\Sigma^+$ separation from this work
(i) $\omega_e x_e$ estimated from linear Birge-Sponer relationship
(j) Spin-orbit coupling constant $A = -37.3$ $cm^{-1}$ from [Coo83]

the correction terms, which will lower them. The addition of an *sp* bond function to the [2*d*1*f*] polarization space however, should increase the direct dissociation energy by about 0.1 eV, and the computed dissociation energy with isogyric correction by about 0.05 eV [Mar89e]. It is possible that a further small increase would result from the addition of a *d*-type bond function. Our determination of 4.31 eV is then perhaps best considered as a lower limit; the BL estimate of 4.4 eV as an upper limit. The actual $D_e$ is probably somewhere in between, so we recommend a preliminary value of 4.36 ± 0.05 eV.

The computed $T_e$ value for the $X\ ^3\Pi$ - $A\ ^3\Sigma^-$ transition is 3790 $cm^{-1}$ at the highest level of theory used, in perfect agreement with the 3781 $cm^{-1}$ value of BL. Neglecting the effect of triple excitations leads to a value of 3390 $cm^{-1}$, which again underscores their importance. Apparently, the multireference CI treatment by BL does include some, but of course not all, of the dominant triple excitation effects.

### 4.4.4 Thermochemistry

The data employed in setting up the partition functions have been summarized in Table XVII. Table XVIII presents the thermodynamic functions for SiC over a 100-6000 K temperature range in increments of 100 K. For the two lowest-lying states, our own

QCISD(T)/MC-311G(2*df*) data were used. For the less prominent $a\ ^1\Sigma^+$ state, we thought the data at the QCISD(T)/MC-311G(*d*) level to be accurate enough. For the three next states, a mixture of data from several other publications was employed; as these states are much less prominent in the total partition function, errors in these spectroscopic constants should not have too severe consequences (*vide infra*).

Some spectroscopic constants were still missing. These were then estimated from the available data using some well-known relationships between spectroscopic constants. More specifically, the harmonic frequency for the $d\ ^1\Sigma^+$ state was estimated from the experimental rotational and centrifugal distortion constants

$$D_e = \frac{4B_e^3}{\omega_e^2} \tag{4.7}$$

or

$$D_0 \approx \frac{4B_0^3}{\omega_0^2} \tag{4.8}$$

from which

$$\omega_e \approx \sqrt{\frac{4B_0^3}{D_0}} \tag{4.9}$$

whereas the anharmonicity constants for all three states were estimated from the computed dissociation and transition energies and a linear Birge-Sponer relationship:

$$\omega_e x_e \approx \frac{\omega_e^2}{4(D_e(X^3\Pi) - T_e)}(6) \tag{4.10}$$

The rotation-vibration coupling constant $\alpha_e$ can be derived from $r_e$, $r_0$, and either an ab initio $B_e$ or an experimental $B_0$, using the relationships

$$\alpha_e = 2B_e(1 - \frac{r_e^2}{r_0^2}) = 2B_e(\frac{r_0^2}{r_e^2} - 1) \tag{4.11}$$

For the $b\ ^1\Pi$ and $d\ ^1\Sigma^+$ states the experimental $B_0$ from BROBM was used; for the $c\ ^1\Delta$ state, we employed the ab initio $B_e$ from the same source.

Figure 4.13 presents the relative abundances for the six electronic states considered as a function of temperature. It is apparent that the ground state, being favored by its additional degeneracy entropy as a $\Pi$ state, remains dominant even at 6000 K, where it still accounts for 76 % of the total. At this same temperature, the $A\ ^3\Sigma^-$ state accounts for some 12 %. Both states are favored against the others by their triplet degeneracy entropies (at these elevated temperatures, the spin-orbit splitting levels of the $X\ ^3\Pi$ state are effectively degenerate). The $a\ ^1\Sigma^+$ state, only slightly higher in energy than the $A\ ^3\Sigma^-$ state but nondegenerate, accounts for 5.1 %, the $b\ ^1\Pi$ state (significantly higher but having degeneracy two) for 4.2 %, and the $c\ ^1\Delta$ state for just under 2 %. The $d\ ^1\Sigma^+$ state fails to reach 1 % of the total, so the approximation to neglect all higher states appears to be justified.

Table XVIII: Thermodynamic functions at 0.1 MPa for SiC (all functions in J/K mol, except $H - H_0$ which is in kJ/mol, and $\log K_f$ which is dimensionless).

| $T$ (K) | $C_p$ | $S^0$ | gef($T$) | $H - H_0$ | $\Delta C_p$ | $\Delta S^0$ | $\Delta$gef($T$) | $\Delta H$ | $-\log K_f$ |
|---|---|---|---|---|---|---|---|---|---|
| 100 | 30.497 | 193.238 | 161.224 | 3.201 | -18.796 | -82.827 | -345.299 | -416.803 | -234.743 |
| 200 | 29.889 | 214.028 | 183.042 | 6.197 | -14.811 | -94.556 | -217.448 | -418.471 | -119.712 |
| 298.15 | 31.057 | 226.150 | 195.357 | 9.181 | -12.302 | -99.929 | -177.967 | -419.782 | -81.980 |
| 300 | 31.085 | 226.343 | 195.548 | 9.238 | -11.987 | -100.001 | -177.484 | -419.805 | -81.506 |
| 400 | 32.585 | 235.494 | 204.436 | 12.423 | -9.843 | -103.141 | -158.538 | -420.890 | -62.458 |
| 500 | 33.819 | 242.904 | 211.412 | 15.746 | -8.301 | -105.162 | -147.673 | -421.793 | -51.055 |
| 600 | 34.763 | 249.157 | 217.195 | 19.177 | -7.189 | -106.571 | -140.712 | -422.565 | -43.468 |
| 700 | 35.513 | 254.574 | 222.156 | 22.692 | -6.339 | -107.613 | -135.914 | -423.240 | -38.057 |
| 800 | 36.152 | 259.359 | 226.513 | 26.276 | -5.641 | -108.413 | -132.428 | -423.838 | -34.006 |
| 900 | 36.731 | 263.651 | 230.405 | 29.921 | -5.032 | -109.041 | -129.796 | -424.370 | -30.858 |
| 1000 | 37.274 | 267.549 | 233.928 | 33.621 | -4.485 | -109.543 | -127.746 | -424.847 | -28.343 |
| 1100 | 37.790 | 271.126 | 237.149 | 37.375 | -3.990 | -109.947 | -126.109 | -425.269 | -26.288 |
| 1200 | 38.282 | 274.435 | 240.120 | 41.179 | -3.544 | -110.275 | -124.777 | -425.645 | -24.577 |
| 1300 | 38.747 | 277.518 | 242.880 | 45.030 | -3.148 | -110.542 | -123.672 | -425.980 | -23.130 |
| 1400 | 39.184 | 280.406 | 245.458 | 48.927 | -2.802 | -110.762 | -122.742 | -426.276 | -21.890 |
| 1500 | 39.593 | 283.124 | 247.879 | 52.866 | -2.503 | -110.944 | -121.951 | -426.542 | -20.817 |
| 1600 | 39.973 | 285.691 | 250.163 | 56.845 | -2.250 | -111.098 | -121.267 | -426.778 | -19.878 |
| 1700 | 40.324 | 288.125 | 252.325 | 60.860 | -2.039 | -111.229 | -120.673 | -426.993 | -19.051 |
| 1800 | 40.648 | 290.439 | 254.379 | 64.909 | -1.868 | -111.340 | -120.152 | -427.187 | -18.315 |
| 1900 | 40.946 | 292.645 | 256.335 | 68.989 | -1.730 | -111.437 | -119.690 | -427.367 | -17.657 |
| 2000 | 41.220 | 294.753 | 258.204 | 73.098 | -1.621 | -111.522 | -119.280 | -427.534 | -17.066 |
| 2100 | 41.471 | 296.770 | 259.993 | 77.233 | -1.539 | -111.600 | -118.912 | -427.691 | -16.531 |
| 2200 | 41.702 | 298.705 | 261.709 | 81.392 | -1.479 | -111.669 | -118.582 | -427.842 | -16.044 |
| 2300 | 41.914 | 300.563 | 263.358 | 85.573 | -1.437 | -111.735 | -118.282 | -427.988 | -15.600 |
| 2400 | 42.108 | 302.351 | 264.946 | 89.774 | -1.412 | -111.795 | -118.011 | -428.130 | -15.194 |
| 2500 | 42.286 | 304.074 | 266.476 | 93.994 | -1.399 | -111.852 | -117.763 | -428.271 | -14.820 |
| 2600 | 42.450 | 305.736 | 267.955 | 98.231 | -1.398 | -111.907 | -117.537 | -428.410 | -14.474 |
| 2700 | 42.601 | 307.341 | 269.384 | 102.484 | -1.403 | -111.960 | -117.330 | -428.549 | -14.155 |
| 2800 | 42.741 | 308.893 | 270.767 | 106.751 | -1.415 | -112.011 | -117.139 | -428.691 | -13.858 |
| 2900 | 42.871 | 310.395 | 272.108 | 111.032 | -1.430 | -112.060 | -116.962 | -428.832 | -13.582 |
| 3000 | 42.992 | 311.851 | 273.409 | 115.326 | -1.448 | -112.109 | -116.799 | -428.975 | -13.324 |
| 3100 | 43.105 | 313.262 | 274.672 | 119.631 | -1.468 | -112.157 | -116.650 | -429.122 | -13.084 |
| 3200 | 43.212 | 314.633 | 275.899 | 123.947 | -1.486 | -112.203 | -116.510 | -429.270 | -12.858 |
| 3300 | 43.314 | 315.964 | 277.093 | 128.274 | -1.504 | -112.250 | -116.380 | -429.418 | -12.646 |
| 3400 | 43.412 | 317.258 | 278.256 | 132.610 | -1.517 | -112.295 | -116.259 | -429.569 | -12.446 |
| 3500 | 43.506 | 318.518 | 279.388 | 136.956 | -1.528 | -112.338 | -116.147 | -429.722 | -12.258 |
| 3600 | 43.599 | 319.745 | 280.492 | 141.312 | -1.534 | -112.382 | -116.042 | -429.874 | -12.081 |
| 3700 | 43.690 | 320.941 | 281.569 | 145.677 | -1.535 | -112.424 | -115.943 | -430.027 | -11.913 |
| 3800 | 43.781 | 322.108 | 282.621 | 150.050 | -1.531 | -112.464 | -115.851 | -430.180 | -11.754 |
| 3900 | 43.873 | 323.246 | 283.648 | 154.433 | -1.519 | -112.504 | -115.764 | -430.333 | -11.603 |
| 4000 | 43.966 | 324.358 | 284.652 | 158.826 | -1.500 | -112.542 | -115.684 | -430.483 | -11.460 |
| 4100 | 44.060 | 325.445 | 285.634 | 163.227 | -1.475 | -112.579 | -115.607 | -430.632 | -11.324 |
| 4200 | 44.157 | 326.508 | 286.594 | 167.638 | -1.442 | -112.613 | -115.536 | -430.778 | -11.195 |
| 4300 | 44.256 | 327.548 | 287.534 | 172.059 | -1.402 | -112.647 | -115.468 | -430.920 | -11.071 |
| 4400 | 44.359 | 328.567 | 288.456 | 176.490 | -1.354 | -112.679 | -115.404 | -431.058 | -10.953 |
| 4500 | 44.464 | 329.565 | 289.358 | 180.931 | -1.298 | -112.709 | -115.343 | -431.190 | -10.841 |
| 4600 | 44.573 | 330.543 | 290.243 | 185.383 | -1.235 | -112.737 | -115.286 | -431.317 | -10.733 |
| 4700 | 44.686 | 331.503 | 291.110 | 189.846 | -1.165 | -112.763 | -115.233 | -431.437 | -10.630 |
| 4800 | 44.802 | 332.445 | 291.962 | 194.321 | -1.088 | -112.786 | -115.182 | -431.549 | -10.531 |
| 4900 | 44.921 | 333.370 | 292.797 | 198.807 | -1.005 | -112.808 | -115.134 | -431.654 | -10.436 |
| 5000 | 45.044 | 334.279 | 293.618 | 203.306 | -0.915 | -112.828 | -115.087 | -431.750 | -10.346 |
| 5100 | 45.170 | 335.172 | 294.424 | 207.816 | -0.820 | -112.845 | -115.043 | -431.836 | -10.258 |
| 5200 | 45.298 | 336.051 | 295.216 | 212.340 | -0.720 | -112.859 | -115.001 | -431.913 | -10.174 |
| 5300 | 45.429 | 336.915 | 295.995 | 216.876 | -0.615 | -112.872 | -114.961 | -431.980 | -10.094 |
| 5400 | 45.562 | 337.765 | 296.761 | 221.426 | -0.506 | -112.883 | -114.922 | -432.036 | -10.016 |
| 5500 | 45.696 | 338.603 | 297.514 | 225.989 | -0.395 | -112.891 | -114.885 | -432.081 | -9.941 |
| 5600 | 45.831 | 339.427 | 298.255 | 230.566 | -0.281 | -112.897 | -114.849 | -432.114 | -9.869 |
| 5700 | 45.967 | 340.240 | 298.984 | 235.156 | -0.165 | -112.900 | -114.815 | -432.136 | -9.799 |
| 5800 | 46.103 | 341.040 | 299.702 | 239.759 | -0.048 | -112.903 | -114.783 | -432.147 | -9.732 |
| 5900 | 46.238 | 341.830 | 300.410 | 244.376 | 0.069 | -112.902 | -114.750 | -432.147 | -9.667 |
| 6000 | 46.373 | 342.608 | 301.107 | 249.007 | 0.187 | -112.900 | -114.719 | -432.133 | -9.604 |

Figure 4.13: Relative abundance of the five lowest states of SiC as a function of temperature.

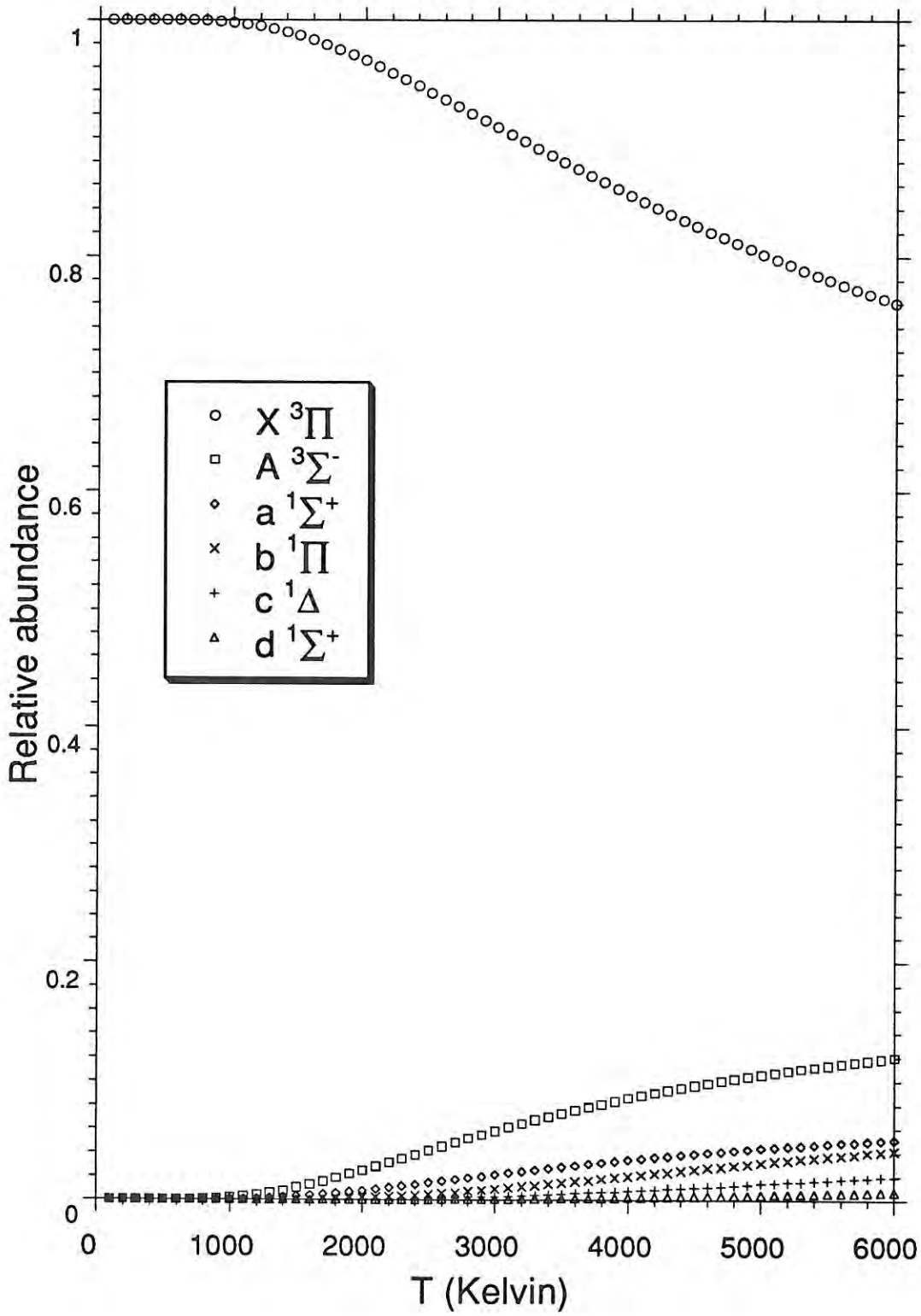

Now considering the 'magical threshold' of 1 % for each state, this occurs around 1500 K for $A\ ^3\Sigma^-$, around 2200 K for $a\ ^1\Sigma^+$, around 3200 K for $b\ ^1\Pi$, and around 4500 K for the $c\ ^1\Delta$ state. For a thumbnail estimate of their effect at these temperatures on the thermodynamic functions $C_p$, $S^0$, gef($T$), and $H - H_0$, one could take their values for the individual states and interpolate linearly[1]. As, for example, the four thermodynamic functions differ by only about 0.1, 2.0, 1.6 J/K mol, and 0.5 kJ/mol at 1500 K for the two lowest-lying states, neglect of a 1 % contribution would result in errors of about 0.001, 0.02, 0.016, and 0.005, respectively, at this temperature. For the $a\ ^1\Sigma^+$ *vs.* $X\ ^3\Pi$ states, errors at 2200 K will only be on the order of 0.0006, 0.012, 0.010, and 0.004. Considering the $b\ ^1\Pi$ state, residuals will (at 3200 K) be on the order of 0.004, 0.006, 0.003, and 0.007 when neglected. Neglect of the $c\ ^1\Delta$ state at 4500 K, finally, would result in errors on the order of 0.01, 0.03, 0.025, and 0.03. This magnitude of errors is certainly negligible against the other errors inherent in this treatment; owever, at elevated temperatures they will become significant (see below).

The thermodynamic functions $\Delta C_p$, $\Delta S^0$, $\Delta$gef($T$), and $\Delta(H - H_0)$, for the association reaction are also tabulated in Table XVIII. Also given is $-\log K_f$ for the association reaction Si(g) + C(g) $\rightarrow$ SiC(g). (The thermodynamic functions used for Si and C atoms were reconstructed from the energy level information given in the JANAF tables [Jan85]. It should be noted that the three components of the ground state of Si are mixed up as printed, and that even with a suggested additional $^3P$ state at 33326 cm$^{-1}$, minor deviations from the JANAF tables are seen above 5500 K.) The primary qualitative information to be deducted from these tables is that SiC is apparently quite stable as a molecule, having a formation constant of the order of $10^{9.6}$ even at 6000 K.

#### 4.4.4.1 Effect of various approximations

Table XIX lists, at temperatures from 1000 to 6000 K in increments of 1000 K, as well as at room temperature, the deviations in the thermodynamic functions introduced by a number of approximations. In the table and the subsequent discussion, all changes are incremental; i.e., we are always discussing the effect of the next approximation with respect to the previous approximate partition function, never the cumulated effect of them all.

The first one is the neglect of the isotope effect. Apparently, this effect is rather small and becomes practically unnoticeable for $C_p$ and $H - H_0$ at practical temperatures. The effect on $S^0$ and gef($T$) is basically constant at these temperatures. It mainly comes from the translation terms.

The second approximation considered is the neglect of the $d\ ^1\Sigma^+$ state, which should give some indication of the effct of neglecting higher excited states. Apparently, the effect

[1] gef($T$) symbolizes the Gibbs energy function gef($T$) $\equiv -(G(T) - H(0))/T$ (Section 1.12).

Table XIX: overview of the effect of different approximations on the computed thermochemical functions.

| T(K) | $\delta C_p$ J/K mol | $\delta S^0$ J/K mol | $\delta$ gef($T$) J/K mol | $\delta H$ kJ/mol | $\delta C_p$ J/K mol | $\delta S^0$ J/K mol | $\delta$ gef($T$) J/K mol | $\delta H$ kJ/mol |
|---|---|---|---|---|---|---|---|---|
| | Neglect of isotope effects | | | | Neglect of highest excited state ($d\ ^1\Sigma^+$) | | | |
| 298.15 | -0.004 | -0.052 | -0.051 | 0.000 | 0.000 | 0.000 | 0.000 | 0.000 |
| 1000 | -0.002 | -0.057 | -0.055 | -0.003 | 0.000 | 0.000 | 0.000 | 0.000 |
| 2000 | 0.000 | -0.058 | -0.056 | -0.004 | -0.023 | -0.003 | 0.000 | -0.006 |
| 3000 | -0.001 | -0.059 | -0.057 | -0.005 | -0.143 | -0.032 | -0.005 | -0.082 |
| 4000 | -0.001 | -0.058 | -0.057 | -0.005 | -0.282 | -0.094 | -0.019 | -0.299 |
| 5000 | 0.000 | -0.058 | -0.057 | -0.005 | -0.362 | -0.167 | -0.042 | -0.628 |
| 6000 | 0.000 | -0.058 | -0.058 | -0.005 | -0.365 | -0.235 | -0.068 | -0.997 |
| | Neglect of all but the first excited states (i.e. $a\ ^1\Sigma^+$, $b\ ^1\Pi$, $c\ ^1\Delta$, and $d\ ^1\Sigma^+$) | | | | Effect of a +100 cm$^{-1}$error in $T_e$ ($X\ ^3\Pi \rightarrow A\ ^3\Sigma^-$) | | | |
| 298.15 | 0.000 | 0.000 | 0.000 | 0.000 | 0.000 | 0.000 | 0.000 | 0.000 |
| 1000 | -0.098 | -0.018 | -0.002 | -0.015 | -0.057 | -0.016 | -0.003 | -0.013 |
| 2000 | -1.032 | -0.328 | -0.07 | -0.516 | -0.035 | -0.060 | -0.022 | -0.076 |
| 3000 | -2.118 | -0.963 | -0.256 | -2.121 | 0.028 | -0.061 | -0.036 | -0.075 |
| 4000 | -2.782 | -1.673 | -0.522 | -4.604 | 0.047 | -0.049 | -0.041 | -0.034 |
| 5000 | -3.181 | -2.341 | -0.82 | -7.603 | 0.047 | -0.038 | -0.042 | 0.013 |
| 6000 | -3.307 | -2.938 | -1.124 | -10.877 | 0.041 | -0.030 | -0.040 | 0.057 |
| | Neglect of all excited states | | | | Neglect of spin-orbit coupling | | | |
| 298.15 | 0.000 | 0.000 | 0.000 | 0.000 | -0.177 | 0.089 | 1.407 | -0.393 |
| 1000 | -0.649 | -0.140 | -0.022 | -0.118 | -0.016 | 0.008 | 0.439 | -0.430 |
| 2000 | -2.365 | -1.223 | -0.331 | -1.785 | -0.004 | 0.002 | 0.222 | -0.439 |
| 3000 | -2.375 | -2.218 | -0.806 | -4.238 | -0.001 | 0.001 | 0.148 | -0.441 |
| 4000 | -1.948 | -2.844 | -1.244 | -6.403 | -0.001 | 0.000 | 0.112 | -0.442 |
| 5000 | -1.590 | -3.237 | -1.606 | -8.161 | -0.001 | 0.000 | 0.089 | -0.443 |
| 6000 | -1.378 | -3.507 | -1.901 | -9.634 | 0.000 | 0.001 | 0.074 | -0.444 |
| | RRHO approximation ($\omega_0 = \omega_e - 2\omega_e x_e$) | | | | Effect of a +10 cm$^{-1}$error in $\omega_e$ for the ground state | | | |
| 298.15 | -0.038 | -0.059 | -0.045 | -0.004 | -0.049 | -0.018 | -0.004 | -0.005 |
| 1000 | -0.314 | -0.233 | -0.109 | -0.125 | -0.028 | -0.076 | -0.041 | -0.036 |
| 2000 | -0.732 | -0.577 | -0.255 | -0.644 | -0.018 | -0.091 | -0.063 | -0.056 |
| 3000 | -1.230 | -0.964 | -0.425 | -1.615 | -0.027 | -0.100 | -0.073 | -0.078 |
| 4000 | -1.903 | -1.404 | -0.614 | -3.162 | -0.048 | -0.109 | -0.082 | -0.114 |
| 5000 | -2.911 | -1.930 | -0.823 | -5.536 | -0.087 | -0.124 | -0.088 | -0.180 |
| 6000 | -4.311 | -2.580 | -1.060 | -9.119 | -0.123 | -0.144 | -0.096 | -0.287 |
| | Effect of a +2 cm$^{-1}$error in $\omega_e x_e$ on ditto | | | | Effect of a +0.005 cm$^{-1}$error in $B_e$ on ditto | | | |
| 298.15 | 0.021 | 0.007 | 0.002 | 0.001 | 0.000 | -0.062 | -0.062 | 0.000 |
| 1000 | 0.062 | 0.053 | 0.022 | 0.030 | -0.002 | -0.063 | -0.063 | -0.001 |
| 2000 | 0.156 | 0.121 | 0.054 | 0.135 | -0.004 | -0.065 | -0.064 | -0.003 |
| 3000 | 0.347 | 0.215 | 0.091 | 0.373 | -0.008 | -0.068 | -0.064 | -0.010 |
| 4000 | 0.733 | 0.364 | 0.139 | 0.897 | -0.013 | -0.070 | -0.066 | -0.020 |
| 5000 | 1.102 | 0.571 | 0.204 | 1.836 | -0.024 | -0.074 | -0.067 | -0.038 |
| 6000 | 0.993 | 0.772 | 0.283 | 2.937 | -0.043 | -0.081 | -0.069 | -0.070 |
| | Effect of a +0.002 cm$^{-1}$error in $\alpha_e$ on ditto | | | | | | | |
| 298.15 | 0.006 | 0.014 | 0.013 | 0.000 | | | | |
| 1000 | 0.040 | 0.038 | 0.021 | 0.016 | | | | |
| 2000 | 0.097 | 0.082 | 0.040 | 0.084 | | | | |
| 3000 | 0.183 | 0.136 | 0.063 | 0.221 | | | | |
| 4000 | 0.365 | 0.211 | 0.090 | 0.482 | | | | |
| 5000 | 0.758 | 0.330 | 0.125 | 1.023 | | | | |
| 6000 | 1.301 | 0.515 | 0.173 | 2.051 | | | | |

on the free energy function is negligible, that on the entropy somewhat less so, whereas the enthalpy might change by about 1 kJ/mol at 6000 K, where $C_p$ changes by 0.37 J/K mol. These effects drop sharply with temperature.

The third one is the neglect of all excited states but the first (i.e. $a\ ^1\Sigma^+$, $b\ ^1\Pi$, $c\ ^1\Delta$, and $d\ ^1\Sigma^+$). It is hardly noticeable at lower temperatures, but at 6000 K, the effect on $H - H_0$ may increase to as much as 11 kJ/mol. The effect on entropy is just under 3 J/K mol, whereas that on the free energy function is about 1.1 J/K mol.

The effects of also neglecting the first excited state $A\ ^3\Sigma^-$ are similar, except that the heat capacity is affected markedly less.

The effect of neglecting the spin-orbit coupling in the ground state is apparently only felt at room or lower temperatures. It may safely be ignored at temperatures of interest for high-temperature chemistry. The enthalpy effect, which has an asymptote at the spin-orbit coupling constant of 37.3 $cm^{-1}$, may basically be seen as the consequence of equal population in the three spin-orbit levels. The effect on the free energy function at these temperatures is readily explained: since $\delta S^0$ is very small, $\delta$gef $\approx$ -$\delta(H - H_0)/T$.

Finally, the RRHO approximation does result in an error of about 8 kJ/mol on the enthalpy, and of grossly 4, 2, and 1 J/K mol on the molar heat, entropy and free energy function, respectively, at 6000 K. Given the drastic nature of this approximation, this relatively low magnitude of errors is quite surprising. The errors in $C_p$ and $H - H_0$ sink drastically with temperature: those in $S^0$ and gef($T$) function appear to decrease linearly.

In order now to assess the effect of errors in our computed spectroscopic constants, we evaluated the partition function for the ground state using small perturbations in the constants.

The effect considered of a +100 $cm^{-1}$ error on the $X\ ^3\Pi \rightarrow A\ ^3\Sigma^-$ transition energy (neglecting all other states) is found to be surprisingly small: only of the order of 0.05 J/K mol on $C_p$, $S^0$ and gef($T$), and 0.05 kJ/mol on $H - H_0$. This implies that the electronic transition energies determined in this work should normally be accurate enough. Note that the error changes sign for $C_p$ and $H - H_0$, and that it appears to pass through a maximum (in absolute value) at different temperatures for all spectroscopic constants.

Increasing the harmonic frequency by 10 $cm^{-1}$ appears to result in only minor effects (less than 0.3 kJ/mol on the enthalpy, about 0.1 J/K mol on the other constants). For the excited state contributions, the effects of such errors would then certainly become negligible. This means that our ab initio frequencies are certainly accurate enough for the present purpose.

Next, the effect of changing the ground-state rotational constant by 0.005 $cm^{-1}$ (which would imply a large error in the bond distance of about 0.006 Å) would result in only petty effects (on the order of 0.05 to 0.08 J/K mol), which are almost constant with temperature, on $S^0$ and gef($T$). For the other two functions, the effect rises with temperature, but can still be safely ignored at 6000 K.

Oddly enough, the partition functions are rather sensitive to the values used for the anharmonicity constant. However, a perturbation of $+2$ cm$^{-1}$ (which would imply a relative error of 33 %), is necessary to produce an enthalpy effect which is about 3 kJ/mol at 6000 K, but which does not exceed 1.2 J/K mol for $C_p$ and $S^0$, and 0.4 J/K mol for gef($T$). Furthermore, the effects drop with temperature. This suggests that some care should be taken in evaluating them for the ground state, but that highly approximate values can safely be used for the excited states. Similar considerations apply for a 0.002 cm$^{-1}$ perturbation (relative error of 40 % !) on the rotation-vibration coupling constant. Here the effect drops steeply with decreasing temperature, so that it becomes quite harmless below even 3000 K.

All this means, that the spectroscopic constants computed ab initio in this work should be quite good enough for the construction of the partition functions even to very high temperatures. If higher accuracy in the partition functions is required, the most desirable step would be to find some approximate parameters for the higher excited states. Even crude SCF values would suffice, given that the electronic transition energy be evaluated at some modest correlated level. However, to make these improvements sensible, it would be even more imperative to obtain a more accurate estimate for the binding energy.

## 4.5 Ab initio spectroscopy and thermochemistry of the BN molecule

### 4.5.1 Introduction

Surface coating by neoceramic materials has become very important in the field of materials science. One compound that has attracted a lot of interest is boron nitride [Gme88]. It has three crystalline modifications, $\alpha$, $\beta$, and $\gamma$, which resemble graphite, cubic diamond, and hexagonal diamond, respectively, in their crystalline structure and physical properties. The $\beta$ and $\gamma$ forms, which are very well suited for surface coating, are metastable under normal conditions of temperature and pressure, just as diamond is metastable compared to graphite.

It has proven extremely difficult to obtain $\beta$ or $\gamma$ BN as thin solid films. (See the introduction of [Mar89c] for references.) Experimental research [Zfi87] as to the relationship between the composition of the plasma in chemical vapor deposition techniques and the nature of the deposited film has been carried out. It has become apparent that the composition of the plasma is of key importance to the final product, and that accurate thermochemical data for the components of the plasma — which are cluster molecules $B_n$, $N_n$, and $B_mN_n$ as well as their ions — are essential for a better understanding and control of the process.

For the atoms B and N there is of course no problem [Jan85], except that the heat

of formation of gaseous boron is not well known because of purification problems. An overwhelming abundance of data is available on the $N_2$ molecule [Hub79, Ric71, Ohn82]. An accurate atomization energy for $N_3$ has recently been computed ab initio [Mar90e], whereas the first published data on $B_3$, $B_2N$ and $BN_2$ were computed by Martin *et al.* (MFG) [Mar89c], where $B_2$, BN, $B_3$, and $N_3$ were also considered. $B_2$ was considered by several authors, including Dupuis and Liu [Dup78], Bruna and Wright [Bru89], Carmichael [Car89], and Knight *et al.* [Kni87]. $B_3$ has since been considered by Marinelli and Pellegatti [Mar89a].

Despite its small size, BN has not been studied in great detail, although it is of some interest to theoretical chemistry (being isoelectronic with $C_2$) besides its importance in materials science. Spectroscopic work is limited to the pioneering work of Douglas and Herzberg [Dou40], work by Thrush [Thr60] and Mosher and Frosch [Mos70], as well as two more recent papers by Bredohl *et al.* (BDHN) [Bre84, Bre85].

The most complete ab initio study to date is the work of Karna and Grein (KG) [Kar85, Kar88], who studied a large number of valence states at the MRD-CI [Bue74] level with a $(9s5p1d)/[5s3p1d]$ basis set [Huz65, Dun70]. Karna and Grein find the ground state to be $X\ ^3\Pi$, with the $a\ ^1\Sigma^+$ state lying only 0.1 eV above. Their computed $r_e$ of 1.327 Åfor the $X\ ^3\Pi$ state, as well as that of 1.397 Å for the $A\ ^3\Pi$ state[2] was in disagreement with the accepted experimental values of 1.281 and 1.326 Å[Dou40], respectively. This prompted BDHN to perform a new analysis [Bre85], which yielded results ($r_0$=1.3291 and 1.3736 Å, respectively) in much better agreement with the KG values. BDHN had previously derived $r_0$=1.283 Å and $\Delta G(\frac{1}{2})$=1712 $cm^{-1}$ for the $a\ ^1\Sigma^+$ state [Bre84]; their $\Delta G(\frac{1}{2})$ values for the $X\ ^3\Pi$ and $A\ ^3\Pi$ states were 1496 and 1292.12 $cm^{-1}$, respectively [Bre85].

Finally, Bhanuprakash and Buenker [Bha88] have studied the electronic transition moments and radiative lifetimes of some band systems. No complete and coherent set of spectroscopic constants $\omega_e$, $\omega_e x_e$, $\alpha_e$, $B_e$, and $D_e$ is known to date for the $X\ ^3\Pi$ and $a\ ^1\Sigma^+$ states.

The dissociation energy is not accurately known either. The most reliable value to date is an estimate by Gaydon [Gay53] of 4.0 ± 0.5 eV, based on a Birge-Sponer like extrapolation of the available spectroscopic data. The one ab initio determination, 4.3 ± 0.25 eV [Mar89c], is in good agreement with this value. Other estimates though (listed in [Jan85]) are in disagreement with this.

The purpose of this Section is to obtain the spectroscopic constants for the two lowest-lying states at a sufficiently high level of theory, to find a more accurate value for the dissociation energy, and finally to set up the partition function with the available data. Our recent work on SiC [Mar90c] has shown that high-level ab initio calculations are

[2]From the results of KG, it should actually be designated $C\ ^3\Pi$, with $A\ ^3\Sigma^-$ and $B\ ^3\Sigma^+$ states in between.

quite capable of producing sufficiently accurate spectroscopic constants for this purpose.

### 4.5.2 Computational methods

All calculations were carried out using the GAUSSIAN 88 program system [Gau88], running both on our DEC VAXstation 3100 under VMS 5.3 and on the IBM 3090/400e VF at the University of Leuven under the MVS/XA operating system.

Electron correlation was treated using the quadratic configuration interaction (QCISD(T)) method (which is actually an approximate coupled cluster method) [Pop87], which includes a quasiperturbative triple excitations correction correct to fifth order [Rag89]. It has recently been shown, that for all but the most pathological cases this method is essentially as good as full CI [Lee90]. Furthermore, it is rigorously size-consistent [Pop87].

While performing such calculations, a number of lower levels of theory, including second-order (MP2 [Bin75b]), third-order (MP3 [Pop76]), partial (MP4(DQ) [Kri78]) and full (MP4 [Kri80b]) fourth-order many-body perturbation theory, as well as spin-projected UHF (PUHF) and MP$n$ energies (PMP$n$) [Sch86], are obtained 'on the fly', as well as the QCISD energy, i.e. QCISD(T) without the quasiperturbative correction.

Two families of basis sets were considered. The first were the standard 6-311G* [Kri80a], 6-311+G* [Cla83], and 6-311G(2$df$) [Fri84] basis sets of the Pople group. It has recently been shown however [Gre89], that the 6-311G basis set is not of valence triple-zeta quality. Therefore calculations were also performed with a Dunning [5$s$3$p$] basis set [Dun71] generated from Huzinaga's (10$s$6$p$) primitive set [Huz65]. Polarization exponents were determined in this work by minimization of the MP4(DQ) [Kri78] atomic energies. The $d$ exponent thus obtained was 0.3478 for B and 0.8060 for N. This exponent was doubled according to the 'even scaling rule' [Fri84, and references therein], and an $f$ exponent was then optimized to go with these two $d$ exponents. Its optimum value was 0.4991 for B, and 1.1064 for N.

The spectroscopic constants were obtained by computing the energy at a number of points around $r_e$, fitting a polynomial of some appropriate degree, re-expanding it about its minimum (the latter determined by a Newton-Raphson method), and performing a Dunham analysis [Dun32]. Errors in the standard deviations on the coefficients were propagated. Considerable experimentation with the fitting procedure has been done. Both regular Dunham and Simons-Parr-Finlan (SPF) [Sim73], as well as polynomials of different degree for SCF and correlation energies [Wil78], were considered. Much to our surprise, a regular fifth-order Dunham expansion, fitted to the unweighted SCF+correlation energies at the points $r_e$-0.055(0.005)$r_e$+0.055 Å, yielded the most well-determined values for the spectroscopic constants. Actually, the faster convergence of SPF expansions compared to Dunham expansions is a mixed blessing when one wants to determine not just the harmonic frequency, but also the higher-order anharmonic constants; with the small range considered here, the smaller convergence radius of the

Dunham expansion is furthermore not an issue.

In one case (the $^1\Sigma^+$ state at 1.25 Å in the [5*s*3*p*2*d*1*f*] basis), deceptive convergence of the QCISD was observed: GAUSSIAN 88 exited the iteration loop because the energy did not change between two iterations, although the gradient of the energy with respect to the cluster amplitudes was still appreciable. This resulted in fitting problems with that curve, which were immediately relieved by eliminating the point involved. Similar (but much less obvious) effect were found at 1.315 and 1.365 Å for the $^3\Pi$ state with the same basis set: these points were also eliminated.

The thermochemical calculations have been performed by direct numerical summation over rovibronic levels. All levels that contribute more than $10^{-8}$ to the partition function are included.

## 4.5.3 Results and discussion

### 4.5.3.1 Ab initio calculations

The computed spectroscopic constants at the QCISD(T) level using the 6-311G*, [5*s*3*p*1*d*], 6-311G(2*df*), and [5*s*3*p*2*d*1*f*] basis sets are given in Table XX. Standard deviations on these constants, obtained by propagating standard deviations in the Dunham coefficients, are given in parentheses.

At the 6-311G* and [5*s*3*p*1*d*] levels, the harmonic frequencies are apparently underestimated, whereas the equilibrium bond distance $r_e$ is overestimated by about 0.01 Å. Increasing the basis set to 6-311G(2*df*) and [5*s*3*p*2*d*1*f*] brings the computed $r_0$ values to within a few milliangstroms of the experimental values; both for the $^3\Pi$ and $^1\Sigma^+$ states, the bond distances are slightly overestimated. Harmonic frequencies are still a few percent too low; some test calculations indicate that including core correlation will increase the computed harmonic frequency by about 4 $cm^{-1}$, whereas shortening the bond distance to the experimental one has an effect of about 7 $cm^{-1}$. The remaining 10–20 $cm^{-1}$ will be due to further basis set incompleteness effects. The next 'correlation consistent' basis set in the Dunning sense [Dun89] would be [5*s*4*p*3*d*2*f*1*g*]; unfortunately, GAUSSIAN 88 does not support *g* functions.

The results with the 6-311G* and [5*s*3*p*1*d*] basis sets differ rather significantly, which is much less the case between 6-311G(2*df*) and [5*s*3*p*2*d*1*f*]. Oddly enough (in the light of [Gre89]), the Pople family yields results for $r_e$ and $\omega_e$ that are generally closer to the experimental $r_0$ and $\Delta G(\frac{1}{2})$ values (which form an upper and a lower bound, respectively, to $r_e$ and $\omega_e$).

Table XXI displays the computed spectroscopic constants as a function of the level of electron correlation. The disappointing performance of all lower theoretical levels is fairly obvious. As for the effect of triple excitations (from the difference between the QCISD and QCISD(T) results), it can be seen that it is apparently fairly large: the effect on the

Table XX: Spectroscopic constants for the lowest $^1\Sigma^+$ and $^3\Pi$ states at the QCISD(T) level.

| Constant | 6-311G* | [5*s*3*p*1*d*] | 6-311G(2*df*) | [5*s*3*p*2*d*1*f*] | Best estimate |
|---|---|---|---|---|---|
| | | $^3\Pi$ state | | | |
| $\omega_e$ | 1463.13(1) | 1440.203(4) | 1483.29(1) | 1479.22(1) | 1529.5 |
| $\omega_e x_e$ | 17.88(3) | 18.09(1) | 16.49(3) | 16.38(3) | 16.76 |
| $r_e$ | 1.34087(2) | 1.34912(1) | 1.33591(2) | 1.33677(3) | 1.3251 |
| $B_e$ | 1.52123(5) | 1.50267(2) | 1.53254(6) | 1.53059(7) | 1.55769 |
| $\alpha_e$ | 0.01962(1) | 0.019491(2) | 0.01884(1) | 0.01882(1) | 0.01887 |
| $r_0$ | 1.34513(3) | 1.35342(1) | 1.33997(3) | 1.34090(4) | 1.329 [Bre85] |
| $10^6 D_e$ | 6.578(1) | 6.5434(3) | 6.544(1) | 6.555(1) | 6.462 |
| $10^{13} H_e$ | -19.19(16) | -20.50(4) | 4.67(23) | 5.50(27) | 4.48 |
| $10^{16} L_e$ | 3.24(3) | 3.50(1) | 2.65(3) | 2.64(4) | 2.47 |
| $Y_{00}$ | -1.786 | -1.865(3) | -1.565(7) | -1.547(8) | -1.591 |
| $10^7 \beta_e$ | -1.75(1) | -1.89(1) | -1.40(1) | -1.38(2) | -1.36 |
| $10^4 \gamma_e$ | -7.28(20) | -9.06(7) | -5.75(25) | -6.81(30) | -5.68 |
| | | $^1\Sigma^+$ state | | | |
| $\omega_e$ | 1687.75(2) | 1663.29(3) | 1694.49(1) | 1689.81(1) | 1737.6 |
| $\omega_e x_e$ | 11.73(6) | 11.25(11) | 12.74(4) | 12.71(3) | 12.81 |
| $r_e$ | 1.29155(4) | 1.29971(7) | 1.28359(3) | 1.28477(2) | 1.2795 |
| $B_e$ | 1.63964(11) | 1.61910(17) | 1.66002(7) | 1.65697(5) | 1.67070 |
| $\alpha_e$ | 0.01907(1) | 0.01880(1) | 0.01915(1) | 0.01926(1) | 0.01920 |
| $r_0$ | 1.29535(5) | 1.30353(8) | 1.28733(3) | 1.28854(2) | 1.283 [Bre84] |
| $10^6 D_e$ | 6.190(1) | 6.137(2) | 6.373(1) | 6.373(1) | 6.178 |
| $10^{13} H_e$ | 1.06(25) | 2.83(21) | 9.21(22) | 6.04(16) | 8.96 |
| $10^{17} L_e$ | -1.93(37) | -2.93(51) | 2.18(27) | 1.76(20) | 2.09 |
| $Y_{00}$ | -0.173(14) | -0.102(26) | -0.454(8) | -0.426(6) | -0.457 |
| $10^8 \beta_e$ | 5.19(20) | 5.96(33) | 2.02(13) | 2.35(9) | 1.98 |
| $10^4 \gamma_e$ | 3.43(34) | 2.95(46) | 1.63(25) | 1.43(19) | 1.61 |
| $T_e$ | -141.95 | +263.54 | -247.15 | -120.79 | +98.6 |

$r_e$ and $r_0$ in Å, all other quantities in $cm^{-1}$.
Figures in parentheses are standard deviations on last digits.

bond distance for the $a\ ^1\Sigma^+$ state is especially noteworthy.

The most striking result, however, is that with all basis sets except [5*s*3*p*1*d*], the $^1\Sigma^+$ state is predicted to be very slightly lower in energy than the $^3\Pi$ state. Given the fact, that the QCISD(T) method predicts an excellent $a\ ^3\Pi$–$X\ ^1\Sigma^+$ transition energy for the isoelectronic $C_2$ molecule (where these two states are also close together) [Rag89b], it is fairly unlikely that we are dealing with an electron correlation artifact. The $T_e$ of only 247 $cm^{-1}$ with the 6-311G(2*df*) and 120 $cm^{-1}$ with the [5*s*3*p*2*d*1*f*] basis set is almost an order of magnitude smaller than that for $C_2$, and should thus be even more valuable as a benchmark for electron correlation methods than the $C_2$ separation commonly used (e.g. [Rag89b, Rag85, Bau87]) for this purpose.

Performing single-point calculations with diffuse functions [Cla83] at the 6-311G(2*df*)

Table XXI: Effect of electron correlation treatment on spectroscopic constants for the lowest $^3\Pi$ and $^1\Sigma^+$ states, using the 6-311G(2*df*) basis set.

| Method | $r_e$ | $T_e$ | $B_e$ | $\omega_e$ | $\omega_e x_e$ | $\alpha_e$ |
|---|---|---|---|---|---|---|
| | | | $^1\Sigma^+$ state | | | |
| RHF | 1.23176 | | 1.80268 | 1895.73 | 21.50 | 0.01983 |
| MP2 | 1.32451 | | 1.55905 | 2037.94 | -13.01 | -0.02231 |
| MP3 | 1.26486 | | 1.70956 | 1784.13 | 12.89 | 0.01696 |
| MP4(DQ) | 1.30633 | | 1.60274 | 1695.46 | -34.57 | -0.01269 |
| MP4(SDQ) | 1.31062 | | 1.59227 | 1779.12 | -11.84 | -0.00415 |
| QCISD | 1.24930 | | 1.75241 | 1718.87 | 27.40 | 0.02565 |
| QCISD(T) | 1.28359 | | 1.66003 | 1694.56 | 13.14 | 0.01930 |
| | | | $^3\Pi$ state | | | |
| UHF | 1.28795 | 23468.58 | 1.64882 | 1757.98 | 16.21 | 0.01416 |
| MP2 | 1.31317 | -3324.95 | 1.58609 | 1752.81 | -58.44 | -0.00187 |
| PUHF | 1.29122 | 24083.09 | 1.64047 | 1707.46 | 31.10 | 0.01778 |
| PMP2 | 1.31772 | -2752.63 | 1.57516 | 1697.42 | -52.06 | -0.00019 |
| PMP3 | 1.31050 | 9283.44 | 1.59255 | 1704.56 | -28.26 | 0.00752 |
| MP3 | 1.30705 | 8871.83 | 1.60096 | 1749.54 | -36.84 | 0.00547 |
| MP4(DQ) | 1.30711 | 4874.53 | 1.60083 | 1739.91 | -34.10 | 0.00620 |
| MP4(SDQ) | 1.31333 | 1038.06 | 1.58570 | 1697.11 | -36.87 | 0.00465 |
| QCISD | 1.32578 | 1886.77 | 1.55607 | 1550.45 | 9.30 | 0.01617 |
| QCISD(T) | 1.33591 | -247.68 | 1.53255 | 1483.29 | 16.72 | 0.01901 |

$r_e$ and $r_0$ in Å, all other quantities in $cm^{-1}$.
All spectroscopic constants are obtained from fitting fourth-degree regular Dunham polynomials to points 1.230(0.005)1.340 for $^1\Sigma^+$, and 1.280(0.005)1.390 for $^3\Pi$ state.

$r_e$ geometries favors the $^3\Pi$ state, making it the ground state by a margin of only 100 $cm^{-1}$. Obviously, more accurate calculations are necessary to make a definitive conclusion about the ground state.

It is obvious from comparison with the experimental $\Delta G(\frac{1}{2})$ values (1496 $cm^{-1}$ for the $X\ ^3\Pi$ and 1712 $cm^{-1}$ for the $a\ ^1\Sigma^+$ states [Bre84, Bre85]) that the computed $\omega_e$ values are still not 'within chemical accuracy'; however, as $\alpha_e$ and $\omega_e x_e$ appear to have stabilized themselves, we may derive $\omega_e$ and $B_e$ values from combining the former two constants with the experimental $\Delta G(\frac{1}{2})$ and $r_0$ values. If we now make the assumption that $a_1$, $a_2$ and $a_3$ are predicted correctly, substituting the 'hybrid' $\omega_e$ and $B_e$ values in the Dunham expressions leads to new values for the other constants, including $\alpha_e$ and $\omega_e x_e$. These in turn may be used to derive new approximations to $r_e$ and $\omega_e$, and the process thus iterated until the set of constants is 'self-consistent'. In the present case, the process converged after two iterations.

There is little to choose between the 6-311G(2*df*) and [5*s*3*p*2*d*1*f*] values; we selected the former as they are associated with the smallest standard deviations. Our 'best estimates' thus derived are given in the last column of Table XX. The anharmonicity constants $\omega_e x_e$ differ considerably from those found by KG; these latter ones, however, are

derived from fourth-or fifth-degree polynomial fits to energies at 2.1(0.1)3.0 bohr. Over such a fairly wide range, higher-order terms in the Dunham expansion become significant and result in artificially large $\omega_e x_e$ values from a low-order fit. (This was found in the initial testing of the fit procedure.)

Some additional constants given in Table XX include the Dunham offset $Y_{00}$, the second-order rotation-vibration coupling constant $\gamma_e$, the centrifugal-vibration coupling constant $\beta_e$, and the second- and third-order centrifugal distortion constants $H_e$ and $L_e$. These constants are less well-determined, and still differ quite considerably with basis set. They have not been retained in the statistical thermodynamics calculation, as their (very small) effect is negligible compared to the errors inherent in the other constants.

The dissociation energy has been computed using the G1 correction of Pople and coworkers, except that QCISD(T) instead of MP4 energies have been used here in the additivity calculations. This latter approach, which has also been followed in our previous work on $N_3$ [Mar90e] as well as (with the related CCD(ST) method [Rag85] instead) on $C_3$ and $C_3^+$ [Mar90e], should normally be more reliable than regular G1 theory as far as additivity is concerned.

With the 6-311G(2*df*) basis set and the G1 correction, we find a $D_e$ of 106.51 kcal/mol; including an additivity correction for the effect of diffuse functions lowers this by 0.46 kcal/mol to 106.06 kcal/mol. A G1-like correction [Mar91] for the [5*s*3*p*2*d*1*f*] basis set leads to a $D_e$ of 105.52 kcal/mol, in very good agreement herewith. Either value should be accurate to ± 2 kcal/mol; combining the former with the zero-point energy of 2.2 kcal/mol for the $X\ ^3\Pi$ state, we finally propose a computed $D_0$ of 103.9±2 kcal/mol. This latter value is in marginal agreement with Gaydon's older estimate [Gay53] of 4.0±0.5 eV, and a previous theoretical calculation of 101.9±4 kcal/mol [Mar89c].

#### 4.5.3.2 Thermochemistry

For the lowest two states, our 'best estimate' spectroscopic constants have been employed. For the $b\ ^1\Pi$ state, new $\omega_e$ and $B_e$ values were derived from the experimental $\Delta G(\frac{1}{2})$ and $r_0$ values [Bre84], and KG's anharmonic and coupling constants.

For the ground state, spin-orbit coupling has been accounted for by assuming the $X\ ^3\Pi$ state to split up in three component states with identical spectroscopic constants. The spin-orbit coupling constant, $A$ = -25.14 $cm^{-1}$, was taken from BDHN [Bre85].

Additionally, the data of Karna and Grein for 20 excited singlet and triplet states [Kar85], and for three additional quintuplet states [Kar88], have been included. These span a range in $T_e$ from 0.50 to 8.37 eV, which should be more than enough for the present purpose. As these lower-lying excited states will normally be much less important, the use of the less accurate MRD-CI/TZP spectroscopic constants will be sufficient for chemical accuracy.

For the singlet and triplet states, anharmonicity and rotation-vibration coupling con-

Table XXII: Thermodynamic functions at 1 bar for BN (all functions in J/K mol, except $H - H_0$ which is in kJ/mol, and log $K_f$ which is dimensionless).

| $T$ | $C_p$ | $S^0$ | gef($T$) | $H - H_0$ | $\Delta C_p$ | $\Delta S^0$ | $\Delta$gef($T$) | $\Delta(H - H_0)$ | log $K_f$ |
|---|---|---|---|---|---|---|---|---|---|
| 100 | 30.371 | 180.868 | 149.333 | 3.154 | -11.296 | -80.403 | -69.244 | -1.115 | 221.180 |
| 200 | 29.914 | 201.759 | 170.935 | 6.165 | -11.681 | -88.363 | -77.030 | -2.266 | 108.375 |
| 298.15 | 29.921 | 213.684 | 183.175 | 9.096 | -11.661 | -93.042 | -81.582 | -3.417 | 71.136 |
| 300 | 29.928 | 213.870 | 183.364 | 9.152 | -11.654 | -93.114 | -81.653 | -3.437 | 70.667 |
| 400 | 30.534 | 222.551 | 192.124 | 12.171 | -11.044 | -96.394 | -84.953 | -4.577 | 51.762 |
| 500 | 31.450 | 229.460 | 198.922 | 15.269 | -10.126 | -98.763 | -87.490 | -5.637 | 40.390 |
| 600 | 32.406 | 235.279 | 204.509 | 18.462 | -9.169 | -100.524 | -89.522 | -6.601 | 32.790 |
| 700 | 33.281 | 240.342 | 209.274 | 21.747 | -8.293 | -101.869 | -91.194 | -7.474 | 27.350 |
| 800 | 34.047 | 244.837 | 213.444 | 25.114 | -7.526 | -102.926 | -92.597 | -8.263 | 23.263 |
| 900 | 34.710 | 248.886 | 217.161 | 28.553 | -6.863 | -103.773 | -93.793 | -8.982 | 20.078 |
| 1000 | 35.287 | 252.574 | 220.520 | 32.054 | -6.286 | -104.465 | -94.828 | -9.639 | 17.526 |
| 1100 | 35.793 | 255.961 | 223.590 | 35.608 | -5.780 | -105.041 | -95.731 | -10.241 | 15.436 |
| 1200 | 36.243 | 259.095 | 226.420 | 39.210 | -5.330 | -105.524 | -96.528 | -10.797 | 13.691 |
| 1300 | 36.649 | 262.013 | 229.047 | 42.855 | -4.924 | -105.934 | -97.236 | -11.309 | 12.213 |
| 1400 | 37.019 | 264.742 | 231.500 | 46.539 | -4.553 | -106.286 | -97.870 | -11.782 | 10.945 |
| 1500 | 37.363 | 267.308 | 233.803 | 50.258 | -4.209 | -106.588 | -98.441 | -12.221 | 9.845 |
| 1600 | 37.685 | 269.730 | 235.973 | 54.011 | -3.887 | -106.849 | -98.958 | -12.625 | 8.881 |
| 1700 | 37.992 | 272.024 | 238.027 | 57.795 | -3.580 | -107.075 | -99.428 | -12.998 | 8.030 |
| 1800 | 38.287 | 274.204 | 239.977 | 61.609 | -3.286 | -107.272 | -99.859 | -13.342 | 7.273 |
| 1900 | 38.572 | 276.282 | 241.833 | 65.452 | -3.002 | -107.441 | -100.255 | -13.656 | 6.595 |
| 2000 | 38.850 | 278.267 | 243.606 | 69.323 | -2.726 | -107.589 | -100.618 | -13.942 | 5.984 |
| 2100 | 39.121 | 280.169 | 245.302 | 73.222 | -2.458 | -107.716 | -100.952 | -14.201 | 5.431 |
| 2200 | 39.387 | 281.995 | 246.929 | 77.147 | -2.196 | -107.824 | -101.262 | -14.435 | 4.929 |
| 2300 | 39.646 | 283.752 | 248.492 | 81.099 | -1.944 | -107.916 | -101.550 | -14.641 | 4.469 |
| 2400 | 39.901 | 285.445 | 249.996 | 85.076 | -1.698 | -107.992 | -101.816 | -14.824 | 4.048 |
| 2500 | 40.149 | 287.079 | 251.447 | 89.079 | -1.463 | -108.057 | -102.066 | -14.981 | 3.661 |
| 2600 | 40.392 | 288.658 | 252.848 | 93.106 | -1.238 | -108.110 | -102.297 | -15.116 | 3.303 |
| 2700 | 40.629 | 290.187 | 254.203 | 97.157 | -1.022 | -108.153 | -102.513 | -15.229 | 2.971 |
| 2800 | 40.860 | 291.669 | 255.515 | 101.232 | -0.818 | -108.187 | -102.714 | -15.320 | 2.663 |
| 2900 | 41.085 | 293.106 | 256.786 | 105.329 | -0.627 | -108.212 | -102.904 | -15.393 | 2.377 |
| 3000 | 41.304 | 294.503 | 258.020 | 109.449 | -0.448 | -108.230 | -103.082 | -15.446 | 2.109 |
| 3100 | 41.517 | 295.861 | 259.219 | 113.590 | -0.284 | -108.242 | -103.249 | -15.483 | 1.858 |
| 3200 | 41.725 | 297.182 | 260.385 | 117.752 | -0.132 | -108.249 | -103.404 | -15.503 | 1.624 |
| 3300 | 41.928 | 298.469 | 261.520 | 121.935 | 0.007 | -108.251 | -103.550 | -15.510 | 1.403 |
| 3400 | 42.127 | 299.724 | 262.625 | 126.137 | 0.132 | -108.248 | -103.689 | -15.503 | 1.196 |
| 3500 | 42.322 | 300.948 | 263.702 | 130.360 | 0.242 | -108.243 | -103.820 | -15.483 | 1.000 |
| 3600 | 42.514 | 302.143 | 264.754 | 134.602 | 0.341 | -108.234 | -103.941 | -15.455 | 0.815 |
| 3700 | 42.704 | 303.310 | 265.780 | 138.863 | 0.427 | -108.225 | -104.057 | -15.416 | 0.640 |
| 3800 | 42.892 | 304.452 | 266.783 | 143.143 | 0.501 | -108.212 | -104.167 | -15.369 | 0.475 |
| 3900 | 43.079 | 305.568 | 267.763 | 147.441 | 0.563 | -108.199 | -104.271 | -15.316 | 0.318 |
| 4000 | 43.266 | 306.661 | 268.722 | 151.759 | 0.615 | -108.183 | -104.369 | -15.257 | 0.168 |
| 4100 | 43.454 | 307.732 | 269.660 | 156.095 | 0.658 | -108.167 | -104.462 | -15.193 | 0.026 |
| 4200 | 43.642 | 308.782 | 270.579 | 160.450 | 0.690 | -108.151 | -104.550 | -15.125 | -0.109 |
| 4300 | 43.833 | 309.811 | 271.480 | 164.823 | 0.715 | -108.134 | -104.632 | -15.056 | -0.237 |
| 4400 | 44.026 | 310.821 | 272.362 | 169.216 | 0.732 | -108.118 | -104.713 | -14.983 | -0.361 |
| 4500 | 44.221 | 311.812 | 273.228 | 173.629 | 0.742 | -108.102 | -104.788 | -14.909 | -0.478 |
| 4600 | 44.420 | 312.786 | 274.077 | 178.061 | 0.746 | -108.085 | -104.860 | -14.834 | -0.590 |
| 4700 | 44.622 | 313.744 | 274.911 | 182.513 | 0.744 | -108.069 | -104.929 | -14.760 | -0.698 |
| 4800 | 44.829 | 314.685 | 275.730 | 186.986 | 0.738 | -108.054 | -104.994 | -14.685 | -0.801 |
| 4900 | 45.039 | 315.612 | 276.535 | 191.479 | 0.727 | -108.038 | -105.055 | -14.613 | -0.900 |
| 5000 | 45.254 | 316.524 | 277.325 | 195.994 | 0.714 | -108.024 | -105.115 | -14.540 | -0.995 |
| 5100 | 45.473 | 317.422 | 278.103 | 200.530 | 0.696 | -108.010 | -105.172 | -14.470 | -1.086 |
| 5200 | 45.696 | 318.308 | 278.867 | 205.089 | 0.676 | -107.995 | -105.227 | -14.401 | -1.173 |
| 5300 | 45.924 | 319.180 | 279.620 | 209.670 | 0.654 | -107.984 | -105.278 | -14.333 | -1.258 |
| 5400 | 46.156 | 320.041 | 280.360 | 214.274 | 0.630 | -107.970 | -105.329 | -14.270 | -1.339 |
| 5500 | 46.392 | 320.890 | 281.090 | 218.901 | 0.604 | -107.960 | -105.376 | -14.208 | -1.417 |
| 5600 | 46.632 | 321.728 | 281.808 | 223.553 | 0.578 | -107.950 | -105.423 | -14.149 | -1.492 |
| 5700 | 46.876 | 322.555 | 282.515 | 228.228 | 0.549 | -107.939 | -105.468 | -14.092 | -1.565 |
| 5800 | 47.123 | 323.373 | 283.213 | 232.928 | 0.520 | -107.930 | -105.510 | -14.039 | -1.635 |
| 5900 | 47.373 | 324.181 | 283.900 | 237.653 | 0.489 | -107.921 | -105.551 | -13.988 | -1.703 |
| 6000 | 47.625 | 324.979 | 284.578 | 242.403 | 0.456 | -107.913 | -105.591 | -13.940 | -1.769 |

stants were available; for the quintuplet states (the lowest of which lies at 3.54 eV), the harmonic approximation had to be adopted. The missing centrifugal distortion constants were computed from the familiar relationship [Dun32, Her50]:

$$D_e = 4\frac{B_e^3}{\omega_e^2} \tag{4.12}$$

The computed functions are listed in Table XXII. Tabulated functions include the heat capacity $C_p$, the entropy $S^0$, the Gibbs energy function gef$(T) \equiv -[G(T) - H(0)]/T$, and the enthalpy function $H - H(0)$, as well as the corresponding functions for the association reaction $B(g) + N(g) \rightarrow BN(g)$ and the logarithm of its equilibrium constant $K_f$. The atomic functions [Jan85] involved were reconstructed from the energy level information given in the JANAF tables for N, and in Odintzova and Striganov [Odi79] for B.

It should be noted that the atomic entropy and free energy function found by ourselves differ by a constant term of about 0.009 J/K mol from the JANAF values. This can be readily traced back to the fact that, whereas we averaged the partition functions over the isotopic masses, the average isotopic mass was used in the JANAF tables, leading to an error of:

$$\delta S = \frac{3}{2} R \ln \frac{\prod_i m_i^{x_i}}{\sum_i x_i m_i} \tag{4.13}$$

where the $m_i$ represent the isotopic masses (in a.m.u.) and the $x_i$ their natural abundances (with $\sum_i x_i = 1$). The case of B, where two isotopes are fairly abundant and have a mass ratio significantly different from unity, is fairly exceptional in this respect.

The principal qualitative concusion to be drawn from the data in Table XXII is that BN is a fairly stable molecule, but will dissociate spontaneously between 4100 and 4200 K.

The relative abundances of the first five states (i.e. $X\ ^3\Pi$, $a\ ^1\Sigma^+$, $b\ ^1\Pi$, $A\ ^3\Sigma^-$, and $B\ ^3\Sigma^+$) and of all the remaining states are depicted in Figure 4.14. At 6000 K, the ground state still makes up about 73% of the total. The $a\ ^1\Sigma^+$ state comes in rapidly, but reaches a maximum of about 11% before 1000 K is reached, after which it starts decaying very slowly beyond 2000 K. At very high temperatures, the $b\ ^1\Pi$ state, which reaches about 8% at 6000 K, benefits from its twofold degeneracy. Likewise, the still higher-lying $A\ ^3\Sigma^-$ state does so, but takes advantage of its lower vibrational frequency and rotational constants to become nearly as important as the $b\ ^1\Pi$ state at 6000 K. At this temperature the higher $B\ ^3\Sigma^+$ state contributes for a little more than 2 %, whereas all the other states together still contribute no more than 0.7 %.

As shown by an error propagation study in [Mar90c] for SiC, the residual errors in good ab initio spectroscopic constants normally do not affect the quality of the partition function significantly. This is even more the case here, where the spectroscopic constants for the three lowest states have been derived with much higher accuracy and the other

Figure 4.14: Relative abundances of the five lowest states of BN as a function of temperature.

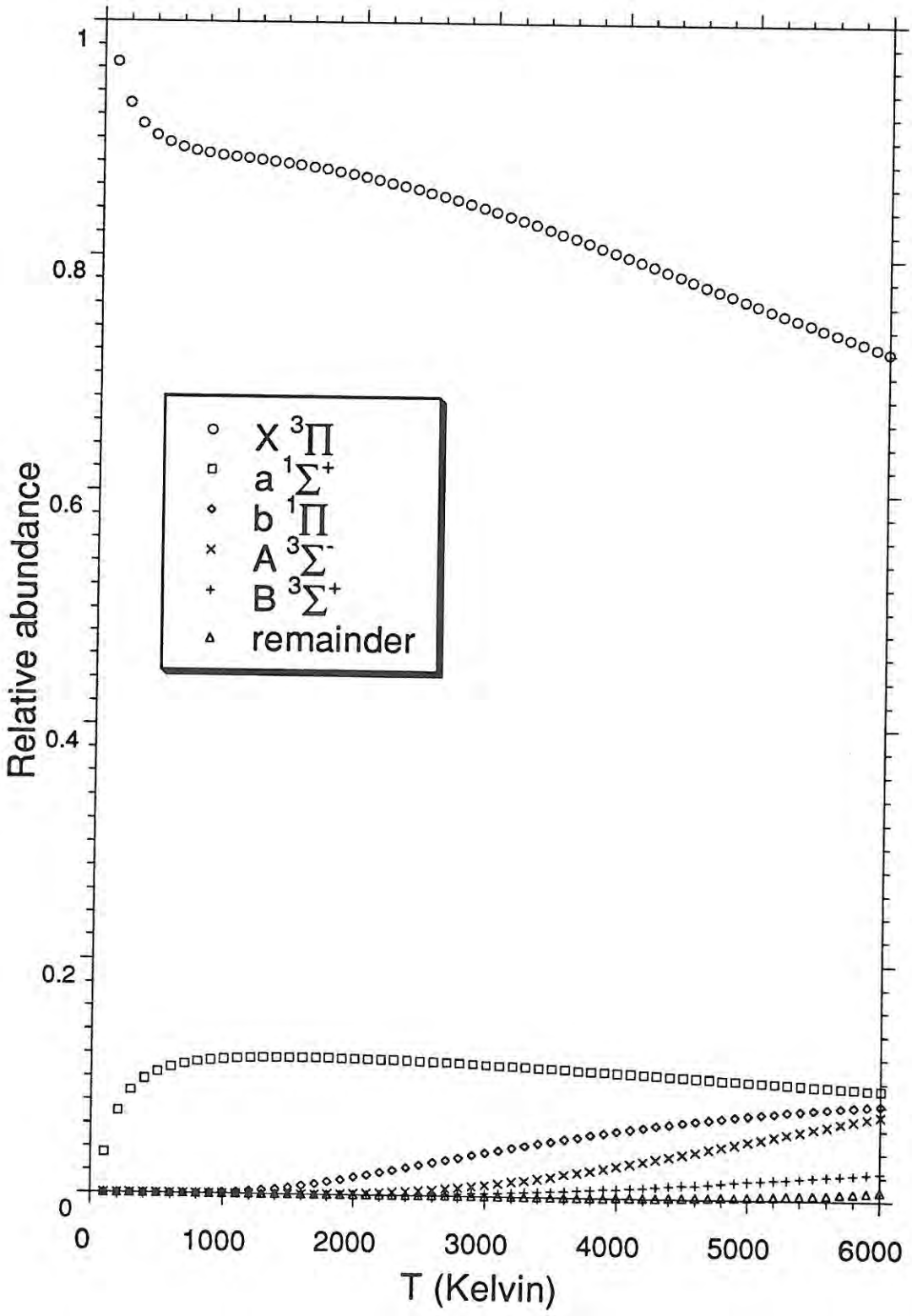

states lie so high that the exact values for these will not be very important anyway. There is one notable exception: the $T_e$ between the two lowest states, and especially the nature of the ground state. Test calculations indicate that a change in $T_e$ from +100 to 0 $cm^{-1}$ will change the free energy function and entropy by a few tenths of a J/K mol at low temperatures, and by virtually nothing at higher temperatures. However, a change to -100 $cm^{-1}$(i.e., reversing the state ordering) will have a very significant effect, on the order of several J/K mol at lower temperatures and still about 0.1 J/K mol at higher temperatures. So the main priority, if these thermodynamic functions are to be improved, is to obtain a reliable value for the transition energy between the two lowest states.

## 4.6 Note on the vibrational spectrum of $C_4$ and $C_5$

### 4.6.1 Introduction

The structure and stability of carbon cluster molecules have been the subject of a lot of theoretical and experimental work [Rag87]. $C_2$ is well characterized spectroscopically [Hub79], and accurate spectroscopic measurements have been performed on the $C_3$ species [Gau65, Wel66, Han74, Cha82], where the spectroscopic analysis was aided by the results of rather sophisticated ab initio treatments [Lis72, Per77, Rom78, Jon85]. The structure of $C_4$, however, is still a matter of controversy.

Bernholdt *et al.* [Ber88b] performed extensive calculations on the linear $^3\Sigma_g^-$ and rhombic $^1A_g$ states of $C_4$. They concluded that the two states are nearly equal in energy, and that the triplet would dominate at higher temperatures. The latter is even true on the basis of earlier calculations by Whiteside *et al.* [Whi81b], which predicted the rhombic form to be about 6 kcal/mol more stable. At high temperatures, this energy difference becomes insignificant, while the effect of the degeneracy entropy on the equilibrium constant of isomerization is independent of temperature, and will thus favor the triplet structure in the high temperature limit [Mar87]. For the linear triplet state, accurate MP2/6-31G* frequencies by Michalska *et al.* [Mic87] are available. Thompson *et al.* [Tho71] trapped several $C_n$ species in rare gas matrices and studied their IR spectra. They assigned a 2164 $cm^{-1}$ value to $C_4$, and a line at 1544 $cm^{-1}$ to $C_5$. However, from the results by Michalska *et al.* , it is seen that linear $C_4$ has a symmetric stretching mode at 2149 $cm^{-1}$, which is not IR active. The antisymmetric mode is located at 1586 $cm^{-1}$(intensity 488.3 km/mol), while the highest IR active frequency of the rhombic structure, the $B_{3u}$ mode, lies even lower at 1428 $cm^{-1}$ (intensity 1262.4 km/mol). Now, MP2 frequencies are generally too high, rather than too low, and are usually within 5 % of the experimental values [Hes86, Sta89]. Therefore, Bernholdt *et al.* arrived at the conclusion that the 2164 $cm^{-1}$frequency is probably due to $C_5$, as supported rather firmly by recent isotopic substitution experiments [Val89], and further agreed with Michalska *et al.*

Table XXIII: Calculated geometry for $C_5$ (Å).

| Theoretical model | Bond lengths | |
|---|---|---|
| | inner | outer |
| HF/6-31G* [Rag87] | 1.275 | 1.271 |
| HF/D95 [Ewi87] | 1.282 | 1.287 |
| HF/D95* [Ewi87] | 1.280 | 1.277 |
| MINDO/3 [Mar87] | 1.313 | 1.270 |
| MP2/6-31G* (this work) | 1.291 | 1.300 |

that the 1544 $cm^{-1}$line should be assigned to $C_4$. They then remarked, that correlated frequencies for $C_5$ would have been helpful to settle the assignment.

The purpose of the present study is to compute these correlated frequencies. The same basis set and theoretical model as in the work of Michalska *et al.* , i.e. MP2/6-31G* (no frozen core), was used in order to facilitate direct comparison.

### 4.6.2 Computational Methods

The calculations were performed using the GAUSSIAN 86 package [Gau86], running on the IBM 3090/300 mainframe[3] with vector facility at the University of Leuven, under the MVS/XA operating system. The standard 6-31G* basis set [Heh72] was used. Only the linear $^1\Sigma_g^+$ state was considered: this was shown to be by far the most stable state in the work of Raghavachari and Binkley [Rag87] and Ewing and Pfeiffer [Ewi87]. The geometry optimization and force constant calculations were carried out using analytical first derivatives [Pop79]. IR intensities were obtained by numerical differentiation of the MP2 dipole moment [Yam86]. To initialize the geometry optimization, analytic [Pop79] HF/3-21G [Bin80] force constants were used.

### 4.6.3 Results and discussion

The MP2 optimized geometry is listed in Table XXIII, along with the Hartree-Fock and MINDO/3 values from literature. It is noted here, that the predicted difference between inner and outer bond lengths is significantly larger at the correlated level than with any of the basis sets at the Hartree-Fock level. Also, the DZP basis sets both predict the outer bond to be shorter than the inner bond, while our MP2/DZP results predict the contrary. A certain dependence on the basis set can be noted for the Hartree-Fock bond lengths. However, it is very probable that our MP2 conclusions are qualitatively correct.

In Table XXIV, MP2/6-31G* vibrational frequencies and IR intensities are presented,

[3]This had not yet been upgraded to a 3090/400e at that time.

Table XXIV: Harmonic frequencies ($cm^{-1}$) and intensities (km/mol) for $^{12}C_5$.

| Symmetry | MINDO/3 | HF/6-31G* | | MP2/6-31G* | |
|---|---|---|---|---|---|
| | | Unscaled | Scaled | Unscaled | Scaled |
| | [Mar87] | [Rag87] | (0.89) | This work[a] | (0.93) |
| $\Sigma_u$ | 2157 | 2344 | 2086 | 2358 (1243) | 2193 |
| $\Sigma_g$ | 2133 | 2220 | 1976 | 2018 (0) | 1877 |
| $\Sigma_u$ | 1671 | 1632 | 1452 | 1471 (64) | 1368 |
| $\Sigma_g$ | 874 | 863 | 768 | 786 (0) | 731 |
| $\Pi_u$ | 660 | 648 | 577 | 487 (1.4) | 453 |
| $\Pi_g$ | 363 | 222 | 198 | 281 (0) | 261 |
| $\Pi_u$ | 189 | 112 | 100 | 130 (18) | 121 |

(a) intensities in km/mol between parentheses

along with the HF/6-31G* frequencies by Raghavachari and Binkley [Rag87]. Also included are the HF frequencies scaled by 0.89, as suggested by Pople *et al.* [Pop81]. In the work of Hout *et al.* [Hou82], it is found that MP2 frequencies overestimate the experimental ones by an average amount of 7.3 %; this suggests a scale factor of 0.93. Scaled MP2 frequencies are found in the last column of Table XXIV.

The very low bending frequencies obtained at the HF/6-31G* level are confirmed here, although their exact values will probably be quite sensitive towards the basis set. Simandiras *et al.* [Sim88] discovered that the bending frequencies of multiply bonded systems are extraordinarily sensitive to the basis set, and that a TZ(2*df*) basis set is in general required to reproduce bending frequencies with high accuracy; this is much less the case for stretching frequencies [Sim87]. Henceforth, our calculated bendings will be much less less accurate than the stretches.

The most striking feature, however, is the very intense $\Sigma_u$ band at 2358 $cm^{-1}$; the MP2 frequency is actually higher than the HF one, as opposed to the general trend [Hou82]. If this IR band is scaled by 0.93, a frequency of 2193 $cm^{-1}$ is obtained, in good agreement with the 2164 $cm^{-1}$ experimental value which was attributed by Thompson *et al.* to $C_4$. Henceforth, the reassignment suggested by Bernholdt *et al.* is confirmed. Another $\Sigma_u$ band is predicted at 1471 $cm^{-1}$ unscaled, and 1368 $cm^{-1}$ scaled. These values are not only too low to correspond to the 1544 $cm^{-1}$ experimental line previously assigned to $C_5$, but the intensity of only 64 km/mol makes it an unlikely candidate too. Thus, these results further confirm the assignment of the 1544 $cm^{-1}$ line to $C_4$. If the 1586 $cm^{-1}$ MP2/6-31G* value of Michalska *et al.* for the highest $\Sigma_u$ mode of $C_4$ is scaled by 0.93, one arrives at a value of 1475 $cm^{-1}$; this magnitude of errors is not exceptional for scaled-down frequencies.

### 4.6.4 Conclusion

The geometry, harmonic frequencies, and IR intensities for $C_5$ have been computed at the MP2/6-31G* level. The outer bond is found to be about 0.01 Å longer than the inner bond. The computed frequencies and intensities confirm that the experimental 2164 $cm^{-1}$ band, formerly assigned to $C_4$ by Thompson *et al.*, corresponds to the highest $\Sigma_u^+$ stretching of $C_5$, and that the 1544 $cm^{-1}$ band previously attributed to $C_5$ is not a part of the $C_5$ spectrum, but rather comes from the $^3\Sigma_g^-$state of $C_4$ as suggested by recent MP2/6-31G* calculations on this system.

## 4.7 A critical comparison of MINDO/3, MNDO, AM1, and PM3 for a model problem: carbon clusters $C_2$-$C_{10}$. An ad hoc reparametrization of MNDO well suited for the accurate prediction of their spectroscopic constants

### 4.7.1 Introduction

Semiempirical methods such as MINDO/3 [Bin75a], MNDO [Dew77a], AM1 [Dew85], and PM3 [Ste89a] have become accepted as useful tools in theoretical chemistry. (For a good review of MINDO/3 and MNDO applications, see e.g. [Cla85, Lew86].). Their chief usefulness lies in the fact, that they are three to four orders of magnitude less expensive than the ab initio methods they offer an alternative to.

The large difference in computational expense is explained by the fact, that all semiempirical methods are based on valence-only minimal basis set Hartree-Fock calculations, combined with INDO [Pop67]-or NDDO [Sus69]-type approximations about the integrals which essentially reduce the $N^4$ dependence (with N representing the basis set dimension) of the integral evaluation to a $N^2$ dependence; the $N^3$ SCF procedure then becomes the dominant step. The remaining quantities in the calculation are replaced by empirical parameters or some function of them; the parameters are evaluated essentially by doing an elaborate least-squares fit of calculated to experimental data (heats of formation, geometries, dipole moments, ionization potentials, ...) for a few hundred reference molecules. This fitting procedure is not only supposed to account for the essential features of basis set expansion and electron correlation but, as the fit is performed to experimental data at 298.15 K, it is even assumed to correct for thermal effects in a quantum mechanical calculation which knows nothing about temperature!

The parametrization is both the principal strength and weakness of semiempirical methods. For 'well-behaved' molecules similar to the parametric set, they allow, for example, a prediction of heats of formation that would otherwise require correlated ab

initio calculations with a medium- to - large basis set. This can even be done for molecules where computer requirements would preclude any decent ab initio work. However, in somewhat more 'exotic' molecules, this similarity can no longer be exploited.

This is perhaps the reason, why all systematic comparisons of several semiempirical methods (see e.g. [Voe89, Voe90, Ste89b]) have hitherto been restricted to 'well-behaved' molecules equal or very similar to the ones used in the parametrization set. All these comparisons indicate a progressive improvement from MINDO/3 to MNDO to AM1 to PM3. However, for a method to be really chemically useful, it should be applicable to nonstandard molecules (such as elemental clusters) as well.

In this light, it appeared interesting to us to attempt a systematic comparison for a class of molecules which is decidedly nonstandard, has never been included seriously in any parametrization, and for which good ab initio and/or experimental data are nevertheless available. One immediate candidate fulfilling all these conditions, and which has aroused a lot of interest both experimentally and theoretically, are neutral carbon clusters $C_n$ (Weltner and Van Zee [Wel89] summarize theoretical and empirical studies up to April 1989). In the present work, we restrict ourselves to $C_2$-$C_{10}$.

Another question we were asking ourselves is: suppose the description is not good, could it be remedied by adjusting the parameters to fit known experimental values? In other terms, is a parametrized semiempirical model hamiltonian capable of giving a good account of this highly unusual set of systems?

Before proceeding, we shall briefly outline a few points about the semiempirical methods considered in this work. This is not an attempt to review semiempirical MO theory; more details can of course be found in the original publications about them.

#### 4.7.1.1 Semiempirical methods

The MINDO/3 method is the only one based on the INDO-approximation [Pop67], the others are based upon NDDO. In INDO (Intermediate Neglect of Differential Overlap), all two-electron integrals involving differential overlap (i.e. of the form $(IJ|KK)$ or $(IJ|KL)$ with $I \neq J$) are neglected, except for the one-center exchange integrals. Among the integrals neglected figure all multi-center exchange integrals and all three-and four-center coulomb integrals. In order to preserve rotational invariance [Pop65], the two-center coulomb integrals then all have to be evaluated using $s$-type functions.

In NDDO (Neglect of Diatomic Differential Overlap) [Sus69], only the integrals involving diatomic differential overlap are neglected, that is to say $(IJ|KK)$ and $(IJ|KL)$ where $I$ and $J$ belong to different atoms. No supplementary conditions have to be introduced to retain rotational invariance. An additional computational expense of only about 20% is thus introduced.

The evaluation of the various one-center terms is similar in all four methods, and will thus not be discussed.

All four methods make a Mulliken-type approximation regarding the off-diagonal $H^0_{kl}$ integrals, except that in MINDO/3 the Mulliken constant $\beta$ is also made proportional to valence-state ionization potentials of the atoms and orbitals involved.

The MINDO/3 method uses a Dewar-Sabelli-Klopman approximation [Dew61] for the two-center repulsion integrals remaining; the other methods use a semiempirical model discussed in detail by Dewar and Thiel [Dew77b].

MINDO/3 and MNDO both use empirical functions for the core-core repulsion which are quite similar at large distances. To correct for overly large repulsions at van der Waals type distances, a number of Gaussians (which decay much faster than the original function) are added to the core in the AM1 method [Dew85], which results in significantly improved performance for molecules involving hydrogen bonds (e.g. Voets *et al.* [Voe89, Voe90]).

The PM3 method [Ste89a] simply represents a consistent global reparametrization of all elements in an AM1 type treatment (as opposed to the partially separate optimizations used hitherto in MNDO and AM1). The difference in performance in PM3 is best seen as an indicator for the sensitivity of the quality of the results to that of the parameter optimization.

Another important difference in the area of parametrization is that in MINDO/3, the $\alpha$ and $\beta$ parameters are taken as bond-dependent in the optimization, whereas they are set to some convenient average of atomic parameters in the other methods. The latter approach has the advantage that no separate parameter has to be determined for each bond type, but the disadvantage that the parametrization suffers some loss in flexibility. In particular, a change in $\alpha$ or $\beta$ that would result in an improved description of one particular bond type might now adversely affect performance for all of the others, resulting in a compromise which satisfies no-one completely.

#### 4.7.1.2 Carbon clusters

We shall now briefly go into the available data on carbon clusters. (A more complete summary can be found in Weltner and Van Zee [Wel89]).

$C_2$ [Hub79] and $C_3$ [Gau65] have been well characterized experimentally. $C_2$ has a $^1\Sigma_g^+$ ground state, but the $^3\Pi_u$ state is only a few kcal/mol above. $C_3$ has a linear structure and a $^1\Sigma_g^+$ ground state. Its most striking feature is the extremely low bending frequency (about 65 $cm^{-1}$), which accounts for some of the molecule's peculiar thermodynamic behavior [Str67]. Detailed ab initio investigations of its optical spectrum have been made [Per77, Rom78, Cha86].

The structure of $C_4$ has been the subject of a lot of controversy, both theoretically (Bernholdt *et al.* [Ber88b] and references therein) and experimentally (Van Zee *et al.* [Van88] and references therein). The experimental studies favor a linear arrangement, whereas the theoretical studies arrive at the conclusion that a linear $^3\Sigma_g^-$ state and a

Table XXV: Predicted heats of formation at 298.15 K (kcal/mol) using the standard parameters.

| Species | MINDO/3 | MNDO | AM1 | PM3 | ab initio [Rag87][e] | Experiment [Jan85] |
|---|---|---|---|---|---|---|
| $C_2$ ($^1\Sigma_g^+$) | 150.57 | 235.43 | 216.25 | 258.23 | 193.8 | 200.22 |
| $C_2(^3\Pi_u)$ | 176.92 | 231.91 | 221.88 | 228.00 | ... | |
| $C_3(^1D_{\infty h})$ | 188.89 | 220.32 | 212.45 | 206.65 | 190.1 | 196.00 |
| $C_3(^1C_{2v})$ | 217.69 | 330.86 | 326.13 | 291.86 | ... | |
| $C_3(^3D_{3h})$ | 201.00 | 310.66[a] | 300.61[a] | 274.73 | ... | |
| $C_4(^1D_{2h})$ | 215.83 | 367.91 | 364.99 | 333.33 | 242.3 | 232.00 |
| $C_4(^1C_{2v})$ | 250.36 | 340.01 | 335.78 | 318.99 | ... | |
| $C_4(^3D_{\infty h})$ | 220.39 | 271.33 | 266.11 | 261.30 | ... | |
| $C_5(^1D_{\infty h})$ | 218.20 | 275.33 | 270.13 | 266.42 | 243.9 | 234.00 |
| $C_6(^3D_{\infty h})$ | 252.34 | 318.00 | 316.70 | 314.66 | ... | |
| $C_6(^1D_{6h})$ | 303.42[c] | 400.80 | 407.21 | 352.82 | ... | |
| $C_6(^1D_{3h})$ | 282.41 | 400.80[b] | 407.21[b] | 352.82[b] | 284.7 | $\geq 282$[f] |
| $C_7(^1D_{\infty h})$ | 257.65 | 331.16 | 330.85 | 327.64 | 298.5 | $\geq 274$[f] |
| $C_8(^1C_{4h})$ | 306.16 | 400.92[d] | 417.89[d] | 378.48[d] | 338.3 | |
| $C_8(^3D_{\infty h})$ | 289.92 | 368.08 | 371.56 | 371.08 | ... | |
| $C_9(^1D_{\infty h})$ | 299.08 | 386.61 | 391.35 | 388.69 | 353.0 | |
| $C_{10}(^1D_{5h})$ | 298.55 | 385.73 | 403.90 | 376.15 | 332.6 | |

(a) False Jahn-Teller distortion observed
(b) Symmetry increased to $D_{6h}$ during optimization
(c) False Jahn-Teller distortion
(d) Symmetry increased to $D_{4h}$ during optimization
(e) Only most stable isomers are given. Binding energies are scaled CCD+ST(CCD)/6-31G* from [Rag87]. $\Delta H_f^0$(C($g$),298.15 K)=170.89 kcal/mol was taken from the 64th edition of the CRC Handbook of Chemistry and Physics (CRC Press, Boca Raton, FL, 1984). Thermal correction was made using the rigid rotor-harmonic oscillator (RRHO) model with UHF/6-31G* frequencies taken from [Rag87].
(f) Upper limits at 0 K from [Dro59].

rhombic $^1A_g$ state are almost isoenergetic; the exact ground state found depends upon details in the computational procedure, but it is fairly certain that it is the rhombus. Augmented coupled cluster calculations in a double-zeta plus polarization basis set yield splittings of 5.2 kcal/mol [Rag87] (CCD+ST(CCD) [Rag85] in a 6-31G* basis) and 5.01 kcal/mol [Mag86] (CCSDT-1 [Lee84] in a DZP basis). In a larger triple-zeta plus polarization basis set, Bernholdt *et al.* [Ber88b] obtain an estimated CCSDT-1 result of -0.7 kcal/mol (i.e., favoring the linear structure). It is uncertain what the effect of further basis set extension will be. As the CCD+ST(CCD)/6-31G* model appears to do a remarkably good job on small state splittings in diatomic molecules (e.g. $C_2$ [Rag87], $B_2$ and BN [Mar89c]), we tend to favor the result of about 5 kcal/mol until further investigations have settled the issue. At practical temperatures however, the linear structure will benefit from the degeneracy entropy of the triplet state, and consequently a mixture

Table XXVI: Some ab initio and experimental isomer and state splittings (all in kcal/mol).

| Species | Isomer | Reference | $T_e$ | ZPE | $E_{\mathrm{vib}}^{298}$ | $T_{298.15}$ |
|---|---|---|---|---|---|---|
| $C_2$ | $^1\Sigma_g^+$ | [Hub79] | 0.0 | 2.7 | 0.0 | 0.0 |
| | | [Bau87] | 0.0 | 2.6 | 0.0 | 0.0 |
| | $^3\Pi_u$ | [Hub79] | 2.0 | 2.3 | 0.0 | 1.6 |
| | | [Sim88] | 0.4 | 2.3 | 0.0 | 0.1 |
| $C_3$ | $D_{\infty h}$ | [Whi81a] | 0.0 | 5.7 | 0.8 | 0.0 |
| | $^3D_{3h}$ | [Whi81a] | 24.4 | 5.7 | 0.0 | 23.9 |
| | $C_{2v}$ | [Whi81a] | 29.9 | 4.8 | 0.1 | 28.5 |
| $C_4$ | $D_{2h}$ | [Rag87] | 0.0 | 8.4[a] | 0.3[a] | 0.0 |
| | $^3D_{\infty h}$ | [Rag87] | 5.2 | 8.4[a] | 0.3[a] | 5.7 |
| | | [Mag86] | 5.0 | 8.4[a] | 1.1[a] | 5.5 |
| | | [Ber88b] | -0.5 | 8.4[a] | 1.1[a] | 0.0 |
| | $C_{2v}$ | [Whi81b] | 29.5 | ... | ... | ... |
| $C_6$ | $D_{3h}$ | [Rag86b] | 0.0 | 18.0 | 0.6 | 0.0 |
| | $^3D_{\infty h}$ | [Rag86b] | 19.3 | 16.9 | 2.0 | 20.4 |
| | | [Rag87] | 15.5 | 16.9 | 2.0 | 20.4 |
| | $D_{6h}$ | [Rag86b] | 3.5 | 17.4 | 0.3 | 2.6 |
| $C_8$ | $^1C_{4h}$ | [Rag87][b] | 0.0 | 24.7 | 1.8 | 0.0 |
| | $^3D_{\infty h}$ | [Rag87][b] | 13.2 | 20.1 | 3.6 | 10.4 |

(a) MP2/6-31G* frequencies from [Mic87]
(b) CCD+ST(CCD) energies are estimated (see [Rag87] for details)
[Bau87] MRCI+Q/[5$s$4$p$3$d$2$f$1$g$]
[Whi81a] $T_e$ MP4(SDTQ)/6-31G*, frequencies UHF/6-31G*
[Whi81b] $T_e$ MP4(SDQ)/6-31G* : no ab initio frequencies available
[Rag86b] $T_e$ MP4(SDTQ)/6-31G*, frequencies UHF/3-21G
[Rag87] $T_e$ CCD+ST(CCD)/6-31G*, frequencies UHF/6-31G*
[Mag86] CCSDT-1/DZP
[Ber88b] CCSDT-1/TZP (estimated)
$T_{298.15}$ represents the state or isomer separation at 298.15 K

of linear and rhombic structures will be found. This conclusion is supported by the very recent detection of a 1544 $cm^{-1}$ IR frequency of $C_4$ [She89] (vide infra), as well as by recent Coulomb explosion experiments [Alg89], "proving unambiguously that many of the [neutral $C_4$ species] measured have the rhombic form". Furthermore, as will be seen at the end of this Section, there is some evidence for an experimental band of rhombic $C_4$ at 1288 $cm^{-1}$.

Ab initio calculations [Ewi87] have made it fairly certain, that the ground state of $C_5$ is a linear $^1\Sigma_g^+$, and that no low-lying excited states or isomers exist. The optical spectra of $C_4$ and $C_5$ have been the subject of an ab initio MRD-CI study [Pac88], in which only

linear structures were considered for both species.

Recently, theoretical and experimental studies have been synergetic in the resolution of the experimental IR spectra of $C_4$ and $C_5$. In an older matrix isolation study of Thompson *et al.* [Tho71] (TDW), IR bands of species $C_2$ to $C_9$ had been obtained; a 1544 $cm^{-1}$ transition had been assigned to $C_5$, a 2164 $cm^{-1}$ band to $C_4$. Theoretical studies [Ber88b, Mic87] appeared to indicate, that the 2164 $cm^{-1}$ band belongs to $C_5$ instead, and that the 1544 $cm^{-1}$ band is caused by the linear isomer of $C_4$; conclusive evidence was given by Martin *et al.* [Mar89b] and Botschwina and Sebald [Bot89]. Guided by these predictions, experimental observations of $C_4$ [She89] and $C_5$ [Ber89] have been made. No definitive spectroscopic characterizations, both theoretically and experimentally, have been made beyond $C_5$.

Heats of formation (reliable to about 0.2–0.4 eV) were obtained by Drowart *et al.* [Dro59] for the species $C_2$ to $C_5$ (and upper limits for $C_6$ and $C_7$), using the Knudsen effusion technique. Later determinations include Zavitsanos and Carlson [Zav73], and Wachi and Gilmartin [Wac72]. The latter two determinations were an attempt to resolve the disagreement between second-and third-law entropies for $C_3$ which was caused by the extremely anharmonic character of the low bending vibration [Str67]. Using an augmented coupled cluster method [Rag85] combined with an empirical scaling procedure, Raghavachari and Binkley (RB) [Rag87] succeeded in theoretical predictions of the binding energies for $C_2$ to $C_{10}$ that they expect to be accurate to $\pm$0.2–0.4 eV.

A correlated study of the potential energy surface (PES) of $C_3$ was first carried out by Whiteside *et al.* [Whi81a]. At the MP4SDTQ/6-31G* level//HF/6-31G* level (i.e. full fourth-order Møller-Plesset energies [Kri80] from a HF stationary point geometry, both obtained using a 6-31G* basis set [Heh72]), a triplet equilateral triangle lies 24.4 kcal/mol above the ground state. The corresponding singlet undergoes Jahn-Teller distortion to an isosceles triangle, which lies 29.9 kcal/mol above the ground state and is the transition state (together with its two Jahn-Teller partners) of a degenerate isomerization of the ground state.

Analogous studies for $C_4$ include Whiteside *et al.* [Whi81b], Magers *et al.* [Mag86], Ritchie *et al.* [Rit86], and Bernholdt *et al.* [Ber88b]. Except for the controversy about the ground state, a singlet $C_{2v}$ structure (a capped triangle) was found to lie 29.5 kcal/mol above the ground state at the MP4SDQ/6-31G*//HF/6-31G* level (i.e, neglecting triple excitations in the fourth-order treatment) [Whi81b].

For $C_5$, a PES study was made by Ewing and Pfeiffer [Ewi87]. It indicated that all other isomers are way above the ground state ($\geq$ 60 kcal/mol).

$C_6$ was studied by Raghavachari *et al.* [Rag86b] and by Parasuk and Almlöf [Par89a]. The findings of both groups are contradictory. At the MP4SDTQ/6-31G*//HF/6-31G* level, a distorted hexagonal structure with $D_{3h}$ symmetry is the ground state [Rag86b]. A linear triplet state lies 19.3 kcal/mol above; a regular hexagonal structure lies only 3.5

Table XXVII: Semiempirical (using standard parameters), ab initio, and experimental geometries (Å, degrees).

| Method/Ref. | Geometry |
|---|---|
| $C_2$ ($^1\Sigma_g^+$) | |
| MINDO/3 | R1=1.163 |
| MNDO | R1=1.169 |
| AM1 | R1=1.164 |
| PM3 | R1=1.189 |
| [Rag87] | R1=1.245 |
| [Bau87] | R1=1.250 |
| [Hub79] | observed:$r_e$=1.243 |
| $C_2$($^3\Pi_u$) | |
| MINDO/3 | R1=1.261 |
| MNDO | R1=1.278 |
| AM1 | R1=1.275 |
| PM3 | R1=1.294 |
| [Bau87] | R1=1.319 |
| [Hub79] | observed:$r_e$=1.312 |
| $C_3$($^1D_{\infty h}$) | |
| MINDO/3 | R1=1.291 |
| MNDO | R1=1.290 |
| AM1 | R1=1.288 |
| PM3 | R1=1.286 |
| [Rag87] | R1=1.278 |
| [Ada89] | R1=1.3027 |
| [Gau65] | observed:$r_0$=1.277 |
| [Han74] | observed:$r_e$=1.287 |
| $C_3$($^1C_{2v}$) | |
| MINDO/3 | R1=1.440, $\theta$1=54.55 |
| MNDO | R1=1.514, $\theta$1=51.40 |
| AM1 | R1=1.487, $\theta$1=52.48 |
| PM3 | R1=1.468, $\theta$1=51.88 |
| [Whi81a] | R1=1.461, $\theta$1=50.66 |
| $C_3$($^3D_{3h}$) | |
| MINDO/3 | R1=1.390 |
| MNDO | R1=1.420 → R1=1.392, $\theta$1=64.66[c] |
| AM1 | R1=1.406 → R1=1.381, $\theta$1=64.14[c] |
| PM3 | R1=1.376 |
| [Whi81a] | R1=1.346 |
| $C_4$($^1D_{2h}$) | |
| MINDO/3 | R1=1.437, $\theta$1=65.27 |
| MNDO | R1=1.478, $\theta$1=62.06 |
| AM1 | R1=1.465, $\theta$1=61.54 |
| PM3 | R1=1.453, $\theta$1=60.50 |
| [Rag87] | R1=1.425, $\theta$1=61.50 |
| [Rit86] | R1=1.448, $\theta$1=62.39 |
| [Mic87] | R1=1.425, $\theta$1=64.60 |
| [Mag86][a] | R1=1.435, $\theta$1=61.85 |
| [Mag86][b] | R1=1.460, $\theta$1=63.20 |
| $C_4$($^1C_{2v}$) | |
| MINDO/3 | R1=1.455, R2=1.310, $\theta$1=151.05 |
| MNDO | R1=1.474, R2=1.316, $\theta$1=149.55 |
| AM1 | R1=1.451, R2=1.313, $\theta$1=149.30 |
| PM3 | R1=1.434, R2=1.315, $\theta$1=149.64 |
| [Whi81b] | R1=1.449, R2=1.308, $\theta$1=151.65 |
| $C_4$($^3D_{\infty h}$) | |
| MINDO/3 | R1=1.310, R2=1.308 |
| MNDO | R1=1.314, R2=1.279 |
| AM1 | R1=1.311, R2=1.276 |
| PM3 | R1=1.310, R2=1.275 |
| [Whi81b] | R1=1.300, R2=1.276 |
| [Rit86] | R1=1.316, R2=1.297 |
| [Mic87] | R1=1.313, R2=1.296 |
| [Mag86][a] | R1=1.308, R2=1.283 |
| [Mag86][b] | R1=1.330, R2=1.305 |
| $C_5$($^1D_{\infty h}$) | |
| MINDO/3 | R1=1.272, R2=1.313 |
| MNDO | R1=1.284, R2=1.281 |
| AM1 | R1=1.280, R2=1.278 |
| PM3 | R1=1.279, R2=1.278 |
| [Rag87] | R1=1.271, R2=1.275 |
| [Mar89b] | R1=1.300, R2=1.291 |
| [Bot89] | R1=1.289, R2=1.283 |
| [Hea89] | observed:$r_{eff}$= 1.283 |
| $C_6$($^3D_{\infty h}$) | |
| MINDO/3 | R1=1.292, R2=1.309, R3=1.301 |
| MNDO | R1=1.300, R2=1.279, R3=1.285 |
| AM1 | R1=1.297, R2=1.275, R3=1.279 |
| PM3 | R1=1.296, R2=1.276, R3=1.281 |
| [Rag86b] | R1=1.293, R2=1.275, R3=1.269 |
| $C_6$($^1D_{6h}$) | |
| MINDO/3 | R1=1.290 → irregular $C_{2v}$ structure |
| MNDO | R1=1.316 |
| AM1 | R1=1.317 |
| PM3 | R1=1.314 |
| [Rag86b] | R1=1.290 |
| $C_6$($^1D_{3h}$) | |
| MINDO/3 | R1=1.051, R2=1.541 |
| MNDO | → $D_{6h}$ |
| AM1 | → $D_{6h}$ |
| PM3 | → $D_{6h}$ |
| [Rag87] | R1=1.078, R2=1.466, $\theta$1=60.00 |
| $C_7$($^1D_{\infty h}$) | |
| MINDO/3 | R1=1.267, R2=1.321, R3=1.289 |
| MNDO | R1=1.283, R2=1.283, R3=1.272 |
| AM1 | R1=1.279, R2=1.280, R3=1.269 |
| PM3 | R1=1.277, R2=1.281, R3=1.270 |
| [Rag87] | R1=1.270, R2=1.280, R3=1.264 |
| $C_8$($^1C_{4h}$) | |
| MINDO/3 | R1=1.474, R2=1.886, $\theta$1=47.47 |
| MNDO | → $D_{4h}$: R1=R2=1.711, $\theta$1=47.97 |
| AM1 | → $D_{4h}$: R1=R2=1.704, $\theta$1=47.84 |
| PM3 | → $D_{4h}$: R1=R2=1.709, $\theta$1=41.86 |
| [Rag87] | R1=1.498, R2=1.840, $\theta$=42.16 |
| $C_8$($^3D_{\infty h}$) | |
| MINDO/3 | R1=1.283, R2=1.314, R3=1.296, R4=1.296 |
| MNDO | R1=1.294, R2=1.281, R3=1.281, R4=1.273 |
| AM1 | R1=1.290, R2=1.277, R3=1.274, R4=1.267 |
| PM3 | R1=1.289, R2=1.278, R3=1.277, R4=1.271 |
| [Rag87] | R1=1.291, R2=1.276, R3=1.268, R4=1.269 |
| $C_9$($^1D_{\infty h}$) | |
| MINDO/3 | R1=1.265, R2=1.325, R3=1.283, R4=1.296 |
| MNDO | R1=1.282, R2=1.284, R3=1.271, R4=1.275 |
| AM1 | R1=1.278, R2=1.281, R3=1.265, R4=1.268 |
| PM3 | R1=1.276, R2=1.283, R3=1.267, R4=1.273 |
| [Rag87] | R1=1.269, R2=1.283, R3=1.261, R4=1.269 |
| $C_{10}$($^1D_{5h}$) | |
| MINDO/3 | R1=R2=2.118, $\theta$1=34.18 |
| MNDO | R1=R2=2.092, $\theta$1=34.19 |
| AM1 | R1=R2=2.080, $\theta$1=34.53 |
| PM3 | R1=R2=2.086, $\theta$1=34.22 |
| [Rag87] | R1=1.895, R2=2.184, $\theta$1=36.00 |

(a) UHF/4s2p2d
(b) MP4(D)/4s2p1d
(c) false Jahn-Teller distortion observed
[Bau87]: MRCI+Q/[$5s4p3d2f1g$]
[Rit86]: CISD/DZP
[Rag87, Whi81a, Whi81b] : UHF/6-31G*
[Mic87, Mar89b, Ada89]: MP2/6-31G*
[Mag86]: MP2/4s2p1d unless indicated otherwise
[Bot89]: CEPA-1/8s4p2d (harmonic values given)
[Rag86b]: UHF/3-21G

kcal/mol above the ground state, but is a second-order saddle point at the HF/3-21G [Bin80] level. At the CASSCF-MRCI/4s3p1d and 4s4p2d levels, on the other hand, the linear triplet is the ground state, and the hexagonal structure distorts by alternating bond distances, not by changing the ring angle. However, Raghavachari pointed out to the authors of [Par89a] (see "note added in proof" there) that the difference would mainly be caused by the fact that only ten to twelve electrons were correlated in [Par89a], whereas all 24 valence electrons were correlated in [Rag86b]. Subsequent CASSCF calculations correlating all 24 valence electrons suggested that the ring angle indeed distorts, and that the distorted cyclic and linear structures become isoenergetic when a larger reference space is used in the CASSCF calculations. Also, as discussed in [Rag86b], removing the rather large spin contamination would result in stabilization of the triplet, whereas improvement of basis set and reference geometry would increase stability of the cyclic structure; finally, an estimated energy difference of ca. 10 kcal/mol is obtained. Further work on this system is apparently called for. This illustrates that even rather sophisticated ab initio treatments may yield qualitatively different results for this type of molecule.

No systematic PES studies have been carried out beyond $C_6$; however, RB considered both linear and cyclic structures for $C_8$ and, using estimated coupled cluster energies for these large species, predicted the linear form to be 13.2 kcal/mol above the cyclic form. This value is likely to be lowered significantly at higher theoretical levels, as the linear forms has significant spin contamination.

Semiempirical studies include the MINDO/2 [Dew70] study of Slanina and Zahradník [Sla77] (who considered $C_2$ to $C_7$), an unpublished MINDO/3 study by Martin [Mar87] (who considered $C_2$ to $C_5$, as well as positive and negative ions), and an incomplete MNDO study by Bernholc and Philips [Ber86] in the framework of a theoretical model for cluster formation kinetics. The MINDO/2 results [Sla77] for the PES are in flagrant qualitative contradiction with other data for $C_3$ and $C_5$; this is not the case for $C_4$. As MINDO/2 is known to produce chemically nonsensical equilibrium geometries (like linear $H_2O$ and planar $NH_3$) [Fla77], this does not come as a surprise. The MINDO/3 study exhibited none of these shortcomings, and a surprisingly good performance for the given problem (see also below). In the MNDO study, only linear and regular cyclic structures with fixed bond lengths were considered; the linear structures were always found to be much more stable.

### 4.7.2 Computational methods

All calculations were performed with a conversion [Mop90] (by the present author) of MOPAC 5.00 [Mop89] on the Control Data Cyber 930-11 computer (1.8 MFLOPS, 64 bit) at the Limburgs Universitair Centrum, under the NOS/VE 1.4.2 operating system. The keyword `PRECISE` was used throughout to improve reproducibility of the results.

Table XXVIII: Predicted vertical ionization potentials (eV) using the standard parameters.

| Species | MINDO/3 | MNDO | AM1 | PM3 | ab initio [Rag87] |
|---|---|---|---|---|---|
| $C_2$ ($^1\Sigma_g^+$) | 11.13 | 11.66 | 12.27 | 11.72 | 12.1[c] |
| $C_2(^3\Pi_u)$ | 9.83 | 10.55 | 11.11 | 10.60 | |
| $C_3(^1D_{\infty h})$ | 8.77 | 11.04 | 11.33 | 11.75 | 11.4[c] |
| $C_3(^1C_{2v})$ | 8.38 | 10.37 | 10.65 | 10.86 | |
| $C_3(^3D_{3h})$ | 8.17 | 9.85[a] | 10.20 | 10.61 | |
| $C_4(^1D_{2h})$ | 8.23 | 10.89 | 11.26 | 11.25 | 10.5[c] |
| $C_4(^1C_{2v})$ | 8.41 | 9.93 | 10.29 | 10.45 | |
| $C_4(^3D_{\infty h})$ | 9.08 | 9.88 | 10.34 | 10.37 | |
| $C_5(^1D_{\infty h})$ | 9.35 | 10.37 | 10.94 | 10.95 | 10.7[c] |
| $C_6(^3D_{\infty h})$ | 8.54 | 9.24 | 9.69 | 9.65 | 9.8[d] |
| $C_6(^1D_{6h})$ | 8.00 | 9.99 | 10.39 | 10.41 | |
| $C_6(^1D_{3h})$ | 9.37 | 9.99[b] | 10.39 | 10.41 | |
| $C_7(^1D_{\infty h})$ | 8.81 | 9.58 | 10.09 | 10.11 | 10.0[e] |
| $C_8(^1C_{4h})$ | 7.78 | 8.97[f] | 9.23[f] | 9.17[f] | 9.2[d] |
| $C_8(^3D_{\infty h})$ | 8.08 | 8.86 | 9.29 | 9.21 | |
| $C_9(^1D_{\infty h})$ | 8.33 | 9.07 | 9.56 | 9.58 | 9.4[e] |
| $C_{10}(^1D_{5h})$ | 7.97 | 9.49 | 9.81 | 9.77 | |

(a) False Jahn-Teller distortion observed
(b) Symmetry increased to $D_{6h}$ during optimization
(c) Adiabatic IPs with the 6-31G(2*d*) basis set
(d) Assuming linear form for the ion
(e) Koopmans' theorem values
(f) Symmetry increased to $D_{4h}$ during optimization

For open-shell systems, the unrestricted Hartree-Fock equations [Pop54] have been used throughout.

For the parameter optimizations, the NLLSQ algorithm of Bartels [Bar72], as implemented in MOPAC 5.00, was incorporated in a small program written for this purpose.

## 4.7.3 Results and discussion

### 4.7.3.1 Standard parameters

Calculated heats of formation for the various structures of $C_2$ to $C_{10}$ considered here are given in Table XXV at the MINDO/3, MNDO, AM1, and PM3 levels, together with the experimental values as given in the JANAF tables [Jan85] and calculated ab initio heats of formation for the most stable isomers. The latter were obtained by correcting the scaled CCD+ST(CCD) [Rag85] $D_0$ values from RB [Rag87] to 298.15 K using UHF/6-31G* frequencies from the same publication: the RRHO (rigid rotor-harmonic oscillator) approximation was made.

Ab initio isomer and state separations for $C_2$, $C_3$, $C_4$, and $C_6$ are presented in Table

Figure 4.15: Considered $C_n$ structures and definition of the geometrical parameters.

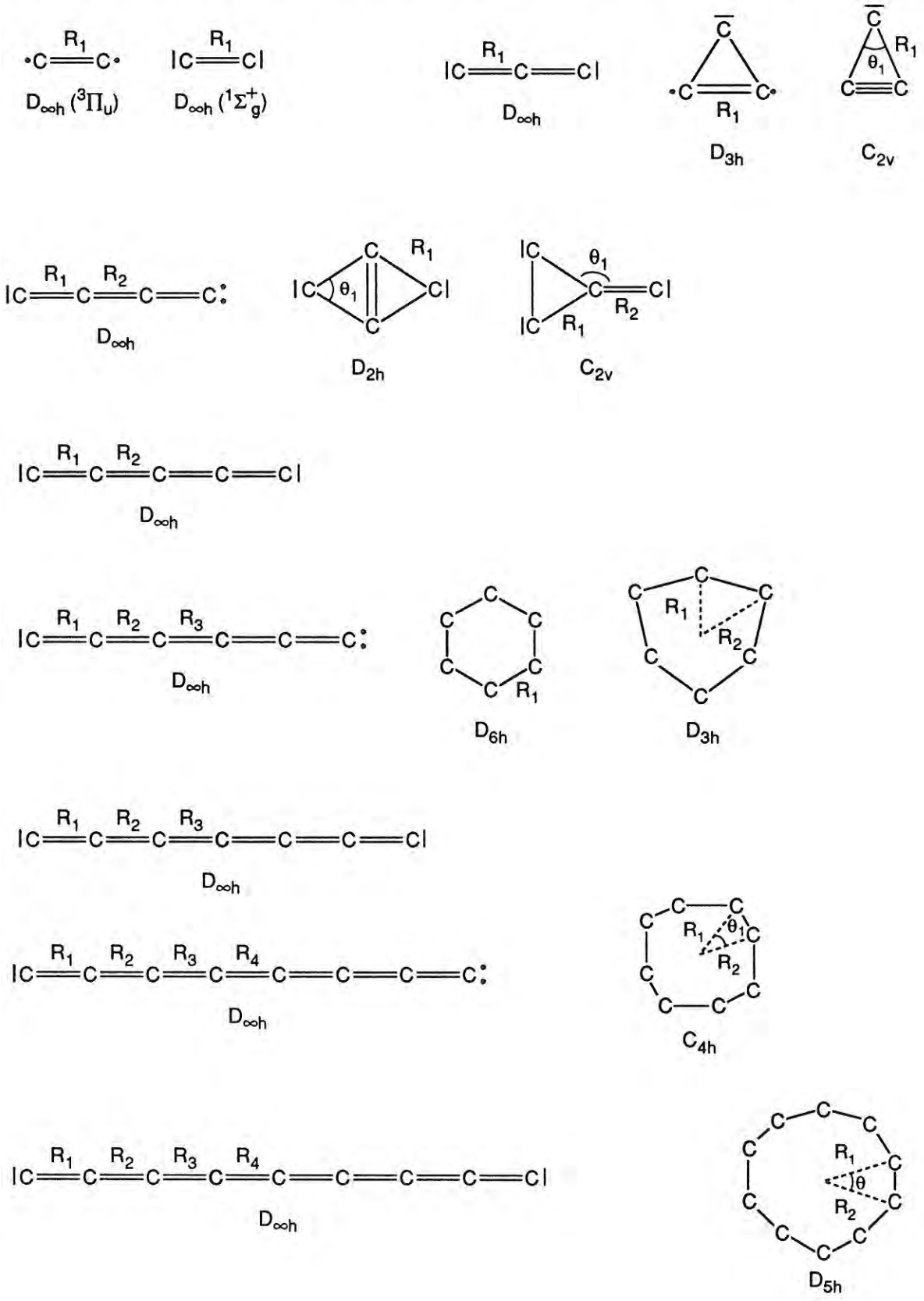

Table XXIX: Modified parameters in semiempirical methods.

| Method | $-\beta_s$ | $-\beta_p$ | $\alpha$ | $\zeta_s$ | $\zeta_p$ | $-U_{ss}$ | $-U_{pp}$ |
|---|---|---|---|---|---|---|---|
| MNDO(partial) | 15.81445 | 9.07434 | 2.61291 | standard | standard | standard | standard |
| AM1(partial) | 14.82667 | 8.22761 | 2.65856 | standard | standard | standard | standard |
| PM3(partial) | 14.18029 | 9.48430 | 2.63427 | standard | standard | standard | standard |
| MNDO(full) | 11.00724 | 6.04922 | 3.15400 | 1.54400 | 1.60397 | 51.63223 | 39.22017 |

XXVI: the reference from which they have been obtained has been included in the table. Insofar as possible, the separations have been corrected to 298.15 K. For the zero-point and thermal corrections, other frequencies than those employed in Table XXV were sometimes chosen, so that the corrections could be evaluated at the same theoretical level for both structures involved in the splitting.

The structures themselves are depicted in Figure 4.15; computed geometric parameters for them are presented in Table XXVII, in which ab initio and experimental results are also summarized. Koopmans' theorem vertical ionization potentials (together with the ab initio values of RB) can be found in Table XXVIII for all four theoretical levels.

Only the lowest electronic state of any given combination of spin and molecular symmetry was considered since MOPAC 5.00 does not allow for manipulation of the initial guess, which makes succesful SCF convergence to a particular excited state a 'blind hit'. In the tables, the isomers and states have therefore been indicated by the point group of the isomer, rather than by the symmetry of the electronic state. The multiplicity is singlet unless indicated otherwise.

It is readily seen from Tables XXV and XXVI, that MINDO/3 holds its own quite well when it comes to reproducing state and isomer splittings. (The only exception is the singlet-triplet splitting in $C_2$; however, being an INDO-based method parametrized for polyatomics, MINDO/3 is expected to fail for diatomics). High points are the barrier towards degenerate isomerization in $C_3$ (MP4/6-31G* 28.5, MINDO/3 28.8 kcal/mol), and the singlet-triplet splitting in $C_4$ (ab initio 5.7, MINDO/3 4.6 kcal/mol). The result for $C_6$ is consistent with Parasuk and Almlöf [Par89a], but not with Raghavachari *et al.* [Rag86b], in that it predicts a linear ground state: the cyclic structure undergoes Jahn-Teller distortion to a highly irregular structure, which is still a saddle point of order one. A linear ground state is predicted for $C_8$, in disagreement with the ab initio calculations of RB.

All splittings and isomeric energy differences are grossly overestimated at the MNDO and AM1 levels, and slightly, but not significantly, less so at the PM3 level. The latter three methods appear to strongly disfavor ring structures in a systematic way.

MNDO and AM1 predict false Jahn-Teller distortions for the triplet equilateral triangle isomer of $C_3$, which is not uncommon: the same phenomenon was e.g. observed for the cyclic ground state of $B_3$ [Mar89c].

Table XXX: Predicted heats of formation at 298.15 K, vertical ionization potentials, and geometries using MNDO with reoptimized $\alpha$, $\beta_s$, and $\beta_p$ parameters.

| Species | $\Delta H_f^0$ (kcal/mol) | VIP (eV) | Geometry (Å, degrees) |
|---|---|---|---|
| $C_2$ ($^1\Sigma_g^+$) | 227.65 | 11.82 | R1=1.170 |
| $C_2(^3\Pi_u)$ | 219.13 | 10.62 | R1=1.281 |
| $C_3(^1D_{\infty h})$ | 196.00 | 11.46 | R1=1.287 |
| $C_3(^1C_{2v})$ | 286.41 | 10.58 | R1=1.510, $\theta$1=51.51 |
| $C_3(^3D_{3h})$ | 276.37 | 10.14 | R1=1.420 |
| $C_4(^1D_{2h})$ | 298.71 | 11.16 | R1=1.475, $\theta$1=62.73 |
| $C_4(^1C_{2v})$ | 289.40 | 10.13 | R1=1.462, R2= 1.312, $\theta$1=149.24 |
| $C_4(^3D_{\infty h})$ | 249.37 | 9.84 | R1=1.314, R2=1.276 |
| $C_5(^1D_{\infty h})$ | 253.11 | 10.50 | R1=1.279, R2=1.277 |
| $C_6(^3D_{\infty h})$ | 300.25 | 8.81 | R1=1.298, R2=1.274, R3=1.278 |
| $C_6(^1D_{6h})$ | 389.31 | 10.10 | R1=1.306 |
| $C_6(^1D_{3h})$ | 386.90 | 10.58 | R1=1.171, R2=1.448 |
| $C_7(^1D_{\infty h})$ | 313.46 | 9.67 | R1=1.278, R2=1.279, R3=1.265 |
| $C_8(^1D_{4h})$ | 402.94 | 8.97 | R1=R2=1.742, $\theta$1=47.07 |
| $C_8(^3D_{\infty h})$ | 355.03 | 8.82 | R1=1.291, R2=1.276, R3=1.273, R4=1.260 |
| $C_9(^1D_{\infty h})$ | 373.59 | 9.15 | R1=1.276, R2=1.281, R3=1.263, R4=1.267 |
| $C_{10}(^1D_{5h})$ | 392.65 | 9.59 | R1=R2=2.080, $\theta$1=34.10 |

MINDO/3 tends towards a systematic underestimate of heats of formation, whereas the three other methods (PM3 slightly less than MNDO and AM1) exhibit a consistent serious overestimate. (The ab initio values of RB appear to tend to an overestimate too, but nowhere nearly as much). Computed geometries at the MNDO, AM1, and PM3 levels appear to agree slightly better with experiment (see Table XXVII) than those at the MINDO/3 level, although the latter preserve the essential qualitative features. Finally, as evident from Table XXVIII, MINDO/3 Koopmans' theorem ionization potentials appear to be less well in agreement with high-quality ab initio values than those at any of the other levels.

It is also readily seen, that MINDO/3 exhibits none of the anomalous results that are found with MINDO/2 [Sla77], which is in agreement with the general conclusion [Bin75a]. The two most important differences between MINDO/2 and MINDO/3 are the use of the Oleari procedure [Ole66] for the empirical determination of one-center integrals in MINDO/3, and the use of optimized STO exponents in the evaluation of the $S_{kl}$ integrals figuring in the Mulliken expression for $H_{kl}^0$.

The small difference in general performance between MNDO and AM1 is readily explained, since there are no significant van der Waals-type interactions to account for in a molecule of this type. The slightly better performance of PM3 can perhaps be attributed to the more thorough optimization of its parameters; however, given the relatively small overall improvement, the importance of this conclusion is debatable.

All this is somewhat puzzling: one would expect MINDO/3 to be significantly worse than the other ones, whereas it is on the whole much better! One explanation would be that there exists an error compensation between the INDO approximation and certain basis set and/or correlation effects: this argument is speculative, to say the least. The other important difference between the two methods, the use of bond-specific $\alpha$ and $\beta$ parameters, appears to be a more likely candidate.

#### 4.7.3.2 Optimal $\alpha$ and $\beta$ parameters

In order to verify this, we determined a set of values for $\alpha$, $\beta_s$, and $\beta_p$ that would lead to exact results for the geometry, ionization potential, and dissociation energy of $C_3$. Whereas these values will always be to some extent dependent upon the exact reference values chosen for each quantity, the global shift in the results for the other molecules should give at least an indication. We finally settled on the following triple. The heat of formation of 196.0 kcal/mol was taken from the JANAF tables [Jan85]. For the bond distance, the experimental $r_e$ value of 1.287 Å [Han74] was selected. The latter value, as opposed to the general trend, is longer than the $r_0$ value of 1.277 Å [Gau65] due to extreme rotation-vibration coupling effects. The experimental values for the ionization potential [Koh70] were shown by Sunil *et al.* [Sun84] to be in error; we finally selected their MRD-CI [Bue74] result of 11.46 eV as a more reliable estimate.

It is perhaps the place to point out that the parameter sets presented in this paper are only to be used for small carbon clusters, not for any other unusual carbon compounds.

Optimal values for the $\alpha$, $\beta_s$, and $\beta_p$ parameters are presented in Table XXIX. Computed MNDO values using the new parameters for heats of formation, vertical ionization potentials, and geometries are given in Table XXX; the AM1 and PM3 values exhibit grosso modo the same tendencies, and are thus not reproduced here.

The vertical ionization potentials appear to be somewhat improved; the heats of formation are now of a slightly better accuracy than those with the MINDO/3 method. Some slight qualitative improvements can be seen in the PES; however, striking computational artefacts such as the abnormally low-lying $C_{10}$ ring in the PM3 method (heat of formation 231.83 kcal/mol, not tabulated) are introduced also. The most important deficiency of the standard parameters however, the highly exaggerated state splittings, is not corrected for properly.

In the course of the optimization, it became clear that increasing the difference between $\beta_s$ and $\beta_p$ leads to increased ionization potentials, and that increasing the mean value of $\beta_s$ and $\beta_p$ leads to decreased heats of formation. Perhaps parameter optimizations could be substantially accelerated by explicitly introducing this coupling into the optimization.

Table XXXI: Predicted heats of formation at 298.15 K, vertical ionization potentials, and geometries using MNDO with fully reoptimized parameters.

| Species | $\Delta H_f^0$ (kcal/mol) | VIP (eV) | Geometry (Å, degrees) |
|---|---|---|---|
| $C_2$ ($^1\Sigma_g^+$) | 228.30 | 11.30 | R1=1.181 |
| $C_2(^3\Pi_u)$ | 217.49 | 10.23 | R1=1.290 |
| $C_3(^1D_{\infty h})$ | 195.92 | 11.11 | R1=1.287 |
| $C_3(^1C_{2v})$ | 248.95 | 10.33 | R1=1.477, $\theta$1=52.68 |
| $C_3(^3D_{3h})$ | 231.88 | 9.97 | R1=1.404 → R1=1.380, $\theta$1=63.83[a] |
| $C_4(^1D_{2h})$ | 231.07 | 10.69 | R1=1.461, $\theta$1=59.89 |
| $C_4(^1C_{2v})$ | 243.91 | 9.88 | R1=1.433, R2=1.310, $\theta$1=148.74 |
| $C_4(^3D_{\infty h})$ | 236.62 | 9.70 | R1=1.314, R2=1.270 |
| $C_5(^1D_{\infty h})$ | 239.47 | 10.18 | R1=1.280, R2=1.270 |
| $C_6(^3D_{\infty h})$ | 274.52 | 9.14 | R1=1.299, R2=1.266, R3=1.272 |
| $C_6(^1D_{6h})$ | 279.98 | 10.14 | R1=1.281 |
| $C_6(^1D_{3h})$ | 265.66 | 10.72 | R1=1.008, R2=1.537 |
| $C_7(^1D_{\infty h})$ | 286.13 | 9.43 | R1=1.279, R2=1.271, R3=1.258 |
| $C_8(^1D_{4h})$ | 302.57 | 8.95 | R1=R2=1.675, $\theta$1=47.80 |
| $C_8(^3D_{\infty h})$ | 315.91 | 8.80 | R1=1.293, R2=1.268, R3=1.266, R4=1.258 |
| $C_9(^1D_{\infty h})$ | 332.54 | 8.95 | R1=1.278, R2=1.272, R3=1.257, R4=1.259 |
| $C_{10}(^1D_{5h})$ | 291.30 | 9.46 | R1=2.054, $\theta$1=34.46 |

(a) false Jahn-Teller distortion observed

#### 4.7.3.3 Fully optimal set of parameters

The last resort was to optimize all the parameters, except the integrals common to all methods, simultaneously. This means four more parameters: $U_{ss}$, $U_{pp}$, $\zeta_s$, and $\zeta_p$. Four more conditions then had to be applied: we chose the CISD/DZP (Configuration Interaction with Single and Double excitations, using a Double Zeta plus Polarization basis set) geometries of the two lowest-lying states of $C_4$ [Rit86], as well as the JANAF heat of formation for $C_4$ (232.00 kcal/mol) and the calculated state splitting of 5.01 kcal/mol [Mag86]. Only the MNDO method was considered.

One would expect, with seven parameters and seven conditions, to obtain a sum of squares of zero with the final parameters. This could not be reached: apparently the state splitting could only be improved at the expense of the agreement in the ionization potential. This might indicate that a minimal basis set Hartree-Fock based model is simply not flexible enough to describe both orbital energies and state splittings well; on the other hand, each geometry condition for $C_4$ actually corresponds to two constraints, thus making nine effective conditions in all. We finally decided to lower the weights for the gradients and the ionization potential by a factor of ten, which did lead to much lower errors in the heats of formation and the state splitting.

Final parameters are again given in Table XXIX; results for heats of formation, vertical ionization potentials, and geometries are presented in Table XXXI.

Table XXXII: MINDO/3 frequencies ($cm^{-1}$) and zero point energies (ZPE, kcal/mol) using standard parameters.

| Species | ZPE | Frequencies |
|---|---|---|
| $C_2(^1\Sigma_g^+)$ | 3.3 | 2327 |
| $C_2(^3\Pi_u)$ | 2.8 | 1993 |
| $C_3(D_{\infty h})$ | 5.7 | 213(2),1410,2181 |
| $C_3(^3D_{3h})$ | | SCF diverges |
| $C_3(C_{2v})$ | 4.8 | 2226$i$,1392,1932 |
| $C_4(C_{2v})$ | 8.6 | 234,265,892,973,1540,1947 |
| $C_4(^3D_{\infty h})$ | 7.9 | 66(2),184,189,1053,1641,2235 |
| $C_4(D_{2h})$ | 9.1 | 339,638,893,1250,1577,1663 |
| $C_5$ | 12.9 | 132(2),308(2),648(2),873,1670,2128,2142 |
| $C_6(D_{3h})$ | 14.0 | 382$i$,381$i$,314,315,436,767,1092,1128(2),1357,1630(2) |
| $C_6(D_{6h})$ | | Jahn-Teller distortion to irregular $C_{2v}$ structure (see text) |
| | 14.6 | 235$i$,443,444(2),465,486,873,930,1361,1597,1643,1756 |
| $C_6(^3D_{\infty h})$ | 15.1 | 93(2),196,197,397(2),536(2),735,1352,1815,1957,2255 |
| $C_7$ | 19.4 | 76(2),189(2),309(2),593(2),596(2),643,1215,1778,2015,2188,2204 |
| $C_8(C_4h)$ | 22.6 | 284$i$,272$i$,372(2),395,399,446(2),460,496,1088,1166(2),1276,1813,1938,1985(2) |
| $C_8(^3D_{\infty h})$ | 21.6 | 61(2),142,144,240,241,396,397,510(2),516(2),565,1068,1535,1808,2035,2084,2237 |
| $C_9$ | 25.8 | 48(2),123(2),226(2),300(2),509,521(2),579(2),587(2),971,1409,1833,1954,2074,2243,2266 |
| $C_{10}$ | 29.6 | 232$i$,214,215,228(2),292(2),332,345,346,357(2),383(2),843,1131,1132, 1531(2),1930,2155(2),2257(2) |

It is readily seen (cf. Table XXVI), that this approach effectively remedies the anomalous state splittings obtained with the standard parameters. All of the results are now at least as good as with the MINDO/3 method, which basically gives the proof that the INDO/NDDO argument suggested above is not valid. Apparently the values for the exponents are highly critical for reproduction of the state splittings: these in turn are coupled to the $\beta$ values through the Mulliken expression.

Computed heats of formation are in fairly good agreement with the experimental data, given the limited accuracy of the latter. The results obtained for the larger clusters differ substantially from their ab initio counterparts; as our semiempirical results do not seem to exhibit the systematic overestimate for the smaller clusters that is seen with the ab initio values, we consider our modified MNDO values to be more reliable.

The principal qualitative features of the PES are now reproduced too, even for $C_6$, where good agreement with RB [Rag87] and [Rag86b] is obtained, and $C_8$, where the linear-cyclic energy difference is in excellent agreement with the ab initio values of RB. One exception is $C_{10}$, for which a $D_{5h}$ structure with alternating bond distances rather than alternating bond angles is predicted; this was also observed with all the other semiempirical methods. Just as with $C_6$, it is not entirely clear which structure is a

Table XXXIII: MNDO frequencies ($cm^{-1}$) and zero point energies (ZPE, kcal/mol) using standard parameters.

| Species | ZPE | Frequencies |
|---|---|---|
| $C_2(^1\Sigma_g^+)$ | 2.9 | 2062 |
| $C_2(^3\Pi_u)$ | 2.5 | 1733 |
| $C_3(D_{\infty h})$ | 6.6 | 478(2),1417,2207 |
| $C_3(^3D_{3h})$ | | Jahn-Teller distortion to $C_{2v}$ structure |
| | 5.9 | 910,1202,1787 |
| $C_3(C_{2v})$ | 4.3 | 1495*i*,1211,1825 |
| $C_4(C_{2v})$ | 8.7 | 386,468,876,936,1401,1950 |
| $C_4(^3D_{\infty h})$ | 9.4 | 246(2),528(2),1069,1673,2303 |
| $C_4(D_{2h})$ | 7.7 | 211,432,691,1026,1458,1565 |
| $C_5$ | 14.0 | 189(2),445(2),760(2),903,1656,2160,2310 |
| $C_6(D_{6h})$ | 17.8 | 399,426,502(2),595(2),1059,1442,1588,1868(2) |
| $C_6(^3D_{\infty h})$ | 16.8 | 129(2),304(2),527(2),665(2),754,1366,1842,2133,2372 |
| $C_7$ | 21.2 | 99(2),259(2),429(2),662,673(2),763(2),1253,1774,2065,2303,2348 |
| $C_8(D_{4h})$ | 26.8 | 324,339,357,406,550,552,555(2),581(2),1064,1268(2),1521,2109,2201(2),2324 |
| $C_8(^3D_{\infty h})$ | 23.9 | 75,76,194,195,337(2),503,504,577,641(2),683(2),1091,1550,1862,2155,2247,2342 |
| $C_9$ | 28.3 | 60(2),161(2),300(2),421(2),520,617(2),716(2),758(2),1003,1442,1812,2090,2114,2337,2404 |
| $C_{10}$ | 34.4 | 236,239,271(2),499,501,506(2),610(2),615,623,628,629,867,1151(2), 1587(2),2031,2175(2),2295(2) |

computational artifact and which is the true one; both structures may even coexist as isomers. (It is remarked, that extended Hückel theory does predict an exceptional stability for a regular decagon [Hof66].) Along the same lines, the other exception is $C_8$, for which an increase of symmetry from $C_{4h}$ (alternating bond angles *and* distances) to $D_{4h}$ (equal angles, alternating bond lengths) is observed. Of the standard methods, only MINDO/3 yielded a $C_{4h}$ structure, whereas all the others found the same $D_{4h}$ with equal angles. Again, it is not clear which structure is the right one.

The agreement for ionization potentials is slightly worse: compared to the ab initio values of RB, they are systematically underestimated by up to 0.5 eV.

Geometries fare better. The bonds for the two lowest states of $C_2$ are much too short, as expected. For $C_3$, an almost perfect agreement with the experimental value is obtained. For the linear form of $C_4$, the large difference between outer (1.314 Å) and inner (1.270 Å) bond is not an artifact of the computational method (as argued in another context in Bernholc and Phillips [Ber86]): large differences were also predicted at the SCF (1.308 and 1.283 Å) and MP4D (1.330 and 1.305 Å) levels by Magers *et al.* [Mag86] using a [4*s*2*p*1*d*] basis set. Ritchie *et al.* [Rit86] find 1.316 and 1.297 Å at the CISD level with a comparable basis set. Michalska *et al.* [Mic87] find 1.313 and 1.296 Å at the MP2/6-31G* level. For the rhombic structure, we find a bond length of 1.461 Å

and an apex angle of 59.9°. Michalska *et al.* found 1.425 Å and an apex angle of 64.6°, compared to 1.460 Å and 63.2° for Magers *et al.* Finally, Ritchie *et al.* came up with 1.448 Å and 62.4°, respectively.

For $C_5$, one experimental result is available in the form of a rotational constant, which produces a mean effective bond length of 1.283 Å [Hea89]. Our calculation finds outer and inner bond lengths of 1.280 and 1.270 Å, respectively. From the definition of the principal moment of inertia for a linear molecule, we find $r_{\text{eff}} = \sqrt{[(r_1 + r_2)^2 + r_2^2]/5}$. This yields an $r_{\text{eff}}$ of 1.274 Å, not corrected for zero-point vibration effects: this value appears to be quite reasonable. Ab initio treatments find $r_1 = 1.300$ Å and $r_2 = 1.291$ Å at the MP2/6-31G* level [Mar89b], $r_1 = 1.297$ and $r_2 = 1.286$ at the CCSD+T(CCSD) [Lee84] level [Ada89], $r_1 = 1.296$ and $r_2 = 1.287$ Å at the CEPA-1 [Kut77] level with a [7*s*3*p*1*d*] basis set [Bot89], and $r_1 = 1.289$ Å, $r_2 = 1.283$ Å at the CEPA-1 level with an [8*s*4*p*2*d*] basis set. These results lead to $r_{\text{eff}}$ values of 1.295, 1.290, 1.291, and 1.285 Å, respectively. Apparently, our semiempirical method holds its own. However, one might argue that since $C_5$ has very low bending frequencies too, the same phenomenon as in $C_3$ might occur, in that $r_0$ might be smaller than $r_e$, and that the values around 1.290 Å are good estimates for the effective $r_e$. In any case, the difference in the bond lengths is reproduced quite well, which cannot be said of SCF-level ab initio calculations [Rag87, Ewi87]: these consistently predict the outer bond to be slightly shorter than the inner bond.

From $C_6$ onwards, the only reference material available is at the Hartree-Fock level [Rag87], except for the $C_6$ CASSCF structures by Parasuk and Almlöf [Par89a] who do not find the $D_{3h}$ structure as the global minimum. Their predicted geometry for the lowest linear state is in partial agreement with ours: 1.298, 1.280, and 1.265 Å from the outside in, compared to 1.299, 1.266, and 1.272 Å in our calculation. Our predicted geometry for the cyclic structure, $r$=1.352 Å and $\theta = 80.42°$, is quite consistent with the expected effects of electron correlation on the HF/6-31G* geometry: the latter [Rag87] was $r$=1.316 Å and $\theta$=90.4°. The angle was quite sensitive towards the basis set: they found 101.4° at the HF/3-21G level. The geometries for $C_7$, linear $C_8$, and $C_9$ agree only partially with their HF/6-31G* counterparts; however, as became clear above, HF/6-31G* bond distances for the linear clusters disagreed both qualitatively and quantitatively with their correlated counterparts. The geometry for cyclic $C_8$ behaves somewhat like that of cyclic $C_6$. The $C_{10}$ system clearly deserves further study. In principle, both our structure and that of RB might be computational artifacts.

#### 4.7.3.4 Harmonic frequencies

Harmonic frequencies using the standard parameters are given in Tables XXXII to XXXV for the MINDO/3, MNDO, AM1, and PM3 methods, respectively. A summary of ab initio and experimental values can be found in Table XXXVI. In this latter table, RRHO zero-

Table XXXIV: AM1 frequencies ($cm^{-1}$) and zero point energies (ZPE, kcal/mol) using standard parameters.

| Species | ZPE | Frequencies |
|---|---|---|
| $C_2(^1\Sigma_g^+)$ | 3.1 | 2146 |
| $C_2(^3\Pi_u)$ | 2.7 | 1906 |
| | | |
| $C_3(D_{\infty h})$ | 6.5 | 432(2),1450,2264 |
| $C_3(^3D_{3h})$ | | Jahn-Teller distortion to $C_{2v}$ structure |
| | 6.3 | 1029, 1295, 1871 |
| $C_3(C_{2v})$ | 4.5 | 1756*i*,1270,1878 |
| | | |
| $C_4(C_{2v})$ | 8.9 | 338,424,966,978,1442,2021 |
| $C_4(^3D_{\infty h})$ | 9.4 | 223(2),465(2),1096,1720,2363 |
| $C_4(D_{2h})$ | 8.3 | 326,441,797,1134,1526,1600 |
| | | |
| $C_5$ | 14.1 | 175(2),417(2),733(2),926,1701,2205,2363 |
| | | |
| $C_6(D_{6h})$ | 18.3 | 351,435(2),587,594(2),1253,1525,1629(2),1884(2) |
| $C_6(^3D_{\infty h})$ | 16.7 | 120,121,280(2),496(2),608(2),775,1407,1893,2183,2434 |
| | | |
| $C_7$ | 21.3 | 93(2),243(2),401(2),652(2),681,706(2),1286,1821,2118,2371,2393 |
| | | |
| $C_8(D_{4h})$ | 26.7 | 256,288,354,405,458,484(2),539,553(2),1117,1322(2),1564,2156,2239,2239,2361 |
| $C_8(^3D_{\infty h})$ | 23.8 | 71,72,183,184,314(2),474(2),595,597,614(2),1124,1596,1916,2209,2310,2411 |
| | | |
| $C_9$ | 28.3 | 57(2),153(2),283(2),393(2),537,592(2),672(2),692(2),1032,1482,1866,2141,2191,2397,2460 |
| | | |
| $C_{10}$ | 31.5 | 237,240,266(2),477(2),484,485,525,535(2),575,583,584,912,1214(2), 1674(2),1855,2211(2),2327,2328 |

point energies (ZPE) and thermal vibrational energies ($E_{\text{vib}}^{298}$)have also been included, for convenience. The latter are computed as:

$$E_{\text{vib}}^{T} = RT \sum_i \frac{u_i}{\exp u_i - 1} \qquad \text{with} \qquad u_i \equiv \frac{hc\omega_i}{kT} \tag{4.14}$$

where the summation index $i$ extends over all the normal modes.

Because the force constant matrix in the semiempirical calculations is constructed from finite differences of the gradient, it may occasionally happen that vibrations belonging to a degenerate pair have frequencies that differ by a wavenumber or more. In such cases, both frequencies are listed in the interest of reproducibility; otherwise, the degeneracies have been given in parentheses.

It is striking again, that the MINDO/3 frequencies are on the whole in better agreement with experiment than any of the three other methods: it even holds its own against a substantial part of the ab initio result. All semiempirical methods, MINDO/3 less than the others, tend towards a systematic overestimate of the frequencies; this property is shared with ab initio HF-level calculations.

Zero-point energies compare quite well with their ab initio HF counterparts. The MINDO/3 values tend to be on the low side, the others on the high side. It should however be remembered, that the ab initio HF values will exhibit a systematic overestimate of

Table XXXV: PM3 frequencies ($cm^{-1}$) and zero point energies (ZPE, kcal/mol) using standard parameters.

| Species | ZPE | Frequencies |
|---|---|---|
| $C_2(^1\Sigma_g^+)$ | 2.9 | 1995 |
| $C_2(^3\Pi_u)$ | 2.5 | 1767 |
| $C_3(D_{\infty h})$ | 6.5 | 410(2),1453,2298 |
| $C_3(^3D_{3h})$ | 6.8 | 1138,1141,1985 |
| $C_3(C_{2v})$ | 4.9 | 1248*i*,1361,2043 |
| $C_4(C_{2v})$ | 9.2 | 335,419,1007,1059,1498,2041 |
| $C_4(^3D_{\infty h})$ | 9.6 | 224(2),526(2),1087,1723,2357 |
| $C_4(D_{2h})$ | 8.8 | 414,473,908,1156,1585,1685 |
| $C_5$ | 14.0 | 166(2),390(2),740(2),909,1695,2232,2348 |
| $C_6(D_{6h})$ | 19.0 | 505,550(2),576,672(2),1155,1496,1638(2),1931,1932 |
| $C_6(^3D_{\infty h})$ | 16.6 | 113(2),172(2),492(2),628(2),756,1388,1888,2164,2387 |
| $C_7$ | 21.1 | 86(2),227(2),376(2),634(2),661,765(2),1265,1807,2124,2306,2401 |
| $C_8(D_{4h})$ | 26.8 | 314,328,342,355,532,558(2),574,582(2),1059,1256(2),1514,2143,2229(2),2365 |
| $C_8(^3D_{\infty h})$ | 23.5 | 65,66,172(2),298,299,461,462,576,602(2),658(2),1098,1575,1904,2195,2256,2332 |
| $C_9$ | 28.1 | 52(2),140(2),263(2),369(2),518,575(2),697(2),1007,1456,1848,2108,2145,2369,2438 |
| $C_{10}$ | 34.2 | 214,217,244(2),481(2),482(2),608,618(2),630,632(2),860,1158,1159, 1614,1615,1916,2197,2198,2313(2) |

about 10 % [Pop81], and that MINDO/3 thus produced again the best results. Some overestimation in the linear species comes from the inaccurate description of the very low bending frequencies; however, ab initio theory with DZP basis sets is also only capable of a qualitative reproduction for these [Sim88].

Summarizing, the agreement with experiment at the various semiempirical levels is certainly no worse than at the ab initio HF level; both are inferior to the correlated ab initio results. A useful agreement with experiment is not really obtained.

With the new parameters, harmonic frequencies were evaluated for all the species considered in this study. The MNDO results are given in Table XXXVII.

They do exhibit one really striking feature: an uncanny agreement with the available experimental results, even for the $C_2$ molecule which, being a diatomic, is supposed not to be described well by an NDDO-based method parametrized for polyatomics! The computed harmonic frequencies of 1883 and 1603 $cm^{-1}$ compare really well with the experimental values [Hub79] of 1855 and 1641 $cm^{-1}$, respectively. For comparison, Bauschlicher and Langhoff [Bau87] obtain ab initio values of 1785 and 1598 $cm^{-1}$ with a Davidson-corrected [Lan74] MRD-CI [Bue74] treatment in a huge [5*s*4*p*3*d*2*f*1*g*] atomic natural orbital [Alm87] basis set: these calculations took several hours on a Cray X-MP/48, while these humble semiempirical runs took about 15 seconds on a Cyber 930. This illustrates again the potential power of a properly parametrized semiempirical method,

even if the parametrization has to be carried out ad hoc: it should be remembered that no adjustment at all for the reproduction of frequencies was made!

The computed IR-active stretching of 2104 $cm^{-1}$ for $C_3$ again compares well with the experimental value of 2040 $cm^{-1}$ [Wel64], which itself is lowered by anharmonic effects. The bending frequency is only qualitatively reproduced, though; however, the same is true for the HF/6-31G* results of RB, and even at the MP2/6-31G* level [Ada89]. It is well known [Sim88], that the reproduction of bending frequencies of multiply-bounded molecules necessitates the use of basis sets with *f* functions, even at sophisticated electron correlation levels.

For the linear form of $C_4$, it is readily seen that our computed harmonic spectrum agrees quite well with the MP2/6-31G* results by Michalska *et al.* [Mic87], even in the low bending frequency. The agreement of the experimental 1544 $cm^{-1}$ band with our computed 1541 $cm^{-1}$ level is almost too good to be true. The agreement with the MP2/6-31G* spectrum for rhombic $C_4$ is somewhat less good: its primary weak spot are the low bending frequencies which would require a more sophisticated ab initio treatment as well. Oddly enough, our computed spectrum is in good agreement with the HF/6-31G* values scaled by a suggested factor of 0.89 [Pop81].

For $C_5$, a really good agreement is observed with the MP2/6-31G* spectrum by Martin *et al.* [Mar89b] (Section 4.6), with a recommended scaling factor of 0.93 [Hou82]. In the former reference, the asymmetric stretching mode has been assigned to the experimental band at 2164 $cm^{-1}$; the value of 2199 $cm^{-1}$ computed here can only be called very satisfactory, given that the MP2/6-31G* spectrum required six hours CPU time on an IBM 3090/300 VF, whereas the present calculation took just under two minutes on the Cyber 930. Good agreement with a more recent CEPA-1 calculation of Botschwina and Sebald [Bot89] is also found.

From $C_6$ onwards, no other material is available than the HF/6-31G* study by RB. A number of IR bands in argon matrix have been tentatively assigned by TDW [Tho71]; however, at least for $C_4$ and $C_5$, their assignment has been proven incorrect. It was also based on linear structures, whereas for $C_6$, $C_8$, and $C_{10}$, the most stable structures are predicted to be cyclic. Correlated ab initio frequencies including IR intensities would be helpful to settle the assignment. Such a study is currently in progress in our laboratory (Section 4.8); however, useful results can even be obtained at this modest level of theory.

MOPAC 5.00 has an undocumented facility for computing dipole moment derivatives (erroneously called 'T-DIPOLE's in the output) of normal vibrations. Although there appear to be some problems with the algorithm, and the absolute values are probably of little use, relative intensities with respect to the 2039 $cm^{-1}$ vibration of $C_3$ appear to be in reasonable agreement with high-level ab initio results. For example, the IR intensities of the two highest active bands of $C_5$ are predicted to differ by a factor 14.7, whereas Botschwina and Sebald found 18.2 (double-harmonic) at their highest theoretical level.

Table XXXVI: ab initio and experimental frequencies ($cm^{-1}$), as well as corresponding zero point energies (ZPE, kcal/mol) and thermal vibrational energies at 298.15 K ($E_{vib}^{298}$, kcal/mol).

| Species | Ref. | ZPE | $E_{vib}^{298}$ | Frequencies |
|---|---|---|---|---|
| $C_2(X\,^1\Sigma_g^+)$ | [Rag87] | 2.8 | 0.0 | $1940(\sigma_g)$ |
| | [Bau87] | 2.6 | 0.0 | $1785(\sigma_g)$ |
| | [Hub79] | 2.7 | 0.0 | observed: $1855(\sigma_g)$ |
| $C_2(a\,^3\Pi_u)$ | [Bau87] | 2.3 | 0.0 | $1598(\sigma_g)$ |
| | [Hub79] | 2.3 | 0.0 | observed: $1641(\sigma_g)$ |
| $C_3(C_{2v})$ | [Whi81a] | 4.8 | 0.0 | $1402i(b_2)$,$1339(a_1)$,$2013(a_1)$ |
| $C_3(D_{\infty h})$ | [Rag87] | 5.7 | 0.8 | $154(\pi_u)$,$1367(\sigma_g)$,$2311(\sigma_u)$ |
| | [Ada89] | | | $190(\pi_u)$,$1220(\sigma_g)$,$2184(\sigma_u)$ |
| | [Gau65] | ... | ... | observed: $65(\pi_u)$,$2040(\sigma_u)$ |
| $C_3(D_{3h})$ | [Whi81a] | 5.7 | 0.0 | $1091(e')$,$1774(a1')$ |
| $C_4(^3D_{\infty h})$ | [Rit86] | 9.1 | 1.1 | $209(\pi_u)$,$408(\pi_g)$,$1022(\sigma_g)$,$1741(\sigma_u)$,$2345(\sigma_g)$ |
| | [Mic87] | 8.4 | 1.1 | $187(\pi_u)$,$419(\pi_g)$,$951(\sigma_g)$,$1586(\sigma_u)$,$2149(\sigma_g)$ |
| | [Ber88b]a | 9.1 | 1.0 | $214(\pi_u)$,$454(\pi_g)$,$1003(\sigma_g)$,$1715(\sigma_u)$,$2300(\sigma_g)$ |
| | [Ber88b]b | 8.5 | 1.0 | $209(\pi_u)$,$449(\pi_g)$,$1014(\sigma_g)$,$1349(\sigma_u)$,$2292(\sigma_g)$ |
| | [She89] | ... | ... | observed: $1544(\sigma_g)$ |
| $C_4(D_{2h})$ | [Rag87] | 8.6 | 0.4 | $350(b_{2u})$,$450(b_{3u})$,$1088(a_g)$,$1103(b_{3g})$,$1431(a_g)$,$1568(b_{1u})$ |
| | [Rit86] | 8.4 | 0.4 | $345(b_{2u})$,$444(b_{3u})$,$1061(a_g)$,$1087(b_{3g})$,$1419(a_g)$,$1541(b_{1u})$ |
| | [Mic87] | 8.4 | 0.3 | $374(b_{2u})$,$712(b_{3u})$,$934(a_g)$,$1103(b_{3g})$,$1298(a_g)$,$1428(b_{1u})$ |
| | [Mag86] | 8.2 | 0.3 | $359(b_{2u})$,$716(b_{3u})$,$912(a_g)$,$1079(b_{3g})$,$1255(a_g)$,$1389(b_{1u})$ |
| $C_5$ | [Rag87] | 12.9 | 1.8 | $112(\pi_u)$,$222(\pi_g)$,$648(\pi_u)$,$863(\sigma_g)$,$1632(\sigma_u)$,$2220(\sigma_g)$,$2344(\sigma_u)$ |
| | [Mar89b] | 12.0 | 1.8 | $130(\pi_u)$,$281(\pi_g)$,$487(\pi_u)$,$786(\sigma_g)$,$1471(\sigma_u)$,$2018(\sigma_g)$,$2358(\sigma_u)$ |
| | [Bot89] | 11.8 | 1.8 | $119(\pi_u)$,$209(\pi_g)$,$570(\pi_u)$,$790(\sigma_g)$,$1477(\sigma_u)$,$2010(\sigma_g)$,$2168(\sigma_u)$ |
| | [Ber89] | ... | ... | observed: $2164(\sigma_u)$ |
| $C_6(^3D_{\infty h})$ | [Rag86b] | 16.9 | 2.0 | $105(\pi_u)$,$228(\pi_g)$,$494(\pi_u)$,$715(\sigma_g)$,$866(\pi_g)$,$1289(\sigma_u)$,$1801(\sigma_g)$, $2184(\sigma_u)$,$2459(\sigma_g)$ |
| $C_6(D_{6h})$ | [Rag86b] | 17.4 | 0.3 | $786i(b_{1u})$,$351i(b_{2g})$,$641(e_{2u})$,$781(e_{2g})$,$1006(b_{2u})$,$1357(a_{1g})$,$1562(e_{1u})$, $1928(e_{2g})$ |
| $C_6(D_{3h})$ | [Rag87] | 18.1 | 0.6 | $458(a_2")$,$575(e")$,$738(e')$,$888(a_1')$,$1269(a_1')$,$1285(e')$,$1349(a_2')$,$1764(e')$ |
| | [Rag86b] | 18.0 | 0.6 | $408(a_2")$,$617(e")$,$750(a_1')$,$753(e')$,$1252(a_2')$,$1269(a_1')$,$1365(e')$,$1726(e')$ |
| $C_7$ | [Rag87] | 19.9 | 2.8 | $73(\pi_u)$,$157(\pi_g)$,$240(\pi_u)$,$598(\pi_g)$,$631(\sigma_g)$,$710(\pi_u)$,$1206(\sigma_u)$, $1745(\sigma_g)$,$2132(\sigma_u)$,$2281(\sigma_u)$,$2376(\sigma_g)$ |
| $C_8(C_4h)$ | [Rag87] | 24.7 | 1.8 | $190(b_g)$,$294(b_u)$,$344(b_u)$,$371(a_u)$,$482(e_g)$,$512(b_g)$,$677(e_u)$,$738(a_g)$, $1014(a_g)$,$1097(e_u)$,$1276(b_g)$,$1957(b_g)$,$2007(e_u)$,$2050(a_g)$ |
| $C_8(^3D_{\infty h})$ | [Rag87] | 20.1 | 3.6 | $819i(\pi_g)$,$67(\pi_u)$,$170(\pi_g)$,$225(\pi_g)$,$293(\pi_u)$,$355(\pi_u)$,$552(\sigma_g)$, $1049(\sigma_u)$,$1495(\sigma_g)$,$1867(\sigma_u)$,$2161(\sigma_g)$,$2330(p_u)$,$2393(\sigma_g)$ |
| $C_9$ | [Rag87] | 26.9 | 3.9 | $49(\pi_u)$,$114(\pi_g)$,$187(\pi_u)$,$252(\pi_g)$,$496(\sigma_g)$,$567(\pi_u)$,$658(\pi_g)$,$783(\pi_u)$, $960(\sigma_u)$,$1393(\sigma_g)$,$1803(\sigma_u)$,$2084(\sigma_u)$,$2134(\sigma_g)$,$2338(\sigma_u)$,$2415(\sigma_g)$ |
| $C_{10}$ | [Rag87] | 30.5 | 2.7 | $184(e_2')$,$253(e_2")$,$419(a_2")$,$497(e_2")$,$555(e_1")$,$568(e_2')$,$577(a_2')$, $661(a_1')$,$690(e_1')$,$946(a_1')$,$1118(e_1')$,$1522(e_2')$,$1971(e_2')$,$2013(e_1')$ |

(a) UHF/4s2p2d
(b) ROHF/4s2p1d
[Bau87]: MRCI+Q/[$5s4p3d2f1g$]
[Rag86b] : UHF/3-21G
[Whi81a, Rag87] : UHF/6-31G*, unscaled (scaling by 0.89 recommended [Ada89], based on a linear regression between calculated and experimental frequencies for a wide range of molecules)
[Mic87, Mar89b, Ada89]: MP2/6-31G*, unscaled (scaling by 0.93 recommended [Wel64] on the same grounds)
[Mag86]: MP2/4s2p1d
[Bot89]: CEPA-1/8s4p2d (harmonic values given)

Table XXXVII: MNDO frequencies ($cm^{-1}$) and zero point energies (ZPE, kcal/mol) using fully reoptimized parameters.

| Species | ZPE | Frequencies |
|---|---|---|
| $C_2(^1\Sigma_g^+)$ | 2.7 | 1883 |
| $C_2(^3\Pi_u)$ | 2.3 | 1603 |
| | | |
| $C_3(C_{2v})$ | 4.3 | 1648*i*,1286,1743 |
| $C_3(D_{\infty h})$ | 6.0 | 383(2),1301,2104 |
| $C_3(^3D_{3h})$ | | Jahn-Teller distortion to $C_{2v}$ structure |
| | 5.7 | 1051,1218,1722 |
| | | |
| $C_4(C_{2v})$ | 8.5 | 274,384,927,1057,1371,1933 |
| $C_4(^3D_{\infty h})$ | 8.5 | 200(2),447(2),966,1541,2171 |
| $C_4(D_{2h})$ | 8.3 | 296,383,852,1157,1536,1551 |
| | | |
| $C_5$ | 12.8 | 151(2),370(2),689(2),813,1528,2015,2199 |
| | | |
| $C_6(^3D_{\infty h})$ | 15.1 | 105(2),248(2),453(2),540(2),677,1240,1694,1999,2245 |
| $C_6(D_{6h})$ | 16.0 | 284*i*,278,361,362,419(2),1310,1356,1510(2),1850(2) |
| $C_6(D_{3h})$ | 14.0 | 272(2),317,364,365,687,1015(2),1189,1229,1527(2) |
| | | |
| $C_7$ | 19.3 | 80(2),212(2),357(2),594,602(2),670(2),1135,1631,1939,2193,2202 |
| | | |
| $C_8(D_{4h})$ | 23.6 | 217,221,232,263,351,356(2),387,424(2),963,1187(2),1450,1984,2113(2),2259 |
| $C_8(^3D_{\infty h})$ | 21.5 | 62,64,161,162,276,277,429(2),518,533(2),557(2),984,1410,1715,2005,2128,2233 |
| | | |
| $C_9$ | 25.7 | 49(2),132(2),248(2),350(2),467,543(2),628(2),657(2),905,1312,1676,1938,2042,2196,2266 |
| | | |
| $C_{10}$ | 30.6 | 190,193,230(2),397,398,403,428(2),443(2),471,484(2),787,1064(2), 1499(2),1819,2030(2),2185(2) |

Also, the relative intensity (RI) of the 2164 $cm^{-1}$ band is found as 4.3, whereas one finds 3.1 from the $C_5$ results of Botschwina and Sebald and the high-level $C_3$ results of Kraemer *et al.* [Kra84]. They should thus give at least a semiquantitative measure of the relative intensities of the vibrations, and so be of considerable use in making the assignments; by the way, this type of accuracy would normally require correlated ab initio calculations.

It should also be kept in mind that the calculations appear to overestimate the experimental frequencies by about 40 $cm^{-1}$ for the linear species; part of this difference could be due to anharmonicity.

Another factor that may aid in assignment is the intensity variation of the bands during annealing. If it is very closely related for two bands, they probably belong to the same species; otherwise, they certainly do not. Spectra at different annealing temperatures may be found in TDW, as well as in Krätschmer and Nachtigall [Kra85] (KN).

Working down from the top, there are two candidates for the 2128 $cm^{-1}$ band: linear $C_9$ (2196 $cm^{-1}$, RI=4.5) and linear $C_7$ (2193 $cm^{-1}$, RI=4.1). The $C_9$ assignment was made by TDW; however, the most striking spectral feature of $C_9$ is an extremely intense band calculated as 2042 $cm^{-1}$, RI=22.9. So assignment of the 2128 $cm^{-1}$ band to $C_9$ would require that, upon annealing, a very large band around 2000 $cm^{-1}$ would increase

in intensity together with the 2128 $cm^{-1}$ line. There is a huge band at 1997 $cm^{-1}$ (see below), but its growing behavior is not at all correlated with that of the 2128 $cm^{-1}$ band, so the $C_9$ assignment may be rejected. For $C_7$, we calculate another intense band at 1939 $cm^{-1}$, RI=3.3. The 1893 $cm^{-1}$ band, also previously assigned to $C_9$, not only has the right intensity, but its growing behavior is well correlated with that of the 2128 $cm^{-1}$ feature (as already noted by TDW). We therefore assign the 2128 and 1892 $cm^{-1}$ band pair to linear $C_7$.

At high annealing rates, a band around 2075-2080 $cm^{-1}$ is observed, which might possibly be due to linear $C_8$. Its growing behavior is correlated with that of bands in the 1800 $cm^{-1}$ region which are most probably due to cyclic $C_8$ (see below).

There are three candidates for the 1997 $cm^{-1}$ band; linear $C_8$ (2128 $cm^{-1}$, RI=4.6), linear $C_6$ (1999 $cm^{-1}$, RI=1.6), and linear $C_9$ (2042 $cm^{-1}$, RI=22.9). The huge intensity for the latter frequency is confirmed at the UHF/6-31G* level [Rag87, RagPC], where a value of no less than 40497 km/mol was found (compared to 1346 km/mol for $C_3$). The computed wavenumber for linear $C_8$ appears to be too high to correspond to the experimental 1997 $cm^{-1}$; also, one would expect $C_9$ to be more abundant because of the odd-even alternation in stability. For linear $C_6$, an additional band is calculated at 1240 $cm^{-1}$, RI=0.18. Such a band is found at 1197 $cm^{-1}$; however, its growing behavior is not at all correlated with that of the 1997 $cm^{-1}$ band, as already noted by KN. The original assignment to $C_6$ should thus be rejected. The only one remaining is then linear $C_9$; it has other intense bands calculated as 2196 $cm^{-1}$ (RI=4.5) and 1676 $cm^{-1}$ (RI=1.5). Bands at 1589 and 1601 $cm^{-1}$ have about the right intensity for the latter, and correlate in their growing behavior with the 1997 $cm^{-1}$ band. Also, several features above 2190 $cm^{-1}$ pile up upon stronger annealing of the matrix (and growth of $C_9$); one of these could be the missing band for $C_9$.

Then comes the 1952 $cm^{-1}$ band erroneously attributed to $C_5$. Its relatively constant intensity correlates well with that of the 1197 $cm^{-1}$ band: we therefore assign both 1952 and 1197 $cm^{-1}$ to linear $C_6$. A possible reaction mechanism explaining the annealing behavior of the 1952, 1997, and 2039 $cm^{-1}$ bands would be:

$$2C_3 \rightarrow C_6 \tag{4.15}$$

$$C_6 + C_3 \rightarrow C_9 \tag{4.16}$$

(two mass spectrometric measurements [Dro59, Zav73] indicated that the trapped vapor consisted for 65 and 75 %, respectively, of $C_3$). In such a mechanism, the $C_9$ intensity would increase with decreasing $C_3$ concentration, whereas the $C_6$ concentration would remain approximately 'steady state'.

Assignments for the remaining bands are a bit more speculative. The 1447 $cm^{-1}$ band could come from the second asymmetric stretch of $C_5$ (calculated as 1528 $cm^{-1}$, RI=0.29). However, again its growing behavior is totally different from that of the 2164

$cm^{-1}$ band, so this assignment should not be retained.

TDW suggested that the bands at 2198, 1893, and 1447 $cm^{-1}$ belong to the same molecule, because of their parallel growing behavior. However, in KN the 1447 $cm^{-1}$ band is seen to grow much faster than the 1893-2128 $cm^{-1}$ pair. Furthermore, the only IR-active band above 1000 $cm^{-1}$ of $C_7$ is predicted to lie at 1206 $cm^{-1}$ by RB, and 1135 $cm^{-1}$ by ourselves, and not to have an appreciable IR intensity. This rules out the assignment of the 1447 $cm^{-1}$ band to $C_7$.

Basically, only the frequencies for the cyclic species then remain; however, our predictions for these are probably not nearly as accurate as for the linear forms. Both 1284 and 1447 $cm^{-1}$ are candidates for cyclic $C_4$, but their growing behavior is totally different from that of the 1544 $cm^{-1}$ band of linear $C_4$. However, kinetic arguments may be invoked to explain this: whereas linear $C_4$ will readily grow to linear $C_5$, $C_6$, or $C_7$ with C, $C_2$, and $C_3$, respectively, the cyclic form would give rise to much less stable capped ring structures. As the linear and cyclic forms do not readily interconvert, cyclic $C_4$ might accumulate while linear $C_4$ is used up in cluster growth (primarily to $C_7$).

Furthermore, the free energy function for isomerization will approximately vary in this temperature range as $\frac{1}{2} \ln T$ (favoring the cyclic structure), since vibrational states are not yet appreciably populated at the temperatures involved whereas the rotors are already approaching classical behavior. This in itself accounts for some, but nearly not all, of the observed intensity variation.

For the 1804, 1818 and 1844 $cm^{-1}$ bands, both cyclic $C_8$ and $C_{10}$ are candidates based on the UHF/6-31G* results of RB. As already noted by KN, the 1804 and 1844 $cm^{-1}$ bands are so closely correlated that they most probably belong to the same molecule. A possible explanation would be the existence of two different distorted forms of the regular ring that lie very close in energy, such as the two $D_{3h}$ structures of $C_6$ found by Raghavachari *et al.* [Rag86b] and Parasuk and Almlöf [Par89a]. Both $C_8$ and $C_{10}$ are candidates for this: further ab initio work on these systems is clearly called for. If the 2075-2080 $cm^{-1}$ band were really linear $C_8$, then we would tend to assign 1818 to cyclic $C_8$ and the 1804,1844 pair to cyclic $C_{10}$, based on the growing behavior of the bands.

A 1595 $cm^{-1}$ band at strong annealing is probably due to $C_3O_2$ because of almost unavoidable contamination by CO.

Finally, the two bands at 1696 and 1715 $cm^{-1}$ might both be due to cyclic $C_6$ (two forms are also possible here). Similar arguments as for $C_4$ apply to explain the lack of correlation with the intensity of the linear $C_6$ bands. The growing behavior of the 1284 $cm^{-1}$ band is correlated with these, so it might also be due to cyclic $C_6$. Again, further ab initio work is called for.

TDW observed substitution patterns with 95 % $^{13}C$-enriched carbon for a number of the bands. We have computed the isotope shifts for single $^{12}C$ substitutions as a final test for the accuracy of our assignments. Both the computed and the observed shifts are

only accurate to a few $cm^{-1}$; only qualitative agreement is expected.

The most intense isotopic band of $C_3$ is predicted at $\Delta = 14.4$ $cm^{-1}$, which is in excellent agreement with the experiental $\Delta$=14 of TDW. All predicted isotope shifts for linear $C_4$ are in very good agreement with the accurate experimental values by Shen and Graham [She89]; the primary bands are predicted at 14.3 and 15.5, and contribute to the $\Delta$=15 peak seen by TDW. Their $\Delta = 30$ peak corresponds to an accumulation of several doubly substituted peaks, which is found theoretically and experimentally [She89].

For $C_5$, the predicted position of all isotopic substituted bands is in excellent agreement with the experimental pattern [Val89]. Primary peaks are predicted at $\Delta = 2.7$, 25.5, and 39.3, with the last peak being only half as intense. This is in good agreement with the $\Delta = 24$ and the weaker band at $\Delta = 37$ $cm^{-1}$ in TDW. Predicted shifts for the lower IR-active band of $C_5$ are $\Delta = 20.2$, 2.8, and 16.2 $cm^{-1}$ from the inside out. The experimental 1447 $cm^{-1}$ feature has $\Delta = 4$ and 6, which again shows that this band does not belong to $C_5$.

The 1197 $cm^{-1}$ band of $C_6$ is predicted to have shifts 9.5, 0.2, and 12.8 $cm^{-1}$, from the inside out, for the three possible distinct substitutions, which is in perfect agreement with the observed $\Delta = 10$ and 12 $cm^{-1}$ (equally strong) seen experimentally. This assignment is thus fairly certain. For the 1952 $cm^{-1}$ companion band, we predict shifts 8.2, 25.1, 4.9 $cm^{-1}$ from the inside out. The first and third band may correspond to the experimental $\Delta = 6$, the second one to $\Delta = 22$ $cm^{-1}$. An observed $\Delta = 38$ $cm^{-1}$ is actually a weak shoulder to the $C_9$ band, and might thus well correspond to a doubly substituted band or merger of these, of which there are several in the right region (see also the results for linear $C_4$).

For the 1997 $cm^{-1}$ band of linear $C_9$, we predict shifts of 0.05, 3.8, 17.7, 15.9, and 2.2 from the inside out. Given the rather broad lines, and the fact noted by TDW that both the parent peak and the isotope peak have shoulders on the high frequency side, the agreement with the single observed $\Delta$=14 $cm^{-1}$ is excellent. Linear $C_8$ has predicted shifts of 4.3, 20.2, 15.2, 1.3, and 0.0 from the inside out, which counterindicates the $C_8$ assignment and thus lends further support to our $C_9$ assignment.

The 1893 $cm^{-1}$ band of linear $C_7$ has computed shifts of 8.3, 0.1, 21.3 and 9.8 $cm^{-1}$ from the inside out, in good agreement with the observed $\Delta$=9 and 11. The $\Delta$=11 band is about half as intense as the $\Delta$=9 band, which means that the inner and outer bands have been exchanged. The changes in force constants required for this would alter the observed shifts of the 2128 $cm^{-1}$ band $\Delta$=7.9, 4.0, 0.7, and 0.0 (from the inside out) sufficiently to obtain good agreement with the single observed band at $\Delta$=13.

Finally, both our force field for cyclic $C_4$ (which we do not consider as reliable as those for the linear species) and its MP2/6-31G* counterpart by Michalska *et al.* [Mic87] lead to isotope shifts in flagrant contradiction with those observed for the 1447 $cm^{-1}$ band. The only candidate remaining for cyclic $C_4$ is thus the 1284 $cm^{-1}$ feature.

Computed zero-point energies are comparable to those obtained at correlated ab initio levels: the same remarks as above apply concerning the linear species.

### 4.7.4 Conclusions

The following salient points appear to emerge from this study:

- MINDO/3 with standard parameters gives a surprisingly good account of the PES of the carbon clusters $C_2$ - $C_{10}$ . The other methods perform very much worse with their standard parameters.
- Possibly, the performance of MNDO-type methods could be enhanced (or at least be made more uniform) by allowing for bond-specific $\alpha$ and $\beta$ parameters as in MINDO/3.
- By parametrizing all MNDO parameters to fit the heat of formation for $C_3$ and $C_4$, as well as the singlet-triplet splitting in the latter, good agreement with experiment can be obtained for the heats of formation, whereas the PES is described consistently with powerful ab initio methods.
- The latter approach yields harmonic frequencies in exceptionally good agreement with available experimental values. The bands at 2128 and 1892 $cm^{-1}$, formerly assigned by TDW to $C_9$, should be reassigned to linear $C_7$. The intense 1997 $cm^{-1}$ feature almost certainly belongs to $C_9$; bands at 1952 and 1197 $cm^{-1}$ both belong to linear $C_6$. Tentative assignments of lines in the 1600-1850 $cm^{-1}$ region to various cyclic structures of $C_6$, $C_8$, and $C_{10}$ have been made.
- The approach outlined above, parametrizing towards known experimental or ab initio data for a small number of molecules in a particular class and then using the new semiempirical model for predictions about the unknown species, could be an inexpensive alternative to the use of ab initio methods combined with various scaling procedures.

## 4.8 Ab initio study of the infrared spectra of linear $C_n$ clusters (n=6–9)

### 4.8.1 Introduction

In view of their large interest in astrophysics, materials science, and in combustion processes, among other subjects, carbon clusters have been studied rather extensively over the years: the situation up to April 1989 has been reviewed by Weltner and Van Zee [Wel89].

$C_2$ [Hub79] and $C_3$ [Gau65] are well characterized spectroscopically; IR bands in argon matrix of the higher species have been studied as early as 1971 by Thompson, DeKock, and Weltner (TDW) [Tho71]. On the basis of simple force field arguments, TDW suggested an assignment for these bands involving linear species $C_4$ to $C_9$. Except for the actual frequencies, isotopic substitution bands from 95 % $^{13}C$-enriched samples, as well as intensity variation upon thermal annealing, were involved in their assignment. In this context, a later study of the annealing behavior of these bands by Krätschmer and Nachtigall (KN) [Kra85] should also be mentioned.

It was only eighteen years later, that the TDW assignment for $C_4$ (2164 $cm^{-1}$) and $C_5$ (1544 $cm^{-1}$) was definitively proven to be wrong by correlated *ab initio* calculations on the force field of $C_4$ [Mic87, Ber88b] and $C_5$ [Mar89b, Bot89, Ada89]. The new assignment, which swapped these frequencies, was experimentally proven by Vala *et al.* [Val89], Bernath *et al.* [Ber89] and Heath *et al.* [Hea89] for $C_5$, and by Shen and Graham [She89] for $C_4$.

Very recently, the Martin *et al.* (MFG) [Mar90g] developed an *ad hoc* modification of the MNDO (modified neglect of diatomic overlap) [Dew77a] method that yields good to excellent results for carbon clusters, especially the harmonic frequencies, which consistently overestimate the available experimental matrix IR frequencies by about 40 $cm^{-1}$ for the linear species (Section 4.7).

In combination with their computed IR intensities and UHF/6-31G* (unrestricted Hartree-Fock) counterparts of these by Raghavachari [RagPC], as well as computed isotope shifts, MFG attempted a new assignment, and arrived at the conclusion that the TDW assignment should be completely revised. In particular, they proposed reassignment of the 2128 and 1893 $cm^{-1}$ pair from $C_9$ to $C_7$, of the 1952 $cm^{-1}$ band from $C_5$ to $C_6$, confirmed the assignment of the 1197 $cm^{-1}$ band to $C_6$, whereas the very intense 1997 $cm^{-1}$ feature was reassigned from $C_6$ to $C_9$.

After going to press of that work, a preprint by Vala *et al.* (VCSP) [Val90] reached us in which an assignment of 1952 $cm^{-1}$ to $C_6$ was proposed on experimental grounds, as well as, "with less certainty", of 1997 $cm^{-1}$ to $C_8$. The former result is in agreement with MFG, the latter is not.

The purpose of the present work is threefold: (a) to seek confirmation for the $C_6$ assignments; (b) to clarify the situation for $C_7$, $C_8$ and $C_9$ on ab initio grounds, and (c) to find out whether the same or different conclusions are reached in the *ad hoc* MNDO study by MFG.

## 4.8.2 Methods, results, and discussion

### 4.8.2.1 The $C_6$ molecule

Table XXXVIII: Computed frequencies ($cm^{-1}$) for $C_2(X\ ^1\Sigma_g^+$ and $a\ ^3\Pi_u)$, $C_3(X\ ^1\Sigma_g^+)$, $C_4(^X\ ^3\Sigma_g^-)$, and $C_5(X\ ^1\Sigma_g^+)$. Infrared intensities (km/mol) are given in parentheses for active vibrations.

| | HF/ 4-21G | MP2/ 4-21G | HF/ 6-31G* | MP2/ 6-31G* | *ad hoc* MNDO[d] | Experiment or high-level ab initio |
|---|---|---|---|---|---|---|
| | | | $C_2(X\ ^1\Sigma_g^+)$ | | | |
| $\Sigma_g$ | 1827 | 1855 | 1940 | 1909 | 1883 | 1828[e] |
| | | | $C_2(a\ ^3\Pi_u)$ | | | |
| $\Sigma_g$ | 1705 | 1556 | 1740 | 1682 | 1603 | 1618[e] |
| | | | $C_3$ | | | |
| $\Sigma_u$ | 2324(1182) | 2106(419) | 2312(1346) | 2184(390)[a] | 2104(RI 1.0) | 2039[f] |
| $\Sigma_g$ | 1349 | 1152 | 1367 | 1220[a] | 1301 | 1224.5[f] |
| $\Pi_u$ | 291(0.11×2) | 128*i* | 153(2.1×2) | 190(20×2)[a] | 383(RI 0.0) | 63.4[f] |
| | | | $C_4$ | | | |
| $\Sigma_g$ | 2357 | 2085 | 2345 | 2149[b] | 2171 | |
| $\Sigma_u$ | 1648(127) | 1437(372) | 1740(142) | 1586(488)[b] | 1541(RI 0.2) | |
| $\Sigma_g$ | 999 | 900 | 1021 | 951[b] | 965 | |
| $\Pi_g$ | 493 | 242*i* | 408 | 419[b] | 447 | |
| $\Pi_u$ | 198(17×2) | 94(13×2) | 210(26×2) | 187(33×2)[b] | 200(RI 0.0) | |
| | | | $C_5$ | | | |
| $\Sigma_u$ | 2405(5811) | 2298(1548) | 2344(6550) | 2358(1243)[c] | 2199(RI 4.2) | 2169[g] |
| $\Sigma_g$ | 2210 | 1931 | 2220 | 2018[c] | 2015 | 2008[g] |
| $\Sigma_u$ | 1601(93) | 1381(63) | 1632(83) | 1471(64)[c] | 1528(RI 0.3) | 1498[g] |
| $\Sigma_g$ | 856 | 754 | 863 | 786[c] | 813 | 792[g] |
| $\Pi_u$ | 825(65×2) | 624*i* | 648(33×2) | 487(1.4×2)[c] | 689(RI 0.0) | – |
| $\Pi_g$ | 301 | 152*i* | 222 | 281[c] | 370 | – |
| $\Pi_u$ | 195(2.7×2) | 125(17×2) | 111(5.2×2) | 130(18×2)[c] | 151(RI 0.0) | – |

(a) L. Adamowicz and J. Kurtz, *Chem. Phys. Lett.* **162**, 342 (1989).
(b) D. Michalska, H. Chojnacki, B. A. Hess Jr., and L. J. Schaad, *Chem. Phys. Lett.* **141**, 376 (1987).
(c) J. M. L. Martin, J. P. François, and R. Gijbels, *J. Chem. Phys.* **90**, 3603(1989).
(d) J. M. L. Martin, J. P. François, and R. Gijbels, *J. Comp. Chem.*, in press.
(e) K. P. Huber and G. Herzberg, *Constants of diatomic molecules* (Van Nostrand Reinhold, New York, 1979).
(f) K. H. Hinkle, J. J. Keady, and P. F. Bernath, *Science* **241**, 1319 (1988).
(g) P. Botschwina and P. Sebald, *Chem. Phys. Lett.* **160**, 485 (1989). These results are anharmonic values derived from a quartic stretching-only CEPA-1/8s4p2d potential, the diagonal force constants being scaled for exact reproduction of the gas-phase value of 2169 $cm^{-1}$ for the highest active band. Corresponding harmonic values are 2198, 2033, 1494, and 800 $cm^{-1}$. Harmonic bending frequencies at the CEPA-1/7s3p1d level are 570, 209, and 119 $cm^{-1}$.

Table XXXIX: Computed bond distances (Å) for linear $C_6$.

| | MP2/6-31G* | UHF/ 6-31G* | UHF/ 4-21G | UHF/ 3-21G | MP2/ 4-21G | CASSCF | *ad hoc* MNDO |
|---|---|---|---|---|---|---|---|
| $R_o$ | 1.3007 | 1.293[a] | 1.2986 | 1.297[a] | 1.3192 | 1.298[b] | 1.299[c] |
| $R_m$ | 1.2940 | 1.275[a] | 1.2672 | 1.266[a] | 1.2938 | 1.280[b] | 1.266[c] |
| $R_i$ | 1.2812 | 1.269[a] | 1.2660 | 1.265[a] | 1.2857 | 1.265[b] | 1.272[c] |
| $R_{\text{eff}}$ | 1.293 | 1.279 | 1.276 | 1.275 | 1.299 | 1.281 | 1.277 |

(a) K. Raghavachari, R. A. Whiteside, and J. A. Pople, *J. Chem. Phys.* **85**, 6623 (1986).
(b) V. Parasuk and J. Almlöf, *J. Chem. Phys.* **91**, 1137 (1989).
(c) J. M. L. Martin, J. P. François, and R. Gijbels, *J. Comp. Chem.*, in press.
$R_o$, $R_m$, and $R_i$ designate the bond distances from the outside in.
$R_{\text{eff}}$ is defined as $\sqrt{[(R_i/2)2 + (R_i/2 + R_m)^2 + (R_i/2 + R_m + R_o)^2]/(35/4)}$

The harmonic force field was computed numerically from analytical MP2 gradients [Pop79] using the GAUSSIAN 86 program system [Gau86] running on the IBM/FPS configuration at the Facultés Universitaires de Namur. The standard 6-31G* basis set [Heh72] was employed. Several bugs in the released FPS version had to be fixed before the calculations could be completed successfully. The final successful calculation, which involved 13 gradient evaluations correlating 36 electrons in 90 orbitals, took about 14 days of CPU time and 800 MB of disk space. Infrared intensities were obtained by numerical differentiation of the MP2 dipole moment [Yam86].

The stationary point geometry, required for these calculations, was first sought again using analytical gradients. An UHF/6-31G* force constant matrix was employed to initiate the optimization.

As the UHF/6-31G* frequencies or IR intensities for linear $C_6$ were included neither in the paper of Raghavachari and Binkley (RB) [Rag87] nor in the personal communication [RagPC], we have computed them ourselves using an analytical force constant matrix [Pop79].

Guo and Karplus [Guo89] found that MP2/4-21G results for stretching frequencies are on the whole quite acceptable, and that the main influence of polarization functions at this level is found on the geometry and the bending frequencies. As we are basically only interested in the stretching frequencies for the carbon clusters, this result may be useful, since 4-21G [Pul79] calculations may still be carried out where MP2/6-31G* would be prohibitive. We have therefore also computed these on the FPS configuration. For comparison, analytical UHF/4-21G frequencies were computed using GAUSSIAN 88 [Gau88] running on a VaxStation 3100 under VMS 5.3.

In order to facilitate comparisons, we have tabulated computed frequencies and IR intensities at all four levels for $C_2$ to $C_5$ in Table XXXVIII. The MP2/6-31G* data are taken from the literature [Ada89, Mic87, Mar89b], the other values were computed in this work. (The HF/6-31G* frequencies were already published by RB [Rag87], but no

Table XL: Theoretical frequencies (unscaled, $cm^{-1}$) and infrared intensities (km/mol) for $C_6$.

| | MP2/ 6-31G* | UHF/ 6-31G* | UHF/ 4-21G | MP2/ 4-21G | UHF/ 3-21G | *ad hoc* MNDO |
|---|---|---|---|---|---|---|
| $\Sigma_g$ | 2167 | 2418 | 2455 | 2137 | 2459[a] | 2245[b] |
| $\Sigma_u$ | 2009(1457) | 2190(1221) | 2179(1377) | 1942(1008) | 2184[a] | 1999(RI 1.6)[b] |
| $\Sigma_g$ | 1759 | 1845 | 1795 | 1654 | 1801[a] | 1694[b] |
| $\Sigma_u$ | 1244(332) | 1327(17) | 1284(25) | 1162(330) | 1289[a] | 1240(RI 0.2)[b] |
| $\Sigma_g$ | 673 | 721 | 718 | 651 | 715[a] | 677[b] |
| $\Pi_g$ | 551 | 134*i* | 845 | 964*i* | 866[a] | 540[b] |
| $\Pi_u$ | 432(0.3×2) | 368(4.3×2) | 487(0.3×2) | 223*i*(4.8) | 494[a] | 453[b] |
| $\Pi_g$ | 223 | 264 | 223 | 41 | 228[a] | 248[b] |
| $\Pi_u$ | 108 | 117(16×2) | 104(11×2) | 128(223×2) | 105[a] | 105[b] |

(a) K. Raghavachari, R. A. Whiteside, and J. A. Pople, *J. Chem. Phys.* **85**, 6623 (1986).
(b) J. M. L. Martin, J. P. François, and R. Gijbels, *J. Comp. Chem.*, in press.

IR intensities were given.) Experimental values for $C_2$ were taken from the Huber and Herzberg compilation [Hub79], those for $C_3$ from the recent work of Hinkle *et al.* [Hin88]. For $C_5$, the nearest thing available are the very-high-level calculations of Botschwina and Sebald [Bot89]. It is evident from Table XXXVIII that HF/4-21G is definitely no worse, and probably better, than HF/6-31G*. MP2/4-21G leads to false bending distortions, but bending frequencies are only qualitatively reproduced at the other levels as well. Quantitative agreement would not only require anharmonic corrections, but also correlated calculations with basis sets including *f* functions [Sim88]. The stretching frequencies, however, are quite good for such a relatively limited theoretical model. Also highlighted is the excellent quality of the *ad hoc* MNDO results, where a substantial part of the remaining error is caused by the harmonic approximation (see e.g. the results for $C_5$)!

The effect of polarization functions on the computed IR intensities is rather large, as could be expected given their importance for dipole moments.

We have also attempted ROHF/4-21G frequency calculations using numerical differentiation of an analytical gradient (since no ROHF analytic second derivatives were available). However, these calculations failed because of symmetry breaking problems that were also encountered for the $C_3^+$ cation by Grev *et al.* [Gre90].

The MP2/6-31G* geometry of $C_6$ is compared in Table XXXIX with the available literature data, being those at the UHF/3-21G and UHF/6-31G* levels by Raghavachari *et al.* [Rag86b], the *ad hoc* MNDO [Mar90g] values by MFG, and the results of Parasuk and Almlöf [Par89a] using a 12/12 complete active space SCF (CASSCF) [Roo80]. All levels of theory except *ad hoc* MNDO yield bond distances that contract from the outside in, as was already found for $C_5$ [Mar89b, Bot89, Ada89] and $C_4$ [Mic87, Ber88b, Mag86,

Rit86].

The 'effective bond distance', as derived from the computed rotational constant, is also included in Table XXXIX, for comparison with experiment. To sketch the accuracy of the MP2/6-31G* results, our MP2/6-31G* geometry for $C_5$ [Mar89b] yields an $r_{eff}$ of 1.2846 Å, compared to the experimental value (including zero-point effects) of 1.283 Å [Hea89], and the 'best theoretical estimate' by Botschwina and Sebald of 1.284 Å. In considering the *ad hoc* MNDO results, it should be remarked that the parametrization was based on an older value of 1.287 Å for the $r_e$ of $C_3$ [Han74], compared to a more recent determination of 1.297 Å [Hin88]. Applying the difference as a correction term, *ad hoc* MNDO leads to an $r_{eff}$ value for $C_5$ of 1.284 Å, in excellent agreement with available data. As far as $C_6$ is concerned, both the MP2/6-31G* and *ad hoc* MNDO values appear to be reasonable; our best estimate is to bracket the experimental value between these.

The MP2/4-21G bond distances, especially the outer one, are apparently seriously overestimated, as would be expected [Guo89].

The harmonic frequencies are presented in Table XL, together with the UHF/3-21G [Rag86b] and *ad hoc* MNDO values from the literature. For the IR active vibrations, intensities in km/mol are given in parentheses; for the *ad hoc* MNDO results, the intensities are relative to the 2039 $cm^{-1}$ band of linear $C_3$.

Taking the customary scaling by 0.89 [Pop81] into account for the UHF/3-21G, UHF/4-21G and UHF/6-31G* values, all levels of theory predict an intense IR band around 2000 $cm^{-1}$, and a less intense band around 1200 $cm^{-1}$. But whereas the HF calculations predict low intensities for the latter, it is found to have a quite appreciable intensity at the MP2/6-31G* level. Scaling the MP2/6-31G* frequencies by the ratio between the observed $C_4$ frequency of 1543.4 $cm^{-1}$ [She89] and the calculated MP2/6-31G* value [Mic87] of 1586 $cm^{-1}$, we find frequencies of 1955 and 1210 $cm^{-1}$, in near-perfect agreement with the proposed 1952 and 1197 $cm^{-1}$ bands. Incidentally, our UHF/4-21G frequencies, scaled by 0.89, are also in good agreement with these band origins. As our reference molecule, linear $C_4$, also has significant spin contamination, the effects hereof are at least partially absorbed in the scaling; they will tend to lower computed frequencies [Mar90a], which is one of the reasons why the generic scaling factor of 0.93 [Mar89b, Hou82] for MP2/6-31G* frequencies produces too low values, both for $C_4$ and $C_6$.

Although MP2/4-21G produces two false imaginary frequencies for the bendings, stretching frequencies, as well as the associated intensity pattern, appear to be quite reasonable. The frequencies are even in excellent agreement with experiment, due to a fortunate error compensation.

Bernath *et al.* [Ber89] derived a column density of $C_5$ in the circumstellar shell of the carbon star IRC+10216 from our computed MP2/6-31G* intensity and an accurate literature value [Kra84] for the IR intensity of the 2039 $cm^{-1}$ band of $C_3$. Botschwina

Table XLI: Computed and experimental isotope shifts for the 1544 and 2164 $cm^{-1}$ bands of $C_4$ and $C_5$, respectively.

| Species | HF/ 4-21G | HF/ 6-31G* | MP2/ 6-31G* | *ad hoc* MNDO | Experiment |
|---|---|---|---|---|---|
| | | $C_4$ | | | |
| 12-12-12-12 | 1543.4 | 1543.4 | 1543.4 | 1543.4 | 1543.4[a] |
| 13-12-12-12 | 1528.6 | 1528.6 | 1528.6 | 1528.7 | 1528.8[a] |
| 12-13-12-12 | 1527.4 | 1527.3 | 1527.3 | 1527.5 | 1527.5[a] |
| 13-13-12-12 | 1511.6 | 1511.2 | 1511.2 | 1511.5 | – |
| 13-12-13-12 | 1513.4 | 1513.4 | 1513.5 | 1513.7 | 1513.8[a] |
| 13-12-12-13 | 1513.3 | 1513.3 | 1513.3 | 1513.5 | 1511.6(??)[a] |
| 12-13-13-12 | 1513.3 | 1513.3 | 1513.3 | 1513.4 | 1513.8[a] |
| 13-13-13-12 | 1498.2 | 1498.2 | 1498.1 | 1498.4 | 1498.8[a] |
| 13-13-12-13 | 1496.9 | 1496.9 | 1497.0 | 1497.2 | 1497.7[a] |
| 13-13-13-13 | 1482.7 | 1482.7 | 1482.7 | 1482.9 | – |
| | | $C_5$ | | | |
| 12-12-12-12-12 | 2164.0 | 2164.0 | 2164.0 | 2164.0 | 2164[b] |
| 13-12-12-12-12 | 2161.2 | 2161.1 | 2161.4 | 2161.8 | 2161[b] |
| 13-12-12-12-13 | 2158.2 | 2157.7 | 2158.6 | 2159.5 | 2158[b] |
| 12-13-12-12-12 | 2145.6 | 2147.0 | 2144.2 | 2146.0 | 2146[b] |
| 12-12-12-13-13 | 2144.0 | 2145.9 | 2142.3 | 2144.9 | 2144[b] |
| 13-12-12-13-12 | 2141.5 | 2141.8 | 2141.0 | 2142.8 | 2142[b] |
| 13-13-12-12-13 | 2139.7 | 2140.4 | 2138.9 | 2141.5 | 2140[b] |
| 12-12-13-12-12 | 2130.3 | 2131.6 | 2129.2 | 2127.8 | 2129[b] |
| 13-12-13-12-12 | 2127.2 | 2128.3 | 2126.2 | 2125.2 | 2128[b] |
| 13-12-13-12-13 | 2123.6 | 2124.2 | 2123.1 | 2122.2 | 2126[b] |
| 12-13-12-13-12 | 2120.5 | 2120.0 | 2121.0 | 2122.2 | 2122[b] |
| 13-13-12-13-12 | 2117.9 | 2117.2 | 2118.4 | 2120.3 | 2120[b] |
| 13-13-12-13-13 | 2115.1 | 2114.1 | 2115.8 | 2118.2 | 2117.5[b] |
| 12-13-13-12-12 | 2112.0 | 2115.7 | 2109.1 | 2109.8 | 2111[b] |
| 13-13-13-12-12 | 2110.4 | 2114.8 | 2108.7 | 2108.6 | 2109[b] |
| 13-12-13-13-12 | 2106.7 | 2109.0 | 2105.3 | 2105.6 | 2106.5[b] |
| 13-13-13-12-13 | 2105.1 | 2107.6 | 2103.0 | 2104.2 | 2104.4[b] |
| 12-13-13-13-12 | 2085.2 | 2085.9 | 2084.7 | 2084.2 | 2086[b] |
| 13-13-13-13-12 | 2082.2 | 2082.7 | 2081.8 | 2081.2 | 2083[b] |
| 13-13-13-13-13 | 2078.8 | 2078.8 | 2078.8 | 2079.1 | 2079.5[b] |

(a) L. N. Shen and W. R. M. Graham, *J. Chem. Phys.* **91**, 5115 (1989).
(b) M. Vala, T. M. Chandrasekhar, J. Szczepanski, R. J. Van Zee, and W. Weltner Jr., *J. Chem. Phys.* **90**, 595 (1989).

and Sebald [Bot89] noted later that the absolute value of the IR intensity is in error by about a factor of three, and presented a revised estimate based on their CEPA1/[8s4p2d] results. However, the relative intensity compared to the MP2/6-31G* value for the 2039 $cm^{-1}$ band of $C_3$ [Ada89] is in fairly good agreement with the value proposed in [Bot89]. For $C_6$, we thus find a relative intensity of 3.74 with respect to $C_3$: this value should be more reliable for the evaluation of column densities.

The spectra in both TDW and KN reveal a relatively constant intensity behavior for both the 1952 and 1197 $cm^{-1}$ bands: any observed variation appears to be correlated. So our assignment of both bands to the same molecule appears to be sound.

A final check can be made by comparing the isotope shifts. In order to assess the accuracy of these first, we compare the calculated shifts at the MP2/6-31G*, UHF/6-31G*, UHF/4-21G*, and *ad hoc* MNDO levels with the available experimental data for $C_4$ [She89] and $C_5$ [Val89].

It is perhaps the place to point out that the methodological requirements for an accurate prediction of isotope shifts are quite different from those for the prediction of actual frequencies. As a meaningful comparison is only possible by scaling the computed bands so that the computed and experimental unsubstituted bands match, any systematic overestimate of *all* frequencies is immaterial: what matters is that the relative magnitudes for the force constants are reasonably well predicted. Consequently, if a method predicts an exaggerated difference between two harmonic frequencies, isotope shifts should be taken with great caution.

Table XLI tabulates the computed and experimental isotope shifts for $C_4$. It can be seen that the agreement is excellent, except for an obvious misassignment by Shen and Graham: the 1511.6 $cm^{-1}$ line clearly comes from the 13-13-12-12 species rather than the 13-12-12-13 species, the band of which accidentally coincides with the 13-12-13-12 and 12-13-13-12 bands at 1513.8 $cm^{-1}$. As all levels of theory produce virtually identical isotope bands that are furthermore all in excellent agreement with experiment, there is little to choose between them.

The cluster of doubly subsituted isotopic bands around 1513 $cm^{-1}$ is the $\Delta = 30$ band seen by TDW and erroneously interpreted as a primary isotopic band with weight one (i.e., the central band for an odd-numbered chain). The two singly substituted bands nearly coincide, leading to the TDW $\Delta = 15$ band.

Table XLI also presents the same analysis for $C_5$, the resolution of the experimental spectrum being much smaller here. Somewhat surprisingly, MP2/6-31G*, *ad hoc* MNDO, and RHF/4-21G all hold their own very well, whereas RHF/6-31G* finds several exaggerated shifts. The band assignment by Vala *et al.* appears to be entirely correct. Regarding the TDW data, the 13-13-13-13-12 peak apparently was absorbed in the parent $^{13}C_5$ peak (which, upon inspection of Figure 4 in TDW, is seen to have a shoulder on the high-frequency side). The 2105 $cm^{-1}$ band comes from the 13-13-13-12-13 species,

Table XLII: Computed and experimental isotope shifts for the 1952 $cm^{-1}$ band of $C_6$.

| Species | MP2/ 6-31G* | Experiment[a] | UHF/ 6-31G* | UHF/ 4-21G | *ad hoc* MNDO |
|---|---|---|---|---|---|
| 12-12-12-12-12-12 | 1952.5 | 1952.5 | 1952.5 | 1952.5 | 1952.5 |
| 13-12-12-12-12-12 | 1948.0 | 1947.5 | 1948.3 | 1948.9 | 1948.7 |
| 12-12-13-12-12-12 | 1943.7 | 1942.5 | 1943.4 | 1942.6 | 1943.2 |
| 13-12-12-12-12-13 | 1943.3 | 1938.5 | 1943.8 | 1945.2 | 1944.7 |
| 13-12-12-13-12-12 | 1939.95 | 1937 | 1939.7 | 1939.4 | 1939.8 |
| 13-12-13-12-12-12 | 1937.9 | 1936.4 | 1938.3 | 1938.3 | 1938.4 |
| 12-12-13-13-12-12 | 1937.4 | 1932.4 | 1936.6 | 1934.8 | 1935.6 |
| 13-12-13-12-12-13 | 1934.1 | 1931.5 | 1934.4 | 1935.0 | 1935.0 |
| 13-12-13-13-12-12 | 1932.5 | 1929.2 | 1932.0 | 1931.0 | 1931.4 |
| 12-13-12-12-12-12 | 1927.6 | 1926.5 | 1927.8 | 1928.0 | 1927.8 |
| 13-12-13-13-12-13 | 1927.5 | 1923.3 | 1927.4 | 1927.0 | 1927.1 |
| 13-13-12-12-12-12 | 1923.7 | 1922.5 | 1924.1 | 1924.8 | 1924.4 |
| 12-13-12-13-12-12 | 1922.9 | 1918.2 | 1921.9 | 1921.0 | 1921.6 |
| 13-12-12-12-13-12 | 1922.5 | 1917.5 | 1923.1 | 1924.1 | 1923.6 |
| 13-13-12-13-12-12 | 1919.5 | 1916.5 | 1918.6 | 1918.1 | 1918.6 |
| 13-13-12-12-12-13 | 1918.4 | 1913.5 | 1919.2 | 1920.7 | 1920.1 |
| 13-12-13-12-13-12 | 1916.8 | 1912.3 | 1916.5 | 1916.5 | 1916.6 |
| 12-13-13-12-12-12 | 1913.6 | 1910.3 | 1914.7 | 1914.5 | 1914.6 |
| 13-12-13-12-13-13 | 1913.2 | 1908.0 | 1912.9 | 1913.4 | 1913.4 |
| 12-13-13-13-12-12 | 1911.0 | 1906.5 | 1910.9 | 1909.6 | 1910.0 |
| 13-12-12-13-13-12 | 1909.6 | 1905.2 | 1910.5 | 1911.0 | 1910.9 |
| 13-13-13-12-12-12 | 1908.4 | 1904.7 | 1910.0 | 1910.6 | 1910.2 |
| 13-13-13-13-12-12 | 1906.3 | 1901.9 | 1906.7 | 1905.9 | 1906.1 |
| 13-12-13-13-13-12 | 1906.1 | 1899.7 | 1906.2 | 1905.5 | 1905.7 |
| 13-12-12-13-13-13 | 1904.1 | 1894.3 | 1905.7 | 1906.9 | 1906.4 |
| 12-13-12-12-13-12 | 1902.9 | 1892 | 1903.0 | 1903.4 | 1903.3 |
| 13-12-13-13-13-13 | 1901.2 | 1891 | 1901.7 | 1901.7 | 1901.2 |
| 13-13-12-12-13-12 | 1898.4 | 1890.2 | 1898.8 | 1899.8 | 1899.4 |
| 12-13-13-12-13-12 | 1893.8 | 1889.5 | 1893.6 | 1893.2 | 1893.6 |
| 13-13-12-12-13-13 | 1893.5 | 1888.2 | 1894.3 | 1896.1 | 1895.5 |
| 13-13-12-13-13-12 | 1890.0 | 1886.3 | 1889.8 | 1889.9 | 1890.3 |
| 13-13-13-12-13-12 | 1888.1 | 1883.7 | 1888.6 | 1888.9 | 1888.9 |
| 12-13-13-13-13-12 | 1887.3 | 1883 | 1886.5 | 1885.1 | 1885.8 |
| 13-13-12-13-13-13 | 1884.1 | 1878.3 | 1884.6 | 1885.5 | 1885.4 |
| 12-13-13-13-13-13 | 1882.3 | 1877.2 | 1882.0 | 1881.2 | 1881.5 |
| 13-13-13-13-13-13 | 1877.2 | | 1877.2 | 1877.2 | 1877.2 |

(a) M. Vala, T. M. Chandrasekhar, J. Szczepanski, and R. Pellow, in: *Materials chemistry at high temperatures* (ed. J. Hastie), Humana Press, Clifton, NJ, 1990.

Table XLIII: Computed isotope shifts for the 1197 $cm^{-1}$ band of linear $C_6$.

| Species | MP2/6-31G* | UHF/6-31G* | UHF/4-21G | *ad hoc* MNDO |
|---|---|---|---|---|
| 12-12-12-12-12-12 | 1197.0 | 1197.0 | 1197.0 | 1197.0 |
| 12-13-12-12-12-12 | 1196.9 | 1196.9 | 1196.7 | 1196.7 |
| 12-13-12-12-13-12 | 1196.8 | 1196.8 | 1196.5 | 1196.6 |
| 12-12-13-12-12-12 | 1185.5 | 1185.8 | 1186.4 | 1186.1 |
| 12-13-13-12-12-12 | 1185.5 | 1185.7 | 1186.2 | 1186.0 |
| 12-13-12-13-12-12 | 1185.5 | 1185.7 | 1186.2 | 1186.0 |
| 12-13-13-12-13-12 | 1185.5 | 1185.6 | 1186.1 | 1185.9 |
| 13-12-12-12-12-12 | 1184.2 | 1184.0 | 1183.6 | 1183.7 |
| 13-12-12-12-13-12 | 1184.1 | 1184.0 | 1183.4 | 1183.6 |
| 13-13-12-12-12-12 | 1183.9 | 1183.7 | 1183.1 | 1183.2 |
| 13-13-12-12-13-12 | 1183.9 | 1183.6 | 1182.9 | 1183.1 |
| 12-12-13-13-12-12 | 1175.1 | 1175.5 | 1176.7 | 1176.2 |
| 12-13-13-13-12-12 | 1175.1 | 1175.5 | 1176.5 | 1176.1 |
| 12-13-13-13-13-12 | 1175.1 | 1175.4 | 1176.4 | 1176.1 |
| 13-12-12-13-12-12 | 1173.3 | 1173.4 | 1173.6 | 1173.5 |
| 13-12-12-13-13-12 | 1173.3 | 1173.4 | 1173.5 | 1173.4 |
| 13-13-12-13-12-12 | 1173.1 | 1173.1 | 1173.2 | 1173.1 |
| 13-13-12-13-13-12 | 1173.1 | 1173.1 | 1173.1 | 1173.1 |
| 13-12-13-12-12-12 | 1172.4 | 1172.5 | 1172.7 | 1172.5 |
| 13-12-13-12-13-12 | 1172.4 | 1172.5 | 1172.6 | 1172.4 |
| 13-13-13-12-12-12 | 1172.3 | 1172.3 | 1172.3 | 1172.1 |
| 13-13-13-12-13-12 | 1172.3 | 1172.2 | 1172.2 | 1172.1 |
| 13-12-12-12-12-13 | 1171.5 | 1171.1 | 1170.3 | 1170.6 |
| 13-13-12-12-12-13 | 1171.3 | 1170.9 | 1169.9 | 1170.2 |
| 13-13-12-12-13-13 | 1171.1 | 1170.7 | 1169.5 | 1169.9 |
| 13-12-13-13-12-12 | 1162.5 | 1162.8 | 1163.5 | 1163.2 |
| 13-12-13-13-13-12 | 1162.5 | 1162.8 | 1163.4 | 1163.1 |
| 13-13-13-13-12-12 | 1162.4 | 1162.6 | 1163.2 | 1162.9 |
| 13-13-13-13-13-12 | 1162.4 | 1162.6 | 1163.1 | 1162.9 |
| 13-12-13-12-12-13 | 1160.3 | 1160.2 | 1159.9 | 1160.0 |
| 13-13-13-12-12-13 | 1160.2 | 1160.0 | 1159.6 | 1159.7 |
| 13-13-12-13-12-13 | 1160.2 | 1160.0 | 1159.6 | 1159.7 |
| 13-13-13-12-13-13 | 1160.0 | 1159.9 | 1159.3 | 1159.5 |
| 13-12-13-13-12-13 | 1150.0 | 1150.1 | 1150.3 | 1150.2 |
| 13-13-13-13-12-13 | 1150.0 | 1150.0 | 1150.1 | 1150.1 |
| 13-13-13-13-13-13 | 1149.9 | 1149.9 | 1149.9 | 1149.9 |

whereas the 2118 $cm^{-1}$ band they dismissed as a shoulder to another band is actually caused by 13-13-12-13-13.

For $C_6$ now, we may compare the various computed isotope spectra to that obtained for the 1952 $cm^{-1}$ band by VCSP. According to the Teller-Redlich rule, the ratio between the $^{13}C_n$ and $^{12}C_n$ frequencies should be $(12.00000/13.00335)^{1/2} = 0.9606$; the actual experimental ratio is slightly higher because of anharmonicity. In order to facilitate comparison with the computed (harmonic) isotope shifts, the latter have been subjected

Table XLIV: Computed bond distances (Å) for linear $C_7$.

| | MP2/6-31G* | RHF/6-31G* | RHF/4-21G | MP2/4-21G | ad hoc MNDO |
|---|---|---|---|---|---|
| $R_o$ | 1.3012 | 1.270[a] | 1.2735 | 1.3174 | 1.279[b] |
| $R_m$ | 1.2953 | 1.280[a] | 1.2728 | 1.2973 | 1.271[b] |
| $R_i$ | 1.2814 | 1.264[a] | 1.2591 | 1.2825 | 1.258[b] |
| $R_{\text{eff}}$ | 1.291 | 1.271 | 1.267 | 1.2953 | 1.267 |

(a) K. Raghavachari and J. S. Binkley, *J. Chem. Phys.* **87**, 2191 (1987).
(b) J. M. L. Martin, J. P. François, and R. Gijbels, *J. Comp. Chem.*, in press.
$R_o$, $R_m$, and $R_i$ designate the bond distances from the outside in.
$R_{\text{eff}}$ is defined as $\sqrt{[R_i^2 + (R_i + R_m)^2 + (R_i + R_m + R_o)^2]/14}$

to a linear transformation, enforcing the $^{12}C_6$ and $^{13}C_6$ bands to coincide with their experimental counterparts. The resulting 36 isotopic frequencies are tabulated in Table XLII, together with the 35 experimental bands reported by VCSP.

We have not attempted an assignment of individual experimental isotopic bands. In the 1952–1920 $cm^{-1}$ range, the bands overlap with isotopic substitutions from the 1997 $cm^{-1}$ feature; below 1893 $cm^{-1}$, they overlap with those of the 1893 $cm^{-1}$ band. Despite the ingenious procedure involving observation of thermal annealing behavior employed by VCSP, some errors in the assignment are simply unavoidable. Two immediate examples are 1878.3 $cm^{-1}$(whose isotopic shift is unrealistically low) and 1886.3 (which is too low in intensity and appears to be 'superfluous' in that range). Also, at least one actual peak will be obscured by the $^{12}C_n$ parent of the 1893 $cm^{-1}$ band.

It is however obvious, that the observed spectrum is unmistakably that of linear $C_6$.

Turning to the TDW data, their $\Delta$ =6 appears to correspond to a merger of the 13-13-13-13-13-12 and 13-13-13-13-12-13 bands (hence the abnormally high intensity), whereas the $\Delta$ = 22 peak corresponds to the 13-13-13-12-13-13 band. Their $\Delta$ = 38, a weak satellite of the very intense parent peak of the original 1997 $cm^{-1}$ feature, may correspond to a cluster of multiply substituted peaks, which is seen both in our theoretical data and in the experimental VCSP spectrum.

For the 1197 $cm^{-1}$ band, all theoretical methods predict primary substitution peaks for $^{13}C_6$ to lie at $\Delta \sim 10$ (13-13-13-12-13-13) and $\Delta \sim 12.5$ (13-13-13-13-13-12) $cm^{-1}$, whereas the 13-13-13-13-12-13 $cm^{-1}$ peak coincides with the parent. This is in excellent agreement with TDW's finding of two equally intense peaks at $\Delta = 10$ and $\Delta = 12$. Furthermore, several doubly substituted peaks cluster around these, leading to the 'smeared' appearance of the double peak. To facilitate future experimental work, we have listed the computed peaks at the various levels considered in Table XLIII.

The fact that a theoretical method as simple as HF/4-21G is apparently quite capable of reproducing experimental isotope spectra rather well is reassuring, in the light of what follows.

Table XLV: Theoretical frequencies ($cm^{-1}$) and infrared intensities (km/mol) for linear $C_7$.

| | RHF/6-31G* | RHF/4-21G | MP2/4-21G | MP2/6-31G* | *ad hoc* MNDO[c] |
|---|---|---|---|---|---|
| $\Sigma_g$ | 2376[a] | 2401 | 2159 | 2216 | 2202 |
| $\Sigma_u$ | 2281[a](11604[b]) | 2364(12984) | 2338(2934) | 2405 | 2193(RI 4.1) |
| $\Sigma_u$ | 2132[a](7169[b]) | 2131(3803) | 1880(613) | 1962 | 1939(RI 3.3) |
| $\Sigma_g$ | 1745[a] | 1717 | 1490 | 1576 | 1631 |
| $\Sigma_u$ | 1206[a](0.14[b]) | 1188(1.26) | 1038(9) | 1098 | 1135 |
| $\Pi_u$ | 710[a](51×2[b]) | 1405(93×2) | 1400*i* | – | 670 |
| $\Sigma_g$ | 631[a] | 629 | 562 | 580 | 594 |
| $\Pi_g$ | 598[a] | 812 | 480*i* | – | 602 |
| $\Pi_u$ | 240[a](0.7×2[b]) | 357(1.25×2) | 144*i* | – | 357 |
| $\Pi_g$ | 157[a] | 157 | 155 | – | 212 |
| $\Pi_u$ | 73[a](5.8×2[b]) | 77(5.0×2) | 79 | – | 80 |

(a) K. Raghavachari and J. S. Binkley, *J. Chem. Phys.* **87**, 2191 (1987).
(b) K. Raghavachari, private communication.
(c) J. M. L. Martin, J. P. François, and R. Gijbels, *J. Comp. Chem.*, in press.

### 4.8.2.2 Higher clusters

With the present hardware and software, MP2/6-31G* analytical gradients for $C_7$ (42 electrons in 105 orbitals, 15 gradients required for harmonic force field) are simply out of the question. We have therefore adopted a different approach at the expense of the infrared intensities: the harmonic force constant matrix for just the stretching frequencies was set up by double numerical differentiation (stepsize 0.01 Å) of the MP2 energy, the latter being evaluated by the fast in-core algorithm (L903 of the GAUSSIAN series) which avoids the separate integral transformation as well as reduces dead I/O time to virtually nil.

The geometry was first optimized at the same level using the energy-only variant [Col76] of the Fletcher-Powell method [Fle63]. Together, these calculations took about two weeks on a VaxStation 3100.

Near-degeneracy effects lead to MO coefficients in excess of 100, which may affect the numerical precision of the MP2 energies. Whereas the amounts involved will still be negligible for an energy calculation, they will introduce considerable noise in the potential energy surface, so that force constants may be seriously affected. This should be kept in mind when considering the accuracy of the reported MP2/6-31G* frequencies.

The geometry is reported in Table XLIV, together with MP2/4-21G and RHF/4-21G results, as well as *ad hoc* MNDO and RHF/6-31G* values from literature. A progressive inward contraction of the bonds is again found at the RHF/4-21G, MP2/4-21G, and MP2/6-31G* levels – as well as, this time, at the *ad hoc* MNDO level – but not at the RHF/6-31G* level. We have again included the $r_{\text{eff}}$ values for comparison with

Table XLVI: HF/4-21G cartesian force constants (atomic units) required to obtain isotope shifts for linear $C_7$, $C_8$, and $C_9$.

| | | | |
|---|---|---|---|
| | $C_7$ RHF/4-21G | | |
| k11=0.809117 | k12=-0.778091 | k13=-0.0636609 | k14=0.0532888 |
| k15=-0.0388330 | k16=0.0285550 | k17=-0.0103760 | k22=1.546210 |
| k23=-0.666597 | k24=-0.157402 | k25=0.108609 | k26=-0.0812862 |
| k33=1.52659 | k34=-0.703169 | k35=-0.162939 | k44=1.61457 |
| | $C_8$ UHF/4-21G | | |
| k11=0.664453 | k12=-0.628233 | k13=-0.0518167 | k14=0.0238131 |
| k15=-0.00703962 | k16=-0.00549874 | k17=0.0139271 | k18=-0.00960450 |
| k22=1.40477 | k23=-0.710519 | k24=-0.0926840 | k25=0.0384642 |
| k26=-0.00206985 | k27=-0.0236519 | k33=1.55450 | k34=-0.717761 |
| k35=-0.106996 | k36=0.0401575 | k44=1.58065 | k45=-0.718448 |
| | $C_9$ RHF/4-21G | | |
| k11=0.808073 | k12=-0.774357 | k13=-0.068529 | k14=0.0577844 |
| k15=-0.0433860 | k16=0.0349307 | k17=-0.0288220 | k18=0.0230841 |
| k19=-0.00877768 | k22=1.52309 | k23=-0.641840 | k24=-0.170535 |
| k25=0.122323 | k26=-0.0949106 | k27=0.0747544 | k28=-0.0616054 |
| k33=1.50502 | k34=-0.690410 | k35=-0.183405 | k36=0.131352 |
| k37=-0.0981207 | k44=1.57922 | k45=-0.656446 | k46=-0.190985 |
| k55=1.52183 | | | |

The atoms are numbered from end to end.
To obtain frequencies in $cm^{-1}$, multiply isotope masses by 1880.860 (number of electron masses in an a.m.u) and frequencies obtained by 219474.8 (twice the Rydberg constant).

experiment: again we propose the MP2/6-31G* value as an upper bound and the *ad hoc* MNDO value as a lower bound.

The previous elimination of the 2164 and 1952 $cm^{-1}$ bands makes the task of vibrational assignment relatively easy even at the Hartree-Fock level, at least when intensities are also included in the interpretation. Although quantitative agreement at this level of theory is probably illusory for these, it is well known that the prime qualitative features are quite well reproduced even for unusual or highly strained molecules [Hes86].

Table XLV lists computed frequencies and IR intensities at the *ad hoc* MNDO, RHF/4-21G and RHF/6-31G* levels, as well as computed frequencies at the MP2/4-21G level and MP2/6-31G* stretching frequencies. Two very intense bands, the upper more intense than the lower, of comparable intensity and about 250 $cm^{-1}$ apart, are predicted at the Hartree-Fock and *ad hoc* MNDO levels. Two such bands exist at 2128 and 1893 $cm^{-1}$. TDW already noted that their intensity variations are so closely correlated that they probably belong to the same molecule, which they thought was $C_9$ (but which has a quite different intensity pattern - *vide infra*). Incidentally, the RHF/4-21G band origins scaled by 0.89 are in quite good agreement with these frequencies. TDW also suggested a band at 1447 $cm^{-1}$ to belong to the same molecule: however, the data of KN do not show any significant intensity correlation between that band and the 1893–2128 twins,

Table XLVII: Theoretical frequencies ($cm^{-1}$) and infrared intensities (km/mol) for linear $C_8$.

| | UHF/6-31G* | UHF/4-21G | *ad hoc* MNDO[b] |
|---|---|---|---|
| $\Sigma_g$ | 2393[a] | 2435 | 2233 |
| $\Sigma_u$ | 2330(3193)[a] | 2345(4073) | 2128(RI 4.6) |
| $\Sigma_g$ | 2161[a] | 2160 | 2005 |
| $\Sigma_u$ | 1867(909)[a] | 1828(1032) | 1715(RI 1.3) |
| $\Sigma_g$ | 1495[a] | 1461 | 1410 |
| $\Sigma_u$ | 1049(9)[a] | 1027(4) | 984 |
| $\Sigma_g$ | 552[a] | 549 | 518 |
| $\Pi_g$ | 355[a] | 528 | 429 |
| $\Pi_u$ | 293(5.6×2)[a] | 264(3.2×2) | 533 |
| $\Pi_u$ | 225(4.5×2)[a] | 888(2.9×2) | 277 |
| $\Pi_g$ | 170[a] | 147 | 162 |
| $\Pi_u$ | 67(10×2)[a] | 66(8×2) | 63 |
| $\Pi_g$ | 819$i$[a] | 1570 | 557 |

(a) K. Raghavachari, private communication.
(b) J. M. L. Martin, J. P. François, and R. Gijbels, *J. Comp. Chem.*, in press.

which are indeed very closely correlated in their spectra. Our calculations furthermore find no such band in the $C_7$ spectrum, which again supports our interpretation.

The MP2 results also predict two IR active frequencies in that region, but their separation appears to be exaggerated; furthermore, the ordering of the highest $\Sigma_g$ and $\Sigma_u$ bands is interchanged. Because of this, predicted isotope shifts will be particularly unreliable. Nevertheless, the deviation between computed and experimental frequencies is still not unusual. The bending part of the potential is again ill reproduced at the MP2/4-21G level, as expected.

A final check is provided by the primary isotope shifts. At the RHF/4-21G level, we predict for the 2128 $cm^{-1}$ band (substituting with $^{12}C$ from the outside in) $\Delta = 0$, 1, 12, 32, and for the 1893 $cm^{-1}$ band 9,21,0,8. Experimentally, TDW found for the 2128 $cm^{-1}$ band a single $\Delta = 13$, as well as a weak shoulder to the parent of the $C_5$ band at $\Delta = 29$, which is in excellent agreement with our data; for the 1893 $cm^{-1}$ band, they saw a pair of bands at $\Delta = 9$ and 11, again in good agreement (the missing band may have been obscured by various contaminants in the spectrum).

Summarizing, we may be quite confident of the assignment. As the table of isotope shifts would be long and not very interesting to read, we have tabulated the symmetry-unique cartesian force constants in Table XLVI: any interested reader may then easily derive any desired frequency by setting up the secular problem.

We now turn to the famous very intense feature at 1997 $cm^{-1}$. VCSP *et al.* reassigned it from TDW's original $C_6$ to $C_8$. However, we feel uncomfortable with this assignment for a number of reasons: (a) because of odd-even alternation in stability discussed at

length in [Rag87], $C_9$ will be much more stable than $C_8$; (b) As seen by comparing Tables XLVII and XLVIII, all levels of theory predict an extremely intense band for $C_9$, whereas the intensities for the strongest band of $C_8$ are an order of magnitude lower; (c) the growth of the 1997 $cm^{-1}$ feature is strongly correlated with the shrinking of the 2039 $cm^{-1}$ band of $C_3$, which already lead TDW to believe that $C_3$ was the 'building block' for the species at 1997 $cm^{-1}$. Brown *et al.* [Bro87] also pointed out that reactions with $C_3$ are the most exergonic way to grow for each cluster. As, according to mass spectrometric measurements [Zav73], the initial carbon vapor consists for about 75 %, 20 %, and 5 % each of $C_3$, C, and $C_2$, the following mechanism seems more logical to us:

$$2C_3 \rightarrow C_6 \tag{4.17}$$

$$C_6 + C_3 \rightarrow C_9 \tag{4.18}$$

In such a mechanism, the $C_6$ concentration would remain relatively constant during depletion of $C_3$ and creation of $C_9$, which agrees with the observed behavior of the bands. Reactions such as

$$C_6 + C_2 \rightarrow C_8 \tag{4.19}$$

will be much less important.

What can be said from the harmonic frequencies? The RHF/4-21G band origin for $C_9$ is in good agreement with the observed 1997 $cm^{-1}$, whereas that for $C_8$ is on the high side. Furthermore, this last frequency is itself lowered by spin contamination effects, making the actual value perhaps still higher. In order to give this reasoning a more firm basis, we apply here a little statistics.

Doing a linear regression with the available experimental values on the abscissa and the 4-21G values on the ordinate, for the two lowest-lying states of $C_2$ and the lowest linear states of $C_3$–$C_7$, and eliminating the $X^1\Sigma_g^+$ state of $C_2$ as a clear outlier, we find (with 9 data points):

$$y = 1.1851x + 143.0; \qquad r = 0.9961 \tag{4.20}$$

For the 1997 $cm^{-1}$ band, this leads to a 'predicted' 4-21G frequency of 2223.8 $cm^{-1}$. Standard statistical techniques lead to:

$$y - 2223.8 = 16.9\sqrt{2F_p(2,7)} \tag{4.21}$$

where $F$ represents the well-known Fisher-Snedecor variance ratio distribution. Its $P$-value for $C_9$ is 17.66 %, that for $C_8$ only 0.06 %. A similar analysis of the *ad hoc* MNDO data (where there is no outlier) leads to $P = 99.83$ and 0.03 %, respectively. The frequency data alone are thus already sufficient for assignment to $C_9$.

A more likely candidate for linear $C_8$ would appear us to be a band at $\sim$ 2075 $cm^{-1}$, which enters the spectra of KN upon strong annealing. For this to be linear $C_8$, a

Table XLVIII: Theoretical frequencies ($cm^{-1}$) and infrared intensities (km/mol) for linear $C_9$.

| | RHF/4-21G | RHF/6-31G* | *ad hoc* MNDO[c] |
|---|---|---|---|
| $\Sigma_g$ | 2465 | 2415[a] | 2266 |
| $\Sigma_u$ | 2373(2945) | 2338[a](433[b]) | 2196(RI 4.4) |
| $\Pi_u$ | 2239(100×2) | 783[a](63×2[b]) | 657(RI 0.1) |
| $\Sigma_u$ | 2188(33883) | 2084[a](40408[b]) | 2042(RI 22.9) |
| $\Sigma_g$ | 2122 | 2134[a] | 1938 |
| $\Sigma_u$ | 1780(681) | 1803[a](867[b]) | 1676(RI 1.5) |
| $\Sigma_g$ | 1375 | 1393[a] | 1312 |
| $\Pi_g$ | 1293 | 658[a] | 628 |
| $\Sigma_u$ | 949(12.5) | 960[a](30[b]) | 905 |
| $\Pi_u$ | 821(19×2) | 567[a](2.7×2[b]) | 543 |
| $\Sigma_g$ | 495 | 496[a] | 467 |
| $\Pi_g$ | 426 | 252[a] | 350 |
| $\Pi_u$ | 198(0.2×2) | 187[a](2.2×2[b]) | 248 |
| $\Pi_g$ | 117 | 114[a] | 132 |
| $\Pi_u$ | 53(5×2) | 49[a](5.2×2[b]) | 49 |

(a) K. Raghavachari and J. S. Binkley, *J. Chem. Phys.* **87**, 2191 (1987).
(b) K. Raghavachari, private communication.
(c) J. M. L. Martin, J. P. François, and R. Gijbels, *J. Comp. Chem.*, in press.

companion band of about one-third that intensity should grow in $\sim$ 1650 $cm^{-1}$: there is one present at 1589 $cm^{-1}$. As far as the predicted companion bands (around 2200 $cm^{-1}$ and 1600 $cm^{-1}$) of $C_9$ go, there is a band with the right behavior and intensity at 1601 $cm^{-1}$, as well as a pile-up of features (upon stronger annealing) beginning at 2200 $cm^{-1}$. These latter assignments are tentative, however, as we do not have experimental isotope shift data at our disposal.

Then come the TDW isotope shift data (as the VCSP spectrum with 50:50 isotope ratios results in an undecipherable plethora of peaks). TDW found a single relatively sharp $\Delta = 14$, with a shoulder on the high frequency side, as well as a very wide (about 10 $cm^{-1}$) parent peak with again a high-frequency shoulder. Computed primary shifts at the HF/4-21G level are $\Delta$ = 3, 15, 16, 7, and 1 $cm^{-1}$ from the outside in for $C_9$, compared to $\Delta$ = 1, 13, 18, 4 for $C_8$. Given the large width of the parent peak, $\Delta$ = 7 is still acceptable for the shoulder, whereas the 15 and 16 $cm^{-1}$ peaks are in good agreement with the sharp peak-cum-shoulder at 14 $cm^{-1}$shift. The $C_8$ data are less easy to fit in, as they would certainly imply a double isotope peak.

The following point is the intensity reduction of the parent peak upon isotopic 50:50 dilution. Given the fact that the parent peak is near the baseline, the intensity ratio can only be used to say that the cluster contains at least eight atoms, not to discriminate between $C_8$ and $C_9$.

The issue of band density is another one. The predicted band densities for $C_8$ and $C_9$

Figure 4.16: Simulated isotopic substitution spectrum for the 1997 $cm^{-1}$ band from the UHF/4-21 force constant matrix for linear $C_8$.

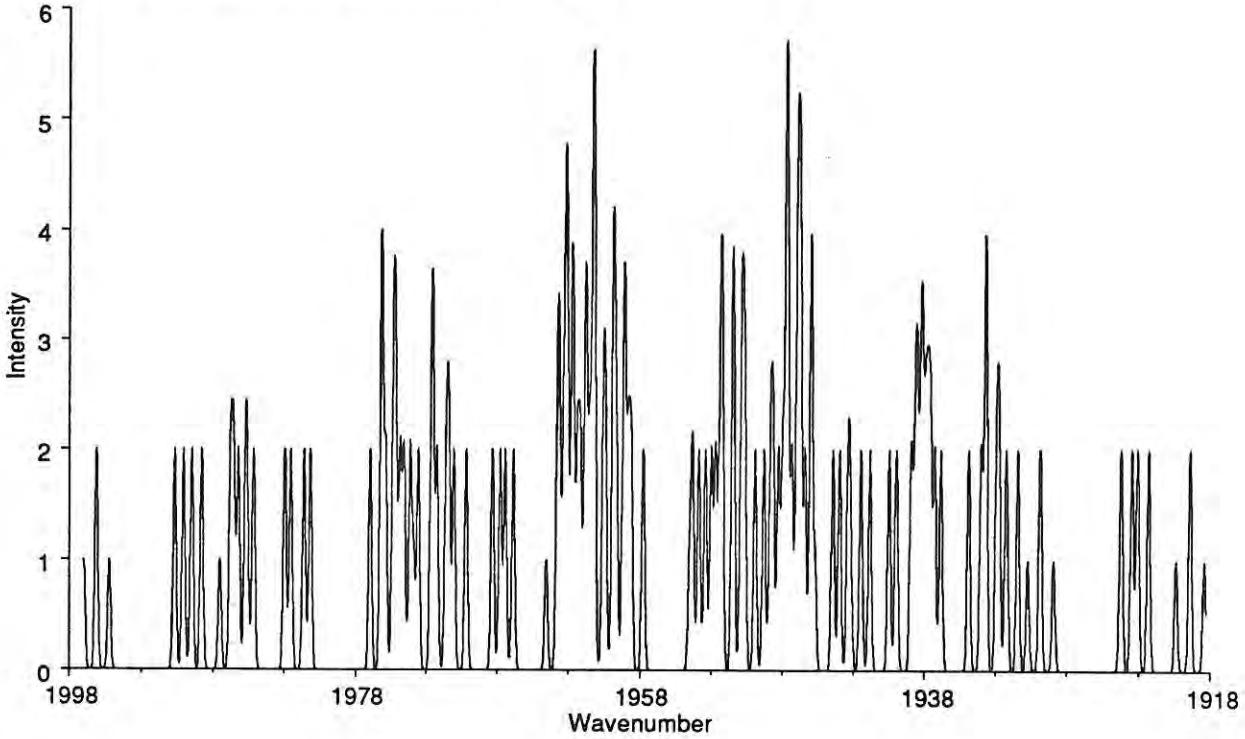


by VCSP are based upon two implicit assumptions: (a) the resolution of the spectrum is small enough to discern all individual peaks; (b) there is little or no coincidence between peaks.

The first is definitely not the case: VCSP quote a resolution of about 0.25 $cm^{-1}$. We have then computed isotopic substitution bands for $C_8$ and $C_9$ from the HF/4-21G force constant matrices (symmetry-unique cartesian force constants again being given in Table XLVI), and found the second assumption not to hold at all: especially for $C_9$, bands often cluster so closely that even the instruments with the highest resolution would not be able to resolve them. Furthermore, if any atoms have zero travel in a given normal vibration (which is nearly the case for the third and sixth atoms in $C_9$), all possible combinations of isotopes for these atoms will give rise to exactly or nearly exactly the same frequency.

Using these data and an estimated mean full width at half maximum (FWHM) of 0.25 $cm^{-1}$ (from Figure 5 of VCSP), we have simulated the spectra assuming Gaussian line shapes. The simulated spectra for $C_8$ and $C_9$ are depicted in Figures 4.16 and 4.17, respectively. The cluttering of bands is especially obvious in Figure 4.17. Even at sight, both spectra are quite different: the $C_8$ spectrum contains several relatively wide 'gaps', none of which (except a small one around 1940 $cm^{-1}$ also seen in Figure 4.17) is present in the experimental spectrum (Figure 5 of VCSP). The 'smear' of bands in several areas of the experimental spectrum (especially around 1960 $cm^{-1}$) is well reproduced in Figure 4.17, but not in Figure 4.16. The behavior near the $^{12}C_n$ peak, where contamination

Figure 4.17: Simulated isotopic substitution spectrum for the 1997 $cm^{-1}$ band from the UHF/4-21 force constant matrix for linear $C_9$.

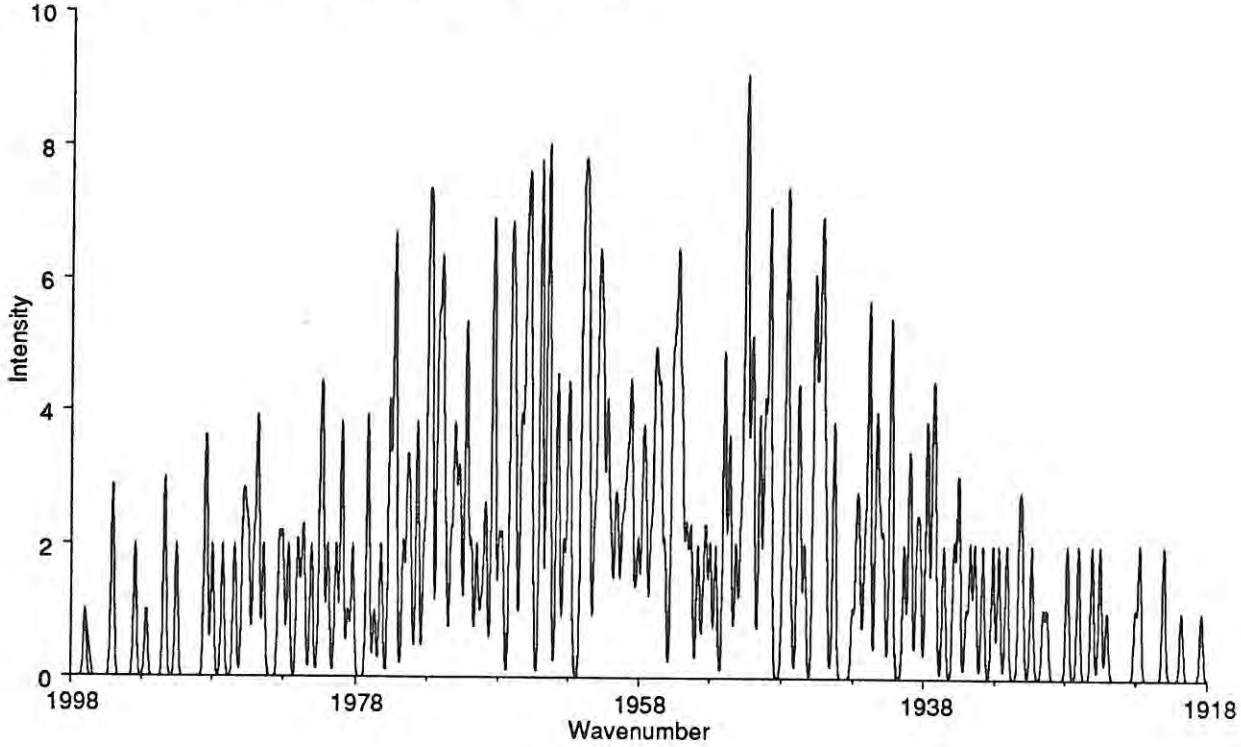


is relatively absent, is relatively well reproduced in Figure 4.17, but not in Figure 4.16. Finally, the locations of several high peaks appear to be better reproduced in Figure 4.17 than in Figure 4.16.

The peak density was subsequently determined by counting the peaks in each spectrum manually. In Figure 4.16, 90 peaks are detected in 78.3 $cm^{-1}$(which corresponds to a smaller area in the experimental spectrum of about 77 $cm^{-1}$ due to anharmonicity), which leads to an approximate band density of $90/77 = 1.169$ per $cm^{-1}$. For $C_9$, 109 distinct peaks and 7 'borderline cases' (that might get lost in the noise of an actual spectrum) are counted, leading to a density between 1.416 and 1.506 per $cm^{-1}$, in excellent agreement with the experimental value of about 1.4 per $cm^{-1}$. A larger FWHM would decrease both densities, as well as the difference.

Summing up, we would be highly surprised if the 1997 $cm^{-1}$ peak turned out to be $C_8$ rather than $C_9$. A high-resolution rotational fine structure such as recorded for $C_5$ by Heath *et al.* [Hea89] could settle the issue: assuming a comparable effective bond length, the predicted rotational constant would be about one-quarter that of $C_5$ for $C_8$, and one-sixth for $C_9$. Another possibility is a high-resolution isotope spectrum with 95:5 $^{12}C$:$^{13}C$ ratio: then primary isotope peaks could be observed in more detail than by TDW, in a range where comparatively little interference from other bands exists.

It was very recently shown [Kur90], that the intensity variation of the 1997 $cm^{-1}$ feature is strongly correlated with that of a band at 307.5 nm in the UV spectrum. This

latter band may consequently also be assigned to $C_9$, as may a band around 246.5 nm be assigned to linear $C_6$ because of its strong correlation with the 1952 $cm^{-1}$ line.

Assignments of the bands around 1700 and 1800 $cm^{-1}$ is more speculative: as discussed by MFG, the most likely candidate for the features around 1700 $cm^{-1}$is cyclic $C_6$, whereas the features between 1800 and 1850 $cm^{-1}$ are probably caused by cyclic $C_8$ and $C_{10}$. As shown by RB, cyclic and linear structures will be nearly isoenergetic for $C_4$, $C_6$, and $C_8$, whereas $C_{10}$ has a distinct cyclic structure. However, the presence of still higher species cannot be ruled out, like $C_{11}$ which is a 'magic number' cluster in mass spectra of graphite [Van87]. Concerning the 1447 $cm^{-1}$band, the only conclusion is negative: the isotope shift pattern completely contradicts assignment to cyclic $C_4$ as well as linear $C_5$, which are about the only species considered that have an IR active band of some intensity in that region. The 1284 $cm^{-1}$ band *may* be caused by the cyclic form of $C_4$ (no experimental isotope data are available): a very-high level study of linear and cyclic $C_4$, which may give conclusive evidence, is presented in Section 4.9. As discussed in MFG, the fact that the growth of the band is not correlated with that of the linear $C_4$ band may be explained on thermodynamic and kinetic grounds. Another possible candidate would be the lower bending frequency of cyclic $C_6$ (computed by RB at 1286 $cm^{-1}$, HF/6-31G*); its IR intensity is on the low side, however.

### 4.8.3 Conclusions

The harmonic frequencies, infrared intensities, and isotopic substitution bands of $C_6$ have been evaluated at the MP2/6-31G* level. They confirm previous assignments of the 1952 and 1197 $cm^{-1}$ matrix IR bands to $C_6$. Isotopic substitution spectra at the MP2/6-31G* and HF/4-21G level, as well as those with a newly developed *ad hoc* MNDO method are shown to be in good agreement with experiment for $C_4$, $C_5$, and $C_6$. On the basis of RHF/4-21G, RHF/6-31G*, MP2/4-21G, MP2/6-31G*, and *ad hoc* MNDO data, including theoretical frequencies, IR intensities, and isotopic substitution spectra, it is shown with virtual certainty that the 2128 and 1893 $cm^{-1}$ matrix IR bands belong to $C_7$. A recent assignment of the very intense 1997 $cm^{-1}$ matrix IR feature to $C_8$ is contradicted on the same grounds, and an alternative assignment to $C_9$ put forward.

### 4.8.4 Aftermath

Independently of ourselves, Heath and coworkers at Berkeley [Hea90a] succeeded in recording gas-phase IR spectra with Doppler-limited resolution of a supersonic carbon cluster bundle. They found a band at 2138.1951(10) $cm^{-1}$ with a rotational fine structure that obviously belongs to linear $C_7$ in a $^1\Sigma_g^+$ state. The effective bond distance reported is 1.2736(4) Å. The gas-phase frequency obviously corresponds to the 2128 $cm^{-1}$ band in argon matrix, confirming our assignment.

After going to press of this Section [Mar90f] and the previous one [Mar90g], Heath and Saykally published further Doppler-limited IR work on carbon clusters. In a first paper [Hea90b], they investigated our hypothesis that the 1997 $cm^{-1}$ matrix IR band was attributable to $C_9$ and found unambiguous confirmation. The gas-phase band origin was found at 2014.3383(10) $cm^{-1}$; the effective bond distance is 1.27868(75) Å.

Two further papers [Hea91a, HeaTBP] report further measurements on $C_7$. The former discusses combination bands of the 2128 $cm^{-1}$ asymmetric stretch with a very low bending frequency, the latter investigated our prediction that the 1893 $cm^{-1}$ band was attributable to $C_7$ and found full confirmation.

The results of these authors reveal yet another intriguing alternating characteristic of the carbon cluster series; whereas $C_3$ and $C_7$ both exhibit floppy behavior with extreme rovibrational coupling and $r_e > r_0$ (contrary to the normal situation), neither $C_5$ nor $C_9$ exhibit this behavior.

## 4.9 Ab initio study of the structure, infrared spectra, and heat of formation of $C_4$ using large basis sets

### 4.9.1 Introduction

Over the last few decades, carbon clusters have aroused a lot of interest both theoretically and experimentally; the review by Weltner and Van Zee [Wel89] extends up to April 1989. Additional progress, made since that review, includes the characterization of linear $C_4$ and $C_5$ by an interaction between theoretical [Mic87, Ber88b, Mar89b, Bot89, Ada89] and experimental [Val89, Ber89, Hea89, She89] groups. Very recently, independent ab initio [Mar90f] and semiempirical [Mar90g] studies have been carried out that propose a revised assignment of the matrix IR bands [Tho71, Kra85] of the linear species up to and including $C_9$. At least for $C_7$ and the 2128 $cm^{-1}$ band, the assignment has been confirmed experimentally by the Berkeley group [Hea90a]. (After going to press of the present Section [Mar91], further confirmations for the assignments of 1998 $cm^{-1}$ to $C_9$ [Hea90b] and of 1893 $cm^{-1}$ to $C_7$ [Hea91a, HeaTBP] have been given.)

In the course of this, an *ad hoc* modification of the MNDO [Dew77a] method has been developed that allows very accurate predictions of the harmonic frequencies for the linear species [Mar90g]. Unfortunately, results for the cyclic species are much less reliable because the minimal basis set on which all current semiempirical models are built does not have the flexibility to describe highly strained rings.

The ground state structure of $C_4$ has long since been a matter of controversy. As early as 1977, it was proposed on the basis of a semiempirical MINDO/2 study [Sla77] that $C_4$ might have a cyclic ground state. A subsequent *ab initio* study by the Pople

group [Whi81b] at the MP4(SDQ) [Kri78] level with a 6-31G* basis set [Heh72] revealed that the linear $^3\Sigma_g^-$ and rhombic $^1A_g$ states of $C_4$ are close together in energy: from an isogyric comparison with triplet methylene, they predicted the rhombus to be about 5 kcal/mol lower in energy.

Ritchie *et al.* [Rit86] studied the two states at the CISD (configuration interaction with all single and double excitations) level with a Davidson correction [Lan74]; the Huzinaga-Dunning $(9s5p1d)/[4s2p1d]$ basis set [Huz65, Dun70] (henceforth denoted DZP) was used. They found the two states to be essentially isoenergetic, with the linear state about 0.2 kcal/mol lower in energy. However, triple excitations, which are very important for this type of molecule, are not included at this level of theory.

Magers *et al.* (MHB) [Mag86] studied the molecule with the same basis set at the MP4(SDTQ) level [Kri80], as well as with various coupled cluster methods [Bar89] up to and including CCSDT-1 [Lee84], at which level they obtained an isomerization energy $\Delta E$ of 5.01 kcal/mol (positive values favoring the rhombus).

Raghavachari and Binkley [Rag87] (RB) obtained a comparable result at the CCD(ST) level [Rag85]. They however remarked, that because of significant spin contamination in the UHF wavefunction for the linear species, the actual value would be significantly lower and the two structures would be very close in energy. MHB made the same remark regarding their own results; however, it has recently been shown that for a single dominant spin contaminant (which is the case for linear $C_4$), the CCSD energy is not affected by the contamination [Sch88, Mar90a]. So the DZP limit will be close to 5 kcal/mol, whereas the 6-31G* limit will be very small. This illustrates that the basis set will have considerable influence on the computed result.

Bernholdt *et al.* [Ber88b] (BMB) performed a coupled cluster investigation with a $[5s3p1d]$ contraction of the MHB primitive set, which is thus of triple-zeta quality. Their best estimate at that level was -0.49 kcal/mol (favoring the linear). It was further argued on thermodynamical grounds [Ber88b, Mar87], that the linear structure would be favored anyway at practical temperatures because of the additional degeneracy entropy.

A further study was at the MRD-CI [Bue74] level with a DZP basis set by Pacchioni and Koutecký [Pac88]. With that method, they found a $\Delta E$ of -2.3 kcal/mol; given the fairly small set of reference configurations, this method will only partially include higher excitation effects.

Up to now, the best results (BMB) indicate thus that the two structures will be very close in energy and may coexist even at low temperatures. Concerning the latter, there is a possibility that a 1284 $cm^{-1}$ matrix IR feature belongs to rhombic $C_4$ [Mar90f, Mar90g]. Experimental isotopic substitution data are absent for this band, so the hypothesis cannot be verified directly. Given however the large basis set effects apparently present, it would also be interesting to investigate the system with some very large basis sets of preferably $[4s3p2d1f]$ quality. Finally, at this level of theory, a theoretical value for the dissociation

energy could be obtained through the G1 procedure [Pop89].

The purpose of this study is thus threefold:

- to investigate the effect of further basis set extension on the linear-rhombic energy difference;
- to provide more accurate harmonic frequencies and isotopic substitution data for the rhombic isomer;
- to obtain a theoretical estimate of the heat of formation of $C_4$.

### 4.9.2 Computational methods

Most computations were performed using the GAUSSIAN 88 package [Gau88] running on the IBM 3090/400e VF at the University of Leuven; some were performed with GAUSSIAN 88 on our VAXstation 3100 under VMS 5.3, as well as using GAUSSIAN 86 [Gau86] on the IBM/FPS configuration at the Facultés Universitaires de Namur.

Both geometry and frequency calculations (the latter through single numerical differentiation) were carried out at the MP2 level using analytical gradients. The latter are computed with the Pople algorithm with the Pople algorithm [Pop79] in GAUSSIAN 86, or the more efficient Z-vector algorithm [Han84] in GAUSSIAN 88.

For the energy calculations, the recently developed QCISD(T) method [Pop87] (quadratic configuration interaction, actually an approximation to CCSD with a quasiperturbative triples correction correct to fifth order [Rag89]) was employed. This method was recently shown to be near full-CI quality even for some 'problem' molecules [Lee90]; the higher-order terms involving the $\hat{T}_1$ operator that are neglected compared to full CI normally only matter for very heavy spin contamination or extreme multireference character. The former is absent here; the latter will be discussed at the end of the present Section.

For some of the larger basis set calculations, even QCISD(T) proved to be beyond our computational power. There, MP4 with multiple spin projection as developed by Schlegel [Sch88, Sch86] was used.

As rigorous size-consistency holds for both QCISD(T) [Pop87] and MP4 [Bar81], dissociation energies are simply computed by subtracting atomic energies rather than through a supermolecular calculation. This procedure may result in very small errors with singly spin-projected MP4 [Sch86]; however, in the same reference, it was indicated that the problem would be remedied by multiple spin projection.

Table XLIX: Total energies (hartree) and isomerization energy $\Delta E$ (kcal/mol) for the $^3\Sigma_u^-$ and $^1A_g$ states of $C_4$.

| Method | $^3\Sigma_u^-$ | $^1A_g$ | $\Delta E$ |
|---|---|---|---|
| RB basis set and geometry | | | |
| CCD(ST)/6-31G*[(a)] | -151.65000 | -151.65827 | 5.19 |
| QCISD/6-31G* | -151.63309 | -151.63106 | -1.27 |
| QCISD(T)/6-31G* | -151.65759 | -151.65928 | 1.06 |
| MP4/6-31G* | -151.65009 | -151.66075 | 6.69 |
| PMP4(1)/6-31G* | -151.65675 | -151.66074 | 2.50 |
| PMP4(2)/6-31G* | -151.65625 | -151.66074 | 2.82 |
| PMP4(3)/6-31G* | -151.65625 | -151.66074 | 2.82 |
| MP2/6-31G* geometry | | | |
| QCISD/6-31G* | -151.63446 | -151.63252[(c)] | -1.21 |
| QCISD(T)/6-31G* | -151.65963 | -151.66237[(c)] | 1.72 |
| MHB basis set and geometry | | | |
| MP4/[4*s*2*p*1*d*] | -151.66354 | -151.68066 | 10.75 |
| PMP4(3)/[4*s*2*p*1*d*] | -151.67006 | -151.68066 | 6.65 |
| QCISD/[4*s*2*p*1*d*] | -151.64721 | -151.64961 | 1.51 |
| QCISD(T)/[4*s*2*p*1*d*] | -151.67179 | -151.67853 | 4.23 |
| CCSD[(b)] | -151.64446 | -151.64836 | 2.45 |
| CCSD+T(CCSD)[(b)] | -151.67176 | -151.67892 | 4.49 |
| CCSDT-1[(b)] | -151.67169 | -151.67967 | 5.01 |
| MP2/6-311G* geometry | | | |
| MP4/6-311G* | -151.70117 | -151.71370 | 7.87 |
| PMP4(3)/6-311G* | -151.70766 | -151.71370 | 3.79 |
| MP4/[5*s*3*p*1*d*] | -151.70528 | -151.71297 | 4.83 |
| PMP4(3)/[5*s*3*p*1*d*] | -151.71196 | -151.71297 | 0.63 |
| QCISD/6-311G* | -151.68117 | -151.67737 | -2.39 |
| QCISD(T)/6-311G* | -151.70852 | -151.71006 | 0.96 |
| QCISD/[5*s*3*p*1*d*] | -151.68564 | -151.67690 | -5.49 |
| QCISD(T)/[5*s*3*p*1*d*] | -151.71297 | -151.70947 | -2.20 |
| MP4/[5*s*4*p*1*d*] | -151.71801 | -151.72755 | 5.99 |
| PMP4(3)/[5*s*4*p*1*d*] | -151.72470 | -151.72755 | 1.79 |
| MP4/6-311+G* | failure | -151.71886 | |
| PMP4(3)/6-311+G* | failure | -151.71886 | |
| MP4/6-311G(2*df*) | -151.77599 | -151.78572 | 6.11 |
| PMP4/6-311G(2*df*) | -151.78292 | -151.78572 | 1.76 |
| MP4/[5*s*3*p*2*d*1*f*] | -151.78241 | -151.79289 | 6.58 |
| PMP4(3)/[5*s*3*p*2*d*1*f*] | -151.78935 | -151.79289 | 2.22 |
| eQCISD(T)/6-311G(2*df*) | -151.78378 | -151.78208 | -1.07 |
| eQCISD(T)/[5*s*3*p*2*d*1*f*] | -151.79036 | -151.78939 | -0.61 |
| eQCISD(T)/[5*s*4*p*2*d*1*f*] | -151.80310 | -151.80397 | 0.55 |

(a) Taken from RB [Rag87].
(b) Taken from MHB [Mag86].
(c) Geometry for $^1A_1$ state from this work (see footnote to Table L). Energies at geometry from [Mic87] are QCISD: -151.63047 and QCISD(T):-151.65950 hartree.
The methods prefixed by an 'e' are extrapolations based on basis set additivity approximations (see text).

## 4.9.3 Results and discussion

### 4.9.3.1 Energetics

All total energies (Hartree) and isomerization energies $\Delta E$ (kcal/mol, plus sign favoring the cyclic) discussed in this section are presented in Table XLIX.

We first redid the CCD(ST) calculations of RB at the QCISD(T) level, in order to assess the effect of spin contamination on their computed $\Delta E$. The UHF/6-31G* reference geometry, used both here and in RB, was taken from Ref. [Whi81b]. We see indeed that there is an appreciable effect; the two structures are nearly isoenergetic at the QCISD(T)/6-31G* level. The PMP4 $\Delta E$ is relatively close to this value (1.76 kcal/mol off). $\langle \hat{S}^2 \rangle$ values for the linear structure range from 2.20 to 2.22 for all calculations reported in this Section; after a single projection, these values no longer exceed 2.01. This highlights the fact, that there is only one major contaminant; QCISD and CCSD should thus do a good job for this molecule as far as being insensitive to spin contamination goes. Application of the second projector changes the total energies by less than a millihartree at the MP4 level; the third changes the energies by only 2 microhartrees. Only the PMP4(3) energies (those with three projectors) will be reported henceforth in Table L. For the sake of completeness, the four core orbitals were frozen in the correlated calculations (as is standard practice with the Pople basis sets, these not being adequate for core correlation anyway).

Use of a correlated geometry does have a small, but appreciable effect. We redid the just mentioned calculations at the MP2/6-31G* geometry reported by Michalska *et al.* [Mic87], to find that the energy difference changes by only +0.08 kcal/mol at the QCISD level, but by +0.66 kcal/mol at the QCISD(T) level. We expect that further optimization of the geometry will result in a very slight additional favoring of the rhombic form.

The fact, that the PMP4(3) $\Delta E$ values are relatively close to the QCISD(T) values comes in handy for the very large basis set calculations.

A second test performed was a comparison with the MHB values. The basis set was DZP, with the polarization exponent $\alpha_D = 0.654$ being taken from MHB. The reference geometries used both here and in MHB were determined at the MP4(D)/DZP level and reported in MHB too. In these calculations, both the four cores and the four highest virtuals were frozen. The *d* shell was a full set of six second-order Gaussians.

The MP4 energies were in complete agreement with those reported in MHB, certifying that all basis set, geometry, and electron correlation details are identical.

At the QCISD(T) level, we predict an energy difference of 4.23 kcal/mol, compared to MHB's CCSD+T(CCSD) [Urb85] value of 4.49 kcal/mol and their CCSDT-1 value of 5.01 kcal/mol.

The difference between QCISD and CCSD total energies should normally be a good measure for the reliability of the QCISD method. The QCISD energies are too low by

Table L: Computed equilibrium geometries (Å, degrees) for the $^3\Sigma_g^-$ and $^1A_g$ states of $C_4$.

| | $^3\Sigma_g^-$ | | $^1A_g$ | |
|---|---|---|---|---|
| Method | $r_o$ | $r_i$ | $r$ | $\theta$ |
| HF/6-31G* | 1.2994 | 1.2758 | 1.4252 | 61.50 |
| MP2/6-31G*[(a)] | 1.313 | 1.296 | 1.425[(c)] | 64.60[(c)] |
| MP2/DZP[(b)] | ... | ... | 1.469 | 63.89 |
| MP4(D)/DZP[(b)] | 1.330 | 1.305 | 1.460 | 63.20 |
| MP2/6-311G* | 1.3132 | 1.2953 | 1.4575 | 63.60 |
| MP2/[5$s$3$p$1$d$] | 1.3165 | 1.2992 | 1.4658 | 63.91 |

(a) Reference [Mic87]
(b) Reference [Mag86]
(c) Our own results at this level are $r = 1.451, \theta = 63.60$ (see text).

2.8 and 1.3 millihartrees for the linear and cyclic structures, respectively. The difference between QCISD(T) and CCSD(T) should normally be much smaller; an important subclass of the diagrams in the difference are Hermitian conjugates of diagrams appearing in the quasiperturbative triples part that comes from the singles, and are thus absorbed in QCISD(T) through double-counting these contributions [Rag89].

Incidentally, the total energies are very close to those obtained at the CCSD+T(CCSD) level. The CCSDT-1 method then, which should give a good estimate of the remaining error, gives a total energy for the linear that is only 100 microhartrees above our QCISD(T) value, whereas for the cyclic, a difference of about 1 millihartree is seen. We think that the difference between the QCISD(T) and CCSDT-1 energies should normally be a good estimate for the error remaining in the electron correlation treatment; the same assumption was made by BMB in their [5$s$3$p$1$d$] study, where the difference between CCSDT-1 and CCSD+T(CCSD) in the [4$s$2$p$1$d$] basis set was used as a correction term to the CCSD+T(CCSD)/[5$s$3$p$1$d$] difference.

The PMP4 energy difference differs by some 2.4 kcal/mol from the QCISD(T) value, which is still acceptably small. The difference with CCSDT-1 is even less.

Since BMB found that the effect of going from a DZP to a TZP basis set was rather sizeable, our next step was to consider a triple-zeta basis set. Grev *et al.* [Gre89] recently showed that the commonly used 6-311G basis set [Kri80a] has two important disadvantages for this purpose: (a) its outer exponents are insufficiently diffuse; (b) the constraint that the $s$ and $p$ exponents be equal lead to optimized exponents that are actually better suited for the core than for the valence region. The conclusion of these authors was that 6-311G is not of triple zeta quality, and that a [5$s$3$p$] Dunning contraction of Huzinaga's (10$s$6$p$) primitive set is to be preferred. We have therefore considered both the 6-311G* basis set and a [5$s$3$p$1$d$] one, based on the Huzinaga/Dunning [5$s$3$p$] contracted set and a single five-membered $d$ function with $\alpha_d$=0.549. The latter has been optimized at the

MP4(DQ) level for carbon atom in its ground state (frozen core) using the G88OPT utility program bundled with GAUSSIAN 88.

For a reference geometry, we have chosen the MP2/6-311G* level, which yields a good geometry for linear $C_3$ [Mar90d], as a reasonable compromise between quality and computational feasability. The geometries are reported in Table L.

As seen from Table XLIX, the difference between the two basis sets is indeed quite appreciable. Whereas the [5*s*3*p*1*d*] predicts a difference of -2.20 kcal/mol at the QCISD(T) level, the 6-311G* basis set yields a difference of +0.96 kcal/mol; i.e., the conclusion is even qualitatively affected!

There is a difference of about 1 kcal/mol between the present QCISD(T)/[5*s*3*p*1*d*] values and the CCSD+T(CCSD)/[5*s*3*p*1*d*] values in BMB. Part of the difference may be due to the different reference geometries; far more importantly, however, the primitive sets are different, the TZP in BMB being a [5*s*3*p*1*d*] contraction from a (9*s*5*p*1*d*) primitive set. (The values for the polarization exponent are also slightly different, but not enough to cause an appreciable difference).

In both cases, the energy difference predicted at the PMP4 level is 2.83 kcal/mol larger than at the QCISD(T) level, compared to 2.42 kcal/mol in the [4*s*2*p*1*d*] basis set discussed above. Given the rather far-reaching consequences of the transition from DZP to TZP basis sets, the relatively small change in this error is a bit reassuring. If the trend continues, we expect that the difference between PMP4 and QCISD(T) will slightly increase further upon additional expansion of the basis set. As the difference favors the cyclic, using the PMP4 level for the basis set calibration should introduce a slight bias towards the cyclic form.

It should be remarked that the 6-31G* basis set apparently yielded values which are relatively close to the 6-311G*, but not to the [5*s*3*p*1*d*] results.

A further extension which might be considered is the addition of diffuse functions [Cla83]. Their effect is expected to be on the order of 1 kcal/mol for the 6-311G*, but negligible for the [5*s*3*p*1*d*] basis set because the latter's outer exponents are already fairly 'diffuse' [Scu89]. Unfortunately, the MP4/6-311+G* calculation for the linear form failed because of near-linear-dependence effects, leading to exceedingly large MO coefficients which cause a numerically unstable integral transform. The energies obtained beyond the MP2 level are so clearly nonsensical that they are not reported here. At the PMP2 level, it appears that the linear gets a boost of 2.52 kcal/mol, which explains a lot of the discrepancy between the 6-311G* and [5*s*3*p*1*d*] results.

The [5*s*3*p*1*d*] calculations were about the maximum we could computationally afford at the QCISD(T) level. However, as the basis set effects do not appear to have converged yet, we have considered two further extensions of the basis set.

Given the fairly large importance of valence set effects, the first thing we considered was loosening the contraction of the (10s6p) set from [5*s*3*p*1*d*] to [5*s*4*p*1*d*]. The polariza-

tion exponent was re-optimized, but could as well have been transferred from the [5*s*3*p*1*d*] calculations: its new value is $\alpha_d = 0.555$. The results show that the cyclic form gets a 'push in the back' by 1.16 kcal/mol. Applying this as a correction term to the −2.20 kcal/mol $\Delta E$ found at the QCISD(T)/[5*s*3*p*1*d*] level, this leaves only −1.04 kcal/mol favoring the linear, or a nearly isoenergetic situation after applying the correction for QCISD(T) inadequacy.

The second extension considered was of course increasing the polarization space. We have considered both the standard 6-311G(2*df*) basis set [Fri84], and a [5*s*3*p*2*d*1*f*] basis set constructed from the [5*s*3*p*1*d*] basis. In the latter, the *d* exponents were doubled by applying the 'even scaling rule' (see [Fri84] and references there), whereas the *f* exponent was optimized with the same procedure as used above, the [5*s*3*p*2*d*] part being held constant. The $\alpha_f$ thus obtained was 0.775.

The results are a bit surprising, in that the extension of the polarization space favors the linear form by 2.03 kcal/mol in the 6-311G(2*df*) case, but the cyclic form by 1.59 kcal/mol in the [5*s*3*p*2*d*1*f*] case. As a result, the extrapolated QCISD(T)/6-311G(2*df*) and QCISD(T)/[5*s*3*p*2*d*1*f*] values are in fairly good agreement, being -1.07 and -0.61 kcal/mol, respectively.

In the latter case, we can now apply the +1.16 kcal/mol correction from the [5*s*3*p*] → [5*s*4*p*] extension, yielding an extrapolated QCISD(T)/[5*s*4*p*2*d*1*f*] value of +0.26 kcal/mol. Finally, applying the 'QCISD(T) inadequacy' correction of 0.78 kcal/mol obtained in the [4*s*2*p*1*d*] basis set, our best estimate for the energy difference in the 'hypothetical motionless state' is +1.33 kcal/mol, or say about 1 kcal/mol, favoring the cyclic isomer.

#### 4.9.3.2 Geometries and harmonic frequencies

Geometries and harmonic frequencies were computed at the MP2/6-311G* level, as well as at the MP2/[5*s*3*p*1*d*] level. MP2 harmonic frequencies in the [4*s*2*p*1*d*] basis set used by MHB were also evaluated for the linear form, for which they did not report them. The geometries obtained are listed in Table L, together with the available literature data. The same is done for the harmonic frequencies in Table LI. For the latter, IR intensities within the double- harmonic approximation were also determined from numerical differentiation of the MP2 dipole moment [Yam86]. Although not recommended for quantitative purposes, the intensities obtained at this level of theory should be good enough to give a qualitative picture of the relative intensities [Hes86].

For bending frequencies of multiply bonded species, at least a [5*s*3*p*2*d*1*f*] basis set is normally required at the MP2 level for quantitative accuracy [Sim88]. However, such a level of theory is beyond our computational power, whereas we are primarily interested in the stretching frequencies.

The only experimental information available is the fact that a band in argon matrix at 1543.4 $cm^{-1}$ belongs to linear $C_4$ [She89], as well as the isotopic substitution spectrum

Table LI: Theoretical harmonic frequencies ($cm^{-1}$) for the $^3\Sigma_g^-$ and $^1A_g$ states of $C_4$. Infrared intensities (km/mol) are given in parentheses for the IR-active modes. Harmonic zero-point energies (ZPEs) are in kcal/mol.

| Symmetry | UHF/6-31G* | MP2/6-31G* | MP2/[4s2p1d] | MP2/6-311G* | MP2/[5s3p1d] |
|---|---|---|---|---|---|
| | | | $^3\Sigma_g^-$ | | |
| $\Sigma_g$ | 2345 | 2149 | 2093 | 2128 | 2115 |
| $\Sigma_u$ | 1740(142.3) | 1586(488.3) | 1544(585.0) | 1562(544.9) | 1551(601.8) |
| $\Sigma_g$ | 1021 | 951 | 922 | 935 | 929 |
| $\Pi_g$ | 408 | 419 | 376 | 401 | 419 |
| $\Pi_u$ | 210(51.2) | 187(33.3) | 174(27.2) | 181(30.4) | 185(31.6) |
| ZPE | 9.07 | 8.43 | 8.09 | 8.28 | 8.30 |
| | | | $^1A_g$ | | |
| $B_{1u}$ | 1568(406.0) | 1428(1262.4) | 1389(*) | 1402(193.4) | 1365(202.7) |
| $A_g$ | 1431 | 1298 | 1255(*) | 1263 | 1229 |
| $B_{3g}$ | 1103 | 1103 | 1079(*) | 1077 | 1048 |
| $A_g$ | 1088 | 934 | 912(*) | 924 | 904 |
| $B_{2u}$ | 450(24.7) | 712(184.5) | 716(*) | 700(26.4) | 679(25.4) |
| $B_{3u}$ | 350(96.4) | 374(316.1) | 359(*) | 355(50.5) | 356(53.1) |
| ZPE | 8.56 | 8.36 | 8.16 | 8.18 | 7.98 |

MP2/6-31G* values are taken from Reference [Mic87]. Our own results for the $^1A_g$ state are: $B_{1u}$ 1429(187.9), $A_g$ 1285, $B_{3g}$ 1103, $A_g$ 950, $B_{2u}$ 713(27.4), $B_{3u}$ 374(47.1).
IR intensities for the $\Pi_u$ mode include the twofold degeneracy.
(*) Taken from MHB [Mag86].

reported in the same reference. It has already been shown in Section 4.8 [Mar90f], that the isotopic substitution bands are in excellent agreement with experiment (deviations on the order of 0.2 $cm^{-1}$) at levels of theory ranging from UHF/4-21G to MP2/6-31G*: the levels of theory presented here form no exception.

The computed frequencies at the MP2/6-311G* and MP2/[5s3p1d] level differ only by a relatively small amount for the linear structure, but rather significantly for the rhombic structure, consistent with the expectation that the latter will put much greater demands on the basis set for frequency evaluations. The MP2/[5s3p1d] prediction of 1551 $cm^{-1}$ for the experimental 1543.4 $cm^{-1}$ band is perhaps a fortunate result of error compensation: further improvement of basis set and electron correlation is expected to lower the frequency, whereas elimination of spin contamination would increase its value [Mar90a]. An even luckier compensation is seen with the MHB basis set, where the calculated value is 'spot on' at 1544 $cm^{-1}$.

The very large intensity predicted at the MP2/6-31G* level [Mic87] for the $B_{1u}$ mode of the rhombus is in disagreement with the fairly moderate values found with other basis sets at the MP2 level. To eliminate the possibility of a misprint in [Mic87], we reran the calculations ourselves. We then also found that the equilibrium geometry reported in [Mic87] was not a stationary point. Our own optimum MP2/6-31G* geometry, which is

Table LII: Computed isotopic substitution spectrum for the hypothetical 1284 $cm^{-1}$band of rhombic $C_4$ (*).

| Isotopomer | Wt. | HF/4-21G | HF/6-31G* | MP2/6-31G* | MP2/6-311G* | MP2/[5*s*3*p*1*d*] |
|---|---|---|---|---|---|---|
| 12-12-12-12 | 1 | 1284.0 | 1284.0 | 1284.0 | 1284.0 | 1284.0 |
| 12-12-12-13 | 2 | 1271.8 | 1271.9 | 1272.1 | 1272.1 | 1272.1 |
| 12-12-13-12 | 2 | 1272.5 | 1272.8 | 1272.7 | 1272.7 | 1272.7 |
| 12-12-13-13 | 4 | 1260.2 | 1260.6 | 1260.8 | 1260.7 | 1260.8 |
| 12-13-12-13 | 1 | 1259.0 | 1259.0 | 1259.0 | 1259.0 | 1259.0 |
| 13-12-13-12 | 1 | 1259.0 | 1259.0 | 1259.0 | 1259.0 | 1259.0 |
| 12-13-13-13 | 2 | 1247.4 | 1247.6 | 1247.6 | 1247.6 | 1247.6 |
| 13-12-13-13 | 2 | 1246.5 | 1246.7 | 1246.9 | 1246.8 | 1246.8 |
| 13-13-13-13 | 1 | 1233.5 | 1233.5 | 1233.5 | 1233.5 | 1233.5 |

(*) The first atom is situated along the largest diagonal of the rhombus. Subsequent atoms are numbered either clockwise or counterclockwise (the two possibilities are equivalent by symmetry).

also in much better agreement with the other MP2 values, is reported in a footnote to Table L. The harmonic frequencies obtained are given as a footnote to Table LI. They are in near-complete agreement with the analytical gradient values given as a footnote to Table II in [Mic87]; the IR intensities, however, are much lower than those previously reported [Mic87], although they are now in good agreement with the other MP2 values.

A practical implication is that, since the IR intensity for the rhombic form is less than half that for the linear form, the two bands will only be detected at a comparable intensity if the ground state is indeed cyclic. (It should be remembered that the linear $^3\Sigma_g^-$ state will benefit from its threefold degeneracy.)

It was already shown before (Sections 4.7 and 4.8) [Mar90f, Mar90g] that the only likely candidate for assignment to the $B_{1u}$ band of the rhombus is a band at 1284 $cm^{-1}$ [Tho71, Kra85]. Application of the well-known generic scaling factors of 0.89 [Pop81] and 0.93 [Hou82], respectively, to the UHF/6-31G* and MP2/6-31G* frequencies supports the assignment, as do the present higher-level results.

One might remark that upon annealing the 1284 $cm^{-1}$ band grows, whereas the 1544 $cm^{-1}$ band even decreases slightly in intensity. However, linear $C_4$ will easily react with $C_3$ to produce linear $C_7$ [Rag87], which is not so evident for the cyclic form. Furthermore, the two forms do not readily interconvert, which means that on kinetic grounds, linear $C_4$ will be depleted much faster than cyclic $C_4$, although both will continue to be formed from the smaller components of the trapped vapor. Furthermore, the additional rotational degree of freedom of the cyclic will by itself displace the isomerization constant in its favor by a factor $\sqrt{T}$, until the linear form starts benefitting from its low bending frequencies at somewhat higher temperatures (> 50–100 K). All this serves mainly to illustrate that the 1284 $cm^{-1}$ assignment cannot necessarily be ruled out on the basis of thermal annealing behavior.

Detection of the band and recording of either a rotational fine structure or an isotopic

Table LIII: Atomic energies (hartree) used in dissociation energy calculations.

| Basis | MP4 | PMP4(1) | QCISD(T) |
|---|---|---|---|
| 6-311G* | -37.764302 | -37.764797 | -37.766695 |
| 6-311+G* | -37.765199 | -37.765808 | |
| 6-311G(2*df*) | -37.774830 | -37.775441 | |
| [5*s*3*p*1*d*] | -37.767208 | -37.767761 | -37.769755 |
| [5*s*4*p*1*d*] | -37.769366 | -37.769913 | |
| [5*s*3*p*2*d*1*f*] | -37.777538 | -37.778186 | |

substitution spectrum should normally give fairly conclusive evidence whether the linear and cyclic isomers coexist or not. In order to facilitate the latter, we have given in Table LII the computed isotopic substitution spectrum at various levels of theory. Evidently, the computed values converge quite rapidly with increasing theoretical level; the MP2/6-311G* and MP2/[5*s*3*p*1*d*] values are even indistinguishable. Because the force constants will not be described as well as for the linear stretching force constants, the agreement with experiment may be somewhat worse than in the latter case, but the spectrum's appearance is itself characteristic enough. The rotational fine structure for an asymmetric top is of course easily distinguished from that of a linear molecule.

Given the difference in oscillator strengths and the additional degeneracy entropy of the linear form, coexistence at these low temperatures normally implies that the rhombus is very slightly below the linear form, as predicted by the present calculations.

Zero point energies (ZPEs) within the RRHO (rigid rotor-harmonic oscillator) approximation may be derived from the computed frequencies (the HF/6-31G* and MP2/6-31G* should be scaled by factors of 0.89 and 0.93, respectively). Their effect on the computed $\Delta E$ is very small (0.1 – 0.3 kcal/mol). All levels of theory except MP2/[4*s*2*p*1*d*] predict that it favors the cyclic structure; however, given the smallness of the effects, no definitive conclusion about that can be made without taking anharmonic corrections into account. Enlarging the basis set will normally lower the computed frequencies for the cyclic a little more than for the linear; on the other hand, the degenerate bending modes of the linear may be significantly affected too, which works in the opposite direction. Our main conclusion regarding the ZPE effect is that its neglect should be negligible compared to the other errors inherent in the calculations.

### 4.9.4 Heat of formation of $C_4$

There are two generally quoted literature sources for the heat of formation of $C_4$: the JANAF tables [Jan85], where a value of 232 kcal/mol is given, and the classic note of Drowart *et al.* [Dro59], who found (using the Knudsen effusion technique) a second-law value of 229.5 ± 7.1 kcal/mol and third-law values (using two different partition

functions) of 240.5 ± 5.8 and 237.5 ± 5.8 kcal/mol, respectively. These values were based on a heat of formation for C(g) of 169.58 kcal/mol, which is listed in the JANAF tables as 169.98 kcal/mol. Hence, another 1.6 kcal/mol should be added to bring the values for $C_4$ on the same scale as our theoretical determination.

The latter follows the standard G1 recipe as outlined in [Pop89]. Atomic energies involved in the calculation may be found in Table LIII. Taking all the customary terms into account, we find a $\Sigma D_e$ of 437.9 and a $\Sigma D_0$ of 430.3 kcal/mol, which means a heat of formation of 249.6 kcal/mol. This value is normally claimed to be accurate to ± 2 kcal/mol. We will not claim this kind of accuracy for such a 'difficult' molecule; however, the 232 and 229.5 kcal/mol values are clearly outside the expected error range. Using PMP4 instead of MP4 energies for the additivity calculation lowers the computed dissociation energies by 0.58 kcal/mol (and of course increases the heat of formation by the same amount).

The free energy functions $-[G(T) - H(0)]/T$ used by Drowart *et al.* in their third-law extrapolation are actually semiempirical estimates by Pitzer and Clementi [Pit59]. Seeing these as a potential error source, we have re-evaluated the free energy functions — within the RRHO (rigid rotor- harmonic oscillator) approximation — ourselves with the available ab initio data. At the temperatures of interest, anharmonic, centrifugal distortion, and rotation-vibration coupling effects may be of some importance; however, even our crude RRHO functions should be much more reliable than the Pitzer-Clementi 'thumbnail estimates'.

Details of the RRHO calculation are as follows. Harmonic frequencies and rotational constants were taken to be unscaled MP2/[5*s*3*p*1*d*] values, with all isotopes $^{12}C$ throughout. The electronic partition function was assumed to be factorizable, and set up separately for the linear and cyclic forms. The necessary transition energies were MRD-CI/DZP values taken from Ref. [Pac88], this data set being the most complete. The isomerization energy at absolute zero was taken to be +1.0 kcal/mol, and the internal partition function thus constructed from those for the linear and cyclic isomers. Finally, the translational contribution was added in, with the molecular weight computed from the natural isotopic abundances.

Computed free energy functions at 2000, 2500, and 3000 K, respectively, are 77.09, 81.19, and 84.66 e.u., in excess of 2 e.u. above the Pitzer- Clementi values. The final values are quite close to those for the linear isomer by itself, illustrating that the latter will dominate at higher temperatures even though it is not the ground state, strictly speaking. Correcting the Drowart *et al.* values for the new free energy functions, we find an average heat of formation of 246.7 kcal/mol. Correcting for the different reference values for the heat of formation of the C(*g*) atom, this even increases to 248.3 kcal/mol, in good agreement with our theoretical determination. (Assuming the linear and cyclic forms to be isoenergetic yields free energy functions of 77.53, 81.55, and 84.96 e.u. at

2000, 2500, and 3000 K, repectively. These values would imply an additional 0.9 kcal/mol increase in the third-law heat of formation.)

Quite surprisingly, redoing the entire G1 procedure with a $[5s3p]$ valence set substituted for the 6-311G one has a rather significant effect on the results. The correction terms have been evaluated according to the same recipe as the ones in the original G1 publication, and are in excellent agreement with them

$$\Delta E_{\mathrm{HLC}} = -0.19 n_\alpha - 5.96 n_\beta \text{ millihartrees} \tag{4.22}$$

where $n_\alpha$ and $n_\beta$ represent the number of spin-up and spin-down electrons, as customary. At the G1/$[5s3p2d1f]$ level, we arrive at $\Sigma D_e$ = 434.3 and $\Sigma D_0$ = 426.7 kcal/mol, or a heat of formation of 253.3 kcal/mol, still in marginal agreement with the revised 'experimental' value. At the G1/6-311G($2df$) level (i.e. ignoring the diffuse functions) we find a $\Sigma D_e$ = 436.9 kcal/mol, which explains part but not all of the discrepancy between the two basis set families. Taking the $[5s3p1d] \rightarrow [5s4p1d]$ extension into account too, however, we arrive at a value in good agreement with both the 'experimental' and G1/6-311+G($2df$) values, namely $\Sigma D_e$ = 438.1, $\Sigma D_0$ = 430.5, and $\Delta H_f^0$ = 249.4 kcal/mol. As a final note, using PMP4 instead of MP4 in the additivity calculations leads to $\Sigma D_e$ lowerings of 0.24, 0.22, and 0.29 kcal/mol for the G1/$[5s3p2d1f]$, G1/$[5s4p2d1f]$, and G1/6-311G($2df$) results, respectively.

In assigning an approximate error bar for the computed heats of formation we should consider a few further possible error sources. These include inadequacy of the electron correlation treatment, which may have an effect on the order of a few kcal/mol at most, and nonadditivity of basis set and electron correlation effects. To assess the possible magnitude of these, we redid our previous calculation of the heat of formation of $C_3$ (Section 4.10) [Mar90f] (where the additivity was assumed only at the CCD(ST) level instead of the MP4 level) using conventional G1 theory and found an error of only 0.5 kcal/mol. A safe error estimate for our theoretical value is then something like $\pm$ 4 kcal/mol.

All this appears to indicate that the heats of formation hitherto assumed for $C_4$ are much too low, that the Drowart *et al.* third-law value might be close to the actual value, and that an experimental redetermination and/or an *ab initio* study at a higher level are indicated.

### 4.9.5 Note

Just before submitting the present work to the Journal of Chemical Physics, we received a preprint from V. Parasuk and J. Almlöf [Par90], where partial-valence CASSCF (complete active space SCF [Roo87]) and partial and full-valence MRCI [Bau90] results are reported for $C_4$. With the MHB basis set (but the redundant $s$ function eliminated from the $d$ shell), these authors found a $\Delta E$ of -2.7 kcal/mol at the MRCI level. This indicates

that a multireference treatment will normally not have a devastating effect on the present results. At their best level of theory (which was MRCI in a [4*s*4*p*2*d*1*f*] atomic natural orbital (ANO) [Alm87] basis set, with all configurations whose coefficients exceed 0.05 in a 10/10 CASSCF being included in the reference set), these authors found the linear form to be 4.5 kcal/mol lower than the cyclic form. However, direct MP2 calculations with basis sets up to [6*s*5*p*4*d*2*f*] indicate that further basis set expansion will favor the cyclic, leading these authors to conclude that the two forms will be nearly isoenergetic. This latter conclusion is in agreement with that reached in the present work.

Dr. Jan Almlöf kindly suggested investigating the effect of basis set superposition error (BSSE), as it tends to artificially favor the cyclic form [ParTBP]. Whereas the last word on the validity of the counterpoise (CP) procedure [Boy70] has not nearly been said (Section 3.4) [Mar89f], we have computed the CP corrections at the PMP4 level using the site-site function counterpoise method [Wel83] (The extension of the CP to interactions involving more than two subsystems, such as $\Sigma D_e$ values for polyatomics, is not unique.) At the PMP4/[5*s*3*p*2*d*1*f*] level, the CP correction favors the linear structure by 0.77 kcal/mol, compared to 2.57 and 2.24 kcal/mol at the PMP4/[5*s*4*p*1*d*] and PMP4/[5*s*3*p*1*d*] levels, respectively. Applying the full CP correction would consequently lead to a nearly vanishing $\Delta E$. On the other hand, the fully CP-corrected $\Delta E$ increases by about 1 kcal/mol each for the two basis set extensions considered. Extrapolating this trend for further basis set extensions suggests that the cyclic form would indeed be slightly below the linear form in the infinite-basis limit. We agree with Dr. Almlöf though, that it is a bit pointless to argue about the ground state on the basis of currently achievable theoretical results alone, and hope that some of the results presented in this paper may aid experimentalists to settle the issue by indirect evidence.

Let it be added that after going to press of the present Section [Mar91], a paper by Andreoni, Scharf, and Giannozzi [And90] appeared in which the geometrical structures of $C_4$ and $C_{10}$ were studied using the Car-Parrinello [Car85] density functional [Par89b] method. Those authors' conclusions for $C_4$ are essentially identical to the ones reached in the present Section [Mar91].

As a final note, again after going to press of the present Section, matrix IR work by Heath and Saykally [Hea91a] provided further unambiguous confirmation for the 1544 $cm^{-1}$ assignment to the $^3\Sigma_g^-$ state of linear $C_4$. The gas-phase band origin was 1548.9368(21) $cm^{-1}$ and the effective bond distance 1.30431(21) Å, in very good agreement with the present ab initio data, our $r_{eff}$ being 1.310 Å at the MP2/6-311G* level and 1.313 Å at the MP2/[5*s*3*p*1*d*] level. As this again implies $r_e$ to be greater than $r_0$, this indicates floppy behavior for linear $C_4$ and possibly absence thereof for linear $C_6$ (by analogy with the alternant behavior observed for the odd-numbered clusters, see end of previous Section).

# 4.10 On the geometrical structure of the $C_3^+$ cation – an ab initio study

## 4.10.1 Introduction

Considerable attention has gone in recent years to the structure and energetics of carbon clusters. The situation up to April 1989, as well as the high significance of this subject, have been reviewed by Weltner and Van Zee [Wel89]. Since then, additional progress has been made, including definitive IR-spectroscopic characterizations of $C_4$ and $C_5$ by an interaction between theory [Mic87, Mar89b, Bot89, Ada89] and experiment [Ber89, She89].

The situation is less clear for the ions than for the neutral clusters. $C_3^+$ is believed to be the building block for the larger clusters [Bro87]; however, its geometrical structure is unknown to date. Previous theoretical studies always assumed a linear structure (see e.g. [Sun84]) by analogy with the neutral species.

Recently, $C_3^+$ has been investigated [Fai87] using the Coulomb explosion technique [Vag89]. The results indicate a cyclic structure; preliminary ab initio calculations by Raghavachari (private communication quoted in [Fai87]) appear to confirm this. However, Vager and Kanter [Vag89b] remarked that the experimental intensity distributions [Fai87] could also be rationalized under the assumption of a linear structure with an extremely low bending frequency (as $C_3$ is since long known to have [Gau65]) with a 'hot' (about 450 K) Boltzmann distribution. We therefore thought it was worthwhile to perform a high-level ab initio study on these species, which might help to settle the issue.

## 4.10.2 Computational methods

The major part of the calculations was performed using the GAUSSIAN 88 program system [Gau88] running on our VAXstation 2000 under VMS 4.7. Some calculations with larger basis set (MP2 geometry optimizations with the 6-311G* basis set, coupled cluster calculations with the 6-311+G* basis set) were too demanding for the VaxStation in terms of both disk space and CPU requirements. These were performed using GAUSSIAN 86 [Gau86] running on an IBM 4381/FPS-X64 configuration at the Facultés Universitaires de Namur. Finally, the largest coupled cluster calculations in the 6-311G(2*df*) basis set (90 contracted Gaussians, all valence electrons correlated in 87 orbitals) were performed using GAUSSIAN 86 on the IBM 3090/400e VF (running under MVS/XA) at the University of Leuven.

Firstly, the potential energy surface was investigated at the UHF/6-31G* level using analytical first and second derivatives [Pop79]. Energy separations between the various stationary points were evaluated using the QCISD(T) model [Pop87], which is actually an approximation to CCSD [Pur82, Bar89] with a perturbative triples correction. It was

Table LIV: Total (hartree; minus sign omitted) and relative (kcal/mol) energies using the 6-31G* basis set for various UHF/6-31G* structures of $C_3^+$.

| Species | UHF | MP2 | MP3 | MP4(D) | MP4(DQ) | MP4(SDQ) |
|---|---|---|---|---|---|---|
| | | Total | energies | | | |
| $C^+(^2P)$ | 37.28708 | 37.33107 | 37.34585 | 37.35206 | 37.35124 | 37.35143 |
| $C(^3P)$ | 37.68086 | 37.73297 | 37.74636 | 37.75064 | 37.74979 | 37.74998 |
| $2C + C^+$ | 112.64880 | 112.79702 | 112.83858 | 112.85334 | 112.85083 | 112.85138 |
| C3P001 | 112.98376 | 113.25712 | 113.27209 | 113.27946 | 113.27139 | 113.27641 |
| C3P002 | 112.95931 | 113.20552 | 113.22180 | 113.22884 | 113.22165 | 113.22980 |
| C3P003 | 112.89324 | 113.29561 | 113.25053 | 113.29112 | 113.26608 | 113.29094 |
| C3P004 | 112.94226 | 113.24907 | 113.26191 | 113.27285 | 113.26245 | 113.27297 |
| C3P005 | 112.93582 | 113.24156 | 113.25482 | 113.26593 | 113.25641 | 113.26582 |
| C3P006 | 112.93084 | 113.28199 | 113.28359 | 113.29139 | 113.28388 | 113.29139 |
| Species | PUHF | PMP2 | PMP3 | QCISD | QCISD(T) | |
| $C^+(^2P)$ | 37.28948 | 37.33214 | 37.34625 | 37.35528 | 37.35599 | |
| $C(^3P)$ | 37.68260 | 37.73383 | 37.74673 | 37.75184 | 37.75277 | |
| $2C + C^+$ | 112.65467 | 112.79979 | 112.83972 | 112.85896 | 112.86153 | |
| C3P001 | 112.98697 | 113.25882 | 113.27297 | 113.28015 | 113.29745 | |
| C3P002 | 112.97228 | 113.21646 | 113.22989 | 113.24155 | 113.25833 | |
| C3P003 | 112.89959 | 113.29959 | 113.25249 | 113.28266 | 113.32360 | |
| C3P004 | 112.96398 | 113.27033 | 113.28173 | 113.29411 | 113.32128 | |
| C3P005 | 112.95299 | 113.25694 | 113.26699 | 113.28982 | 113.31463 | |
| C3P006 | 112.93811 | 113.28778 | 113.28731 | 113.29680 | 113.32361 | |
| | | Relative | energies | | | |
| Species | UHF | MP2 | MP3 | MP4(D) | MP4(DQ) | MP4(SDQ) |
| $2C + C^+$ | 210.19 | 312.87 | 279.25 | 274.87 | 271.75 | 276.11 |
| C3P001 | 0.00 | 24.15 | 7.22 | 7.48 | 7.84 | 9.40 |
| C3P002 | 15.34 | 56.53 | 38.78 | 39.25 | 39.05 | 38.65 |
| C3P003 | 56.80 | 0.00 | 20.75 | 0.17 | 11.17 | 0.28 |
| C3P004 | 26.04 | 29.20 | 13.61 | 11.63 | 13.45 | 11.56 |
| C3P005 | 30.08 | 33.92 | 18.06 | 15.98 | 17.24 | 16.04 |
| C3P006 | 33.21 | 8.55 | 0.00 | 0.00 | 0.00 | 0.00 |
| Species | PUHF | PMP2 | PMP3 | QCISD | QCISD(T) | |
| $2C + C^+$ | 208.52 | 313.63 | 280.87 | 274.74 | 289.96 | |
| C3P001 | 0.00 | 25.58 | 9.00 | 10.45 | 16.41 | |
| C3P002 | 9.22 | 52.17 | 36.03 | 34.67 | 40.96 | |
| C3P003 | 54.83 | 0.00 | 21.85 | 8.87 | 0.00 | |
| C3P004 | 14.42 | 18.36 | 3.50 | 1.69 | 1.46 | |
| C3P005 | 21.32 | 26.76 | 12.75 | 4.38 | 5.63 | |
| C3P006 | 30.66 | 7.41 | 0.00 | 0.00 | 0.00 | |

Table LV: Expectation values of $\hat{S}^2$, term symbols, and configurations for various structures of $C_3^+$.

| Species | $\langle\hat{S}^2\rangle$ | $\langle\hat{S}^2\rangle_1$ | $\langle\hat{S}^2\rangle_A$ | Term | Electronic configuration |
|---|---|---|---|---|---|
| C3P001 | 3.765 | 3.751 | 3.750 | $^4A_1'$ | $(a_1')^2(e')^4(a_1')^2(e')^4(a_2")^2(a_1')(e')^2$ |
| C3P002 | 3.991 | 3.913 | 3.759 | $^4\Pi_u$ | $(\sigma_g)^2(\sigma_u)^2(\sigma_g)^2(\sigma_g)^2(\sigma_u)^2(\pi_u)^4(\sigma_g)(\sigma_u)(\pi_g)$ |
| C3P003 | 0.780 | 0.757 | 0.750 | $^2\Sigma_u^+$ | $(\sigma_g)^2(\sigma_u)^2(\sigma_g)^2(\sigma_g)^2(\sigma_u)^2(\pi_u)^4(\sigma_g)^2(\sigma_u)$ |
| C3P004 | 1.495 | 1.459 | 0.917 | $^2B_2$ | $(a_1)^2(b_2)^2(a_1)^2(a_1)^2(a_1)^2(b_2)^2(a_1)^2(b_1)^2(b_2)$ |
| C3P005 | 1.038 | 0.977 | 0.760 | $^2A_1$ | $(a_1)^2(b_2)^2(a_1)^2(a_1)^2(a_1)^2(b_2)^2(a_1)^2(b_1)^2(a_1)$ |
| C3P006 | 0.807 | 0.783 | 0.752 | $^2B_2$ | $(a_1)^2(b_2)^2(a_1)^2(a_1)^2(a_1)^2(b_2)^2(a_1)^2(b_1)^2(b_2)$ |

$\langle\hat{S}^2\rangle$, $\langle\hat{S}^2\rangle_1$, and $\langle\hat{S}^2\rangle_A$ represent the expectation values of $\hat{S}^2$ for the UHF wave function, the first-order MBPT wavefunction, and the PUHF wave function, respectively.

shown very recently [Lee90], that QCISD is quite comparable to CCSD for nonpathological cases. During the course of the QCISD calculation, MP2 [Bin75b], MP3 [Pop76], and MP4(SDQ) [Kri78] energies, as well as their spin-projected counterparts [Sch86], are obtained 'on the fly'; these allow for assessment of convergence of the MBPT series as well as of spin contamination effects.

For the most stable states, geometries were then optimized at the MP2 level using the 6-311G* basis set [Kri80a] and analytical gradients [Pop79]. From these geometries, both QCISD(T) and CCD+ST(CCD) [Rag85] calculations were performed. (In keeping with the recent nomenclature for perturbatively corrected coupled cluster methods [Rag89], we will henceforth denote CCD+ST(CCD) as CCD(ST)). The latter method was available on the FPS configuration as well as on the IBM 3090, and could thus be used with much larger basis sets. The prime difference with QCISD(T) is in the account for infinite-order single substitution effects and coupling terms thereof: comparison allows their assessment.

Using the CCD(ST) model, calculations were then performed with the 6-311+G* basis set [Cla83] to assess the effect of diffuse functions, and with the 6-311G(2*df*) basis set [Fri84] to evaluate the effect of polarization set expansion. On these final energies, a G1 correction [Pop89] was applied to obtain dissociation energies accurate to about 2 kcal/mol [Pop89].

## 4.10.3 Results and discussion

### 4.10.3.1 Potential energy surface of $C_3^+$

Equilibrium geometries obtained at the UHF/6-31G* level are depicted in Figure 4.18. For these same structures, total energies at various levels of electron correlation, as well as the relative energies with respect to the lowest-lying state, are given in Table LIV. Electronic configurations, term symbols, and expectation values for the $\hat{S}^2$ operator are

Figure 4.18: Stationary point geometries for $C_3^+$ at the UHF/6-31G* level. Bond distances are in Ångstrom units.

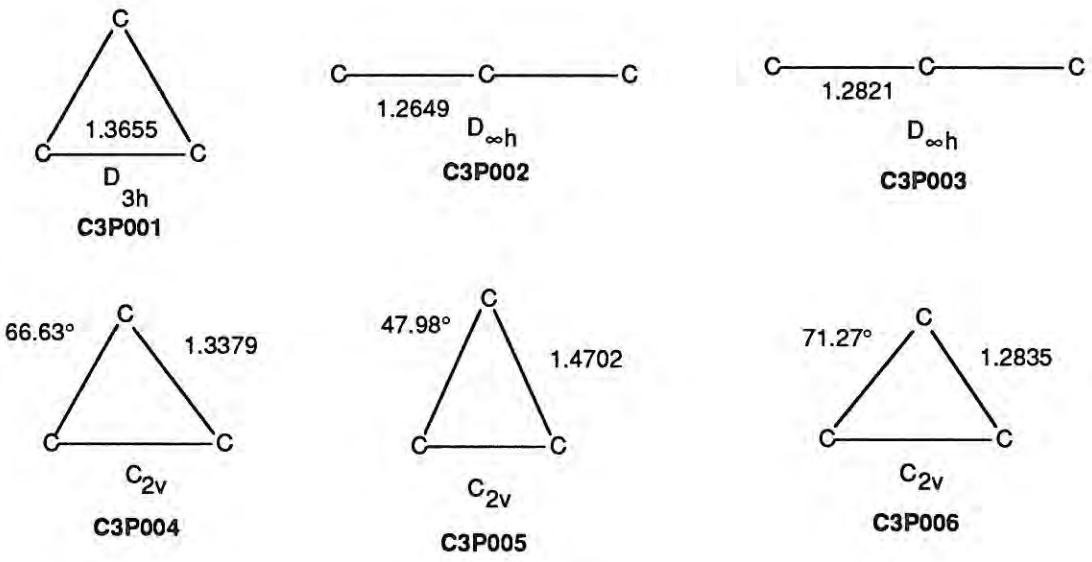


presented in Table LV, whereas harmonic frequencies at the UHF/6-31G* level, as well as the corresponding double-harmonic infrared and Raman intensities, are listed in Table LVI.

It can immediately be seen, that electron correlation effects are very prominent for this system. Even qualitative conclusions such as the nature of the ground state are profoundly affected by the electron correlation model selected.

At the Hartree-Fock level, the quartet surface appears to be the lowest one. The equilateral triangle is the ground state, followed at 15.34 kcal/mol by the linear structure C3P002. The latter has the low bending frequency now familiar for linear carbon clusters, which also undergoes a 'weak' Renner-Teller splitting here. This implies that there will be another low-lying $D_{3h}$ state C3P001′ ($^2A_2''$) , which correlates with the other component of the Renner-Teller pair. The potential energy surface (PES) is thus markedly similar to the doublet surface of $B_3$ (Section 4.2.3) [Mar89c, Mar89a]. However, the very heavy spin contamination that was seen in both the $^2\Pi_g$ and the $^2A_1'$ states of $B_3$ [Mar89c] is absent here, apparently because the additional two unpaired electrons fill up the low-lying virtual orbitals that cause the problem in $B_3$ ($\pi_g$ for the $^2\Pi_g$ state, $e''$ for the $^2A_1'$ state).

The doublet surface is considerably higher in energy at the UHF level. For the triangular structure (a $^2E'$ state), the Jahn-Teller theorem applies. This leads to two isosceles triangles, namely the $^2B_2$ state C3P004 (apex angle 66.63°) and the $^2A_1$ state C3P005 (apex angle 49.98°). However, whereas C3P004 is a local minimum, C3P005 is a first-order saddle point on the PES. The latter will be the transition state for a degenerate

Table LVI: Harmonic frequencies for various structures of $C_3^+$.

| Species | $\omega_4$ ($cm^{-1}$) | $\omega_3$ ($cm^{-1}$) | $\omega_2$ ($cm^{-1}$) | $\omega_1$ ($cm^{-1}$) | ZPE (kcal/mol) |
|---|---|---|---|---|---|
| | | | UHF/6-31G* | | |
| C3P001 | | 1327($e'$,34,1) | 1327($e'$,34,1) | 1774($a_1'$,0,50) | 6.33 |
| C3P002 | 233($\pi_u$,23,0) | 330($\pi_u$,16,0) | 1380($\sigma_g$,0,35) | 1956($\sigma_u$,543,0) | 5.57 |
| C3P003 | 145$i$ ($\pi_u$,18,0) | 145i ($\pi_u$,18,0) | 1301($\sigma_g$,0,124) | 2496($\sigma_u$,3932,0) | 5.43 |
| C3P004 | | 767($b_2$,56,19) | 891($a_1$,43,86) | 1500($a_1$,1,20) | 4.51 |
| C3P005 | | 89$i$ ($b_2$,132,91) | 1080($a_1$,29,14) | 2057($a_1$,6,470) | 4.48 |
| C3P006 | | 793($a_1$,18,302) | 1690($b_2$,1106,241) | 1893($a_1$,20,505) | 6.26 |
| | | | UHF/6-311G* | | |
| C3P003 | 163$i$ ($\pi_u$,16,0) | 163i ($\pi_u$,16,0) | 1286($\sigma_g$,0,129) | 2480($\sigma_u$,4056,0) | 5.38 |
| C3P006 | | 787($a_1$,17,499) | 1668($b_2$,1203,230) | 1868($a_1$,23,568) | 6.18 |
| | | | UHF/6-31G(2d) | | |
| C3P003 | 228$i$ ($\pi_u$,8,0) | 228i ($\pi_u$,8,0) | 1288($\sigma_g$,0,106) | 2463($\sigma_u$,3769,0) | 5.36 |
| C3P006 | | 752($a_1$,17,390) | 1695($b_2$,1147,118) | 1845($a_1$,20,506) | 6.14 |

The numbers between parentheses are the IR intensity (km/mol) and the Raman activity (Å$^4$/a.m.u.) within the double-harmonic approximation.

isomerization between the three equivalent Jahn-Teller distortions of the equilateral triangle: this situation is peculiarly akin to that in $B_3$ (cfr. the $^4B_1$ and $^4A_2$ states there), and, to a lesser extent, to the degenerate isomerization of the $^1\Sigma_g^+$ state in neutral $C_3$ (which has a $^1$E′ Jahn-Teller state) [Whi81a]. The linear $^2\Sigma_u^+$ state (C3P003), which has the same electronic configuration as the ground state of $B_2N$, lies much higher in energy at the UHF level, and is also a transition state.

It was only at a much later stage, that an additional stationary point C3P006 for the $^2B_2$ state was accidentally discovered. It lies much higher in energy than C3P004 at the UHF level; however, it is definitely much lower in energy at all levels of electron correlation, having a markedly higher correlation energy. Incidentally, C3P004 has a extremely high degree of spin contamination, which is only modest in C3P006. As the stationary point geometry of C3P004 resembles that of the quartet state C3P001, which is much lower in energy than C3P006, we believe that C3P004 is an artifact of the UHF method, caused by admixture of a lower-lying $^4A_1$ state which is essentially a distortion of C3P001. The Mulliken charge distributions [Mul55] in Figure 4.19 clarify this point: those of C3P004 are almost those of an equilateral triangle, whereas C3P006 has a significantly lowered positive charge on the apical C atom.

Similar 'false stationary points' were encountered in a PES study of $B_4$ [MarTBP], and may be encountered for other molecules. A trick for locating the 'true' state which may sometimes work is thus to find the equilibrium geometry of the contaminating state, and then restart the geometry optimization for the state to be located with a geometry significantly different from that of the contaminant, but still reasonable for the target

Figure 4.19: Mulliken charge distributions (UHF/6-31G*).

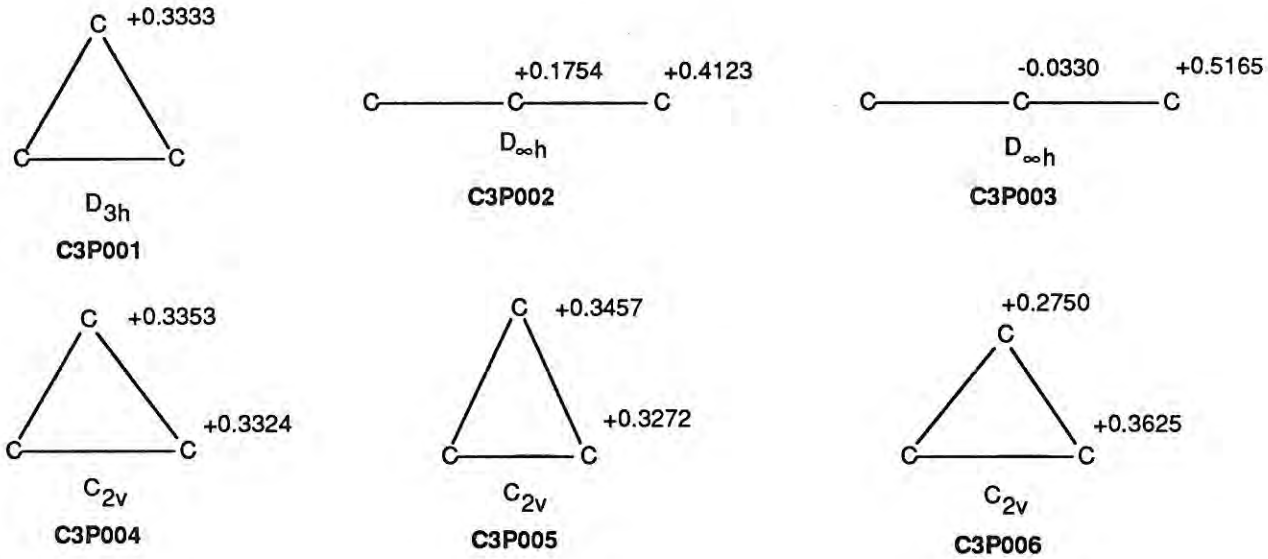


state.

The rationale behind preferring C3P006 over C3P004 is somewhat comparable to that behind the annihilated UHF method of Baker [Bak89]; an older paper by Farnell *et al.* [Far83] is also worth mentioning here. In the latter reference, an asymmetric solution with high spin contamination was invariably found to yield poor geometry predictions,for homonuclear diatomics; this problem was completely remedied by enforcing symmetry on the wavefunction, which incidentally also greatly reduced spin contamination.

At all levels of electron correlation except MP2 (where C3P003 lies lowest in energy), C3P006 is found to be the ground state.

Introduction of electron correlation favors the doublet over the quartet, as expected. Less obvious is, that the linear structure C3P003 gets favored by some 30 kcal/mol over C3P004 at the MP2 level. The sequence found here is C3P002 > C3P005 > C3P001 > C3P006 > C3P003. Except for the position of C3P003, this sequence is found at all subsequent levels of theory. At the MP3 level, C3P003 seats itself between C3P002 and C3P005. At the MP4(D) level, C3P003 is situated very close (0.17 kcal/mol) to the ground state. This phenomenon is primarily caused by heavy oscillation in the MP series for C3P003 (cfr. Table LIV). At the MP4(DQ) level then, C3P003 and C3P001 change places, whereas the introduction of fourth-order single excitations brings C3P003 close (0.28 kcal/mol) to the ground state again. It is apparent, that coupled-cluster calculations are indispensible here, because the MP series is far from converged at fourth order.

Application of Schlegel's spin projection technique has a rather profound effect. Neglecting the artifact C3P004, the ordering of structures remains unchanged. Both C3P004

and C3P005 apparently benefit greatly; for the same reason as C3P004, the latter also suffers from high spin contamination, which is however removed for the greatest part by a single spin annihilation (cfr. Table LV). The barrier height for degenerate isomerization is very strongly reduced by the spin projection.

This conclusion is confirmed when higher-order effects are included by the QCISD(T) procedure. A relatively large barrier between C3P006 and C3P003 is found at the QCISD level: the inclusion of triple excitations flattens it so much that the two structures are energetically degenerate at the QCISD(T) level. The C3P001-C3P006 separation is also significantly increased through the triple excitations (see Table LIV), which are much more important for C3P003 and C3P004/6 than they are for C3P001 (cfr. Table LIV). (Their effect on the C3P001-like ground state of $B_3$ is not that large either.) Both QCISD and QCISD(T) find C3P004 only sightly higher in energy than C3P006, about the amount one would expect from a purely geometric distortion. This attests the capability of CCSD-type methods to correct even very heavy spin contamination, as well as the very high significance of higher-order single excitation effects for spin-contaminated species [Pop88, Mar90a].

The C3P002-C3P003 pair does exhibit some analogy with the $^2\Sigma_u^+$ - $^4\Pi_u$ pair in $B_2N$ [Mar89c]. As can be seen from Figure 4.19, C3P003 has the same very polar charge distribution as $B_2N$ in its ground state. It also has an extremely intense asymmetric stretch, just as the ground state of $B_2N$. The changes in the harmonic frequencies between C3P003 and C3P002 strongly parallel those in $B_2N$ too. The bending frequency of the $^2\Sigma_u^+$ state of $B_2N$ was extremely low: here it is imaginary. The infrared intensity of the asymmetric $b_2$ stretch of C3P006 is significantly lower than that of the $\sigma_u$ stretch of C3P003, due to the much more even charge distribution. It is however still about as strong as the intense 2164 $cm^{-1}$ band of $C_5$, quite unlike C3P004, which only exhibits a relatively weak $b_2$ IR intensity.

The $\sigma_u$ HOMO of C3P003 correlates with the $b_2$ HOMO of C3P004/C3P006. Its negative orbital energy decreases markedly from C3P003 to C3P006. Note that the Koopmans electron affinity (EA) of C3P003, 11.69 eV ($\sigma_u$, leading to the $^1\Sigma_g^+$ ground state of $C_3$) is in unexpectedly good agreement with the most reliable vertical IP [Sun84] for $C_3$ of 11.46 eV. C3P006 has three low-lying virtual orbitals: 9.33 eV ($b_2$, leading to a $^1A_1$ state that will spontaneously stretch itself to the linear ground state [Whi81a]), 9.23 eV ($a_1$, leading to a $^3B_2$ state which is a distortion of the $^3A_2'$ equilateral triangle of $C_3$), and 8.62 eV ($a_1$, leading to the corresponding open-shell singlet). C3P001 has a Koopmans EA of 8.32 eV ($a_1'$, leading to the $^3A_2'$ state).

Subsequently, calculations using both the 6-311G* and 6-31G(2d) basis sets were performed. All conclusions at the 6-31G* level are confirmed. The imaginary frequency of the linear structure is even increased (cf. Table LVI), so C3P003 will certainly be a transition state at the Hartree-Fock limit. C3P006 is lower in energy than C3P003

Figure 4.20: Stationary point geometries for C3P003 and C3P006 at the UHF/6-311G*, UHF/6-31G(2*d*), and MP2/6-311G* levels. Bond distances are in Ångstrom units.

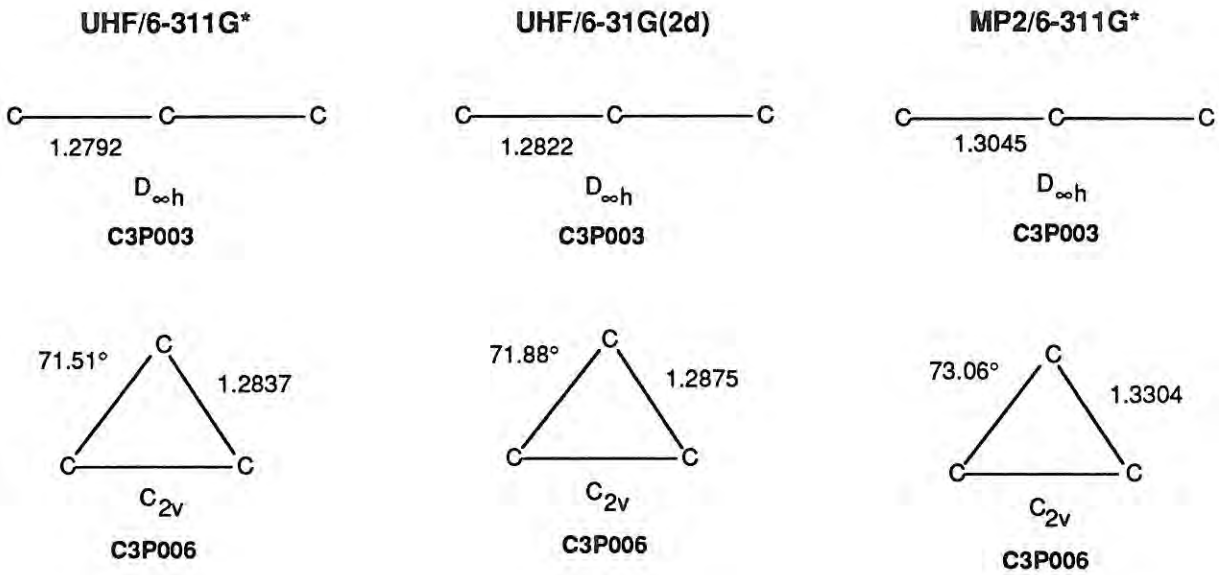


at all levels of electron correlation except MP2. However, triple excitations again have a profound effect on the barrier, leading to the conclusion that $C_3^+$ might perhaps be quasilinear: the energy difference might be so small that a few vibrational quanta suffice to obtain a linear structure. However, for a more serious estimate of the barrier, a correlated reference geometry is necessary.

As expected, the bond distances are significantly lengthened at the MP2/6-311G* level (cfr. Figure 4.20). An especially spectacular change of 0.0467 Å is seen for C3P006: that for C3P003 is more modest at 0.0264 Å. The bond angle of C3P006 is increased by 1.55°. At these reference geometries, the degree of spin contamination is rather small ($\langle S^2 \rangle$=0.785 and 0.782 for C3P003 and C3P006, respectively; for the first-order MBPT wavefunction, we found 0.760 and 0.761) , as well as being almost equal for the two species. It might then be that higher-order single excitation effects cancel between the two. This assumption was tested by running both CCD(ST) and QCISD(T) calculations from both geometries. As witnessed from Table LVII, the differences indeed cancel to some extent. This enables us to use CCD(ST) (which was available on the FPS system) for the larger basis set calculations.

One might not expect MP2/6-311G* geometries to be accurate because of the significance of higher-order effects. However, MP2/6-31G* performed quite well for geometries and harmonic frequencies of other carbon clusters [Mic87, Mar89b, Ada89]. In general, MP2/6-31G* A-B bond distances tend to be overestimated [DeF79]; enlargement of the

Table LVII: Total (hartree;minus sign omitted) and dissociation (kcal/mol) energies of $C_3$ and $C_3^+$ using large basis sets (MP2/6-311G* reference geometry unless indicated otherwise).

| Species | UHF | CCD | CCD(S) | CCD(ST) | QCISD | QCISD(T) |
|---|---|---|---|---|---|---|
| | | Total | energies | | | |
| | | | 6-311G* | | | |
| $C^+(^2P)$ | 37.29180 | 37.36110 | 37.36157 | 37.36238 | 37.36168 | 37.36248 |
| $C(^3P)$ | 37.68905 | 37.76512 | 37.76551 | 37.76659 | 37.76562 | 37.76669 |
| $C_3(^1\Sigma_g^+)$ | 113.37616 | 113.73672 | 113.74364 | 113.77084 | 113.74622 | 113.77400 |
| $C_3^+(^2\Sigma_u^+)$ | 112.90870 | 113.29011 | 113.30348 | 113.34836 | 113.30855 | 113.35266 |
| (a) | 112.91034 | NA | NA | NA | 113.30702 | 113.34960 |
| $C_3^+(^2B_2)$ | 112.94485 | 113.31376 | 113.32084 | 113.35165 | 113.32364 | 113.35446 |
| (b) | 112.95760 | 113.29147 | 113.30240 | 113.32731 | NA | NA |
| (a) | 112.95097 | NA | NA | NA | 113.32264 | 113.35088 |
| | | | 6-311+G* | | | |
| $C^+(^2P)$ | 37.29248 | 37.36196 | 37.36244 | 37.36325 | | |
| $C(^3P)$ | 37.68957 | 37.76599 | 37.76640 | 37.76753 | | |
| $C_3(^1\Sigma_g^+)$ | 113.37839 | 113.74010 | 113.74710 | 113.77453 | | |
| $C_3^+(^2\Sigma_u^+)$ | 112.91004 | 113.29180 | 113.30524 | 113.35025 | | |
| $C_3^+(^2B_2)$ | 112.94643 | 113.31561 | 113.32275 | 113.35367 | | |
| | | | 6-311G(2*df*) | | | |
| $C(^3P)$ | 37.68968 | 37.77502 | 37.77545 | 37.77738 | | |
| $C^+(^2P)$ | 37.29226 | 37.36522 | 37.36574 | 37.36686 | | |
| $C_3(^1\Sigma_g^+)$ | 113.38333 | 113.78692 | 113.79331 | 113.82449 | | |
| $C_3^+(^2\Sigma_u^+)$ | 112.91647 | 113.33191 | 113.34466 | 113.39308 | | |
| $C_3^+(^2B_2)$ | 112.95384 | 113.35600 | 113.36315 | 113.39720 | | |
| | | Dissociation | energies | | | |
| | | | 6-311G* | | | |
| $C_3(^1\Sigma_g^+)$ | 193.91 | 276.95 | 280.57 | 295.61 | 281.99 | 297.38 |
| $C_3^+(^2\Sigma_u^+)$ | 149.85 | 250.23 | 257.84 | 284.14 | 260.81 | 286.64 |
| $C_3^+(^2B_2)$ | 172.54 | 265.07 | 268.73 | 286.21 | 270.28 | 287.77 |
| | | | 6-311+G* | | | |
| $C_3(^1\Sigma_g^+)$ | 194.32 | 277.44 | 281.05 | 296.14 | | |
| $C_3^+(^2\Sigma_u^+)$ | 149.61 | 249.66 | 257.28 | 283.59 | | |
| $C_3^+(^2B_2)$ | 172.45 | 264.60 | 268.26 | 285.74 | | |
| | | | 6-311G(2*df*) | | | |
| $C_3(^1\Sigma_g^+)$ | 197.22 | 289.83 | 293.02 | 308.96 | | |
| $C_3^+(^2\Sigma_u^+)$ | 153.64 | 261.46 | 268.58 | 295.84 | | |
| $C_3^+(^2B_2)$ | 177.09 | 276.58 | 280.19 | 298.43 | | |
| | | | Combined | | | |
| Species | UHF | CCD | CCD(S) | CCD(ST) | QCISD(T)x | G1 |
| $C_3(^1\Sigma_g^+)$ | 197.64 | 290.32 | 293.51 | 309.48 | 311.26 | 322.11 |
| $C_3^+(^2\Sigma_u^+)$ | 153.40 | 260.88 | 268.02 | 295.30 | 297.80 | 305.04 |
| $C_3^+(^2B_2)$ | 177.00 | 276.11 | 279.72 | 297.96 | 299.52 | 306.76 |

QCISD(T)x denotes QCISD(T) values estimated assuming additivity of the basis set extension effects and the QCISD(T)-CCD(ST) difference.

(a) at UHF/6-311G* geometry

(b) C3P004 at the geometry of C3P006

basis set diminishes the effect [Sim88]. In cases with spin contamination, infinite-order single excitations tend to lengthen the bond distances [Mar90a]; however, for the small contamination mentioned in the previous paragraph the effect would amount to a few thousands of an Ångstrom at most. As both effects are of the same order of magnitude and work in opposite directions, some error cancellation will occur. This is just as well, since QCISD or QCISD(T) geometry optimizations were out of the question with the present computer facilities. For our main purpose, which is the evaluation of energies, the geometries will certainly be accurate enough.

The assumption was tested anyway with the 6-31G* basis set for C3P003, by computing the energy at five points 1.26(0.015)1.32. Equilibrium geometries obtained (3 decimal places maximum accuracy) were 1.306 Å at the MP2 level, 1.307 Å at the QCISD level, and 1.318 Å at the QCISD(T) level. Enlargement of the basis set will tend to shorten the computed bond distance, so the MP2/6-311G* geometry might be close to one obtained, say, at the QCISD(T)/6-311G(2*df*) level.

Faibis *et al.* [Fai87] obtained an $R_s$ distribution in their Coulomb explosion measurements, with $R_s$ being defined as

$$R_s = \frac{v_a + v_b}{v_c} \tag{4.23}$$

where $v_a$, $v_b$, and $v_c$ represent the velocities of the three fragment ions with respect to the center of mass, ordered as $v_a < v_b < v_c$. For an isosceles triangle, one finds

$$R_s = 1 + \frac{2}{\sqrt{(1 + 9\tan^2(\theta/2))}} \tag{4.24}$$

where $\theta$ represents the apex angle of the triangle. A rigid linear structure would correspond to $R_s = 1$; a rigid $D_{3h}$ structure to $R_s = 2$.The MP2/6-311G* equilibrium geometry for C3P006 leads to an $R_s$ value of 1.821, in excellent agreement with the experimental distribution [Fai87] which peaks around $R_s = 1.82$.

Attempts to compute MP2 harmonic frequencies by finite differences of the gradient failed, because of SCF convergence difficulties in the displaced geometries. As anharmonicity and rotation-vibration coupling are prone to be quite large for this molecule, we plan to perform an energy grid calculation, and subsequently an anharmonic analysis, in the near future, provided enough supercomputer time is available to us.

#### 4.10.3.2 Cyclic-linear barrier

When the basis set is enlarged from 6-31G* to 6-311G*, the cyclic isomer ( C3P006) is favored, lying 0.81 kcal/mol below the linear structure ( C3P003) at the QCISD(T)/6-311G*//HF/6-311G* level (see Table LVII). When triple excitations are neglected, the separation increases to 9.80 kcal/mol; this again illustrates the exceptional importance of triple excitations for this potential surface. As expected from the large geometry change,

the use of MP2/6-311G* reference geometries increases the separation: it is 1.13 kcal/mol at the QCISD(T) level. The separation is 2.07 kcal/mol at the CCD(ST) level; given the large difference between CCD(S) and QCISD energies, this implies that the errors cancel to a large extent between linear and cyclic states. It would be interesting to compare the results with those of a full CCSDT [Nog87] calculation, so the effect of the complete $\hat{T}_3$ *ansatz* could be assessed.

Note that the CCD(ST) result for C3P004 at the C3P006 geometry differs very significantly from that for C3P006: this is mainly due to the exceptional importance of $\hat{T}_1$ effects for heavily spin-contaminated species such as C3P004.

Addition of diffuse functions has a relatively small effect on the separation, favoring the cyclic structure by an additional 0.08 kcal/mol. (It is perhaps worth mentioning, that the polarity of the Mulliken charge distribution is reversed with respect to that in Figure 4.19; this phenomenon was not seen with any of the other basis sets.) Finally, expanding the polarization space to (2*df*) yields a barrier of 2.59 kcal/mol, which is an increase of 0.52 kcal/mol over the 6-311G* basis set. Assuming additivity of the effects of diffuse and additional polarization functions (which is quite reasonable because of their great similarity), we obtain a separation of 2.67 kcal/mol at the CCD(ST) level; correction for the QCISD(T) effects then finally yields a value of 1.73 kcal/mol.

This difference is of the same order of magnitude as our claimed accuracy for the dissociation energy. However, the *ab initio* determination of total atomization energies (TAEs) is a much more demanding problem than the prediction of energy differences between different structures of the same molecule, so the uncertainty on the barrier should be much smaller than that on the TAE. We expect that further enhancement of the basis set, as well as reoptimization of the geometry at a higher level, would result in further increases of the barrier, so the present result is best regarded as a lower bound (at least at the levels of electron correlation considered). This also implies, that at least at the levels of electron correlation involved, the qualitative conclusion that the ground state is cyclic is very unlikely to be wrong.

It should be noted that the S(CCD) ($= E_{\mathrm{CCD(S)}} - E_{\mathrm{CCD}}$) contribution sinks markedly when the polarization space is increased to (2*df*). It is not entirely unreasonable to expect S(QCISD) ($=E_{\mathrm{QCISD}} - E_{\mathrm{CCD}}$) to follow the same trend. Also, in the 6-311G* basis, the ratios between S(QCISD) and S(CCD) are comparable for the two structures: 1.379 for the linear, and 1.395 for the cyclic structure. For neutral $C_3$ (*vide infra*), a value of 1.373 is found. Now assuming that these ratios are approximately transferable across basis sets, we find extrapolated S(QCISD) contributions of 17.69 and 10.05 millihartrees, respectively, for the linear and cyclic structures, compared to the values of 17.90 and 10.00 millihartrees obtained using plain additivity. This would favor the cyclic structure by an additional 0.16 kcal/mol. Analogous considerations for the $\hat{T}_3$ effect lead to conclusions not significantly different from assuming plain additivity (the cyclic structure is

favored by an additional 0.03 kcal/mol), mainly because the differences between T(CCD) and T(QCISD) are relatively small. Our 'best theoretical estimate' for the barrier then becomes 1.92 kcal/mol.

It is very likely that the HF/6-31G* frequencies scaled by a recommended factor of 0.89 [Pop81] are in error by a substantial amount (especially the bending frequency): however, an estimate of the ZPE difference from them should normally be reliable enough to give an indication. It leads to a barrier at 0 K of 1.21 kcal/mol, or 423 $cm^{-1}$. This means that, just like triplet methylene [Bun85], the molecule will be quasilinear, since one or two quanta in the bending vibration will suffice to yield an effective linear structure. Taking the scaled HF/6-31G* bending frequency as an upper bound and assuming a rigid rotor-harmonic oscillator (RRHO) partition function, we obtain a (100)/(000) population ratio of 0.0332 at room temperature and 0.1047 at 450 K. Combining the fact that 97.68% and 89.53%, respectively, of the molecules will still reside in the (000) state, with the expectation that the 'linearized' (100) state will have an extremely low bending frequency with large amplitude motions, the experimental $R_s$ distribution is readily explained. At very high temperatures, high populations of $(nkl)$ $(n > 0)$ states will combined with the relatively low barrier towards degenerate isomerization to create an extremely floppy molecular system.

#### 4.10.3.3 Dissociation energy of neutral $C_3$

The MP2/6-311G* bond distance of neutral $C_3$ is found as 1.3030 Å, in very good agreement with the latest experimental $r_e$ value [Hin88] of 1.2968 Å. Applying the difference as a correction term, we predict $r_e$ geometries of r=1.2983 Å and ($r$=1.3242 Å, $\theta$=73.06°) for linear and cyclic $C_3^+$ , respectively. Because of small spin-contamination effects discussed above, we expect these values to be too low, rather than too high; a conservative error bar would be $\pm 0.005 \mathring{A}$.

Peculiarly enough, the difference between QCISD and CCD(S) energies is quite significant (Table LVII), unlike what is expected for a closed-shell singlet state. The cause for this is readily found in the low-lying $\pi_g$ orbitals, which are the source of similar albeit smaller effects in the $N_2$ molecule, as well as in the $a^1\Sigma_g^+$ state of SiC (Section 4.4.3) [Mar90d].

Table LVII reveals that addition of diffuse functions has a rather small effect of 0.53 kcal/mol on the $\Sigma D_e$ (at the CCD(ST) level). As expected, the contribution of additional polarization functions is rather large at 13.35 kcal/mol. An analogous correction for QCISD(T) higher order effects as discussed in the previous section leads to a $\Sigma D_e$ value of 311.06 kcal/mol. (Assuming simple additivity of the QCISD(T) correction would lead to the value of 311.26 kcal/mol listed in Table LVII.)

The G1 correction then yields a $\Sigma D_e$ of 321.93 kcal/mol, which should be accurate to $\pm$ 2 kcal/mol. As the procedure followed here actually involves much less far-reaching

Table LVIII: Ionization potentials of $C_3$ at various theoretical levels.

| hline Species | UHF | CCD | CCD(S) | CCD(ST) | QCISD | QCISD(T) |
|---|---|---|---|---|---|---|
| | | | 6-311G* | | | |
| C | 10.81 | 10.99 | 10.99 | 11.00 | 10.99 | 11.00 |
| $C_3$(vert) | 12.72 | 12.15 | 11.98 | 11.50 | 11.91 | 11.46 |
| $C_3$(adia) | 11.74 | 11.51 | 11.50 | 11.41 | 11.50 | 11.42 |
| | | | 6-311+G* | | | |
| C | 10.80 | 10.99 | 10.99 | 11.00 | | |
| $C_3$(vert) | 12.74 | 12.20 | 12.02 | 11.54 | | |
| $C_3$(adia) | 11.75 | 11.55 | 11.55 | 11.45 | | |
| | | | 6-311G(2*df*) | | | |
| C | 10.81 | 11.15 | 11.15 | 11.17 | | |
| $C_3$(vert) | 12.70 | 12.38 | 12.21 | 11.74 | | |
| $C_3$(adia) | 11.69 | 11.73 | 11.70 | 11.63 | | |
| | | | Combined | | | |
| Species | UHF | CCD | CCD(S) | CCD(ST) | QCISD(T)x | G1 |
| C | 10.81 | 11.15 | 11.15 | 11.17 | 11.17 | 11.18 |
| $C_3$(vert) | 12.73 | 12.43 | 12.25 | 11.79 | 11.76 | 11.92 |
| $C_3$(adia) | 11.70 | 11.77 | 11.75 | 11.67 | 11.68 | 11.84 |

QCISD(T)x denotes QCISD(T) values estimated assuming additivity of the basis set extension effects and the QCISD(T)-CCD(ST) difference.

assumptions about higher order effects than conventional G1 theory, the error bar is even a bit conservative. Using experimental frequencies from the JANAF tables [Jan85], an RRHO estimate for the zero-point energy results in $\Sigma D_0 = 317.08$ kcal/mol. Combined with $\Delta H^0_{f,0}(\mathrm{C(g)}) = 169.98 \pm 0.11$ kcal/mol from the same source, we obtain a $\Delta H^0_{f,0}$ value of 192.86 $\pm$ 2 kcal/mol. The JANAF enthalpy functions for C and $C_3$ finally lead to a $\Delta H^0_{f,298} - \Delta H^0_{f,0}$ difference of 2.06 kcal/mol, or a $\Delta H^0_{f,298}$ of 194.9 $\pm$ 2 kcal/mol, in excellent agreement with the experimental value of 196 $\pm$ 4 kcal/mol, but with a much smaller error margin. A previous theoretical determination of Raghavachari and Binkley [Rag87] (scaled CCD(ST)/6-31G* $\Sigma D_e$ combined with HF/6-31G* frequencies scaled by 0.89) yielded a value of 190 $\pm$ 4 kcal/mol. Admittedly our theoretical procedure required roughly twenty times as much computer time. However, $C_3$ should now be added to the list of cluster molecules for which reasonably accurate thermochemical data are available.

### 4.10.3.4 Ionization potential of $C_3$

As the geometries of linear $C_3$ and $C_3^+$ are hardly different, the energy difference between both can be taken as the first vertical IP, whereas the energy difference between linear $C_3$ and cyclic $C_3^+$ would be the first adiabatic IP. In order to assess the accuracy of the theoretical procedure, let us first consider the carbon atom.

At the CCD(ST)/6-311G* and QCISD(T)/6-311G* levels, the IP of C($^3P$) is found

to be 11.00 eV (Table LVIII), compared to a very precise experimental determination of 11.26 eV [Jan85]. Addition of diffuse functions has no significant effect, whereas expansion of the polarization space to (2*df*) leads to a value of 11.17 eV (at the CCD(ST) level). ΔSCF values fail obviously (10.81 eV); this is even more the case with Koopmans' theorem values (both IP of C($^3P$) and EA of $C^+(^2P)$).

Again at the QCISD(T)/6-311G* level, the VIP1 of $C_3$ is found to be 11.46 eV, in excellent agreement with the MRCI result of Sunil *et al.* [Sun84], obtained using a 6-31G basis set supplemented with a diffuse *p* function and a contraction of two *d* functions. $\hat{T}_1$ effects on the VIP1 amount to a rather high 0.24 eV; triple excitations are even more important, contributing 0.45 eV. Use of the CCD(ST) procedure results in an error of only 0.04 eV. Apparently, the MRCI treatment of Sunil *et al.* includes some dominant triple excitation effects through the choice of the reference space.

Addition of diffuse functions increases the VIP1 by no more than 0.04 eV; however, expansion of the polarization space increases VIP1 by no less than 0.24 eV (Table LVIII). Finally, assuming additivity of corrections, one arrives at a best direct VIP1 of 11.76 eV, which is significantly higher that the Sunil *et al.* result. A G1 correction would then finally lead to a 'best theoretical VIP1' of 11.92 ± 0.1 eV. This value is in good agreement with the older experimental result of 12.1 ± 0.3 eV [Koh70], but a bit above more recent determinations of 9.98-11.61 eV [Sun84, note added in proof] and 11.1 ± 0.5 eV [Gup79]. The adiabatic IP would be 0.08 eV lower at 11.84 ± 0.1 eV, which is in marginal agreement with these determinations (and might imply that the linear-cyclic energy difference predicted in this paper is indeed a lower bound). Raghavachari and Binkley [Rag87] found an adiabatic IP of 11.4 eV at the CCD(ST)/6-31G(2d) level: apparently, the basis set has considerable influence on the result.

As expected, Koopmans's theorem and ΔSCF values are hopelessly out of range: the former even wrongly predicted a $^2\Pi_u$ state for the cation. Oddly, the Koopmans' EA of the cation produces very good VIP values of 11.72 eV at the UHF/6-311G* level, and 11.76 eV at the UHF/6-311+G* and UHF/6-311G(2*df*) levels (11.80 eV combined). The cause for this is unclear.

### 4.10.4 Conclusions

The potential energy surface of the $C_3^+$ cation has been investigated using coupled cluster techniques and large basis sets. The results are particularly sensitive towards the level of electron correlation. Spin contamination even produces a 'false stationary point' at the UHF/6-31G* level. $C_3^+$ has a cyclic $^2B_2$ ground state with predicted geometry $r$=1.3242 Å, $\theta$ = 73.06° (MP2/6-311G*, empirically corrected bond distance). At the highest level of theory considered, the linear structure ($^2\Sigma_u^+$ state) lies about 2 kcal/mol above the ground state: this might imply quasilinearity. There is also a low barrier towards degenerate isomerization: at high temperatures, $C_3^+$ will be extremely floppy. Harmonic

frequencies (UHF/6-31G*) as well as double-harmonic IR and Raman intensities are given for various structures of $C_3^+$. Interesting analogies of $C_3^+$ with $B_3$ and $B_2N$ are pointed out. The heat of formation at 298.15 K, vertical and adiabatic ionization potentials of $C_3$ are predicted as 194.9 ± 2 kcal/mol, 11.92 ± 0.1 eV, and 11.84 ± 0.1 eV, respectively.

## 4.11 $C_3^+$ revisited: an ab initio study using multireference methods

*Important note: contrary to the remainder of Chapters 3, 4, and 5 of this work, the results and discussion presented in this section are only partially the work of the present author. The majority of the results, and a substantial part of the interpretation, are due to Dr. Peter R. Taylor of NASA Ames. The inclusion of this section does not imply a claim to intellectual property; it only serves to fulfill the need for a 'sequel to the $C_3^+$ story'.*

### 4.11.1 Introduction

Over the last few decades, carbon clusters have aroused considerable interest both theoretically and experimentally; the review by Weltner and Van Zee [Wel89] extends up to April 1989. A brief update of that review may be found in the introduction to Section 4.8 [Mar90f]; as a result of the latest development, linear carbon clusters $C_3$, $C_4$, $C_5$, $C_6$, $C_7$, and $C_9$ have so far been characterized.

The situation is less clear for the ions than for the neutral clusters. The "building block" of the ions is believed to be $C_3^+$ [Bro87], although its geometrical structure is not currently known. Older theoretical studies always assumed a linear structure (see, e.g., [Sun84]) by analogy with the neutral species.

The Coulomb explosion [Vag89] experiments of Faibis *et al.* [Fai87] at first sight appeared to indicate unambiguously that the structure was cyclic: preliminary *ab initio* calculations by Raghavachari (private communication quoted in [Fai87]) corroborated this conclusion. However, Vager and Kanter [Vag89b] remarked that the experimental intensity distribution of Faibis *et al.* could also be rationalized by assuming a linear structure with large amplitude bendings similar to those of neutral $C_3$[Hin88], combined with a fairly high Boltzmann temperature of about 450 K. It therefore seemed desirable to perform an *ab initio* study to settle the issue.

No less than three such studies were performed independently, namely by Grev *et al.* (GAS) [Gre90], Raghavachari [Rag90], and Martin *et al.* (MFG) [Mar90e], in order of appearance. GAS used various CI methods, including single, double, triple, and quadruple excitations (CISDTQ) in some cases, as well as full CI in the valence orbital space. They predicted a fairly large energy separation ($\Delta E$) of 7 ± 4 kcal/mol (positive sign favoring

the cyclic form throughout this Section) using a combination of 11/35 CISDTQ (the notation signifying 11 electrons correlated in 35 orbitals), 11/12 full CI, and 11/45 CISD, all in the Huzinaga-Dunning DZP basis set [Huz65, Dun70]. However, GAS afterwards detected input errors in their computer program and have recently published substantially revised data as an erratum [Gre90, erratum], in which they propose a barrier of $4 \pm 4$ kcal/mol. This value actually leaves open the question whether $C_3^+$ is cyclic.

Raghavachari and MFG used more or less comparable theoretical methods, namely the 6-311+G(2*df*) basis set [Fri84] and the recently proposed QCISD(T) method [Pop87], which can be viewed as a good approximation [Lee90] to CCSD(T) [Rag89], i.e., coupled cluster with all single and double substitutions and a quasiperturbative account of connected triples. For technical reasons, MFG used additivity approximations at the CCD(ST) level [Rag85] for assessing the effects of diffuse and additional polarization functions. The main difference between these two papers is the choice of reference geometry, which was determined at the QCISD(T)/6-31G* level by Raghavachari and at the MP2/6-311G* level by MFG.

Raghavachari found a barrier of 3 kcal/mol at the QCISD(T)/6-311+G(2*df*) level from QCISD(T)/6-31G* geometries, but considered his results unreliable as he found that the bending potential of the cyclic form went through a maximum around 100 degrees at the QCISD(T)/6-31G* level. He then concluded that the QCISD(T) method artificially favored the linear form and that the barrier would be larger, in agreement with the original GAS value (apparently known to Raghavachari through a preprint) of $7 \pm 4$ kcal/mol.

Unaware of the other work, MFG simply proposed a "best estimate" for the barrier of 2 kcal/mol on the basis of their calculations. Such a barrier height would indicate that the ion is on the borderline of quasilinearity.

These three papers were followed by the work of Scuseria [Scu90], who studied $C_3^+$ as a test-case for his newly developed ROHF-based CCSD(T) code [Scu90]. (The use of an ROHF reference eliminates all possible problems with spin contamination, and consequently the UHF bifurcation noted in the previous Section [Mar90e].) For basis sets similar to those of MFG and Raghavachari, CCSD(T) arrived at results similar to QCISD(T), as could be expected from the work of Lee *et al.* [Lee90]. Scuseria however also considered ANO basis sets [Alm87] up to [5*s*4*p*3*d*2*f*1*g*], and found that the $\Delta E$ increased still further, to reach a value of 6.8 kcal/mol in the largest basis set.

One significant limitation of all the results quoted so far is that they were obtained with single-reference wave functions. GAS actually performed CASSCF [Roo87] calculations of the energy separation, obtaining 2.2 kcal/mol with a TZ2P basis set, but discarded this result as supposedly being less reliable than their CI results.

The rather low energy separation at the CASSCF level — to be compared with the high $\Delta E$ found at the single-reference Hartree-Fock level (Table LIX) — suggests that

non-dynamical (near-degeneracy) correlation effects favor the linear state; on the other hand, the results by Scuseria show that basis set extension and — by implication — dynamical correlation effects favor the cyclic form. This means that, in order to predict a reliable separation, a balanced description of nondynamical and dynamical correlation effects is essential. It therefore seems imperative to investigate the separation with a multireference method.

A comparison with the coupled cluster results by MFG, Raghavachari, and Scuseria would furthermore allow an assessment of the ability of these single-reference methods to handle strong near-degeneracy effects.

We therefore decided to undertake a study of the $C_3^+$ ion using multireference methods, which is reported in the present Section. The methods considered were multireference CI (MRCI) (see [Bau90] for a review) with and without a multireference analog of the Davidson correction [Blo83], and multireference augmented coupled pair functional (MR-ACPF or just ACPF) [Gda88].

## 4.11.2 Computational methods

Two basis sets were employed throughout the present work. The first is the DZP set used by GAS, and consists of Dunning's [4$s$2$p$] contraction [Dun70] of the Huzinaga (9$s$5$p$) primitive set [Huz65], supplemented by a single six-membered $d$ function with exponent 0.75. The second basis set considered was a [5$s$3$p$2$d$1$f$] basis set constructed from Dunning's [5$s$3$p$] contraction [Dun71] of Huzinaga's (10$s$6$p$) primitive set [Huz65], supplemented by two sets of pure $d$ and one set of pure $f$ functions. The polarization exponents were optimized at the MP4(DQ) level for the C atomic ground state, and are given as: $\alpha_d = 0.549$, $\alpha_f = 0.775$. The $d$ exponent was split using the 'even scaling rule' $\alpha/2$ and $2\alpha$. In some calculations, an $f$ exponent of 0.966 was used. This has little or no consequence for the computed energy separations.

The Dunning-type basis set was considered because the commonly used 6-311G basis set [Kri80a] was recently shown by Grev and Schaefer [Gre89] to have some important deficiencies.

The CASSCF calculations all employed an active space comprising the 2$s$ and 2$p$ orbitals and electrons, that is, 11 electrons in 12 active orbitals. Such a CASSCF expansion involves on the order of 85,000 configuration state functions (CSFs), which is obviously intractable as a reference wavefunction. Therefore a selection procedure was applied to them, with reference CSFs only being included if their expansion coefficients in the CASSCF wavefunction were larger than some threshold. Selection was carried out at both the cyclic and linear geometries. CSFs at the cyclic geometry that fell below the selection threshold but are symmetry-correlated with selected CSFs in the linear form were included also, and conversely. All calculations were carried out without correlating the core electrons.

Table LIX: Total and relative energies with the [4*s*2*p*1*d*] basis set for various single-reference electron correlation models.

| Number of MOs | Method | $^2\Sigma_u^+$ hartree | $^2B_2$ hartree | $\Delta E$ kcal/mol |
|---|---|---|---|---|
| | RHF | −112.89028 | −112.92951 | 24.62 |
| 12 | CISD | −113.04280 | −113.05366 | 6.81 |
| | (a) | -113.04280 | -113.05279 | 6.27 |
| | CISD+Q | −113.06858 | −113.06823 | -0.22 |
| | (a) | -113.06858 | -113.06722 | -0.85 |
| | CISDTQ | −113.06950 | −113.06973 | 0.14 |
| | (a) | -113.07110 | -113.07037 | -0.46 |
| | full CI | −113.07219 | −113.07056 | -1.02 |
| | (a) | -113.07399 | -113.07142 | -1.61 |
| | UCISD | −113.04826 | −113.05658 | 5.22 |
| | QCISD | −113.06232 | −113.06532 | 1.88 |
| | QCISD(T) | −113.07382 | −113.06979 | -2.53 |
| 24 | CISD | −113.14591 | −113.16670 | 13.05 |
| | CISD+Q | −113.18694 | −113.19696 | 6.29 |
| | CISDTQ | −113.20289 | −113.20829 | 3.39 |
| | (a) | -113.21412 | -113.22220 | 5.07 |
| | QCISD | −113.18517 | −113.19596 | 6.77 |
| | QCISD(T) | −113.21344 | −113.21121 | -1.40 |
| 35 | CISD | −113.21383 | −113.23692 | 14.49 |
| | CISD+Q | −113.26488 | −113.27775 | 8.08 |
| | CISDTQ | −113.28696 | −113.29354 | 4.13 |
| | (a) | -113.29870 | -113.30970 | 6.90 |
| | QCISD | −113.26193 | −113.27580 | 8.70 |
| | QCISD(T) | −113.29803 | −113.29863 | 0.38 |
| 45 | CISD | −113.23245 | −113.25745 | 15.69 |
| | CISD+Q | −113.28563 | −113.30054 | 9.36 |
| | UCISD | −113.23517 | −113.25848 | 14.63 |
| | QCISD | −113.28333 | −113.29828 | 9.38 |
| | QCISD(T) | −113.32258 | −113.32397 | 0.87 |
| | MP4(SDQ) | −113.29109 | −113.29259 | 0.94 |
| | MP4(SDTQ) | −113.35983 | −113.32058 | -24.63 |
| | CISD (e) | −113.23244 | −113.25749 | 15.72 |
| | CISD+Q (e) | −113.28562 | −113.30061 | 9.41 |
| | (b) | −113.29541 | −113.30714 | 7.36 |
| | (c) | −113.30961 | −113.31599 | 4.00 |
| | (d) | −113.29042 | −113.30226 | 7.43 |

+Q denotes a Davidson correction [Lan74]
CISD, CISD+Q, CISDTQ, and full CI values are taken from the GAS erratum [Gre90, erratum] except where indicated otherwise; other values are computed in this work.
(a) Corresponding data in the original GAS publication [Gre90]. Data identical to or within roundoff of that in the erratum have been omitted.
(b) using renormalized Davidson correction [Sie78]
(c) using Davidson-Silver correction [Dav77]
(d) using Pople correction [Pop77]
(e) This work. Due to roundoff errors in geometry or basis set exponents, the energies differ by a few units in the fifth decimal place from the GAS values. Re-evaluation was necessary because the ROHF value involved in the size-consistency correction formulas had not been given in the GAS paper and had to be taken from this work.

As the molecule is bent from its linear geometry (i.e., the bond angle is decreased from 180°), the molecular point group changes from $D_{\infty h}$ to $C_{2v}$, to pass through $D_{3h}$ at a bond angle of 60° and return to $C_{2v}$ as the angle is decreased further. To ensure smoothness of the potential energy surface, it would be desirable that the MOs display full point group symmetry for all these situations. As the $^2\Sigma_u^+$ and $^2B_2$ states are symmetry-correlated, no problem arises there. But at 60°, the $^2B_2$ state becomes one component of a Jahn-Teller $^2E'$ state, the other being the $^2A_1$ state that has the lowest energy below 60°. (This same $^2A_1$ state was found as the transition state towards degenerate isomerization in the previous Section.) So in order to make the MOs display the full $D_{3h}$ symmetry at 60°, they have to be averaged over the $^2A_1$ and $^2B_2$ states [Bau88]. This however creates another problem at the linear geometry, as the $^2A_1$ state corresponds to one component of the $^2\Pi_u$ state at the linear geometry; the other component corresponds to the first excited state of $^2B_2$ symmetry at $C_{2v}$ geometries. Hence, to make the MOs display full symmetry and equivalence at all possible geometries, the MOs are obtained from a state-averaged CASSCF calculation in $C_{2v}$ symmetry, with the averaging being carried out over the 1 $^2B_2$, 2 $^2B_2$, and 1 $^2A_1$ states. Such state-averaged CASSCF wavefunctions were used for all multireference work reported here, with the exception of the CASSCF vibrational frequencies where no root averaging was carried out.

CASSCF, MRCI and ACPF energy calculations at NASA Ames were performed using the MOLECULE-SWEDEN program system [Mol90] running on the NASA Ames Central Computing Facility CRAY Y-MP/832 and NAS Facility CRAY Y-MP/8128. CASSCF vibrational frequencies were determined using the SIRIUS/ABACUS program system running on the NASA Ames Computational Chemistry Branch CONVEX C-210 and an IBM RISC 6000 model 530 workstation on loan from IBM Corporation.

The QCISD(T) calculations at the LUC were performed using GAUSSIAN 88 [Gau88] running on the IBM 3090/400e VF at the University of Leuven.

## 4.11.3 Results and discussion

### 4.11.3.1 Calibration of the $n$-particle space

Results using single-reference methods and the [4*s*2*p*1*d*] basis set are presented in Table LIX. As GAS considered the behavior of the computed $\Delta E$ as a function of the number of virtual orbitals, we have done the same at the QCISD and QCISD(T) levels. The "full CI" result is actually obtained with the same MO space as the CASSCF results discussed below, so it has limited value as a benchmark for dynamical correlation treatments.

The most striking feature of these results is the extreme variation of $\Delta E$ with the electron correlation method. Triple excitations have an especially large effect. The MP4 method breaks down completely, which illustrates the importance of higher-order effects.

The reason for this is readily seen from Table LX; the molecule does indeed exhibit exceptional multireference character. (For comparison with these figures, we note that the RHF configuration comprises less than 87% of the CISD wave functions computed by GAS.) As a further illustration, the computed CISD $\Delta E$ changes by 5.5 kcal/mol depending on which size-consistency correction formula (Davidson [Lan74], renormalized Davidson [Sie78], Davidson-Silver [Dav77], or Pople [Pop77] correction) is applied to the CISD results. As this scatter in the results is of the same order of magnitude as the quantity to be computed, the use of CISD+Q results in investigating basis set expansion and basis set additivity corrections is questionable.

When comparing the QCISD(T) and full CI results of Table LIX, it should be recalled that the former are computed from a UHF, and the latter from an RHF reference wave function. The difference between the GAS CISD results and our UHF-CISD calculation (denoted UCISD in Table LIX) can be used as an approximate correction: it suggests that the computed QCISD(T) $\Delta E$ should be raised by approximately 1.59 kcal/mol to bring it on the same scale as the RHF-based calculations, leading to an approximate "RHF-QCISD(T)" result of $-0.94$ kcal/mol. This is in excellent agreement with the 11/12 full CI value of $-1.02$ kcal/mol.

As the virtual orbital space increases in size, the CISDTQ and QCISD(T) results diverge from each other. The rather large difference of 3.75 kcal/mol with 35 MOs may be caused by the following deficiencies of QCISD(T) with respect to CISDTQ; neglect of higher-order terms in $\hat{T}_1$, neglect of diagrams involving more than one connected triply-excited intermediate state, and neglect of connected quadruple excitations. On the other hand, CISDTQ is not, in general, size-consistent, and given the very large effect of size-consistency corrections on the CISD results, and the extreme multireference character, it is not at all clear a priori that unlinked diagrams involving quintuple and higher excitations (which enter at sixth order in MBPT) can be neglected.

The QCISD(T) method in the full 45 MOs, corrected with the 12 MO QCISD(T)/full CI difference would give an estimated $\Delta E$ of 2.38 kcal/mol; the CISDTQ method in 35 MOs corrected with the 12 MO CISDTQ/full CI difference plus an estimate of the extension from 35 to 45 MOs from the Davidson-corrected CISD result yields an estimated $\Delta E$ of 4.25 kcal/mol. The difference between these estimates is still on the order of magnitude of $\Delta E$ itself.

The logical step is then to consider multireference methods. Both MRCI and averaged coupled-pair functional (ACPF) [Gda88] were considered. The latter is size consistent; to the former, a multireference analog [Blo83] of the Davidson correction was applied. (These energies are denoted MRCI+Q.) CASSCF results are also included as these allow us to distinguish between internal and external correlation effects. All results are given in Table LX.

A first set of calculations included reference occupations selected at a threshold of 0.05

Table LX: Total and relative energies with the [4*s*2*p*1*d*] basis set for various multireference electron correlation models.

| Method | $^2\Sigma_u^+$ | $^2B_2$ | $\Delta E$ | $^2\Sigma_u^+$ | $^2B_2$ |
|---|---|---|---|---|---|
| | hartree | hartree | kcal/mol | %ref | %ref |
| CASSCF | −113.16869 | −113.17101 | 1.46 | | |
| Val(0.05e) | −113.16153 | −113.16619 | 2.93 | 94.2 | 93.4 |
| Val+Q(0.05e) | −113.16778 | −113.17372 | 3.73 | | |
| Val(0.025) | −113.16650 | −113.16838 | 1.19 | 96.4 | 95.8 |
| Val+Q(0.025) | −113.16888 | −113.17174 | 1.79 | | |
| Val(0.01) | −113.16817 | −113.17027 | 1.32 | 98.6 | 98.4 |
| Val+Q(0.01) | −113.16861 | −113.17081 | 1.38 | | |
| MRCI(0.05) | −113.30085 | −113.30565 | 3.01 | 90.1 | 89.4 |
| MRCI+Q(0.05) | −113.32562 | −113.33345 | 4.91 | | |
| ACPF(0.05) | −113.32624 | −113.33596 | 6.10 | 87.0 | 83.7 |
| MRCI(0.05e) | −113.30223 | −113.30733 | 3.20 | 90.6 | 90.1 |
| MRCI+Q(0.05e) | −113.32557 | −113.33253 | 4.37 | | |
| ACPF(0.05e) | −113.32550 | −113.33305 | 4.74 | 88.3 | 87.2 |
| MRCI(0.025) | −113.31107 | −113.31346 | 1.50 | 92.2 | 91.8 |
| MRCI+Q(0.025) | −113.32750 | −113.33186 | 2.74 | | |
| ACPF(0.025) | −113.32685 | −113.33134 | 2.82 | 90.7 | 90.0 |
| MRCI(0.01) | −113.31647 | −113.31902 | 1.60 | 93.7 | 93.7 |
| MRCI+Q(0.01) | −113.32775 | −113.33043 | 1.68 | | |

+Q denotes a multireference analog [Blo83] of the Davidson correction [Lan74]
(0.05e) represents the (0.05) reference space augmented with five configurations that have coefficients above 0.05 in the ACPF(0.05) calculation (see text).
%ref is the percentage of the wave function contributed by the reference configurations

in the CASSCF wave function (merged from calculations on the cyclic and linear forms). However, in an ACPF calculation employing all single and double excitations from this reference space five additional CSFs appear with final ACPF coefficients greater than 0.05. All these CSFs are valence occupations, and so were added to the reference space. Results obtained with this expanded reference space are denoted 0.05e. An ACPF calculation based on the expanded reference space does not show any new CSFs with coefficients greater than 0.05. We should also note that at the tighter selection thresholds of 0.025 and 0.01 that were also used no problems with additional references arise.

The 0.05 threshold results for the $\Delta E$ are all rather large; comparisons with the tighter selection thresholds show several trends. First, the computed $\Delta E$ decreases on expansion of the reference space. Concomitantly, the effect of the size-consistency correction decreases, and the MRCI+Q and ACPF values approach each other. The latter two effects are readily explained by considering the weight of the reference configurations given in Table LX: MRCI(0.05) and especially ACPF(0.05) show large deviations from unity for this quantity. The weight of the reference configurations is considerably smaller

Table LXI: Total and relative energies with the $[5s3p2d1f]$ basis set.

| Method | $^2\Sigma_u^+$ hartree | $^2B_2$ hartree | $\Delta E$ kcal/mol |
|---|---|---|---|
| CASSCF | −113.19311 | −113.19818 | 3.18 |
| CASSCF[a] | −113.19406 | −113.19926 | 3.27 |
| Val(0.025) | −113.19087 | −113.19556 | 2.94 |
| Val+Q(0.025) | −113.19330 | −113.19894 | 3.54 |
| MRCI(0.025)[b] | −113.38360 | −113.38985 | 3.92 |
| MRCI+Q(0.025)[b] | −113.40633 | −113.41459 | 5.18 |
| QCISD | −113.35484 | −113.37495 | 12.62 |
| QCISD(T) | −113.40164 | −113.40709 | 3.42 |

+Q denotes a multireference analog [Blo83] of the Davidson correction [Lan74]
[a] Cartesian rather than spherical harmonic basis functions
[b] Three highest virtual orbitals were excluded from the calculation

for ACPF(0.05) than for MRCI(0.05), but this situation improves with expansion of the reference space.

MRCI calculations have also been carried out in a space of 12 MOs — these are denoted Val(0.05e), etc, since they correspond to valence space calculations. By comparison with the CASSCF results, which represent a full CI in this MO space, it can then be assessed whether the method is capable of a balanced treatment of internal correlation. While the Val(0.05e) $\Delta E$ differs significantly from the CASSCF result, the MRCI(0.025) and MRCI+Q(0.025) values bracket it. (The Val(0.025) wave function has a sum of squared reference coefficients of about 96%.)

As a final $n$-particle calibration step, an MRCI calculation at a reference selection threshold of 0.01 has been performed. The resulting MRCI wave function comprises more than 3.3 million CSFs. (As the ACPF(0.025) calculation converged rather slowly, an ACPF(0.01) calculation was not attempted since it would have severely strained our computing resources.) The MRCI(0.01) results further reduce $\Delta E$ to 1.68 kcal/mol (1.60 kcal/mol without the Davidson correction). The difference between the various size-consistency correction formulas becomes on the order of 0.01 kcal/mol, and is thus negligible. The Val(0.01) results, both for the total energies and the $\Delta E$, nearly coincide with the CASSCF values, verifying that the treatment of internal correlation is effectively complete. Table LX shows that the reference configurations comprise about 98.5% of the Val(0.01) wave function and about 93.5% of MRCI(0.01).

Most strikingly, the final MRCI+Q(0.01) $\Delta E$ is very close to the CASSCF result. Hence in this basis set the differential effect (between the two structures) of external correlation is essentially negligible. Of all the single-reference methods in Table LIX, QCISD(T) is closest to the MRCI+Q(0.01) $\Delta E$, whereas CISDTQ appears to seriously

overshoot. This again attests to the ability of single-reference coupled-cluster methods to overcome near-degeneracy problems. The QCISD(T) total energies, however, differ from the MRCI+Q(0.01) energies by amounts similar in magnitude to $\Delta E$, so some error compensation is certainly involved. Given its very substantial multireference character, $C_3^+$ should be valuable as a test system for electron correlation methods (see [Scu90], for example). Our MRCI+Q(0.01) energies should be useful as a benchmark for this purpose.

#### 4.11.3.2 One-particle basis set calibration

Carrying out an MRCI(0.01) calculation in the $[5s3p2d1f]$ basis is considerably beyond our current resources: the wave function would involve well over twenty million CSFs. We have performed calculations at three levels, QCISD(T), CASSCF, and MRCI(0.025) (these calculations employed an $f$ exponent of 0.966). The MRCI(0.025) calculation is at the limit of our computational capabilities, even with the three highest virtual orbitals excluded from the correlation treatment and only the pure spherical harmonic components of the basis functions retained. The final MRCI wave functions comprise almost six million CSFs.

Results are given in Table LXI. Val(0.025) calculations have also been performed, in order to assess the quality of the internal correlation treatment. Once again, the MRCI(0.025) and MRCI+Q(0.025) values bracket the CASSCF $\Delta E$. To assess the effect on internal correlation of using Cartesian Gaussians instead of spherical harmonics, a CASSCF result using the former is also reported. The CASSCF total energies are lowered by about 1 millihartree, and the $\Delta E$ is increased by less than 0.1 kcal/mol.

It is apparent from a comparison of Tables LX and LXI that expansion of the basis set favors the cyclic form, as expected from the single-reference results. The scatter in the $\Delta E$ values of Table LX (excluding QCISD) is about 2 kcal/mol, with Val(0.025) producing the lowest and the MRCI+Q(0.025) the highest result. If we assume that the difference between the MRCI+Q(0.01) and MRCI+Q(0.025) results in the DZP basis is transferable to the larger basis (this is certainly preferable to making no correction for the effect of the selection threshold) we obtain an estimated $\Delta E$ of 4.12 kcal/mol, while the same approach applied to the MRCI(0.025) result gives 4.10 kcal/mol. Finally, if we correct the larger basis QCISD(T) result by the difference between the QCISD(T)/DZP and MRCI+Q(0.01)/DZP values we obtain an estimated $\Delta E$ of 4.23 kcal/mol. Part of the very small difference with the MRCI results may even be caused by the inclusion of the three highest virtuals (that were deleted in the MRCI calculations).

Comparison of Tables LIX, LX, and LXI gives a direct measurement of the effect of expanding the one-particle basis for given correlation treatments. At the CASSCF, Val(0.025), or Val+Q(0.025) level, $\Delta E$ increases by 1.7 kcal/mol on going from the $[4s2p1d]$ to the $[5s3p2d1f]$ basis. At the MRCI+Q(0.025) or QCISD(T) level, the in-

Table LXII: Variation of QCISD(T)/6-31G* results (hartree, kcal/mol) with choice of reference geometry (Å, degrees).

| Level of theory for | $^2\Sigma_u^+$ | | $^2B_2$ | | | |
|---|---|---|---|---|---|---|
| reference geometry | $r_e$ | E | $r_e$ | $\theta$ | E | $\Delta E$ |
| UHF/6-31G* [Mar90e, Rag90] | 1.282 | −113.32364 | 1.283 | 71.3 | −113.32359 | -0.03 |
| CISD/TZ2P [Gre90] | 1.283 | −113.32376 | 1.296 | 71.0 | −113.32569 | 1.21 |
| MP2/6-311G* [Mar90e] | 1.305 | −113.32620 | 1.330 | 73.1 | −113.32630 | 0.06 |
| QCISD(T)/6-31G* [Rag90] | 1.318 | −113.32658 | 1.333 | 67.0 | −113.32832 | 1.09 |

crease is 2.5 kcal/mol (the increase is almost the same at the MRCI(0.025) level). This implies that the basis set effect on *dynamical* correlation here is only 0.8 kcal/mol. Using the approach outlined above to correct for $n$-particle space improvements, we expect that the MRCI(0.01) or MRCI+Q(0.01) result in the $[5s3p2d1f]$ basis set would be about 4.2 kcal/mol. This could still be an overestimate of the full CI result in the $[5s3p2d1f]$ basis, since 1 kcal/mol may be an underestimate of the effects of $n$-particle space truncation. The major remaining source of error, however, is undoubtedly the one-particle basis set.

Given that non-dynamical correlation is apparently more important than dynamical correlation in determining $\Delta E$, the basis set effects computed by Scuseria [Scu90] may be something of an overestimate, but they should certainly supply a good guide to the maximum probable $\Delta E$. At the CCSD(T) level, he finds $\Delta E$=4.54 kcal/mol with a $[5s3p2d1f]$ basis set, and 6.81 kcal/mol with a $[5s4p3d2f1g]$ basis set; this is an increase of 2.27 kcal/mol. Erring on the safe side, we set an approximate upper bound of 2.6 kcal/mol to the effect of further basis set saturation. Even if neglected correlation effects (i.e., beyond MRCI+Q(0.025)) have been underestimated above, it seems very improbable that $\Delta E$ could be smaller than 4.2 kcal/mol, and it could be as large as 6.8 kcal/mol. Our best estimate, given our computed numbers, is thus 5.5±1.3 kcal/mol.

Our best estimate is 2.5 kcal/mol higher than the QCISD(T)/6-311+G(2$df$) value computed by Raghavachari, and 3.5 kcal/mol higher than the best estimate of MFG. The $n$-particle calibration accounts for much of the difference with the Raghavachari value, and most of the remainder will be due to basis set differences; there may be some effect from different choices of reference geometry, as illustrated by Table LXII, where QCISD(T)/6-31G* values are tabulated for various reference geometries. The fairly large effect on $\Delta E$ of using MP2/6-311G* reference geometries is explained by the fact that although the bond length is close to the QCISD(T)/6-31G* optimum value, the bond angle differs by about 6 degrees. There is some compensation of errors in bond length and angle in the CISD/TZ2P geometry, leading to a predicted $\Delta E$ that is in close agreement with the value at the QCISD(T)/6-31G* optimum geometry. It is also worth noting that

Table LXIII: CASSCF geometries (Å, degrees), harmonic frequencies ($cm^{-1}$), and zero-point energies (ZPE, kcal/mol) for $C_3^+$.

| State | E(hartree) | $r_1$ | $r_2$ | $\theta$ | Harmonic frequencies | | | ZPE |
|---|---|---|---|---|---|---|---|---|
| | | | | [4s2p1d] basis set | | | | |
| $^2B_2$ | −113.17879 | 1.350 | 1.350 | 66.4 | $742(a_1)$ | $945(b_2)$ | 1610 $(a_1)$ | 4.71 |
| $^2\Sigma_u^+$ | −113.17664 | 1.330 | 1.330 | 180.0 | $46.5i(\pi_u)$ | $2852i(\sigma_u)$ | 1146 $(\sigma_g)$ | 1.64 |
| $^2\Sigma^+$ | −113.17850 | 1.283 | 1.373 | 180.0 | $112(\pi)$ | $1766(\sigma)$ | 1136 $(\sigma)$ | 4.47 |
| | | | | [5s3p2d1f] basis set | | | | |
| $^2B_2$ | −113.20483 | 1.331 | 1.331 | 66.6 | $760(a_1)$ | $980(b_2)$ | 1612 $(a_1)$ | 4.79 |
| $^2\Sigma_u^+$ | −113.19953 | 1.314 | 1.314 | 180.0 | $107i(\pi_u)$ | $5114i(\sigma_u)$ | $1154(\sigma_g)$ | 1.65 |

the QCISD(T)/6-31G* geometry reported by Raghavachari is in close agreement with the CASSCF/TZ2P geometry reported by GAS.

Finally, our estimate is smaller than Scuseria's best computed value [Scu90], although our uncertainty essentially encompasses it. Our [4s2p1d] MRCI(0.01) result is over 1 kcal/mol smaller than his DZP CCSD(T) result [Scu90], and it seems very likely that the CCSD(T) method overestimates $\Delta E$ by at least this amount, although part of the difference may be due to the use of different reference geometries. It is interesting to note in passing that while this seems to be a case where CCSD(T) and QCISD(T) disagree, since $\Delta E$ from the two methods differs by 2 kcal/mol, this probably reflects mainly the fact that the QCISD(T) treatment is UHF-based, while the CCSD(T) is RHF-based. Making the RHF/UHF correction referred to in Section 4.11.3.1 halves the difference.

#### 4.11.3.3 Is linear $C_3^+$ a local minimum or a transition state?

Raghavachari observed that, when the bond distance was kept fixed at 1.32 Å and the bond angle was varied, the QCISD(T)/6-31G* energy went through a maximum at about 100 degrees. More specifically, the energy at 100 degrees was 4.98 kcal/mol above that at 70 degrees (corresponding to the cyclic structure), and 4.24 kcal/mol above the linear structure. Raghavachari expected the barrier to increase upon enlargement of the basis set, and saw this as indicating that the QCISD(T) treatment was of dubious quality for this molecule. (It should be remembered, however, that this conclusion was based on the erroneous GAS results.)

Given the apparently good performance of the QCISD(T) method, compared to MRCI, for $C_3^+$ , we are no longer convinced that Raghavachari's doubts were justified. Three explanations can be advanced to explain the double minimum: (a) it is a basis set artifact; (b) it is a correlation method artifact; (c) it is an actual physical feature of the potential surface. Possibility (b) seems remote, in view of our calibration studies above; in order to eliminate (a), we have performed a single QCISD(T)/[5s3p2d1f] calculation

at $r$=1.290 Å, $\theta$=100.0 degrees. The computed energies are: QCISD −113.36132 hartree, QCISD(T) −113.39867 hartree. So there is indeed a double minimum at the QCISD(T) level not seen at the QCISD level, and thus coming from the triple excitations. The energy is 5.29 kcal/mol above that of the cyclic form, but only 1.87 kcal/mol above the linear form. This corresponds to a linear isomer with a large-amplitude very low bending frequency. It is possible that further improvement of basis set and electron correlation treatment would remove the hump, but the actual potential surface may well exhibit a double minimum.

We have also performed CASSCF geometry optimization and harmonic frequency calculation in both the [4$s$2$p$1$d$] and [5$s$3$p$2$d$1$f$] basis sets, the results of which are summarized in Table LXIII. We note that the use of our optimized CASSCF geometries instead of the GAS CISD structures would have lowered our computed CASSCF $\Delta E$ above by 0.11 kcal/mol. The linear structure exhibits symmetry breaking, which is probably an artifact but does occur in both basis sets. Symmetry breaking of the linear structure was also noted by GAS at the CISD/TZ2P level and by Raghavachari at the QCISD(T)/6-31G* level. We have located the broken-symmetry solution in the [4$s$2$p$1$d$] basis: a $^2\Sigma^+$ state with all frequencies real. Its bending frequency is very low (112 cm$^{-1}$). Estimating the zero-point energies from these latter frequencies and those for the cyclic form, we find that they will shift the $\Delta E$ by −0.24 kcal/mol, i.e., favoring the linear form. However, there is considerable uncertainty in this zero-point correction given the symmetry breaking for the linear structure. The basis set effect on the CASSCF frequencies is rather small for the cyclic structure, with the largest change being a 35 cm$^{-1}$ increase in the asymmetric stretch. The one real frequency of the symmetric linear structure is also only slightly increased by expanding the basis set. If we assume that all frequencies of the symmetry-broken linear form would be increased proportionally by this factor, we would obtain an estimated [5$s$3$p$2$d$1$f$] zero-point correction of −0.29 kcal/mol, but again this result should be viewed with some scepticism. Elementary reasoning suggests that zero-point vibration will favor the linear form, of course, but it is difficult to say by how much with only the results given here.

The $B_2$ vibration of the cyclic form has a large IR intensity [Mar90e], and could thus in principle be detected experimentally. Our CASSCF/[5$s$3$p$2$d$1$f$] value of 980 cm$^{-1}$ for the harmonic frequency may aid experimentalists in identifying it. This value should normally be a lower bound, as only internal correlation is included, with the QCISD(T)/6-31G* value of 1194 cm$^{-1}$ found by Raghavachari serving as an upper bound. The cause of the discrepancy between the GAS CASSCF/TZ2P value of 1124 cm$^{-1}$ and our present results is not clear.

As an additional aid to experimentalists, we have computed the isotopic substitution shifts for the $B_2$ vibration from the CASSCF/[5$s$3$p$2$d$1$f$] force constant matrix. They are (the middle atom corresponding to the apical one): $\Delta(13-12-12) = -12.2$,

$\Delta(12-13-12) = -14.3$, $\Delta(13-12-13) = -23.9$, and finally $\Delta(13-13-12) = -26.7$ $cm^{-1}$. As shown in [Mar90f] for carbon clusters, such ab initio isotope shifts are normally in excellent agreement with the experimental ones if they are scaled by the ratio between the computed and observed frequency, and are thus quite useful in confirming or rejecting an assignment.

One practical implication of the double minimum in the bending coordinate being an actual potential surface feature would be that quasilinear behavior of the $^2B_2$ state can be completely ruled out at the temperatures involved in the Coulomb explosion experiments [Fai87] (about 450 K). Hence the ambiguity pointed out by Vager and Kanter [Vag89b] can be resolved in favor of an unambiguous interpretation as a cyclic $^2B_2$ state. Actually, as the $^2A_1$ transition state (the other Jahn-Teller component of the equilateral triangular structure) was found by all three previous theoretical studies, GAS, MFG and Raghavachari, to be lower in energy than the barrier towards the linear state, the effective structure would become $^2E'$ before the molecule starts exhibiting quasilinear behavior, as the temperature is increased. At high temperatures, the two effects will combine to make $C_3^+$ into one of the most fluxional covalent molecular systems known.

## 4.11.4 Conclusions

We have definitively shown that the ground state of $C_3^+$ is a cyclic $^2B_2$ state. The linear $^2\Sigma_u^+$ structure lies 5.5±1.3 kcal/mol higher in energy, and is probably not a transition state but a local minimum. The computed isomerization energy is exceptionally sensitive to the electron correlation treatment, particularly to accounting for connected triple excitations in single-reference-based treatments. From our multireference studies, it appears that non-dynamical correlation effects are more important than dynamical correlation effects in determining $\Delta E$. We have confirmed that the wave functions for both the cyclic and linear structures show extreme multireference character. Of all the single-reference treatments considered, CCSD(T) and QCISD(T) appear to agree best with our multireference results. The MRCI+Q(0.01)/[4*s*2*p*1*d*] $\Delta E$ value, which should be very close to the full CI limit in this basis set, is 1.68 kcal/mol; this result may provide a useful benchmark for other electron correlation treatments.

# References


[Ada88] L. Adamowicz, personal communication quoted in [Bra88].

[Ada89] L. Adamowicz and J. Kurtz, *Chem. Phys. Lett.* **162**, 342 (1989).

[Alg89] M. Algranati, H. Feldman, D. Kella, E. Malkin, E. Miklazky, R. Naaman, Z. Vager, and J. Zajfman, *J. Chem. Phys.* **90**, 4617 (1989).

[Alm87] J. Almlöf and P. R. Taylor, *J. Chem. Phys.* **86**, 4070 (1987).

[And90] W. Andreoni, D. Scharf, and P. Giannozzi, *Chem. Phys. Lett.* **173**, 449 (1990).

[Ang83] J. Anglada, P. J. Bruna, S. D. Peyerimhoff, and R. J. Buenker, *J. Phys. B* **16**, 2469 (1983).

[Bac81] G. B. Bacskay, *Chem. Phys.* **61**, 385 (1981).

[Bak86] J. Baker, R. H. Nobes, and L. Radom, *J. Comp. Chem.* 7, 349 (1986).

[Bak89] J. Baker, J. Chem. Phys. **91**, 1789 (1989); Chem. Phys. Lett. **152**, 227 (1988).

[Bar72] R. H. Bartels, University of Texas Center for Numerical Analysis, Report CNA-44 (1972).

[Bar81] R. J. Bartlett, *Ann. Rev. Phys. Chem.* **32**, 359 (1981).

[Bar89] R. J. Bartlett, *J. Phys. Chem.* **93**, 1697 (1989).

[Bau87] C. W. Bauschlicher Jr. and S. R. Langhoff, *J. Chem. Phys.* **87**, 2919 (1987).

[Bau88] C. W. Bauschlicher and P. R. Taylor, *Theoret. Chim. Acta* **74**, 63 (1988).

[Bau90] C. W. Bauschlicher, Jr., S. R. Langhoff, and P. R. Taylor, *Adv. Chem. Phys.* **77**, 103 (1990).

[Bec86] S. Becker and H. J. Dietze, *Int. J. Mass Spectr. Ion Proc.* **73**, 157 (1986).

[Ber86] J. Bernholc and J. C. Phillips, *Phys. Rev.* **B 33**, 7395 (1986); *J. Chem. Phys.* **85**, 3258 (1986).

[Ber88a] P. F. Bernath, S. A. Rogers, L. C. O'Brien, C. R. Brazier, and A. D. McLean, *Phys. Rev. Lett.* **60**, 197 (1988).

[Ber88b] D. E. Bernholdt, D. H. Magers, and R. J. Bartlett, *J. Chem. Phys.* **89**, 3612 (1988).

[Ber89] P. F. Bernath, K. H. Hinkle, and J. J. Keady, *Science* **244**, 562 (1989) and references therein.

[Bha88] K. Bhanuprakash and R. J. Buenker, *Chem. Phys. Lett.* **152**, 215(1988).

[Bie85] W. Bieger, G. Seifert, H. Eschrig, and G. Grossmann, *Z. Phys. Chem. (Leipzig)* **266**, 751 (1985); G. Seifert, H. Eschrig, W. Bieger, *Z. Phys. Chem. (Leipzig)* **267**, 529 (1986).

[Bin75a] R. C. Bingham, M. J. S. Dewar, and D. H. Lo, *J. Am. Chem. Soc.* **97**, 1285 (1975).

[Bin75b] J. S. Binkley and J. A. Pople, *Int. J. Quantum Chem.* **9**, 229 (1975).

[Bin80] J. S. Binkley, J. A. Pople, and W. J. Hehre, *J. Am. Chem. Soc.* **102**, 939 (1980).

[Bin83] J. S. Binkley and M. J. Frisch, *Int. J. Quantum Chem. Symp.* **17**, 337 (1983).

[Blo83] M. R. A. Blomberg and P. E. M. Siegbahn, *J. Chem. Phys.* **78**, 5682 (1983).

[Bot89] P. Botschwina and P. Sebald, *Chem. Phys. Lett.* **160**, 485 (1989).

[Boy70] S. F. Boys and F. Bernardi, *Mol. Phys.* **19**, 553 (1970).

[Bra88] C. R. Brazier, P. F. Bernath, J. B. Burkholder, and C. J. Howard, *J. Chem. Phys.* **89**, 1762 (1988).

[Bre84] H. Bredohl, I. Dubois, Y. Houbrechts, and P. Nzohabonayo, *J. Phys. B* **17**, 95 (1984).

[Bre85] H. Bredohl, I. Dubois, Y. Houbrechts, and P. Nzohabonayo, *J. Mol. Spectr.* **112**, 430 (1985).

[Bro87] W. L. Brown, R. R. Freeman, K. Raghavachari, and M. Schlüter, *Science* **235**, 860 (1987).

[Bru80] P. J. Bruna, S. D. Peyerimhoff, and R. J. Buenker, *J. Chem. Phys.* **72**, 5437 (1980).

[Bru81] P. J. Bruna, C. Petrongolo, R. J. Buenker, and S. D. Peyerimhoff, *J. Chem. Phys.* **74**, 4611 (1981).

[Bru89] P. J. Bruna and J. S. Wright, *J. Chem. Phys.* **91**, 1126 (1989).

[Bue74] R. J. Buenker, S. D. Peyerimhoff, and W. Butscher, *Mol. Phys.* **35**, 771 (1978). R. J. Buenker and S. D. Peyerimhoff, *Theor. Chim. Acta* **35**, 33 (1974). R. J. Buenker and S. D. Peyerimhoff, *Theor. Chim. Acta* **39**, 217 (1975).

[Bun85] P. R. Bunker, in *Comparison of ab initio quantum chemistry with experiment for small molecules* (ed. R. J. Bartlett), D. Reidel, Dordrecht, Boston, 1985, p.141.

[Car85] R. Car and M. Parinello, *Phys. Rev. Lett.* **55**, 2471 (1985).

[Car89] I. Carmichael, *J. Chem. Phys.* **91**, 1072 (1989).

[Cha75] M. W. Chase, J. L. Curnutt, A. T. Hu, H. Prophet, A. N. Syverud, and L. C. Walker, *J. Phys. Chem. Ref. Data* **4**, 1 (1975).

[Cha82] K. W. Chang and W. R. M. Graham, *J. Chem. Phys.* **77**, 4300 (1982).

[Cha86] C. F. Chabalowski, R. J. Buenker, and S. D. Peyerimhoff, *J. Chem. Phys.* **84**, 268 (1986).

[Cla70] T. C. Clark and M. A. A. Clyne, *Trans. Faraday Soc.* **66**, 877 (1970).

[Cla83] T. Clark, J. Chandrasekar, G. W. Spitznagel, and P. von Ragué Schleyer, *J. Comp. Chem.* **4**, 294 (1983).

[Cla85] T. Clark, *A Handbook of Computational Chemistry* (J. Wiley, New York, 1985).

[Cla88] D. A. Clabo Jr., W. D. Allen, R. B. Remington, Y. Yamaguchi, and H. F. Schaefer III, *Chem. Phys.* **123**, 187 (1988) and references therein.

[Col76] J. B. Collins, P. von Ragué Schleyer, J. S. Binkley, and J. A. Pople, *J. Chem. Phys.* **64**, 5142 (1976): appendix.

[Coo83] D. L. Cooper, *Astrophys. J.* **265**, 808 (1983).

[Crc84] *Handbook of Chemistry and Physics*, 64th edition (CRC Press, Boca Raton, Florida, 1984).

[Dav77] E. R. Davidson and D. W. Silver, *Chem. Phys. Lett.* **52**, 403 (1977).

[DeF79] D. J. DeFrees, B. A. Levi, S. K. Pollack, W. J. Hehre, J. S. Binkley, and J. A. Pople, *J. Am. Chem. Soc.* **101**, 4086 (1979); *erratum* **102**, 2513 (1980).

[Dew61] M. J. S. Dewar and N. L. Hojvat, *J. Chem. Phys.* **34**, 1232 (1961).

[Dew70] M. J. S. Dewar and E. Haselbach, *J. Am. Chem. Soc.* **92**, 590 (1970).

[Dew77a] M. J. S. Dewar and W. Thiel, *J. Am. Chem. Soc.* **99**, 4899 (1977).

[Dew77b] M. J. S. Dewar and W. Thiel, *Theor. Chim. Acta* **46**, 89 (1977).

[Dew85] M. J. S. Dewar, E. G. Zoebisch, E. F. Healy, and J. J. P. Stewart, *J. Am. Chem. Soc.* **107**, 3902 (1985).

[Die85] H. J. Dietze and S. Becker, *Fresenius Z. Anal. Chem.* **321**, 490 (1985).

[Dou40] A. E. Douglas and G. Herzberg, *Can. J. Res. A* **18**, 179 (1940).

[Dou65] A. E. Douglas and W. J. Jones, *Can. J. Phys.* **43**, 2116 (1965); M. Polak, M. Gruebele, and R. J. Saykally, *J. Am. Chem. Soc.* **109**, 2884 (1987).

[Dro59] J. Drowart, R. P. Burns, G. DeMaria, and M. G. Inghram, *J. Chem. Phys.* **31**, 1131 (1959).

[DucPC] G. Ducarroir, personal communication.

[Dun32] J. L. Dunham, *Phys. Rev.* **41**, 721 (1932); A. C. Hurley, *Introduction to the electron theory of small molecules* (Academic Press, London, 1976).

[Dun70] T. H. Dunning Jr., *J. Chem. Phys.* **53**, 2823 (1970).

[Dun71] T. H. Dunning Jr., *J. Chem. Phys.* **55**, 716 (1971).

[Dun89] T. H. Dunning Jr., *J. Chem. Phys.* **90**, 1007 (1989).

[Dup78] M. Dupuis and B. Liu, *J. Chem. Phys.* **68**, 2902 (1978).

[Dyk82] J. M. Dyke, N. B. H. Jonathan, A. E. Lewis, and A. Morris, *Mol. Phys.* **47**, 1231 (1982).

[Ewi87] D. W. Ewing and G. Pfeiffer, *Chem. Phys. Lett.* **134**, 413 (1987).

[Fai87] A. Faibis, E. P. Kanter, L. M. Tack, E. Bakke, and B. J. Zabransky, *J. Phys. Chem.* **91**, 6445 (1987).

[Far83] L. A. Farnell, J. A. Pople, and L. Radom, *J. Phys. Chem.* **87**, 79 (1983).

[Fla77] M. C. Flanigan, A. Komornicki, and J. W. McIver, Jr., "Ground State Potential Energy Surfaces and Thermochemistry", in *Modern Theoretical Chemistry vol. 8* (ed. G. A. Segal, Plenum Press, New York, London, 1977), p.1.

[Fle63] R. Fletcher and M. J. D. Powell, *Computer Journal* **6**, 163 (1963).

[Fri84] M. J. Frisch, J. A. Pople, and J. S. Binkley, *J. Chem. Phys.* **80**, 3265 (1984).

[Gau63] L. Gausset, G. Herzberg, A. Lagerqvist, and B. Rosen, *Disc. Faraday Soc.* **35**, 113 (1963).

[Gau65] L. Gausset, G. Herzberg, A. Lagerqvist, and B. Rosen, *Astrophys. J.* **142**, 45 (1965).

[Gau86] M. J. Frisch, J. S. Binkley, H. B. Schlegel, K. Raghavachari, C. F. Melius, R. L. Martin, J. J. P. Stewart, F. W. Bobrowicz, C. M. Rohlfing, L. R. Kahn, D. J. DeFrees, R. Seeger, R. A. Whiteside, D. J. Fox, E. M. Fluder, and J. A. Pople, GAUSSIAN 86 release C, Carnegie-Mellon University, Pittsburgh, PA, 1987.

[Gau88] M. J. Frisch, M. Head-Gordon, H. B. Schlegel, K. Raghavachari, J. S. Binkley, C. Gonzalez, D. J. DeFrees, D. J. Fox, R. A. Whiteside, R. Seeger, C. F. Melius, J. Baker, R. L. Martin, L. R. Kahn, J. J. P. Stewart, E. M. Fluder, S. Topiol, and J. A. Pople, GAUSSIAN 88 release C, Gaussian, Inc., Pittsburgh, PA, 1989.

[Gaw86] J. F. Gaw and N. C. Handy, *Chem. Phys. Lett.* **128**, 182 (1986).

[Gay53] A. G. Gaydon, *Dissociation energies*, 2nd ed., Chapman & Hall Ltd., London, 1953.

[Gda88] R. J. Gdanitz and R. Ahlrichs, *Chem. Phys. Lett.* **143**, 413 (1988).

[Gme88] *Gmelins Handbook of Inorganic Chemistry*, 8th Edition, Boron compounds, 3rd supplement, Volume 3, (Springer Verlag, Berlin, 1988).

[Gre89] R. S. Grev and H. F. Schaefer III, *J. Chem. Phys.* **91**, 7305 (1989).

[Gre90] R. S. Grev, I. L. Alberts, and H. F. Schaefer III, *J. Phys. Chem.* **94**, 3379 (1990); *erratum* **94**, 8744 (1990).

[Guo89] H. Guo and M. Karplus, *J. Chem. Phys.* **91**, 1719 (1989).

[Gup79] S. K. Gupta and K. A. Gingerich, *J. Chem. Phys.* **71**, 3072 (1979).

[Han74] C. F. Hansen, B. J. Henderson, and W. E. Pearson, *J. Chem. Phys.* **60**, 754(1974).

[Han84] N. C. Handy and H. F. Schaefer III, *J. Chem. Phys.* **81**, 5031 (1984); N. C. Handy, R. D. Amos, J. F. Gaw, J. E. Rice, and E. D. Simandiras, *Chem. Phys. Lett.* **120**, 151 (1985); E. D. Simandiras, N. C. Handy, and R. D. Amos, *Chem. Phys. Lett.* **133**, 324 (1987).

[Han85] N. C. Handy, P. J. Knowles, and K. Somasundram, *Theor. Chim. Acta* **68**, 87 (1985).

[Har72] P. C. Hariharan and J. A. Pople, *Chem. Phys. Lett.* **16**, 217 (1972); see also: R. A. Whiteside, R. Krishnan, M. J. Frisch, J. A. Pople, Paul von Ragué Schleyer, *Chem. Phys. Lett.* **80**, 547 (1981) for the effect on $C_3$.

[Hea89] J. R. Heath, A. L. Cooksy, M. H. W. Gruebele, C. A. Schmuttenmaer, and R. J. Saykally, *Science* **244**, 564 (1989).

[Hea90a] J. R. Heath, R. A. Sheeks, A. L. Cooksy, and R. J. Saykally, *Science* **249**, 895 (1990).

[Hea90b] J. R. Heath and R. J. Saykally, *J. Chem. Phys.* **93**, 8392 (1990).

[Hea91a] J. R. Heath and R. J. Saykally, *J. Chem. Phys.* **94**, xxxx (1990).

[Hea91b] J. R. Heath and R. J. Saykally, *J. Chem. Phys.* **94**, yyyy (1990).

[HeaTBP] J. R. Heath and R. J. Saykally, to be published.

[Heh72] W. J. Hehre, R. Ditchfield, and J. A. Pople, *J. Chem. Phys.* **56**, 2257 (1972). P. C. Hariharan and J. A. Pople, *Chem. Phys. Lett.* **16**, 217 (1972). P. C. Hariharan and J. A. Pople, *Theor. Chim. Acta* **28**, 213 (1973).

[Her45] G. Herzberg, *Infrared and raman spectra* (Van Nostrand Reinhold, New York, 1945), p. 521 ff.

[Her50] G. Herzberg, *Spectra of diatomic molecules* (Van Nostrand Reinhold, New York, 1950).

[Hes86] B. A. Hess Jr., L. J. Schaad, P. Čársky, and R. Zahradník, *Chem. Rev.* **86**, 709 (1986).

[Hil60] See e. g. T. L. Hill, *Introduction to Statistical Thermodynamics*, (Addison-Wesley, Reading, MA, 1960).

[Hin88] K. W. Hinkle, J. J. Keady, and P. F. Bernath, *Science* **241**, 1319 (1988).

[Hof66] R. Hoffmann, *Tetrahedron* **22**, 521 (1966).

[Hou82] R. F. Hout, Jr., B. A. Levi, and W. J. Hehre, *J. Comp. Chem.* **3**, 234 (1982).

[Hub79] K. P. Huber and G. Herzberg, *Constants of diatomic molecules* (Van Nostrand Reinhold, New York, 1979).

[Huz65] S. Huzinaga, *J. Chem. Phys.* **42**, 1293 (1965).

[Jan71] D. R. Stull and H. R. Prophet (eds.), JANAF Thermochemical Tables (2nd ed.), NSRDS-NBS 37, National Bureau of Standards, Washington DC, 1971.

[Jan80] K. Jankowski and J. Paldus, *Int. J. Quantum Chem.* **18**, 1243 (1980).

[Jan85] M. W. Chase, Jr., C. A. Davies, J. R. Downery, Jr., D J. Frurip, R. A. McDonald, and A. N. Syverud, *J. Phys. Chem. Ref. Data* **14** (1985) supplement 1: *JANAF Thermochemical Tables*, Third Edition (2 volumes).

[Jon85] R. O. Jones, *J. Chem. Phys.* **82**, 5078 (1985).

[Kar85] S. P. Karna and F. Grein, *Chem. Phys.* **98**, 207 (1985).

[Kar88] S. P. Karna and F. Grein, *Chem. Phys. Lett.* **144**, 149 (1988).

[Kas36] L. S. Kassel, *Chem. Rev.* **18**, 277 (1936).

[Kes87] G. Kessler, H. D. Bauer, W. Pompe, and H. J. Scheibe, *Thin Solid Films* **147**, L45 (1987).

[Kir78] *Kirk-Othmer Encyclopedia of Chemical Technology*, 3rd ed. (Wiley, New York, 1978), Vol. 4, pp. 520-535.

[Kni87] L. B. Knight Jr., B. W. Gregory, S. T. Cobranchi, D. Feller, and E. R. Davidson, *J. Am. Chem. Soc.* **109**, 3521 (1987).

[Koh70] F. J Kohl and C. A. Stearns, *J. Chem. Phys.* **52**, 6310 (1970).

[Koo34] T. Koopmans, *Physica* **1**, 69 (1934).

[Kra84] W. P. Kraemer, P. R. Bunker, and M. Yoshimine, *J. Mol. Spectr.* **107**, 191 (1984).

[Kra85] W. Krätschmer and K. Nachtigall, in *Polycylic aromatic hydrocarbons and astrophysics* (eds. A.Léger *et al.*), D. Reidel, Dordrecht, 1985.

[Kri78] R. Krishnan and J. A. Pople, *Int. J. Quantum Chem.* **14**, 91 (1978).

[Kri80] R. Krishnan, M. J. Frisch, and J. A. Pople, *J. Chem. Phys.* **72**, 4244 (1980) and references therein.

[Kri80a] R. Krishnan, J. S. Binkley, R. Seeger, and J. A. Pople, *J. Chem. Phys.* **72**, 650 (1980).

[Kri80b] R. Krishnan, M. J. Frisch, and J. A. Pople, *J. Chem. Phys.* **72**, 4244 (1980).

[Kur90] J. Kurtz and D. R. Huffmann, *J. Chem. Phys.* **92**, 30 (1990).

[Kut77] W. Kutzelnigg, "Pair Correlation Theories", in: *Modern Theoretical Chemistry vol. 3* (ed. H. F. Schaefer III, Plenum Press, New York, London, 1977), p.129. A. Szabo and N. S. Ostlund, *Modern quantum chemistry: introduction to advanced electronic structure theory* (Revised First Edition, McGraw-Hill, New York, 1989).

[Lan74] S. R. Langhoff and E. R. Davidson, *Int. J. Quantum Chem.* **8**, 61 (1974).

[Lar86] M. Larsson, *J. Phys. B* **19**, L261 (1986).

[Lee84] Y. S. Lee, S. A. Kucharski, and R. J. Bartlett, *J. Chem. Phys.* **81**, 5906 (1984). M. Urban, J. Noga, S. J. Cole, and R. J. Bartlett, *J. Chem. Phys.* **83**, 4041 (1985). J. Noga, R. J. Bartlett, and M. Urban, *Chem. Phys. Lett.* **134**, 126 (1987).

[Lee84a] T. J. Lee, D. J. Fox, H. F. Schaefer III, and R. M. Pitzer, *J. Chem. Phys.* **81**, 356 (1984).

[Lee90] T. J. Lee, A. P. Rendell, and P. R. Taylor, *J. Phys. Chem.* **94**, 5463 (1990).

[Lew86] D. F. Lewis, *Chem. Rev.* **86**, 1111 (1986).

[Lis72] D. H. Liskow, C. F. Bender, and H. F. Schaefer III, *J. Chem. Phys.* **56**, 5075 (1972).

[Lut74] B. L. Lutz and J. A. Ryan, *Astrophys. J.* **194**, 753 (1974).

[Mag86] D. H. Magers, R. J. Harrison and R. J. Bartlett, *J. Chem. Phys.* **84**, 3284 (1986).

[Mar87] J. M. L. Martin, M. Sc. thesis (University of Antwerp, Wilrijk, 1987).

[Mar89a] F. Marinelli and A. Pellegatti, *Chem. Phys. Lett.* **158**, 545 (1989).

[Mar89b] J. M. L. Martin, J. P. François, and R. Gijbels, *J. Chem. Phys.* **90**, 3403 (1989).

[Mar89c] J. M. L. Martin, J. P. François, and R. Gijbels, *J. Chem. Phys.* **90**, 6469 (1989); *Colloque de Physique* **50 C 5**, 873 (1989).

[Mar89d] J. M. L. Martin, J. P. François, and R. Gijbels, *J. Comp. Chem.* **10**, 152 (1989).

[Mar89e] J. M. L. Martin, J. P. François, and R. Gijbels, *J. Comp. Chem.* **10**, 875 (1989).

[Mar89f] J. M. L. Martin, J. P. François, and R. Gijbels, *Theor. Chim. Acta* **76**, 195 (1989) and references therein.

[Mar90a] J. M. L. Martin, J. P. François and R. Gijbels, *Chem. Phys. Lett.* **166**, 295 (1990).

[Mar90b] J. M. L. Martin, J. P. François and R. Gijbels, *Chem. Phys. Lett.* **172**, 354 (1990).

[Mar90c] J. M. L. Martin, J. P. François, and R. Gijbels, *J. Chem. Phys.* **92**, 6655 (1990).

[Mar90d] J. M. L. Martin, J. P. François and R. Gijbels, *J. Chem. Phys.* **93**, 4485 (1990).

[Mar90e] J. M. L. Martin, J. P. François, and R. Gijbels, *J. Chem. Phys.* **93**, 5037 (1990).

[Mar90f] J. M. L. Martin, J. P. François and R. Gijbels, *J. Chem. Phys.* **93**, 8850 (1990).

[Mar90g] J. M. L. Martin, J. P. François and R. Gijbels, *J. Comp. Chem.* **11**, xxxx (1990).

[Mar91] J. M. L. Martin, J. P. François, and R. Gijbels, *J. Chem. Phys.* **94**, xxxx (1991).

[MarTBP] J. M. L. Martin, J. P. François, and R. Gijbels, to be published.

[McL80] A. D. McLean and G. S. Chandler, *J. Chem. Phys.* **72**, 5639 (1980).

[Mic87] D. Michalska, H. Chojnacki, B. A. Hess Jr., and L. J. Schaad, *Chem. Phys. Lett.* **141**, 376 (1987).

[Mol34] C. Møller and M. S. Plesset, *Phys. Rev.* **46**, 618 (1934).

[Mol90] MOLECULE-SWEDEN is an electronic structure program system written by J. Almlöf, C. W. Bauschlicher Jr., M. R. A. Blomberg, D. P. Chong, A. Heiberg, S. R. Langhoff, P.-Å. Malmqvist, A. P. Rendell, B. O. Roos, P. E. M. Siegbahn, and P. R. Taylor.

[Mop89] J. J. P. Stewart, MOPAC *5.00: a general purpose molecular orbital package* (QCPE 455).

[Mop90] J. J. P. Stewart, J. M. L. Martin, and J. P. François, MOPAC *5.00, CDC version* (QCPE 455/CDCM); see also *QCPE Bulletin* **10**, 9(1990) for announcement.

[Mos70] O. A. Mosher and R. P. Frosch, *J. Chem. Phys.* **52**, 5781 (1970).

[Mue89] F. Müller-Plathe and L. Laaksonen, *Chem. Phys. Lett.* **160**, 175 (1989).

[Mul55] R. S. Mulliken, *J. Chem. Phys.* **23**, 1833, 1841, 2338, 2343 (1955).

[Mur82] J. N. Murrell, O. Novaro, and S. Castillo, *Chem. Phys. Lett.* **90**, 421 (1982); O. Novaro and S. Castillo, *Int. J. Quantum Chem. Symp.* **26**, 41 (1984).

[Nog87] J. Noga and R. J. Bartlett, *J. Chem. Phys.* **86**, 7041 (1987); *erratum* **89**, 3401 (1988).

[Odi79] G. A. Odintzova and A. R. Striganov, *J. Phys. Chem. Ref. Data* **8**, 63(1979).

[Ohn82] K. Ohno and K. Morokuma (eds.), *Quantum chemistry literature data base – Bibliography of ab initio calculations for 1978-1980*, (Elsevier, Amsterdam, 1982); Supplement for 1981, *J. Mol. Struct. (THEOCHEM)* **91**, 1 (1982); Supplement for 1982, *ibid.* **106**, 1 (1983); Supplement for 1983, *ibid.* **119**, 1 (1984); Supplement for 1984, *ibid.* **134**, 1 (1985); Supplement for 1985, *ibid.* **148**, 1 (1986); Supplement for 1986, *ibid.* **154**, 1 (1987); Supplement for 1987, *ibid.* **182**, 1 (1988); Supplement for 1988, *ibid.* **203**, 1 (1989); Supplement for 1989, *ibid.* **211**, 1 (1990).

[O'e66] L. Oleari, L. Di Sipio, and L. De Michelis, *Mol. Phys.* **10**, 97 (1966).

[Pac79] *Pure and Applied Chemistry* **51**, 1 (1979).

[Pac88] G. Pacchioni and J. Koutecký, *J. Chem. Phys.* **88**, 1066 (1988).

[Par85] J. D. Parsons, R. F. Bunshah, and O. M. Stafsudd, *Solid State Technol.* **28**, 133 (1985).

[Par89a] V. Parasuk and J. Almlöf, *J. Chem. Phys.* **91**, 1137 (1989).

[Par89b] R. G. Parr and W. Yang, *Density-functional theory of atoms and molecules* (Oxford University Press, Oxford, 1989).

[Par90] V. Parasuk and J. Almlöf, *J. Chem. Phys.*, in press.

[ParTBP] V. Parasuk and J. Almlöf, to be published.

[Pel81] M. J. Pellerite, R. L. Jackson, and J. I. Braumann, *J. Phys. Chem.* **85**, 1624 (1981).

[Per77] J. Perič-Radič, J. Römelt, S. D. Peyerimhoff, and R. J. Buenker, *Chem. Phys. Lett.* **50**, 344 (1977).

[Pet88] C. Petrongolo, *J. Mol. Struct. (THEOCHEM)* **175**, 215 (1988).

[Pit59] K. S. Pitzer and E. Clementi, *J. Am. Chem. Soc.* **81**, 4477 (1959).

[Pit61] K. S. Pitzer and L. Brewer, *Thermodynamics* (McGraw-Hill, New York, 1961).

[Pol87] M. Polak, M. Gruebele, and R. J. Saykally, *J. Am. Chem. Soc.* **109**, 2884 (1987) and references therein.

[Pop54] J. A. Pople and R. K. Nesbet, *J. Chem. Phys.* **22**, 571 (1954).

[Pop65] J. A. Pople, D. P. Santry, and G. A. Segal, *J. Chem. Phys.* **43 S**, 129 (1965).

[Pop67] J. A. Pople, D. L. Beveridge, and P. A. Dobosh, *J. Chem. Phys.* **47**, 2027 (1967).

[Pop76] J. A. Pople, J. S. Binkley, and R. Seeger, *Int. J. Quantum Chem. Symp.* **10**, 1 (1976).

[Pop77] J. A. Pople, R. Seeger, and R. Krishnan, *Int. J. Quantum Chem. Symp.* **11**, 149 (1977).

[Pop79] J. A. Pople, R. Krishnan, H. B. Schlegel, and J. S. Binkley, *Int. J. Quantum Chem. Symp.* **13**, 225 (1979).

[Pop81] J. A. Pople, H. B. Schlegel, R. Krishnan, D. J. DeFrees, J. S. Binkley, M. J. Frisch, R. A. Whiteside, R. F. Hout, and W. J. Hehre, *Int. J. Quantum Chem. Symp.* **15**, 269 (1981).

[Pop83] J. A. Pople, M. J. Frisch, B. T. Luke, and J. S. Binkley, *Int. J. Quantum Chem. Symp.* **17**, 307 (1983).

[Pop87] J. A. Pople, M. Head-Gordon, and K. Raghavachari, *J. Chem. Phys.* **87**, 5968 (1987).

[Pop88] J. A. Pople, M. Head-Gordon, and K. Raghavachari, *Int. J. Quantum Chem. Symp.* **22**, 377 (1988).

[Pop89] J. A. Pople, M. Head-Gordon, D. J. Fox, K. Raghavachari, and L. A. Curtiss, *J. Chem. Phys.* **90**, 5622 (1989).

[Pul79] P. Pulay, G. Fogarasi, F. Pang, and J. E. Boggs, *J. Am. Chem. Soc.* **101**, 2550 (1979).

[Pur82] G. D. Purvis III and R. J. Bartlett, *J. Chem. Phys.* **76**, 1910 (1982).

[Rag85] K. Raghavachari, *J. Chem. Phys.* **82**, 4607 (1985) and references therein.

[Rag86a] K. Raghavachari, *J. Chem. Phys.* **84**, 5672 (1986).

[Rag86b] K. Raghavachari, R. A. Whiteside, and J. A. Pople, *J. Chem. Phys.* **85**, 6623 (1986).

[Rag87] K. Raghavachari and J. S. Binkley, *J. Chem. Phys.* **87**, 2191 (1987).

[Rag89] K. Raghavachari, G. W. Trucks, J. A. Pople, and M. Head-Gordon, *Chem. Phys. Lett.* **157**, 479 (1989).

[Rag89b] K. Raghavachari, J. A. Pople, and M. Head-Gordon, in: *Many-body methods in quantum chemistry* (Ed. U. Kaldor), Lecture Notes in Chemistry 52, Springer,Berlin, 1989, p. 215.

[Rag90] K. Raghavachari, *Chem. Phys. Lett.* **171**, 249 (1990).

[RagPC] K. Raghavachari, private communication. The unpublished data comprise: (a) UHF/6-31G* IR intensities and Raman activities for linear $C_7$, $C_8$, and $C_9$, as well as cyclic $C_8$; (b) UHF/6-31G* frequencies for linear $C_8$.

[Ric71] W. G. Richards, T. E. H. Walker, and R. K. Hinkley, *A bibliography of ab initio molecular wave functions* (Clarendon Press, Oxford, 1971); W. G. Richards, T. E. H. Walker, L. Farnell, and P. R. Scott, *Supplement for 1970-1973* (Clarendon Press, Oxford, 1974); W. G. Richards, P. R. Scott, E. A. Colbourn, and A. F. Marchington, *Supplement for 1974-1977* (Clarendon Press, Oxford, 1978); W. G. Richards, P. R. Scott, V. Sackwild, and S. A. Robins, *Supplement for 1978-1980* (Clarendon Press, Oxford, 1981).

[Rit86] J. P. Ritchie, H. F. King, and W. S. Young, *J. Chem. Phys.* **85**, 5175 (1986).

[Roh86] C. M. Rohlfing and R. L. Martin, *J. Phys. Chem.* **90**, 2043 (1986).

[Rom78] J. Römelt, S. D. Peyerimhoff, and R. J. Buenker, *Chem. Phys. Lett.* **58**, 1 (1978).

[Roo77] B. Roos, in: *Computational Methods in Quantum Chemistry and Molecular Physics vol. 15* (eds. G. H. F. Diercksen, B. T. Sutcliffe, A. Veillard), D. Reidel, Dordrecht, Boston, 1977, p. 251.

[Roo80] B. O. Roos, P. R. Taylor, and P. E. M. Siegbahn, *Chem. Phys.* **48**, 157 (1980). B. O. Roos, *Int. J. Quantum Chem. Symp.* **14**, 175 (1980).

[Roo87] B. O. Roos, *Adv. Chem. Phys.* **69**, 399 (1987).

[Rot85] B. Rother and C. Weissmantel, *Phys. Status Solidi* **A 87**, K119 (1985).

[San84] H. J. Sanders, *Chem. Eng. News* **62**, 26 (1984).

[Sat83] M. Satou and F. Fujimoto, *Japan. J. Appl. Phys. II* **22**, 171 (1983).

[Sat85] K. Sattler, in: *Current Topics in materials science vol. 12* (ed. E. Kaldis), Elsevier, Amsterdam, 1985.

[Sch77] M. E. Schwartz, in: *Modern Quantum Chemistry vol. 4* (ed. H. F. Schaefer III), Plenum Press, New York, 1977, p.357.

[Sch82] H. B. Schlegel, *J. Comp. Chem.* **3**, 214 (1982).

# Additions and corrections

**page 1.3** Line after equation (1.15): change "F S, and P" to "F, S, and P".

**page 1.52** Last line: change "Sections 3.9 and 3.10" to "Sections 4.10 and 4.11".

**page 1.116** Section 1.12.2.1, second paragraph, third line: "splitting them up in $2S+1$ component states with spin-orbit quantum number $J = L - S_z$" should read "splitting them up in $2S + 1$ (if $L \geq S$) or $2L + 1$ (if $L < S$) component states, with spin-orbit quantum number $J = L + S_z$".

**page 1.124** Equation (1.442) should read

$$Q_{\rm rot} = e^{y/3}\sqrt{\frac{\pi}{xy^2}}(1 + \frac{z^2}{90} + \frac{8z^3}{2835} + \frac{5z^4}{4536} + \frac{148z^5}{280665} + \ldots)$$

instead of

$$Q_{\rm rot}(y) = \frac{e^{y/3}}{y}\sqrt{\frac{\pi}{xy^2}}(1 + \frac{z^2}{90} + \frac{8z^3}{2835} + \frac{5z^4}{4536} + \frac{148z^5}{280665} + \ldots)$$

**page 3.44** Second paragraph, 10th line: read "it is readily seen" instead of "it it readily seen".

**page 4.46** Equation (4.6): delete "(4)" in right-hand side.

**page 4.54** Equation (4.10): delete "(6)" in right-hand side.

**page 4.148** Footnote (a) to table, second line: "within roundoff of that in" should become "within roundoff of those in".

**page 4.164** Entry [Mar90g] should be updated to: J. M. L. Martin, J. P. François, and R. Gijbels, *J. Comp. Chem.* **12**, 52 (1991).

**page 4.165** Entry [ParTBP] should be updated to: V. Parasuk, J. Almlöf, and B. DeLeeuw, *Chem. Phys. Lett.* **176**, 1 (1991).

**page 4.167** Entry [Scu90] should be updated to: G. E. Scuseria, *Chem. Phys. Lett.* **176**, 27 (1991).

**page xxxii** Entry 19: update reference to: JOURNAL OF COMPUTATIONAL CHEMISTRY **12**, 52–70 (1991).

**page xxxiii** Entry 22: change "JOURNAL OF CHEMICAL PHYSICS" to "JOURNAL OF PHYSICAL CHEMISTRY".

**page xxxiii** Entry 23: change "CHEMICAL PHYSICS" to "ZEITSCHRIFT FÜR PHYSIK D: ATOMS, MOLECULES, AND CLUSTERS".

**page xxxiv** Append "Vaalsbroek, 16-18.5.1990." to final sentence.

[Sch84] H. B. Schlegel, *Theor. Chim. Acta* **66**, 333 (1984).

[Sch86] H. B. Schlegel, *J. Chem. Phys.* **84**, 4530 (1986).

[Sch88] H. B. Schlegel, *J. Phys. Chem.* **92**, 3075 (1988).

[Scu89] G. E. Scuseria and H. F. Schaefer III, *J. Chem. Phys.* **90**, 3629 (1989).

[Scu90] G. E. Scuseria, *Chem. Phys. Lett.*, submitted for publication.

[See76] R. Seeger and J. A. Pople, *J. Chem. Phys.* **65**, 265 (1976).

[See77] R. Seeger and J. A. Pople, *J. Chem. Phys.* **66**, 3045 (1977).

[Sei88] G. Seifert, B. Schwab, S. Becker, and H. J. Dietze, *Int. J. Mass Spectr. Ion Proc.* **85**, 327 (1988).

[She89] L. N. Shen and W. R. M. Graham, *J. Chem. Phys.* **91**, 5115 (1989).

[Sie78] P. E. M. Siegbahn, *Chem. Phys. Lett.* **55**, 386 (1978).

[Sim73] G. Simons, R. G. Parr, and J. M. Finlan, *J. Chem. Phys.* **59**, 3229 (1973).

[Sim87] E. D. Simandiras, N. C. Handy, R. D. Amos, *Chem. Phys. Lett.* **133**, 324 (1987).

[Sim88] E. D. Simandiras, J. E. Rice, T. J. Lee, R. D. Amos, and N. C. Handy, *J. Chem. Phys.* **88**, 3187 (1988) and references therein.

[Sla75] Z. Slanina, *Collect. Czech. Chem. Commun.* **40**, 1997 (1975).

[Sla77] Z. Slanina and R. Zahradník, *J. Phys. Chem.* **81**, 2252 (1977).

[Sok79] M. Sokolowski, *J. Cryst. Growth* **46**, 136 (1979).

[Spi87] G. W. Spitznagel, T. Clark, and P. von Ragué Schleyer, *J. Comp. Chem.* **8**, 1109 (1987).

[Sta89] J. F. Stanton, W. N. Lipscomb, D. H. Magers, and R. J. Bartlett, *J. Chem. Phys.* **90**, 3241 (1989).

[Ste89a] J. J. P. Stewart, *J. Comp. Chem.* **10**, 209 (1989).

[Ste89b] J. J. P. Stewart, *J. Comp. Chem.* **10**, 221 (1989).

[Str67] H. L. Strauss and E. Thiele, *J. Chem. Phys.* **46**, 2473 (1967).

[Sun84] K. K. Sunil, A. Orendt, K. D. Jordan, and D. J. DeFrees, *Chem. Phys.* **89**, 245 (1984).

[Sus69] R. Sustmann, S. F. Williams, M. J. S. Dewar, L. C. Allen, and P. von Ragué Schleyer, *J. Am. Chem. Soc.* **91**, 5350 (1969).

[Suz79] H. Suzuki, *Prog. Theor. Phys.* **62**, 936 (1979).

[Szm83] J. Szmidt, A. Jakubowski, A. Michalski, and A. Rusek, *Thin Solid Films* **110**, 7 (1983).

[Tak86] T. Takagi, *Vacuum* **36**, 27 (1986).

[TayPC] P. R. Taylor, personal communication.

[Tho71] K. R. Thompson, R. L. DeKock, and W. Weltner Jr., *J. Am. Chem. Soc.* **93**, 4688 (1971).

[Thr60] B. A. Thrush, *Proc. Chem. Soc. (London)*, 339 (1960); *Nature* **186**, 1044 (1960).

[Tia88] R. Tian, J. C. Facelli, and J. Michl, *J. Phys. Chem.* **92**, 4073 (1988).

[Tsu65] T. Tsuji, *Ann. Tokyo Astron. Obs.* **9**, 1 (1965); E. M. McCabe, *Mon. Not. Roy. Astron. Soc.* **200**, 71 (1982).

[Tur87] B. E. Turner, in: *Physics and chemistry of small clusters* (ed. P. Jena, B. K. Rao, and S. N. Khanna), Plenum Press, New York, 1987, p.915.

[Urb85] M. Urban, J. Noga, S. J. Cole, and R. J. Bartlett, *J. Chem. Phys.* **83**, 4041 (1985).

[Vag89] Z. Vager, R. Naaman, and E. P. Kanter, *Science* **244**, 426 (1989).

[Vag89b] Z. Vager and E. P. Kanter, *J. Phys. Chem.* **93**, 7745 (1989).

[Val89] M. Vala, T. M. Chandrasekhar, J. Szczepanski, R. Van Zee, and W. Weltner Jr., *J. Chem. Phys.* **90**, 595 (1989).

[Val90] M. Vala, T. M. Chandrasekhar, J. Szczepanski, and R. Pellow, in: *Materials chemistry at high temperatures* (ed. J. Hastie), Humana Press, Clifton, NJ, 1990.

[Van87] J. A. Van Vechten and D. A. Keszler, *Phys. Rev. B* **36**, 4570 (1987) and references therein.

[Van88] R. J. Van Zee, R. F. Ferrante, K. J. Zeringue, W. Weltner Jr., and D. W. Ewing, *J. Chem. Phys.* **88**, 3465 (1988).

[Voe89] R. Voets, J. P. François, J. M. L. Martin, J. Mullens, J. Yperman, and L. C. Van Poucke, *J. Comp. Chem.* **10**, 449 (1989).

[Voe90] R. Voets, J. P. François, J. M. L. Martin, J. Mullens, J. Yperman, and L. C. Van Poucke, *J. Comp. Chem.* **11**, 269 (1990).

[Wac72] F. Wachi and D. E. Gilmartin, *High Temp.Sci.* **4**, 423 (1972).

[Wel64] W. WeltnerJr. and D. McLeod Jr., *J. Chem. Phys.* **40**, 1305 (1964).

[Wel66] W. Weltner Jr. and D. McLeod Jr., *J. Chem. Phys.* **45**, 3096 (1966).

[Wel83] B. H. Wells and S. Wilson, *Chem. Phys. Lett.* **101**, 429 (1983).

[Wel89] W. Weltner Jr. and R. J. Van Zee, *Chem. Rev.* **89**, 1713 (1989).

[Whi81] R. A. Whiteside, Ph.D. Thesis (Carnegie-Mellon University, Pittsburgh, PA, 1981): UMI Dissertation Services # 8118449 (Ann Arbor, MI, 1990).

[Whi81a] R. A. Whiteside, R. Krishnan, M. J. Frisch, J. A. Pople, and P. Von Ragué Schleyer, *Chem. Phys. Lett.* **80**, 547 (1981).

[Whi81b] R. A. Whiteside, R. Krishnan, D. J. DeFrees, J. A. Pople, and P. Von Ragué Schleyer, *Chem. Phys. Lett.* **78**, 538 (1981).

[Wig84] M. D. Wiggins, C. R. Aita, and F. S. Hickernell, *J. Vac. Sci. Technol.* **A2**, 322 (1984).

[Wil78] S. Wilson, *Mol. Phys.* **35**, 1 (1978).

[Won88] M. W. Wong, P. W. M. Gill, R. H. Nobes, and L. Radom, *J. Phys. Chem.* **92**, 4875 (1988).

[Yam86] Y. Yamaguchi, M. Frisch, J. Gaw, H. F. Schaefer III, and J. S. Binkley, Nobes, and L. Radom, *J. Chem. Phys.* **84**, 2262 (1986).

[Zah74] R. Zahradník, Z. Slanina, and P. Čársky, *Collect. Czech. Chem. Commun.* **39**, 63 (1974); Z. Slanina and R. Zahradník, *Collect. Czech. Chem. Commun.* **39**, 729 (1974).

[Zav73] P. D. Zavitsanos and G. A. Carlson, *J. Chem. Phys.* **59**, 2966 (1973).

[Zfi87] ZFI Mitteilungen, nr. 134: *Beiträge zur Clusterforschung* (Akademie der Wissenschaften der DDR, September 1987).

# Chapter 5

# Miscellaneous methodological issues

*Science is nothing but trained and well organised common sense.*

*Thomas H. Huxley, 1825–1895*

## 5.1 Summary and general introduction

During the course of the preceding work, a number of methodological issues that could not be 'dealt with on the fly' cropped up. All three were related to the fact that most cluster molecules investigated are open-shell molecules with low-lying excited states. The combination of these two results in substantial spin contamination. As discussed in Chapter 1, it was shown recently [Pop88] that for such molecules single excitation effects become unusually important, and that they cannot be dealt with adequately at the MP4 or even CCD(ST) level: less than half of the single excitation effect is recovered at the MP4 level for these molecules.

The obvious remedy would be to use CCSD [Pur82] or CCSD(T) [Rag89], the latter of which had just been published; QCISD(T) [Pop87] was also a valid option. However, no program capable of any of these three methods was available to us, whereas implementing them for oneself would require the development, debugging, and testing of a FORTRAN code in excess of perhaps 20,000 statements. This could impossibly be completed within the available time span; furthermore, most of this work would have been obsolete by the time it was completed.

The one treatment that includes $\hat{T}_1$ effects to infinite order, and that could be performed with the available software, was CISD. Of course CISD is not size-consistent, and some preliminary calculations showed that even the difference between CISD and CID energies — taken as a measure for the $\hat{T}_1$ effects — is plagued by very serious size consistency errors. However, various correction formulas exist [Lan74, Pop77, Dav77, Sie78] which are supposed to remedy the problem. Then, it was found that the computed $\hat{T}_1$ energy was to a fairly large extent dependent on the choice of the correction formula. Literature study revealed that, although the regular Langhoff-Davidson correction formula

[Lan74] is almost universally employed (most of the remaining papers use the Pople correction [Pop77]), no serious theoretical or numerical comparison of the available formulas had ever been made. Consequently, this was definitely a matter to be looked into.

At the same time, given the importance of $\hat{T}_1$ effects in the energy for the type of molecules at hand, the question was raised whether neglect of $\hat{T}_1$ effects would affect the computed geometry. Again this issue had not been investigated before, except for some more 'well-behaved' molecules where the effect was found to be negligible [DeF82].

In Section 5.2[a], the effect of single excitations on the computed geometries and harmonic frequencies is investigated for some species selected for their pathologically large degree of spin contamination. These include BO, CCH, CN, $CO^+$, NO, $N_3$, and BN. It is shown that single excitations have a large effect, up to several hundreds of an Ångstrom, on calculated bond distances. The effect decreases with increasing basis set size. Harmonic frequencies may be affected by as much as 200 $cm^{-1}$. It is also shown that CCSD, CISD, CID, and CCD energies are effectively invariant under single spin annihilation when no major higher contaminants are present. It can be concluded from our work that for species with heavy spin contamination, CISD is presently the method to be preferred over MP2 and even spin-projected MP2.

In Section 5.3[b], four common size-consistency corrections for limited CI, i.e. the Davidson [Lan74], renormalized Davidson [Sie78], Davidson-Silver [Dav77], and Pople [Pop77] formulas, are critically compared both numerically and on perturbation and coupled-cluster theoretical grounds. The Pople correction is shown to give a lower bound to CCD total energies, and to reproduce them relatively well. The Davidson-Silver formula provides an upper bound for the LCCD total energy, and is definitely superior to the regular and renormalized Davidson corrections. The regular Davidson formula is shown to have important deficiencies with respect to both regular and linearized coupled cluster energies.

Meanwhile, we acquired GAUSSIAN 88 [Gau88], which includes the QCISD(T) method and thus dealt with the problem of $\hat{T}_1$ inclusion for once and for all. It also however enabled us to benchmark the computed $\hat{T}_1$ energy, as obtained from a size-consistency corrected CISD calculation, to the rigorously size-consistent values obtained from the difference between CCD and QCISD energies. Additionally, this quantity was interesting as a demanding test-case for the various size-consistency correction formulas, and allowed a less 'academic' assessment of the conclusions reached in Section 5.3. This was investigated in Section 5.4[c]. Our finding there is that CISD supplemented with Pople's size-consistency correction reproduces QCISD binding energies surprisingly well. The single excitation energy, as obtained by various methods, is discussed in terms of

[a] This section has been adapted from J. M. L. Martin, J. P. François, and R. Gijbels, *Chem. Phys. Lett.* **166**, 295 (1990).

[b] Adapted from J. M. L. Martin, J. P. François, and R. Gijbels, *Chem. Phys. Lett.* **172**, 346 (1990).

[c] Adapted from J. M. L. Martin, J. P. François, and R. Gijbels, *Chem. Phys. Lett.* **172**, 346 (1990).

higher-order perturbation theory. For molecules in which they are important, such as spin-contaminated radicals, a relatively accurate method for estimating single excitation energies is presented that avoids CCSD or QCISD calculations.

Whereas full CCSD (or, by default, QCISD) calculations are of course more satisfying to perform, reasons of cost or availability may preclude their application. For example with GAUSSIAN 88, which is the most commonly used quantum chemistry suite, CISD calculations take about a quarter of the time of the equivalent QCISD calculation. When low-lying excited states are present, the convergence behavior of the CISD iterations is not seriously affected, whereas QCISD may well require five times as many iterations as the corresponding CISD calculation. This means that for large molecules, the ability to use CISD with a Pople correction instead of QCISD may well make the difference between an affordable and an impossible study.

It should be added that a very efficient reformulation of both CISD and CCSD has recently been published [Scu88]. The CISD algorithm described there is even faster than the shape-driven GUGA algorithm [Sax82], whereas CCSD can be done in less than twice the time of the equivalent CISD calculation. The code involved is not generally available, however, and a factor of two still does make a considerable difference in cost when large systems are treated.

## 5.2 Unusually large effects of single excitations on the geometry of radical species and limiting spin-projection invariance of some correlated methods

### 5.2.1 Introduction

The evaluation of correlated geometries is presently becoming a standard tool of theoretical chemistry, at least for small molecules. Just as in the case of correlated energy evaluation, the problem of convergence towards the basis set full CI limit imposes itself.

Thanks to Handy and Schaefer's Z-vector method [Han84], MP2 [Bin75] is now computationally by far the most efficient method. Contrasting with the case of energy evaluation, basis set and correlation method seem to be synergetic in derivative evaluation [Sim88]. More specifically, it was found in refs. [DeF79] and [Pop79] that only half of the correlation effects are recovered at the MP2 level using a double-zeta plus polarization (DZP) basis set, whereas very accurate geometries have been obtained at the same level using triple-zeta plus double polarization (TZ2P) or larger basis sets [Sim88]. Also, a very significant improvement was seen by DeFrees *et al.* [DeF82] upon going from MP2 to MP3 [Pop76] with the same DZP basis set, whereas no improvement at all was found using large basis sets [Alb88]. The main similarity between these two methods lies in the fact, that both of them only account for double excitations.

In certain types of molecules, such as those with multiple bonds or highly electronegative elements, triple excitations are well known to be very important in the energy [Fri80]. In derivative evaluation, similar, albeit smaller effects were noted, such as in the seminal paper of Bartlett and coworkers on the potential energy surface of water [Bar87]. However, a general consensus appeared to exist that the effect of single excitations on the geometry was very small. DeFrees *et al.* [DeF82] reported that only insignificant changes (less than 0.001 Å) were observed upon going from CISD to CID geometries. Since most experimental geometry data are not even accurate to 0.001 Å, let alone that present-day theoretical methods can claim such an accuracy, such differences seem to be of only academic importance.

However, in a recent paper by Pople *et al.* [Pop88] an interesting component analysis of the contributions of various excitation levels on a medium-sized class of compounds was made. A surprising phenomenon was observed there with the CN and CCH radicals: the single excitation contributions were not only very high, but they were also underestimated by 50% or more at the fourth-order [Fri80] Møller-Plesset level (in which they first appear). Nobes *et al.* [Nob87] had previously noted that whereas MBPT was notoriously unsuccessful in computing the electron affinity of CN, a very satisfactory result was obtained at the Davidson-corrected [Lan74] CISD level. Both radical species exhibit

Table I: Geometries (Å) for some radical and singlet species at several correlated levels.

| Species | CISD/3-21G | CID/3-21G | CISD/6-31G* | CID/6-31G* | CCD/3-21G |
|---|---|---|---|---|---|
| BO | 1.2382 | 1.2300 | 1.2074 | 1.2032 | 1.2327 |
| $^3$CH | | | | | |
| $r_{CC}$ | / | / | 1.1995 | 1.1866 | / |
| $r_{CH}$ | / | / | 1.0653 | 1.0649 | / |
| CN | 1.1704 | 1.1488 | 1.1558 | 1.1408 | 1.1483 |
| $CO^+$ | 1.1299 | 1.1125 | 1.1118 | 1.1010 | 1.1131 |
| NO | 1.1650[a] | 1.1393[a] | (1.1486)[a] | (1.1423)[a] | 1.1396[a] |
| $N_3$ | 1.2016 | 1.1956 | 1.1764 | 1.1732 | 1.2016 |
| BN | 1.3491 | 1.3323 | 1.3181 | 1.3099 | 1.3350 |
| BH | 1.2575 | 1.2558 | 1.2322 | 1.2308 | 1.2582 |
| $H_2O$ | 0.9895 | 0.9881 | 0.9574 | 0.9568 | 0.9914 |
| | 105.21° | 105.34° | 104.33° | 104.41° | 105.09° |
| $N_2$ | 1.1131 | 1.1112 | 1.1050 | 1.1034 | 1.1192 |

(a) Numerical instability of the Dunham analysis was observed

a large degree of spin contamination, so it did not appear unlikely to us that a similar phenomenon would occur with the geometry.

The relationship between spin contamination and slow convergence of the Møller-Plesset series is well known [Han85]. Actually, spin contamination in radical species is most likely to occur when low-lying excited states of a higher multiplicity than the reference state exist at the Hartree-Fock level [Gil88]. When this is the case, such low-lying states of the same multiplicity usually exist too, which will have large cluster amplitudes or CI coefficients. The latter are responsible for the slow convergence of the Møller-Plesset series, since they cause large contributions to powers of the substitution operators ($\hat{T}_2^2$ first appears at fourth order) and cross-terms (which only start appearing in fifth order). Actually, some of the lowest-lying among these states will be single excitations with respect to the reference state. Since the interaction among the singly excited configurations themselves (they do not interact with the ground state as a consequence of Brillouin's theorem) is generally rather small, and it is the only interaction which is accounted for at the MP4 level, the underestimate at the MP4 level is readily understood: the most important terms will be the contributions of these large amplitudes in $\hat{T}_1$ to $\hat{T}_1^2$ and $\hat{T}_1\hat{T}_2$, both of which appear for the first time in fifth order. Now, $\hat{T}_1^2$ is included in a CISD calculation, so the difference between CISD and CID geometries will give some indication of the magnitude of the effect.

### 5.2.2 Computational methods

All calculations were performed using the GAUSSIAN 86 program package [Gau86] running on a VAXstation 2000 under the VMS 4.7 operating system. Since only unfinished code

Table II: Expectation values of the $\hat{S}^2$ operator for the SCF wavefunction, the first-order MBPT wavefunction, and the SCF wavefunction with single spin annihilation, respectively*.

| | 3-21G | | | 6-31G* | | |
|---|---|---|---|---|---|---|
| | $\langle\hat{S}^2\rangle$ | $\langle\hat{S}^2\rangle_1$ | $\langle\hat{S}^2\rangle_A$ | $\langle\hat{S}^2\rangle$ | $\langle\hat{S}^2\rangle_1$ | $\langle\hat{S}^2\rangle_A$ |
| BO | 0.82–0.88 | 0.79–0.85 | 0.75–0.76 | 0.79–0.83 | 0.78–0.80 | 0.75–0.75 |
| CCH | N/A | N/A | N/A | 1.13 | 1.05 | 0.85 |
| CN | 0.99–1.33 | 0.93–1.22 | 0.78–0.98 | 0.93–1.28 | 0.89–1.18 | 0.77–0.94 |
| $CO^+$ | 0.92–1.19 | 0.87–1.10 | 0.77–0.87 | 0.87–1.11 | 0.83–1.03 | 0.76–0.83 |
| NO | 0.76–1.06 | 0.76–1.00 | 0.75–0.76 | 0.76–1.01 | 0.75–0.96 | 0.75–0.76 |
| $N_3$ | 0.91 | 0.85 | 0.76 | 0.88 | 0.83 | 0.75 |
| BN | 2.10 | 2.08 | 2.00 | 2.05 | 2.04 | 2.00 |

* For the cases in which a potential curve was evaluated, the variation over the range considered is given.
$\langle\hat{S}^2\rangle_1 = \langle\hat{S}^2\rangle + \langle\psi_0|\hat{S}^2|\psi_1\rangle$ (using intermediate normalization), in which $|\psi_0\rangle$ represents the Hartree-Fock wavefunction and $|\psi_1\rangle$ the first- order MBPT correction to the wavefunction as obtained in an MP2 calculation.

for open-shell CID and CISD gradients is present in this program, the optimizations were run using a derivative-free modification [Col76] of the Davidon-Fletcher-Powell [Fle63] method. Convergence criteria were tightened to increase numerical precision using the `TIGHT` keyword.

In certain cases (especially NO), the optimization presented difficulties; the bond distance was then determined by evaluating the energy at six points at a spacing of 0.02 Å, and finding the interpolation polynomial through these points, and performing a Dunham analysis [Dun32] on it.

### 5.2.3 Results and discussion

Table I presents the computed geometries at several electron correlation levels using the 3-21G [Bin80] and 6-31G* basis sets [Heh72] for the molecules BO, CCH, CN, $CO^+$, $N_3$ and BN, all of them selected for their high degree of spin contamination, as well as the closed-shell molecules BH, $H_2O$, and $N_2$. Table II lists expectation values of $\hat{S}^2$ at the corresponding levels; spin-projected values and expectation values from the first-order MBPT wavefunction are also included. The former is a qualitative indicator for multiple-contaminant character, the latter for improvement of spin-contamination with inclusion of electron correlation.

We are well aware of the fact, that the basis sets used are far too small to achieve any useful agreement with experiment for these molecules, and will therefore not go into any comparison with experimental bond lengths. Our sole intention is to demonstrate the anomaly discussed in the present Section using some appropriate model systems.

Table III: Harmonic frequencies ($cm^{-1}$) for some spin-contaminated diatomic radicals.

| | 3-21G | | 6-31G* | |
|---|---|---|---|---|
| | CISD | CID | CISD | CID |
| BO | 1723 | 1664 | 1780 | 1747 |
| CN | 1917 | 2102 | 2103 | 2282 |
| $CO^+$ | 2049 | 2243 | 2278 | 2448 |
| NO | 1807[a] | 3272[a] | 2632[a] | 2407[a] |

(a) numerical instability of the Dunham analysis was observed for this case.

It is immediately clear from Table I, that the effect is anything but minimal: for the NO, CN, $CO^+$, and BN radicals, a change in bond length of 0.02 Å or more is observed, which is twice as large as the SCF bond distance error in most molecules! Upon going from the 3-21G to the 6-31G* basis set, the effect decreases by as much as 30 to 50 %. This may indicate that very large basis sets would result in an acceptable error: a significant deviation will however most probably still remain. From the results for CCH, it is apparent that mainly the multiple bond is involved: the C-H bond hardly changes. It is also clear, that the effect increases with increasing contamination: the deviations for BO and $N_3$, which have a much lower deviation in $\langle \hat{S}^2 \rangle$ than the others, are also significantly smaller.

In view of the earlier discussion, it would be interesting to see whether the same phenomenon occurs in a closed-shell species with low-lying excited states. However, for BH a change in bond length of only 0.0017 Å is seen with the 3-21G basis set, compared to 0.0014 Å with the 6-31G* basis set. Noticeable as such an error would be in high-precision work, it is hardly as spectacular as any of the others. By comparison: the corresponding change for the bond-length of water, which is a singlet without any low-lying excited states, is 0.0014 Å with the 3-21G basis, and only 0.0006 Å with the 6-31G* basis. This suggests that with basis sets sufficiently large to obtain experimentally useful results, the error would be negligible. The effect on $N_2$, a well-behaved molecule with multiple bonds, is 0.0019 Å and 0.0016 Å with the 3-21 and 6-31G* basis sets, respectively.

The effects of unlinked clusters are also significant, though much smaller, as witnessed by the CCD results in Table I. They are also much more spurious.

The effect of single excitations on harmonic frequencies can also be studied since these are obtained as a by-product when the bond distance is being computed from a polynomial interpolation. Table III presents some of these frequencies. Again, it can be seen that the effect is sometimes quite significant, and may exceed 10 % of the calculated frequencies. In the case of NO, the Dunham analysis is numerically highly unstable, exhibiting clearly nonsensical values for the anharmonicity constant. Incidentally, this molecule has an enormous variation in $\langle \hat{S}^2 \rangle$ over the range considered.

In the light of these results, some doubt is cast on recent attempts [McD89] at cal-

culating radicaloid transition state structures with projected MP2 methods (using the 6-31G* basis set). Such methods do correct for spin-contamination effects on the double excitations, but cannot possibly account for the effect of single excitations. Furthermore, it is shown in the Appendix that the CISD energy is invariant under single spin annihilation. At the present time, the cheapest way of incorporating single excitation effects in gradient calculations appears to be CISD. CCSD [Pur82] would actually be the method of choice since it also eliminates the unlinked cluster contribution; however, its gradient evaluation is far from routine, as well as being computationally very demanding. Another solution, when no gradients are available, would be to perform CISD calculations and to correct with the Davidson-Silver formula [Dav77], which we have recently shown [Mar90b] to be markedly superior over other size-consistency corrections. Since no analytical derivatives of the size-consistency correction are obtained, this procedure would be more useful if a potential curve is also required.

### 5.2.4 Appendix: single spin projection invariance of CISD, CID and CCD energies

Using intermediate normalization for convenience, the spin-projected energy is defined as (following Schlegel [Sch88]):

$$E_p = \frac{\langle \hat{P}_s\psi_0|\hat{H}|\hat{P}_s\psi\rangle}{\langle \hat{P}_s\psi_0|\hat{P}_s\psi\rangle} \tag{5.1}$$

$$= \frac{\langle \psi_0|\hat{P}_s\hat{H}|\psi\rangle}{\langle \psi_0|\hat{P}_s|\psi\rangle} \tag{5.2}$$

The latter definition is also valid because $\hat{H}$ and $\hat{P}_s$ commute, and $\hat{P}_s$ is idempotent. $\hat{P}_s$ here represents the Löwdin spin projection operator [Low55]

$$\hat{P}_s = \prod_{k\neq s} \frac{\hat{S}^2 - k(k+1)}{s(s+1) - k(k+1)} \tag{5.3}$$

Applying the closure relationship, which states that the identity operator $\hat{I}$ may be written as

$$\hat{I} = |\psi_0\rangle\langle\psi_0| + \sum_i |\psi_i\rangle\langle\psi_i| \tag{5.4}$$

where the summation extends over all possible excited determinants, we obtain:

$$E_p = \frac{\langle \psi_0 | \hat{P}_s\hat{I}\hat{H} | \psi\rangle}{\langle \psi_0 | \hat{P}_s\hat{I} | \psi\rangle} = \frac{\langle \psi_0 | \hat{P}_s | \psi_0\rangle \langle \psi_0 | \hat{H} | \psi\rangle + \sum_i \langle \psi_0 | \hat{P}_s | \psi_i\rangle \langle \psi_i | \hat{H} | \psi\rangle}{\langle \psi_0 | \hat{P}_s | \psi_0\rangle + \sum_j \langle \psi_0 | \hat{P}_s | \psi_j\rangle \langle \psi_j | \psi\rangle} \tag{5.5}$$

If the Löwdin spin-projection operator $\hat{P}_s$ is approximated by annihilation of just a single spin contaminant, i.e. by

$$\hat{A}_{s+n} = \frac{\hat{S}^2 - (s+n)(s+n+1)}{s(s+1) - (s+n)(s+n+1)} \tag{5.6}$$

then $i$ and $j$ in (5.5) are restricted to single and double excitations (compare [Sch88], Eq.10). It is easily seen that $\hat{A}_{s+n}$ and $\hat{H}$ also commute, but $\hat{A}_{s+n}$ is no longer idempotent. This can be shown by writing $|\psi\rangle$ in terms of pure spin states:

$$|\psi\rangle = \sum_{m=0}^{\infty} d_m |\psi_{s+m}\rangle \tag{5.7}$$

$$\hat{S}^2|\psi\rangle = \sum_{m=0}^{\infty} (s+m)(s+m+1) d_m |\psi_{s+m}\rangle \tag{5.8}$$

With

$$(s+m)(s+m+1) - (s+n)(s+n+1) = 2s(m-n) + (m^2-n^2) + (m-n) \tag{5.9}$$

this yields

$$\hat{A}_{s+n}|\psi\rangle = \sum_{m=0}^{\infty} \left[\frac{2s(m-n) + m^2 - n^2 + m - n}{-2ns - n^2 - n}\right] d_m |\psi_{s+m}\rangle \tag{5.10}$$

$$= \sum_{m=0}^{\infty} \left[1 - \frac{2ms + m^2 + m}{2ns + n^2 + n}\right] d_m |\psi_{s+m}\rangle \tag{5.11}$$

It is then obvious that

$$\hat{A}^2_{s+n}|\psi\rangle = \hat{A}_{s+n}\left(\hat{A}_{s+n}|\psi\rangle\right) = \sum_{m=0}^{\infty} \left[1 - \frac{2ms + m^2 + m}{2ns + n^2 + n}\right]^2 d_m |\psi_{s+m}\rangle \tag{5.12}$$

The expression in square brackets is only equal to its square if m=0 (where it becomes unity) or m=n (where it becomes zero). For the other components, the idempotency does *not* hold, which is a consequence of the fact that the annihilator *does* affect states other than the one to be annihilated. Now Schlegel [Sch88] constructed a proof that CCSD is invariant under single spin projection upon the assumption that (5.1) and (5.2) are still equivalent when $\hat{P}_s$ is approximated by $\hat{A}_{s+n}$: we now see that this, and consequently the proof, is not generally valid since $\hat{A}_{s+n}$ is not idempotent. We may however investigate under what circumstances it does hold, exactly or approximately.

In practice, the principal contaminant is the next higher spin (i.e., triplet for an open-shell singlet, quartet for a doublet state, ...), so $\hat{A}_{s+n}$ is taken as $\hat{A}_{s+1}$

$$\hat{A}_{s+1} = \frac{\hat{S}^2 - (s+1)(s+2)}{s(s+1) - (s+1)(s+2)} \tag{5.13}$$

Then (5.12) becomes:

$$\hat{A}_{s+1}\,|\psi\rangle = \sum_{m=0}^{\infty}\left[1 - \frac{2ms + m^2 + m}{2s+2}\right] d_m\,|\psi_{s+m}\rangle \tag{5.14}$$

Now when $d_m (m \geq 2)$ goes to zero (i.e. when no appreciable higher contamination is present), $|\psi_{s+m}\rangle (m \geq 2)$ will make a negligible contribution both to $\hat{A}_{s+1}|\psi\rangle$ and $\hat{A}^2_{s+1}|\psi\rangle$. Under this condition:

$$\lim_{d_m \to 0} \hat{A}^2_{s+1}\,|\psi\rangle = \lim_{d_m \to 0} \hat{A}_{s+1}\,|\psi\rangle = d_0\,|\psi_s\rangle \quad \text{with all } m \geq 2 \tag{5.15}$$

Then under these circumstances (5.1) and (5.2) are effectively equivalent, and the invariance for CCSD holds approximately (exactly in the limiting case). One important practical situation where this happens is the breaking of a single bond: it is well known, that CCSD performs very well for this problem. A simple check whether the condition is fulfilled can be made by inspection of $\langle \hat{S}^2 \rangle$ for the annihilated wavefunction: it should be close to $s(s+1)$.

The same limiting invariance properties as for CCSD can be proven for CISD. Under the conditions stated above, (5.5) holds in the limit for $\hat{A}_{s+1}$ (we will omit the "lim" from now on):

$$E_p = \frac{\left\langle \psi_0 \middle| \hat{A}_{s+n} \middle| \psi_0 \right\rangle \left\langle \psi_0 \middle| \hat{H} \middle| \psi \right\rangle + \sum\limits_{S,D} \left\langle \psi_0 \middle| \hat{A}_{s+n} \middle| \psi_i \right\rangle \left\langle \psi_i \middle| \hat{H} \middle| \psi \right\rangle}{\left\langle \psi_0 \middle| \hat{A}_{s+n} \middle| \psi_0 \right\rangle + \sum\limits_{S,D} \left\langle \psi_0 \middle| \hat{A}_{s+n} \middle| \psi_j \right\rangle \langle \psi_j | \psi \rangle} \tag{5.16}$$

Using intermediate normalization, the CISD method is defined by the equations

$$|\psi\rangle = |\psi_0\rangle + \sum_S c_s\,|\psi_S\rangle + \sum_D c_D\,|\psi_D\rangle \tag{5.17}$$

$$E_{\text{CISD}} = \left\langle \psi_0 \middle| \hat{H} \middle| \psi \right\rangle \tag{5.18}$$

$$c_S E_{\text{CISD}} = \left\langle \psi_S \middle| \hat{H} \middle| \psi \right\rangle \tag{5.19}$$

$$c_D E_{\text{CISD}} = \left\langle \psi_D \middle| \hat{H} \middle| \psi \right\rangle \tag{5.20}$$

Substitution in (5.16) yields:

$$\begin{aligned}
(E_p)_{\text{CISD}} &= \frac{\left\langle \psi_0 \middle| \hat{A}_{s+1} \middle| \psi_0 \right\rangle \left\langle \psi_0 \middle| \hat{H} \middle| \psi \right\rangle + \sum\limits_S \left\langle \psi_0 \middle| \hat{A}_{s+1} \middle| \psi_S \right\rangle \left\langle \psi_S \middle| \hat{H} \middle| \psi \right\rangle}{\left\langle \psi_0 \middle| \hat{A}_{s+1} \middle| \psi_0 \right\rangle + \sum\limits_S \left\langle \psi_0 \middle| \hat{A}_{s+1} \middle| \psi_S \right\rangle \langle \psi_S | \psi \rangle + \sum\limits_D \left\langle \psi_0 \middle| \hat{A}_{s+1} \middle| \psi_D \right\rangle \langle \psi_D | \psi \rangle} \\
&\quad + \frac{\sum\limits_D \left\langle \psi_0 \middle| \hat{A}_{s+1} \middle| \psi_D \right\rangle \left\langle \psi_D \middle| \hat{H} \middle| \psi \right\rangle}{\left\langle \psi_0 \middle| \hat{A}_{s+1} \middle| \psi_0 \right\rangle + \sum\limits_S \left\langle \psi_0 \middle| \hat{A}_{s+1} \middle| \psi_S \right\rangle \langle \psi_S | \psi \rangle + \sum\limits_D \left\langle \psi_0 \middle| \hat{A}_{s+1} \middle| \psi_D \right\rangle \langle \psi_D | \psi \rangle} \\
&= \frac{\left( \left\langle \psi_0 \middle| \hat{A}_{s+1} \middle| \psi_0 \right\rangle + \sum\limits_S \left\langle \psi_0 \middle| \hat{A}_{s+1} \middle| \psi_S \right\rangle c_S + \sum\limits_D \left\langle \psi_0 \middle| \hat{A}_{s+1} \middle| \psi_D \right\rangle c_D \right) E_{\text{CISD}}}{\left\langle \psi_0 \middle| \hat{A}_{s+1} \middle| \psi_0 \right\rangle + \sum\limits_S \left\langle \psi_0 \middle| \hat{A}_{s+1} \middle| \psi_S \right\rangle c_S + \sum\limits_D \left\langle \psi_0 \middle| \hat{A}_{s+1} \middle| \psi_D \right\rangle c_D} \\
&= E_{\text{CISD}}
\end{aligned} \tag{5.21}$$

The CID equations follow from (5.17), with $c_s \equiv 0$ and $E_{\text{CISD}}$ then becoming $E_{\text{CID}}$. Because $c_s$ vanishes, the middle terms in numerator and denominator of (5.16) vanish too and one obtains

$$(E_p)_{\text{CID}} = E_{\text{CID}} \tag{5.22}$$

An analogous point concerning CCD vs. CCSD leads to

$$(E_p)_{\text{CCD}} = E_{\text{CCD}} \tag{5.23}$$

It was already noted [Sch88] that

$$(E_p)_{QCISD} = E_{QCISD} \tag{5.24}$$

$$(E_p)_{\text{CCSD}} = E_{\text{CCSD}} \tag{5.25}$$

As a final note, it is remarked that the equality does *not* hold exactly for linearized coupled cluster (L-CCA) energies, even in the limiting case.

An alternative definition of the projected energy could have been given as follows:

$$E_p = \frac{\left\langle \hat{P}_s\psi \middle| \hat{H} \middle| \hat{P}_s\psi \right\rangle}{\left\langle \hat{P}_s\psi \middle| \hat{P}_s\psi \right\rangle} \tag{5.26}$$

$$= \frac{\left\langle \psi \middle| \hat{H}\hat{P}_s \middle| \psi \right\rangle}{\langle \psi | \hat{P}_s | \psi \rangle} \tag{5.27}$$

in which (5.26) and (5.27) are again equivalent for the full Löwdin operator $\hat{P}_s$ but not when $\hat{P}_s$ is approximated by a single annihilator $\hat{A}_{s+n}$. Again using intermediate normalization for $|\psi\rangle$ (which may be done because the intermediate and fully normalized wavefunctions differ only in a constant factor which cancels between numerator and denominator), it is easily verified that, upon going through the same steps as in the present derivation, the same result is obtained.

If $\hat{P}_s$ were approximated by annihilation of the next two contaminants, i.e.

$$\hat{P}_s \approx \hat{A}_{s+1}\hat{A}_{s+2} \tag{5.28}$$

then $\hat{A}_{s+1}\hat{A}_{s+2}$ is again not idempotent, but behaves effectively so when no appreciable higher contaminants are present (i.e. $d_m \to 0 (m \geq 3)$). Realizing that two extra excitation levels are introduced for every extra projector [Kno88], it is easily seen that under these circumstances CCSDTQ and CISDTQ would be effectively invariant under double spin annihilation. A practical situation would be the breaking of a double bond or the simultaneous breaking of two single bonds. The same conclusion was already suggested in [Sch88].

## 5.3 On size consistency corrections for limited configuration interaction calculations

### 5.3.1 Introduction

Limited configuration interaction (CI) theory [Sha77], the oldest electron correlation method, has always retained a certain popularity. It is possible with all commonly available quantum chemistry program suites, including the GAUSSIAN series [Gau82, Gau86, Gau88], HONDO [Hon87], CADPAC [Cad87], and GAMESS [Gam88]. Although driven from first place by Møller-Plesset based many-body perturbation methods [Kri80b, and references therein], it still has retained a comfortable second place, even with the advent of coupled cluster [Bar89] methods.

Easy availability is one factor contributing to its wide use. Computational cost, a problem with earlier implementations, is now very much decreased through shape-driven GUGA [Sax82, Sie84] techniques. Thirdly, evaluation of gradients is relatively inexpensive, because the energy is already stationary with respect to the excitation coefficients [Kri80c], and coupled-perturbed Hartree Fock (CPHF) equations [Ger68] need only be solved for the Hartree-Fock orbitals. This is certainly not true for Møller-Plesset or coupled cluster methods. Whereas MP2 derivatives can be efficiently computed through Handy's Z-vector scheme [Han84], they only contribute (except with very large basis sets [Sim88]) for about half the difference between Hartree-Fock and exact (full CI) wavefunctions [DeF79]. Higher order MP gradients become progressively more difficult, whereas coupled cluster gradients are computationally very demanding. A final advantage of CI is its being variational: consequently, the limited CI energy is always an upper limit to the exact basis set (or full CI) energy. Neither for MBPT, nor for coupled cluster wavefunctions is this necessarily true.

However, limited CI has the unfortunate disadvantage of not being size-extensive: the CI energy for two systems at infinite distance is not equal to the sum of the individual CI energies, which makes the method as it is unusable for the evaluation of dissociation energies. Even for small systems, the error is far from academic [Ahl74]; for large systems, it may exceed the interaction energy to be evaluated.

Over the years, various simple correction formulas have been proposed. The four most important ones are the Davidson correction [Lan74], the renormalized Davidson correction [Bar77, Sie78], the Davidson-Silver correction [Dav77], and the Pople correction [Pop77]. In practical applications, the Davidson correction [Lan74] is used almost exclusively, although none of the four formulas requires additional computation time beyond the limited CI calculation and the other formulas may be expected to work better on theoretical grounds (see below for discussion). It is therefore unfortunate that no systematic numerical comparisons between these formulas have ever been performed, except

for a very recent paper by Knowles *et al.* [Kno90] where Davidson- and Davidson-Silver corrected MRD-CI energies have been compared with full CI results. Such a comparison is not entirely valid since (a) the multireference analogues of the Davidson and Davidson-Silver formulas have no firm theoretical basis; (b) even with an exact correction for size inconsistency, the MRD-CI energy is not equivalent to the full CI energy because the ansatz is still incomplete (see also below).

The purpose of this Section is a critical assessment of the four formulas, based both on numerical computations and a theoretical comparison within MBPT and coupled cluster frameworks.

### 5.3.2 Size-consistency corrections

At any order of perturbation theory, the correlation energy contains four types of contributions:

(a) linked, connected diagrams

(b) diagrams that are linked, but disconnected

(c) renormalization terms

(d) unlinked disconnected diagrams

Furthermore, both (b) and (d) may be of the 'exclusion principle violating' (EPV) variety [Kel69], in which two or more occupied or virtual indices coincide between the disconnected parts of the diagram.

One formulation [Rob75] of the famous 'linked cluster theorem' [Bru55, Gol69] states that the sum of the renormalization and unlinked cluster terms cancels at any order of perturbation theory. It is perhaps the place to point out [Rob75], that this is only true if the EPV diagrams are included properly.

In a CID calculation, renormalization terms are present, but no unlinked cluster diagrams. The CID equations in iterative form are given by

$$c_D \Delta E = \langle \psi_D | \hat{H}' | (1 + \hat{C}_2) \psi_0 \rangle \tag{5.29}$$

$$\Delta E = \langle \psi_0 | \hat{H}' | \hat{C}_2 \psi_0 \rangle \tag{5.30}$$

in which $\Delta E$ represents the CID correlation energy, and $\hat{H}' \equiv H - H_0$. $\psi_0$ is the Hartree-Fock wavefunction; the zero-order Hamiltonian $H_0$ is the sum of the Fock operators for the electrons. $\hat{C}_2$ represents the double excitation operator, $\hat{C}_2 |\psi_0\rangle = \sum_D c_D |\psi_D\rangle$.

Term (a) is a consequence of the left-hand part of (5.29), and consequently of the $\Delta E$ expression, which may be seen as an intermediate normalization condition (hence the name). If unlinked EPV and non-EPV terms are added, we obtain

$$\Delta E = \sum_D t_D \langle \psi_0 | \hat{H}' | \psi_D \rangle \tag{5.31}$$

$$
\begin{aligned}
t_D \Delta E &= \langle \psi_D | \hat{H}' | (1 + \hat{T}_2 + (\hat{T}_2^2/2)_{UL}) \psi_0 \rangle \\
&= \langle \psi_D | \hat{H}' | (1 + \hat{T}_2) \psi_0 \rangle + \frac{1}{2} \sum_{D'} t_D t_{D'} [\langle \psi_D | \hat{H}' | \psi_{DD'} \rangle + \langle \psi_D | \hat{H}' | \psi_{D'D} \rangle] \\
&= \langle \psi_D | \hat{H}' | (1 + \hat{T}_2) \psi_0 \rangle + \sum_{D'} t_D t_{D'} \langle \psi_D | \hat{H}' | \psi_{DD'} \rangle \\
&= \langle \psi_D | \hat{H}' | (1 + \hat{T}_2) \psi_0 \rangle + \sum_{D'} t_D t_{D'} \langle \psi_0 | \hat{H}' | \psi_{D'} \rangle \\
&= \langle \psi_D | \hat{H}' | (1 + \hat{T}_2) \psi_0 \rangle + t_D \Delta E
\end{aligned} \tag{5.32}
$$

from which

$$
\langle \psi_D | \hat{H}' | (1 + \hat{T}_2) \psi_0 \rangle = 0 \tag{5.33}
$$

Eq. (5.33) is none other than the amplitude equation for L-CCD = D-MBPT($\infty$).

Analogously, size-consistency correction of the CISD equations would lead to the L-CCSD = SD-MBPT($\infty$) method. So assessment of any size-consistency correction formula can only be made by comparison to the L-CCA result, not to ordinary CCA and certainly not to full CI, as is sometimes done.

One way to derive a correction formula for size inconsistency is an approximate evaluation of the renormalization terms, or of the unlinked cluster terms (in the latter case, one assumes that EPV diagrams may be neglected). It was discovered quite early on [Bru55], that the first unlinked diagrams appear at fourth order, and that they could be computed as

$$
E^{(2)} \langle 1 | 1 \rangle \tag{5.34}
$$

where $E^{(2)}$ is the second-order MBPT energy, and $|1\rangle$ the first-order MBPT wave function. By approximating $E^{(2)}$ by the CID correlation energy $E_{\mathrm{CID}}$ and $\langle 1|1\rangle$ by $1 - C_0^2$ (where $C_0$ represents the coefficient of the Hartree-Fock reference state $|0\rangle$), the familiar Davidson formula [Lan74] is obtained[1]

$$
E_{\mathrm{DC}} = (1 - C_0^2) E_{\mathrm{CID}} \tag{5.35}
$$

Because of its simplicity, and of its apparent usefulness when the perturbation series converges quickly and $C_0$ is not too far from unity (the two usually occur together because multireference character and slow PT series convergence are both linked to the existence of low-lying excited states [Gil88]), (5.35) has become so popular that [Lan74] appeared as a 'citation classic' in Current Contents. However, when low-lying excited states exist, the formula becomes a poor approximation to an approximation for two reasons. The first (which will be shown below is not important) is the fact that $E_{\mathrm{CID}}$ has little to do with $E^{(2)}$ anymore. More importantly, the expression $(1 - C_0^2)$ for the wavefunction

[1] This and related formulas are given here for CID, but are also valid for CISD.

overlap disregards the intermediate normalization used in perturbation theory. Taking it into account leads to the so-called renormalized Davidson correction [Bar77, Sie78]:

$$E_{\mathrm{RDC}} = [(1 - C_0^2)/C_0^2]E_{\mathrm{CID}} \tag{5.36}$$

It is at least correct to fourth order in MBPT: however, as pointed out by Siegbahn [Sie78], it is much more accurate than it looks (*vide infra*).

Neither (5.36) nor (5.35) is exact for a two-electron system, where the correction should vanish. Seeing this as an important deficiency, Pople *et al.* [Pop77] derived a different formula from consideration of the CI matrix for $N$ noninteracting minimal basis set two-electron systems. Manipulating the expression for the correlation energy to eliminate the integrals, they obtained the expression:

$$E_{\mathrm{PC}} = E_{\mathrm{CID}}\left[\frac{(2C_0^2 - 1)N}{2(1 - C_0^2)}\left(\sqrt{1 + \frac{4C_0^2(1 - C_0^2)}{(2C_0^2 - 1)^2}\frac{1}{N}} - 1\right) - 1\right] \tag{5.37}$$

or, more readably (with $z \equiv (1 - C_0^2)/(2C_0^2 - 1)$)

$$E_{\mathrm{PC}} = E_{\mathrm{CID}}\left[\frac{N}{2z}\left(\sqrt{1 + \frac{4z(1+z)}{N}} - 1\right) - 1\right] \tag{5.38}$$

where they took $N$ to be $n/2$, with $n$ representing the number of electrons correlated in the CI calculation. Numerical tests were reported to indicate [Luc78], that this formula was inferior to the simple Davidson correction. However, as the tests were limited to two electronic transition energies of glyoxal (with a relatively small basis set), they hardly warrant such far-reaching conclusions.

Davidson and Silver [Dav77] considered the same model, but chose to eliminate $N$ rather than the integrals. Sacrificing the exactness for a two-electron system (the deviation of which is very small in practice), they made various assumptions about the integrals in the low and high $N$ limits, and thus obtained the formula carrying their names:

$$E_{\mathrm{DSC}} = \frac{(1 - C_0^2)E_{\mathrm{CID}}}{2C_0^2 - 1} = zE_{\mathrm{CID}} \tag{5.39}$$

They expected this formula to hold for larger values of N and smaller values of $C_0^2$ than (5.35), but presented no numerical tests. It is easily seen by expanding the square root in (5.37) in a power series, that $E_{\mathrm{PC}}$ is an upper bound to $E_{\mathrm{DSC}}$, and that it approaches $E_{\mathrm{DSC}}$ in the high-$N$ limit.

Siegbahn [Sie78] derived an exact expression for the renormalization energy

$$E_{\mathrm{R}} = \Delta E\langle\psi'|\psi'\rangle + (\Delta E)^2 \sum_{K=0}^{\infty} \langle\psi'|\hat{R}(\hat{V}\hat{R})^K|\psi'\rangle \tag{5.40}$$

where $|\psi'\rangle \equiv |\psi\rangle - |0\rangle$ and $\hat{R}$ is the so-called propagator or resolvent

$$\hat{R} = \sum_i \frac{|\psi_i\rangle\langle\psi_i|}{E_i^{(0)} - E_0^{(0)}} \tag{5.41}$$

Furthermore

$$\langle\psi'|\psi'\rangle = (1 - C_0^2)/C_0^2 \tag{5.42}$$

By approximating $\Delta E$ by $E_{CID}$ and neglecting the term involving the propagator series, the renormalized Davidson correction is recovered. The leading term of the propagator series is $(\Delta E)^2\langle\psi'|\hat{R}|\psi'\rangle$, which appears for the first time in sixth order. As the wavefunction overlap starts out at second order and the CID (or CISD) energy is correct to third order, the first deviation there appears at sixth order. Consequently, the renormalized Davidson correction is correct to fifth order in perturbation theory.

However, it is more elegant (and not much more difficult) to substitute $E_{\rm CID} + E_{\rm R}$ for $\Delta E$. If the propagator series is then neglected and the resulting equation is solved for $E_{\rm R}$, one obtains:

$$E_{\rm R} = \frac{\langle\psi'|\psi'\rangle E_{\rm CID}}{1 - \langle\psi'|\psi'\rangle} = \frac{(1 - C_0^2)E_{\rm CID}}{2C_0^2 - 1} \tag{5.43}$$

which is of course just the Davidson-Silver correction. Considering the terms of $E_{\rm R}$ at different orders of MBPT

$$E_{\rm R} = E_{\rm R}^{(4)} + E_{\rm R}^{(5)} + E_{\rm R}^{(6)} + \ldots \tag{5.44}$$

( $E_{\rm R}^{(1)} = E_{\rm R}^{(2)} = E_{\rm R}^{(3)} = 0$), we find that the two correction formulas differ for the first time at sixth order, with leading term $E_{\rm R}^{(4)}\langle 1|1\rangle$. As both the first-order wavefunction overlap and the fourth-order renormalization energy can become quite substantial in practice, the difference is far from academic.

The difference with the regular Davidson formula may be found by expanding $1 - C_0^2$ in terms of the wavefunction overlap:

$$1 - C_0^2 = \frac{\langle\psi'|\psi'\rangle}{1 + \langle\psi'|\psi'\rangle} = \langle\psi'|\psi'\rangle - \langle\psi'|\psi'\rangle^2 + \ldots \tag{5.45}$$

It is then found that

$$E_{\rm RDC} - E_{\rm DC} = E_{\rm CID}\langle\psi'|\psi'\rangle^2 - \ldots = E^{(2)}\langle 1|1\rangle^2 + \ldots \tag{5.46}$$

which is of sixth order too. With $E_{\rm CID}$ and the wavefunction overlap potentially both becoming quite large, this means that the difference certainly cannot be neglected.

Notating the correction formulas as power series in $x \equiv 1 - C_0^2$ or $y \equiv (1 - C_0^2)/C_0^2$,

$$E_{\rm DC} = E_{\rm CID}x \tag{5.47}$$

$$E_{\rm RDC} = E_{\rm CID}(x + x^2 + x^3 + \ldots) = E_{\rm CID}y \tag{5.48}$$

$$E_{\rm DSC} = E_{\rm CID}(x + 2x^2 + 4x^3 + \ldots) = E_{\rm CID}(y + y^2 + y^3 + \ldots) \tag{5.49}$$

and taking into account that the propagator series term $(\Delta E)^2 \sum_{K=0}^{\infty} \langle\psi'|\hat{R}(\hat{V}\hat{R})^K|\psi'\rangle$ will be negative from its mathematical form, we obtain the inequalities

$$E_{\rm CID} > E_{\rm CID} + E_{\rm DC} > E_{\rm CID} + E_{\rm RDC} > E_{\rm CID} + E_{\rm DSC} > E_{L-CCA} \tag{5.50}$$

This conclusion appears to be anomalous for a two-electron system: it is however a consequence of the fact, that a L-CCA calculation includes certain EPV diagrams that are not present in a CI calculation [Pal82]. We will digress a bit on this point as it serves to justify the Pople correction from a MBPT/CC viewpoint.

Compared to a CID calculation, the LCCD calculation contains the unlinked part of $\hat{T}_2^2/2$. However, as there are only two electrons, this contains only terms in which the same electrons have been annihilated twice. Compared to the CCD calculation, the only thing that is lacking is the linked part of $\hat{T}_2^2/2$, in which there are also only terms of the EPV variety. As CID and CCD results are both equivalent to a full CI for a two-electron system, this implies that the two sets of EPV terms are equal but opposite in sign. If we now partition $\hat{T}_2^2/2$ for a system with more than two electrons in an EPV part and a non-EPV part, Pople's correction is equivalent to (a) neglecting the non-EPV part; and (b) assuming that the linked EPV diagrams cancel their unlinked counterparts in the same way as in the two-electron case. It should thus be regarded as an approximation to CCD, not to LCCD.[2] As the neglected non-EPV linked diagrams are disconnected, they will raise the energy and the Pople-corrected CID energy should thus normally be a lower bound to the CCD energy.

Expansion of the Pople correction in $x$ and $y$, respectively, yields

$$E_{\mathrm{PC}} = E_{CID}\left[x(\frac{N-1}{N}) + 2x^2(\frac{N-1}{N})^2 + x^3(\frac{N-1}{N})^2(\frac{4N-5}{N}) + \ldots\right] \tag{5.51}$$

$$E_{\mathrm{PC}} = E_{CID}\left[y(\frac{N-1}{N}) + y^2(\frac{N-1}{N})(\frac{N-2}{N}) + y^3(\frac{N-1}{N})(\frac{5-5N+N^2}{N^2}) + \ldots\right] \tag{5.52}$$

By truncating both series after the quadratic term, expanding the products involving $N$, and neglecting higher-order terms in $1/N$, we obtain the following inequalities:

$$E_{\mathrm{PC}} > E_{\mathrm{DC}} \quad \text{for} \quad N < 2 + \frac{1}{2x} \tag{5.53}$$

$$E_{\mathrm{PC}} > E_{\mathrm{RDC}} \quad \text{for} \quad N < 3 + \frac{1}{y} = 3 + \frac{x}{1-x} \tag{5.54}$$

Numerical tests for various values of $x$ ranging from $1/200$ to $1/3$ showed both inequalities to be correct to the nearest integer $N$.

Let us now verify our conclusions with some numerical results.

### 5.3.3 Numerical results and discussion

LCCD results were compiled from the literature [Bar77, Jan80, Pal82, Pal72, Kva82, Pop78]; details on basis sets and reference geometries may be found there. In [Jan80,

[2] Because the difference between L-CCA ≡ CEPA-0 and CID+PC is essentially an approximate EPV account, the Pople correction actually is most closely related to CEPA($n$) with $n > 0$ (Section 1.8.1).

Table IV: Correlation energies (millihartree; minus sign omitted) at the CID, CCD, and L-CCD levels, as well as with a number of different size-consistency correction formulas.

| Species | CID | x | DC | RDC | DSC | PC | L-CCD | CCD |
|---|---|---|---|---|---|---|---|---|
| $H_2O$ | 274.020[a] | 0.052952 | 288.530[a] | 289.341 | 290.249 | 286.696 | 290.750[a] | – |
| $H_4(\alpha{=}.5)$ | 52.515[b] | 0.061773 | 55.759[b] | 55.973 | 56.216 | 54.242 | 56.260[b] | 53.572[b] |
| $H_4(\alpha{=}.2)$ | 55.861[b] | 0.070783 | 59.815[b] | 60.116 | 60.467 | 57.986 | 60.553[b] | 57.233[b] |
| $H_4(\alpha{=}.1)$ | 63.340[b] | 0.093338 | 69.252[b] | 69.861 | 70.609 | 66.592 | 71.017[b] | 65.318[b] |
| $H_4(\alpha{=}.05)$ | 73.785[b] | 0.142319 | 84.286[b] | 86.028 | 88.464 | 79.865 | 91.829[b] | 76.635[b] |
| $P_4(\alpha{=}10)$ | 53.013[b] | 0.058231 | 56.100[b] | 56.291 | 56.507 | 54.650 | 56.507[b] | 54.650[b] |
| $P_4(\alpha{=}4)$ | 55.504[b] | 0.060987 | 58.889[b] | 59.109 | 59.359 | 57.305 | 59.364[b] | 57.258[b] |
| $P_4(\alpha{=}2.2)$ | 81.300[b] | 0.191390 | 96.860[b] | 100.543 | 106.510 | 90.790 | 125.211[b] | 84.897[b] |
| $D_4(\alpha{=}6)$ | 53.076[b] | 0.058200 | 56.165[b] | 56.356 | 56.572 | 54.714 | 56.572[b] | 54.714[b] |
| $D_4(\alpha{=}4)$ | 53.105[b] | 0.057452 | 56.156[b] | 56.342 | 56.552 | 54.722 | 56.555[b] | 54.697[b] |
| $D_4(\alpha{=}2)$ | 52.515[b] | 0.061773 | 55.759[b] | 55.973 | 56.216 | 54.242 | 56.260[b] | 53.572[b] |
| $D_4(\alpha{=}1.5)$ | 56.790[b] | 0.076404 | 61.129[b] | 61.488 | 61.912 | 59.135 | 62.001[b] | 57.644[b] |
| $D_4(\alpha{=}1)$ | 67.575[b] | 0.104654 | 74.647[b] | 75.474 | 76.519 | 71.511 | 76.704[b] | 68.255[b] |
| CO(large CI) | 253.290[c] | 0.070986 | 271.270[c] | 272.644 | 274.245 | 270.823 | 275.610[c] | – |
| CO(small CI) | 131.450[c] | 0.045873 | 137.480[c] | 137.770 | 138.089 | 137.058 | 138.200[c] | – |
| $BH_3$ | 47.150[d] | 0.030329 | 48.580[d] | 48.625 | 48.672 | 48.273 | 48.675[d] | 48.048[d] |

(a) [Bar77]
(b) [Jan80]. $H_4$ represents two $H_2$ molecules in a trapezoidal configuration with the three shorter distances equal to 2 a.u. The inner bond angle is taken as $\pi(\alpha{+}1/2)$. $D_4$ stands for a rectangular arrangement, the shorter distance again equal to 2 a.u., the larger to $\alpha$ a.u.. $P_4$ finally represents a linear arrangement, with outer bond distances 2 a.u. and inner bond distance $\alpha$ a.u..
(c) [Pal82]
(d) [Pal72]
Further details about basis set and geometry may be found in these references.

Kva82, Pop78], CCD results are also given; [Bar77, Jan80, Pal82, Pal72] also list CID and Davidson-corrected CID energies. From the latter, the renormalized Davidson, Davidson-Silver and Pople-corrected CID energies could be derived without further calculations. For the cases treated in Refs.[Kva82, Pop78], CID calculations were performed with the specified basis sets and geometries using the GAUSSIAN 86 program [Gau86], running on a VaxStation 2000 under MicroVMS 4.7. The `NORM(A)` found in the GAUSSIAN 86 output is easily verified to be $1/C_0$ from comparing the regular and intermediate normalization expressions; the various size-consistency corrected energies could then easily be obtained. All results may be found in Table IV.

The energy sequence (5.50) is confirmed throughout. It is also found throughout the whole Table (except for HF, where the difference is very small) that $E_{\mathrm{CCD}} > E_{\mathrm{PC}}$, as predicted, as well as that $E_{\mathrm{PC}} > E_{\mathrm{DC}}$, which is a consequence of the small value of $N$ for these systems. Large values of $N$ would lead to violation of the last equality, with $E_{\mathrm{PC}} > E_{\mathrm{DSC}}$ still holding, however.

The results for $H_2$ illustrate our remarks on two-electron systems: $E_{\mathrm{CID}}$ is equal to $E_{\mathrm{CCD}}$, whereas $E_{\mathrm{CID}} > E_{\mathrm{LCCD}}$. It is also seen, that the Davidson, renormalized Davidson and Davidson-Silver energies for $H_2$ are indistinguishable from the LCCD result to the accuracy given. Similar conclusions can be drawn for LiH (the core electrons were frozen

Table IV: (continued)

| Species | CID | x | DC | RDC | DSC | PC | L-CCD | CCD |
|---|---|---|---|---|---|---|---|---|
| $CH^+$ | 68.581[e] | 0.061549 | 72.802[e] | 73.078 | 73.394 | 71.643 | 73.61[e] | 70.31[e] |
| $BeH_2$ | 39.786 | 0.027072 | 40.863 | 40.893 | 40.924 | 40.530 | 40.93[e] | 40.23[e] |
| LiH(1.20Å) | 17.688 | 0.015185 | 17.956 | 17.960 | 17.965 | 17.824 | 17.97[e] | 17.69[e] |
| LiH(1.40Å) | 17.472 | 0.016098 | 17.754 | 17.758 | 17.763 | 17.615 | 17.76[e] | 17.48[e] |
| LiH(1.6409Å) | 18.393 | 0.019260 | 18.747 | 18.754 | 18.761 | 18.573 | 18.76[e] | 18.40[e] |
| LiH(1.80Å) | 19.468 | 0.022476 | 19.905 | 19.916 | 19.926 | 19.692 | 19.93[e] | 19.47[e] |
| LiH(2.0Å) | 21.194 | 0.027800 | 21.783 | 21.800 | 21.818 | 21.497 | 21.82[e] | 21.20[e] |
| LiH(2.50Å) | 26.776 | 0.047617 | 28.051 | 28.114 | 28.185 | 27.445 | 28.20[e] | 26.78[e] |
| BH(0.80Å) | 52.800 | 0.069676 | 56.479 | 56.754 | 57.075 | 55.500 | 57.37[e] | 53.93[e] |
| BH(1.00Å) | 55.751 | 0.068687 | 59.580 | 59.863 | 60.190 | 58.557 | 60.48[e] | 57.09[e] |
| BH(1.2313Å) | 60.241 | 0.070071 | 64.462 | 64.780 | 65.150 | 63.341 | 65.43[e] | 61.91[e] |
| BH(1.40Å) | 63.783 | 0.073241 | 68.454 | 68.824 | 69.256 | 67.229 | 69.49[e] | 65.73[e] |
| BH(1.60Å) | 68.216 | 0.079478 | 73.638 | 74.106 | 74.662 | 72.252 | 74.88[e] | 70.61[e] |
| BH(2.00Å) | 78.308 | 0.100712 | 86.195 | 87.078 | 88.184 | 84.363 | 88.47[e] | 82.01[e] |
| $B(^2P)$ | 93.626 | 0.057954 | 99.052 | 99.386 | 99.764 | 97.122 | 100.2[f] | 95.5[f] |
| $B(^4P)$ | 48.351 | 0.009865 | 48.828 | 48.833 | 48.838 | 48.641 | 48.8[f] | 48.6[f] |
| $Be(^1S)$ | 75.266 | 0.074277 | 80.857 | 81.305 | 81.832 | 78.281 | 82.6[f] | 77.7[f] |
| $Be(^3P)$ | 38.202 | 0.006329 | 38.444 | 38.446 | 38.447 | 38.324 | 38.5[f] | 38.3[f] |
| BeH | 71.993 | 0.027352 | 73.962 | 74.017 | 74.076 | 73.214 | 74.2[f] | 72.9[f] |
| $BeH_2$ | 100.549 | 0.038134 | 104.383 | 104.535 | 104.700 | 103.241 | 104.8[f] | 103.0[f] |
| BH | 120.532 | 0.067877 | 128.713 | 129.309 | 129.998 | 126.521 | 131.3[f] | 125.3[f] |
| $BH_2$ | 122.183 | 0.042387 | 127.362 | 127.591 | 127.842 | 126.119 | 128.0[f] | 125.3[f] |
| $C(^3P)$ | 112.309 | 0.041098 | 116.925 | 117.123 | 117.338 | 115.563 | 117.6[f] | 114.1[f] |
| $C(^5S)$ | 64.864 | 0.011693 | 65.622 | 65.631 | 65.640 | 65.377 | 65.7[f] | 65.3[f] |
| $CH(^2\Pi)$ | 142.839 | 0.052459 | 150.332 | 150.747 | 151.210 | 148.621 | 151.9[f] | 147.2[f] |
| $CH_2(^1A_1)$ | 173.553 | 0.061176 | 184.170 | 184.862 | 185.650 | 182.313 | 187.7[f] | 181.1[f] |
| $CH_2(^3B_1)$ | 151.686 | 0.042835 | 158.183 | 158.474 | 158.792 | 156.891 | 159.0[f] | 155.8[f] |
| $CH(^4\Sigma^-)$ | 115.623 | 0.032109 | 119.335 | 119.458 | 119.590 | 118.401 | 119.7[f] | 117.5[f] |
| F | 206.410 | 0.025981 | 211.772 | 211.915 | 212.066 | 210.756 | 212.1[f] | 210.6[f] |
| HF | 257.772 | 0.036439 | 267.166 | 267.521 | 267.904 | 265.750 | 268.1[f] | 266.0[f] |
| $H_2$ | 35.782 | 0.016574 | 36.375 | 36.385 | 36.395 | 35.782 | 36.4[f] | 35.8[f] |
| Li | 32.763 | 0.003369 | 32.874 | 32.874 | 32.875 | 32.800 | 32.9[f] | 32.8[f] |
| LiH | 62.265 | 0.025439 | 63.849 | 63.890 | 63.934 | 63.078 | 64.0[f] | 63.1[f] |
| N | 130.878 | 0.027166 | 134.434 | 134.533 | 134.638 | 133.520 | 134.8[f] | 132.6[f] |
| NH | 165.963 | 0.038663 | 172.380 | 172.638 | 172.918 | 171.070 | 173.1[f] | 170.0[f] |
| $NH_2$ | 203.910 | 0.048496 | 213.799 | 214.303 | 214.861 | 212.225 | 215.2[f] | 211.1[f] |
| O | 166.223 | 0.026842 | 170.685 | 170.808 | 170.938 | 169.710 | 171.0[f] | 169.1[f] |
| OH | 210.363 | 0.038317 | 218.423 | 218.745 | 219.092 | 217.028 | 219.3[f] | 216.4[f] |
| $H_2O$ | 255.231 | 0.047594 | 267.379 | 267.986 | 268.657 | 265.746 | 269.0[f] | 265.5[f] |

(e) [Kva82]
(f) [Pop78]
Further details about basis set and geometry may be found in these references.

both in [Kva82] and this work, so it is a two-electron system as far as the correlation energy is concerned).

The results from [Jan80] are actually for two $H_2$ molecules in various geometrical configurations, with the large values of $\alpha$ representing two $H_2$ molecules at large distances. For these latter cases, the Pople formula does an excellent job at reproducing the correlation energies; for lower values of $\alpha$, the agreement worsens, apparently because linked, disconnected, non-EPV diagrams start contributing to the energy.

Compared to the CCD results, the Pople corrected energies are in general reasonably accurate: the deviation becomes worse as $x$ increases, but is 2 millihartree or less for the practical cases from Table IV. For molecules such as HF and $H_2O$, the deviation is even only a few hundred microhartrees; for the others, considerable error cancellation between atom and molecule, as well as between different states, is even involved, so CID and CISD with a Pople correction may be an alternative to CCD and CCSD, repectively, for well-behaved molecules, when actual CCD or CCSD calculations are impossible for reasons of cost or unavailablilty of the methods. (In our own experience, computer times for CISD, CCD, and QCISD increase roughly as 1:2:4 in favorable cases, and as bad as 1:10:20 in cases of difficult coupled cluster convergence[3]).

As expected, all other correction formulas severely overestimate (in absolute value) the CCD correlation energy; any better agreement with full CI or experiment obtained with the Davidson formula (compared to the Pople formula) can only be a result of error compensation, notably with the neglect of connected triple excitations and (in the case of a comparison with experiment) basis set incompleteness.

Comparing the Davidson correction to the LCCD results, we find very good agreement for small values of $x$, but deviations of several millihartrees (that do *not* cancel between atom and molecule, or states) as $x$ becomes larger. For the 'large' CI calculation [Pal82] on CO, the error is even no less than 4.34 millihartrees. This case illustrates the fact, that $x$ will tend to rise with increasing basis set; Davidson-corrected CI calculations will thus not even be capable of reproducing basis set extension effects properly!

The error in the renormalized Davidson correction appears to be roughly half that of the regular Davidson correction. The Davidson-Silver formula tends to cut the remaining error again in half, but may also reduce the total error by no less than an order of magnitude [see e.g. $BH_3$, $CH^+$ and BH(r=2.00 Å)]! For many systems, the error is reduced to below 1 millihartree.

Summarizing, the Davidson-Silver formula is clearly superior when the LCCD energies are taken as a criterion. The traditional Davidson formula is 'neither fish nor fowl': it seriously overestimates the CCD correlation energy, and seriously underestimates (in

[3]After publication of the paper on which this Section is based, Gustavo E. Scuseria pointed out that the timing ratios between CISD and CCSD given here are an artifact of the GAUSSIAN program series. In another implementation [Scu88], the ratio CISD:CCSD varies from 1:0.5 to 1:2.

absolute value) its linearized counterpart. So depending on the actual application, we recommend that either the Pople correction or the Davidson-Silver correction be used instead of the traditional Davidson correction.

In the following Section [Mar90c], we shall investigate an actual application of our findings to some heavily spin-contaminated radical species - a type of molecules that puts very heavy demands on the electron correlation model used.

## 5.4 Some cost-effective approximations to CCSD and QCISD

### 5.4.1 Introduction

It has recently been discovered that $\hat{T}_1$ effects on the energy [Pop88], and potential energy surfaces [Mar90a], are very large for UHF cases with heavy spin contamination, as well as in ROHF cases with multireference character [Lee90]. Their proper inclusion requires CCSD (coupled cluster with all singles and doubles) [Pur82] or QCISD (quadratic configuration interaction with all singles and doubles) [Pop87] treatments that are not always available or practical to perform.

Another way of estimating the single excitation energy would be to take the difference between CISD and CID energies, both with a size-consistency correction applied. The author was involved in a study of some heavily spin-contaminated cluster molecules (see e.g.[Mar89b]) without having CCSD or QCISD treatments available. After a critical analysis [Mar90b] of the four most important size consistency corrections in literature, namely the regular [Lan74] and renormalized [Bar77, Sie78] Davidson corrections, the Pople correction [Pop77], and the Davidson-Silver correction [Dav77], the following approximate model was settled for:

$$\Delta E = E_{\mathrm{CCD(T)}} + E_{\mathrm{CISD+DSC}} - E_{\mathrm{CID+DSC}} \tag{5.55}$$

as a tolerable alternative to QCISD(T). (We recall that CCD(T) represents coupled cluster theory with all doubles and a quasiperturbative correction for triples [Rag85]) In the meantime, we acquired QCISD through the GAUSSIAN 88 program [Gau88]. It was recently shown [Lee90], that QCISD and CCSD perform comparably for nonpathological cases; significant differences are only present for cases where both QCISD and CCSD treatment are too limited anyway. Comparing single excitations energies obtained using the above approximate model with the 'exact' value (the difference $E_{\mathrm{CCSD}} - E_{\mathrm{CCD}}$) or a very good approximation to that (the difference $E_{\mathrm{QCISD}} - E_{\mathrm{CCD}}$) would then not only serve to test the validity of the approximation: using different size consistency corrections in the approximate calculation would also allow to assess the relative ability of the corrections to accurately estimate an infinite-order energy difference.

Before presenting numerical results, we will first try to look at the single excitation energy thus obtained from a purely theoretical viewpoint.

### 5.4.2 The single excitation energy in a MBPT/CC framework

A first relevant question is: how accurate would an LCCSD-LCCD difference be? This is easily found by generating the various PT terms according to the Kucharski-Bartlett procedure [Kuc86].

The QCISD equations in operator form are (Section 1.6):

$$D_1 T_1 = \hat{W}_N[\hat{T}_1 + \hat{T}_2 + \hat{T}_1\hat{T}_2] \quad (5.56)$$

$$D_2 T_2 = \hat{W}_N[1 + \hat{T}_1 + \hat{T}_2 + \hat{T}_2^2/2] \quad (5.57)$$

$$\Delta E = \langle 0|\hat{W}_N|\hat{T}_2 0\rangle \quad (5.58)$$

compared to the LCCSD equations[4]:

$$D_1 T_1 = \hat{W}_N[\hat{T}_1 + \hat{T}_2] \quad (5.59)$$

$$D_2 T_2 = \hat{W}_N[1 + \hat{T}_1 + \hat{T}_2] \quad (5.60)$$

$$\Delta E = \langle 0|\hat{W}_N|\hat{T}_2 0\rangle \quad (5.61)$$

$\hat{T}_1$ and $\hat{T}_2$ are the usual cluster operators; $\hat{W}_N$ is $\hat{H} - E_{SCF}$ in normal operator form, whereas $D_1$ and $D_2$ represent the appropriate many-body perturbation theory denominators.

Now expanding the cluster operators in a perturbation series [Kuc86]:

$$\hat{T}_n = \hat{T}_n^{(1)} + \hat{T}_n^{(2)} + \hat{T}_n^{(3)} + \ldots \quad (5.62)$$

we start out with all amplitudes equal to zero, and start iterating the equations. To second order in the amplitudes (third order in the energy), the two give identical results.

At third order, $\hat{T}_1^{(3)}$ is still equal between the two methods, whereas $\hat{T}_2^{(3)}$ differs by a term $\hat{T}_2^{(3)}(Q)$, caused by $(\hat{T}_2^{(1)})^2/2$ in the QCISD equations. This translates itself in a fourth-order energy difference, $E_Q^{(4)}$, as is well known.

Limiting ourselves to terms that will be present in the single excitation part of the correlation energy, we find that at the following iteration, $\hat{T}_2^{(3)}(Q)$ introduces a term $\hat{T}_1^{(4)}(DQ)$, which together with the $\hat{T}_1^{(4)}(T_{sd})$ term coming from $\hat{T}_1^{(2)}\hat{T}_2^{(1)}$ causes a fifth-order difference in $\hat{T}_2$, which finally translates in a sixth-order difference in the single-excitation energies. Both terms will generally be positive due to their disconnected

[4]Peter R. Taylor [TayPC] rightly points out that LCCSD was never unambiguously defined: one may equally well write $\Delta E = \langle 0|\hat{W}_N|\hat{T}_2 0\rangle$ or $\Delta E = \langle 0|\hat{W}_N|(\hat{T}_1^2/2 + \hat{T}_2)0\rangle$. (The definitions differ at fifth order). However, this would introduce not only a nonlinear term (which contradicts the 'linear' character of LCCSD), but would also introduce fifth-and higher-order diagrams with intervertex excitation levels above two, which contradicts the logical equivalence $E_{LCCSD} = SD-MBPT(\infty)$, analogous to $E_{LCCD} = D-MBPT(\infty)$. Kucharski and Bartlett [Kuc86], who considered LCCSD in the context of a fifth-order comparison of various approximate coupled cluster methods, used the same definition considered in the present Section.

nature, so the LCCSD single excitation energy will generally be an upper bound to the QCISD singles energy.

What is the difference between the QCISD singles energy and its 'exact' CCSD counterpart? The CCSD equations in operator form are (Section 1.6):

$$D_1 T_1 = \hat{W}_N[\hat{T}_1 + \hat{T}_2 + \hat{T}_1\hat{T}_2(+\hat{T}_1^2/2 + \hat{T}_1^3/6)] \tag{5.63}$$

$$D_2 T_2 = \hat{W}_N[1 + \hat{T}_1 + \hat{T}_2 + \hat{T}_1^2/2 + \hat{T}_1\hat{T}_2 + \hat{T}_2^2/2 (+\hat{T}_1^3/6 + \hat{T}_1^4/24 + \hat{T}_1^2\hat{T}_2/2)] \tag{5.64}$$

$$\Delta E = \langle 0|\hat{W}_N|\hat{T}_1^2/2 + \hat{T}_2 0\rangle \tag{5.65}$$

The terms in round parentheses only contribute beyond sixth order. The $\hat{T}_1\hat{T}_2$ term in the $\hat{T}_2$ equation will affect $\hat{T}_2$ in fourth order, and consequently the energy in fifth. It will normally be the leading term in the CCSD-QCISD energy difference. Both terms being disconnected and thus generally 'positive', the QCISD correlation energy will normally be a lower bound for the CCSD correlation energy (as found in the results by Lee *et al.* [Lee90]). The $\hat{T}_1^2/2$ term in the energy equation should normally be small for HF reference cases, as pointed out by Paldus *et al.* [Pal89]. Both terms give rise (*inter alia*) to diagrams of the $E_{ST}^{(5)}$ class. Peculiarly, these diagrams are Hermitian conjugates of diagrams generated by the quasiperturbative treatment of triple excitations in QCISD(T) and CCSD(T) [Rag89]:

$$\text{QCISD(T)} - \text{QCISD} = (2\sum_s^S + \sum_s^D)\sum_t^T\sum_u^D \frac{a_s V_{st} V_{tu} a_u}{D_t} \tag{5.66}$$

$$\text{CCSD(T)} - \text{CCSD} = (\sum_s^S + \sum_s^D)\sum_t^T\sum_u^D \frac{a_s V_{st} V_{tu} a_u}{D_t} \tag{5.67}$$

It is easily seen that either formula generates, besides $E_T^{(4)}$, all fifth-and higher order diagrams that only have one intervertex excitation level of three. To fifth order one obtains

$$E_T^{(4)} + E_{DT}^{(5)} + E_{TD}^{(5)} + 2E_{ST}^{(5)} \tag{5.68}$$

and

$$E_T^{(4)} + E_{DT}^{(5)} + E_{TD}^{(5)} + E_{ST}^{(5)} \tag{5.69}$$

respectively. The double-counting in the QCISD(T) case ensures that the $E_{ST}^{(5)}$ term is included correctly anyway: similar arguments apply at sixth order. This explains the finding by Lee *et al.* [Lee90], that the QCISD(T)-CCSD(T) difference is generally much smaller than the QCISD-CCSD difference. The effects of $\hat{T}_2^{(4)}(Tds)$, of $\hat{T}_1^{(2)}\hat{T}_2^{(2)}$ and $\hat{T}_1^{(3)}\hat{T}_2^{(1)}$, and finally of $(\hat{T}_1^{(2)})^2/2$ on $\hat{T}_2^{(5)}$ will translate in a sixth-order difference between the QCISD and CCSD singles energies: their effect on $\hat{T}_1^{(5)}$ will only affect the energy at seventh order.

Table V: Exact and approximate CCD energies (hartree; minus sign omitted).

| Species | MP4(DQ) | CCD | CID | PC | DC | RDC | DSC |
|---|---|---|---|---|---|---|---|
| B | 24.57542 | 24.57835 | 24.57835 | 24.57951 | 24.58169 | 24.58190 | 24.58214 |
| C | 37.76364 | 37.76512 | 37.76477 | 37.76685 | 37.76807 | 37.76822 | 37.76838 |
| $N^a$ | 54.47272 | 54.47291 | 54.47229 | 54.47385 | 54.47480 | 54.47487 | 54.47495 |
| $N^a$ | 54.49026 | 54.49038 | 54.48969 | 54.49200 | 54.49230 | 54.49237 | 54.49245 |
| Si | 288.90960 | 288.91035 | 288.91010 | 288.91192 | 288.91308 | 288.91323 | 288.91341 |
| $B_3$ | 73.98791 | 73.99026 | 73.97253 | 73.99460 | 73.99585 | 73.99892 | 74.00291 |
| $BN_2(^2\Pi)$ | 133.81618 | 133.81823 | 133.78207 | 133.81958 | 133.81831 | 133.82274 | 133.82840 |
| $B_2N$ | 103.97866 | 103.97974 | 103.95219 | 103.98361 | 103.98359 | 103.98758 | 103.99273 |
| $N_3$ | 163.69063 | 163.69141 | 163.64896 | 163.69529 | 163.69250 | 163.69777 | 163.70449 |
| CN | 92.47453 | 92.47585 | 92.46100 | 92.47743 | 92.47957 | 92.48115 | 92.48304 |
| CCH | 76.39456 | 76.39628 | 76.38262 | 76.39810 | 76.40003 | 76.40157 | 76.40341 |
| BN | 79.18266 | 79.18371 | 79.17447 | 79.18570 | 79.18784 | 79.18888 | 79.19010 |
| BO | 99.75339 | 99.75367 | 99.74114 | 99.75372 | 99.75568 | 99.75670 | 99.75787 |
| NO | 129.56163 | 129.56130 | 129.54100 | 129.56309 | 129.56450 | 129.56653 | 129.56896 |
| $CO^+$ | 112.51038 | 112.51126 | 112.49729 | 112.51201 | 112.51415 | 112.51544 | 112.51694 |
| SiC(r=1.72) | 326.79353 | 326.79449 | 326.78574 | 326.79729 | 326.79914 | 326.80043 | 326.80198 |

(a) 6-31G* basis set
(b) 6-311G* basis set

So far we have thus obtained the result, that the QCISD singles energy, which itself is known to estimate the CCSD singles energy quite well, is estimated correctly to fifth order by an L-CCSD calculation. Furthermore, the difference terms at sixth order partly involve the same quantities that occur in the small QCISD-CCSD difference. Let us now investigate, in how far the various size-consistency corrections are capable of reproducing the singles energy.

Subtracting the renormalization errors of Davidson-Silver [Dav77] corrected CISD and CID calculations, we obtain as the leading error term

$$E^2_{\mathrm{LCCD}}\langle\psi'|\hat{R}|\psi'\rangle_{\mathrm{D}} - E^2_{\mathrm{LCCSD}}\langle\psi'|\hat{R}|\psi'\rangle_{\mathrm{SD}} \tag{5.70}$$

which, when expanded in a PT series, becomes

$$\begin{aligned} &-(E^{(2)}+E^{(3)}+E^{(4)}_{\mathrm{D}}+\ldots)^2(\langle 1|\hat{R}|1\rangle+\langle 1|\hat{R}|2_{\mathrm{D}}\rangle+\langle 1|\hat{R}|3_{\mathrm{D}}(\mathrm{D})\rangle \\ &\quad+\langle 2_{\mathrm{D}}|\hat{R}|2_{\mathrm{D}}\rangle+\ldots)+(E^{(2)}+E^{(3)}+E^{(4)}_{\mathrm{D}}+E^{(4)}_{\mathrm{S}}+\ldots)^2(\langle 1|\hat{R}|1\rangle+\langle 1|\hat{R}|2_{\mathrm{D}}\rangle \\ &\quad+\langle 1|\hat{R}|3_{\mathrm{D}}(\mathrm{D})\rangle+\langle 1|\hat{R}|3_{\mathrm{D}}(\mathrm{S})\rangle+\langle 2_{\mathrm{D}}|\hat{R}|2_{\mathrm{D}}\rangle+\langle 2_{\mathrm{S}}|\hat{R}|2_{\mathrm{S}}\rangle+\ldots) \\ &= E^{(4)}_{\mathrm{S}}E^{(2)}\langle 1|\hat{R}|1\rangle+\ldots+(E^{(2)})^2(2\langle 1|\hat{R}|3_{\mathrm{D}}(\mathrm{S})\rangle+\langle 2_{\mathrm{S}}|\hat{R}|2_{\mathrm{S}}\rangle)+\ldots \end{aligned} \tag{5.71}$$

where $|2_{\mathrm{S}}\rangle$ represents the single excitation part of $|2\rangle$, and $3_{\mathrm{D}}(\mathrm{S})$ represents the part of $|3_{\mathrm{D}}\rangle$ caused by the effect of $\hat{T}^{(2)}_1$ on $\hat{T}_2$. $|2_{\mathrm{D}}\rangle$ and $|3_{\mathrm{D}}(\mathrm{D})\rangle$ are defined similarly.

Both sets of terms start at order eight. So the singles energy as calculated from a Davidson-Silver corrected CISD calculation is identical to seventh order with that from LCCSD!

Table VI: Exact and approximate QCISD energies (hartree; minus sign omitted).

| Species | MP4(SDQ) | QCISD | CISD | PC | DC | RDC | DSC |
|---|---|---|---|---|---|---|---|
| B | 24.57562 | 24.57895 | 24.57893 | 24.58014 | 24.58240 | 24.58262 | 24.58288 |
| C | 37.76378 | 37.76562 | 37.76477 | 37.76655 | 37.76815 | 37.76831 | 37.76848 |
| $N^a$ | 54.47280 | 54.47314 | 54.47250 | 54.47408 | 54.47505 | 54.47512 | 54.47520 |
| $N^b$ | 54.49033 | 54.49060 | 54.48989 | 54.49153 | 54.49253 | 54.49261 | 54.49269 |
| Si | 288.90986 | 288.91099 | 288.91070 | 288.91234 | 288.91381 | 288.91398 | 288.91417 |
| $B_3$ | 73.99701 | 74.02453 | 73.98521 | 74.02341 | 74.02161 | 74.02910 | 74.04049 |
| $BN_2(^2\Pi)$ | 133.82256 | 133.82917 | 133.78701 | 133.82915 | 133.82697 | 133.83232 | 133.83934 |
| $B_2N$ | 103.98554 | 103.98784 | 103.95646 | 103.99151 | 103.99088 | 103.99565 | 104.00196 |
| $N_3$ | 163.70142 | 163.70752 | 163.65602 | 163.70978 | 163.70527 | 163.71199 | 163.72083 |
| CN | 92.48291 | 92.50213 | 92.47238 | 92.49902 | 92.50063 | 92.50428 | 92.50901 |
| CCH | 76.39994 | 76.41153 | 76.39044 | 76.41206 | 76.41377 | 76.41650 | 76.41996 |
| BN | 79.18663 | 79.19331 | 79.17956 | 79.19441 | 79.19672 | 79.19842 | 79.20049 |
| BO | 99.75932 | 99.76262 | 99.74590 | 99.76146 | 99.76351 | 99.76499 | 99.76675 |
| NO | 129.56830 | 129.57022 | 129.54601 | 129.57148 | 129.57265 | 129.57525 | 129.57842 |
| $CO^+$ | 112.51872 | 112.53098 | 112.50738 | 112.52955 | 112.53160 | 112.53423 | 112.53750 |
| SiC(r=1.72) | 326.79734 | 326.81330 | 326.79440 | 326.81450 | 326.81596 | 326.81927 | 326.82378 |

(a) 6-31G* basis set
(b) 6-311G* basis set

The difference between the singles energies as estimated using the Davidson-Silver and the renormalized Davidson [Bar77] formulas is readily found to be

$$E_{\mathrm{R,CISD}}\langle\psi'|\psi'\rangle_{\mathrm{CISD}} - E_{\mathrm{R,CID}}\langle\psi'|\psi'\rangle_{\mathrm{CID}} = E_{\mathrm{R}}^{(4)}[\langle 2_{\mathrm{S}}|2_{\mathrm{S}}\rangle + 2\langle 1|3_{\mathrm{D}}(\mathrm{S})\rangle] + O(\lambda^9) \tag{5.72}$$

So the difference is only of order eight; however, both $E_{\mathrm{R}}^{(4)}$ and $\langle 2_{\mathrm{S}}|2_{\mathrm{S}}\rangle$ are expected to be large for the cases of interest, as opposed to the eighth-order term in the previous paragraph.

For the regular Davidson correction [Lan74], one obtains after some manipulations the result:

$$\Delta E_{\mathrm{R,RDC}} - \Delta E_{R,DC} = E_{\mathrm{S}}^{(4)}\langle 1|1\rangle^2 + \ldots + 2E^{(2)}\langle 1|1\rangle\langle 2_{\mathrm{S}}|2_{\mathrm{S}}\rangle + \ldots \tag{5.73}$$

Again, the terms in both series start at order eight: however, once more all factors involved are quite substantial for the cases of interest.

We will now look at the results of some numerical computations.

### 5.4.3 Numerical results and discussion

CCD(ST) and QCISD(T) calculations were performed using the GAUSSIAN 88 program package [Gau88] running on a VaxStation 2000 under MicroVMS 4.7. Calculations for $B_3$, $B_2N$, $BN_2(^2\Pi)$ and $N_3$ were done using the 6-31G* basis set from their UHF/6-31G* geometries [Mar89b]. Those for BN, BO, NO, and $CO^+$ were performed using the 6-31G* basis set [Dit71, Har73] from CISD/6-31G* equilibrium geometries [Mar90a]. Results for

Table VII: Total atomization energies (kcal/mol) at various theoretical levels.

| Species | CCD | CID +PC | CID +DC | CID+ RDC | CID+ DSC | QCISD | CISD +PC | CISD +DC | CISD +RDC | CISD +DSC |
|---|---|---|---|---|---|---|---|---|---|---|
| BN | 83.11 | 83.05 | 82.43 | 82.90 | 83.47 | 88.61 | 87.97 | 87.39 | 88.27 | 89.36 |
| $B_3$ | 160.15 | 160.69 | 157.37 | 158.90 | 160.96 | 180.51 | 177.59 | 172.20 | 176.48 | 183.14 |
| $BN_2(^2\Pi)$ | 184.53 | 183.47 | 180.12 | 182.67 | 185.97 | 190.72 | 188.79 | 184.79 | 187.91 | 192.05 |
| $B_2N$ | 219.71 | 220.10 | 216.75 | 218.95 | 221.83 | 223.89 | 224.12 | 220.28 | 222.94 | 226.53 |
| $N_3$ | 171.11 | 171.78 | 168.24 | 171.40 | 175.47 | 180.79 | 180.42 | 175.78 | 179.86 | 185.25 |
| SiC | 74.68 | 74.76 | 74.05 | 74.66 | 75.42 | 85.77 | 85.10 | 84.09 | 85.96 | 88.56 |
| CN | 138.27 | 137.82 | 137.55 | 138.40 | 139.43 | 154.32 | 151.19 | 150.57 | 152.71 | 155.52 |
| CCH | 229.81 | 229.23 | 228.47 | 229.24 | 230.19 | 238.76 | 237.92 | 236.98 | 238.50 | 240.45 |

SiC at r=1.72 Å were taken from [Mar90d]. Finally, QCISD(T) results for CN and CCH were taken from [Pop88], and supplemented with CCD(ST), CID and CISD calculations in this work. These values were obtained using the 6-311G* basis set [Kri80a] from MP2/6-31G* geometries.

Total energies at various levels of theory are given in Table V. Single excitation contributions obtained using the four size consistency corrections, as well as the QCISD-CCD difference, are given in Table VI. Finally, total atomization energies (TAE's) at various theoretical levels for the species BN, $B_3$, $B_2N$, $BN_2(^2\Pi)$, $N_3$ , CN, CCH, and SiC are given in Table VII.

Firstly, we compare CCD and the Pople-corrected [Pop77] CID energies. From Table V, we find that there are significant (1.5 – 5 millihartree) overestimates (in absolute value) of the total energy. However, as witnessed from Table VII, very substantial error compensation exists between the atoms and the molecules. Except for $BN_2$, the TAE's are in error by 0.5 kcal/mol or less! This makes CID with a Pople correction an economic alternative to CCD for large molecules (a CID calculation usually takes less than half the time of a CCD calculation, at least with the GAUSSIAN 8x series of programs. In cases of difficult CCD convergence, the difference is much larger. For large systems, this may make the difference between a calculation that is affordable and one that is not.). On this account, the Davidson-corrected CID fails badly, underestimating TAE's by as much as 4.4 kcal/mol. CID with a renormalized Davidson corrections fares better, but still underestimates the TAE's by as much as 1.86 kcal/mol (for $BN_2$). Finally, the Davidson-Silver correction appears to lead to an overshoot, by as much as 4.4 kcal/mol (for $N_3$). As an overestimate would be expected for LCCD, this latter result is at least methodologically correct.

It should be remarked that most of the species considered have large to very large amounts of spin contamination, and that the MP4(DQ) binding energies sometimes differ very significantly from the CCD results (as much as 4 kcal/mol in the case of $B_3$!). MP4(DQ), which would be even less expensive than a CID calculation, is thus not an option.

Table VIII: Total atomization energies (kcal/mol) at the QCISD(T) level and using various approximate triple excitation corrections.

| Species | PC+T (MP4) | DSC+T (MP4) | PC+T (CCD) | DSC+T (CCD) | QCISD(T) | MP4DTQ +S(PC) | MP4DTQ +S(DSC) | CCD(T) +S(PC) | CCD(T) +S(DSC) |
|---|---|---|---|---|---|---|---|---|---|
| BN | 87.49 | 88.88 | 91.89 | 93.28 | 92.49 | 93.18 | 94.15 | 91.95 | 92.93 |
| $B_3$ | 186.12 | 191.67 | 186.66 | 192.21 | 192.94 | 189.62 | 194.91 | 186.12 | 191.41 |
| $BN_2(^2\Pi)$ | 197.41 | 200.67 | 196.96 | 200.22 | 198.85 | 199.26 | 200.02 | 198.01 | 198.77 |
| $B_2N$ | 237.62 | 240.03 | 235.90 | 238.31 | 235.99 | 240.35 | 241.03 | 235.52 | 236.20 |
| $N_3$ | 193.84 | 198.67 | 191.44 | 196.27 | 191.58 | 193.05 | 194.17 | 190.78 | 191.91 |
| SiC | 87.43 | 90.90 | 87.93 | 91.39 | 90.59 | 88.16 | 90.96 | 87.85 | 90.65 |
| CN | 158.00 | 162.33 | 157.20 | 161.52 | 160.60 | 158.63 | 161.35 | 157.65 | 160.36 |
| CCH | 243.16 | 245.69 | 242.83 | 245.36 | 242.92 | 244.53 | 246.10 | 243.41 | 244.98 |

Secondly, we compare QCISD and Pople-corrected CISD energies. Performance is again relatively good, but the Pople correction no longer gives a lower bound. This is partly a consequence of the fact that QCISD is itself a lower bound to CCSD, to which the Pople-corrected CISD energy should be an approximate lower bound. The error is most significant for the $B_3$ molecule, which has $\langle S^2 \rangle = 1.55$ at the UHF/6-31G* geometry; the difference between CCSD and QCISD should then be rather significant. Davidson's correction is even more deficient here than in the CID case; the renormalized correction again fares better. The Davidson-Silver formula exhibits the same overshooting tendency as in the CID case.

Taking the single excitation contribution as the difference between Tables V and VI, it is seen that the Davidson correction severely underestimates single excitation contributions. The Pople correction fares better, but nevertheless still underestimates them significantly. The renormalized Davidson correction tends towards a minor underestimate (except for CN and $B_3$, where the underestimate is more serious), whereas the Davidson-Silver correction tends towards a slight overestimate. On the whole, however, the Davidson-Silver single excitation energies appear to agree best with the QCISD-CCD difference.

Now turning to the total atomization energies (Table VII), the largest deviations (3 kcal/mol or more) are seen for the CN and $B_3$ molecules. As both of them exhibit extreme amounts of spin contamination ($\langle S^2 \rangle = 1.04$ for CN, 1.55 for $B_3$), the QCISD binding energies are only upper bounds to the CCSD values, and the latter should be much closer to the Pople-corrected CISD values. The error of 2 kcal/mol in $BN_2$ was also seen in the CCD-CID case, and has thus nothing to do with the single excitations, but everything with the linked non-EPV part of $\hat{T}_2^2/2$.

The conclusion reached at this point is that CISD with a Pople correction is a relatively accurate and very cost-effective approximation to QCISD or CCSD. It is then a viable alternative in cases where the latter two methods are precluded on grounds of cost or availability. As CCSD is known to describe the breaking of a single bond very well, a practical application would be the evaluation of single bond dissociation energies in large

Table IX: Total energies (hartree; minus sign omitted) involved in triple excitation corrections.

| | MP4(SDTQ) | CCD(T) | QCISD(T) |
|---|---|---|---|
| B | 24.57594 | 24.57912 | 24.57971 |
| C | 37.76430 | 37.76620 | 37.76669 |
| $N^a$ | 54.47326 | 54.47359 | 54.47381 |
| $N^b$ | 54.49087 | 54.49122 | 54.49143 |
| Si | 288.91040 | 288.91134 | 288.91194 |
| $B_3$ | 74.01157 | 74.00704 | 74.04661 |
| $BN_2(^2\Pi)$ | 133.83753 | 133.83338 | 133.84422 |
| $B_2N$ | 104.00814 | 104.00074 | 104.00931 |
| $N_3$ | 163.72416 | 163.71101 | 163.72674 |
| CN | 92.49482 | 92.48733 | 92.51406 |
| CCH | 76.40933 | 76.40625 | 76.42032 |
| BN | 79.19353 | 79.19140 | 79.20092 |
| SiC(r=1.72) | 326.80212 | 326.80105 | 326.82300 |

(a) 6-31G* basis set
(b) 6-311G* basis set

molecules.

Extension to multiple bonds or total atomization energies requires some account of the effect of connected triple substitutions. Full CCSDT calculations are presently out of the question for any but the smallest molecules; QCISD(T) or CCSD(T) [Rag89] are the next best alternative. More cost-effective approximations are the quasiperturbative treatment based on converged CCD amplitudes CCD(T) [Rag85], and particularly a full MP4 calculation, the triple excitation contribution being found from $E_{\mathrm{MP4(SDTQ)}} - E_{\mathrm{MP4(SDQ)}}$.

The results of such approximations are listed in Table VIII, together with the 'exact' QCISD(T) values. (Some energies involving triple excitations necessary for reconstructing this table are found in Table IX.) Both T(MP4) and T(CCD) are considered; also, the approximate CCSD energy is taken as both CISD with a Pople correction and CCD+CISD(PC)-CID(PC). The latter method is more accurate in cases where the linked disconnected non-EPV part of $\hat{T}_2^2$ is likely to be important.

For three molecules, namely BN, $B_2N$, and $N_3$, the energies involving T(MP4) are totally unsatisfactory, whereas quite good results are obtained using T(CCD). The approximations involving only the single excitation increment in the CI offer no clear advantage over those using only the triple excitation contribution from MP4 and CCD, except for the $BN_2$ molecule (vide supra). The energies involving the Pople correction differ significantly from their QCISD(T) counterparts for $B_3$ and CN, whereas the Davidson-Silver corrected energies are closer there. However, as discussed above, the ones involving the Pople correction are likely to be closer to the CCSD(T) result for these particular

cases. This finding may be useful for the situation that neither QCISD(T) nor CCSD(T) treatments are available for molecules which require them. However, a separate CCD(T) calculation is still required, which is not very efficient computationally.

This leaves the approximate methods discussed in the present Section as useful primarily if the triple excitation contribution is not too large, and can consequently be evaluated at the MP4 level without gross errors. Alternatively, a Pople-corrected CISD calculation should be a much more accurate (and not overly expensive) alternative to Pople's infinite-order extrapolation formula [Pop83, Mar89a]. Of course, if CCSD(T) or QCISD(T) methods are simply not available, and both MP4 and CISD are - for example for users of the HONDO package [Hon87], GAUSSIAN 82 [Gau82], or GAUSSIAN 86 [Gau86] (in the latter case, CCD(ST) is also possible) - the present method is certainly preferable over using plain MP4 energies - or not treating the problem altogether.

# References


[Ahl74] R. Ahlrichs, *Theor. Chim. Acta* **35**, 59 (1974).

[Alb88] I. L. Alberts and N. C. Handy, *J. Chem. Phys.* **89**, 2107 (1988).

[Bar77] R. J. Bartlett and I. Shavitt, *Int. J. Quantum Chem. Symp.* **11**, 165 (1977); *erratum* **12**, 543 (1978).

[Bar87] R. J. Bartlett, S. J. Cole, G. D. Purvis, W. C. Ermler, H. C. Hsieh, and I. Shavitt, *J. Chem. Phys.* **87**, 6579 (1987).

[Bar89] R. J. Bartlett, *J. Phys. Chem.* **93**, 1697 (1989).

[Bin75] J. S. Binkley and J. A. Pople, *Int. J. Quantum Chem.* **9**, 229 (1975).

[Bin80] J. S. Binkley, J. A. Pople, and W. J. Hehre, *J. Am. Chem. Soc.* **102**, 939 (1980).

[Bru55] K. A. Brueckner, *Phys. Rev.* **97**, 1353 (1955).

[Cad87] R. D. Amos and J. E. Rice, *CADPAC, the Cambridge Analytical Derivatives Packages* (University Chemical Laboratory, Cambridge, 1987).

[Col76] J. B. Collins, P. von Ragué Schleyer, J. S. Binkley, and J. A. Pople, *J. Chem. Phys.* **64**, 5142 (1976): appendix.

[Dav77] E. R. Davidson and D. W. Silver, *Chem. Phys. Lett.* **52**, 403 (1977).

[DeF79] D. J. DeFrees, B. A. Levi, S. K. Pollack, W. J. Hehre, J. S. Binkley, and J. A. Pople, *J. Am. Chem. Soc.* **101**, 4086 (1979); *erratum* **102**, 2513 (1980).

[DeF82] D. J. DeFrees, K. Raghavachari, H. B. Schlegel, and J. A. Pople, *J. Am. Chem. Soc.* **104**, 5576 (1982).

[Dit71] W. J. Hehre, R. Ditchfield, and J. A. Pople, *J. Chem. Phys.* **56**, 2257 (1972).

[Dun32] J. L. Dunham, *Phys. Rev.* **41**, 721 (1932); A. C. Hurley, *Introduction to the electron theory of small molecules* (Academic Press, London, 1976).

[Fle63] R. Fletcher and M. J. D. Powell, *Computer Journal* **6**, 163 (1963).

[Fri80] M. J. Frisch, R. Krishnan, and J. A. Pople, *Chem. Phys. Lett.* **75**, 66 (1980); R. Krishnan, M. J. Frisch, and J. A. Pople, *J. Chem. Phys.* **72**, 4244 (1980).

[Gam88] M. W. Schmidt and S. T. Elbert, GAMESS (North Dakota State University, 1988).

[Gau82] J. S. Binkley, M. J. Frisch, D. J. DeFrees, K. Raghavachari, R. A. Whiteside, H. B. Schlegel, E. M. Fluder, and J. A. Pople, GAUSSIAN 82, Carnegie-Mellon University, Pittsburgh, PA, 1983.

[Gau86] J. S. Binkley, M. J. Frisch, K. Raghavachari, D. J. DeFrees, H. B. Schlegel, R. A. Whiteside, E. M. Fluder, R. Seeger, D. J. Fox, M. Head-Gordon, S. Topiol, and J. A. Pople, GAUSSIAN 86 Release C, Carnegie-Mellon University, Pittsburgh, PA, 1987.

[Gau88] M. J. Frisch, M. Head-Gordon, H. B. Schlegel, K. Raghavachari, J. S. Binkley, C. Gonzalez, D. J. DeFrees, D. J. Fox, R. A. Whiteside, R. Seeger, C. F. Melius, J. Baker, R. L. Martin, L. R. Kahn, J. J. P. Stewart, E. M. Fluder, S. Topiol, and J. A. Pople, GAUSSIAN 88 release C, Gaussian, Inc., Pittsburgh, PA, 1989.

[Ger68] J. Gerratt and I. M. Mills, *J. Chem. Phys.* **49**, 1719, 1730 (1968).

[Gil88] P. M. W. Gill, J. A. Pople, L. Radom, and R. H. Nobes, *J. Chem. Phys.* **89** 7307 (1988).

[Gol69] J. Go'dstone, *Proc. Royal Soc. (London)* **A 239**, 267 (1957).

[Han84] N. C. Handy and H. F. Schaefer III, *J. Chem. Phys.* **81**, 5031 (1984); N. C. Handy, R. D. Amos, J. F. Gaw, J. E. Rice, and E. D. Simandiras, *Chem. Phys. Lett.* **120**, 151 (1985); E. D. Simandiras, N. C. Handy, and R. D. Amos, *Chem. Phys. Lett.* **133**, 324 (1987).

[Han85] N. C. Handy, P. J. Knowles, and K. Somasundram, *Theor. Chim. Acta* **68**, 87 (1985).

[Har73] P. C. Hariharan and J. A. Pople, *Theor. Chim. Acta* **28**, 213 (1973).

[Heh72] W. J. Hehre, R. Ditchfield, and J. A. Pople, *J. Chem. Phys.* **56**, 2257 (1972). P. C. Hariharan and J. A. Pople, *Chem. Phys. Lett.* **16**, 217 (1972). P. C. Hariharan and J. A. Pople, *Theor. Chim. Acta* **28**, 213 (1973).

[Hon87] H. F. King and M. Dupuis, HONDO 7, QCPE 544 (Quantum Chemistry Program Exchange, Bloomington, IN).

[Jan80] K. Jankowski and J. Paldus, *Int. J. Quantum Chem.* **18**, 1243 (1980).

[Kel69] H. P. Kelly, *Adv. Chem. Phys.* **14**, 129 (1969).

[Kno88] P. J. Knowles and N. C. Handy, *J. Chem. Phys.* **88**, 6991 (1988).

[Kno90] D. B. Knowles, J. R. Alvarez-Collado, G. Hirsch, and R. J. Buenker, *J. Chem. Phys.* **92**, 585 (1990).

[Kri80a] R. Krishnan, J. S. Binkley, R. Seeger and J. A. Pople, *J. Chem. Phys.* **72**, 650 (1980).

[Kri80b] R. Krishnan, M. J. Frisch, and J. A. Pople, *J. Chem. Phys.* **72**, 4244 (1980).

[Kri80c] R. Krishnan, H. B. Schlegel, and J. A. Pople, *J. Chem. Phys.* **72**, 4654 (1980).

[Kuc86] S. A. Kucharski and R. J. Bartlett, *Adv. Quantum Chem.* **18**, 281 (1986).

[Kva82] V. Kvasnicka, *Phys. Rev.* **A 25**, 671 (1982).

[Lan74] S. R. Langhoff and E. R. Davidson, *Int. J. Quantum Chem.* **8**, 61 (1974).

[Lee90] T. J. Lee, A. P. Rendell, and P. R. Taylor, *J. Phys. Chem.* **94**, 5463 (1990).

[Low55] P. O. Löwdin, *Phys. Rev.* **97**, 1509 (1955).

[Luc78] C. E. Dykstra, R. R. Lucchese, and H. F. Schaefer III, J. Chem. Phys. 67 (1977) 2422.

[Mar89a] J. M. L. Martin, J. P. François, and R. Gijbels, *Chem. Phys. Lett.* **157**, 217 (1989).

[Mar89b] J. M. L. Martin, J. P. François, and R. Gijbels, *J. Chem. Phys.* **90**, 6469 (1989).

[Mar90a] J. M. L. Martin, J. P. François, and R. Gijbels, Chem. Phys. Lett. **166**, 295 (1990).

[Mar90b] J. M. L. Martin, J. P. François, and R. Gijbels, *Chem. Phys. Lett.* **172**, 346 (1990).

[Mar90c] J. M. L. Martin, J. P. François, and R. Gijbels, *Chem. Phys. Lett.* **172**, 354 (1990).

[Mar90d] J. M. L. Martin, J. P. François, and R. Gijbels, *J. Chem. Phys.* **92**, 6655 (1990).

[McD89] J. J. W. McDouall and H. B. Schlegel, *J. Chem. Phys.* **90**, 2363 (1989) and references therein.

[Nob87] R. H. Nobes, J. A. Pople, L. Radom, N. C. Handy, and P. J. Knowles, *Chem. Phys. Lett.* **138**, 481 (1987).

[Pal72] J. Paldus, J. Cizek, and I Shavitt, *Phys. Rev. A* **5**, 50 (1972).

[Pal82] J. Paldus, P. E. S. Wormer, F. Visser, and A. van der Avoird, *J. Chem. Phys.* **76**, 2458 (1982).

[Pal89] J. Paldus, J. Cizek, and B. Jeziorski, *J. Chem. Phys.* **90**, 4356 (1989).

[Pop76] J. A. Pople, J. S. Binkley, and R. Seeger, *Int. J. Quantum Chem. Symp.* **10**, 1 (1976).

[Pop77] J. A. Pople, R. Seeger, and R. Krishnan, *Int. J. Quantum Chem. Symp.* **11**, 149 (1977).

[Pop78] J. A. Pople, R. Krishnan, H. B. Schlegel, and J. S. Binkley, *Int. J. Quantum Chem.* **14**, 545 (1978).

[Pop79] J. A. Pople, R. Krishnan, H. B. Schlegel, and J. S. Binkley, *Int. J. Quantum Chem. Symp.* **13**, 225 (1979).

[Pop83] J. A. Pople, M. J. Frisch, B. T. Luke, and J. S. Binkley, *Int. J. Quantum Chem. Symp.* **17**, 307 (1983).

[Pop87] J. A. Pople, M. Head-Gordon, and K. Raghavachari, *J. Chem. Phys.* **87**, 5968 (1987).

[Pop88] J. A. Pople, M. Head-Gordon, and K. Raghavachari, *Int. J. Quantum Chem. Symp.* **22**, 377 (1988).

[Pur82] G. D. Purvis III and R. J. Bartlett, *J. Chem. Phys.* **76**, 1910 (1982).

[Rag85] K. Raghavachari, *J. Chem. Phys.* **82**, 4607 (1985).

[Rag89] K. Raghavachari, G. W. Trucks, J. A. Pople, and M. Head-Gordon, *Chem. Phys. Lett.* **157**, 479 (1989).

[Rob75] M. A. Robb, in *Computational Methods in Quantum Chemistry and Molecular Physics* (eds. G. H. F. Diercksen, B. T. Sutcliffe, and A. Veillard), D. Reidel, Dordrecht, Boston, 1975, p.435.

[Sax82] P. Saxe, D. J. Fox, H. F. Schaefer III, and N. C. Handy, *J. Chem. Phys.* **77**, 5584 (1982).

[Sch88] H. B. Schlegel, *J. Phys. Chem.* **92**, 3075 (1988).

[Scu88] G. E. Scuseria, C. L. Janssen, and H. F. Schaefer III, *J. Chem. Phys.* **89**, 7382 (1988).

[Sha77] I. Shavitt, in *Modern Theoretical Chemistry* (ed. H. F. Schaefer III), Plenum Press, New York, London, 1977, p.189.

[Sie78] P. E. M. Siegbahn, *Chem. Phys. Lett.* **55**, 386 (1978).

[Sie84] P. E. M. Siegbahn, *Chem. Phys. Lett.* **109**, 417 (1984); P. J. Knowles and N. C. Handy, *Chem. Phys. Lett.* **111**, 315 (1984).

[Sim88] E. D. Simandiras, J. E. Rice, T. J. Lee, R. D. Amos, and N. C. Handy, *J. Chem. Phys.* **88**, 3187 (1988) and references therein.

[TayPC] P. R. Taylor, personal communication.

# Summary and general conclusions

In principle, any chemically interesting property of a molecule can be obtained exactly and quantitatively by solving the molecular Schrödinger equation. However, the presence of many-body interactions makes an exact solution impossible analytically, and intractable numerically. Approximate solutions are always a trade-off between desired accuracy and computational cost. Recent improvements in computer technology, as well as methodological advances, have currently created a situation where the accuracy of ab initio results becomes competitive with experiment for small molecules. Contrary to experiments however, no restrictions with respect to abundance, lifetime, or reactiveness have to be reckoned with.

Through the construction of the molecular partition function, statistical thermodynamics allows extending this accuracy to macroscopic thermodynamic properties.

The present work deals with the application of ab initio methods to a number of practical problems in materials science and astrophysics, as well as with some improvements in the general methodology.

Chapter 1 reviews the current state (December 1990) of the general theory. No claim of completeness is made; however, all aspects that are relevant to the remainder of the work are discussed inasmuch as possible. Special attention has been given to electron correlation techniques such as configuration interaction, many-body perturbation theory, and coupled cluster methods.

Chapter 2 briefly discusses the hardware and computer programs employed in the remainder of the work.

In Chapter 3, the accurate ab initio computation of molecular dissociation energies (total atomization energies, heats of formation, ...) is addressed. To this end, a new family of finite basis sets, denoted *combined bond-polarization basis sets*, has been introduced. All practical ab initio calculations expand the solution in terms of a finite set of basis functions that are usually centered on the nuclei. For molecules, the anisotropic nature of chemical bonding (as opposed to the isotropic environment of an atom) necessitates the addition either of polarization functions (basis functions with higher angular momentum centered on the atoms) or of bond functions (basis functions with lower angular momentum placed along the bond axis). Either type of function has its pros and cons. The author showed however (Section 3.2) that by applying them jointly, dissociation energies of 'chemical accuracy' (errors $\leq$ 2 kcal/mol) can be obtained at a much lower cost (factor 4–20 depending on the case) than with a polarization-only basis set of comparable quality. An often raised objection against bond functions, namely the pathological basis set superposition errors associated with them, was explained in terms of intra-atomic external correlation. It was shown in Section 3.3 that by admitting at least $f$ functions to the polarization complement (in the case of $sp$ bond functions), this problem is greatly alleviated. Such basis sets involve a computational cost comparable to that of common polarization-only basis sets, but exhibit markedly superior performance. The problem of many-body BSSE for polyatomic systems, for which no unique well-defined measure exists, has been discussed in Section 3.4. Empirical arguments in favor of neglecting BSSE altogether are presented there. By improving the electron correlation treatment (Section 3.5) and using correlated reference geometries (Section 3.6), an accuracy of 0.12 kcal/mol per bond has been achieved for the dissociation energies of the closed-and open-shell hydrides $AH_n$ (A=Li–F). As an example application, definitive proof for an experimental misinterpretation in the dissociation energy of BH has been given (Section 3.7).

Cluster molecules have aroused a lot of interest recently in several fields, such as

materials science and astrophysics. In materials science, particularly surface coating with neoceramic materials by means of chemical vapor deposition techniques, clusters form the 'natural bridge' between a gaseous plasma and a thin solid film. Most of these materials have several crystalline modifications, of which only one or two have the desired properties of hardness and corrosion resistance (e.g., diamond for solid carbon, $\beta$-BN in the case of boron nitride, carborundum for solid SiC). Experimental research has shown that the nature of the deposited material is strongly dependent on the cluster growth processes in the plasma; if sufficient thermochemical data on the clusters were available, the process could be simulated and possibly controlled.

These same cluster molecules (notably $C_n$ and SiC) crop up in astrophysics, where they occur in stellar atmospheres and interstellar clouds. They are seen by IR and radio astronomers as mostly unidentified bands; the spectroscopic characterization of the molecules involved would enable these workers to identify these molecules and to draw conclusions (as regards age, chemical processes, ...) about the abovementioned celestial bodies.

The experimental characterization of these molecules is difficult because of their reactivity and short lifetime. Theoretical methods, for which these considerations are irrelevant, are an obvious alternative. Furthermore, the spectroscopic properties needed by the astrophysicists are also essential in setting up the partition functions for the (high-temperature) thermochemical data needed by the materials scientists.

In Section 4.2, the cluster molecules $B_3$, $B_2N$, $BN_2$, and $N_3$ have been studied. For the former three, these ab initio calculations constitute the first published data altogether. $B_3$ is an equilateral triangle in its ground state; $B_2N$ is an exceptionally stable linear molecule. The four lowest states of $BN_2$ are very close together; the global minimum of these is a cyclic structure. The molecule will however dissociate in B and $N_2$ at all temperatures. Findings for $N_3$ are in fair agreement with experiment for the spectroscopic constant; however its heat of formation was in disagreement with all three literature values that additionally disagreed with each other. To settle the issue for once and for all, the total atomization energy of $N_3$ was computed with very large basis sets in Section 4.3.

In Sections 4.4 and 4.5, respectively, the diatomics SiC and BN are treated. As they are only diatomics, accuracy was pushed to the limit of what is technically possible. Spectroscopic constants for the lowest few states, including anharmonic ones, were obtained with large basis sets and coupled cluster techniques. Using these data, partition functions have been set up by direct numerical summation and thermodynamic functions up to 6000 K tabulated. The latter include anharmonicity, rovibrational coupling, centrifugal distortion, and spin-orbit coupling effects. In the case of SiC, an error analysis of the thermodynamic functions has been carried out; it has been found that the accuracy of good ab initio calculations is more than enough for the purpose at hand. In the case of BN, the lowest $^3\Pi$ and $^1\Sigma^+$ states are found to lie extremely closely together ($T_e \approx 100$ cm$^{-1}$).

As early as 1971, carbon vapor had been trapped in an argon matrix, IR spectra recorded, and various bands assigned to various clusters using simple force field arguments. Most importantly, the 2164 cm$^{-1}$ band was assigned to $C_4$; 1544 cm$^{-1}$ to $C_5$; 1997 cm$^{-1}$ and 1197 cm$^{-1}$ to $C_6$; 2128, 1893, and 1447 cm$^{-1}$ to $C_9$. Ab initio calculations on $C_4$ found no IR-active band near 2164 cm$^{-1}$; in Section 4.6, a correlated ab initio calculation of the harmonic frequencies and IR intensities of $C_5$ shows definitively that the 2164 and 1544 cm$^{-1}$ assignments should be swapped. This prediction was confirmed by the subsequent detection of $C_5$ in the atmosphere of carbon star IRC +10 216, as well as Doppler-limited IR spectroscopy of the 2164 cm$^{-1}$ band. At that time, cost

considerations precluded extension of the treatment to the larger clusters.

Therefore, the performance of the semiempirical methods MINDO/3, MNDO, AM1, and PM3 — which are four orders of magnitude less expernsive than the corresponding ab initio calculations — for the clusters $C_2$–$C_{10}$ was critically compared (Section 4.7) with the available (very incomplete) experimental and ab initio data. MINDO/3 performed acceptably but no more than that; the other methods broke down completely. This could be traced back to the parametrization procedure; an ad hoc reparametrization of MNDO provided results in good agreement with available data. Peculiarly, excellent agreement with the available harmonic frequencies could be achieved for the linear structures (mean overestimate of 40 $cm^{-1}$). By comparing computed frequencies, IR intensities, and isotope shifts with the available experimental spectra, a completely revised assignment was suggested, namely of 1952 and 1197 $cm^{-1}$ to $C_6$; of 2128 and 1893 $cm^{-1}$ to $C_7$; and of the very intense 1997 $cm^{-1}$ feature to $C_9$. Various other bands were tentatively assigned to cyclic structures.

An independent confirmation by ab initio techniques is presented in Section 4.8. Assignments for $C_6$ and $C_7$ were straightforward; an extensive list of arguments for assigning the 1997 $cm^{-1}$ band to $C_9$ is presented, which contradicts its recent assignment to $C_8$. Meanwhile, all of these assignments have been proven experimentally by Doppler-limited IR work.

The ground state of $C_4$ — which has a linear and a rhombic structure very close together in energy — has been a matter of controversy for almost a decade. All previous studies, however, neglected consideration of basis set effects. Therefore, an investigation using large basis sets of $[5s4p2d1f]$ quality is reported in Section 4.9. It is found that the cyclic structure is approximately 1 kcal/mol lower in energy than the linear one. Arguments favoring assignment of the 1284 $cm^{-1}$ matrix IR feature to cyclic $C_4$ are found, with the proviso that the cyclic structure indeed be lower in energy than the linear one; this allows experimental verification. The computed heat of formation (expected accuracy ±4 kcal/mol) is about 20 kcal/mol higher than the experimental (Knudsen effusion) value; however, the cause of the discrepancy is shown to be the use of rough estimates for the partition functions in the experimental third-law analysis. Using more accurate functions brings the revised experimental value in close agreement with the theoretical one.

$C_3^+$ is considered to be the 'building block' for the carbon cluster ions. Its structure was investigated by Coulomb explosion techniques, the data of which could be interpreted both in terms of a cyclic and a linear structure. In an attempt to settle the issue, ab initio calculations are presented in Section 4.10. It is shown there that $C_3^+$ is cyclic, but will be very fluxional at higher temperatures as both the linear structure and a Jahn-Teller transition state towards degenerate isometrization are very close in energy. Two other groups arrived, simultaneously and independently, at the same conclusion. However, the computed energy difference $\Delta E$ between the linear and cyclic structures differs considerably between the three studies. Apparently the $\Delta E$ is extremely sensitive to the electron correlation method employed, which is caused by very prominent near-degeneracy effects. In a joint effort with NASA Ames Research Center (Section 4.11), a multireference study of this molecule was therefore undertaken. Together with new results using an open-shell CCSD(T) method, this allowed to put forward a more or less definitive value of 5.5±1.3 kcal/mol.

During the course of the work on cluster molecules, some methodological issues cropped up which are dealt with in Chapter 5. It was previously known that in cases of heavy spin contamination (which occurs when a UHF reference wavefunction is used for an open-shell molecule with low-lying excited states), single excitations become very im-

portant and cannot adequately be dealt with by perturbational methods. In Section 5.2 is it shown that their effect on geometries and harmonic frequencies also becomes fairly large for these molecules, whereas it is usually taken for granted that their contribution is negligible. The limiting invariance of some electron correlation methods with respect to contamination by the next higher spin state is also discussed there.

Limited configuration interaction, the oldest electron correlation method, has the main disadvantage that it is not size-consistent, i.e. computed energy does not scale properly with the size of the system. Several correction formulas have been proposed over the years, but these were never critically compared. Such a comparison, both numerically and by a perturbation theory analysis, is presented in Section 5.3. It is shown that the linearized coupled cluster energy, which corresponds to the limited CI energy after cancellation of the renormalization term by unlinked cluster terms, is best approximated by the Davidson-Silver formula, whereas the regular coupled cluster energy is best approximated by the Pople formula, which includes an approximate mutual cancellation of linked and unlinked exclusion principle violating (EPV) terms. An example application is considered in Section 5.4, where it is shown that for most practical cases, the CCSD (coupled cluster with all singles and doubles) energy can be conveniently approximated by CISD with a Pople correction.

Summarizing, it has been shown that even at the present state of the art, ab initio methods are a valuable tool in solving practical chemical problems arising in widely diverging fields such as astrophysics and materials science, and that their accuracy may equal and even surpass that of the best experimental techniques. And this, as the reader should be reminded time and again, is only the beginning.

# Samenvatting en algemene conclusies

In principe kan elke chemisch interessante moleculaire grootheid exact en kwantitatief worden bekomen door de moleculaire Schrödingervergelijking op te lossen. De aanwezigheid van veeldeeltjesinteracties maakt evenwel een analytische oplossing principieel onmogelijk, en een exacte numerieke oplossing technisch niet haalbaar. Benaderde oplossingen zijn steeds een compromis tussen de gewenste nauwkeurigheid en de rekenkundige kostprijs. Recente verbeteringen in de computertechnologie, alsmede methodologische vorderingen, hebben op het ogenblik een situatie gecreëerd waar de nauwkeurigheid van ab initio resultaten voor kleine moleculen competitief wordt met de experimentele. In tegenstelling met het experiment evenwel, behoeft men geen rekening te houden met beperkingen aangaande zeldzaamheid, levensduur, of reactiviteit.

De statistische theormodynamica laat toe, via het opstellen van de moleculaire partitiefunctie, deze nauwkeurigheid uit te breiden tot macroscopische thermodynamische grootheden.

Het onderhavige werk behandelt de toepassing van ab initio-methoden op een aantal praktische problemen in de materiaalwetenschappen en de astrofysica, alsmede enkele verbeteringen op het gebied van de algemene methodologie.

Hoofdstuk 1 geeft een overzicht van de huidige (december 1990) stand van de algemene theorie. Dit overzicht maakt geen aanspraak op volledigheid; alle aspecten die relevant zijn voor de rest van het werk worden evenwel in de mate van het mogelijke besproken. Speciale aandacht wordt geschonken aan elektronencorrelatietechnieken zoals configuratie-interactie, veeldeeltjesstoringsrekening, en 'coupled cluster' methoden.

In Hoofdstuk 2 worden de computerapparatuur en -programmatuur, die in de rest van het werk worden gebezigd, kort toegelicht.

In Hoofdstuk 3 wordt de nauwkeurige ab initio berekening van moleculaire dissociatie-energieën (totale atomisatie-energieën, vormingswarmten) aangesneden. Hiertoe wordt een nieuwe familie van eindige basissets, de *combined bond-polarization* basissets, ingevoerd. In alle praktische ab initioberekeningen wordt de oplossing ontwikkeld in termen van een eindig stel basisfuncties die gewoonlijk op de atoomkernen gecentreerd zijn. Voor moleculen maakt het anisotrope karakter van een chemische binding (in tegenstelling tot de isotrope omgeving in een vrij atoom) het noodzakelijk om hetzij polarisatiefuncties (basisfuncties met hoger hoekmoment, die gecentreerd zijn op de atomen), hetzij bondfuncties (basisfuncties met lager hoekmoment, geplaatst langsheen de bindingsas), aan de basisset toe te voegen. Beide types van basisfunctie hebben hun voor- en nadelen. De auteur toonde echter aan (Sectie 3.2) dat door ze gezamenlijk toe te passen, bindingsenergieën van 'chemische nauwkeurigheid' (fouten $\leq$ 2 kcal/mol) kunnen worden bekomen tegen een veel lagere rekenkundige kostprijs (een factor 4 tot 20 naargelang het geval) dan met een 'alleen polarisatie' basisset van vergelijkbare kwaliteit. Een vaak gemaakt bezwaar tegen het gebruik van bondfuncties, namelijk de pathologische basissetsuperpositiefouten die ermee gepaard gaan, werd uitgelegd in termen van atomaire externe correlatie. Er werd aangetoond in Sectie 3.3 dat door tenminste $f$-functies in de polarisatieruimte toe te laten (in het geval van *sp* bondfuncties), dit probleem grotendeels verholpen wordt. Zulke basissets brengen een rekenkundige kost met zich mede vergelijkbaar met deze van veelgebruikte 'alleen polarisatie' basissets, doch performeren duidelijk superieur. Het probleem van BSSE voor polyatomische moleculen, waarvoor geen eenduidige goedgedefinieerde maat bestaat, werd besproken in Sectie 3.4. Empirische argumenten voor het totaal verwaarlozen van BSSE worden daar eveneens voorgesteld. Door het beter in rekening brengen van elektronencorrelatie (Sectie 3.5) en het gebruik van referentiegeometrieën op gecorreleerd niveau (Sectie 3.6) kon een nauwkeurigheid

van 0,12 kcal/mol per binding worden bereikt voor de dissociatie-energieën van de $AH_n$ (A=Li–F) hydriden en hydrideradicalen. Als een voorbeeld van toepassing werd het definitief bewijs geleverd voor een foutieve experimentele interpretatie bij het bepalen van de dissociatie-energie van BH (Sectie 3.7).

Clustermoleculen hebben recent heel wat belangstelling opgewekt in diverse gebieden, waaronder materiaalwetenschappen en astrofysica. In de materiaalwetenschappen, in het bijzonder bij oppervlakteveredeling met neokeramische materialen middels 'chemical vapor deposition' technieken, vormen clusters de 'natuurlijke brug' tussen een gasvormig plasma en de dunne oppervlaktelaag. De meeste neokeramische materialen komen in diverse kristallijne modificaties voor, waarvan slechts één de vereiste eigenschappen van hardheid en corrosiebestendigheid heeft (bv. diamant voor vast koolstof, $\beta$-BN in het geval van boornitride, carborundum voor vast SiC). Experimenteel onderzoek heeft aangetoond dat de aard van het afgezette materiaal in belangrijke mate afhangt van de clustergroeiprocessen in het plasma; indien voldoende thermodynamische gegevens beschikbaar waren, kon het proces worden gesimuleerd en mogelijk gecontroleerd.

Diezelfde clustermoleculen (in het bijzonder $C_n$ en SiC) duiken op in de astrofysica, waar zij voorkomen in steratmosferen en interstellaire gaswolken. Zij worden gezien door IR- en radio-astronomen als merendeels ongeïdentificeerde banden; de spectroscopische karakterisatie van de moleculen zou deze wetenschappers toelaten deze moleculen te identificeren en conclusies te trekken (aangaande ouderdom, chemische processen, ...) over de hogervermelde hemellichamen.

De experimentele karakterisatie van deze moleculen is moeilijk wegens hun reactiviteit en korte levensduur. Theoretische methoden, waarvoor deze beschouwingen van geen tel zijn, vormen een voor de hand liggend alternatief. Daarbij zijn de spectroscopische eigenschappen vereist door de astrofysicus ook essentieel voor het opstellen van de partitiefunctie, teneinde de door de materiaalwetenschappers vereiste thermochemische gegevens (bij hoge temperatuur) te bekomen.

In Sectie 4.2 werden de clustermoleculen $B_3$, $B_2N$, $BN_2$ en $N_3$ bestudeerd. Voor de drie eerstgenoemde species vormen deze ab initioberekeningen de eerste gepubliceerde gegevens in de literatuur. $B_3$ is in de grondtoestand een gelijkzijdige driehoek; $B_2N$ is een uitzonderlijk stabiel lineair molecuul. De vier laagstliggende toestanden van $BN_2$ liggen zeer dicht bij elkaar; het globale minimum hiervan is een ringstructuur. Het molecuul zal dissociëren in B en $N_2$ bij alle temperaturen. De bevindingen voor $N_3$ zijn in redelijke overeenkomst met het experiment voor wat de spectroscopische constanten aangaat; de vormingswarmte is evenwel in tegenspraak met alledrie de literatuurwaarden, die bovendien onderling niet overeenstemmen. Teneinde deze kwestie voor eens en voor altijd op te helderen, werd in Sectie 4.3 de totale atomisatie-energie van $N_3$ met zeer grote basissets berekend.

In Secties 4.4 en 4.5 werden de diatomische moleculen SiC en BN behandeld. Daar zij slechts diatomisch zijn, werd getracht de nauwkeurigheid tot de grens van het technisch mogelijke op te voeren. Spectroscopische constanten voor enkele van de laagstliggende toestanden, inclusief de anharmonische, werden bekomen met behulp van grote basissets en 'coupled cluster' technieken. Gebruikmakend van deze gegevens werden de partitiefuncties opgesteld d.m.v. rechtstreekse numerieke sommatie en tabellen aangelegd van de thermodynamische functies tot 6000 K. Bij deze laatste zijn correcties inbegrepen voor anharmoniciteit, rotatie-vibratiekoppeling, centrifugaalvervorming, en spin-baan koppeling. In het geval van SiC werd een foutenanalyse van de thermodynamische functies gemaakt, en gevonden dat de nauwkeurigheid van goede ab initioberekeningen meer dan voldoende is voor het gestelde doel. In het geval van BN werd gevonden dat de laagste $^3\Pi$ en $^1\Sigma^+$ toestanden extreem dicht bij elkaar liggen ($T_e \approx 100$ cm$^{-1}$).

Reeds in 1971 werd koolstofdamp gevangen in een argon-matrix, werden IR-spectra opgenomen, en diverse banden toegekend aan diverse clustermoleculen op basis van eenvoudige krachtveld-argumentaties. Als belangrijkste conclusie werd de 2164 $cm^{-1}$ band toegekend aan $C_4$; 1544 $cm^{-1}$ aan $C_5$; 1997 $cm^{-1}$ en 1197 $cm^{-1}$ aan $C_6$; 2128, 1893, en 1447 $cm^{-1}$ aan $C_9$. Ab initioberekeningen op $C_4$ vonden geen IR-actieve band nabij 2164 $cm^{-1}$; in Sectie 4.6 toonde een ab initioberekening op gecorreleerd niveau van de harmonische frequenties en IR-intensiteiten van $C_5$ definitief aan dat de toekenningen van de 2164 en 1544 $cm^{-1}$-banden moesten omgewisseld worden. Deze voorspelling werd bevestigd door de daaropvolgende detectie van $C_5$ in de atmosfeer van koolstofster IRC +10 216, zowel als door IR-spectroscopie met Doppler-beperkte resolutie van de 2164 $cm^{-1}$-band. Op dat ogenblik sloten kostprijs-overwegingen de uitbreiding van deze behandeling naar de grotere clusters uit.

Daarom werden resultaten bekomen met de semi-empirische methoden MINDO/3, MNDO, AM1 en PM3 — die vier orden van grootte goedkoper zijn dan de overeenkomstige ab initio-berekeningen — kritisch vergeleken (Sectie 4.7) met de beschikbare (zeer onvolledige) experimentele en ab initiogegevens. MINDO/3 performeerde aanvaardbaar, maar niet meer dan dat; de andere methoden lieten het totaal afweten. Dit kon worden teruggevoerd op de parametrisatieprocedure; een ad hoc herparametrisatie van MNDO leverde resultaten in goede overeenkomst met de beschikbare experimentele gegevens. Merkwaardig genoeg kon voor de lineaire structuren een uitstekende overeenkomst met de beschikbare experimentele harmonische frequenties worden bereikt (gemiddelde overschatting van 40 $cm^{-1}$); door berekende frequenties, IR-intensiteiten, en isotoopverschuivingen te vergelijken met de beschikbare experimentele spectra kon een volledig herziene toekenning worden voorgesteld, namelijk van 1952 en 1197 $cm^{-1}$ aan $C_6$; van 2128 en 1893 $cm^{-1}$ aan $C_7$; en van de zeer intense 1997 $cm^{-1}$ band aan $C_9$. Diverse andere banden werden tentatief toegekend aan ringstructuren.

Een onafhankelijke bevestiging via ab initiotechnieken is weergegeven in Sectie 4.8. Toekenningen voor $C_6$ en $C_7$ waren voor de hand liggend; in tegenspraak met een recent voorgestelde toekenning van de 1997 $cm^{-1}$ band aan $C_8$ werd een uitgebreide reeks argumenten aangedragen voor een toekenning aan $C_9$. Sindsdien werden al deze toekenningen experimenteel bewezen door middel van IR-spectroscopie met Doppler-beperkte resolutie.

De grondtoestand van $C_4$ — waarvoor een lineaire en een ruitvormige structuur zeer dicht bijeen liggen in energie — is een punt van controverse sinds bijna een decennium. Alle voorgaande studies verwaarloosden evenwel het beschouwen van basisset-effecten. Daarom werd een studie met zeer grote basissets van $[5s4p2d1f]$ kwaliteit uitgevoerd (Sectie 4.9). Er werd gevonden dat de cyclische vorm ongeveer 1 kcal/mol lager in energie ligt dan de lineaire. Argumenten voor het toekennen van de 1284 $cm^{-1}$ matrix-IR band aan cyclisch $C_4$ worden gevonden, vooropgesteld dat de cyclische structuur inderdaad lager in energie dan de lineaire zou zijn; dit laat experimentele verificatie toe. De berekende vormingswarmte (verwachte nauwkeurigheid $\pm$ 4 kcal/mol) is ongeveer 20 kcal/mol hoger in energie dan de experimentele waarde (d.m.v. Knudsen-effusie); het wordt evenwel aangetoond dat de oorzaak van de discrepantie ligt in het gebruik van ruwe schattingen voor de partitiefunctie in de experimentele derde-wet analyse. Het gebruik van meer nauwkeurige partitiefuncties brengt de herziene experimentele waarde in nauwe overeenstemming met het experiment.

$C_3^+$ wordt beschouwd als de 'bouwsteen' van de positieve ionen van de koolstofclusters. De structuur ervan werd experimenteel onderzocht middels Coulomb-explosietechnieken; de gegevens hieruit konden worden geïnterpreteerd in termen van zowel een lineaire als een cyclische structuur. In een poging de kwestie op te helderen, worden ab initioberekenin-

gen op dit systeem voorgesteld in Sectie 4.10. Er wordt aangetoond dat $C_3^+$ cyclisch is, maar zeer flexibel zal zijn bij hoge temperaturen aangezien zowel een lineaire structuur als een Jahn-Teller transitietoestand t.o.v. ontaarde isomerisatie zeer dichtbij liggen in energie. Twee andere groepen kwamen tegelijk en onafhankelijk van ons tot dezelfde conclusie. Nu bleek echter het berekende energieverschil $\Delta E$ tussen de lineaire en de cyclische structuren serieus te verschillen tussen de drie studies. Kennelijk is de $\Delta E$ zeer gevoelig aan de gebruikte electronencorrelatiemethode, hetgeen veroorzaakt wordt door zeer prominente bijna-ontaardingseffecten. Daarom werd in een gemeenschappelijke krachtsinspanning (Sectie 4.11) met het Ames Research Center van de NASA een multireferentie-studie van dit molecuul ondernomen. Tesamen met resultaten bekomen met een nieuwe CCSD(T) methode voor radicalen, liet dit toe een min of meer definitieve waarde van 5.8±1.3 kcal/mol voorop te stellen.

In het verloop van het werk op de clustermoleculen doken een aantal methodologische problemen op die besproken worden in Hoofdstuk 5. Het was tevoren bekend dat in gevallen van zware spin-contaminatie (hetgeen optreedt wanneer een UHF-referentiedeterminant wordt gebruikt voor een onpaar molecuul met laagliggende aangeslagen toestanden), enkelvoudige excitaties zeer belangrijk worden en niet bevredigend kunnen worden behandeld via storingsrekening. In Sectie 5.2 wordt aangetoond dat hun effect op geometrieën en harmonische frequenties dan ook tamelijk groot wordt, terwijl het gewoonlijk als vaststaand wordt aangenomen dat hun bijdrage verwaarloosbaar is. De invariantie-in-de-limiet van een aantal elektronencorrelatiemethodes ten opzichte van contaminatie door de volgende hogere spintoestand wordt aldaar eveneens besproken.

Beperkte configuratie-interactie, de oudste elektronencorrelatiemethode, heeft het nadeel dat zij niet extensief is, d.w.z. de berekende energie neemt niet correct toe met de grootte van het systeem. Diverse correctieformules werden voorgesteld, maar nooit kritisch vergeleken. Zulk een vergelijking, zowel numeriek als door middel van een storingstheoretische analyse, wordt gegeven in Sectie 5.3. Er wordt aangetoond dat de gelineariseerde 'coupled cluster' energie, die overeenkomt met de beperkte CI energie na het elimineren van de renormalisatieterm, het best wordt benaderd door de Davidson-Silver formule, terwijl de gewone 'coupled cluster' energie het best wordt benaderd door de Pople-formule, die ook de wederzijdse opheffing van 'linked' en 'unlinked' Pauliverbodschendende (EPV) termen benaderd in rekening brengt. Een voorbeeld van toepassing wordt beschouwd in Sectie 5.4, waar wordt aangetoond dat in de meeste praktische gevallen de CCSD ('coupled cluster' met alle enkelvoudige en dubbele substituties) energie handig kan worden benaderd door CISD met een Pople-correctie.

Samengevat werd er aangetoond dat, zelfs bij de huidige stand van het domein, ab initiomethoden een waardevol werktuig zijn voor het oplossen van chemische problemen in zo ver uiteenlopende gebieden als materiaalwetenschappen en astrofysica, en dat hun naukeurigheid die van de beste experimentele technieken kan evenaren en zelfs overtreffen. En dit — de lezer zij hieraan telkens en telkens weer herinnerd — is nog slechts het begin.

# Publication list

## Scientific papers

1. J.M.L. Martin, J.P. François, and R. Gijbels, *Combined bond-polarization function basis sets for accurate ab initio calculations of the dissociation energies of $AH_n$ molecules (A = Li to F)*, JOURNAL OF COMPUTATIONAL CHEMISTRY **10**, 152–162 (1989).

2. J.M.L. Martin, J.P. François, and R. Gijbels, *Combined bond-polarization function basis sets for accurate determination of dissociation energies. 2. Basis set superposition error as a function of the parent basis set.*, JOURNAL OF COMPUTATIONAL CHEMISTRY **10**, 875–886 (1989).

3. J.M.L. Martin, J.P. François, and R. Gijbels, *Combined bond-polarization function basis sets for accurate determination of dissociation energies. 3. Basis set superposition error for polyatomic systems*, THEORETICA CHIMICA ACTA **76**, 195–209 (1989).

4. J.M.L. Martin, J.P. François, and R. Gijbels, *On the validity of Pople's infinite-order Møller-Plesset extrapolation and an alternative formula within MBP/CC theories*, CHEMICAL PHYSICS LETTERS **157**, 217–223 (1989); *erratum* **159**, 122 (1989).

5. J.M.L. Martin, J.P. François, and R. Gijbels, *Accurate ab initio predictions of the dissociation energy and heat of formation of first-row hydride species*, CHEMICAL PHYSICS LETTERS **163**, 387–391 (1989).

6. J.M.L. Martin, J.P. François, and R. Gijbels, *Comment on "A theoretical study of the dissociation energy of BH using quadratic configuration interaction"*, JOURNAL OF CHEMICAL PHYSICS **91**, 4425–4426 (1989).

7. J.M.L. Martin, J.P. François, and R. Gijbels, *Note on the vibrational spectrum of $C_4$ and $C_5$*, JOURNAL OF CHEMICAL PHYSICS **90**, 3603–3605 (1989).

8. J.M.L. Martin, J.P. François, and R. Gijbels, *Ab initio study of boron, nitrogen, and boron-nitrogen clusters. I.Isomers and thermochemistry of $B_3$, $B_2N$, $BN_2$, and $N_3$*, JOURNAL OF CHEMICAL PHYSICS **90**, 6469–6485 (1989).

9. J.M.L. Martin, J.P. François, and R. Gijbels, *Isomers and thermochemistry of $B_3$, $B_2N$, $BN_2$, and $N_3$*, COLLOQUE DE PHYSIQUE **50 C5**, 873–885 (1989).

10. R. Voets, J.P. François, J.M.L. Martin, J. Mullens, J. Yperman, and L.C. Van Poucke, *Theoretical study of the proton affinities of 2-, 3-, and 4-monosubstituted*

*pyridines in the gas phase by means of MINDO/3, MNDO, and AM1*, JOURNAL OF COMPUTATIONAL CHEMISTRY **10**, 449–468 (1989).

11. J.M.L. Martin, J.P. François, and R. Gijbels, *Ab initio study of the proton affinity of a number of ortho-substituted pyridines*, JOURNAL OF COMPUTATIONAL CHEMISTRY **10**, 346–357 (1989).

12. J.M.L. Martin, J.P. François, and R. Gijbels, *Unusually large effects of single excitations on the geometry of radical species and limiting spin-projection invariance of some correlated methods*, CHEMICAL PHYSICS LETTERS **166**, 295–302 (1990).

13. R. Voets, J.P. François, J.M.L. Martin, J. Mullens, J. Yperman, and L.C. Van Poucke, *Theoretical study of the proton affinities of 2-, 3-, and 4-monosubstituted phenolate ions in the gas phase by means of MINDO/3, MNDO, and AM1*, JOURNAL OF COMPUTATIONAL CHEMISTRY **11**, 269–290 (1990).

14. J.M.L. Martin, J.P. François, and R.Gijbels, *Accurate ab initio spectroscopic and thermodynamic properties for the SiC molecule*, JOURNAL OF CHEMICAL PHYSICS **92**, 6655–6667(1990).

15. J.M.L. Martin, J.P. François, and R. Gijbels, *On size consistency corrections for configuration interaction calculations*, CHEMICAL PHYSICS LETTERS **172**, 346–353 (1990).

16. J.M.L. Martin, J.P. François, and R. Gijbels, *Some cost-effective approximations to CCSD and QCISD*, CHEMICAL PHYSICS LETTERS **172**, 354–360 (1990).

17. J.M.L. Martin, J.P. François, and R. Gijbels, *The dissociation energy of $N_3$*, JOURNAL OF CHEMICAL PHYSICS **93**, 4485–4487 (1990).

18. J.M.L. Martin, J.P. François, and R. Gijbels, *On the geometrical structure of the $C_3^+$ cation — an ab initio study*, JOURNAL OF CHEMICAL PHYSICS **93**, 5037-5045 (1990).

19. J.M.L. Martin, J.P. François, and R. Gijbels, *A critical comparison of MINDO/3, MNDO, AM1, and PM3 for a model problem: carbon clusters $C_2$-$C_{10}$. An ad hoc reparametrization of MNDO well suited for the accurate prediction of their spectroscopic constants*, JOURNAL OF COMPUTATIONAL CHEMISTRY **11**, xxxx-xxxx+18 (page proofs corrected).

20. J.M.L. Martin, J.P. François, and R. Gijbels, *Ab initio study of the infrared spectra of linear $C_n$ clusters (n=6–9)*, JOURNAL OF CHEMICAL PHYSICS **93**, 8850–8861 (1990).

21. J.M.L. Martin, J.P. François, and R. Gijbels, *Ab initio study of the structure, infrared spectra, and heat of formation of* $C_4$, JOURNAL OF CHEMICAL PHYSICS, accepted and in press.

22. P.R. Taylor, J.M.L. Martin, J.P. François, and R. Gijbels, *An ab initio study of the* $C_3^+$ *cation using multireference methods*, JOURNAL OF CHEMICAL PHYSICS, submitted.

23. J.M.L. Martin, J.P. François, and R. Gijbels, *Ab initio spectroscopy and thermochemistry of the BN molecule*, CHEMICAL PHYSICS, submitted.

## Published computer programs

24. J.J.P. Stewart, J.M.L. Martin and J.P. François, MOPAC *5.0: A general purpose molecular orbital package (CDC version)*, QCPE 455/CDCM (Quantum Chemistry Program Exchange, Bloomington, IN); see also QCPE BULLETIN **10**, 9 (1990) for announcement.

## Oral and poster presentations

25. J.M.L. Martin, *Efficiënte ab initio berekening van dissociatie-energieën met hoge nauwkeurigheid door middel van gecombineerde bond-polarisatiebasissets*, oral presentation at the VCV DAG DER JONGEREN '89, Vrije Universiteit Brussel, 24.5.1989.

26. J.M.L. Martin, J.P. François, and R. Gijbels, *Ab initio studie van boor-, stikstof- en boor-stikstofclusters en hun ionen in verband met dunnelaagbereiding*, poster presentation at the DAG DER JONGEREN '89.

27. J.M.L. Martin, J.P. François, and R. Gijbels, *Combined bond-polarization basis sets for efficient and accurate computation of molecular dissociation energies and other properties*, poster presentation at the SECOND SCF USERS GROUP MEETING, Facultés Universitaires de Namur, 18-19.5.1989.

28. J.M.L. Martin, J.P. François, and R. Gijbels, *Ab initio study of boron-nitrogen clusters in relation to thin layer preparation*, poster presentation at the SECOND SCF USERS GROUP MEETING.

29. J.M.L. Martin, J.P. François, and R. Gijbels, *Ab initio study of boron, nitrogen, and boron-nitrogen clusters and their ions in relation to thin layer preparation*, poster presentation at the SEVENTH EURO-CVD CONFERENCE, Perpignan, 19-23.6.1989.

30. J.M.L. Martin, J.P. François, and R. Gijbels, *An efficient and accurate ad hoc semiempirical method and its application to carbon clusters* $C_n$ *(n=2-10)*, poster

presentation at the THIRD SCF USERS GROUP MEETING, Facultés Universitaires de Namur, 11-13.6.1990

31. J.M.L. Martin, J.P. François, and R. Gijbels, *Chemically accurate ab initio calculations on small cluster molecules*, poster presentation at the THIRD SCF USERS GROUP MEETING.

32. J.M.L. Martin, J.P. François, and R. Gijbels, *Assignment of the infrared spectrum of carbon vapor trapped in an argon matrix, guided by ab initio and ad hoc MNDO calculations*, poster presentation at the ISSPIC 5 CONFERENCE, Konstanz, 10-14.9.1990.

## Scientific prize

33. Second prize in DSM CONTEST FOR CHEMISTRY AND TECHNOLOGY 1990 with entry entitled: *Ab initio studie van clusters in verband met de bereiding van dunne neokeramische lagen. Ontwikkeling van efficiënte en accurate theoretische methoden voor de berekening van spectroscopische en thermodynamische eigenschappen*,

# Glossary of acronyms

| | |
|---|---|
| **ACPF** | Averaged coupled pair functional (Section 1.9.2). |
| **AO** | Atomic orbital. |
| **AM1** | Austin model 1, a semiempirical method (Section 4.7.1.1). Essentially MNDO with modified core repulsion functions. |
| **BD** | Brueckner doubles theory, or CCD based on Brueckner orbitals (Section 1.6.7). |
| **BD(T)** | Same with a quasiperturbative triples correction. |
| **BSSE** | Basis set superposition error (Section 1.11.4). |
| **CASSCF** | Complete active space SCF (Section 1.4.2). |
| **CC** | Coupled cluster theory (Section 1.6). |
| **CCD** | Coupled cluster theory with all double substitutions (1.6.1). |
| **CCD(ST)** | CCD with quasiperturbative singles and triples corrections (Section 1.6.6). |
| **CCD+ST(CCD)** | See CCD(ST). |
| **CCSD(T)** | CCSD with a quasipertubative correction for triple excitations composed of both a fourth-order like term involving the double excitation amplitudes and a fifth-order like term involving the single excitation amplitudes (Section 1.6.6). An excellent approximation to full CI. |
| **CCSD+T(CCSD)** | CCSD with a quasipertubative correction for triple excitations composed of only the fourth-order like term involving the double excitation amplitudes (Section 1.6.6). Significantly degraded performance over CCSD(T). |
| **CCSD** | Coupled cluster theory with all single and double substitutions (Section 1.6.2). |
| **CEPA** | Coupled electron pair approximation (Section 1.9.1). |
| **CID** | Limited configuration interaction with all double excitations (Section 1.3.4). |

| | |
|---|---|
| **CISD** | Limited configuration interaction with all single and double excitations (Section 1.3.4). |
| **CP** | Counterpoise (method), an approximate BSSE correction scheme (1.11.4). |
| **CPF** | Coupled pair functional (Section 1.9.2). |
| **CPHF** | Coupled perturbed Hartree-Fock (Section 1.10.4). |
| **DIIS** | Direct inversion of the iterative subspace, a convergence accelerator (Section 1.1.7.1). |
| **EA** | Electron affinity. |
| **EPV** | Exclusion principle violating (Section 1.5.6). |
| **FCI** | Full configuration interaction, the exact determination of the basis set correlation energy (Section 1.3.1). |
| **G1 theory** | An isogyric correction scheme for atomization energies, with a general accuracy of $\pm$ 2 kcal/mol (Section 1.11.8). |
| **GHF** | Generalized Hartree-Fock (Section 1.1.5). |
| **HF** | Hartree-Fock (Section 1.1.1). |
| **HOMO** | Highest occupied molecular orbital. |
| **IEPA** | Independent electron pair approximation (Section 1.9.1). |
| **INDO** | Intermediate neglect of differential overlap, a semiempirical method (Section 4.7.1.1). |
| **IP** | Ionization potential. |
| **LCCD** | Linearized coupled cluster theory with all double substitutions (Section 1.6.1). |
| **LCCSD** | Linearized coupled cluster theory with all single and double substitutions (Section 5.4.2). |
| **LUMO** | Lowest unoccupied molecular orbital. |
| **MBPT** | Many-body perturbation theory (Section 1.5). |
| **MCSCF** | Multiconfigurational SCF (Section 1.4.2). |

| | |
|---|---|
| **MINDO/3** | Modified INDO version 3, a semiempirical method (Section 4.7.1.1). |
| **MNDO** | Modified neglect of diatomic overlap, a semiempirical method (Section 4.7.1.1). |
| **MO** | Molecular orbital. |
| **MP2** | Second order MBPT (Section 1.5.4). |
| **MP3** | Third order MBPT (Section 1.5.5). |
| **MP4(DQ)** | Fourth order MBPT neglecting the contributions of single and triple excitations at fourth order (Section 1.5.6). |
| **MP4(SDQ)** | Fourth order MBPT neglecting the contributions of triple excitations at fourth order (Section 1.5.6). |
| **MP4(SDTQ)** | See MP4. |
| **MP4** | Full fourth order MBPT (Section 1.5.6). |
| **MP** | Møller-Plesset theory. See MBPT. |
| **MRD-CI** | Multireference double excitation configuration interaction (Section 1.4.1). |
| **MRCI** | The NASA Ames multireference CI procedure. Basically CISD from a subset of the CASSCF determinants (Section 1.4.4). |
| **NDDO** | Neglect of diatomic differential overlap, a semiempirical method (Section 4.7.1.1). |
| **PM3** | Parametrization 3, a semiempirical method (Section 4.7.1.1). A reparametrization of AM1. |
| **PMP2** | Spin-projected MP2 (Section 1.8). |
| **PMP3** | Spin-projected MP3 (Section 1.8). |
| **PUHF** | Spin-projected unrestricted Hartree-Fock (Section 1.8). |
| **PUMP2** | See PMP2. |
| **PUMP3** | See PMP3. |

| | |
|---|---|
| **QCISD(T)** | QCISD with a quasiperturbative correction for triple excitations composed of both a fourth-order like term involving the double excitation amplitudes and a fifth-order like term involving the single excitation amplitudes (Section 1.6.6). A very good approximation to CCSD(T). |
| **QCISD** | Quadratic configuration interaction with all singles and doubles, a good approximation to CCSD (Section 1.6.2). |
| **QCSCF** | Quadratically convergent SCF, an implicit Newton-Raphson SCF iteration algorithm (Section 1.1.7.2). |
| **RHF** | Restricted Hartree-Fock (Section 1.1.2). Usually (but not always) closed-shell. |
| **ROHF** | Restricted open-shell Hartree-Fock (Section 1.1.3). |
| **SCF** | Self-consistent field (Section 1.1.1). |
| **SOCI** | Second order CI. CISD from a CASSCF wavefunction (Section 1.4.4). |
| **UHF** | Unrestricted Hartree-Fock (Section 1.1.1). |
| **VIP** | Vertical (as opposed to 'adiabatic') ionization potential. |